解析代谢密码，洞见生命健康

——SCIEX 代谢组学应用文集

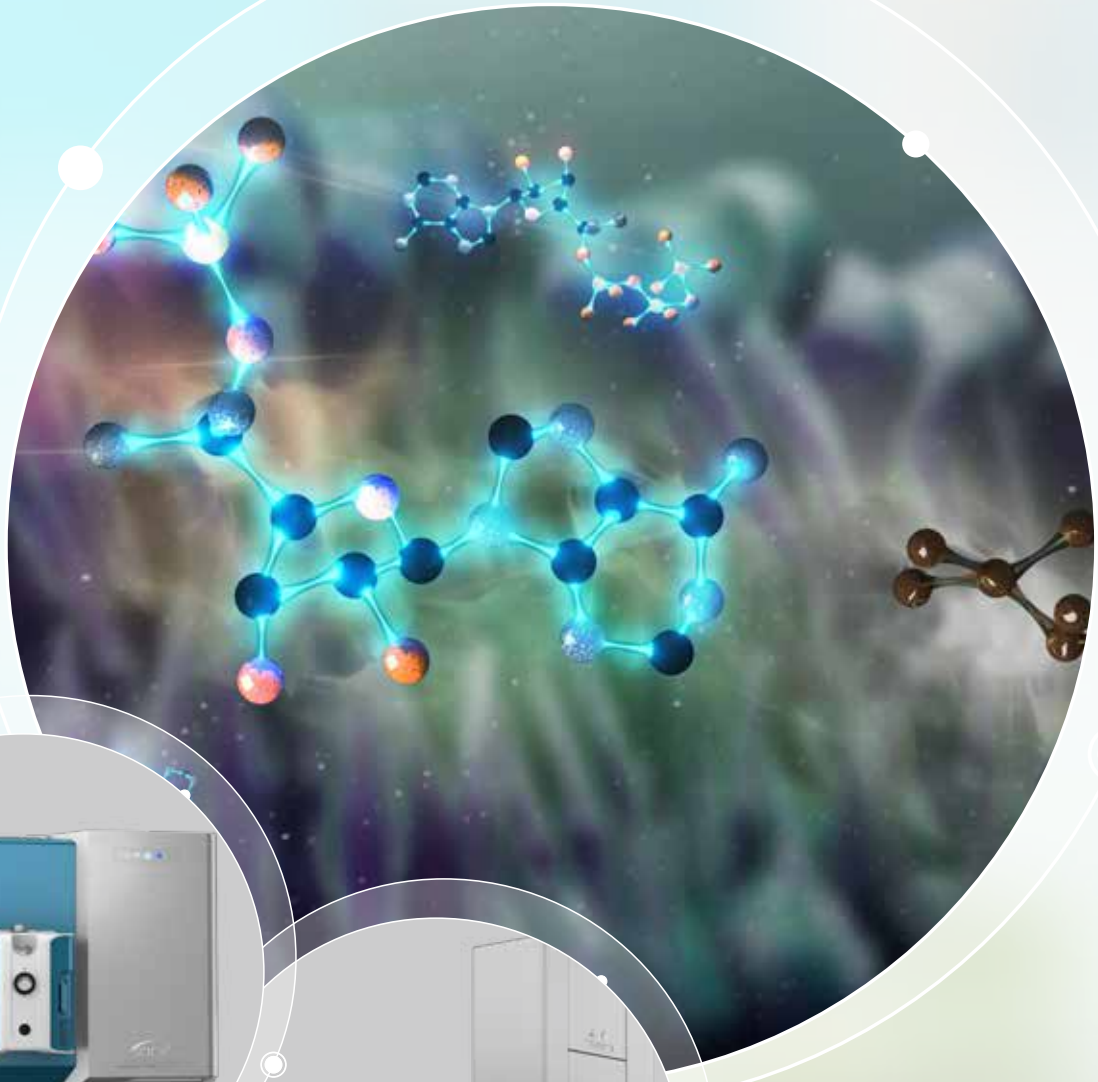

SCIEX

The power of precision

超过 50 年的创新历程

1970

SCIEX 公司创立
Barry French 和 William Breukelman 创立于多伦多大学

1981

发布第一款 SCIEX 商用三重四极杆 (MS/MS) 质谱仪器

1989

发布 API III
第一款 SCIEX 商业化 LC-MS/MS

2001

发布 API 4000™ LC-MS/MS 系统

发布 Echo MS
声波激发耦合质谱系统 AEMS，具备超高通量检测能力

2021

发布 7500系列
LC-MS/MS 系统

2019

发布 5500+系列
LC-MS/MS 系统

2019年发布
TripleTAF 6600+

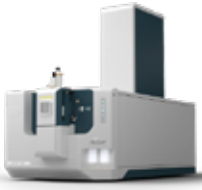

发布 ZenoTOF 7600
多重碎裂高分辨质谱

发布全新软件操作平台
SCIEX OS

发布 中国本土化产品
4500/5500+ LC-MS/MS 系统

发布在线毛细管电泳-质谱联用仪器 Intabio™ ZT 系统

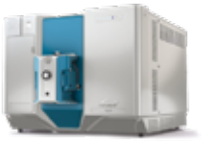

2024

发布 7500+系列
LC-MS/MS 系统
开创灵敏度新时代

2022

发布 Zeno SWATH DIA
全新一代数据非依赖质谱采集技术

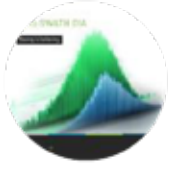

2023

发布临床质谱
Citrine™ Triple Quad™ System
注册证编号：国械注进(20232220176)

ZT Scan DIA
全新一代数据非依赖质谱采集技术

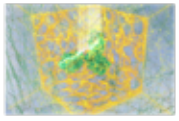

SCIEX
The power of precision

发布 QTRAP 线性离子阱将三重四极杆和线性离子阱技术相结合

2002

发布 API 5000™ LC-MS/MS 系统

2005

2010年发布 TripleTOF 5600 首次提出高分辨质谱具备三重四极杆定量能力

2010

发布 4500 系列 LC-MS/MS 系统

发布 SWATH 数据非依赖质谱采集技术

2012

2013年发布 TripleTOF 5600+

2013

发布 QTRAP 6500+系列 LC-MS/MS 系统

2016

发布 X500系列 台式高分辨QTOF质谱仪

2015

发布 3500系列 LC-MS/MS 系统

2014

发布 中国本土化产品6500+ LC-MS/MS 系统

发布 ZenoTOF 8600 系统 极速超敏多重碎裂高分辨质谱系统

2025

发布中国本土化产品 高分辨质谱 X500R QTOF 系统、ZenoTOF 7600 系统和 ZenoTOF 7600+ 系统

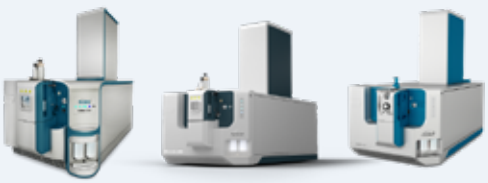

发布 ZenoTOF 7600+ 多重碎裂高分辨质谱

发布中国本土化产品 Triple Quad™ 7500+ 系列 LC-MS/MS系统

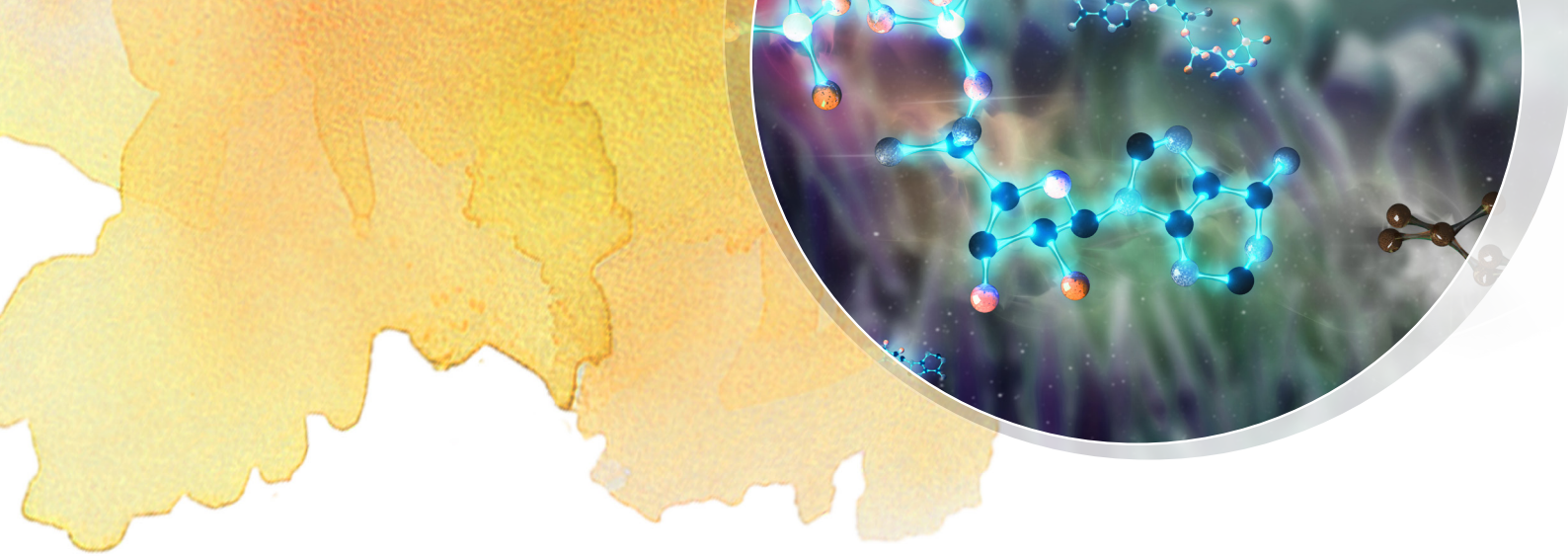

先进的代谢组学整体解决方案

ZenoTOF 系列多重碎裂高分辨质谱

- **858 Hz** 的卓越采集速度，让样品中的代谢组一览无余，实现更多代谢物的检测；
- Zeno Trap 显著提高离子占空比，灵敏度提升高达 **20 倍**，让样品中超痕量代谢物无处遁形，实现更多低丰度代谢物的发现；
- 配置 CID（碰撞诱导碎裂）和 **EAD（电子活化解离）**，多重碎裂模式生成丰富的 MS/MS 谱图，明察秋毫，区分代谢物中的同分异构体。

QTRAP/QQQ 系列高端定量质谱

- 采集速度高达 **800 MRM 每秒**，一次进样实现数千个代谢物的精准定量分析；
- 创新 **Mass Guard 技术**，提升质谱耐受性，满足更大队列代谢组学样品的分析需求；
- 开发高覆盖代谢组学全流程整体解决方案，实现用户端的“即插即用”。

完整的整体解决方案

- 支持非靶向代谢组学、靶向代谢组学、拟靶向代谢组学等不同代谢组学分析策略；
- 配套代谢组学工作站，实现端到端整体解决流程，即导入数据，自动完成数据评价校正、代谢物注释、统计分析、代谢网络分析、整合分析等功能，最终生成生物学洞见；
- 代谢组学工作站另外支持高覆盖靶向定量数据分析和拟靶向代谢组学工作流程。

内容提要

提高二级灵敏度对非靶向代谢组学工作流程的影响

基于 ZenoTOF™ 7600 系统的Zeno™ 数据依赖型采集(IDA）技术

Impact of increased MS/MS sensitivity on the untargeted metabolomics workflow

Kranthi Chebrolu[1], Jason Causon[2], Shaokun Pang[1], David Cox[2], Christie Hunter[1]

[1] SCIEX, USA;[2] SCIEX, Canada

数据依赖型采集模式（DDA 或 IDA）被广泛应用于质谱法非靶向代谢组学分析流程。通常，DDA包含两个步骤。第一步，在特定的质量范围内进行一级探测性扫描，同时可用作后续定量。第二步，根据用户设定的判定标准，对于第一步中符合要求的一级离子，触发采集二级信息。一个高效的DDA工作流程，需要尽可能多的触发采集二级信息，并根据这些二级信息对不同样本中的化合物进行准确鉴定。

QTOF系统的二级采集速率较高，能够在一次样本采集中实现化合物鉴定流程。然而，过高的采集速率可能会降低二级信息的数据质量，这是因为过高的采集速度必然会造成积累时间变短，从而影响数据库匹配鉴定化合物的结果。理想状态下，即使在非常高速率进行二级信息采集时，也能够保持良好的数据质量和分辨率。

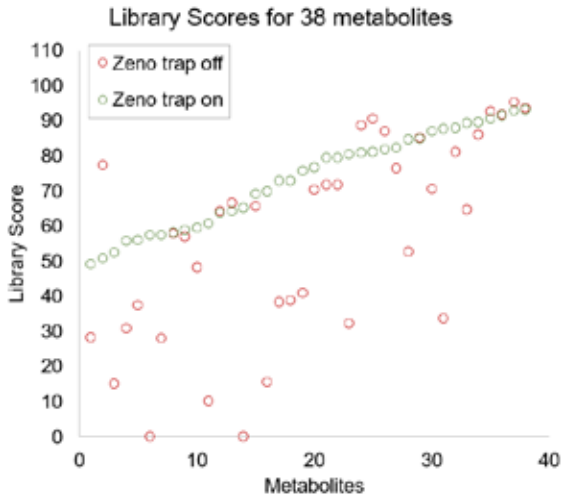

图 1. 在Zeno MS/MS模式下，灵敏度提升明确，谱库匹配得分提高。尿液中代谢物在Zeno trap模式开启（绿）和关闭（红）时的数据库匹配得分。Zeno trap模式开启时，数据库匹配得分提高。更多细节见图4。

当连续的离子流通过脉冲信号推入垂直的TOF区域时，会存在占空比损失（占空比通常为5%-25%）。然而，在ZenoTOF™ 7600系统中，Zeno™ trap(Zeno阱)能够提高占空比至90%以上，在保证高分辨率的同时显著提高二级灵敏度[1]。本文以分析尿液样本中代谢物为例，探索一次进样Zeno IDA工作流程策略，在保证二级高采集速率的前提下，对二级灵敏度提升的影响。

ZenoTOF™ 7600 系统用于非靶向代谢组学研究的主要特点

- ZenoTOF 7600 系统在扫描速度快（133 Hz）条件下，能同时保证高分辨率和高质量的质谱数据，一次进样完成非靶向代谢组学流程。

RUO-MKT-02-13434-ZH-A

- 在Zeno IDA模式下，Zeno trap可以显著提高低丰度母离子的二级灵敏度
- 在DDA流程下，开启Zeno trap功能，采集到评分大于95的二级谱图成倍提高。
- 更高质量的质谱图，显著提高（15%）数据库匹配数目。
- 两种非靶向流程进行数据处理：SCIEX OS软件的数据库匹配功能； MarkerView™软件的数据统计功能。

方法

样本制备：共计四组大鼠尿液样本：ZDF大鼠雄性组，ZDF大鼠雌性组，SD大鼠雄性组，SD大鼠雌性组。雄性和雌性（每组n=5）。取尿液样本20 µL，以流动相A稀释10倍后上机分析，进样体积2 µL。

色谱条件：液相色谱为ExionLC™ AD系统。色谱柱为Phenomenex Luna Omega Polar C18, 3 µm 150 x 2.1 mm (00F-4760-AN)。流动相 A 为含 0.1% 甲酸 的水溶液，流动相 B为含 0.1% FA 的乙腈。梯度洗脱，流动相B在13.1 min从0%升至95%（线性梯度），流速为0.3 mL/min。 柱温箱温度为 40 ℃。

质谱条件：采用SCIEX ZenoTOF™ 7600系统的DDA数据采集流程，SCIEX OS软件进行数据采集。ESI源，正离子模式。离子源参数如下：CUR 35, GS1 55, GS2 55, IS 5500, TEM 600℃。每个循环同时采集60个高分辨二级质谱信息，二级累积时间为10 ms。DP 50 V，CE 30 V。二级扫描范围10-1000Da。对比Zeno™ trap（Zeno阱）开启和关闭的灵敏度区别。每个样本，每个采集方法重复三次。

数据处理：采用SCIEX OS软件和MarkerView™软件进行数据处理。流程一，采用SCIEX OS软件对IDA数据进行数据库检索，包括AMMSL[2]和NIST数据库。流程二，采用MarkerView™软件进行峰提取，并对差异性成份在SCIEX OS软件中进行数据库匹配。

Zeno trap提高谱图质量

除了高分辨率和高质量精度外，二级数据质量（信噪比）也是用于数据库匹配的关键指标。当Zeno trap开启进行MS/MS数据采集时，二级碎片离子信号强度和谱图质量显著提升（图2），从而导致鸟嘌呤更高的数据库匹配得分（图3）。

测试的第一个数据处理工作流程是使用AMMSL数据库从混合样本中搜索DDA数据，然后利用SCIEX数据库进行核心生物代谢物的鉴定的样本。在Zeno trap开启时，在 SD雄性和雌雄大鼠样本中共计鉴定到74个代谢物，较Zeno trap关闭模式下，提升15%。

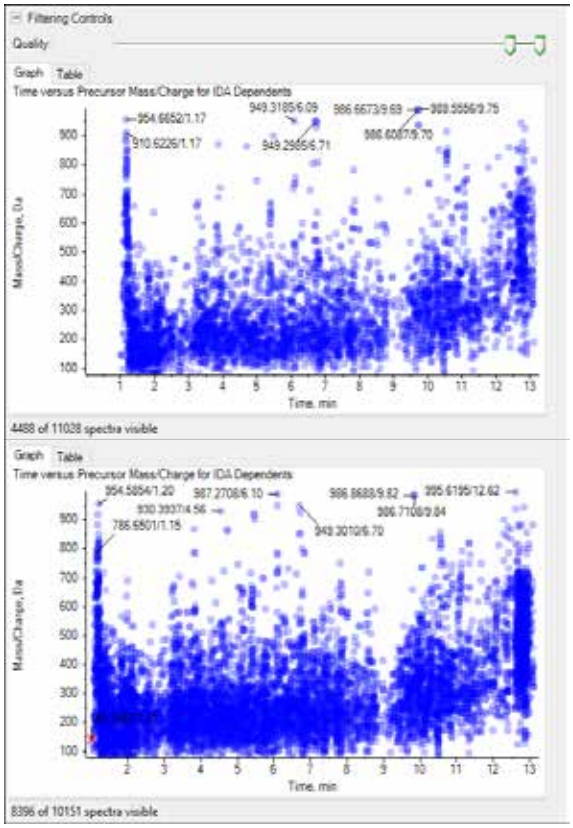

图2. Zeno trap启开，使用数据依赖型采集（DDA）策略，显著提高了谱图质量。Zeno trap关闭模式下，约40%（4488/11028）的二级谱图得分≥ 95（上图）。Zeno trap开启时，约83%（8395/10151）的二级谱图得分≥ 95（下图）。展示的数据是在DDA采集策略下的ZDF雄性大鼠混合样本数据。

只有当一级母离子的信号强度低于Zeno阈值时，Zeno trap功能自动开启用于二级信息采集。因此，二级谱图质量的提高和数据库得分的提升将主要针对一级信号低的待测物。

在Zeno trap开启和关闭模式下，通过数据库匹配，在ZDF雄性大鼠尿液样本中共计鉴定到153个代谢物。详细结果根据数据库匹配得分被分成3组，用以评估Zeno trap开启时对数据库得分的影响（图4）。

1. 组1包括Zeno trap启开时，数据库匹配得分< 50的代谢物。与Zeno trap启开相比，Zeno trap关闭时，数据库匹配得分范围宽，这是因为二级质谱数据质量很差。如图中红色圆点所示，Zeno trap关闭时，大量代谢物无二级匹配，得分为0。

RUO-MKT-02-13434-ZH-A

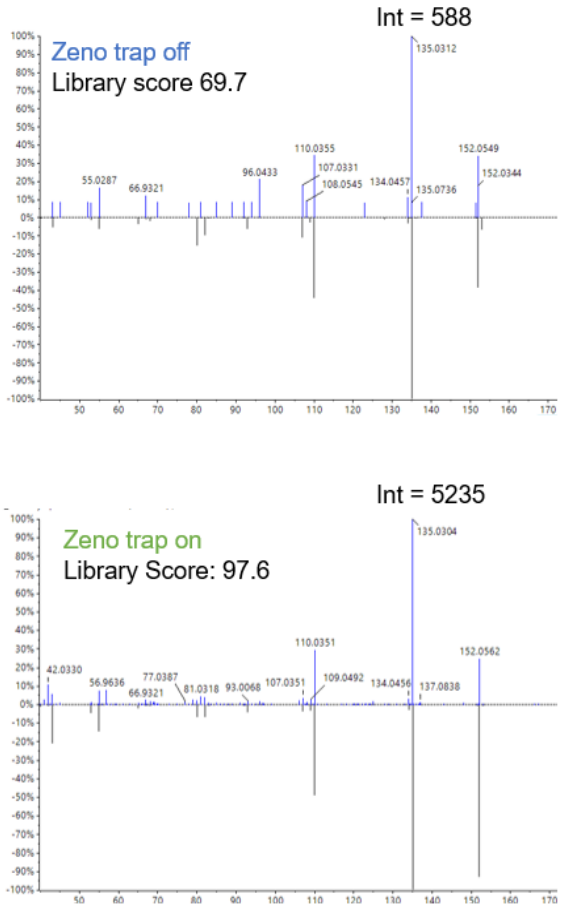

图3. 二级谱库质量的提高带来更好的数据库匹配得分。以鸟嘌呤为例，Zeno trap关闭时，数据库匹配得分为69.7（上图）；Zeno trap开启时，数据库匹配得分为97.6（下图）。在上图标记的质谱图中，碎片离子m/z=135.03信号强度在Zeno trap开启时有显著提升。

2. 组2包括Zeno trap启开时，数据库匹配得分在50-90的代谢物以及大量低丰度代谢物所获得的的代谢物匹配结果。这组代谢物是在Zeno trap开启模式下采集到了高质量二级质谱数据鉴定而来。也得到较高的数据库匹配得分（图1）。
3. 组3为数据库匹配得分>90的代谢物，代谢物含量相对较高。因该类代谢物本身能够采集到高质量的二级信息，Zeno trap提升的二级灵敏度对于数据库匹配得分影响不大。

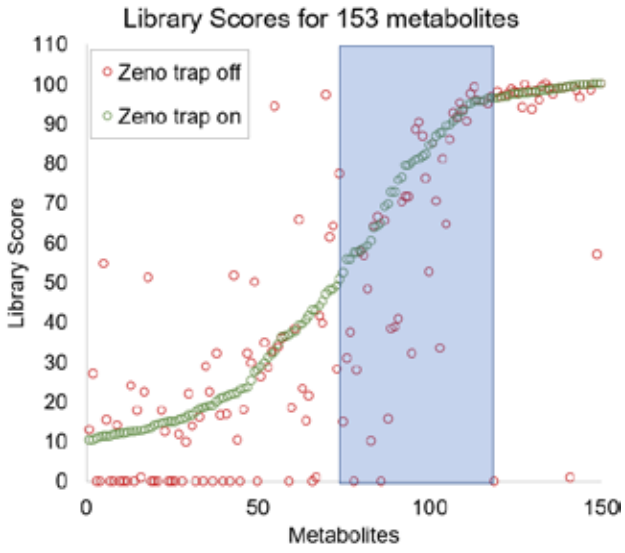

图4. 在Zeno trap开启和关闭模式下，共计鉴定到153个代谢物。这些代谢物被分为3组。组1为在Zeno trap开启模式下数据库匹配得分< 50的代谢物。组2为数据库匹配得分在50-90的代谢物，并与Zeno trap关闭时的数据进行了比较，具有更可信的数据库匹配度。组3为数据库匹配得分>90的代谢物。

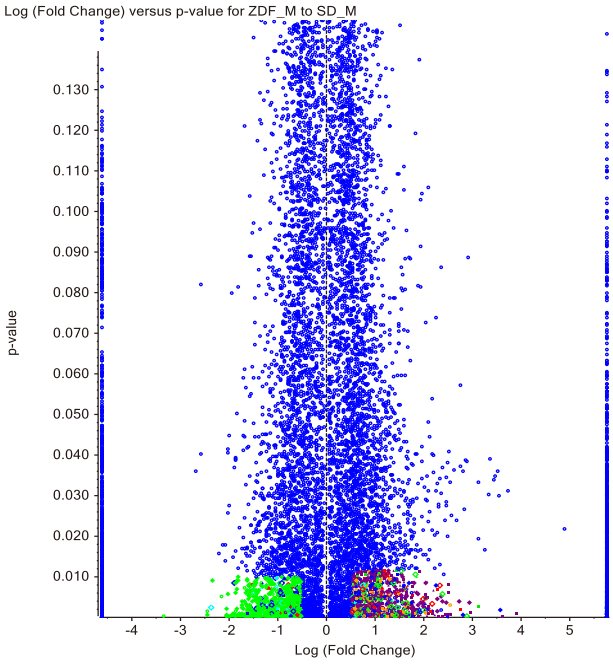

图5. 一级特征母离子检测。利用MarkerView™软件，以p ≤ 0.01, ± Log fold change(差异倍数) ≥ 0.5为标准，提取一级特征母离子。共计4222个差异特征被识别，利用SCIEX OS软件进行鉴定。

RUO-MKT-02-13434-ZH-A

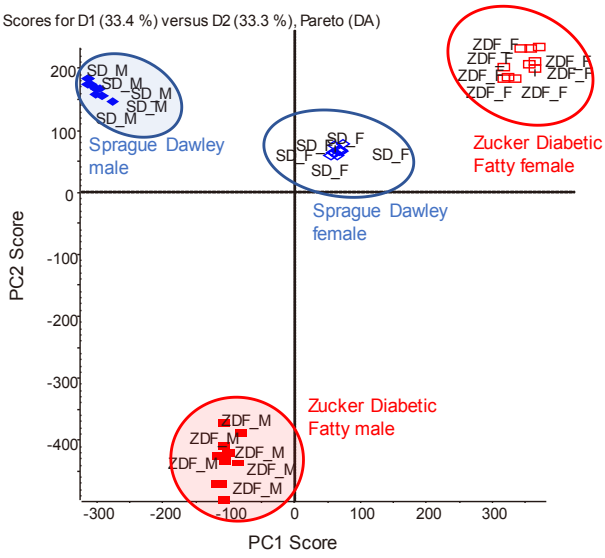

图6. 主成分分析（PCA)给出明确的分组差异。用4222（p ≤ 0.01, ± Log fold change(差异倍数) ≥ 0.5）个提取识别离子进行主成分分析，实验组之间有非常好的离散度，而且每组中10个大鼠样品有非常好的重现性聚集

差异成份识别

用MS1的DDA数据进行定量分析，因此这实际上可以单独用于数据库检索，根据MS1的差异来寻找不同的特征，然后用用数据库检索方式确定次级特征。这种统计驱动的非靶向分析方法能简化数据处理，因此用MarkerView™软件处理数据并在各实验组的大鼠间收集的DDA数据（n=10, ZDF 雄鼠，ZDF 雌, SD 雄鼠和 SD 雌鼠)

初始提取到29270个特征峰，经过对一系列实验数据配对t-检验（图5）以及特征离子的定位，以p ≤ 0.01, ± Log fold change(差异倍数) ≥ 0.5为标准，共计4222个差异特征峰被识别。这些差异特征峰在PCA分析中离散度非常好好，在一个实验组内也具仍良好的重复性。（图6）

鉴定到的4222个特征峰列表导入SCIEX OS软件中进行数据库匹配鉴定。根据AMMSL和NIST数据库检索结果，最终鉴定到的50个代谢物具有非常视的置信度。

结论

本实验在ZenoTOF™ 7600系统中进行DDA数据采集策略，分别在Zeno™ trap（Zeno 阱）开启和关闭状态下采集二级质谱信息。用两种非靶向数据处理流程对数据进行处理，并探讨了Zeno trap技术对生物样本中重要的差异化代谢物鉴定结果的影向。

- Zeno trap开启时，二级灵敏度显著提升，谱图质量提高，代谢物鉴定数目提高了15%。
- 在快速MS/MS信息采集（10 ms累积时间）条件下，也可获得高质量的谱图信息。
- 当分析物信号极低，MS/MS质谱图质量不好进，通过Zeno MS/MS也可以获得数据库匹配很高的分数。
- 在样本量很少时，也希望获得高质量的谱图。
- 二级采集速度快（10 ms）可以提供更多的数据点用以准确鉴定。
- 使用SCIEX OS软件和MarkerView™软件，可以使用多种数据处理方法来解释样本组的DDA数据。

参考文献

1. Qualitative flexibility combined with quantitative power. SCIEX technical note, RUO-MKT-02-13053-A.
2. Automated Targeted Screening of Hundreds of Metabolites -Using an Accurate Mass Metabolite Spectral Library with SCIEX OS Software. SCIEX technical note, RUO-MKT-02- 2201-B.
3. What is Zeno-On-Demand and what does it do? SCIEX community post, RUO-MKT-18-13325-A.

RUO-MKT-02-13434-ZH-A

SCIEX ZenoTOF™ 7600系统Zeno Trap功能在代谢组学分析中的应用

Zeno Trap Application in Metabolomics

刘婷[1]；郭立海[1]

[1] *SCIEX 中国应用部*

SCIEX ZenoTOF™ 7600系统 (后面简称，7600系统)在硬件设计上主要有4方面的改进：使用全新0号四极杆（Q0）设计，新加入电子活化解离碰撞池（EAD Cell, Electron activated dissociation Cell），采用Zeno™ Trap（Zeno 阱）设计，最后使用了高频模数转化器（Analog-to-Digital Converter, ADC）和时间数字转化器（Time-to-Digital Converter, TDC）(图1)； 这4方面硬件上的改进，使其具备了某些独特功能（表1）。

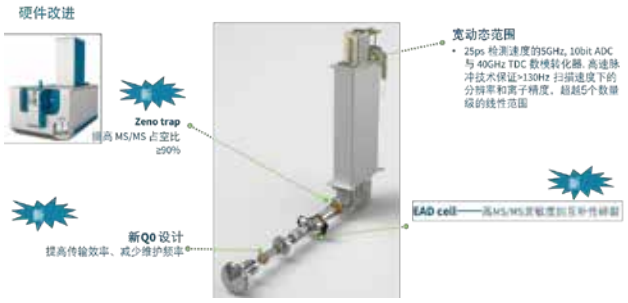

图1. SCIEX ZenoTOF™ 7600系统内部构造和硬件改进

表1. 7600系统硬件改变和其对应功能

硬件改进	对应功能
新Q0设计	提高离子传输效率，减少仪器维护频率；
EAD cell	提供EAD碎裂技术，与CAD(Collision-activated dissociation, 碰撞活化解离) 碎裂技术具有互补性；
Zeno Trap	提高离子占空比，富集MS/MS碎片离子，提高MS/MS灵敏度；
宽动态范围	5GHz, 10bit ADC和40GHz TDC数模转换器，提供5个数量级线性范围；高频脉冲技术保证130Hz扫描速度下的分辨率和离子精度；

SCIEX ZenoTOF 7600系统硬件的改进，对应用功能的提升，一些文章已经报道过[1-2]。本文主要就Zeno Trap在代谢组学中的应用展开研究。Zeno Trap的设计主要是通过提高离子占空比[3]，来提高MS/MS的灵敏度；我们可以简单的认为：在Q2（第二根三重四极杆）后的Zeno Trap对离子有个富集作用，保证90%以上的离子能够进入飞行时间管（TOF, Time of flight）中检测，从而提高了MS/MS的灵敏度。本文选用包含85种小分子化合物的细胞上清液样本，来设计实验，讨论Zeno Trap在实际工作中的潜在应用。

Zeno Trap在代谢组学中的应用特点

- 定量实验，提高MRM^{HR}（高分辨多重反应监测）定量灵敏度；
- 定性实验，提高数据库匹配的置信度； 特别是对低含量化合物，也能获得优异的数据库匹配；
- 大队列实验中，配合130Hz (5ms/ scan)快速扫描速度，保证化合物的覆盖率和MS/MS谱图质量的前提下，至少可以缩减一半的样品运行时间；

实验样本

细胞上清液样本，含有85种化合物，包含氨基酸，有机酸，核苷，维生素，糖等化合物。其中90%的化合物母离子小于500Da, 88%的化合物定量碎片离子小于300Da。这个分子量范围，与体内代谢组学主要化合物的分布范围很相似。

Zeno Trap在代谢组学定量研究中的应用

靶向代谢组学，需要对目标代谢物进行相对或绝对定量。获得优异的灵敏度，至关重要。在Zeno On（开启Zeno Trap 功能）和Zeno Off（关闭Zeno Trap 功能）下，分别使用MRM^{HR}采集模式，对代谢物进行定量分析，比较Zeno Trap功能对灵敏度的影响。

RUO-MKT-02-14196-ZH-A

本实验采用梯度洗脱，20min 液相运行时间，7600系统使用MRM^{HR} 采集模式。TOF MS（一级高分辨质谱）采集范围：50-800 Da，累加时间（Accumulation Time）为100ms; MRM^{HR}子离子采集范围：30-800 Da，累加时间为8ms; 分别比较Zeno On和Zeno Off 条件下，Zeno On 与TOF MS条件下，85个化合物的灵敏度变化。

图2中展示了三个化合物的测试结果，结果表明：1）Zeno On与Zeno Off比较，灵敏度显著提高5-15倍；说明Zeno On能大大提高碎片离子的灵敏度；2）Zeno On 下的MRM^{HR}，与一级质谱下的提取离子流图（XIC）比较，灵敏度提高11-79倍，这也说明：对于某些化合物而言，MRM^{HR}采集模式能更好地去噪音，获得更优异的灵敏度，配合Zeno Trap功能，更能大大提高碎片离子的灵敏度。3）为了获得更全面的数据，对85个化合物的Zeno On与Zeno Off下的MRM^{HR}结果比较，Zeno On条件下峰面积平均提高11X。

定量实验结果表明：Zeno On能显著提高MRM^{HR}定量灵敏度，对于小分子化合物，可以提高10X左右灵敏度。

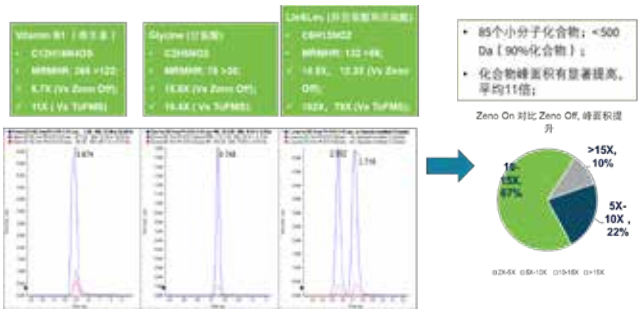

图2. 三个化合物Zeno On-MRM^{HR}，Zeno Off-MRM^{HR}和TOF MS采集下XIC色谱图 (左图)，统计85个化合物结果，Zeno On平均提高11X灵敏度.

Zeno Trap 在代谢组学定性研究中的应用

代谢组学定性实验中，快速和便捷进行代谢物的鉴定的方式是：MS/MS数据库匹配。当化合物获得高质量的MS/MS谱图时，MS/MS数据库匹配就可以获得更高的匹配分值。但对于低含量代谢物，由于响应较低，也获得高质量的MS/MS谱图就变成了非常大的挑战。

本实验采用梯度洗脱，20min 液相运行时间，7600系统使用IDA-Top10 (信息依耐性扫描-触发10个二级谱图采集)采集模式，使用DBS（动态背景扣除）功能，TOF MS采集范围：50-1000 Da, 累加时间为200 ms; TOF MS/MS（二级高分辨谱图）采集范围：30-1000 Da，累加时间为50ms; 比较Zeno On 和Zeno Off 条件下，85个化合物的MS/MS谱图，数据库匹配情况，特别关注低含量化合物的匹配情况。

测定结果显示：1). 85个化合物，Zeno On 和Zeno Off条件下, 均能采集到每个化合物保留时间下的MS/MS谱图；2) Zeno On条件下采集到的MS/MS谱图，谱图质量明显优于Zeno Off，因此，Zeno On条件下，85个化合物的数据库匹配分值均高于80%，即使LOD（最低检出线）附近的代谢物，也能获得良好的谱库检索结果（图3和图4）。

图3. 谷胱氨肽（氧化型）在IDA-Top10 MS/MS采集模式下，母离子绝对信号500cps (强度不高)，Zeno On采集MS/MS 谱图的数据库匹配分值为90.8%，Zeno Off 采集MS/MS匹配分值为41.5%.

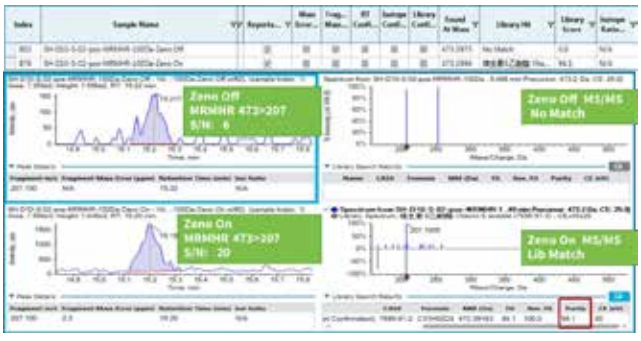

图4. LOD浓度下维生素E酯在Zeno Off和Zeno On条件下获得的MS/MS谱图，数据库匹配得分结果。Zeno Off条件下的 MS/MS谱图，由于LOD下信号强度太低，无法获得高质量的MS/MS谱图，而匹配失败；Zeno On 条件下获得的MS/MS谱图，碎片离子强度的提高，确保了MS/MS谱图质量，从而维生素E酯的匹配分值高达94%.

RUO-MKT-02-14196-ZH-A

定性实验结果表明：Zeno Trap功能能大大提高MS/MS谱图质量，MS/MS谱图数据库匹配准确率大大提高。

Zeno Trap 配合130Hz扫描速度，在代谢组学大队列中的应用

代谢组学大队列，是消除个体差异的有效手段。但大队列研究也对仪器提出了更高的要求，即在保证化合物覆盖率（即灵敏度）和化合物鉴定质量（即MS/MS谱图的质量）的前提下，尽可能缩短采集运行时间，提高样品采集效率。7600系统采用的高脉冲技术可以保证在130Hz（相当于5ms 扫描时间）的扫描速度下，也可以获得优异的分辨率和灵敏度。

本实验采用IDA采集模式，方法设定上，将依此缩短采集运行时间，提高MS/MS采集个数，缩短TOF MS 和MS/MS累加时间，实验具体设计见图6。

图6. 不同梯度运行时间（20min, 10min, 5min, 2.5min）下的TOF MS和TOF MS/MS累加时间设定

	20min 运行时间 IDA-Top10	10min 运行时间 IDA-Top20	5min 运行时间 IDA-Top40	2.5min 运行时间 IDA-Top80
累加时间 TOF MS	200 ms	150 ms	100 ms	50 ms
累加时间 TOF MS/MS	50 ms	25 ms	15 ms	5 ms

实验评价2个指标：1）细胞上清液样本中，85个化合物在不同运行时间下，覆盖率是否有变化；具体操作为：计算不同梯度条件下化合物峰面积，均与20min梯度下的峰面积进行比较，若峰面积小于75%，即认为该化合物在该梯度条件下未被检出和覆盖；2）85个化合物在不同运行时间下，MS/MS数据库匹配的鉴定率是否有变化；具体操作为：不同梯度条件下，检出的85个化合物，其MS/MS谱图与数据库匹配，匹配值>80%，认为该化合物被成功鉴定。

图5中的结果展示20min, 10min, 5min，2.5min运行时间下，85个化合物的覆盖率和鉴定率的变化。该实验结果表明，该实验的运行时间由20 min缩短到5 min，即缩减2倍的运行时间下，化合物检测的灵敏度和MS/MS谱图质量基本一致；但考虑到代谢组学样本基质的复杂性，我们可以预测：将原有梯度时间缩减1倍，到10min左右，针对代谢组学大队列研究是非常可行的。这样即大大提高样本通量，又节省了仪器成本和试剂成本。

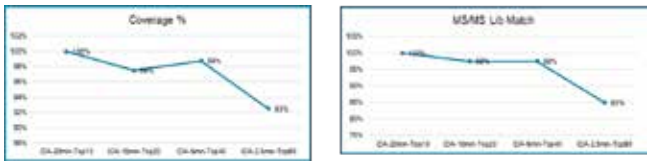

图5. 不同梯度运行时间下，85个化合物的覆盖率和鉴定率；20min, 10min,5min运行时间下，覆盖率和鉴定率没有显著性差异.

图6展示了在20min, 10min, 5min梯度下，生物素的TOF MS-XIC和MS/MS谱库匹配结果。可以看出，三个梯度条件下，XIC色谱图的强度和峰面积并没有显著变化，MS/MS谱图质量良好，匹配分值均在90%以上； 图7展示了黄嘌呤核苷在20min, 10min, 5min梯度下的TOF MS XIC（提取离子流图）和MS/MS谱图匹配结果； 可以看出，黄嘌呤核苷含量较低，即使一级母离子仅在1000cps强度下，三个条件也可以获得优异的MS/MS谱图质量，匹配分值均大于90%。

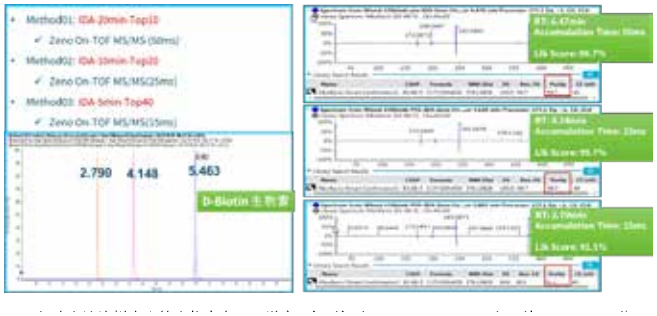

图6. 细胞上清液样本中的生物素在不同梯度运行时间（20min, 10min, 5min）下的TOF MS XIC谱图，和MS/MS谱图匹配情况.

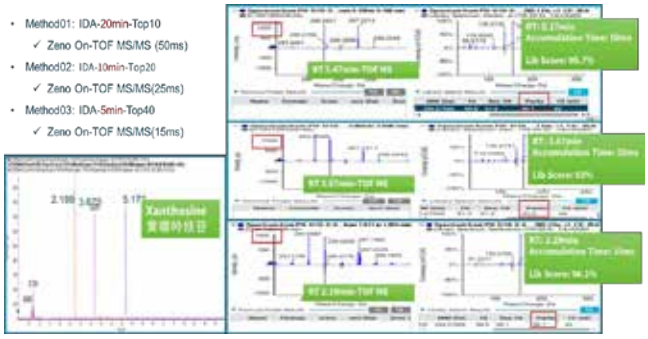

图7. 细胞上清液样本中的黄嘌呤核苷，在不同梯度运行时间（20min, 10min, 5min）下的TOF MS XIC谱图，和MS/MS谱图匹配情况.

RUO-MKT-02-14196-ZH-A

这些结果都表明，Zeno Trap结合130Hz的扫描速度，在不损失灵敏度和MS/MS谱图质量的前提下，即在不影响代谢组学覆盖率和鉴定率的前提下，将样本运行时间缩减一倍，是完全可以实现的。

结论

本研究使用细胞上清液样本评价Zeno Trap功能在代谢组学中的应用，主要考察定量灵敏度，定性鉴定率和大队列应用三个方面。

- Zeno Trap提高小分子MRM^{HR}定量10x左右
- Zeno Trap能更好的提高MS/MS谱图质量，特别是对于低含量化合物，大大提高数据库匹配的准确率，从而提高鉴定效率；
- Zeno Trap结合Zeno TOF 7600 130Hz的扫描速度，在保证覆盖率和鉴定准确率的情况下，缩减运行时间1倍，大大提高大队列样本的检测效率。

参考文献

1. Impact of increased MS/MS sensitivity on the untargeted metabolomics workflow. SCIEX technical note, RUO-MKT-02-13434-ZH-A.
2. Complete structural elucidation of lipids in a single experiment using electron activated dissociation (EAD). SCIEX technical note, RUO-MKT-02-13050-ZH-B.
3. Zeno trap white paper. SCIEX technical paper, RUO-MKT-19-13373-B.

RUO-MKT-02-14196-ZH-A

Improved metabolite identification using the ZenoTOF 8600 system to analyze NIST SRM 1950 plasma by DDA analysis

Paul RS Baker[1], Suya Liu[2], Robert Proos[1], Jason Causon[2], Rebekah Sayers[3], Sahana Mollah[1], Elliott Jones[1],

[1] SCIEX, USA, [2]SCIEX, Canada, [3]SCIEX, UK,

This technical note introduces a novel high-resolution mass spectrometer, the ZenoTOF 8600 system, which was used to identify metabolites in human plasma using an untargeted mass spectrometry approach.

Untargeted metabolomics using a data-dependent acquisition (DDA) scan mode is a common approach to studying the metabolites in biological samples. The experiment is based on a cycle of identifying potential precursor molecules via an MS1 scan and selecting the top candidates for product ion analysis to generate spectra for database matching to identify compounds. To improve the identification of metabolites, two instrument qualities are equally essential: high sensitivity and fast acquisition speed. High sensitivity increases the likelihood of triggering high-quality product ion spectra for low-concentration analytes, and a faster acquisition allows for more DDA cycles during the experiment, improving the chance that the low-level metabolites will be analyzed.

The ZenoTOF 8600 system is a high-resolution QTOF mass spectrometer with a fast analytical speed (~100 MS/MS events/s), and an improved front end to enable a high ion influx paired with a novel optical detector to increase the instrument's sensitivity ~10-fold compared to the ZenoTOF 7600 system, as determined by signal-to-noise (S/N). Here, human plasma was analyzed using the ZenoTOF 7600 and 8600 instruments to evaluate the improved identification of analytes in untargeted metabolomics analysis on human plasma using reversed-phase (RP) chromatography (**Figure 1**).

Key features of untargeted metabolomics analysis using the ZenoTOF 8600 system

- Using untargeted analysis, the SCIEX ZenoTOF 8600 system identified 1.4-fold more metabolites than the ZenoTOF 7600 system in human plasma extract (274 vs. 203, analyzing 1 µL plasma equivalents)
- The ZenoTOF 8600 system demonstrated ~10-fold greater sensitivity at the TOF MS and TOF MS/MS levels than the ZenoTOF 7600 system

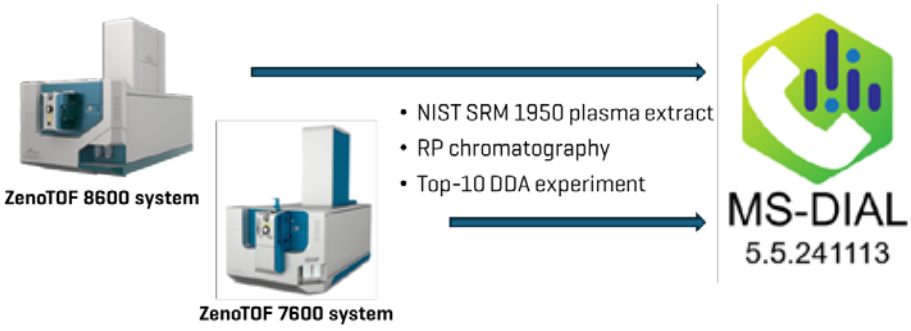

Instrument	Vol plasma (µL)	Features	TOF MS/MS acquired	Reference matched metabolites
ZenoTOF 8600 system	0.1	13250	3678	**145**
ZenoTOF 7600 System	0.1	3652	1661	134
ZenoTOF 8600 system	0.4	20248	5073	**217**
ZenoTOF 7600 System	0.4	5790	2418	183
ZenoTOF 8600 system	1	25413	6064	**274**
ZenoTOF 7600 System	1	11002	3932	203

Figure 1. A comparative study to evaluate the identification of metabolites using DDA analysis. Human plasma extracts were analyzed on the ZenoTOF 7600 or 8600 system using a top-10 DDA experiment in the positive ion mode. Data were processed using MS-DIAL 5.5 software to identify reference-matched metabolites. Due to its greater sensitivity, data acquired on the ZenoTOF 8600 system enabled the identification of ~1.4-fold more metabolites than the ZenoTOF 7600 system.

MKT-34922-A

Introduction

Metabolomics research has heavily relied on untargeted MS-based analytical methods (i.e., DDA) to detect and potentially quantify small biomolecules within a sample (1,2). High-resolution mass spectrometry (HRMS) analysis using a DDA scan mode is the primary tool for this type of experiment, which is based on an initial survey scan, such as a TOFMS scan, to select potential precursor molecules for product ion analysis. Individual MS/MS scans are acquired for each chosen precursor, and the cycle repeats itself throughout the whole experiment. Algorithms are in place to minimize repetitive measurements of the same compound, but multiple MS/MS spectra for an individual compound are typically acquired. The time for each cycle depends on the number of dependent MS/MS scans, which must be balanced with the chosen chromatographic separation strategy and the speed and sensitivity of the instrument to maximize coverage.

The primary criterion for DDA precursor ion selection is intensity—ions will be chosen in decreasing order from the most intense peak within the survey scan spectrum, provided it has not been excluded based on the experimental exclusion criteria. A plasma-derived metabolomics sample typically has hundreds of precursor ions in each survey scan, so the DDA duty cycle must be as short as possible, the exclusion criteria algorithm carefully balanced, and the instrument must be sensitive for low-level analytes to be present in the spectra for optimal untargeted analysis. The ZenoTOF 8600 system can execute an MS/MS scan in < 10 ms, enabling a scan rate of ~100/s. This rate for a top-10 DDA experiment results in a duty cycle of 600 ms (100 ms for the survey scan and 500 ms for the 50 dependent MS/MS scans). That means for a 6-second-wide eluting peak, there is a strong chance that an MS/MS spectrum would be acquired for any given peak, if it is detected at the precursor ion level. This rate also suggests that for a 20 min gradient, there could be > 40,000 MS spectra acquired. This is not the case. For the ZenoTOF 7600 system, analyzing 0.2 µL plasma equivalents, the number is ~9,000. This means that provided the DDA exclusion criteria were optimally set, the detection capacity of the instrument exceeds the number of detected precursors. It is this aspect of untargeted metabolomics that can benefit from improved instrument sensitivity.

Two instrument qualities are essential for the accurate and comprehensive identification of metabolites using DDA: a high speed of analysis and high sensitivity. Better sensitivity increases the likelihood of triggering product ion analysis for low-concentration analytes, and a faster analysis speed allows for more DDA cycles, which improves the chance that the low-level metabolites will be analyzed. The ZenoTOF 8600 system is a high-resolution QTOF mass spectrometer with fast analytical speed, a reconfigured front end to increase ion flux, and a novel optical detector that combine to increase the instrument's sensitivity ~10-fold compared to the ZenoTOF 7600 system. It is hypothesized that the increased instrument sensitivity will result in an increase in the number of triggered MS/MS events.

Furthermore, the MS/MS spectra acquired from the low-level metabolites will be of better quality due to the better sensitivity. Both improvements are expected to increase the number of reference-matched metabolites.

The NIST SRM 1950 human plasma standard was used in these studies to provide a common reference for comparison. Recently, a comprehensive metabolomic/lipidomic profile of the NIST 1950 standard was performed using high-resolution NMR spectroscopy (700 MHz), direct injection tandem mass spectrometry (DI-MS/MS), liquid chromatography-tandem mass spectrometry (LC-MS/MS), and inductively coupled plasma mass spectrometry (ICP-MS) (3). Using these diverse methods, the authors identified and quantified ~ 500 metabolites (lipid molecular species were also quantified, bringing the target list to 1058). The mass spectrometry methods were targeted, which is advantageous in terms of quantitative sensitivity, but they lacked the ability to characterize known- and unknown-unknown compounds. Untargeted analysis is better suited to this type of discovery-based analysis.

A significant challenge associated with untargeted metabolomics is data processing. As is the case for lipidomics data processing, robust interpretation of untargeted metabolomics data is still, effectively, in its early development. For the results presented here, MS-DIAL 5.5 software was used to match DDA-derived MS/MS spectra to its compound database. Because of the diverse programs available to process DDA data and the data themselves having been acquired uniquely despite the sample being the same, direct comparisons of data presented here with literature-based studies should be approached with caution and not necessarily considered an "apples-to-apples" comparison.

Here, human plasma was analyzed using the ZenoTOF 7600 and 8600 instruments to compare the extent and quality of analyte identification in untargeted metabolomics analyses. Due to its improved sensitivity, the ZenoTOF 8600 system identified ~ 1.4-fold more analytes than the ZenoTOF 7600 system under similar analytical conditions and generated superior quality scores, as defined by the MS-DIAL 5.5 software match score.

Materials and methods

Sample preparation: NIST SRM 1950 plasma was extracted using 4 volumes of ice-cold methanol, vortexing for 10 s, centrifuging at 15,000 x g for 10 min, and decanting the supernatant. The supernatant was dried using a speedvac, and the metabolites were resuspended in water to a final concentration of 1 µL extract = 0.1 µL plasma equivalents. The supernatant was directly analyzed by high-performance liquid chromatography electrospray ionization tandem mass spectrometry (HPLC-ESI-MS/MS).

MKT-34922-A

Chromatography: Samples were analyzed using an Exion LC system with a Kinetex F5 column (2.1 × 150 mm, 2.6 µm, Phenomenex). A simple linear gradient from 0 to 95% B was used with standard reversed phase mobile phases at a flow rate of 200 µL/min. Mobile phase A was 0.1% formic acid in water, and mobile phase B was 0.1% formic acid in acetonitrile. The HPLC rinse solvent was water/methanol/iso-propanol/acetonitrile (1:1:1:1, v/v). The flow rate was 0.200 µL/min, and the gradient conditions are shown in **Table 1**. A 1 to 10 µL injection volume was used (0.1 to 10 µL plasma equivalents), and the column temperature was maintained at 30°C throughout the analysis. The total runtime was 23 min.

Table 1 Chromatographic gradient

Time (min)	Mobile phase A (%)	Mobile Phase B (%)
0	100	0
2	100	0
14	5	95
16	5	95
18.5	100	0
23	100	0

Mass spectrometry: Metabolomics analysis on human plasma extracts was performed on two instruments: a ZenoTOF 7600 system and a ZenoTOF 8600 system, both equipped with an Optiflow Turbo V ion source and an electrospray ionization (ESI) probe. Instrument calibration was maintained using the automated calibrant delivery system (CDS), which calibrated every five samples with an ESI calibration solution specific for the positive ionization mode. DDA experiments were performed using CID-based fragmentation in the positive ion mode.

The systems were configured for CID-based DDA experiments to select the top 10 most abundant ions for fragmentation. Dynamic background subtraction (DBS) with a mass tolerance of 50 mDa was applied to both experiments to minimize noise and maximize the MS/MS quality. Once a precursor ion was selected and fragmented, it was dynamically excluded from candidate selection for 6 s. The TOF MS accumulation time was set to 100 ms, and the accumulation time for the dependent TOFMS/MS analysis was 50 ms. The TOF MS and TOFMS/MS instrument parameter settings are shown in **Table 2**. A detailed description of the ZenoTOF 7600 system instrument parameters and their relevance to metabolomics DDA experiments has been previously published (9); the parameter descriptions therein are applicable to the ZenoTOF 8600 system.

To test the ZenoTOF 8600 system's sensitivity improvement, a high-resolution multiple reaction monitoring (MRMHr) scan mode was employed. From the untargeted data, 14 analytes were selected to cover a wide range of masses and peak intensities. The same plasma sample was used, and n=5 replicates were run using the MRMHr scan mode. Instrument parameter settings were the same as those used for the DDA experiments (**Table 2**).

Data processing: All DDA data were processed using MS-DIAL 5.5 software (4). Optimal parameter settings used for MS-DIAL software processing are presented in a recent SCIEX technical note (5), with some exceptions: the DOT product score and the reverse DOT product score thresholds were set to 500, and the TOFMS threshold was set to 100 counts per second (cps). Metabolite coverage determined from data generated by each instrument is given as reference-matched identifications; the total number of spectra acquired far exceeds these numbers. (For a detailed explanation of match scores, see reference 6.) Quantitative data acquired using the MRMHr scan mode were processed using the Analytics module in SCIEX OS software; Qualitative data were visualized using the Explorer module.

Table 2. Instrument parameter settings

Parameter	ZenoTOF 7600 system	ZenoTOF 8600 system
Curtain gas (CUR)	40 psi	40 psi
Ion source gas 1 (GS1)	40	40
Ion source gas 2 (GS2)	60	60
CAD gas (CAD)	7	7
Source temperature (TEM)	500	500
Ion spray voltage (IS)	4000 V	4000 V
Declustering potential (DP)	80 V	80 V
Collision energy (CE)	30 V	30 V
Zeno threshold	100,000 cps	100,000 cps
CE (V) - TOFMS	10 V	12 V
CE (V) - TOFMS/MS	30 V	30 V
Declustering potential (DP)	40 V	40 V
TOFMS accumulation time (Acc)	100 ms	100 ms
TOFMS/MS accumulation time (Acc)	50 ms	50 ms
Time bins to sum	6	6

MKT-34922-A

Results

Quantitative performance of the ZenoTOF 8600 system

The ZenoTOF 8600 system was designed with an optical detector that can process more ion current than the detector used in the ZenoTOF 7600 system. This ability, along with the upgraded front-end ion optics, imparts greater sensitivity to the instrument. To measure the impact of improved sensitivity on metabolomics analysis, two different approaches were used: a comparison of the peak areas (and their respective S/N ratios) from a small set of metabolites as measured in the TOFMS dimension, and a targeted MRMHr experiment to measure sensitivity improvements in the MS2 dimension.

Figure 2 shows the combined TICs (TOFMS in blue and dependent product ion scans in pink) for the ZenoTOF 7600 and 8600 systems (top and bottom panels, respectively). A cursory inspection of each instrument's TICs indicates an approximately 10-fold increase in ion intensity for the ZenoTOF 8600 system, reflecting the improved sensitivity of the instrument. Because the two instruments perform at the same data acquisition speed, the improved sensitivity is likely responsible for the significant increase in the number of features acquired using the ZenoTOF 8600 system compared to the ZenoTOF 7600 system (25413 vs. 11002 for 1 µL human plasma equivalents; **Fig. 1**). The improved sensitivity also enabled more triggered dependent scans on the ZenoTOF 8600 system (6064 vs. 3932 MS/MS spectra acquired using 1 µL human plasma equivalents; **Fig. 1**).

The increased peak intensities acquired on the ZenoTOF 8600 system do not necessarily mean the instrument is more sensitive. Sensitivity improvements should be reported in terms of a relative increase in the S/N. Because DDA experiments are not quantitative at the TOF MS/MS level, sensitivity was assessed by comparing the TOF MS XIC peak intensities and their concordant S/N from metabolites detected on each instrument. An evaluation of the peak areas with S/N calculations for 5 example metabolites is presented in **Table** 3. The S/N values were calculated using SCIEX OS software using the Explorer data analysis module and represent the average value for each analyte from n=5 injections. The noise region from each TOFMS XIC used to calculate the S/N was selected using the following criteria: the "blank"

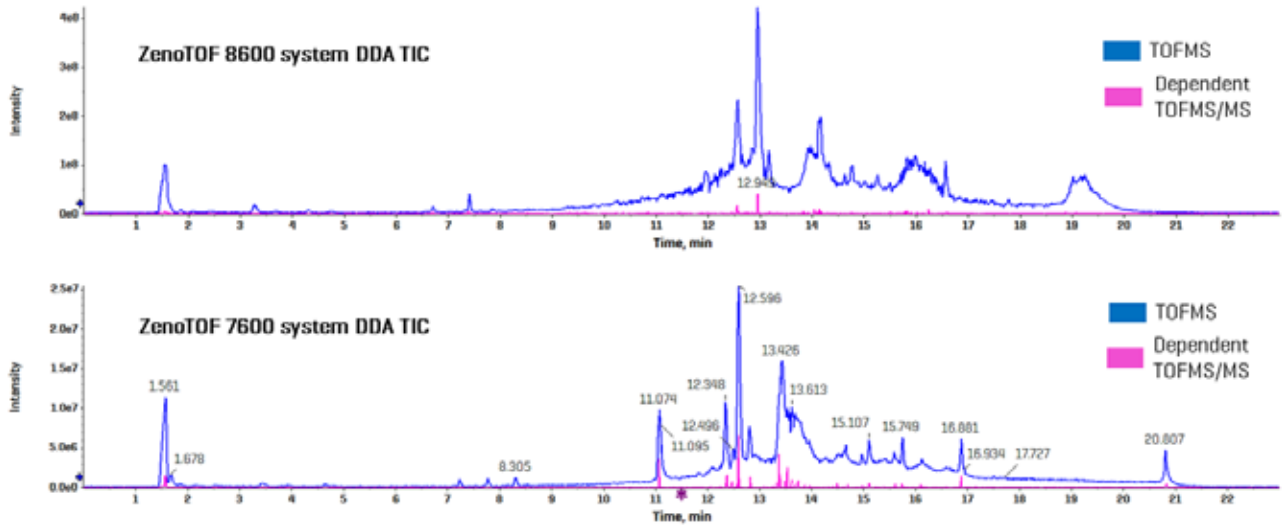

Figure 2. Untargeted (DDA) analysis of metabolites in human plasma on the ZenoTOF 7600 and 8600 systems using DDA analysis. The top panel shows a combined TIC for TOFMS (blue) and dependent product ion scans (pink) acquired on the ZenoTOF 7600 system. The lower panel shows the same for data acquired on the ZenoTOF 8600 system. The overall intensities of the TICs from the ZenoTOF 8600 system are > 10-fold higher than those acquired on the ZenoTOF 7600 system. The number and intensities of the triggered product ion scans are significantly higher using the ZenoTOF 8600 system—6064 vs. 3932 dependent MS/MS scans on the ZenoTOF 7600 analyzing 1.0 µL plasma equivalents. The 1.4-fold increase in the number of dependent scans contributed to the greater number of identified metabolites.

Table 3. TOFMS-derived S/N ratios for 5 example metabolites analyzed by DDA analysis

ID	m/z	8600 ZenoTOF system		7600 ZenoTOF system		Fold increase (8600 vs. 7600)
		Peak area avg	S/N avg	Peak area avg	S/N avg	S/N
Arginine	175.1185	1.18E+06	14493	6.611E+05	3316	4.4
Citruline	176.1037	1.37E+05	2700	2.884E+04	222	12.1
Hypoxanthine	137.0462	1.85E+06	2122	2.215E+04	46	46.5
Pantothenate	220.1174	2.32E+04	866	9.556E+03	95	9.2
Hippuric acid	180.0655	6.40E+04	773	1.372E+04	98	7.9

MKT-34922-A

Table 4. MRMHr-derived peak areas (with respective S/N ratios) for 12 example metabolites

Metabolite	ZenoTOF 8600 system		ZenoTOF 7600 system		Average fold-improvement using the ZenoTOF 8600 system	
	Peak area avg (n=5)	S/N avg (n=5)	Peak area avg (n=5)	S/N avg (n=5)	Peak area	S/N
Tyrosine	1.66E+07	1220	2.53E+06	236	6.5	5.2
Naproxen	1.54E+06	2311	9.32E+04	351	16.5	6.6
Piperine	2.81E+06	4514	2.41E+05	1073	11.6	4.2
Octonoyl carnitine	1.33E+06	2765	2.89E+04	111	46.0	25.0
Methionine	3.36E+06	3060	4.60E+05	832	7.3	3.7
Bilirubin	2.05E+07	153222	1.03E+07	6724	2.0	22.8
Thyroxine	2.68E+05	791	1.70E+04	172	15.8	4.6
Sphinganine-1-phosphate	4.95E+04	234	3.59E+03	6	13.8	42.4
Gabapentin	6.34E+04	111	9.44E+03	11	6.7	10.4
Cortisone	3.93E+04	365	3.51E+03	19	11.2	18.8
Indole-3-carbinol	1.54E+05	43	4.05E+03	4	38.0	9.7
Proline	9.73E+07	12424	1.44E+07	2454	6.7	5.1

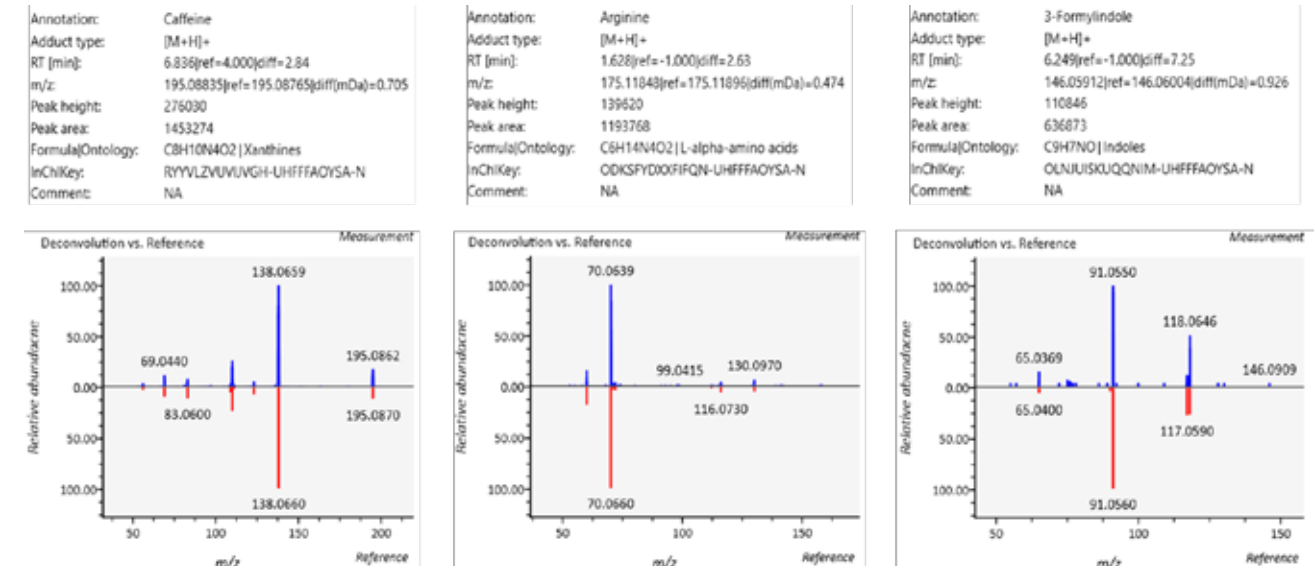

Figure 3. Spectral matching by MS-DIAL 5.5 software. Presented here are three examples of metabolites identified in human plasma by MS-DIAL 5.5 software. More information is available within the software's user interface, but highlighted here are the acquired MS/MS spectra (in blue) compared to the reference spectra (inverted, in red).

chromatographic region was > 1 min in length and within 2 min of the targeted peak elution time, and the region needed to be devoid of any extraneous isobaric peaks. The S/N of the TOFMS XIC peaks was improved by an average of 16-fold (range = 4.4- to 46-fold) on the ZenoTOF 8600 system compared to the ZenoTOF 7600 system.

To compare the sensitivity of the two instruments at the MS/MS level, an MRMHr experiment was performed on 12 representative metabolites that cover a broad mass range and diverse peak intensities and areas. **Table 4** shows an overall increase in peak areas and calculated s/n values for all compounds, with an average peak area increase of 15.5-fold (range of 2 to 46-fold) and an average S/N value increase of 13.2 (range of 3.7 to 42-fold). These data indicate that the ZenoTOF 8600 system is more sensitive than the ZenoTOF 7600 system for metabolomics studies.

Identification of metabolites using MS-DIAL 5.3 software

The improved sensitivity of the ZenoTOF 8600 system and the increased number of features should translate to better coverage of the metabolome from untargeted metabolomics experiments. In general, better sensitivity allows for detecting less prominent

fragment ions, improving the quality of the product ion spectra, and leading to a better match and more confident metabolite identification. To test this hypothesis, DDA experiments were performed on the ZenoTOF 7600 and 8600 systems to compare the numbers of identified metabolites in human plasma lipid extracts.

The MS-DIAL user interface provides a comprehensive view of the processed DDA data. **Figure 3** shows an abridged example of data that is generated for reference-matched metabolites. Of note is the comparison of experimental data (lower panels, blue spectra) to reference data (red spectra). The enhanced sensitivity of the latter instrument resulted in a 136% increase (~1.4-fold increase) in coverage of the human plasma metabolome in these experiments (274 vs. 203 reference-matched IDs). These identified metabolites have match scores ranging from 2.2 to 1.1. Importantly, in all the comparative experiments performed on the ZenoTOF 7600 and 8600 systems, the latter instrument consistently generated more features, and more MS/MS dependent scans were triggered (**Figure 1**). This observation is likely due to the enhanced sensitivity in both the MS1 and MS/MS modes of the ZenoTOF 8600 system. The higher MS1 sensitivity logically leads to more candidate ions for the dependent product ion scan, and the enhanced MS/MS sensitivity will impart better fragment intensities and a better overall quality of MS/MS spectrum.

In summary, the ZenoTOF 8600 system is shown to generate superior untargeted metabolomics results compared to the ZenoTOF 7600 system. Although it is challenging to find true equivalent data sets in the metabolomics literature, a study using NIST 1950 plasma analyzed in the positive ion mode, with analytes resolved using RP chromatography, reported 72 distinct metabolites were found using MS-DIAL software for data processing [7], which is less than found here using either instrument. As mentioned above, it is problematic to do a numbers comparison, especially in metabolomics, where there is little standardization and many different software platforms by which the data are analyzed. In the data presented here, the strongest conclusions should be made from the direct comparison of the two instruments' performances, analyzing the same sample under the same experimental conditions and data processing parameters.

Conclusions

- In comparative studies, the ZenoTOF 8600 system is ~10-fold more sensitive than the ZenoTOF 7600 system at the TOFMS and TOF MS/MS levels of analysis
- The SCIEX ZenoTOF 8600 system identified ~1.4-fold more metabolites than the ZenoTOF 7600 system in human plasma extract (275 vs. 203)
- Using the same analytical method, the improved sensitivity of the ZenoTOF 8600 system generated an increased number of features and dependent product ion scans compared to the ZenoTOF 7600 system (6064 vs. 3932 for 1 µL human plasma equivalents)

References

1. Broeckling, C. D., Beger, R. D., Cheng, L. L., Cumeras, R., Cuthbertson, D. J., Dasari, S., Davis, W. C., Dunn, W. B., Evans, A. M., Fernández-Ochoa, A., Gika, H., Goodacre, R., Goodman, K. D., Gouveia, G. J., Hsu, P. C., Kirwan, J. A., Kodra, D., Kuligowski, J., Lan, R. S., Monge, M. E., ... Mosley, J. D. (2023). Current Practices in LC-MS Untargeted Metabolomics: A Scoping Review on the Use of Pooled Quality Control Samples. *Analytical chemistry*, *95*(51), 18645–18654. https://doi.org/10.1021/acs.analchem.3c02924
2. Defossez, E., Bourquin, J., von Reuss, S., Rasmann, S., & Glauser, G. (2023). Eight key rules for successful data-dependent acquisition in mass spectrometry-based metabolomics. *Mass spectrometry reviews*, *42*(1), 131–143. https://doi.org/10.1002/mas.21715
3. Rupasri Mandal, Jiamin Zheng, Lun Zhang, Eponine Oler, Marcia A. LeVatte, Mark Berjanskii, Matthias Lipfert, Jun Han, Christoph H. Borchers, and David S. Wishart. *Analytical Chemistry* **2025** *97* (1), 667-675. https://doi.org/10.1021/acs.analchem.4c05018
4. Takeda, H., Matsuzawa, Y., Takeuchi, M., Takahashi, M., Nishida, K., Harayama, T., Todoroki, Y., Shimizu, K., Sakamoto, N., Oka, T., Maekawa, M., Chung, M. H., Kurizaki, Y., Kiuchi, S., Tokiyoshi, K., Buyantogtokh, B., Kurata, M., Kvasnička, A., Takeda, U., Uchino, H., ... Tsugawa, H. (2024). MS-DIAL 5 multimodal mass spectrometry data mining unveils lipidome complexities. *Nature communications*, *15*(1), 9903. https://doi.org/10.1038/s41467-024-54137-w
5. Ozbalci, C., Baker, P. R., & Sayers, R. MS-DIAL software parameters for processing untargeted metabolomics data acquired on the ZenoTOF 7600 system. MKT-30320-A_SCIEX-Technical-Note_metabolomics_ZenoTOF_DDA_parameters-FINAL_1-11-2024.pdf
6. Tsugawa, H., Cajka, T., Kind, T., Ma, Y., Higgins, B., Ikeda, K., Kanazawa, M., VanderGheynst, J., Fiehn, O., & Arita, M. (2015). MS-DIAL: data-independent MS/MS deconvolution for comprehensive metabolome analysis. *Nature methods*, *12*(6), 523–526. https://doi.org/10.1038/nmeth.3393
7. Barbier Saint Hilaire, P., Rousseau, K., Seyer, A., Dechaumet, S., Damont, A., Junot, C., & Fenaille, F. (2020). Comparative Evaluation of Data Dependent and Data Independent

MKT-34922-A

Acquisition Workflows Implemented on an Orbitrap Fusion for Untargeted Metabolomics. *Metabolites*, *10*(4), 158. https://doi.org/10.3390/metabo10040158

MKT-34922-A

Untargeted data-dependent acquisition (DDA) metabolomics analysis using the ZenoTOF 7600 system

Source, compound and experimental parameters to perform DDA experiments using collision-induced dissociation

Paul RS Baker and Robert Proos
SCIEX, USA

This technical note details instrument settings and best practices for untargeted metabolomics using the ZenoTOF 7600 system. The ion flow path of this instrument is different from any other QTOF instrument available. Therefore, untargeted metabolomics method development requires unique instrument settings to achieve success. Here, appropriate parameter settings are provided and these settings are explained in the context of how the device functions and is designed. Understanding how the hardware is used to generate untargeted metabolomics data can dramatically improve data quality and increase the number of metabolites detected and identified during data processing.

Ideally, untargeted metabolomics experiments are designed to detect and potentially quantify all biomolecules in a sample. These data represent a snapshot of the metabolic state of the organism studied. A typical results file for DDA metabolomics analysis is shown in Figure 1. In practice, the quality of the data and the extent of metabolite coverage depend on the parameter settings used on the instrument and the experimental method. For targeted analysis experiments, in which internal and primary reference standards are typically available, instrument parameter settings can be optimized empirically. In contrast, generalized parameter settings are required for global analysis to maximize coverage of the diverse compounds present in the biome.

Key features of untargeted metabolomics analysis using the ZenoTOF 7600 system

- The unique instrument design that enables electron-activated dissociation (EAD) and the use of the Zeno trap requires specific instrument parameter settings for untargeted metabolomics
- Parameter setting suggestions and their detailed explanations are provided to optimize metabolomic coverage and spectral quality
- The untargeted metabolomics method described here leverages the speed and sensitivity of the ZenoTOF 7600 system to maximize throughput while maintaining data quality

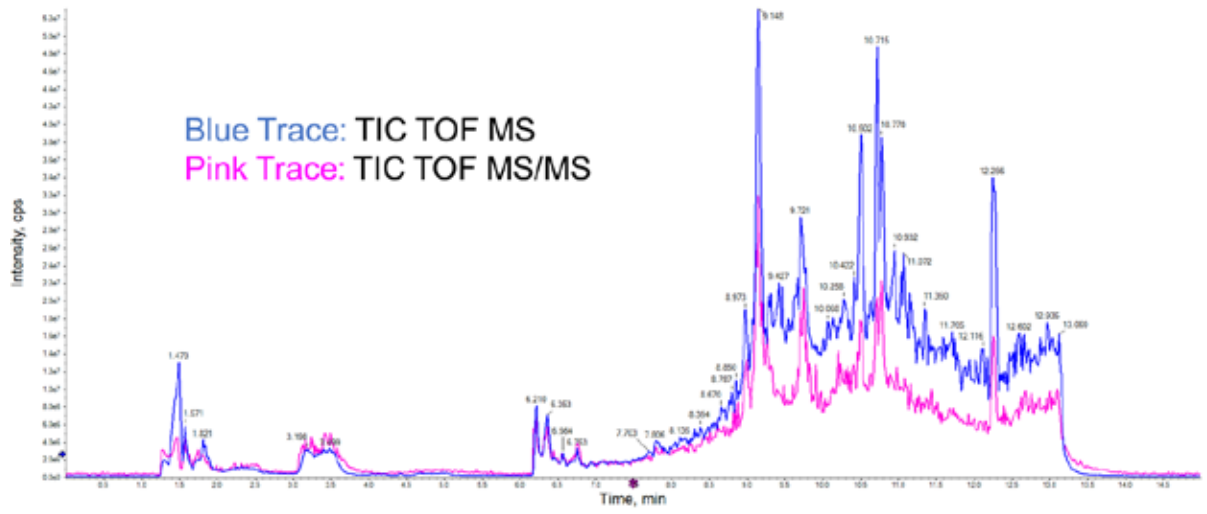

Figure 1. TIC from a 15 min untargeted metabolomics experiment using the IDA scan mode. The speed and sensitivity of the ZenoTOF 7600 system enable high-throughput analysis while maintaining high MS/MS spectral quality.

RUO-MKT-02-15367-A

Methods

Sample preparation: NIST SRM 1950 plasma was extracted using 4 volumes of methanol. After centrifugation to separate the precipitated proteins, the supernatant was analyzed directly.

Chromatography: Samples were analyzed using an ExionLC system with a Kinetex F5 column (2.1 × 150 mm, 1.7 µm, Phenomenex). A simple linear gradient from 0 to 95% B was used with standard reversed phase mobile phases (A = 0.1% formic acid in water and B = 0.1% formic acid in acetonitrile) with a flow rate of 200µL/min. A 1µL injection volume was used and the column temperature was maintained at 30°C throughout the analysis. The total run time was 15 min.

Mass spectrometry: The extracted sample was analyzed on the ZenoTOF 7600 system equipped with the OptiFlow Turbo V ion source. Data were collected using DDA methods designed to vary from top 20 to top 100 candidate ions, with dynamic background subtraction (DBS), and exclusion criteria of 6s after 3 occurrences, both activated and deactivated. The TOF MS accumulation time was set to 100 ms, and a collision energy (CE) of 30 V was used. A 5 ms accumulation time was used for TOF MS/MS experiments.

Data processing: All data were analyzed using the Analytics module in SCIEX OS software. The MS/MS spectra were compared to the library spectra using version 2.0 of the SCIEX All-in-One and SCIEX Accurate Mass Metabolite spectral libraries and the NIST 17 spectral library.

Instrument calibration

The first step in developing an untargeted metabolomics method is to ensure that the ZenoTOF 7600 system is operating at peak performance. Instrument performance depends on several factors but can be distilled down to 2 requirements: 1) the instrument must be correctly calibrated, and 2) it must be free from contamination. Below are steps that should be taken before any analytical experiments are performed.

1. Open the MS Tuning tab
2. Every 1-2 weeks, run EI Background Reduction to help clean the EAD cell, even if the EAD fragmentation function has not been used. The precursor ions travel through the EAD cell to get to the CID portion of Q2 and, subsequently, to the accelerator, TOF and detector. If the EAD cell is dirty, it may affect the sensitivity and resolution of the system in CID mode.
3. Every day, run MS Quick Check for the polarity that will be used. When using the TwinSpray ion source, there is no need to change any source parameters from the default settings. However, if using the OptiFlow Turbo V ion source, the source temperature should be changed to 500°C. Important note: Changing this value in the box does not change the temperature setting in real time. To implement this change, proceed to Step 2-Achieve Stable Signal, change the value from 200°C to 500°C, then click in another of the setting boxes. Press Stop, click on Step 1, then click Next to proceed back to Step 2. The value will then be appropriately set to 500°C. The system might take a couple of minutes to equilibrate to the new temperature.
4. During the MS Quick Check, observe the intensity of the MS/MS product ion when the Zeno trap is deactivated (*m/z* 520 in the negative ion mode or *m/z* 494 in the positive ion mode). Ideally, this signal must be above 1e5 counts per second (cps). If the Zeno trap is activated during this step, the signal will be variable because it depends on the MS-level sensitivity as a function of different ion transmission control (ITC) values and therefore will not be consistent over time. Save the tuning reports to a dedicated folder so that the signal of this third ion can be tracked as a measure of overall instrument performance.
5. If the mass accuracy calibration fails (for example, is >2 ppm) but is outside the tolerance range (for example, within 4 ppm), the system is likely suitable to use. The in-run calibration employs a mass tolerance range of 5 ppm.
6. If the sensitivity or resolution fails during calibration, perform the ADC Initialization and run EI Background Reduction, followed by TOF Tuning. These functions all appear in the MS Tuning tab. Below are the steps to take in response to failures during calibration. Note: If there is a need to proceed to steps (e) and (f), these steps can be performed in any order, depending on timing constraints and familiarity with venting and cleaning the QJet. A flow chart is presented in Figure 2 that summarizes these actions.

RUO-MKT-02-15367-A

a. **ADC Initialization.** ADC initialization re-establishes proper communication between the detector and the computer. Once reset, rerun MS Quick Check. If it passes, then start sample analysis. If it fails, proceed to step (b).
b. **EI Background Reduction**. The Background Verification Level process will almost always fail the first time. Press next and perform the Background Reduction Scan. The signal should decrease significantly over the first few minutes. After 5-10 minutes, press Next to proceed to the final check. Save the tuning report, including the optional steps. Re-check MS Quick Check. If it passes, then start sample analysis. If it fails, proceed to step (c).
c. **TOF Tuning**. Select TOF tuning and allow the process to proceed. Re-run MS Quick Check. If it passes, then start sample analysis. If it fails, proceed to step (d).
d. **Zeno Calibration.** After TOF Tuning, the Zeno trap should be re-calibrated by clicking Zeno Calibration. Once this test is complete, run MS Quick Check again. If the instrument fails this last check, please clean the Qjet.
e. **QJet Cleaning.** If the instrument sensitivity test still fails, vent the system and clean the curtain plate, the orifice plate and the QJet. SCIEX has an official QJet cleaning procedure and detergent, bags and brushes. Do not perform any cleaning or maintenance of the instrument beyond the QJet. Once vented, the QJet is cleaned and the instrument is reassembled, the system will need time (2 - 8 min) to re-achieve the suitable operating vacuum pressure in the TOF chamber. After restarting and allowing the pressure to stabilize, run ADC Initialization and run MS Quick Check.
f. **Detector Optimization**. If the instrument fails the sensitivity test after re-running MS Quick Check, then run Detector Optimization. This test varies the voltage on the detector to ensure it is held at the correct voltage. As detectors age, the voltage required to maintain sensitivity increases. There is a voltage limit and the detector must be replaced when the limit is reached. In this situation, the analytical quadrupoles or other ion path components might also be contaminated and deep cleaning will need to be performed by a service engineer.

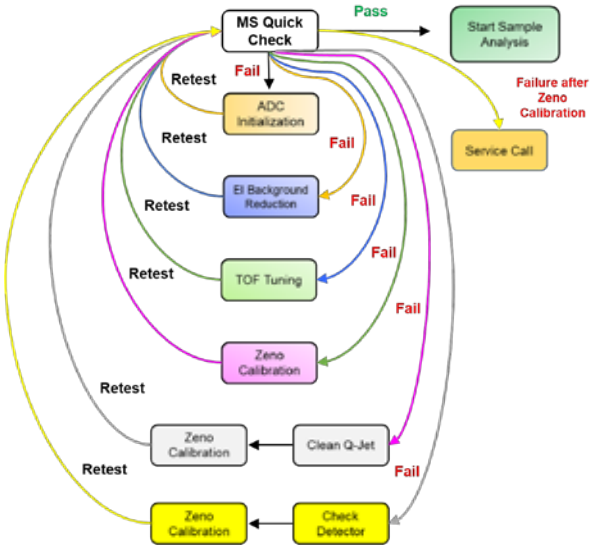

Figure 2. Flowchart depicting the correct order of MS tuning procedures to follow if the initial MS Quick Check experiment fails at any stage of the run. At each stage of the process, re-run MS Quick Check to see if the issue is resolved. If it is, proceed with sample analysis. If not, continue to troubleshoot by performing the next tuning procedure in the list and re-testing via MS Quick Check.

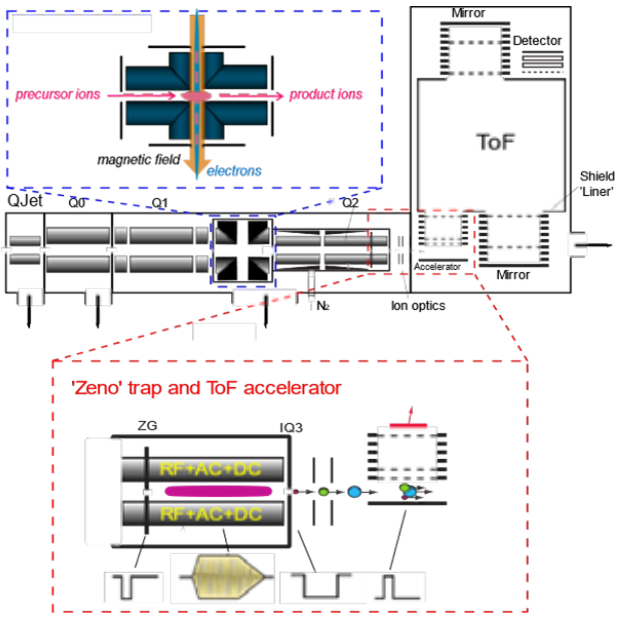

Figure 3. Assembly diagram of the ZenoTOF 7600 system. The integrated MS/MS assembly supports both CID and EAD fragmentation. Fragment ions can be trapped by the Zeno trap, which increases the instrument duty cycle to >90%.

ZenoTOF 7600 system hardware configuration

The functions and mechanisms of several features on the ZenoTOF 7600 system will be explained here to better understand how specific parameter settings are set to optimally run untargeted metabolomics in a DDA experiment using the information-dependent acquisition (IDA) scan mode. Figure 3 shows the assembly of the primary ion rail components, through

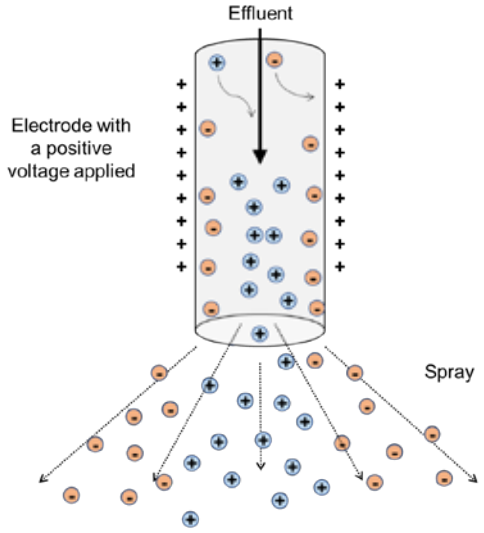

which the ions flow from left to right. As with all LC-ESI MS/MS instruments, ions are generated in the source, the ion beam is created and refined in the interface region, which comprises the

Figure 4. Diagram of the ionization process in the electrospray electrode. Note that both positive and negative ions are produced during the process. In this example, a positive voltage is applied, causing negative ions to migrate to the edges of the electrode and the positive ions to migrate to the center. The spray is not homogeneous, so it is important to consider the position of the electrode and the drying gas (GS2) when tuning the source parameters to maximize signal intensity.

QJet and Q0 region, and ions are selected for product ion analysis in Q1. In the ZenoTOF 7600 system, ions leave Q1 and enter the EAD cell, which can trap and fragment ions or transfer precursor ions to Q2 for CID-based fragmentation. In either case, fragment ions enter the Zeno trap, where they are collected and sent to the TOF accelerator in a mass-dependent manner. EAD-based fragmentation will not be discussed in the context of untargeted metabolomics in this technical note.

The Zeno trap functions by trapping ions generated by EAD- or CID-based fragmentation. The Zeno trap is not used during TOF MS scans because the ion current is already attenuated via ion transmission control (ITC) and the likelihood of detector saturation is high. Once the ions are trapped (t < 1 ms), they are sequentially scanned from the trap to the TOF accelerator in a mass-dependent manner. High molecular weight ions are scanned out first and are followed by lower molecular weight ions, such that they all arrive at the TOF accelerator at the same time. This eliminates the mass intensity bias that results in other instruments only taking a portion of the fragment ions. Once the ions are accelerated into the TOF, the Zeno trap fills and repeats the cycle. This process improves the instrument duty cycle and ~90-95% of all fragment ions hit the detector.

A key parameter to consider regarding the Zeno trap is the Zeno threshold, which is a measure of the precursor ion intensity. If the precursor ion intensity is below this value, the Zeno trap is used and fragment ions from that precursor ion are trapped and sent to the TOF accelerator. If the precursor ion intensity is above the threshold value, the Zeno trap is not used. In this case, the fragment ions that hit the detector without the Zeno trap activated are scaled according to the set Zeno calibration values. Therefore, the visualized data are corrected to what the intensity would have been if the Zeno trap had been used.

Parameter settings for DDA experiments

The parameter settings for untargeted metabolomics on the ZenoTOF 7600 system will differ from those used on other SCIEX instruments. The primary reason for this is that the ion path is different from other instruments due to the incorporation of the EAD cell and the Zeno trap. For example, the EAD cell and the Zeno trap occupy a portion of Q2 and therefore make the collision cell shorter. Consequently, the collision energy (CE) parameter setting should be higher than that used on other SCIEX instruments to compensate for the shorter collision cell dimensions.

Figure 5 shows a screencap of the parameter settings that were optimized for untargeted metabolomics on the ZenoTOF 7600 system in the positive ion mode. For the experiments performed in the negative ion mode, the absolute value for each setting is the same and further discussion points are provided below. In the sections below, many of the critical parameters are discussed, starting with source parameters.

Spray voltage. Typically, the ESI voltage is set at or near its maximum. It is essential to recognize that during ionization, both positive and negative ions are produced (conservation of charge). If a positive voltage is applied (for example, in positive ion mode), positive ions will migrate toward the center of the effluent stream and negative ions will migrate toward the walls of the electrode (Figure 4). When the spray is created, the plume is not homogenous. Negative ions will be at the outside edges of the plume and positive ions will be at its center. This segregation of the ions makes it essential to always adjust the position of the probe on the ZenoTOF 7600 system. The position of the OptiFlow Turbo V ion source does not need to be adjusted, however, because its geometry is already optimized. Other key source parameters include the nebulizing gas (GS1), which affects droplet size, and the drying gas (GS2), which evaporates

RUO-MKT-02-15367-A

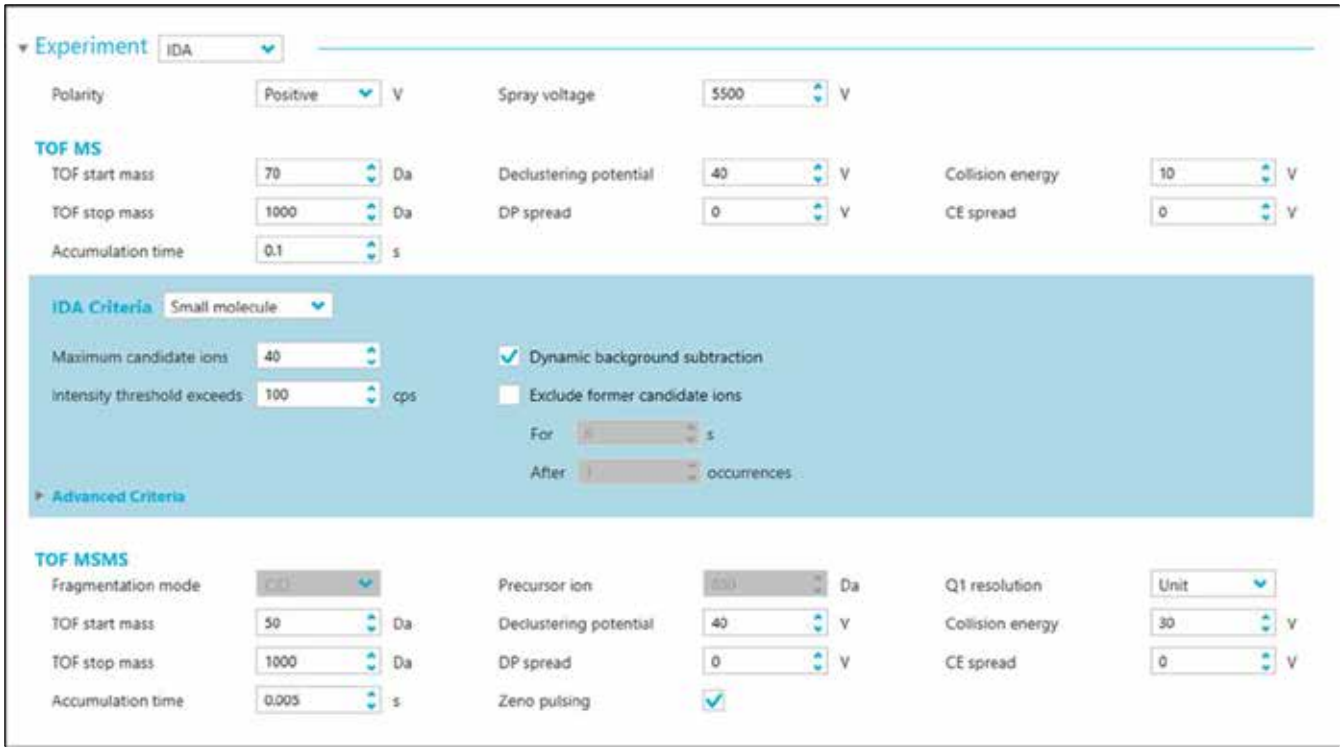

Figure 5. User interface screencap showing the specific recommended settings for global untargeted metabolomics experiments in the positive ion mode. The experimental set up includes parameter settings for the source, TOF MS, TOF MS/MS and important considerations for IDA criteria. These considerations include whether to use DBS and/or exclusion criteria. For the negative ion mode, the absolute value of each setting is the same.

the solvent to generate gas-phase ions. Subtle changes in either or both parameters can affect instrument sensitivity. In samples with heavy matrix contamination, as is common in metabolomics experiments, one can slightly lower the ESI voltage to reduce the ionizing species that come from the matrix. With a high voltage setting, highly ionizable species in the matrix may crowd out the lower ionizable species and suppress the analyte signal.

Declustering potential. The declustering potential (DP) is the voltage potential between the orifice and the front of the QJet. It acts as the motive force to draw ions into the instrument and helps disrupt any solvent clusters surrounding the ions. If the DP setting is too high, it can lead to source fragmentation. For both the TOF MS and the dependent TOF MS/MS portions of the DDA experiment, the DP should be set to 40 V in untargeted metabolomics experiments. Ion intensity does not change significantly with changes to DP but a higher setting (~60 V) might be preferred for larger compounds. In contrast, small molecules such as amino acids, are better analyzed at a lower DP (~20 V). The 40 V setting is a middle ground and gives the best results for a diverse set of analytes.

The parameters below affect the ion flow through and fragment generation by the ZenoTOF 7600 system. Differences between TOF MS and TOF MS/MS experiments are explained.

Collision energy. The collision energy (CE) setting affects the acceleration of ions through Q2. During CID, CE is responsible for imparting enough energy to the ions to fragment when they collide with nitrogen in the collision cell. However, CE also serves as a motive force for ions in non-MS/MS experiments. For the TOF MS survey scan in the DDA method, note that the CE is set to 10 V, even though no fragmentation is desired. As ions move along the ion path, they cool down. This is notable at the entrance to Q2, where nitrogen gas is present and

Table 1. Effects of varying IDA criteria on the features identified, MS/MS events triggered, library hits, and cycle time.

Experiment	DBS	Exclusion list	Peaks (features)	Peaks w/ MS/MS spectra	Formula Finder hits	Library hits with >70% purity score	% MS/MS with library match	Average cycle time (s)
Blank	*Yes*	*No*	*3781*	*2319*	*2499*	*71*	*3.06*	*255*
POS IDA Top 30	*Yes*	*No*	*6811*	*4435*	*4200*	*216*	*4.87*	*321*
POS IDA Top 40	*Yes*	*No*	*6065*	*4184*	*3771*	*204*	*4.88*	*327*
POS IDA Top 50	*Yes*	*No*	*5576*	*3978*	*3524*	*221*	*5.56*	*376*
POS IDA Top 60	*Yes*	*No*	*4879*	*3524*	*3011*	*198*	*5.62*	*392*
POS IDA Top 70	*Yes*	*No*	*4404*	*3294*	*2724*	*208*	*6.31*	*420*
POS IDA Top 80	*Yes*	*No*	*4025*	*3060*	*2528*	*188*	*6.14*	*439*
POS IDA Top 90	*Yes*	*No*	*3825*	*2918*	*2429*	*190*	*6.51*	*446*
POS IDA Top 100	*Yes*	*No*	*3641*	*2838*	*2314*	*192*	*6.77*	*464*
POS IDA Top 30	*Yes*	*Yes*	*5363*	*3614*	*3349*	*210*	*5.81*	*308*
POS IDA Top 40	*Yes*	*Yes*	*4924*	*3510*	*3070*	*219*	*6.24*	*336*
POS IDA Top 50	*Yes*	*Yes*	*4644*	*3398*	*2902*	*216*	*6.36*	*357*
POS IDA Top 60	*Yes*	*Yes*	*4346*	*3264*	*2734*	*230*	*7.05*	*384*
POS IDA Top 70	*Yes*	*Yes*	*4127*	*3134*	*2583*	*209*	*6.67*	*391*
POS IDA Top 80	*Yes*	*Yes*	*4028*	*3114*	*2566*	*197*	*6.33*	*423*
POS IDA Top 90	*Yes*	*Yes*	*3804*	*2937*	*2423*	*199*	*6.78*	*436*
POS IDA Top 100	*Yes*	*Yes*	*3555*	*2783*	*2254*	*197*	*7.08*	*451*
POS IDA Top 30	*No*	*No*	*5225*	*1808*	*3254*	*216*	*11.95*	*624*
POS IDA Top 40	*No*	*No*	*4718*	*2139*	*2958*	*216*	*10.10*	*777*
POS IDA Top 50	*No*	*No*	*4376*	*2319*	*2729*	*227*	*9.79*	*928*
POS IDA Top 60	*No*	*No*	*4073*	*2485*	*2591*	*196*	*7.89*	*1082*
POS IDA Top 70	*No*	*No*	*3820*	*2554*	*2435*	*203*	*7.95*	*1235*
POS IDA Top 80	*No*	*No*	*3641*	*2616*	*2326*	*203*	*7.76*	*1380*
POS IDA Top 90	*No*	*No*	*3336*	*2584*	*2123*	*212*	*8.20*	*1515*
POS IDA Top 100	*No*	*No*	*3278*	*2685*	*2122*	*172*	*6.41*	*1651*
POS IDA Top 30	*No*	*Yes*	*5120*	*3291*	*3220*	*264*	*8.02*	*629*
POS IDA Top 40	*No*	*Yes*	*4765*	*3341*	*2978*	*246*	*7.36*	*773*
POS IDA Top 50	*No*	*Yes*	*4366*	*3306*	*2793*	*244*	*7.38*	*915*
POS IDA Top 60	*No*	*Yes*	*4089*	*3219*	*2596*	*218*	*6.77*	*1051*
POS IDA Top 70	*No*	*Yes*	*3816*	*3095*	*2454*	*223*	*7.21*	*1181*
POS IDA Top 80	*No*	*Yes*	*3573*	*3042*	*2241*	*217*	*7.13*	*1320*
POS IDA Top 90	*No*	*Yes*	*3406*	*2915*	*2172*	*194*	*6.66*	*1449*
POS IDA Top 100	*No*	*Yes*	*3189*	*2776*	*2063*	*198*	*7.13*	*1587*

RUO-MKT-02-15367-A

collisional cooling is significant. By adding a small amount of CE voltage, the ions are pushed through Q2 without significant fragmentation and arrive at the TOF accelerator.

The CE voltage is set to 30 V for CID-based MS/MS analysis. This value gives similar MS/MS spectra to the SCIEX metabolomics library collected using SCIEX TripleTOF systems (4600, 5600 and 6600 series). These instruments were run at 35 V with a collision spread of 15-20 V. Note that on the ZenoTOF 7600 system, the CE spread is set to 0, meaning that all the spectra will be acquired at the designated 30 V. The main reason for this, compared to the instrument settings using the TripleTOF systems, is that it takes approximately 15-20 ms to enable the CE spread function. The ZenoTOF 7600 system significantly improves the instrument duty cycle, sensitivity and detection of low *m/z* fragments. It was more advantageous to shorten the accumulation time and decrease the cycle time to improve coverage, than it was to use a collision energy spread.

Accumulation time. For global metabolomics experiments, accumulation time is one of the most important parameters to consider. In general, increasing accumulation time will improve the signal-to-noise ratio (S/N), which improves the quality of the MS and MS/MS spectra. Higher-quality spectra generally have increased library hits. However, if the accumulation time is too long, the cycle time of the DDA experiment is extended and fewer MS/MS spectra are acquired. For the MS TOF experiments, it was empirically determined that the best balance is achieved using 0.100 s (100 ms) for untargeted metabolomics experiments. At the MS/MS level, it was determined that 5 ms is the best accumulation time. Although the latter setting might seem too small, the ZenoTOF 7600 system was designed to be fast (133 CID MS/MS per second, 133 Hz). The 8- to 10-fold improvement in the instrument duty cycle from the Zeno trap compensates and enables high-quality MS/MS spectra at high-speed acquisition rates. In general, with this instrument, faster accumulation times are better and there do not appear to be significant gains in spectral quality at accumulation times >10 ms.

Zeno pulsing. The function of the Zeno trap is explained above. By clicking the Zeno pulsing box, the Zeno trap will be activated, provided that the precursor ion intensity is below the set Zeno threshold. For untargeted metabolomics experiments, it is recommended that the Zeno threshold is set to 20,000 cps.

IDA criteria. One of the more challenging aspects of any DDA experiment is selecting the optimal settings that control which precursor ions are selected for subsequent MS/MS analysis. In SCIEX DDA experiments, this group of parameters is controlled by the IDA criteria panel (Figure 4, blue box). To determine the best IDA criteria parameter settings, a series of experiments was performed to vary the maximum number of candidate precursor ions per cycle (“maximum candidate ions”), whether DBS was used and whether exclusion criteria were enforced (Table 1). In all experiments, the TOF MS and TOF MS/MS instrument parameter settings were set, as shown in Figure 4.

The comprehensive dataset shown in Table 1 is separated into 4 sections, divided by the darker lines within the table. Each section shows 8 experiments that were performed in the positive ion mode, in which the maximum number of candidate ions was varied from the top 30 to 100 candidates. The 4 sections differ by whether DBS and/or exclusion criteria were applied. Each variable and its effects on the data are discussed below. For this type of experiment, no advanced IDA criteria parameters are used.

1. **Maximum candidate ions.** Ideally, DDA experiments are designed to maximize the coverage of unknown molecules while still maintaining high MS/MS spectral quality. Balancing coverage and spectral quality are most affected by the number of candidate ions chosen. Table 1 shows the numbers of peaks (features) detected, peaks detected that generated MS/MS spectra, Library and Formula Finder hits and the average cycle time as a function of candidate ions. Figure 6 shows a comparison of the MS/MS spectral quality for tyrosine acquired with 30, 70 and 100 candidate ions selected. From these data, the best number of candidate ions was determined to be between 30 and 50. As the number of candidate ions increased above 50, the number of features identified decreased.
2. **Dynamic background subtraction.** DBS is a function that improves the detection of precursor ions in a DDA experiment. The algorithm creates an extracted ion chromatogram (XIC) of the candidate ion over the preceding data points. It takes the first derivative of the curve and determines whether the candidate ion is at the apex of the first derivative. If it is at the apex, the MS/MS-dependent scan will be triggered. This algorithm is designed for small molecules and minimizes redundant MS/MS collection. Additionally, it reduces background contamination from triggering dependent MS/MS scans.
3. **Exclusion criteria.** Exclusion criteria are parameters that limit redundant MS/MS spectra from individual precursor ions. At least 1 MS/MS scan should be triggered near or at

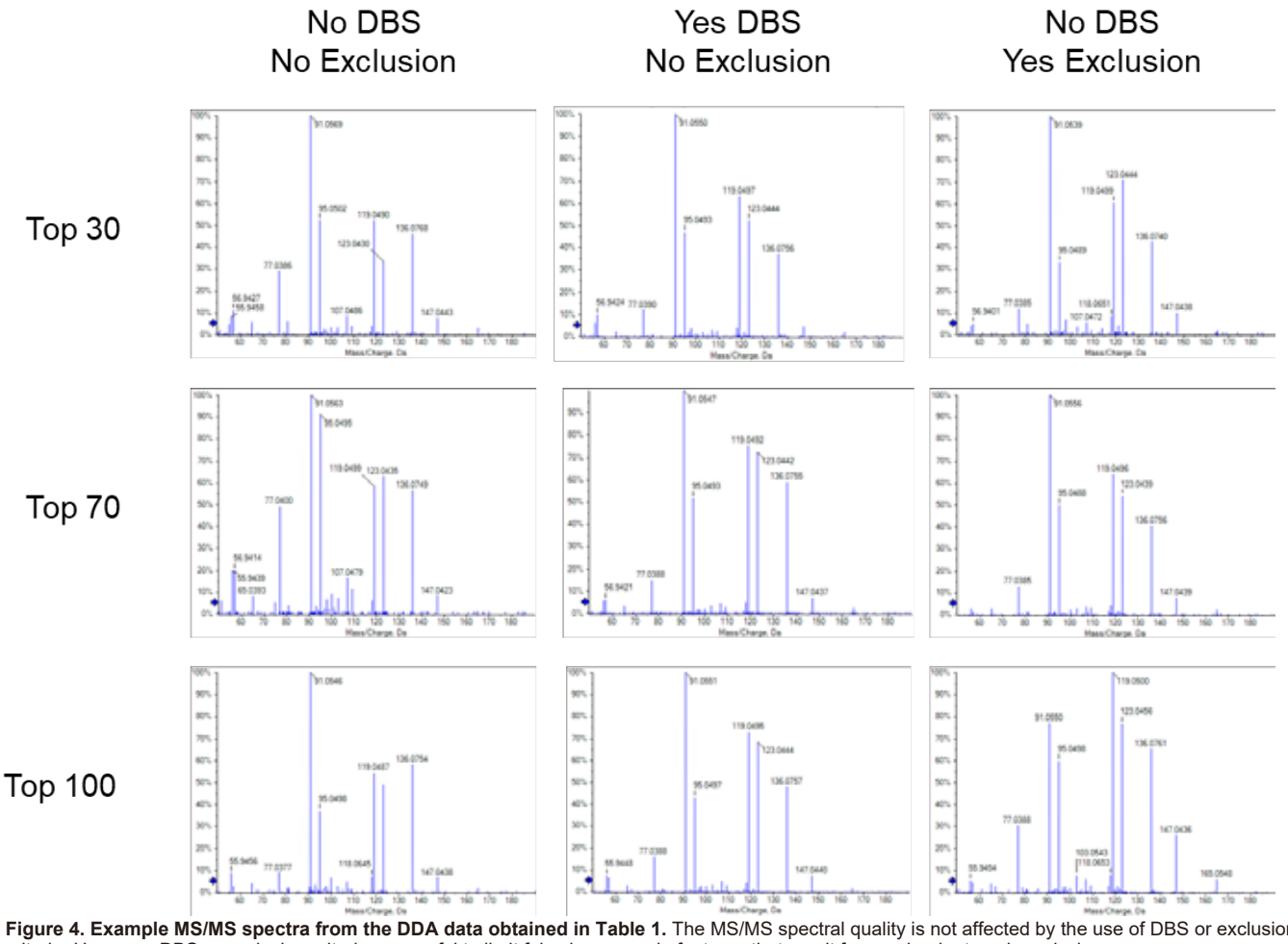

Figure 4. Example MS/MS spectra from the DDA data obtained in Table 1. The MS/MS spectral quality is not affected by the use of DBS or exclusion criteria. However, DBS or exclusion criteria are useful to limit false increases in features that result from redundant peak analysis.

the apex of the peak. If a product ion scan is triggered from a candidate ion, that precursor ion will be ignored for the exclusion period, which should be entered as half of the peak width in seconds. Typically, this exclusion is triggered after 1 or 2 triggered MS/MS scans. This feature works well for large- and small-molecule applications.

The effects of DBS and exclusion criteria on global metabolomics results are detailed in Table 1. The use of DBS resulted in more features with MS/MS spectra, however, the number of library matches from the data did not increase correspondingly. As the MS/MS spectral quality was not impacted (Figure 6), this outcome might be attributed to the spectral libraries used not including the lower intensity analytes. The use of exclusion criteria without DBS resulted in slightly more library matches, as additional features included MS/MS data. When no filtering is used for precursor selection, the most intense ions will be continually selected for the MS/MS scans at the expense of less intense ions, except at the highest number of candidate ions. In this case, the fewest peaks with MS/MS spectra and the fewest library matches are observed. In general, using either DBS or exclusion criteria in the acquisition method will increase both the number of peaks with MS/MS data and the number of library matches.

Conclusions

- Source parameters, including the probe position, drying and nebulizing gases and the electrospray voltage on the ZenoTOF 7600 system must be optimized for untargeted metabolomics experiments. The optimization of these parameters can be affected by the flow rate and the matrix composition of the sample.
- Due to the unique hardware configuration of the instrument, parameter settings, such as collision energy and

RUO-MKT-02-15367-A

accumulation, must be adjusted to accommodate diverse metabolites

- The ZenoTOF 7600 system is ideal for untargeted metabolomics due to its speed, sensitivity, and ability to perform complementary EAD experiments

RUO-MKT-02-15367-A

SWATH DIA and library driven compound identification revealed upregulation of flavonoids in *Ocimum basilicum* L. flowers

Identification of differentially regulated metabolites using SWATH DIA

Marialuce Maldini[1], Kranthi Chebrolu[2], Paola Montoro[3], Luigi d'Aquino[4] and Christie Hunter[2]
[1]SCIEX, Italy, [2]SCIEX, US, [3]University of Salerno, Fisciano (SA), [4]ENEA, Portici (NA)

Indoor plant growing is increasing in urban environments to deal with increasing soil loss and to shorten food chains. Light is among the most important environmental factors to be addressed in indoor cultivations, since it is the main driver for basic plant processes such as growth and development but also for directional movement, circadian rhythms, seed germination, etc. Different plant species are differently affected by light conditions (spectra, photon flux, light / dark ratio) and different phenological stages display different optima about light conditions. A better understanding of the effect of different light wavelengths on plant growth and development in indoor environment is, therefore, needed to better drive plant cultivation.[1] Metabolomics has served as a powerful tool to elucidate gene functions, enzyme activity and provide a detailed blueprint of overall plant health. In this study, basil (*Ocimum basilicum* L.) was grown from seedling to flowering stages in a new concept microcosm (EP 3 236 741 B1) in which the effects of different light spectrums on the growth and metabolome of different plant parts are investigated.[2, 3] SWATH DIA, a data independent acquisition workflow, was used to generate a comprehensive signature of the metabolome of each sample.

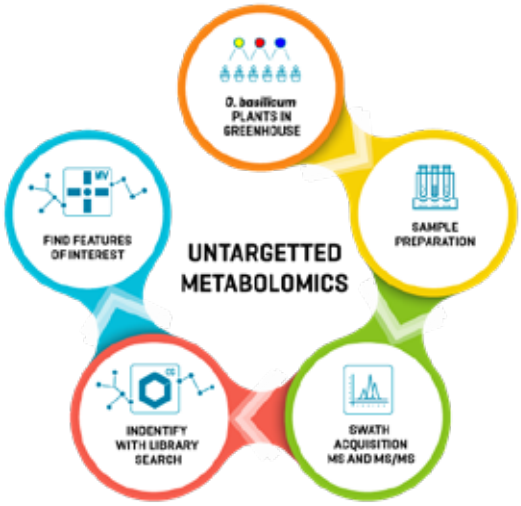

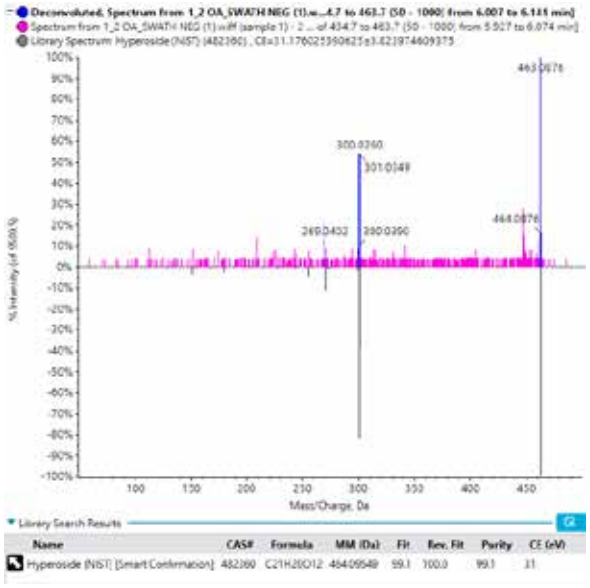

Figure 1. Deconvoluted MS/MS spectrum matching with library spectrum. (Top) The blue colored spectrum is the deconvoluted MS/MS spectrum from the SWATH acquisition data which is overlayed with raw MS-MS spectrum (pink) for parent mass 464.0876 at 5.9 min. (Bottom) Grey colored spectrum represents MS/MS spectra of Hyperoside from NIST library. The fit and purity score of 99 indicate the confidence of the identification for hyperoside from the library match.

In the previously proposed metabolomic workflow, the untargeted identification step was avoided by reduction of total number of features to a smaller feature list that are significantly different across biological samples.[2] Later, a complete compound annotation of a selected feature list is carried out through targeted identification using library spectral match.

Here, an untargeted data processing pipeline was used where all unknown features present in data that match with library spectrum are identified prior to performing multivariate statistical analysis. High confident identification of features utilizes MS1, MS/MS and deconvoluted spectrum for library spectral matching (Figure 1).

RUO-MKT-02-14667-A

In the current workflow, metabolites identified with high confidence in SCIEX OS software are plotted in MarkerView software to visualize statistical differences through PCA-DA and volcano plots. A great similarity in identified features in the proposed workflow (SCIEX OS to MarkerView software) to the conventional workflow (MarkerView to SCIEX OS software) illustrates a robust data processing workflow.[2]

Key features of data acquisition and processing workflow

- Metabolic features from high-resolution, accurate mass MS and MS/MS data acquired using SWATH DIA were identified by leveraging spectral libraries in SCIEX OS software.
  - Natural products HR-MS/MS and NIST libraries were used to identify key metabolites with high confidence
  - Identified metabolite panel were passed through to MarkerView software for multivariate statistical analysis including PCA and T-test
  - Graphical displays allow easy determination of differentiating metabolites

Methods

Sample preparation: The plants were cultivated for approximately 60 days under either white (W) or blue/red (B/R) light. The top leaves (apical, Ap L), middle leaves (median, Me L) and inflorescences (flower) were harvested and extracted with a solution of 1:1, ethanol/water. A Sep-Pak C18 was used to extract chlorophyll.[2]

Chromatography: An ExionLC system equipped with an HSS T3 column (100×1.0mm, particle size 1.8µm, Waters) was used for metabolite separation at a flow rate of 0.45 mL/min.[2]

Mass spectrometry: Data were acquired in positive and negative modes using a TripleTOF 6600 system using SWATH DIA. Details of the acquisition strategy are summarized in this technical note.[2]

Data processing: SWATH DIA data were processed in SCIEX OS software 1.6 using the Natural Products HR-MS/MS, Accurate Mass High Resolution and NIST spectral libraries. Feature identification step was conducted using a non-targeted workflow through Analytics section in SCIEX OS software. Sample data (.wiff files) were uploaded in Analytics, and a new processing method was created using a representative quality control sample. In contrast to the first technical note, here the metabolites were first identified, and then identified metabolites were used in the statistical analysis to find differentiating features. For this workflow type, non-targeted screening was selected, and components selection can be left blank (Figure 2). In the Library Search section, the Smart Confirmation Search is selected for the library search algorithm. Purity was selected for how the results would be sorted. Then, all the libraries used in compound identification were selected.

The mass tolerance for both MS and MS/MS was set to 0.02 Da (Figure 2). Finally, the polarity box was checked which enables the software to recognize the mode in which data is acquired. Under flagging rules, Mass Error (ppm), Library hit score and Formula finder score boxes were selected, and appropriate weighting percent are input in the boxes while the percent difference isotope ratio is optional.

Figure 2. Building a processing method for non-targeted metabolomics workflow for SWATH DIA data. The left panel depicts the selection of workflow type and selection of a representative sample for building a processing method. In the middle panel, the components section can be left empty or only first row should be filled with a known endogenous compound. The right panel shows the parameter settings, where smart confirmation search is selected. The results are sorted by purity of the spectrum. All libraries that are relevant for the sample types are selected, and precursor and fragment mass tolerances are selected as 0.02 Da. Finally, by checking the polarity box, software recognizes the polarity mode in which SWATH DIA data is acquired.

RUO-MKT-02-14667-A

In Formula Finder section, since these are plant samples, only naturally occurring compounds option was chosen because the data acquired is on plant samples. In Max element section, S (sulfur) was de-selected because sulfur compounds are uncommon in plants. Under non-targeted peaks, the retention time range was set to 2 min to 26 min, peak detection sensitivity was set to two steps away from “exhaustive” to avoid peak detection at noise level.

The result file consists of features that are identified through MS/MS spectral matching with library at various confidence levels, and features with only MS spectrum alone. The features that were identified with high confidence were exported from SCIEX OS software. Further, these identified features were copied into Excel where a vlookup function was used to consolidate the data into a single list of unique compounds with peak areas from each sample associated.

After consolidation of the data, this data was imported as text into MarkerView software for multivariate statistical analysis and generation of 2D graphical plots.

Comprehensive data collection using SWATH DIA

The study of the metabolome is key to understanding the basic biological mechanisms that regulate plant growth and stress responses, however the metabolome is highly complex and comprehensive interrogation is difficult using traditional data dependent approaches. The SWATH DIA workflow was used here because it can acquire high-resolution MS and MS/MS data on all detectable precursors in the sample.[2] The method is sensitive and reproducible and provides a comprehensive view of the metabolome using a relatively short 30-minute run. Both the high-resolution MS and MS/MS spectra are used for metabolite identification by library search (Figure 1), and quantitative peak areas can be obtained from both the MS and MS/MS data.

Identifying metabolites using library matching

Feature identification through library matching was performed using Analytics in SCIEX OS software, using the NIST 2017, Natural product and Metabolite_HR-MS-MS libraries. Overall, 508 metabolites were identified across the dataset with high confidence.

Hyperoside (Quercetin 3-galactoside/Hyperin), m/z of 463.0891 eluted at chromatographic retention time of 5.87 min, was one of several features that was identified with very high confidence using NIST library MS-MS spectrum that showed significant difference apical leaves to flowers (Figure 3).

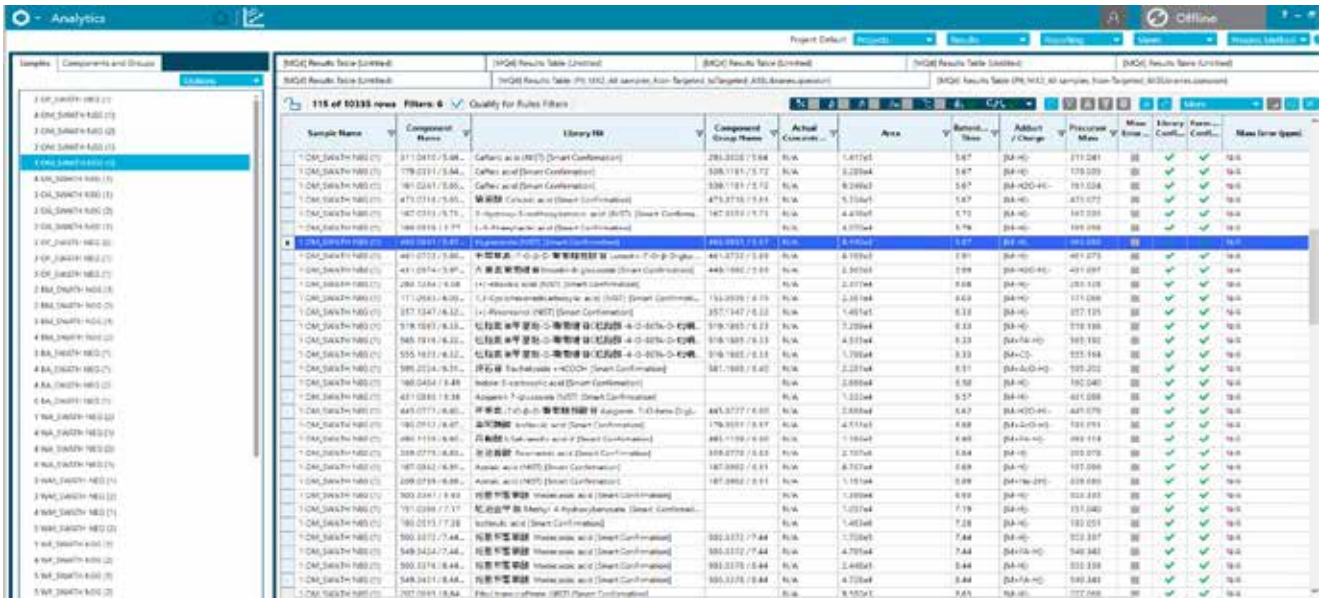

Figure 3. Results from library search in Analytics module of SCIEX OS software. Result file consists of sample name, component name (m/z and retention time information), library hit, compound ID, the data used to search the feature and library confidence and formula confidence. SCIEX OS software provides flexibility of sorting the compounds with high library confidence and formula confidence.

RUO-MKT-02-14667-A

Statistical analysis of identified features through MarkerView software

The peak areas of metabolites identified with high confidence from the library search performed in SCIEX OS software were formatted in excel and imported into MarkerView software for multivariate statistical analysis.

Figure 4 (left) displays the Scores plot (left) for Partial Least Squares Discriminant Analysis (PLS-DA) and Loadings plot (right) for all the biological replicates studied to understand compounds that significantly differentiate sample groups and replicates. Features with higher D1 and D2 loading scores are more differentiating. On a closer examination, flower samples exposed to white or blue/red light have (Figure 4, left) clustered together in second (top right) and fourth (bottom right) quadrants and clearly separated from the leaf samples exposed to white of blue/red light.

All the metabolites that have contributed to sample variation are displayed on the Loadings plot (Figure 4, right) by compound name, library from which it was identified, and the identification algorithm. For instance, hyperoside had higher D1 and D2 scores making it one of the key compounds differentiating flowers exposed to different wavelengths as opposed to leaves.

Several other compounds, luteolin 7- glucoside, betulinic acid, salvianolic acid and cichoric acid seem be more important compounds that are separating flower and leaf samples apart.

T-test analysis

Next, the pairwise *t*-test was performed to find specific differences between individual groups of interest. Figure 5 (left) shows the volcano plot with log fold change on x axis and p-value on y axis constructed from a pairwise *t*-test for 2 groups from batch 2, specifically the apical leaf samples grown under white light (AP L_WL) and the flower samples grown under white light (F_B/R). Compounds with a low *p*-value and high fold change are ones that differ in abundance between the groups with high confidence. Hyperoside and salvionic acid with *p*-value ≤ 0.05 and fold change ≥ 3, are compounds of interest for future experiments. Furthermore, about 85% of all the compounds in the Figure 5 (left) in red text were comparable to those identified in the previous work with the alternative workflow[4,5] suggesting robustness of both data processing workflows.

Peak area response plots comparing peltatoside (Quecetin-3-O-arabioglucoside) and luteolin 7- glucoside for apical leaves and

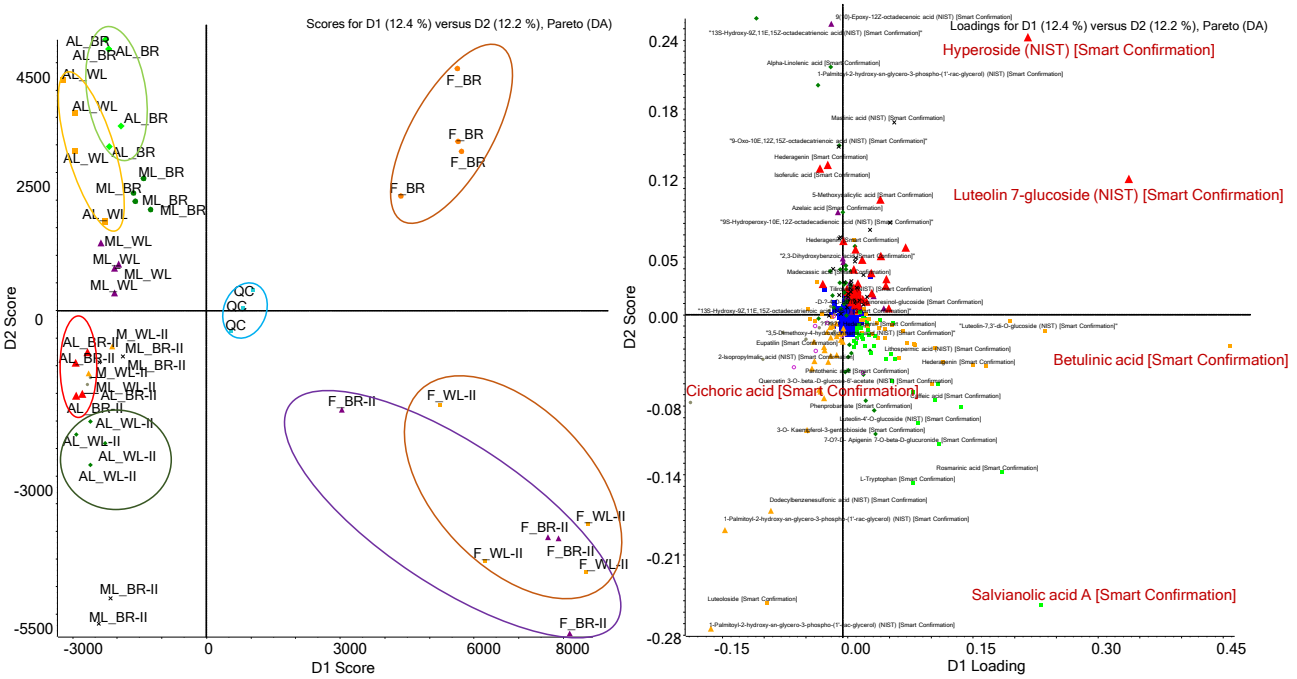

Figure 4. PCA analysis of identified metabolites from SWATH DIA data. (Left) Scores plot. PLS-DA showed the distinguishable segregation of flower (F) and apical leaf (AL) samples exposed to white and blue/red right wavelengths. (Right) Loadings plot of supervised multivariate statistical analysis (dimension reduction), shows all the compounds identified with high confidence that were used in performing PLS-DA. From the PLS-DA plots, the compounds that are highlighted in red color seems to have significantly impacted the groups that are observed in the score plots.

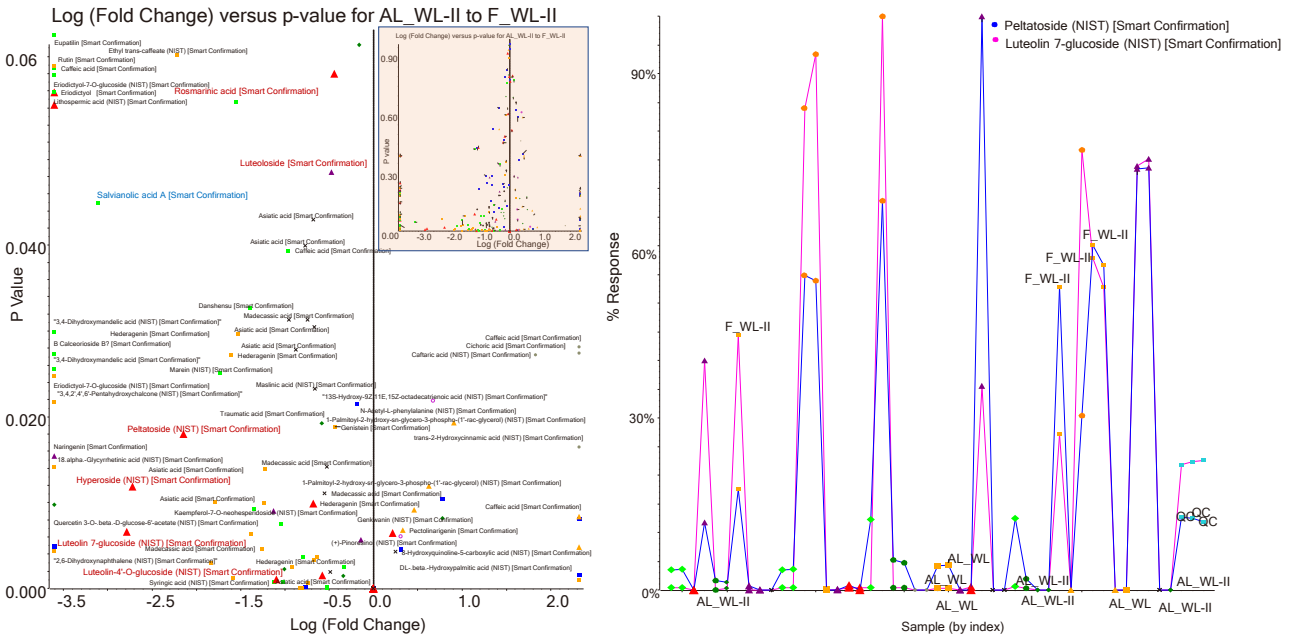

Figure 5. T-test analysis of leaf vs. flower grown under white light. The volcano plot (left) provides both statistical significance (p-value) on the Y axis and fold change for compounds on x-axis used in t-test. The compounds names marked in red are same compounds identified from the interest list generated from MarkerView software in previous technical note[2], suggesting the robustness of the of both workflows. Area response plots (right) from various samples depict higher levels of peltatoside and luteolin 7- glucoside in flowers compared to apical leaves.

flowers exposed to white light showed higher levels of these compounds in flowers as opposed to leaves (Figure 5, right).

In this study, popular flavonoids such as hyperoside, peltatoside, naringenin, quercetin, luteolin glucosides are upregulated in flowers. It can be also established that flowers either exposed to white or blue/red light have shown higher levels of flavonoids than leaves. Flavonoids are well known for their UV protection and their functional role ROS scavenging under high light stress conditions.[6] Additionally, these compounds are largely responsible for colors and aroma of the flower.[7] Further, it will be interesting to investigate the role of Eriodictyol-7-O-glucoside in flower tissues due to its relative abundance in flowers exposed to white light compared to blue/red light.

Conclusions

In this study, *O. basilicum* plants grown under different light wavelengths and SWATH DIA was used to examine the metabolic changes that occurred in different plant parts. Here, an alternative data processing approach was used for metabolite identification through library searching in SCIEX OS software.[2] Then the identified metabolites were analyzed using MarkerView software to find the differentially regulated plant metabolites. Both workflows are supported within SCIEX OS software.

- Rich dataset for untargeted plant metabolomics was collected using data independent acquisition (SWATH DIA), providing high-resolution MS and MS/MS data for all detectable precursors in a sample in a single run
- Metabolites were identified using a library searching that leverages the MS and MS/MS from SWATH DIA data
- Statistically significant metabolite differences and trends were easily visualized using MarkerView software, using the various multivariate statistical analysis and visualization tools (PCA, PLS-DA, t-test) to distinguish biological samples. With this workflow, metabolite names are displayed rather than m/z / RT features with the previously described workflow.[2]

RUO-MKT-02-14667-A

References

1. d'Aquino L. *et al.* (2022). *Growth and metabolism of basil grown in a new-concept microcosm under different lighting conditions.* *Scientia Horticulturae* **299**:111035.
2. Global metabolite profiling of leaves and flowers of *Ocimum basilicum* L. grown in a microcosm under different light wavelengths. SCIEX technical note, RUO-MKT-02-14157-A.
3. K Patel, *et al.* (2018) New insights into the medicinal importance, physiological functions and bioanalytical aspects of an important bioactive compound of foods 'Hyperin': Health benefits of the past, the present, the future" *Beni-Suef University Journal of Basic and Applied Sciences*, **7(1)**, 31-42.
4. MarkerView software - SCIEX community posts.
5. Natural Products HR-MS/MS Spectral Library 1.1.
6. *BMC Plant Biology* **volume 17**, Article number: 64 (2017)
7. Torawane SD *et al.* (2020) Controlled release of functional bioactive compounds from plants. *Enc. Active Mol. Del System* 103-110.

RUO-MKT-02-14667-A

Analysis of untargeted metabolomics data from an untargeted Zeno data-dependent acquisition (DDA) workflow using SCIEX OS software

A metabolomics data processing pipeline for DDA data acquired on the ZenoTOF 7600 system

Rebekah Sayers[1], Robert Proos[2] and Paul RS Baker[2]
[1]SCIEX UK; [2]SCIEX US

This technical note describes the best practices for analyzing untargeted metabolomics data acquired using the ZenoTOF 7600 system. Previous work has provided a step-by-step overview of instrument parameter settings to obtain optimal untargeted data[1]. This work explains the settings and the subtle changes to the processing method in SCIEX OS software that are needed to maximize coverage of the metabolome.

Metabolites are chemically and structurally diverse compounds that are found endogenously at a wide dynamic concentration range, which makes the metabolome challenging to characterize.

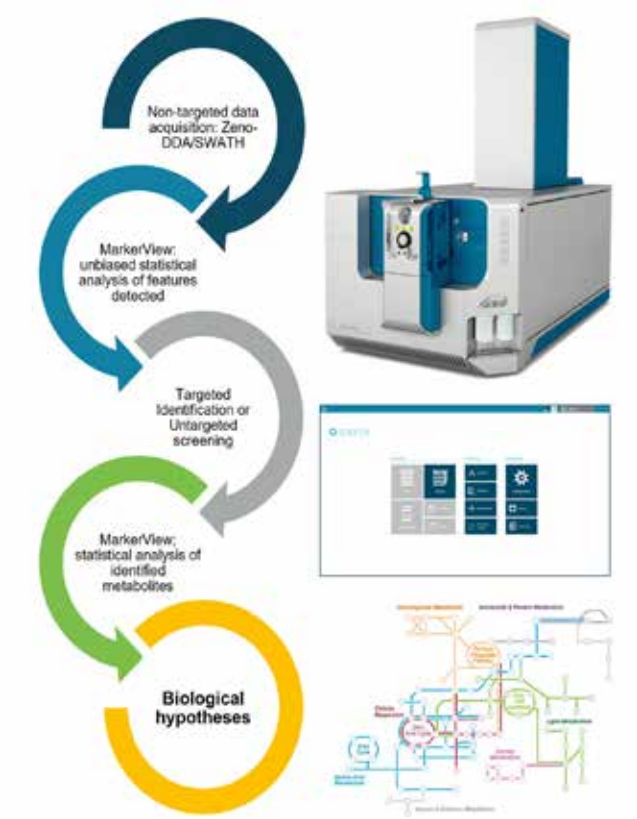

Figure 1. Targeted and untargeted metabolite screening workflows on the ZenoTOF 7600 system.

Mass spectrometry is typically used for metabolomics analysis in complex biological samples. DDA is a commonly used analytical technique for untargeted metabolomics to detect and potentially quantify all metabolites in a sample (Figure 1). In this experiment, a TOF MS scan detects all precursor ions within a specified mass range, and MS/MS scans are triggered for those precursors that pass pre-defined criteria. Based on adjustments to the criteria, an ideal experiment should provide as much coverage of the metabolites as possible, while maintaining good MS/MS spectral quality. A complementary technical note detailing the optimal instrument parameter settings for DDA analysis using the ZenoTOF 7600 system is available online[1].

Many metabolites are present at low endogenous concentrations due to the nature of the metabolome, which can lead to low-quality spectra and poor coverage. However, the Zeno trap provides significant gains in MS/MS sensitivity and improves MS/MS spectral quality. The use of the Zeno trap can therefore result in higher confidence spectral matching and greater metabolite coverage. Spectral matching is currently reliant on libraries obtained from instruments without a Zeno trap. Therefore, the processing methods must be optimized to realize the true potential and impact of the data.

Key features of processing Zeno DDA data using SCIEX OS software

- An untargeted metabolomics workflow with the Zeno trap enabled provides high-quality MS/MS spectra
- Current MS/MS spectral libraries contain fragmentation data acquired on platforms without a Zeno trap, which differ in the ratio/intensity of fragment ions
- To maximize the impact of metabolomics data acquired on the ZenoTOF 7600 system, specific parameter settings within the data processing method should be used

RUO-MKT-02-15619-A

Methods

Sample preparation: NIST SRM 1950 plasma was extracted using 4 volumes of ice-cold methanol. After centrifugation to separate the precipitated proteins, the supernatant was directly analyzed by liquid chromatography electrospray ionization tandem mass spectrometry (HPLC-ESI-MS/MS).

Chromatography: Samples were analyzed using an Exion LC system with a Kinetex F5 column (2.1 × 150 mm, 2.6 µm, Phenomenex). A simple linear gradient from 0 to 95% B was used with standard reversed phase mobile phases at a flow rate of 200 µL/min. Mobile phase A was 0.1% formic acid in water and mobile phase B was 0.1% formic acid in acetonitrile. A 1 µL injection volume was used and the column temperature was maintained at 30°C throughout the analysis. The total runtime was 20 min.

Mass spectrometry: The extracted sample was analyzed on the ZenoTOF 7600 system equipped with the OptiFlow Turbo V ion source. Data were collected using a top-40 DDA method, with dynamic background subtraction (DBS) and exclusion for 6 s after 3 occurrences. The method used a TOF MS accumulation time of 100 ms, collision energy (CE) of 30 V and a TOF MS/MS accumulation time of 5 ms. For a detailed explanation of parameter settings used for DDA analysis on the ZenoTOF 7600 system, see reference 1.

Data processing: All data were analyzed using the Analytics module in SCIEX OS software. The MS/MS spectra were compared to the library spectra using the SCIEX All-in-One HR-MS/MS library version 2.0, SCIEX Accurate Mass Metabolite Spectral Library version 2.0 and NIST 2017 MS/MS library. Statistical analysis was performed using MarkerView software.

SCIEX OS software: Project Default Settings

Quantitative processing parameters (peak integration)

SCIEX OS software can be used to process all data types acquired on both triple quadrupole and QTOF instruments, and processing parameters can be adjusted depending on the type of analysis and data processing used (Fig. 2). SCIEX OS software has 3 integration algorithms that can be used to integrate peaks. These options are listed in the Project Default Settings in the Analytics module of SCIEX OS software (Fig. 3).

MQ4: This algorithm selects a low, but not the lowest, concentration standard or quality control sample as the representative sample for the analytical run. This algorithm requires some user input to define the integration parameters but can enable faster searching. This algorithm is therefore preferentially used for targeted and untargeted identification workflows.

AutoPeak: This algorithm selects a high, but not saturated, concentration standard or quality control sample as the representative sample of the analytical run. Chromatograms within the batch being processed are evaluated to determine which sample is the best peak model for each transition. The peak model is constructed based on a model of 3 Gaussian peaks. This algorithm requires little user input because few parameters are adjustable. This is the optimal choice for targeted quantitative analysis.

Summation: This algorithm does not perform a normal peak search and instead assumes that a peak is present close to the expected retention time. This algorithm works well with flow-injection analysis (FIA) or infusion data.

When performing quantitative mass spectrometry data processing, it is important to determine whether a given peak is significant and exceeds background noise. There are 3 signal-to-noise algorithms available in the software, including relative noise, standard deviation and peak-to-peak. The latter 2 require the noise region and the peak of interest to be selected on the

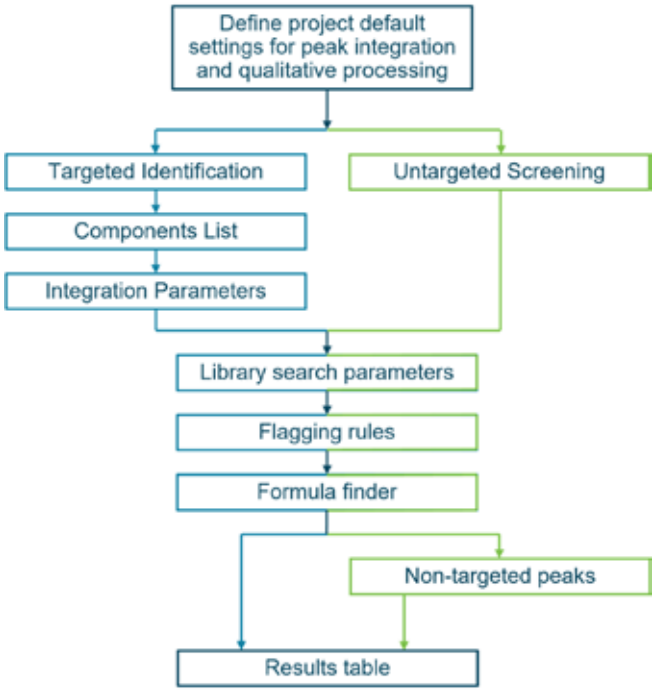

Figure 2. Process for defining processing parameters in SCIEX OS software, according to workflow

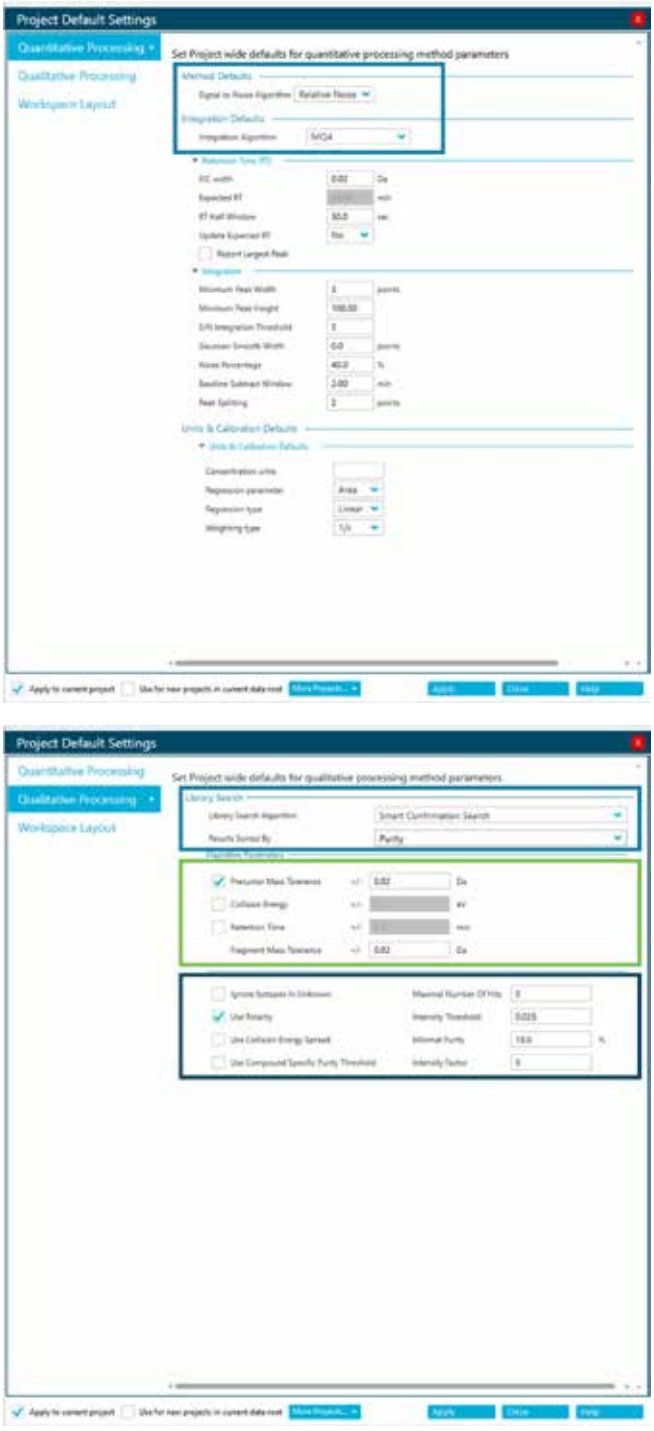

Figure 3. Project default settings. Top: Peak integration and signal-to-noise algorithms and **Bottom:** library searching algorithm, filtering and scoring settings.

chromatogram and are therefore not suitable for untargeted data analysis. The relative noise algorithm provides a less subjective means of determining signal-to-noise calculations and allows a background to be calculated even when no peak-free part of the chromatogram is available.

For targeted and untargeted metabolite screening, the MQ4 integration and relative noise algorithms should be selected.

Qualitative processing method parameters

The quantitation and targeted identification workflow can be used for both the quantitative and qualitative analyses of known analytes and uses library searching to confirm the identity of analytes in the sample. There are 3 types of library searches that can be performed.

Candidate search finds the best spectral match from all compounds in the selected libraries. This search will take the longest time to process.

Confirmation search uses the name in the components list to match against compound names in the libraries. The name in the XIC list must exactly match the name in the library or no hit will be found. This should only be used in a targeted identification search, where the target list has been generated from the library compound list.

Smart confirmation search first searches for matching names, and then searches using the spectra if no match is found. Smart confirmation search is recommended for this workflow as the processing time will be the same as the confirmation search if the compound name exists in the library. This search strategy comes with the added flexibility to perform candidate searching when needed. This is the most used search algorithm.

Once the results have been obtained from the library search, it is important to assess the confidence of each of the identifications. There are 3 scores can be computed to sort the results.

Purity score uses all peaks from both spectra when calculating the score. A high value indicates a high probability that the unknown spectrum has been correctly identified and does not contain significant amounts of peaks from additional compounds. A lower value indicates that the match is less certain or additional fragment ion peaks from another compound are present in the unknown spectrum. This is the most used method to sort results.

Fit score is calculated based on the library spectrum and it ignores peaks that are present only in the unknown spectrum. The fit score describes how well the library spectrum is represented in the unknown spectrum. A high fit score with a low purity score indicates that the unknown spectrum is likely impure but contains library compounds.

RUO-MKT-02-15619-A

Reverse fit score is calculated based on peaks that are present in the unknown spectrum and it ignores peaks present only in the library spectrum. The reverse fit score describes how well the unknown spectrum is represented in the library spectrum.

Default settings for quantitative processing and peak integration should be set for each project and cannot be altered within the processing method. Qualitative processing method parameters can be set for the project and can also be modified in the processing method.

SCIEX OS software: Targeted and non-targeted metabolite screening

When performing untargeted data analysis, select either the quantitation and targeted identification or non-targeted screening workflow. The selected project default parameters are used for peak integration and are saved in the processing method file.

For targeted identification, a component list must be entered. This can be inputted manually, imported from a text file or generated from a library database. Inputting the chemical formula and selecting the adduct/charge will automatically calculate the precursor mass (Da). The peak integration will then be performed using an example data file. This can be reviewed before proceeding or found later in the results table.

If non-targeted screening is used, a component list can be used if desired but the non-targeted search parameters must be defined. If the processing method contains the targeted analytes, then the customized integration parameters for the targeted components will not affect the non-targeted peak integration. To change the project default parameters, the user must create a new non-targeted method. If the parameters are changed in an existing method, the changed parameters will not be implemented.

Library search parameters

Library search parameters have a big impact on the coverage and the quality of spectral matching (Fig. 4). Precursor mass tolerance, collision energy, retention time and polarity settings can be used to filter the data. Precursor mass tolerance should be set according to data type. For accurate mass data acquired on a high-resolution instrument, the precursor mass tolerance should be set to 0.02 Da. Unchecking the Collision Energy and Collision Energy Spread boxes will allow more spectra to be

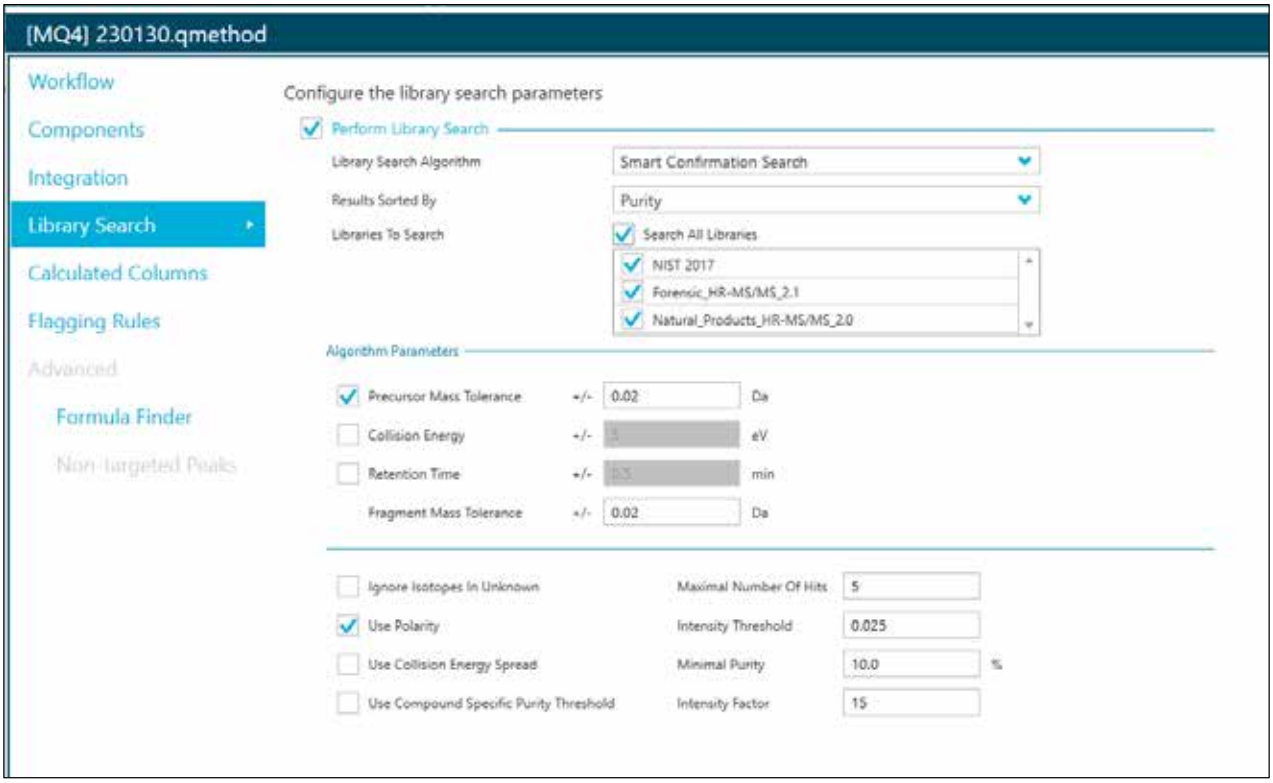

Figure 4. Library search parameters for DDA data acquired on the ZenoTOF 7600 system

returned. Using CE and CES is recommended if the experimental conditions are the same as those used to build the library, as this will return the most reliable results. Retention time (RT) should only be selected if the search is against a library that includes RTs and if the same chromatographic separation conditions are used. Metabolomics data are typically acquired in both polarities, so selecting this filter will allow library components to be matched correctly to data acquired in the same polarity.

These settings will determine which spectra in the library will be evaluated against the acquired spectra. Good filtering will improve processing time and reduce false positives. Incorrect filtering will cause false negatives. The remaining parameters will affect how the results are scored. Fragment mass tolerance, intensity threshold, minimal purity and intensity are important to consider when comparing data to a library acquired without using the Zeno trap because of differences in the intensities of fragments.

Intensity threshold sets which fragment ions are used in the search. The default 0.05 value corresponds to 5% and any peak below 5% of the base peak will be ignored. This value can be used to remove small noise peaks from the spectrum and improve purity scores. Decreasing this will allow more of the smaller peaks to be considered during spectral searching, which might be important to identify a compound. For processing our Zeno DDA data, this number is set to 0.025%.

Minimal purity indicates how well the sample and library spectra match. All peaks from both spectra are used. High values indicate a higher likelihood that the unknown spectrum has been correctly identified and that it does not contain significant amounts of peaks from additional compounds. Lower values indicate that the match is less certain or that fragment ion peaks from another compound are present in the unknown spectrum. Increasing the value of this setting reduces the frequency of lower quality hits.

Intensity factor compensates for differences in peak height between the unknown spectrum and the library spectra. The larger the intensity factor, the greater the difference allowed between the unknown spectrum and the library while still getting a high score. Increasing this value will remove the significance of relative intensity. When comparing spectra generated with the Zeno trap, the intensity factor should be set to 20 to reduce the importance of variation in the ratio of fragment ions between the unknown and the library spectra. Increasing the intensity factor also increases the purity and these settings change the score calculation. A low intensity factor can yield low scores for true hits, whereas a large intensity factor might introduce false positives.

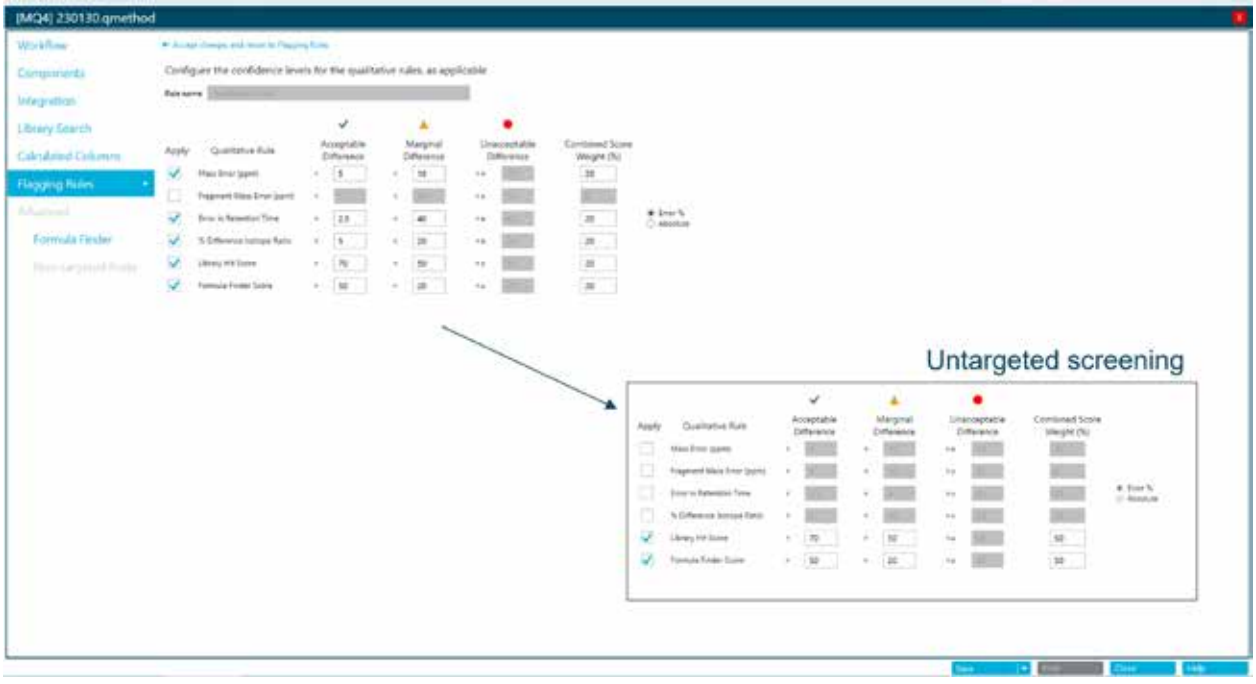

Figure 5. Confidence level settings. Found under the Flagging Rules tab, these settings enable easy identification of compounds in the results table that may require further investigation before assigning identity

RUO-MKT-02-15619-A

Confidence level settings – Flagging rules

Confidence level settings establish the acceptable boundaries by which data is matched to the spectral libraries and are used to filter any proposed metabolite identifications and characterize the quality of the match. These levels can be set in the Flagging Rules tab (Fig. 5). A score is calculated for the sample metabolite for all criteria selected. A combined score can be generated based on weighting all parameters. The weighing of each qualitative rule can be adjusted according to the number of rules but should total 100%. The results table can be filtered using this traffic light system in which metabolites that fall within the defined confidence intervals will be highlighted in green for acceptable, yellow for marginal and red for unacceptable.

Qualitative rules include mass error (ppm), fragment mass error (ppm), error in retention time, % difference in isotope ratio, library hit score and formula finder score. When performing targeted identification, all but the fragment mass error qualitative rule can be selected. To include a fragment mass error, it must be entered in the components list.

Formula finder

The formula finder algorithm tries to predict the possible chemical formula based on the MS and MS/MS spectra, precursor mass accuracy, isotopic pattern and MS/MS fragmentation.

Formula predictions are made from a defined list of elements and mass tolerance that can be found under the Advanced Tab (Fig. 6). First, select from either naturally occurring compounds or synthetic compounds. In either case, the type of element and/or number of elements to consider must be entered in the Limits section. Proposed formulas are scored based on precursor mass accuracy and average MS/MS mass accuracy of matching fragments. The MS spectrum contributes 67% to the final formula finding score and the MS/MS spectrum contributes 33%. As a result, the ability of the formula to predict the MS mass is the primary influence on the score. However, the matching of the MS/MS fragments also influences the score. The isotope pattern is used to generate the list of found formulas but it is not used to generate the final score. Therefore, a formula with the wrong isotope pattern will probably not be included in the list. A list of possible formulas is determined using precursor mass accuracy, isotopic pattern and MS/MS fragmentation. A high formula finding score does not guarantee that the sample compound is the one identified by the formula finding algorithm because several formulas often match within the mass error. Care must be taken and other confirmatory testing must be done before a compound is identified using formula finding.

SCIEX OS software: Results

After defining the required algorithms and processing parameters discussed above, a results table will be generated (Fig. 7). Extracted ion chromatograms (XICs) are generated for all

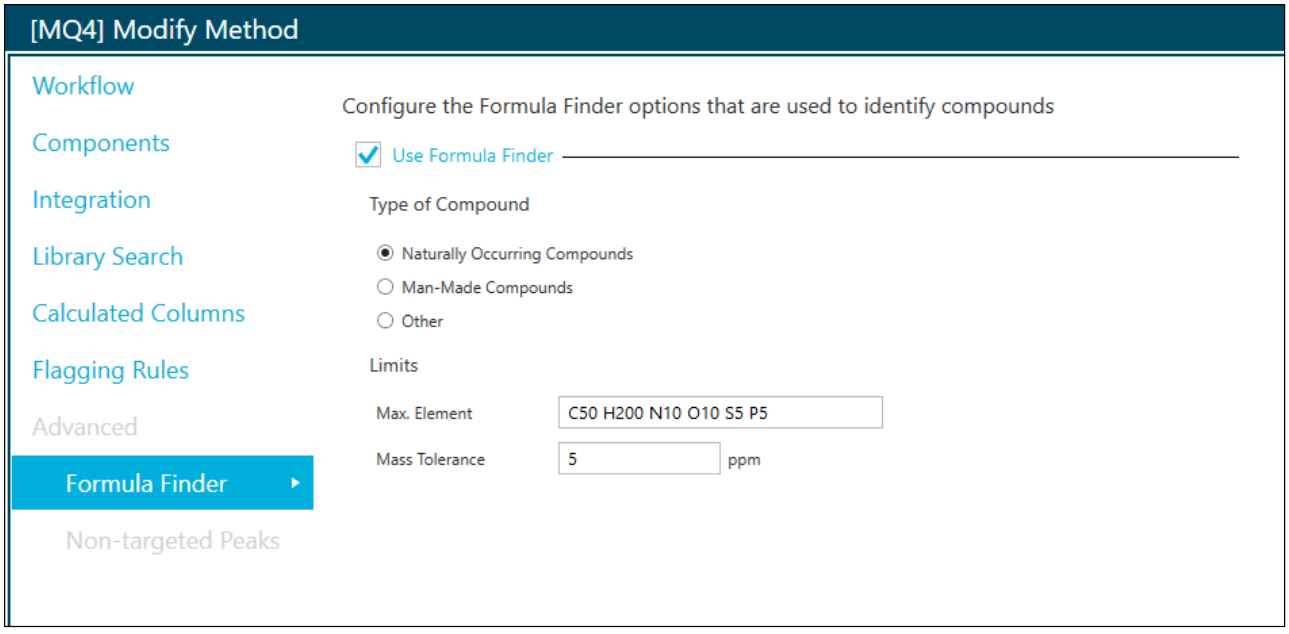

Fig 6. Formula Finder settings. An empirical formula can be predicted based on the TOF MS and TOF MS/MS spectra acquired for DDA experiments. These predictions are influenced by the limits on the elemental composition and mass tolerance settings

RUO-MKT-02-15619-A

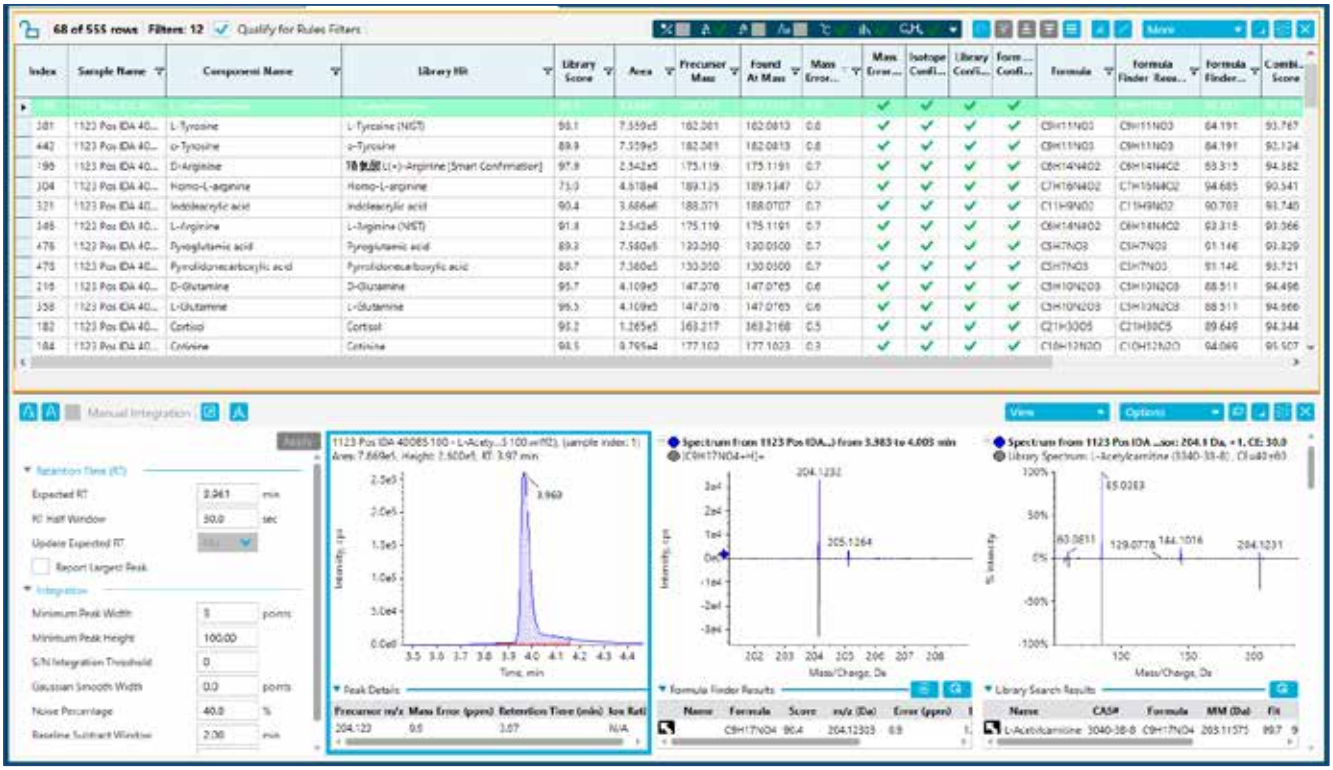

Figure 7. Results table generated from a targeted identification workflow in SCIEX OS software. Results have been filtered to show only those meeting the highest confidence for each criterion.

metabolites in the library based on thresholds set by the user, such as formula and expected retention time of all target analytes. The MS and MS/MS information is automatically evaluated if the detected XIC signal exceeds the user-defined intensity threshold or signal-to-noise (Figure). Data processing results are ranked based on 4 selectivity criteria to provide a high degree of confidence in assigning compound identifications to detected compounds:

- Retention time matching
- Mass accuracy
- Isotope pattern fit
- MS/MS library searching

In addition, the peak intensity of the analyte can be compared to that of a standard sample of known concentration to obtain quantitative information.

Formula finder results are shown in Figure 7. Clicking on Formula Finder Results will show additional potential candidates. The chemical structure of the selected formula finder results is also shown in the table if the compound has been updated from ChemSpider. By clicking on the ChemSpider icon in the results table, a ChemSpider session is initiated, and a list of all suggested compounds that match the selected formula will be generated. Selecting a compound in the results list in the app will display the chemical structure, acquired vs matched spectra and a table of matching fragments, together with their mass errors and elemental composition

MarkerView software: Statistical analysis

The MarkerView software is designed to allow the data from several samples to be compared so that differences can be identified. The program uses multivariate analysis (MVA) techniques to compare the samples and provides both supervised and unsupervised methods (Figs. 8 and 9). Supervised methods use prior knowledge about the sample groups (for example, healthy vs diseased) to determine the variables that distinguish the groups. In contrast, unsupervised methods allow the structure within the data to be determined and visualized. The 2 approaches can be combined, for example, as unsupervised methods can be used to determine the groups and then supervised methods can be used to confirm the important variables.

The first stage of data analysis is to perform an unbiased review of the detected features. Using the wizard, the raw data files (*.wiff or *.wiff2) are imported into the software without any prior processing. Data can be assessed by performing a PCA

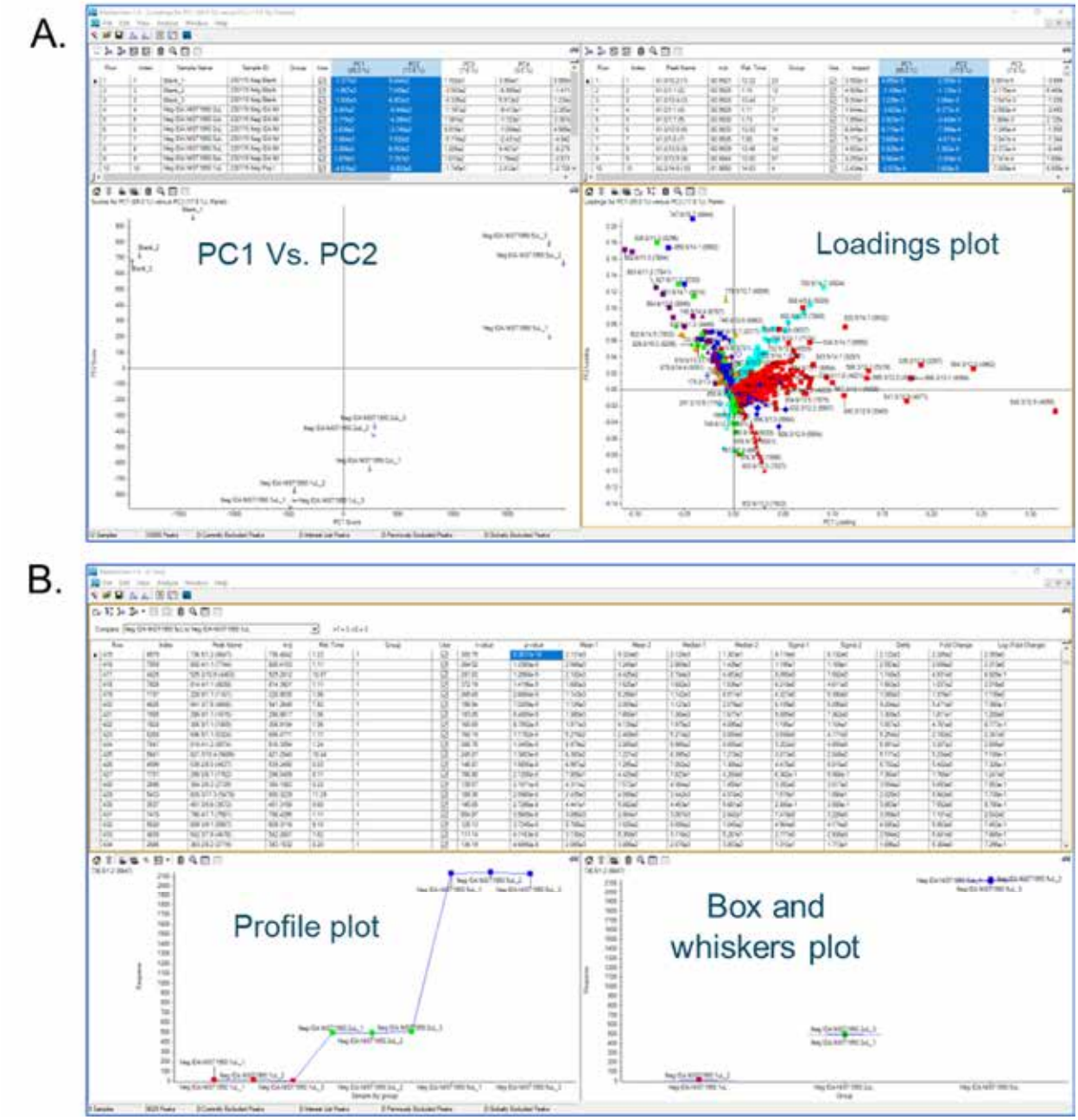

Figure 8. Unsupervised PCA Analysis. Panel A: Two groups of data, for example treated Vs. control samples can be processed via PCA analysis to identify outlier metabolites in the treated group from the loadings plot. These data can be visualized by highlighting the data point(s) form the loadings plot and to generate either a profile plot or a box and whiskers plot as shown in **Panel B.**

analysis. The resulting scores and loading plots enable us to check data reproducibility and quickly identify any outliers. A t-test between groups of interest can show differences between individual features across samples. A volcano plot of p value vs fold-change highlights any significant changes across the samples. These metabolites can be added to an interest list.

These processing steps are used to identify putative features of interest. Data must then be processed in SCIEX OS software using a spectral library to identify the selected features.

Once the features have been identified, a second statistical analysis using the peak list of identified metabolites can be

RUO-MKT-02-15619-A

performed. When the peak list is imported into MarkerView software, the names of the metabolites are shown instead of the feature's m/z and RT. PCA analysis and t-tests on our sample sets. The resulting volcano plot shows which metabolites have the largest fold-change and which are significantly different between the samples. This approach can enable fast identification of features of interest, which may reveal important biological insights.

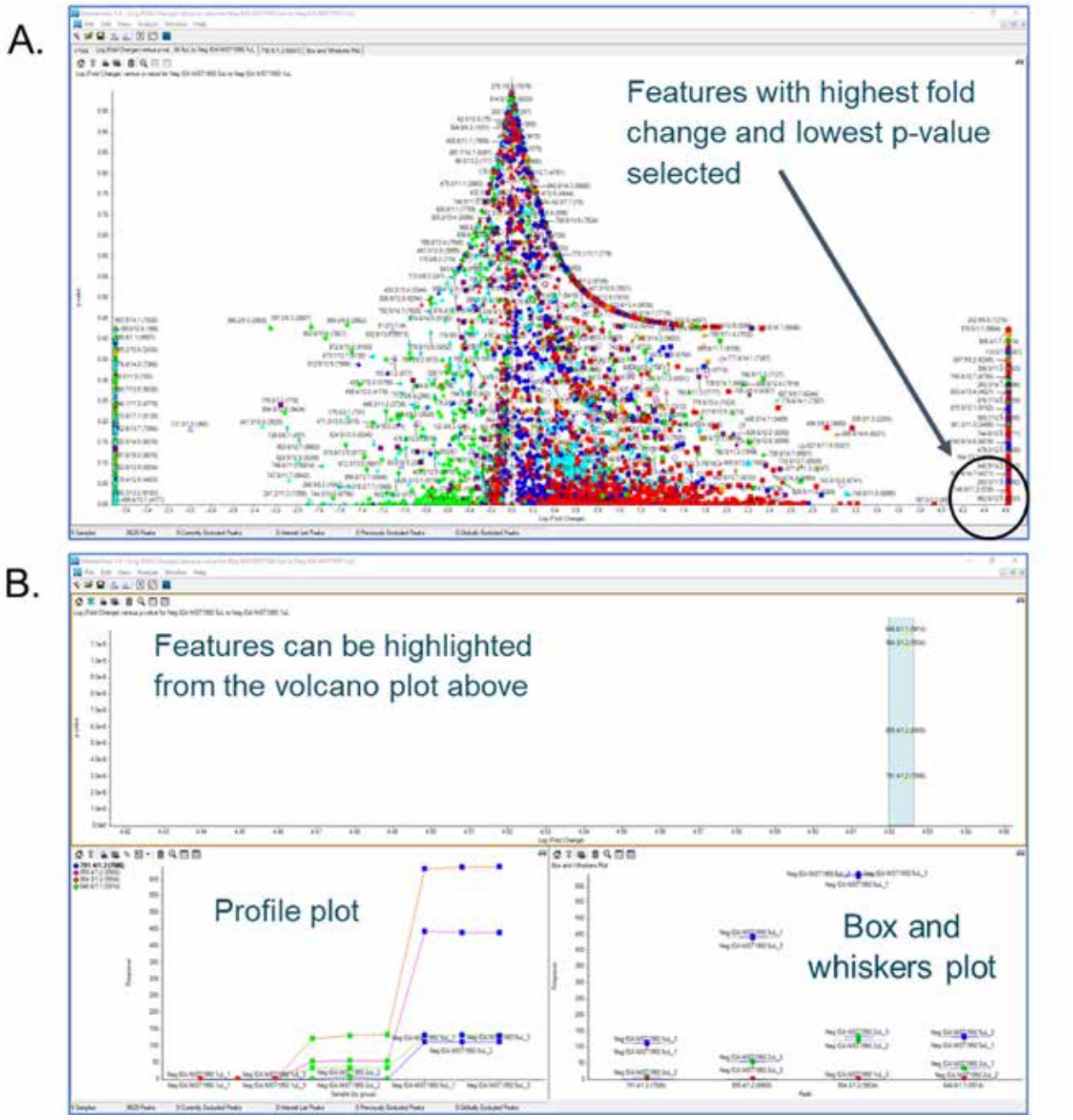

Figure 9. Volcano plot data visualization form MarkerView software. Data can be visualized via a volcano plot **(Panel A),** and as in figure 8, highlighted data can be visualized quantitatively as a profile plot or a box and whiskers plot as shown in **(Panel B)**.

RUO-MKT-02-15619-A

Conclusions

- High-resolution, accurate mass MS/MS data acquired on the ZenoTOF 7600 system at a fixed collision energy may not match as confidently to spectral libraries acquired without the Zeno trap. Herein, optimized parameter settings are provided
- SCIEX OS software allows targeted identification and quantitation and untargeted screening of metabolites. This high degree of flexibility enables the user to optimize processing parameters for a given workflow and/or data type.
- Algorithm and processing parameter choices will impact how many metabolites are confidently identified when comparing Zeno DDA data with conventional spectral libraries
- MarkerView software together with SCIEX OS software provides a complete solution to a metabolomics workflow

References

1. Baker, PRS and Proos R. Untargeted data-dependent acquisition (DDA) metabolomics analysis using the ZenoTOF 7600 system. SCIEX technical note, RUO-MKT-02-15367-A

RUO-MKT-02-15619-A

MExplorer Ultimate新一代非靶向代谢组学数据分析软件助力痛风疾病研究

MExplorer Ultimate: Next-Generation Non-Targeted Metabolomics Data Analysis Software Empowers Gout Disease Research

满卓[a]，郝亚芳[b]，司丹丹[a]，龙志敏[a]，刘冰洁[a]，陈爱明[b]
Zhuo Man[a], Yafang Hao[b], Dandan Si[a], Zhimin Long[a], Bingjie Liu[a], Aiming Chen[b]
[a] SCIEX应用支持中心，中国；[b] 大连达硕

关键词： MExplorer Ultimate; Metabolomics; 一站式分析; 人工智能

前言

痛风是常见代谢性疾病，发病率上升，发病机制尚未完全明确，寻找有效诊断标志物和治疗靶点迫在眉睫。代谢组学为痛风研究提供新视角，能挖掘潜在生物标志物和揭示发病机制。SCIEX和大连达硕公司联合推出了MExplorer Ultimate软件，实现从峰提取、定性鉴定、统计分析、通路分析、正负整合分析等一系列全面丰富的解决方案。采用MExplorer Ultimate软件一站式分析代谢组学实验数据，在痛风研究中关键作用。本文通过介绍其在痛风代谢组学研究中的应用案例，为相关研究提供参考。

MExplorer Ultimate软件具有以下主要特点

1. 一站式代谢组学数据处理流程，从质谱数据到机理阐释，操作简单方便；
2. 一键式峰提取，包括保留时间校正及峰匹配、QC校正等；
3. 具有上千种标准品谱库以及配合上百万种网络谱库进行代谢物鉴定，包括代谢物和脂质等，化合物检索方便，鉴定结果丰富可靠；
4. 可以实现丰富的统计学分析，如t-test，PCA等，并进行通路分析，从而对生物学意义有更好的阐释；
5. 非靶向定性结果可以一键式转化为拟靶向MRM离子对，快速方便；
6. 生成的数据报告全面丰富，谱图质量满足出版要求；
7. 工作流程清晰简单，能够满足处理大样品量的数据分析；

图1. MExplorer Ultimate软件登录界面展示

仪器设备

SCIEX Exion LC™超高效液相系统联用SCIEX QTOF四极杆串联飞行时间质谱系统

RUO-MKT-02-34589-ZH-A

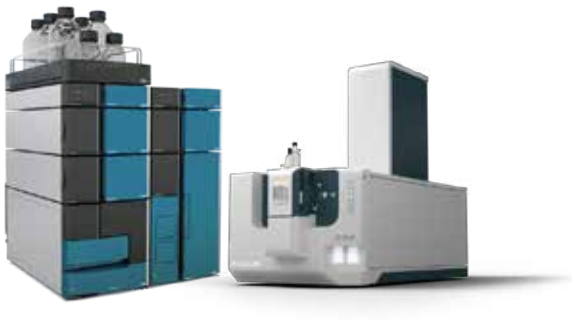

图2. Exion LC™液相系统联用SCIEX QTOF系统

样品及试剂

样本处理：冰上取50 µL血浆样本于1.5 mL EP管，加4倍体积含内标甲醇，涡旋、静置后，4℃、13,000 g离心15 min沉淀蛋白。取上清液浓缩，-20℃保存。上机前用100 µL甲醇/水(2:8)复溶，振荡离心后，取上清用于分析。

样品信息：对照组（Con）36个；痛风组（Gout）32个；尿酸组（HUA）30个；痛风石组（UAN）9个。

色谱分析：

色谱柱：正离子模式使用BEH C8 2.1×100 mm, 1.7 µm，负离子模式使用HSS T3 2.1×100mm, 1.8 µm

梯度洗脱30 min。

质谱分析：

离子源：ESI电喷雾电离源　　扫描方式：POS和NEG

气帘气CUR：30psi　　喷雾电压IS：5500v/-4500v

源温度 Temp：500℃　　雾化气Gas1：50psi

辅助气GAS2：50psi　　碰撞气 CAD：7psi

IDA信息依赖型采集模式

TOFMS扫描范围：60-1300Da

MS/MS二级碎片采集模式：

每个时间点触发15个MS/MS二级扫描；

TOF MS/MS扫描范围40-1300 m/z；

DBS(Dynamic Background Subtraction)启用：使用实时动态扣除背景，获得高效率的二级子离子，碰撞能量CE和步阶CES：35 ± 15eV（即收集CE20/35/50低中高三个不同碰撞能量的子离子质谱信息，获得全面丰富的子离子碎片信息）

代谢组学分析流程图

图3.非靶向代谢组学分析流程图

数据分析结果展示

1. 软件界面整体展示

采用一站式软件平台，从一级峰表提取至成份鉴定，至统计学分析，通路分析，阐述生物学意义。如图4所示。

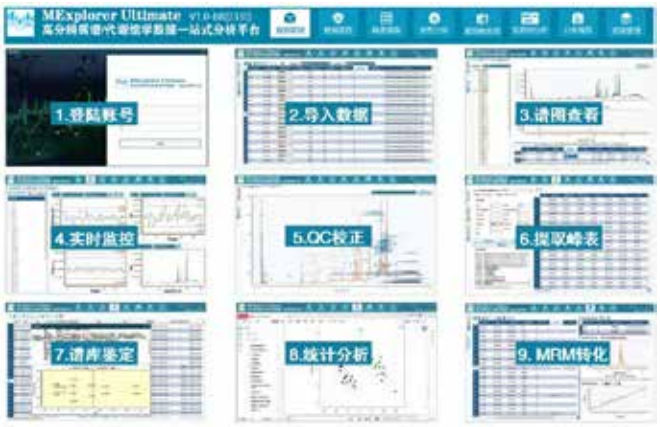

图4. MExplorer Ultimate软件各个模块界面总览

2. 峰提取与数据校正

MExplorer Ultimate软件系统可快速实现单样本中代谢物特征的识别与提取，以及多样本间质谱特征的匹配。峰提取时，只需

RUO-MKT-02-34589-ZH-A

点击简单按钮即可将wiff文件转换为质谱文件，并更进一步实现峰匹配分析；数据校正则利用QC样本结合内标校正保留时间和质谱强度等参数；样本批次间则通过对比内标和QC样本特征离子建立校正模型，对不同批次数据标准化处理，有效消除批次效应，为研究提供可靠数据支持。如图5-7所示。

图5.提交数据界面

图6. 谱图查看界面展示

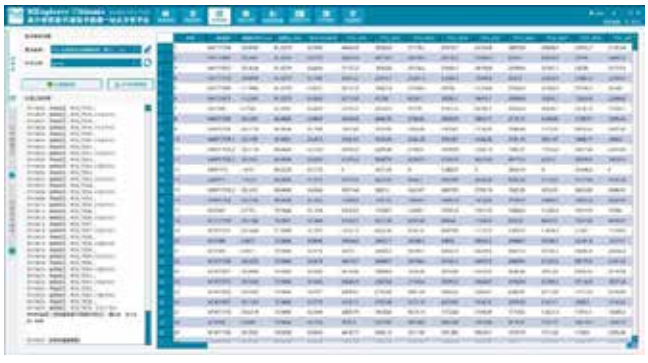

图7. 峰提取界面展示

3. 定性鉴定分析

MExplorer Ultimate软件系统开展定性鉴定分析，亮点突出。其能精准筛选二级质谱特征，提供本地库和云端全库两种定性模式，前者准确快速，后者定性数量多，满足不同需求。软件通过匹配二级质谱与峰表完成色谱峰定性，还能将未匹配的二级质谱添加到峰表并自动提取峰面积，同时利用多库对未匹配色谱峰重新定性，全面提升定性的准确性与全面性，有力推动高尿酸血症和痛风相关代谢物的研究。如图8-9所示。

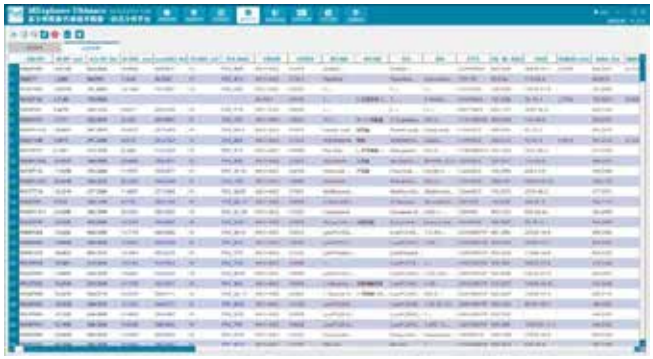

图8.定性结果展示

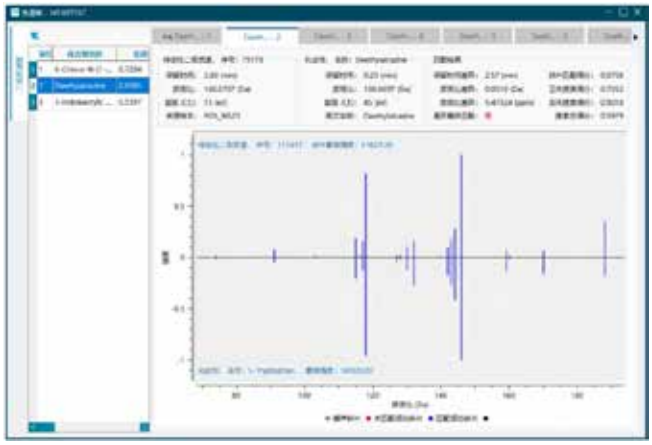

图9.定性结果谱图展示

4. 差异代谢物统计与通路分析

采用MExplorer Ultimate软件可实现快速高效的差异代谢物统计与通路分析。本案例中先按HUA vs Gout分组设置对比项，在One-MAP平台构建项目及适配算法链，执行分析后获取结果。结果显示，HUA 与 Gout组间分别有551种、428种、293种差异代谢

物，各富集于不同数量的代谢通路。软件还能验证结果，为研究发病机制、开发生物标志物和治疗靶点提供数据支撑。如图10-15所示。

图10. 正负峰表统一的操作界面

图11. 差异物发现模块展示

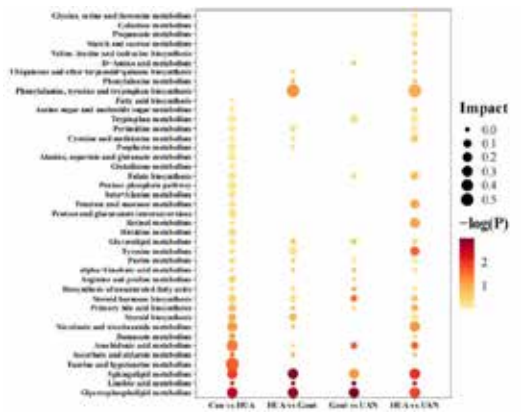

图12. 差异通路汇总展示（Con：对照；HUA：尿酸；Gout：痛风；UAN：痛风石）

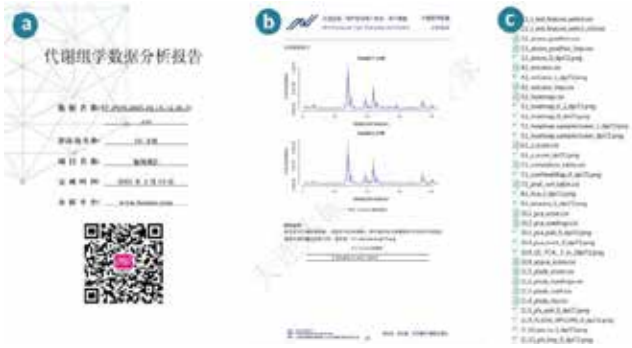

图13. 统计学结果部分展示；a.分析报告；b.报告详细内容；c.详细图表；

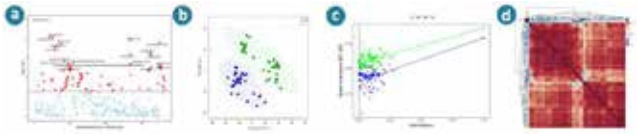

图14. 统计学分析及通路分析展示；a.t-test检验；b.plsda得分图；c.置换检验；d.热图

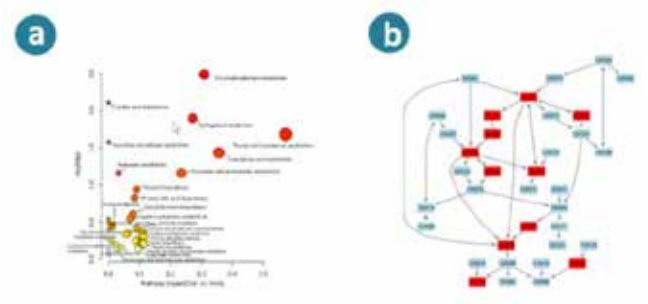

图15. a.pathway通路气泡图；b.差异通路示例

5. 拟靶向分析

借助MExplorer Ultimate软件可开展拟靶向数据分析。在探究痛风发生发展分子机制的研究中，首先采用SCIEX QTOF高分辨系统结合本软件进行非靶向数据分析，确定MRM离子对。再利用软件对SCIEX的UHPLC-HRMS与UHPLC-TQMS进行保留时间校准和TQMS参数优化。最后输出离子对表后，依特定条件分析样本，借助软件提取峰面积、筛选代谢物，再经统计分析发现患者和健康对照者的代谢差异，为疾病研究提供线索。如图16所示。

RUO-MKT-02-34589-ZH-A

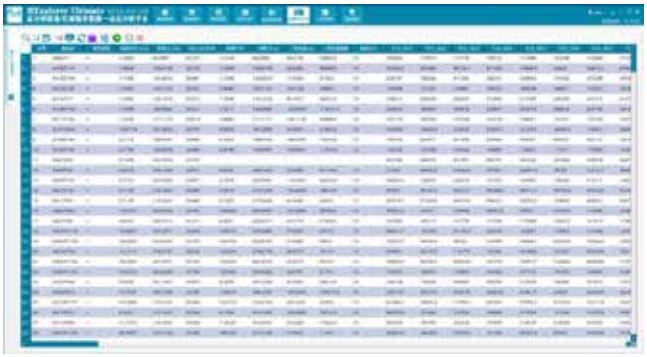

图16. 拟靶向分析界面展示

6. 报告输出

MExplorer Ultimate软件的报表输出内容丰富，涉及数据各关键环节。它记录数据基础信息，展示质量监控结果，呈现峰表提取详情、定性分析结果、差异物与通路分析成果、拟靶向分析数据，还包含分析报告汇总信息，方便用户查看和获取原始数据，了解分析全貌。如图17所示。

图17. 报告展示

总结

在痛风代谢组学研究中，研究人员收集血浆样本，借助MExplorer Ultimate软件开展系统分析。在数据管理环节，运用手动导入和动态监控功能载入原始数据，设置实验条件并完善样本信息。质量监控时，通过多维度参数设置和多指标实时监控保证数据质量。峰表提取阶段，完成文件转换、校准和曲线建立，对比样本峰面积。定性分析利用本地库和云端库，实现色谱峰精准定性。差异物发现和通路分析，设定对比项，在One-MAP平台分析，揭示关键代谢物和通路。拟靶向分析精准提取并优化离子对。最后，软件生成全面报告，为研究提供决策依据，有力推动痛风研究发展。

RUO-MKT-02-34589-ZH-A

MS-DIAL software parameters for processing untargeted metabolomics data acquired on the ZenoTOF 7600 system

Cagakan Ozbalci[1], Paul RS Baker[2], and Rebekah Sayers[1]

[1]SCIEX, UK; [2]SCIEX, USA

This technical note demonstrates the importance of parameter settings in MS-DIAL version 4.92 to process untargeted metabolomic data acquired using the ZenoTOF 7600 system. Previous technical notes[1-2] have shown the importance of instrumental settings for data acquisition and best practices for data processing using SCIEX OS software to produce the highest quality data with broad metabolome coverage. However, different software programs have different algorithms that process data with uniquely defined parameters and settings (**Figure 1**). Furthermore, parameter settings can be instrument-dependent, which requires comprehensive testing to determine the best parameter settings for a particular data set. Herein, MS-DIAL 4.92 software[3], a widely used processing tool for metabolomics and lipidomics data analysis, was used to interpret untargeted metabolomics data. Parameter settings were sequentially adjusted through iterative data processing to reveal how setting changes affect metabolomics results. Optimal MS-DIAL software parameter setting values are presented for data acquired using the ZenoTOF 7600 system.

Key features of optimizing MS-DIAL software parameters for processing metabolomics data acquired using the ZenoTof 7600 system

- MS-DIAL software rapidly processes untargeted metabolomics data acquired on the ZenoTOF 7600 system
- The high sensitivity of the ZenoTOF 7600 system enables low threshold settings within MS-DIAL software that improves the overall coverage of the metabolomics experiment
- MS-DIAL software is compatible with most metabolomic compound libraries

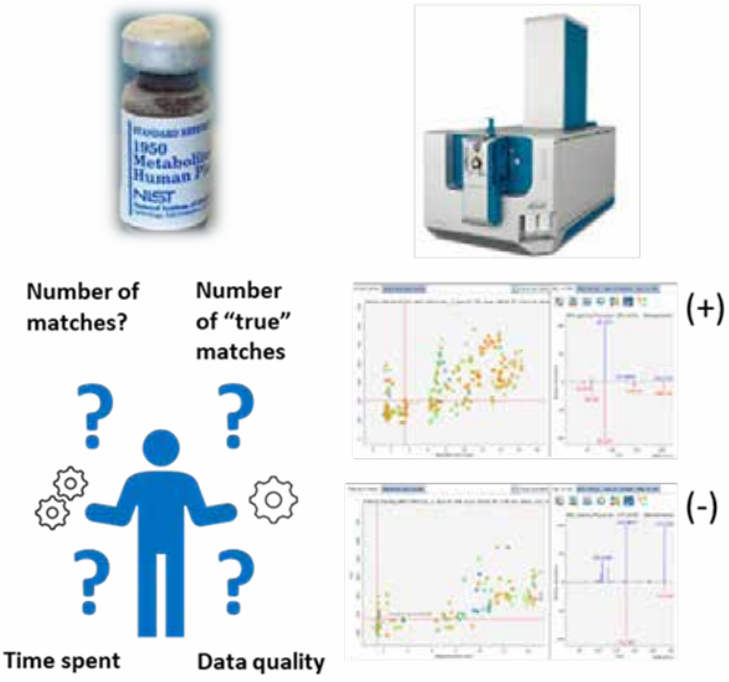

Figure 1. A major bottleneck for untargeted metabolomics workflows is time spent data processing. Understanding the software-specific parameter settings and how they should be adjusted to accommodate specific instrument data is essential to maximize coverage while maintaining high confidence in a timely manner. Herein optimal parameter settings for MS-DIAL 4.92 software are described for untargeted metabolomics data acquired on the ZenoTOF 7600 system.

MKT-30320-A

Introduction

Untargeted metabolomics aims to detect and quantify all observable small biomolecules within a sample to define the metabolic state of an organism and potentially identify biomarkers of disease[4]. High-resolution mass spectrometry (HRMS) analysis using a data-dependent acquisition (DDA) mode is the primary tool for untargeted metabolomics experiments. To increase compound detection and identification (i.e., coverage), experiments are typically run in both positive and negative ion modes. Acquired data are generally processed using software that matches MS/MS spectra to small molecule databases for compound identification.

The breadth of coverage of metabolic compounds by mass spectrometry depends on several factors. First, instrument performance and hardware parameter settings affect metabolomics data quality. Optimal parameter settings for the ZenoTOF 7600 system have been previously reported[1] that leverage the speed and sensitivity of the instrument to maximize coverage from a DDA experiment. Second, data processing parameters significantly impact the identification of metabolites. These parameters can be related to library match score, minimum intensity threshold, etc. Incorrect parameter settings may result in misidentification or missing a compound altogether. Software parameter settings for SCIEX OS software for untargeted metabolomics data acquired using the ZenoTOF 7600 system have been previously determined[2]. MS DIAL software can also process these data; however, its parameter settings are unique from SCIEX OS software. Systematic adjustment of parameter settings and data review are required to find the optimal software parameter settings.

In this technical note, untargeted metabolomics data were acquired from NIST SRM plasma samples using the ZenoTOF 7600 system. Data were processed by MS DIAL 4.92 software using iterative permutations of different parameter settings for *minimum threshold, mass slice width,* and *identification cut-off* tabs in the processing workflow. From these processed data, optimal software processing parameters were identified and are reported herein.

Methods

Sample preparation: NIST SRM 1950 samples were extracted by a one-phase liquid extraction. Four volumes of ice-cold ethanol were added to 1 sample volume and vortexed for 30 seconds. Extraction mixtures were centrifuged to separate the precipitated protein debris, and the supernatant was used directly for metabolomics analysis. The supernatant can be stored at -20 °C for future analysis.

Chromatography: Extracted metabolites were resolved using an Exion UHPLC instrument equipped with a Kinetex F5 column (2.1 × 150 mm, 2.6 µm; Phenomenex). The column oven temperature was 40°C with a constant flow rate of 0.2 mL/min. Gradient details are shown in **Table 1.**

Table 1: Chromatographic gradient (flow rate = 0.20 mL/min)

Time (min)	Mobile phase A (%)	Mobile Phase B (%)
0.0	100	0
2.1	100	0
14	5	95
16	5	95
16.1	0	0
20	0	0

Mass spectrometry: Extracted samples were analyzed using a ZenoTOF 7600 system with an OptiFlow Turbo V ion source. A top-40 DDA method with dynamic background subtraction (DBS) and exclusion for 6 s after 3 occurrences was employed for both positive and negative ion modes. Electrospray ionization voltages were set to 5500 V and -4500 V for positive and negative ion modes, respectively. The collision energy (CE) was set to 30 V for positive and -25 V for negative ion mode, and the accumulation time was set to 5ms. The automated calibrant delivery system (CDS) performed automated calibration every 9 samples. A summary of the MS instrument parameters is presented in **Table 2**.

Table 2: ZenoTOF 7600 system source and gas parameters

Parameter	Setting (Pos)	Setting (Neg)
Curtain gas (CUR)	35	35
Ion source gas 1 (GS1)	50	50
Ion source gas 2 (GS2)	70	70
CAD Gas (CAD)	7	7
Source temperature (TEM)	500 °C	500 °C
Ion spray voltage (IS)	5500 V	-4500 V
TOF MS mass range	60-1000 Da	60-1000 Da
Declustering Potential (DP)	40	-40
Time bins to sum	6	6
Accumulation time	5 ms	5 ms
IDA max candidate ions	40	40
Dynamic background subtraction (DBS)	Yes	Yes
Collision energy (CE)	30	-25
Zeno pulsing	Yes	Yes
Zeno threshold	20000	20000

Data processing: All data were processed using MS-DIAL 4.92 open-source software. For identification, two different libraries (*ExpBioInsilico_NEG_VS17.msp* and *ExpBioInsilico_Pos_VS17.msp*) were employed. These libraries can be downloaded from (http://prime.psc.riken.jp/compms/msdial/main.html) and can easily be selected in the "Identification" tab of the software.

MKT-30320-A

Project creation and analysis of parameter settings

Project creation

Initial "new project" creation is illustrated in **Figure 2**. Selecting the project file path where the raw files are stored is critical. WIFF and WIFF2 files can be submitted to MS-DIAL without conversion. Click "Soft ionization," "Chromatography," and "Conventional LC/MS or dependent MS/MS" for the first three tabs. Other noteworthy options to consider are "Data type" (MS1 and MS2). Choose "Centroid data" for both sections. Lastly, select "Metabolomics" for the target omics and "negative" or "positive" for the ion mode.

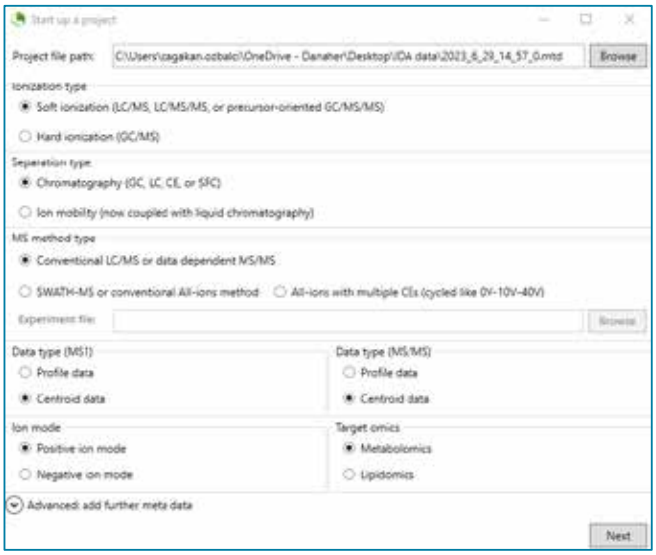

Figure 2. New project creation page

Analysis parameter settings

Data collection tab:

In this section, MS-DIAL software parameter settings critically affect coverage and the time needed to process the data files. Significantly, these settings also affect the number of false positive results. In the "Mass accuracy" settings, the default values are recommended. Next, click the "advanced" button, as shown in **Figure 3**. To limit the data processing mass range and potentially reduce the time required for processing, enter the appropriate MS1 and MS2 mass ranges. It is also recommended to define when retention time starts and ends to remove unnecessary data points, such as the washing step, from the analysis. The other settings can be kept as default values. If a powerful workstation computer is used, the "Number of threads" setting can be set to more than 2.

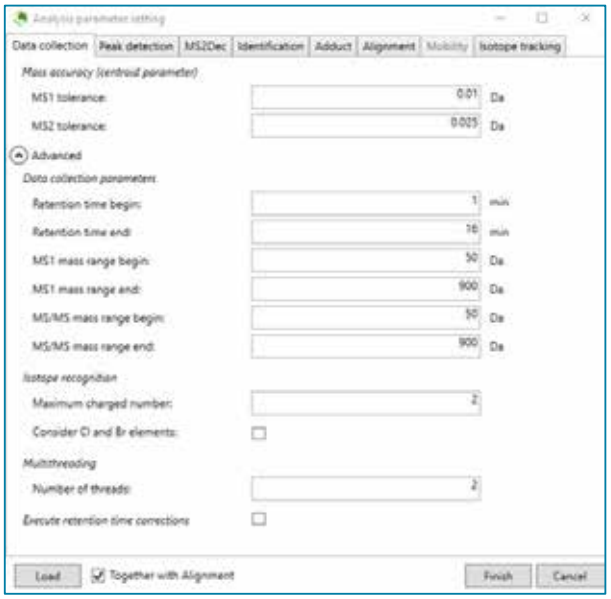

Figure 3. Data collection tab with advanced settings

Peak detection tab:

Under the "Peak detection" tab, there are two parameters to be adjusted for optimal peak detection: "Minimum peak height" and "Mass slice width" (**Figure 4**). One of the goals of this technical note was to investigate how varying these parameters affects the data quality and the overall processing time. For "minimum peak height," 50, 250, 500, and 1000 amplitude were sequentially selected, and the mass slice was set to 0.05 or 0.1 Da. If the smoothing method needs to be changed, click Advanced in this section for detailed smoothing settings.

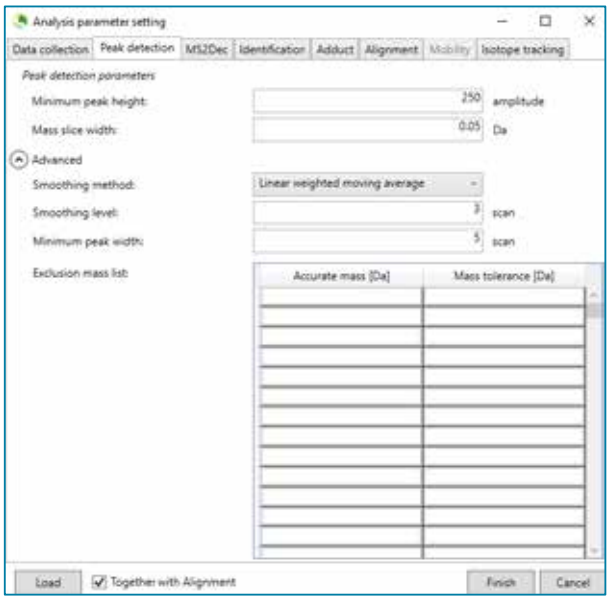

Figure 4. Peak detection settings tab with smoothing method details

Identification tab:

In the identification section, an MSP file, which can be downloaded from MS-DIAL's website, should be selected, and the identification cut-off value should be set. The default value for this parameter is 80%, but in this study, values of 70% and 60% were also used to observe the effect on the final results. The remaining parameter settings can be set as shown in Figure 5. If a custom library is to be used, click on the advanced button and select the library. (The library should be stored as a *.txt file.)

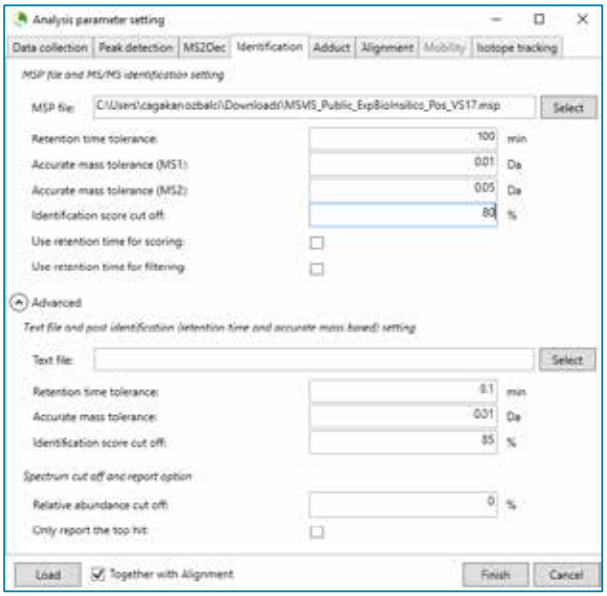

Figure 5. Identification tab

Adducts tab:

Metabolite adducts can vary depending on the modifiers added to solvents. For example, in the positive ion mode, a compound can appear as a protonated ion or as a sodium, potassium, or ammonium adduct. The recommended adducts to be selected in both positive and negative ion modes are presented in **Figure 6**.

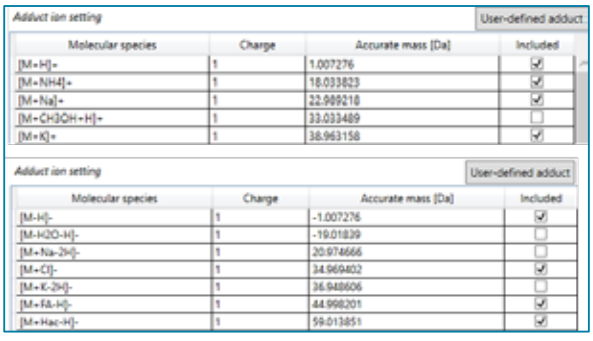

Figure 6. Adduct ion setting tab

Alignment tab:

This is the final section to be completed before processing a sample or a sample batch (**Figure 7**). A reference sample file should be chosen from a pooled QC sample or from the sample with the highest metabolite concentration. The remaining parameters (and those under the Advanced tab) were set to the default values since they are compatible with the ZenoTOF 7600 system data acquisition. Once all parameters have been set, click "Finish" and wait until the results screen appears.

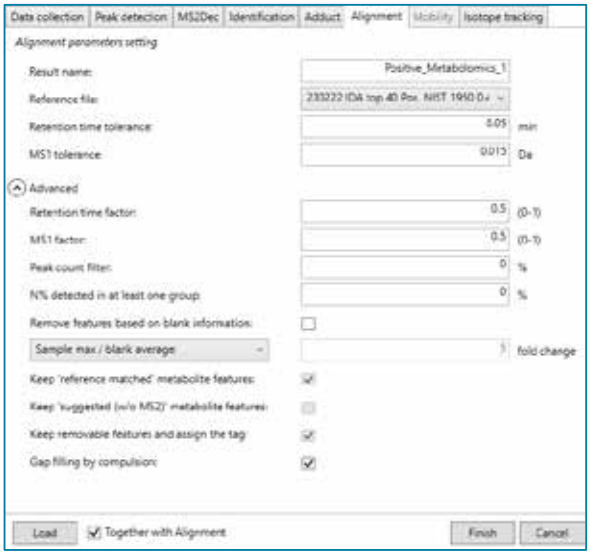

Figure 7. Alignment tab

Results and discussion

Metabolites extracted from NIST SRM 1950 plasma samples were analyzed in positive and negative ion modes, with two different injection volumes for each polarity. For the positive ion mode, 0.4 µL and 2 µL of the extract were analyzed, whereas 1 µL and 5 µL were injected in the negative ion mode. **Tables 3 and 4** show how adjusting the different parameter settings affects the numbers of identified metabolites in the positive and negative ion modes. Only the higher volume injection results are displayed in these tables. For both polarities, the higher injection volume resulted in approximately 1.4 more annotated metabolites than the lower volume injections (data not shown).

Table 3. Coverage, time for analysis, and confidence under different parameter settings in the positive ion mode.

Polarity	Volume	Min Threshold	Mass slice widh	Identification cut off	Number of hits	Time for analysis
Positive	2 µL	50	0.1	60%	573	Very long
Positive	2 µL	50	0.05	60%	651	Very long
Positive	2 µL	250	0.1	60%	505	Long
Positive	2 µL	250	0.05	60%	556	Long
Positive	2 µL	500	0.1	60%	432	Normal
Positive	2 µL	500	0.05	60%	470	Normal
Positive	2 µL	1000	0.1	60%	342	Short
Positive	2 µL	1000	0.05	60%	367	Short
Positive	2 µL	50	0.1	70%	257	Very long
Positive	2 µL	50	0.05	70%	276	Very long
Positive	2 µL	250	0.1	70%	237	Long
Positive	2 µL	250	0.05	70%	258	Long
Positive	2 µL	500	0.1	70%	213	Normal
Positive	2 µL	500	0.05	70%	224	Normal
Positive	2 µL	1000	0.05	70%	176	Short
Positive	2 µL	1000	0.1	70%	173	Short
Positive	2 µL	50	0.1	80%	135	Very long
Positive	2 µL	50	0.05	80%	141	Very long
Positive	2 µL	250	0.1	80%	129	Long
Positive	2 µL	250	0.05	80%	134	Long
Positive	2 µL	500	0.1	80%	119	Normal
Positive	2 µL	500	0.05	80%	119	Normal
Positive	2 µL	1000	0.1	80%	100	Short
Positive	2 µL	1000	0.05	80%	100	Short

Each row in **Tables 3 and 4** is color-coded according to their identification confidence. Dark orange and light orange coded rows denote high confidence, while blue coded rows denote lower confidence and may contain more false positive results. Grey-coded rows represent little increase in the number of hits but indicate significantly increased analysis time. For context, the time for analysis of a single sample is presented in **Table 5**. Changes in the "Min Threshold" parameter can dramatically affect the analysis time but have less affect the number of hits. The identification cut-off percentage has a significant impact on the number of hits. And the "mass slice width" affects the number of hits only for data with low confidence.

Table 5. Typical times for analysis of 1 sample at different threshold values

Threshold	Analysis time (min)	Descriptor
50	12	Very long
250	1.7	Long
500	1.4	Normal
1000	1.2	Short

Table 4. Coverage, time for analysis, and confidence under different parameter settings in the negative ion mode

Polarity	Volume	Min Threshold	Mass slice widh	Identification cut off	Number of hits	Time for analysis
Negative	5 µL	50	0.05	60%	343	Very long
Negative	5 µL	50	0.1	60%	307	Very long
Negative	5 µL	250	0.05	60%	295	Long
Negative	5 µL	250	0.1	60%	273	Long
Negative	5 µL	500	0.05	60%	239	Normal
Negative	5 µL	500	0.1	60%	231	Normal
Negative	5 µL	1000	0.05	60%	177	Short
Negative	5 µL	1000	0.1	60%	172	Short
Negative	5 µL	50	0.05	70%	217	Very long
Negative	5 µL	50	0.1	70%	198	Very long
Negative	5 µL	250	0.05	70%	202	Long
Negative	5 µL	250	0.1	70%	189	Long
Negative	5 µL	500	0.05	70%	174	Normal
Negative	5 µL	500	0.1	70%	168	Normal
Negative	5 µL	1000	0.05	70%	134	Short
Negative	5 µL	1000	0.1	70%	132	Short
Negative	5 µL	50	0.05	80%	95	Very long
Negative	5 µL	50	0.1	80%	94	Very long
Negative	5 µL	250	0.05	80%	91	Long
Negative	5 µL	250	0.1	80%	91	Long
Negative	5 µL	500	0.05	80%	87	Normal
Negative	5 µL	500	0.1	80%	87	Normal
Negative	5 µL	1000	0.05	80%	76	Short
Negative	5 µL	1000	0.1	80%	75	Short

As shown in **Tables 3 and 4**, a balance must be struck between the analysis time, coverage, and confidence. In the positive ion mode, a minimum threshold of >50 and <250 appears to give the best coverage. Due to the high sensitivity and the high signal-to-noise ratio of the data acquired on the ZenoTOF 7600 system, a value of 250 cps was chosen to give the best coverage using an "identification cutoff" value of 70%. As seen in the tables, however, small changes can significantly affect the overall data, so it is recommended that

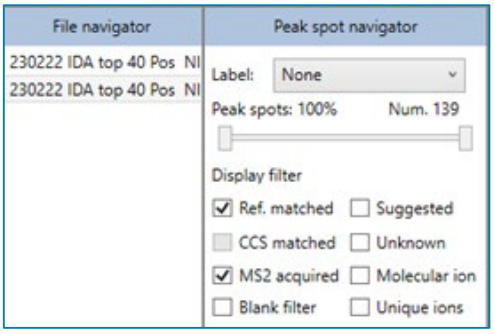

Figure 8. Peak spot navigator. MS2 acquired and Ref. matched are selected to filter the metabolites with the most confident annotation.

MKT-30320-A

these software processing parameters be a starting point from which adjustments can be made to generate the best data for a given data set. For example, for data processed from a large cohort study. In that case, increasing the "minimum threshold" to 500-1000 cps may be reasonable to decrease the time needed for analysis. As expected, the data also indicate that a higher sample load (i.e., higher analyte concentration) generates higher-quality data.

The confidence level in the processed data can be adjusted in the "Peak spot navigator." Clicking on the "Ref. matched" display option will only show compounds with a matching MS/MS reference spectrum in the compound library (**Figure 8)**.

Although MS-DIAL's MS/MS fragment library algorithm matches acquired data with a high degree of confidence, it is recommended to manually validate the metabolite annotations from the right bottom panel (Identification) and change the annotation, if necessary, as shown in **Figure 9.**

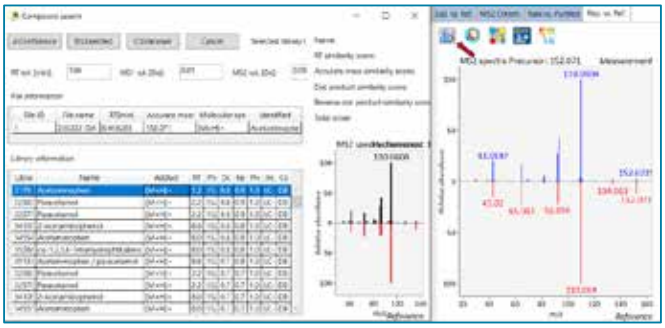

Figure 9. Identification panel. Annotated metabolites can be reviewed from this panel. If the annotation is not correct, it can be easily changed using the MS/MS look-up button (red arrow)

Conclusions

- The speed and sensitivity of the ZenoTOF 7600 system enable the generation of reproducible and high-quality data for untargeted metabolomic analysis
- In MS-DIAL 4.92 software, the "Minimum threshold" value of 250 cps and the "Identification cut off" value of 70% are good initial settings for untargeted metabolomics data acquired on the ZenoTOF 7600 system
- For extensive cohort studies, or in situations where it is necessary to minimize the overall analysis time, the "Minimum threshold" parameter setting value can be increased up to 1000 cps
- The number of analytes identified in a sample is proportional to the concentration of the sample; higher sample volume and concentration are recommended

References

1. Baker, PRS and Proos R. Untargeted data-dependent acquisition (DDA) metabolomics analysis using the ZenoTOF 7600 system. SCIEX technical note, RUO MKT-02-15367-A
2. Sayers R, Proos R, and PRS Baker. Analysis of untargeted metabolomics data from an untargeted Zeno data-dependent acquisition (DDA) workflow using SCIEX OS software. SCIEX technical note, RUO-MKT-02-15619-A
3. Tsugawa H, Cajka T, Kind T, Ma Y, Higgins B, Ikeda K, Kanazawa M, VanderGheynst J, Fiehn O, Arita M. Nat Methods. 2015; 12(6):523-6. Doi: 10.1038/nmeth.3393
4. Alseekh, S et al. Mass spectrometry-based metabolomics: a guide for annotation, quantification and best reporting practices. Nat Methods. 2021; 18(7):747-756. Doi 10.1038/s41592-021-01197-1

MKT-30320-A

全球天然产物社会分子网络系统（GNPS）结合SCIEX高分辨质谱系统进行天然产物研究

Global Natural Products Social Molecular Networking system (GNPS) is combined with SCIEX High Resolution Mass Spectrometry system to study natural products

谢亚平，司丹丹，龙志敏
Yaping Xie, Dandan Si, Zhimin Long
SCIEX 应用支持中心，中国

Key words: Global Natural Products Social Molecular Networking system, SCIEX High Resolution Mass Spectrometry system, Natural Products

引言

全球天然产物分子网络系统（Global Natural Products Social Molecular Networking，简称GNPS）是近年发展起来的天然产物可视化鉴定技术，结构类似的天然产物，在相同的质谱裂解条件下，会产生相似的特征碎片离子，通过计算机计算这些碎片离子的相似度，按相似度大小，合成一张可视化的网络图谱，其中每一个节点表示一个化合物的MS/MS 质谱图，结构类似的化合物分子会在一个分子网络中聚集成簇。目前，分子网络技术作为研究工具广泛在天然产物领域使用。应用的主要方向包括中药化学成分定性表征、药物代谢方面的研究、化学成分定量表征及质量控制、活性成分的分离与制备、培养方法和提取工艺的优化、疾病诊断和个性化治疗等方向。GNPS数据库主要来源包括第三方数据库MassBank、HMDB、ReSpect、NIST（2014）等，Dorrestein实验室和Sirenas MD单位采集的化合物和谱图，全球多个科研群体提供的化合物和谱图等。GNPS质谱数据库不仅具有鉴定已知化合物（dereplication）、类似物（variable dereplication）和自动分析MN（Molecular Networking）中化合物的功能，还具有对多来源的MS/MS数据进行存储管理及更新数据的功能等。

本文本研究采用分子网络技术，将SCIEX高分辨质谱系统采集样品数据上传至GNPS，构建忍冬四个不同部位（S1-S4）化合物的的分子网络关系，可获得四个部位最终成分鉴定结果、结构类似物分子网络关系以及不同化合物成分在四个部位中的分布规律，为忍冬中不同部位的有效成分的研究提供依据。

技术特点

1. SCIEX高分辨质谱系统超快的扫描速度（最高133HZ或100HZ）保证采集到天然产物中更多的MS和MS/MS质谱信息，保证数据采集的全面性
2. SCIEX高分辨质谱系统独有的IDA+DBS采集模式，保证采集到更高质量的MS/MS质谱信息，保证数据采集的有效性
3. GNPS分子网络分析主要依赖高质量的MS/MS进行峰对齐及相似度分析，结合SCIEX高分辨质谱更全面有效的MS/MS信息，可获得更可靠全面的分析结果

仪器设备

SCIEX ExionLC™ AD系统和SCIEX 高分辨质谱系统

图1. ExionLC™ AD系统和SCIEX 高分辨质谱系统

MKT-30320-A

液相条件

液相系统：SCIEX ExionLC™ AD系统

色谱柱：Phenomenex Kinetex C18(100 × 2.1mm, 2.6 μm)

流动相：A: 水 (含0.025%甲酸)
B: 甲醇:乙腈 =1:1（含0.025%甲酸）

流速：0.3 mL/min

柱温：40 ℃

液相梯度：

时间(min)	A(%)	B(%)
0	98	2
2	98	2
20	40	60
22	5	95
25	5	95
25.1	98	2
30	98	2

质谱条件

扫描模式：ESI+/- TOF MS-IDA-15TOF MS/MS

扫描范围：一级m/z 60-1300 二级m/z 40-1300

CDS自动校正

动态背景扣除（DBS）开启

离子源参数：

喷雾电压: 5500V/-4500 V　　气帘气 CUR: 35 psi

雾化气 GS1: 55 psi　　雾化气 GS2: 55 psi

源温度：550 ℃　　DP电压：±60 V

碰撞能量：±40 ± 20

实验流程

SCIEX高分辨质谱系统IDA+DBS采集模式获得的高质量数据上传至GNPS网站，在IDA+DBS采集模式下可获得大量的高质量MS/MS质谱信息，GNPS通过计算机算法计算这些MS/MS质谱数据的相似度，然后根据相似度的大小将这些质谱图整合成一张可视化的网络图谱，如图2所示。

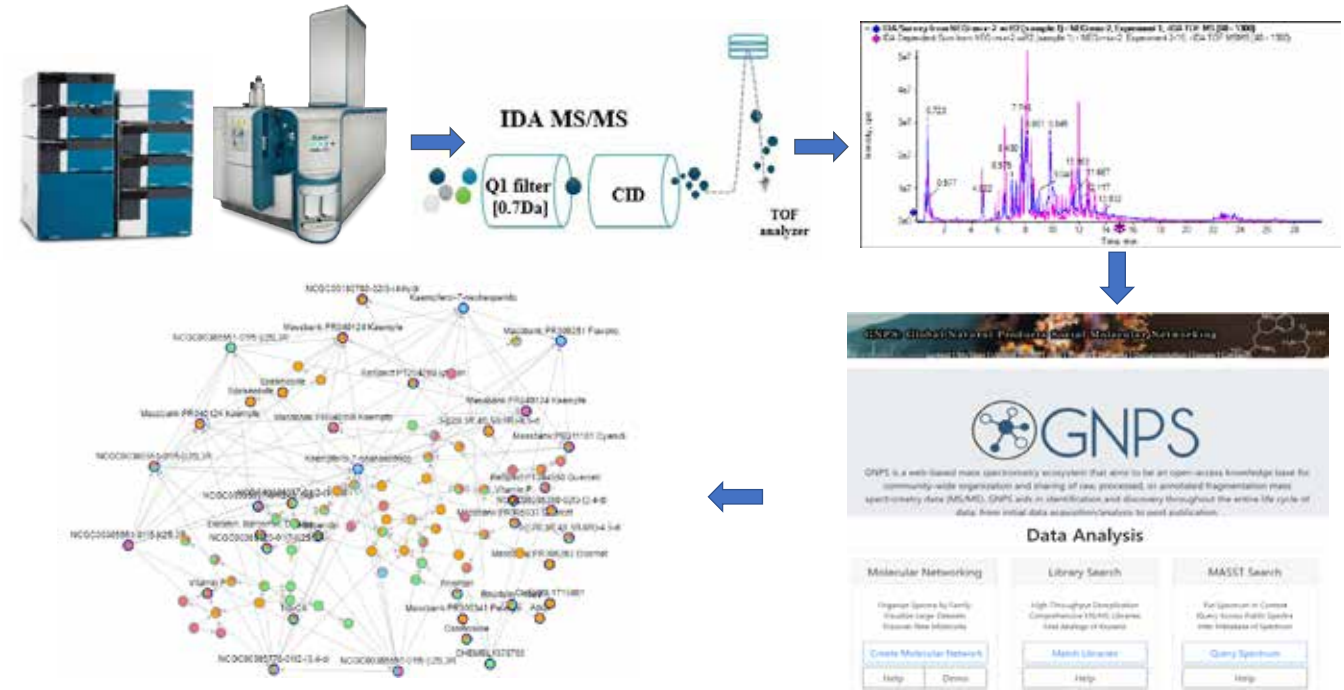

图2. 实验流程

RUO-MKT-02-14562-ZH-A

实验结果

1. 天然产物成分鉴定结果

上传数据至GNPS网站进行数据处理之后可获得天然产物成分鉴定结果表，如图3所示

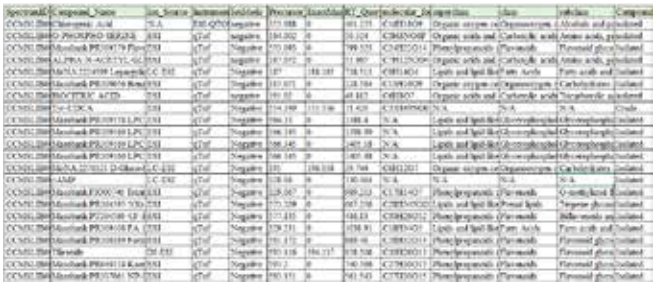

图3. GNPS谱库鉴定结果

2. 天然产物中结构类似物分析结果

上传数据至GNPS网站进行分子网络数据处理之后可获得可视化分子网络图，如图4所示。其中可以看到蓝色标记区域内为化合物m/z 447.096及其结构类似物，与m/z 447.096结构类似的化合物包括m/z 593.151、m/z 579.135、m/z 493.099、m/z 531.148、m/z 483.837，MS/MS结构相似度采用余弦值表示，五个化合物与化合物m/z 447.096的相似度分别为0.92、0.90、0.90、0.86、0.88（如图中蓝色字体标注余弦值）。其中m/z 447.096 GNPS谱库匹配结果为木犀草苷（luteolin-7-O-glucoside），m/z 593.151 GNPS谱库匹配结果为山柰酚-3-O-芸香糖苷（Kaempferol-3-o-rutinoside），以这两种化合物为例展示其MS/MS及结构相似性，可见两者具有多个相同的主要碎片离子（图中黄色区域标记）并且具有相似化合物结构，图5所示。

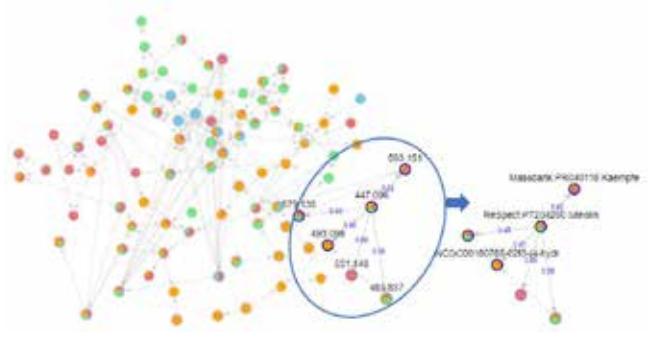

图4. GNPS结构类似物分析结果

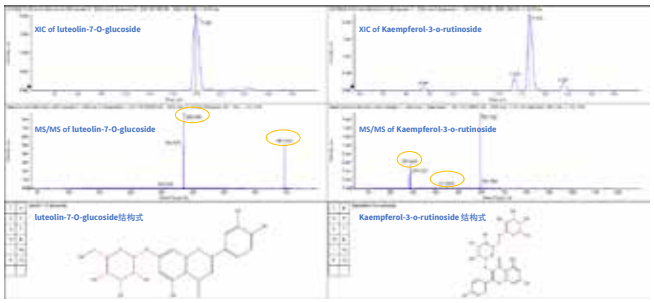

图5. luteolin-7-O-glucoside和Kaempferol-3-o-rutinoside 相似性对比

3. 天然产物成分差异分析

上传数据至GNPS网站进行分子网络数据处理之后可获得可视化分子网络图，如图6所示。其中可以看到蓝色标注区域为绿原酸（Chlorogenic acid）及其结构类似物分子网络图，在该区域可以看到，每种成分（即每个节点）均含有一种甚至几种不同颜色，例如绿原酸（Chlorogenic acid）含有红蓝绿黄四种不同颜色，这四种颜色分别代表不同部位忍冬样品S1-S4，因此我们可以快速直观看到忍冬S1-S4四个不同部位均含有中药成分绿原酸（Chlorogenic acid）。每个节点的不同颜色以饼状图显示，其中所占饼图的比例越大代表该成分在样品中含量越高，因此可以直观看到绿原酸（Chlorogenic acid）在S1（红色）样品中含量最高，在S2（蓝色）样品中含量最低。通过可视化的分子网络图可以快速发现不同样品之间的成分差异，与目前应用较多的 PCA、PLS-DA、OPLS-DA 等方法相比，分子网络技术具有数据分析能力强、可视化程度高、数据兼容性强、结果准确可靠等优势。

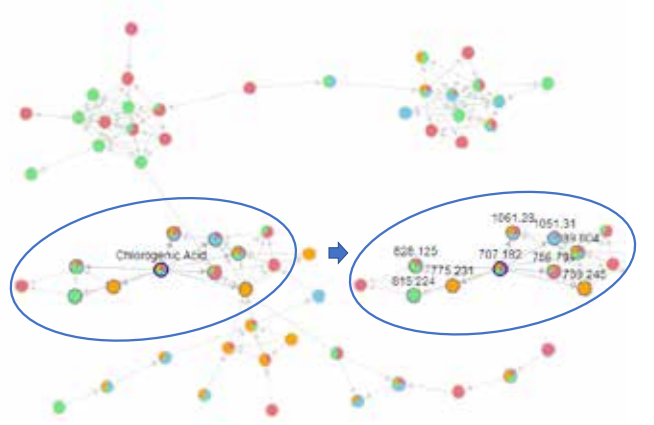

图6. 绿原酸在不同样品中（S1-S4）含量分布差异（其中红蓝绿黄四种颜色分别代表S1-S4）

RUO-MKT-02-14562-ZH-A

总结

本文使用SCIEX 高分辨质谱系统获得高质量的MS及MS/MS信息，SCIEX高分辨质谱系统在超快的扫描速度下保证了数据的高灵敏度，全面性和有效性。GNPS利用SCIEX高质量的MS/MS数据可快速进行天然产物的鉴定、结构类似物分析以及差异成分分析，为天然产物的研究提供了更加快速便捷可视化的分析方法，可很好地应用于天然产物的多方向研究分析。

RUO-MKT-02-14562-ZH-A

Zeno MS/MS技术在大鼠尿液靶向代谢组学研究中的应用

利用SCIEX ZenoTOF™ 7600系统分析

Targeted metabolomics in rat urine using Zeno MS/MS

Kranthi Chebrolu[1], Jason Causon[2], Robert Di Lorenzo[2], Christie Hunter[1]

[1] SCIEX，美国；[2] SCIEX，加拿大

通常，学术实验室和临床试验的研究人员只能得到非常少量的样本，并且需要从体积有限的样本中获得最多的信息。这一要求推动了对高灵敏度和高特异性的靶向分析方法的需求，以便在复杂的生物样品中获得高质量的定量的结果，并根据结果提出生物学见解。高分辨率高质量精度质谱系统（HRMS）由于其高特异性和高质量的二级全扫描能力，在非靶向代谢组学和复杂基质中的化合物鉴定方面具有良好的应用前景。然而，HRMS仪器由于灵敏度相对较低，通常不是对目标分析物进行精确定量的首选。此外，一些高分辨系统无法在快速分析所需的高扫描速度下保持高分辨率。

随着SCIEX ZenoTOF™ 7600系统的发布，科学家们现在可以在高扫描速度速下获得高质量精度的定量结果。ZenoTOF 7600系统的核心创新是Zeno™ trap（Zeno阱），激活Zeno trap后，由于优化了从碰撞池到加速器的离子传输，占空比得到了显著改善[1]。这

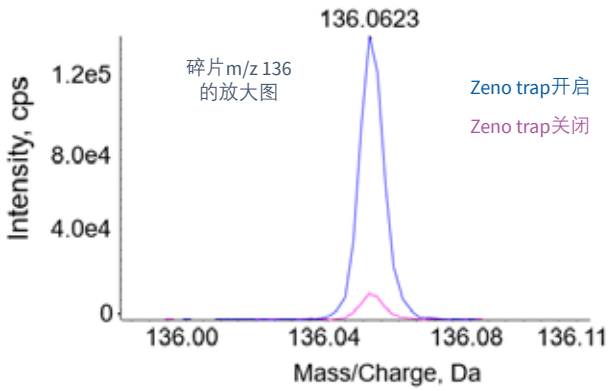

图 1. MS/MS 灵敏度显著提高。在Zeno trap开启（蓝色）和Zeno™ trap关闭（粉色）情况下，cAMP二级碎片的提取离子流图（XIC）对比。当Zeno™ trap开启时，信噪比提高了约12.5倍。这是经稀释的尿液进样2 µl的结果。

种占空比的改善大大提高了MS/MS灵敏度，从而使靶向高分辨率工作流程成为现实。本实验创建了一个小的靶向分析方法，用于糖尿病大鼠模型尿液中代谢物的检测，从而展示MRM^{HR}工作流程和Zeno MS/MS对定量结果质量的影响。

尿液样本来自Zucker糖尿病大鼠模型，并建立了13种代谢物的靶向分析方法。比较了Zeno trap开启和关闭两种方法之间的灵敏度，Zeno trap开启时MS/MS信号明显增加（例如：图1中的环磷酸腺苷（cAMP）碎片响应增加了约12倍）。本文介绍了此实验从数据采集到结果统计分析的完整工作流程。

ZenoTOF™ 7600系统用于靶向代谢组学的主要特点

- Zeno trap通过提高占空比到≥ 90 % [1]，可在高采集速度（高达133 Hz）的同时，显著提高MS/MS 灵敏度
- 在代谢物的高灵敏度定量实验中，激活Zeno trap后，MS/MS 提取离子流图（XIC）峰面积增加约13倍

RUO-MKT-02-13297-ZH-B

- QTOF 系统的灵活性，可扩展适用于其他工作流程
  - SWATH®采集技术、数据依赖采集、电子活化解离（EAD）
- SCIEX OS软件中强大的数据处理工具，用于精确定量，随后使用MarkerView™软件进行多元统计分析

方法

样品制备：从四个不同的大鼠组收集尿液样品：Zucker 糖尿病脂肪（ZDF）大鼠，雄性和雌性； Sprague Dawley（SD）大鼠，雄性和雌性。每组5只大鼠。取 20 µL 尿液用流动相 A 稀释 10 倍，用于 LC-MS/MS 分析。

色谱条件：使用配备 Phenomenex Luna Omega Polar C18, 3 µm 150 × 2.1 mm（00F-4760-AN）色谱柱的 ExionLC AD HPLC 液相系统 (SCIEX) 进行样品分离。从 0 到 95% B 的简单线性洗脱梯度结合标准的反相洗脱流动相（A = 0.1% 甲酸水溶液和 B = 0.1% 甲酸乙腈溶液），流速为 300 µL/min。进样体积为 0.2 或 2 µL，整个分析过程中柱温保持在 40 ℃。总运行时间为 13.1 分钟，包括 2 分钟的平衡时间。

质谱条件：在 SCIEX ZenoTOF™ 7600 系统上，使用 SCIEX OS 软件，以 ESI 正模式采集 MRM^{HR}数据。离子源条件如下：CUR35、GS1 55、GS2 55、ISVF 5500、TEM 600 ℃。每个代谢物的高分辨率 MS/MS的采集累积时间为10 ms。碰撞能量（CE）均为30。分别建立Zeno™ trap开启和关闭的方法，以便进行灵敏度比较。每个方法的每个样品重复采集三次。

数据处理：在SCIEX OS软件中进行MS/MS峰识别、积分和定量分析，然后将结果导入MarkerView™软件进行多元统计分析（图2）。为了建立MRM^{HR}数据的处理方法，首先要在Explorer模块中对MS/MS质谱图进行分析，以选择适合的碎片离子。选择的结果也与安装了SCIEX高分辨代谢物库（AMMSL 2.0）的LibraryView™软件中的谱图进行了比较。从ChemSpider获得的结构信息也被用来确认碎片的一致性，并从中获得感兴趣碎片的理论m/z。在Explorer模块（图3）中获得的这些碎片的精确质量信息被用于在SCIEX OS软件的Analytics模块中构建最终的处理方法。然后将碎片离子的峰面积导入MarkerView™软件进行统计分析。

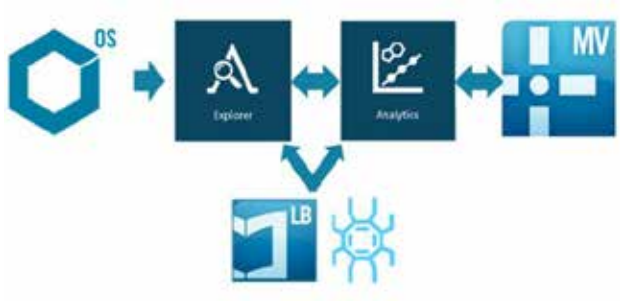

图2.工作流程图。数据采集和处理均使用SCIEX OS软件。MS/MS使用Explorer和Analytics模块进行分析，谱库搜索使用library View™软件和ChemSpider功能进行。

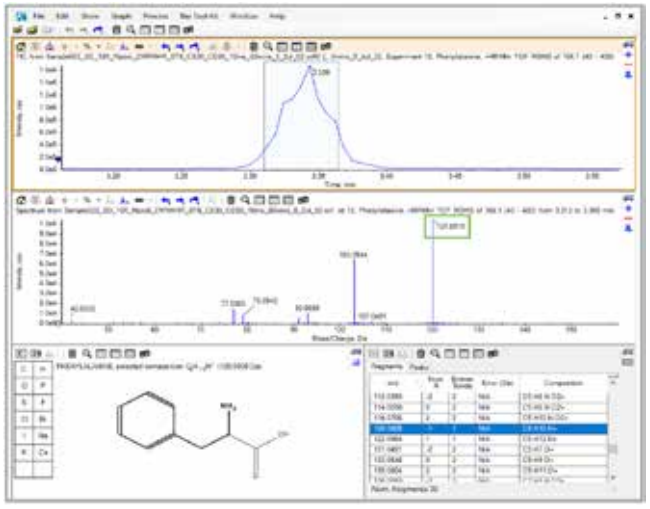

图3.SCIEX OS软件中用于代谢物鉴定的Explorer模块。顶部栏显示苯丙氨酸的提取离子色谱图（XIC），而中间栏显示可用于从LibraryView™软件中选择感兴趣碎片的实际高分辨MS/MS谱图。底部栏显示了从ChemSpider获得的结构，该结构提供了拟合的（理论）碎片和精确的质量信息，后者随后用于质量误差的计算。

用于靶向定量的 Zeno MRM^{HR}工作流程

Zeno trap激活后，可显著增加 ZenoTOF™ 7600 系统上的 MS/MS 信号，同时在不牺牲分辨率的情况下保持非常高的采集速度。利用尿液中 13 种代谢物的靶向 MRM^{HR}分析结果，对 Zeno trap激活造成的灵敏度增加进行了研究。对打开和关闭 Zeno trap情况下采集到的提取离子色谱图（XIC）进行了比较，以计算灵敏度的增益。如图 1 所示，cAMP 产生的主要碎片离子为 m/z 136.0618，观察到信号增益超过 10 倍。

RUO-MKT-02-13297-ZH-B

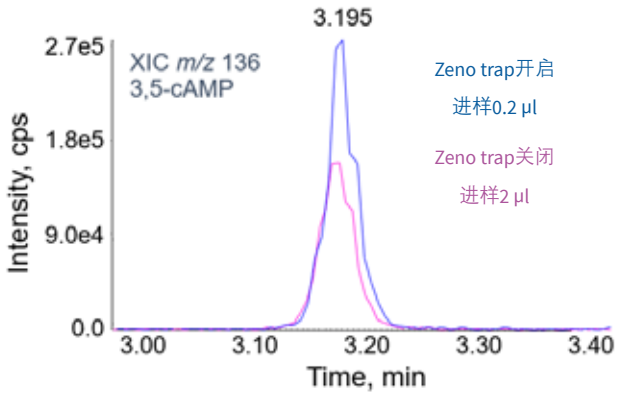

图4. 样本量减少10倍的情况下，获得了更好的MS/MS灵敏度。图为开启Zeno trap（进样0.2 µL，蓝色）和关闭 Zeno trap（进样2 µL，粉红色）获得的XIC图的对比结果。当开启Zeno trap时，信噪比提高了约1.5倍。MS/MS采集速率非常快（累计时间为10 ms），在整个色谱峰上提供了15个数据点。

为了解决样品量有限的问题，我们对开启 Zeno trap进样0.2 µL和关闭 Zeno trap进样2 µL，两种方式进行了对比实验（图 4）。即使柱上进样量低了 10 倍，使用 Zeno trap的 m/z 136.0618 碎片质量的 XIC 峰面积也比不用Zeno trap时高出约 1.5 倍。复杂基质样品使用更高的稀释倍数或更低的柱上的进样量，基质效应会降低，因而可提高数据质量。此外，对于一些非常珍贵的样品，对更低样品量的检测能力对研究人员来说可能是一个优势。

本研究对所分析的13种代谢物分别进行Zeno trap关闭和开启的效果比较，结果汇总见表1。如表1所示，数据质量（如碎片质量误差、谱库匹配结果和峰面积）在开启Zeno trap时都变得更好。本研究分析的13种化合物中，有12种化合物碎片离子的质量误差小于3 ppm。平均而言，与关闭Zeno trap相比，开启Zeno trap时获得的MS/MS峰面积提高了14倍。值得注意的是，在此过程中仪器保持非常高的MS/MS采集速率（每个MS/MS累计时间为10 ms）。

MarkerView™软件用于统计分析

本实验利用一个小样本集来检验从定量到统计分析的工作流程（图 5，表 2）[3,4]。请注意，这些代谢物是根据之前对同一样本集的 SWATH®采集结果选择的[2]。这些感兴趣的代谢物被选中并用于上述靶向检测研究中。在 MarkerView™ 软件 (MV) 中用无监督主成分分析 (PCA) 生成二维评分图。四种类型的小鼠模型，ZDF-雄性和雌性、SD-雄性和雌性分别聚类，且明显互相分开，他们之间97% 的差异来自PC1 和 PC2（图 5，顶部）。

表1. Zeno trap的使用，使MS/MS质谱图质量提高。Zeno trap的激活使MS/MS信号显著增加，因而碎片离子XIC图峰面积也显著增加（平均增加13.6倍）。得到的Zeno MS/MS质谱图具有很高的质量精度和谱库匹配度。

代谢物	碎片离子 (m/z)	谱库匹配	MS/MS碎片质量偏差	Zeno trap带来的面积变化（开/关）
Acetylglutamate	*84.0444*	√	*-0.14*	*12.51*
Arginine	*70.0651*	√	*3.73*	*13.18*
Carnitine	*103.0401*	√	*-4.52*	*11.12*
Creatine	*43.0291*	√	*3.87*	*18.11*
Cyclic AMP	*136.0618*	√	*2.56*	*10.00*
Glutamine	*84.0444*	√	*1.72*	*18.08*
Histidine	*110.0713*	√	*0.24*	*26.72**
Leucine	*69.0699*	√	*0.56*	*15.83*
Methyladenosine	*150.0778*	√	*1.28*	*10.28*
Phenylalanine	*120.0808*	√	*2.37*	*10.38*
Tryptophan	*118.0651*	√	*0.26*	*11.93*
Tyrosine	*119.0495*	√	*-3.81*	*8.89*
Uric acid	*141.0407*	√	*4.24*	*10.29*
			平均峰面积增加倍数	***13.64***

** 关闭Zeno trap时峰面积太小无法积分*

载荷图显示了四个 PCV 组（数据未显示）。选择在载荷图上显示出较大变化的代谢物，并将其显示为箱线图（图 5 底部）。cAMP 和甲基腺苷（methyladenosine）在样本中具有相似的差异模式，而肌酸（creatine）在 ZDF 和 SD 尿液样本中显示出不同的模式。

从SWATH® 采集到 MRM^{HR}工作流程

由于SWATH®采集流程是在同一仪器的同一样本集上进行的，因此还展示了从SWATH®采集到 MRM^{HR}的工作流程。本实验从SWATH®采集的数据中选择了实验组间丰度存在差异的代谢物以及一些额外的代谢物，并用于建立有靶向的MRM^{HR}方法。在两个采集方式获得的数据中，有8种代谢物在不同糖尿病小鼠与SD雄性样本之间的倍数变化结果具有良好的相关性（所有组间比较的$r^2 \geq 0.92$，见图6）。这展示了在同一台HRAM系统上执行非靶向筛查工作流程以及靶向定量分析的可行性。

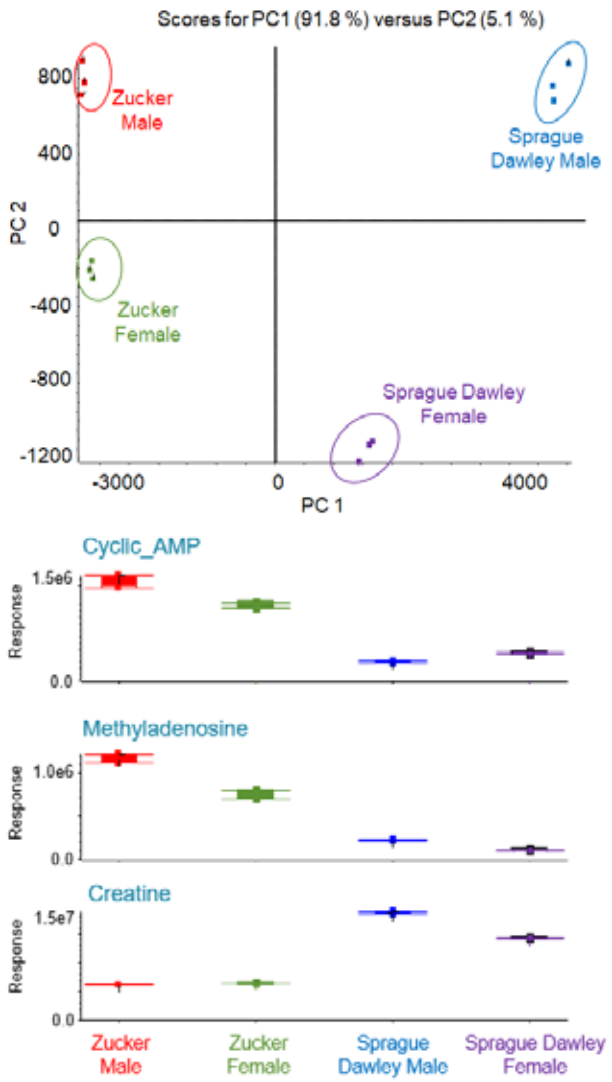

图 5. 主成分分析 (PCA) 突出了样本之间的明显差异。将 MRM^{HR}数据的峰面积导入 MarkerView™ 软件并执行 PCA-PCVG分析。（顶部）PCA-PCVG分数图显示了重复进样的良好重现性，且即使只有 13 种目标代谢物，不同大鼠尿液样品依然明显分离。（底部）选定分析物的箱线图突出显示了整个分析中的样品的差异。

利用SWATH®采集流程，可以实现一次进样定量测定大量代谢产物，并提供初步定量结果，以发现样品之间的差异。当下一步为同一分析物开发MRM^{HR}分析方法时，使用更窄的Q1窗口可提供更高的检测特异性，从而对筛选结果进行进一步确认。值得一提的时，两种检测方法均可以在ZenoTOF™ 7600系统上完成。

表2.大鼠尿液样本中代谢物丰度的差异。以雄性SD大鼠为对照，计算峰面积倍数变化（用log 2峰面积比表示）。

	Log2峰面积比率		
代谢物	SD 雌/雄	ZDF雌 /SD雄	ZDF雄 /SD雄
Acetylglutamate	*-0.94*	*0.40*	*0.36*
Arginine	*-1.32*	*-4.42*	*-1.44*
Carnitine	*1.77*	*3.59*	*2.90*
Creatine	*-0.38*	*-1.53*	*-1.60*
Cyclic AMP	*0.56*	*1.97*	*2.39*
Glutamine	*3.62*	*6.34*	*4.92*
Histidine	*-0.09*	*-1.08*	*-2.33*
Leucine	*-1.35*	*-2.06*	*-2.47*
Methyladenosine	*-1.11*	*1.78*	*2.39*
Phenylalanine	*-0.76*	*-2.04*	*-3.48*
Tryptophan	*-0.51*	*-3.50*	*-3.49*
Tyrosine	*-0.83*	*-3.01*	*-3.94*
Uric acid	*0.17*	*1.71*	*0.73*

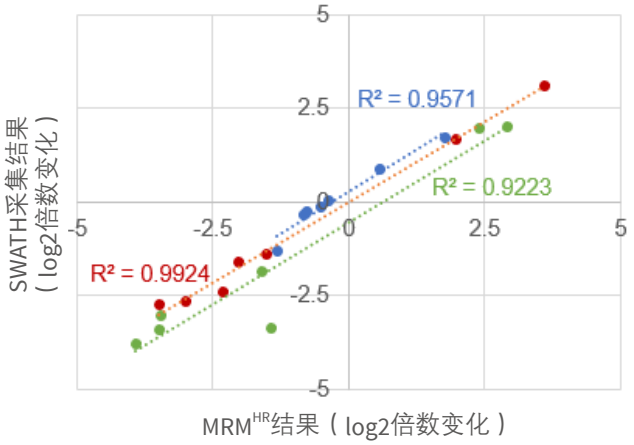

图6. SWATH®采集流程与MRM^{HR}工作流程的定量结果的相关性。计算了三组对比样本（SD雌性/SD雄性、ZDF雌性/SD雄性和ZDF雄性/SD雄性）中8种化合物的log2倍数变化结果。两种定量流程之间有很好的相关性。

RUO-MKT-02-13297-ZH-B

结论

本文探讨了利用ZenoTOF™ 7600系统的靶向MRM^{HR}工作流程对生物样品中代谢物进行定量的过程。

- Zeno MS/MS 将 MS/MS 灵敏度平均提高了 13 倍，从而为每种代谢物提供了高质量的 MS/MS 全扫描数据，以实现可靠的化合物鉴定，同时，碎片离子 XIC 峰面积的大幅增加提高了仪器的定量灵敏度
- Zeno™ trap对仪器灵敏度的增强为用户提供了更多的工作流程选择；例如，通过更大倍数的样品稀释来减少基质效应，或更小体积的进样以分析体积有限的样品
- 利用SCIEX OS软件进行原始数据处理，再利用MarkerView™软件进行多元统计分析的可视化，ZenoTOF™ 7600系统提供了从鉴定到定量的完整工作流程
- 此外，本实验还展示了在同一台质谱上从非靶向SWATH®采集研究过渡到靶向MRM^{HR}工作流程的能力。

参考文献

1. Qualitative flexibility combined with quantitative power -Using the SCIEX ZenoTOF 7600 LC-MS/MS system, powered by SCIEX OS software. SCIEX technical note, RUO-MKT-02-13053-A.
2. Rapid analysis and interpretation of metabolomics SWATH acquisition data using a cloud-based processing pipeline. SCIEX technical note RUO-MKT-02-13056-A.
3. What is principal component analysis and how does it work?SCIEX community post RUO-MKT-18-12137-A.
4. What is principal component variable grouping (PCVG) and how do I use it? SCIEX community post RUO-MKT-18- 12137-A.

RUO-MKT-02-13297-ZH-B

利用SCIEX ZenoTOF™ 7600质谱建立玉米中小分子代谢物的分析方法

Development of a method on research metabolites in Zea mays L. by SCIEX ZenoTOF™ 7600

雷敏，龙志敏，郭立海
Lei Min, Long Zhimin, Guo Lihai

SCIEX，中国

Keywords: Zea mays L., metabolites, ZenoTOF™ 7600

引言

玉米（Zea Mays L.）是中国重要的粮食作物、饲料作物和经济作物，在中国农业生产中起着重要的作用。为了更好的研究不同品种玉米在不同区域生长过程中，应对生物胁迫和非生物胁迫，以及生长机制和规律等，因此越来越多农学领域的科研者通过多种组学的研究手段更深入的探究这些机制。玉米中含有大量的小分子代谢物，包括初生代谢物和次生代谢物。初生代谢物的作用主要是维持植物生命活动和生长发育，次生代谢物则更多参与植物抗病、抗逆等应答。因此，尽可能全面的了解和鉴定出玉米中的小分子代谢物，是开展植物代谢组学研究工作中的重要环节。

本方案使用非靶向代谢组学的流程尽可能全面鉴定出两种不同品种玉米（1号：普通黄金玉米；2号：甜玉米）中的代谢物，然后进行统计分析，筛选两种品种间的差异代谢物，以挖掘两个玉米品种间的差异代谢物，可应用于研究优选育种及作物生长规律和机制。

本文实验方法特点

本文展示了使用SCIEX ZenoTOF™ 7600系统鉴定出玉米中的代谢物，并统计找出两种品种之间的差异代谢物。该方案具有以下特点：

1. 本实验采用SCIEX ZenoTOF™ 7600系统进行数据采集，该仪器具有扫描速度快（高达133 HZ），以及ZenoTrap 富集二级离子，提高占空比，最终极大提高二级灵敏度的特点。结合IDA(数据依赖性采集)和DBS功能(动态背景扣除)的采集方式，可在一针进样过程中，尽可能全面的采集高质量的二级谱图，以实现更全面鉴定小分子代谢物的目的。
2. 该方法鉴定结果，以一级质荷比偏差，同位素比例偏差和二级碎片匹配度三个维度进行定性确认。总共鉴定出330个小分子代谢物，正、负模式下分别鉴定到183和147个不重复代谢物。
3. 该方法采集效率高，仅30 min的方法即可完成一针样品的检测，实现高通量检测。总共鉴定的330个小分子代谢物，正、负模式下分别鉴定到183和147个不重复成分，包括初生代谢物和次生代谢物，如氨基酸、核苷、糖类、酚酸类及大量糖苷类等，覆盖度高。
4. 采用QC样本对方法进行稳定性考察，3个QC样本中的330个脂质进行RSD统计。统计结果，97 %代谢物成分RSD在20 %之内，远满足代谢组学QC样本重复性要求，表明仪器和方法的重现性好。
5. 该方法通过非靶向代谢组学方法，尽可能全面的获得两种玉米中的代谢物，为农学领域的科研客户开展非靶向代谢组学和高覆盖靶向代谢组学研究均可以提供代谢物信息和参考，便于快速筛选差异代谢物。

仪器设备

SCIEX Exion LC™系统 + ZenoTOF™ 7600 系统

RUO-MKT-02-15366-ZH-A

液相方法

色谱柱：HSS T3 (100×2.1 mm, 1.8 µm)

流动相：

A相：水（含2 mmol/L 醋酸铵+0.1 %甲酸）

B相：乙腈

流速：0.3 ml/min

柱温：40 ℃

Time(min)	A (%)	B (%)
0.00	98	2
2.00	98	2
14.0	60	40
22.0	2	98
26.0	2	98
26.1	98	2
30.0	98	2

离子源：电喷雾离子源ESI源，正、负离子模式

采集方式：TOF MS（飞行时间质谱一级扫描）-30 MS/MS（飞行时间质谱二级扫描）

飞行时间质谱一级扫描TOF MS: 质荷比范围(Da) 100-1500

飞行时间质谱二级扫描TOF MS/MS: 质荷比范围(Da) 50-1250

自动校正系统(CDS)开启

动态背景扣除(DBS)开启

Zeno 阈值：200000 cps

离子源参数

电喷雾电压: 5500 V(正离子) / -4500 V(负离子)

气帘气 CUR: 35 psi　　雾化气 GAS1: 55 psi

雾化气 GAS2: 55 psi　　源温度 TEM：500 ℃

去簇电压 DP：80 V (正离子) / -80 V (负离子)

碰撞能量 CE ± CES：35 ± 15 V(正离子) / -35 ± 15 V(负离子)

供试品溶液制备

取两种不同品种的玉米冻干粉末约1 g，每个品种平行称量3份，分别加入5 ml 80 %甲醇，涡旋1 min，超声20 min，4000 rpm离心15 min后，取上清液，分别直接进样分析。

QC制备(质控样本)

两种品种的总共六份样品，分别取100 µl混合成一个QC样本。

实验结果

1. QC样品溶液

分别从所有样品中取100 µl溶液混合，作为QC样本，考察仪器的稳定性。正、负离子总离子流图分别见图1和图2。

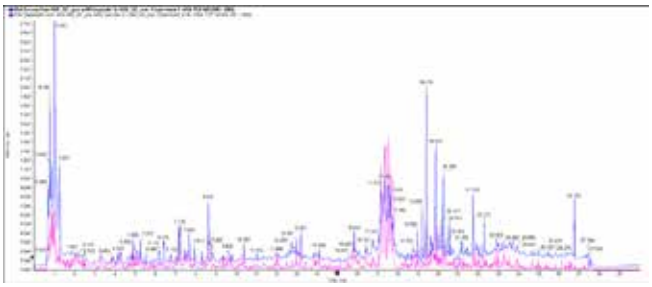

图1. QC样本正离子总离子流图

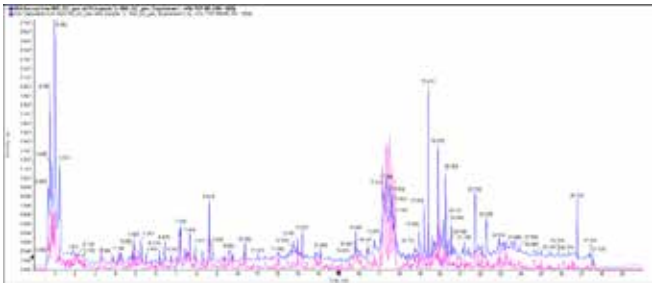

图2. QC样本负离子总离子流图

RUO-MKT-02-15366-ZH-A

2. QC样本重现性评估

QC样本穿插在进样序列中，每三针样品中穿插一针QC样品，最后使用QC样品来评估序列进样中仪器的稳定性和重复性。

以3个QC样本重叠图考察保留时间和总离子流信号强度的重现性。3针QC样品的重叠图，正、负离子模式分别见图3和图4。从重叠图可以看出，化合物保留时间波动在0.1min以内，总离子流图的响应强度重叠好，满足代谢组学对于QC的要求。

从以上考察结果来看，仪器在序列运行过程中，状态稳定，样品结果可用于代谢组学分析。

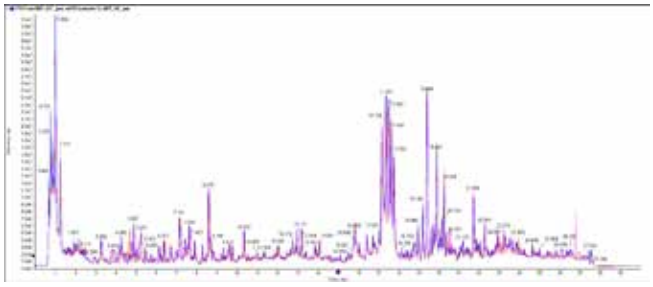

图3. 3针QC样品正离子总离子流重叠图

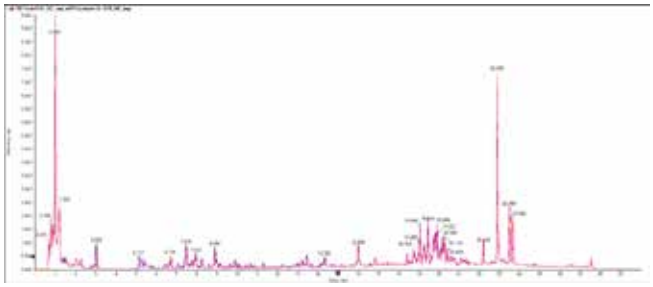

图4. 3针QC样品负离子总离子流重叠图

3. 代谢物鉴定信息（部分）：

3.1 代谢物成分鉴定列表

本实验中，使用SCIEX OS软件（版本号3.0）结合SCIEX天然产物数据库，对QC样本进行小分子代谢物鉴定。通过一级质荷比偏差，同位素比例偏差和二级碎片匹配度三个维度进行定性确认。总共鉴定出330个小分子代谢物，正、负模式下分别鉴定到183和147个不重复成分，包括初生代谢物和次生代谢物，如氨基酸、核苷、糖类、酚酸类及大量糖苷类等。详细鉴定结果列表如表1：

3.2 代谢物结构解析过程

1. 以阿魏酰基-1,4-丁二胺二级谱图为例，进行碎片归属，确认结构式。推测碎片归属如图5。

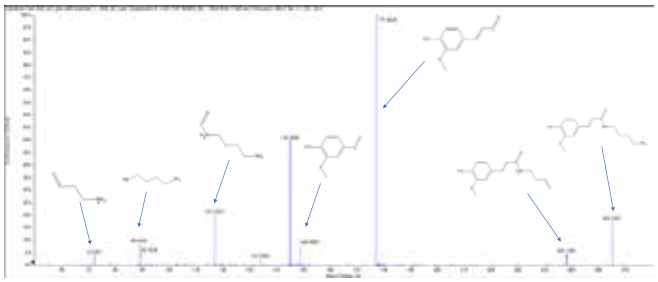

图5. 阿魏酰基-1,4-丁二胺碎片解析

2. 以3-Indoleacetic acid-o-葡萄糖苷的二级谱图为例，进行碎片归属，确认结构式。推测碎片归属如图6。

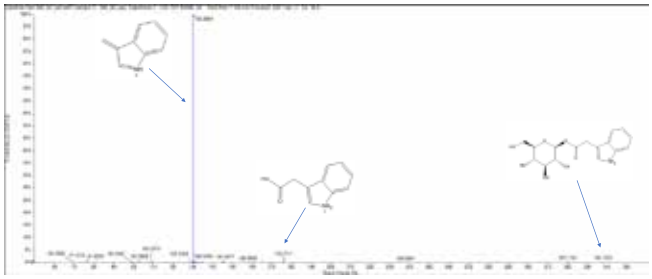

图6. 3-Indoleacetic acid-o-葡萄糖苷碎片解析

4. 统计结果：

2种不同品种的玉米，每组3个样本，每个样本进样1针，最后寻找两个品种的差异代谢物。本文中的数据使用MetaboAnalyst (版本号5.0，https://www.metaboanalyst.ca) 对334个代谢物进行统计，筛选差异代谢物。

4.1 PCA统计图

对2组样本进行PLS-DA统计，PLS-DA得分图见图7。从PLS-DA得分图可以看出2组样本有明显的区分，表明样本之间有明显的差异。

4.2 火山图

以Fold Change>2 或<0.5，及p<0.05为筛选条件绘制火山图，见图8。从火山图中可以看到大量代谢物在两组样本之间存在差异。

RUO-MKT-02-15366-ZH-A

表1. 正离子鉴定列表（部分）

Component Name	Formula	Adduct / Charge	Area	Retention Time(min)	Precursor Mass	Mass Error (ppm)
香豆酰基 -1,4- 丁二胺 1	$C_{13}H_{18}N_2O_2$	[M+H]+	6.97E+04	6.47	235.1441	-0.4
香豆酰基 -1,4- 丁二胺 2	$C_{13}H_{18}N_2O_2$	[M+H]+	4.22E+05	7.1	235.1441	0.4
阿魏酰基 -1,4- 丁二胺 1 N-feruloylputrescine 1	$C_{14}H_{20}N_2O_3$	[M+H]+	3.49E+05	7.01	265.1547	0.7
阿魏酰基 -1,4- 丁二胺 1 N-feruloylputrescine 2	$C_{14}H_{20}N_2O_3$	[M+H]+	2.06E+06	7.61	265.1547	-0.2
阿魏酰基 - 戊二胺 1	$C_{15}H_{22}N_2O_3$	[M+H]+	4.27E+05	7.51	279.1703	0.2
阿魏酰基 - 戊二胺 2	$C_{15}H_{22}N_2O_3$	[M+H]+	1.51E+05	8.36	279.1703	-0.8
N- 反式 - 对香豆酰酪胺 1 paprazine 1	$C_{17}H_{17}NO_3$	[M+H]+	2.56E+06	12.76	284.1281	0.6
Glutamylphenylalanine 1	$C_{14}H_{18}N_2O_5$	[M+H]+	3.55E+05	7.58	295.1288	2.9
N - feruloyltyramine N- 阿魏酰酪胺 1	$C_{18}H_{19}NO_4$	[M+H]+	1.92E+05	12.53	314.1387	0.2
N - feruloyltyramine N- 阿魏酰酪胺 2	$C_{18}H_{19}NO_4$	[M+H]+	1.82E+06	13.09	314.1387	0.9
3-Indoleacetic acid +Glu 1	$C_{16}H_{19}NO_7$	[M+H]+	1.60E+06	7.44	338.1234	1.6
3-Indoleacetic acid +Glu 2	$C_{16}H_{19}NO_7$	[M+H]+	1.86E+06	7.66	338.1234	1.2
3-Indoleacetic acid +Glu 3	$C_{16}H_{19}NO_7$	[M+H]+	1.15E+06	8.3	338.1234	0.9
3-Indoleacetic acid +Glu 4	$C_{16}H_{19}NO_7$	[M+H]+	1.80E+06	8.62	338.1234	0.9
阿魏酰基 - 丙二胺 + 香豆酰基	$C_{22}H_{24}N_2O_5$	[M+H]+	3.25E+04	11.54	397.1758	-0.9
阿魏酰基 -1,4- 丁二胺 + 香豆酰基 1	$C_{23}H_{26}N_2O_5$	[M+H]+	1.84E+06	12.65	411.1914	0.6
阿魏酰基 -1,4- 丁二胺 + 香豆酰基 2	$C_{23}H_{26}N_2O_5$	[M+H]+	4.73E+06	12.99	411.1914	0.7
阿魏酰基 - 羟基丁二胺 + 香豆酰基 1	$C_{23}H_{26}N_2O_6$	[M+H]+	1.67E+05	11.56	427.1864	0.5
阿魏酰基 - 羟基丁二胺 + 香豆酰基 2	$C_{23}H_{26}N_2O_6$	[M+H]+	2.40E+04	11.79	427.1864	-0.2
阿魏酰基 -1,4- 丁二胺 +Glu	$C_{20}H_{30}N_2O_8$	[M+H]+	1.18E+05	6.28	427.2075	-0.8
阿魏酰基 -1,4- 丁二胺 + 阿魏酰基 1	$C_{24}H_{28}N_2O_6$	[M+H]+	1.10E+06	12.49	441.202	0.8
阿魏酰基 -1,4- 戊二胺 + 阿魏酰基 1	$C_{25}H_{30}N_2O_6$	[M+H]+	7.71E+04	13.27	455.2177	0.6
3-Indoleacetic acid +Glu+Xyl 1	$C_{21}H_{27}NO_{11}$	[M+NH4]+	6.27E+05	7.56	487.1922	0.9

备注：Glu 为葡萄糖基，xyl 为木糖基。

表2. 负离子鉴定列表（部分）

Component Name	Formula	Adduct / Charge	Area	Retention Time(min)	Precursor Mass	Mass Error (ppm)
allantoin	$C_4H_6N_4O_3$	[M-H]-	8.01E+04	0.9	157.0367	-1
2-oxoadipate	$C_6H_8O_5$	[M-H]-	1.95E+05	2.22	159.0299	-2
Urate	$C_5H_4N_4O_3$	[M-H]-	3.15E+05	2.29	167.0211	-0.5
Fructose	$C_6H_{12}O_6$	[M-H]-	3.97E+05	0.85	179.0561	-2.0
Galactitol	$C_6H_{14}O_6$	[M-H]-	3.98E+06	0.84	181.0718	-0.5
Mannitol	$C_6H_{14}O_6$	[M-H]-	3.98E+06	0.84	181.0718	-0.5
azelaic acid	$C_9H_{16}O_4$	[M-H]-	5.15E+05	12.09	187.0976	-1.8
4-hydroxy-2-quinolinecarboxylic acid	$C_{10}H_7NO_3$	[M-H]-	1.78E+05	8.25	188.0353	-2.3
Quinic acid	$C_7H_{12}O_6$	[M-H]-	3.75E+05	0.96	191.0561	-2.0
D-glucuronic acid	$C_6H_{10}O_7$	[M-H]-	8.83E+05	0.86	193.0354	-2.0
异阿魏酸 Isoferulic acid	$C_{10}H_{10}O_4$	[M-H]-	3.40E+05	10.82	193.0506	-2.3
巴豆苷 2-Hydroxyadenosine	$C_{10}H_{13}N_5O_5$	[M-H]-	7.88E+05	5.28	282.0844	-1
鸟苷guanosine	$C_{10}H_{13}N_5O_5$	[M-H]-	3.04E+05	5.41	282.0844	-1.1
亚油酸 Linoleic acid	$C_{18}H_{32}O_2$	[M-H]-	1.52E+08	22.88	279.233	-1.1
柠檬酸 Citric acid	$C_6H_8O_7$	[M-H]-	7.91E+06	2.03	191.0197	-0.3
D-甘露糖 D-(+)-Mannose	$C_6H_{12}O_6$	[M-H]-	9.57E+05	0.97	179.0561	-2.2
p-香豆酸 p-Coumaric acid	$C_9H_8O_3$	[M-H]-	1.81E+05	10.21	163.0401	-2.3
原儿茶酸 Protocatechuic acid	$C_7H_6O_4$	[M-H]-	6.89E+04	8.94	153.0193	-2.1
水杨酸salicylic acid	$C_7H_6O_3$	[M-H]-	7.20E+04	7.65	137.0244	-2.2
L-苹果酸 L-Malic acid	$C_4H_6O_5$	[M-H]-	2.74E+06	1.03	133.0142	-1.1

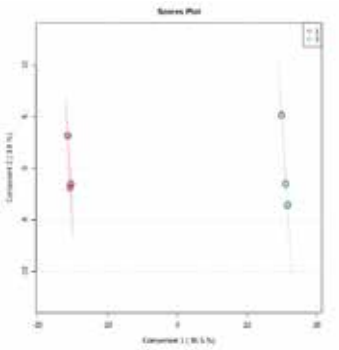

图7. PCA-DA得分图

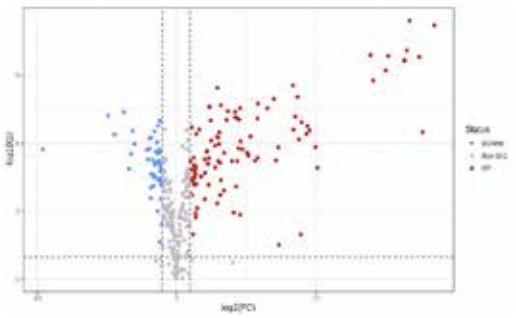

图8. 火山图（FC>2 或<0.5, p<0.05）

RUO-MKT-02-15366-ZH-A

4.3 差异代谢物统计

以p值<0.05，Fold change>2或<0.5，及VIP>1筛选两组间的差异物。两组间的差异代谢物总共是148个，部分差异代谢物信息见表3。表明两个品种玉米中的代谢物差异很大。

表3. 1组和2组之间的差异物列表（部分）

Compound name	p	Fold change	VIP
阿魏酰基-乙胺 1	4.03E-12	108770	1.0754
阿魏酰基-乙胺 2	6.51E-12	372910	1.0754
narcotin	8.16E-11	94224	1.0754
4'-Methoxy-7-O-(6''-acetyl)-D-glucopyranosyl-8,3'-dihydroxyflavanone	1.33E-10	15716	1.0754
Kamebanin+Glu+Gluc	1.45E-10	37569	1.0754
马钱子碱 Brucine	1.62E-10	174220	1.0754
异绿原酸（3,5-二咖啡酰奎宁酸）（Isochlorogenic acid A）3,5-Di-O-caffeoylquinic acid	2.31E-10	84029	1.0754
阿魏酰基-羟基丁二胺+香豆酰基2	6.24E-10	33196	1.0753
Chrysoeriol (Luteolin 3'-methyl ether)	1.76E-09	17975	1.0753
阿魏酰基-1,4-丁二胺+香豆酰基 1	2.9E-09	328.2	1.0753
urate	3.74E-09	7.6725	1.0753
阿魏酰基-1,4-丁二胺+阿魏酰基 1	9.35E-09	411.69	1.0753
阿魏酰基-羟基丁二胺+香豆酰基1	1.13E-08	127.12	1.0753
Carnosic acid+Glu+Gluc	1.85E-08	57.671	1.0752
Androsin 2	2.12E-08	9.1087	1.0752
Homovanillic acid	2.52E-08	5.1605	1.0752
3-(4-hydroxyphenyl)-lactate	2.52E-08	5.1605	1.0752
M2BOA	2.87E-08	23.826	1.0752
HM2BOA+Glu+Glu	2.88E-08	91.8	1.0752

备注：Glu为葡萄糖基，Gluc为葡萄糖醛酸基。

RUO-MKT-02-15366-ZH-A

总结

本文展示了使用SCIEX ZenoTOF™ 7600系统建立了鉴定玉米中小分子代谢物的方法，同时该方案中鉴定到的代谢物的一级母离子和二级碎片离子可建立MRM 离子对应用于玉米高覆盖靶向代谢组学研究。该方案体现出SCIEX ZenoTOF™ 7600系统扫描速度快，二级灵敏度高的特点，并结合IDA结合DBS功能采集方式，一针进样，尽可能全面的采集高质量的二级谱图用于鉴定小分子代谢物。该方案通过一级质荷比偏差，同位素比例偏差和二级碎片匹配度总共鉴定出330个小分子代谢物，包括初生代谢物和次生代谢物，代谢物覆盖度高。其中，大量的代谢物在两个品种玉米中均表现出差异。该方法通过非靶向代谢组学方法，尽可能全面的获得两种玉米中的代谢物信息，为农学领域的科研客户开展非靶向代谢组学和高覆盖靶向代谢组学研究均可以提供代谢物成分信息和参考，便于快速筛选差异物。

RUO-MKT-02-15366-ZH-A

基于高分辨质谱X500R QTOF系统油菜籽的代谢组和脂质组学分析

Metabolomic and lipidomic profilig of rapeseed based on X500R QTOF High Resolution Mass Spectrometry

贾金茹，司丹丹，龙志敏，郭立海
Jia Jinru, Si Dandan, Long Zhimin, Guo Lihai
SCIEX应用支持中心，中国
SCIEX，China

Keywords: X500R QTOF, Metabolomics, Lipidomics, Rapeseed

前言

植物中含有较为丰富的代谢物，包括负责植物生长发育的初级代谢产物和与植物抗胁迫密切相关的次生代谢产物。而植物代谢组学作为代谢组学一个重要的分支，以植物为研究对象，主要研究不同物种、不同基因类型或不同生态类型的植物在不同生长时期或受某种刺激前后的所有小分子代谢产物，并通过液质联用技术对其进行定性或定量分析，找出其代谢的变化规律，深度挖掘植物代谢信息[1]。

油菜花籽是世界上重要的农业油料作物，也是世界上第三大植物油来源。油菜籽中含有丰富的不饱和脂肪酸，由于多不饱和脂肪酸的存在，使其具有较高的营养价值。除了不饱和脂肪酸外，菜籽油还含有多种微量营养成分，包括植物甾醇、生育酚、类黄酮等，也受到了消费者和营养学家的关注[2,3]，因此对油菜籽中代谢产物和脂质进行分析和鉴定有助于对其生产和加工提供知识基础。

本实验采用高分辨质谱X500R QTOF系统并结合数据依赖性采集模式（IDA）的采集方法，实时动态背景扣除（DBS）技术进行油菜花籽的非靶向数据采集，一次进样即可同时得到一级精确质量数和二级碎片图谱。数据结果使用SCIEX OS软件进行分析，根据自建的代谢物以及脂质的二级标准谱库可以极大的提高数据处理效率，最终通过一级精确质量数、同位素分布和二级碎片从油菜籽中共确认代谢物299个、脂质387个。

方法特点

1. X500R QTOF具备高扫描速度，采用TOF MS-IDA-MS/MS模式，结合独有的实时动态背景扣除（DBS）技术，一针进样可实现有效且高质量的一级和二级信息全面采集，可满足后续定性和组学分析的要求。
2. SCIEX OS软件结合天然产物高分辨二级数据库和脂质二级数据库，极大地提高数据分析速度，并准确对检测到的化合物进行鉴定，为后续寻找不同产地油菜籽的差异标志物提供基础。
3. X500R高分辨质谱具备较强的抗污染能力，且在长时间的样品采集过程中，仪器仍能保证数据的稳定性和重现性。

样品及试剂

实验所用油菜花籽样品：粉橙（1）、白花（2）、紫红（3）、红橙（4）、紫茎金黄（5）、亮紫（6）、洋红（7）、红橙（8）、紫叶白花（9）

样品前处理

代谢组学样品前处理：将油菜籽样品研磨成粉末备用，称取适量粉末加20倍量的乙醇和水混合溶液（70/30，v/v），冰浴超声提取30 min，在4 ℃下12000 rpm离心15 min。离心完成后，取上清1.5 mL，40 ℃水浴下氮气流下吹干上清，加200 µl乙腈和水混合溶液（50/50，v/v）复溶后，在4 ℃下12000 rpm离心15 min，取上清待分析。

RUO-MKT-02-15719-ZH-A

脂质组学样品前处理：将油菜籽样品研磨成粉末备用，称取100 mg样品，加入400 µl冰甲醇和水混合溶液（75/25, v/v），冰浴超声30 min；加入1 ml冰甲基叔丁基醚充分涡旋振荡；继续冰浴超声15 min，加入250 µl水，涡旋振荡1 min，室温静置10 min后，在4 ℃下12000 rpm离心15 min。离心完成后，取上层液体，置于真空浓缩离心机中挥干，挥干后的样品用400 µl异丙醇/甲醇（1:1, v/v）复溶，复溶后的样品在4 ℃下12000 rpm离心15 min，离心后的上清转移至进样瓶中待分析。

仪器设备

ExionLC™系统+SCIEX高分辨质谱X500R QTOF系统

色谱条件

代谢组学

色谱柱：Waters HSS T3（100 mm × 2.1 mm, 1.8 µm）

柱温：40 ℃

进样体积：2 µL

流动相：A为水（含0.05%FA），
B为乙腈和甲醇混合溶液（1:1, v/v）

流速：0.3 ml/min

梯度程序：见下表

Time (min)	A（%）	B（%）
0	95	5
1	95	5
25	5	95
27	5	95
27.1	95	5
30	95	5

脂质组学

色谱柱：Kinetex C18 column（100 mm × 2.1 mm, 2.6 µm）

柱温：40 ℃

进样体积：2 µL

流动相：A为甲醇、乙腈和水混合溶液（1:1:1, v/v/v，含5 mM乙酸铵），B为异丙醇（含5 mM乙酸铵）

流速：0.3 ml/min

梯度程序：见下表

Time (min)	A（%）	B（%）
0	80	20
1	80	20
5	60	40
7	40	60
20	10	90
21	10	90
21.1	80	20
23	80	20

质谱条件

代谢组学&脂质组学

SCIEX高分辨质谱X500R QTOF系统;

离子源：ESI源;

扫描模式：ESI+/-TOF MS-IDA 15TOF MS/MS; 一级扫描时间：0.15 s; 二级扫描时间：0.035 s;

扫描范围：MS1, m/z, 100-1500; MS2, m/z, 50-1500;

DBS动态背景扣除开启

离子源参数：

电喷雾电压(IS): 5500 V/-4500 V;

气帘气(CUR): 35 psi;

雾化气(GS1): 55 psi;

辅助加热气(GS2): 50 psi;

离子源温度(TEM): 550 ℃;

碰撞气(CAD): 9 psi;

去簇电压(DP): ± 60 V;

碰撞能量(CE): ± 40 ± 20 V

RUO-MKT-02-15719-ZH-A

数据处理及数据分析

采用SCIEX OS软件对油菜籽样品的数据采集，并对得到的高质量一级和二级高分辨质谱数据进行分析，鉴定油菜籽中的代谢物和脂质成分。

通过主成分分析（PCA）和方差分析（ANOVA）等统计分析方法对从样本中鉴定到的代谢物和脂质进行分析，寻找存在显著差异的标志物。

代谢组学&脂质组学分析流程图

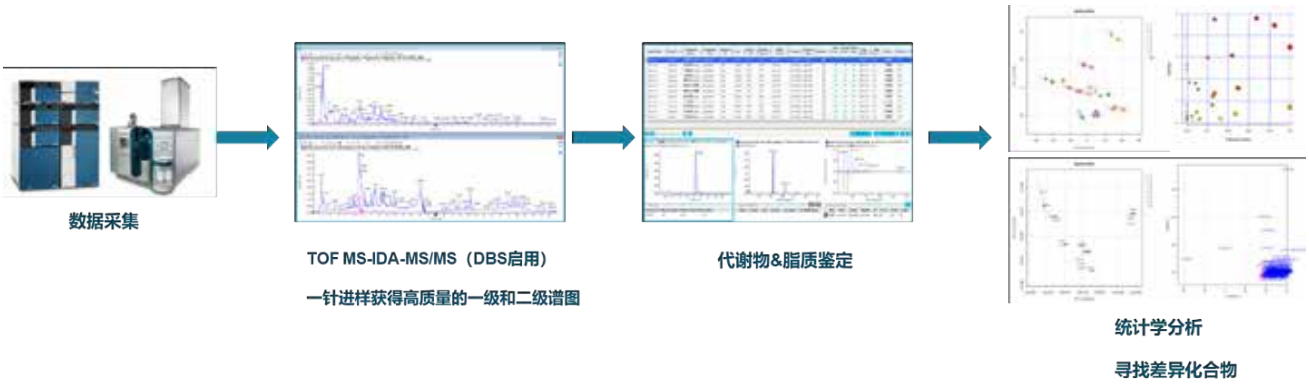

图1. 代谢组学&脂质组学分析流程图

实验结果与讨论

1. 油菜籽代谢物和脂质的鉴定

本实验通过SCIEX OS软件采用数据依赖性采集（IDA）和实时动态背景扣除（DBS）模式，一针进样，完成样本的一级精确质量数和二级图谱信息的采集。采用靶向数据处理流程结合高分辨天然产物数据库、代谢物数据库和脂质数据库对油菜籽中主要成分进行分析。图2展示了SCIEX OS软件靶向二级谱库检索结果，采用红绿灯判断系统，根据一级精确质量数、同位素分布以及二级谱图匹配得分进行化合物准确鉴定，实现满足设定条件的化合物信息的快速过滤，极大减少了分析时间。图3-5中列举苯丙素类、黄酮类、硫代葡萄糖苷类代谢物的二级图谱解析。

对数据库中没有的代谢物，我们采用非靶向的鉴定流程，按峰面积从大到小进行排序，对其二级质谱图进行解析。根据方法中设定的最大元素组成，软件可自动拟合满足条件的分子式信息，并以MS/MS的匹配度进行判断。最终从油菜籽样品中共鉴定299个代谢物，主要包括氨基酸类、脂肪酸类、硫代葡萄糖苷类、苯丙素类、黄酮及其苷类等，以及387个脂质成分，包括甘油磷脂、甘油酯、糖脂、鞘脂等23个亚类。表1展示了油菜籽中典型的代谢物（硫代葡萄糖苷类）。

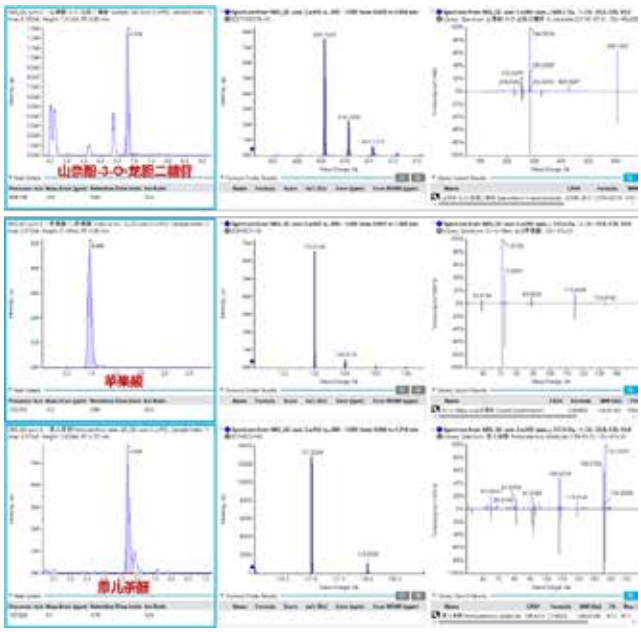

图2. OS软件靶向二级谱库检索结果展示

RUO-MKT-02-15719-ZH-A

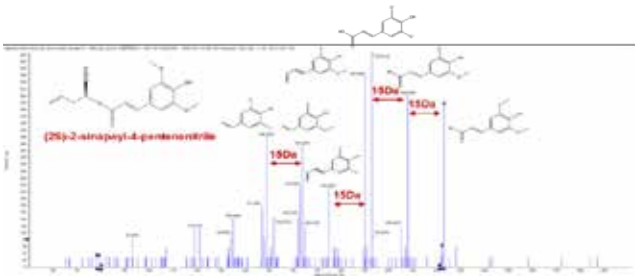

图3. 苯丙素类化合物二级图谱解析

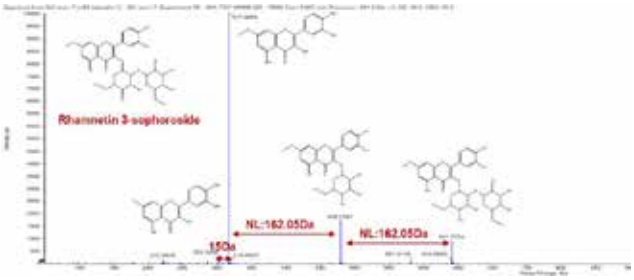

图4. 黄酮类化合物二级图谱解析

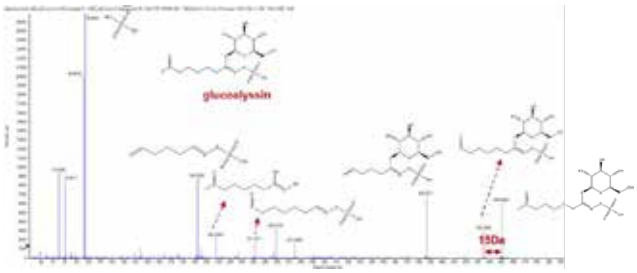

图5. 硫代葡萄糖苷类化合物二级图谱解析

2. 统计分析

代谢组学数据结果

根据上述鉴定到的代谢产物结果对多组油菜籽样本进行无监督的主成分分析，图6展示了主成分分析结果。从图中可以看出QC样本（所有组别样本的混合物）点紧密的 在中心附近，说明在样品采集周期内仪器具有较高的精密度，且样品稳定。不同组别的样本可以完全分离，初步说明样本之间存在显著的差异。进一步通过Anova分析，以P < 0.01为标准进行差异代谢物筛选，在设定的筛选条件下找到134个组间差异的代谢物（见表2），主要为脂

表1. 油菜籽中典型的代谢物（硫代葡萄糖苷类）

Component Name	Area	RT/min	Adduct	Formula	Precursor Mass	Found At Mass	Mass Error (ppm)
Glutathione (oxidized form)	4.69E+05	1.08	[M-H]-	$C_{20}H_{32}N_6O_{12}S_2$	611.1450	611.1451	0.6
glucotropaeolin	1.19E+06	4.46	[M-H]-	$C_{14}H_{19}NO_9S_2$	408.0426	408.0424	1.0
Glucobarbarin	1.89E+06	3.67	[M-H]-	$C_{15}H_{21}NO_{10}S_2$	438.0528	438.0527	1.5
glucohesperin	2.65E+06	2.85	[M-H]-	$C_{14}H_{27}NO_{10}S_3$	464.0720	464.0718	-1.3
Methylpentyl glucosinolate	3.96E+06	6.03	[M-H]-	$C_{13}H_{25}NO_9S_2$	402.0891	402.0893	-1.0
Neoglucobrassicin isomer	8.36E+06	5.63	[M-H]-	$C_{17}H_{22}N_2O_{10}S_2$	477.0643	477.0641	0.4
Methylpentyl glucosinolate isomer	9.18E+06	6.31	[M-H]-	$C_{13}H_{25}NO_9S_2$	402.0891	402.0892	-1.0
Methylpentyl glucosinolate isomer	1.19E+07	6.13	[M-H]-	$C_{13}H_{25}NO_9S_2$	402.0891	402.0889	-1.0
Glucobrassicin	1.54E+07	5.30	[M-H]-	$C_{16}H_{20}N_2O_9S_2$	447.0540	447.0534	0.7
Neoglucobrassicin	1.79E+07	6.57	[M-H]-	$C_{17}H_{22}N_2O_{10}S_2$	477.0636	477.0636	1.5
glucoraphanin	3.47E+07	0.92	[M-H]-	$C_{12}H_{23}NO_{10}S_3$	436.0405	436.0404	1.7
glucoberteroin	3.49E+07	5.63	[M-H]-	$C_{13}H_{25}NO_9S_3$	434.0620	434.0615	-0.8
glucoalyssin	3.71E+07	1.08	[M-H]-	$C_{13}H_{25}NO_{10}S_3$	450.0560	450.0559	2.1
gluconapoliferin	3.72E+07	1.09	[M-H]-	$C_{12}H_{21}NO_{10}S_2$	402.0530	402.0526	2.0
gluconasturtiin	4.86E+07	5.64	[M-H]-	$C_{15}H_{21}NO_9S_2$	422.0582	422.0582	0.8
glucobrassicanapin	1.07E+08	3.41	[M-H]-	$C_{12}H_{21}NO_9S_2$	386.0580	386.0575	-3.9
glucobrassicanapin isomer	1.50E+08	3.88	[M-H]-	$C_{12}H_{21}NO_9S_2$	386.0580	386.0575	-2.1
gluconapin	4.04E+08	1.12	[M-H]-	$C_{11}H_{19}NO_9S_2$	372.0420	372.0425	-1.7

RUO-MKT-02-15719-ZH-A

表2. 不同品种鉴定的差异代谢物列表

Component Name	Area	RT/min	Formula	Found At Mass
(11E)-Octadecenoic acid	2.48E+06	25.33	$C_{18}H_{34}O_2$	283.2635
(2S)-2-sinapoyl-4-pentenenitrile	1.08E+06	12.30	$C_{16}H_{17}NO_5$	302.1030
(9E)-9-Octadecenedioic acid	3.24E+06	14.99	$C_{18}H_{32}O_4$	311.2223
(9Z,12Z,15Z)-9,12,15-Octadecatrieneperoxoic acid	1.07E+06	19.66	$C_{18}H_{30}O_3$	295.2268
1-O-b-D-glucopyranosyl sinapate	3.86E+05	6.24	$C_{17}H_{22}O_{10}$	387.1292
2-Furoic acid	9.60E+05	1.08	$C_5H_4O_3$	111.0089
2-Oxooctadecanoic acid	4.32E+06	19.70	$C_{18}H_{34}O_3$	297.2429
2-Piperidinylphosphonic acid	2.98E+06	7.45	$C_5H_{12}NO_3P$	164.0479
3,4,5-TRIETHOXYBENZOIC ACID	4.16E+06	6.50	$C_{13}H_{18}O_5$	253.1079
Caffeic acid 3-glucoside	5.39E+06	4.92	$C_{15}H_{18}O_9$	341.0877
Caffeoylcholine	2.21E+06	4.41	$C_{14}H_{20}NO_4$+	266.1385
Coniferyl alcohol	1.01E+06	7.45	$C_{10}H_{12}O_3$	179.0713
Coumaric acid	6.90E+05	3.59	$C_9H_8O_3$	165.0545
FA 18:2	5.12E+06	18.59	$C_{18}H_{32}O_3$	295.2271
glucoalyssin	3.71E+07	1.08	$C_{13}H_{25}NO_{10}S_3$	450.0559
glucoberteroin	3.49E+07	5.63	$C_{13}H_{25}NO_9S_3$	434.0615
gluconasturtiin	4.86E+07	5.64	$C_{15}H_{21}NO_9S_2$	422.0582
glucoraphanin	3.47E+07	0.92	$C_{12}H_{23}NO_{10}S_3$	436.0404
Glutathione (oxidized form)	4.69E+05	1.08	$C_{20}H_{32}N_6O_{12}S_2$	611.1451
hydroxyferuloylcholine	9.39E+06	4.77	$C_{15}H_{22}NO_5$+	296.1488
Iridin	8.32E+05	8.40	$C_{24}H_{26}O_{13}$	521.1301
isorhamnetin-3-O-glucoside	4.53E+05	8.13	$C_{22}H_{22}O_{12}$	477.1036
Isoswertisin 2''-rhamnoside	6.55E+06	9.94	$C_{28}H_{32}O_{14}$	591.1708
Kaempferol 3-O-Hydroxyferuloylsophoroside 7-O-Glucoside	4.29E+05	5.11	$C_{43}H_{48}O_{25}$	963.2423
Kaempferol 3-sophorotrioside	5.53E+06	4.80	$C_{33}H_{40}O_{21}$	773.2138
……	……	……	……	……

肪酸类、硫代葡萄糖苷类成分、黄酮类、苯丙素类等成分，这些差异化合物在不同品种的油菜花籽之间含量均有明显的差异。进一步对组间差异的生物标志物所涉及的代谢通路进行分析，选择合适的代谢库进行匹配。按照P < 0.05且FDR < 0.05筛选代谢通路，涉及的主要代谢通路包括亚油酸代谢、黄酮和黄酮醇类的生物合成、苯丙素类化合物生物合成、糖代谢（见图 7）。查阅文献发现[3]，所涉及到的代谢通路与报道相符，不同来源或品种的油菜花籽主要差异来源可能是与生长条件或应对应激条件相关，同时这些差异代谢物均是油菜籽主要的营养性成分，具有其独特的生物学功能。此外，不仅不同产地或品种会由于其生长环境或条件导致营养成分的差异，在油菜籽加工过程中也会存在一部分营养成分的流失，所以可通过根据上述几类差异化合物的变化进行加工工艺的优化，以最大限度的保留其营养价值。后续可通过广泛拟靶向代谢组学实现差异代谢物的相对定量分析，深入研究不同品种油菜花籽的代谢物差异表现。

RUO-MKT-02-15719-ZH-A

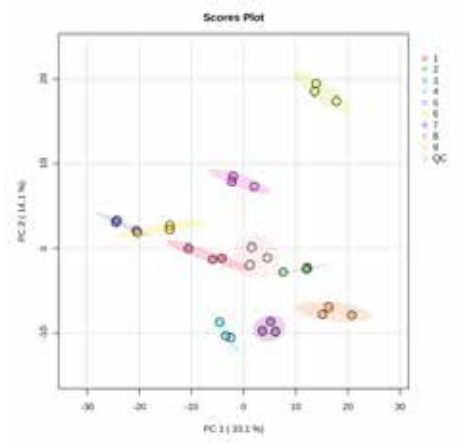

图6. PCA得分图

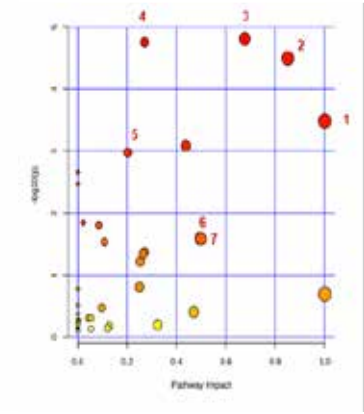

图7. 差异代谢通路结果

饱和脂肪酸具有多种生理功能，例如抗癌、抗心血管疾病、降血脂等，而多不饱和脂肪酸无法在人体合成，只有通过从植物中获取，所以选择富含丰富的不饱和脂肪酸的油菜籽进行加工更有助于人们的健康。因此通过上述找到的差异代谢物初步评价不同产地或品种油菜籽的营养价值，可为其后续生产和加工提供依据。

代谢组学的结果显示，差异化合物中包括不饱和脂肪酸且涉及到的主要代谢通路是亚油酸代谢和亚麻酸代谢，说明不同品种或不同生长环境中油菜籽中的亚油酸和亚麻酸含量的变化较为明显。据文献报道，油菜籽中富含大量的油酸、亚油酸、亚麻酸等不饱和脂肪酸以及棕榈酸和硬脂酸等饱和脂肪酸，其中所含的不饱和脂肪酸对人体有较多益处，例如对糖尿病、代谢综合征等疾病具有促健康作用，且促进健康人及患者的脂质代谢。尤其是亚油酸和亚麻酸，其结构中含有一个或多个不饱和双键，抗氧化的效果更佳，并且由于人体内缺乏特定的酶，所以只能从饮食中获取。因此从食用方面来说，亚油酸和亚麻酸含量丰富的油菜籽营养价值更高，食用可促

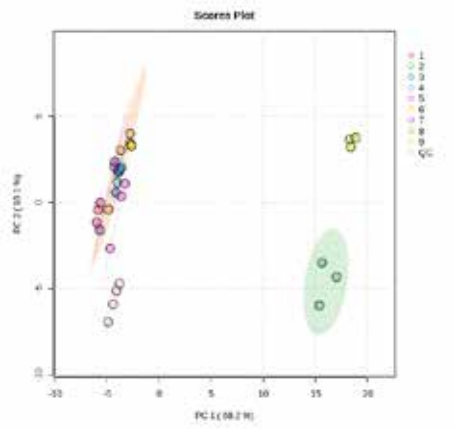

图8. PCA分析结果

脂质组学结果

脂质组学的数据同样是按照代谢组学的流程进行数据处理，寻找差异化合物。根据前期鉴定到的脂质结果对多组油菜籽样本进行无监督的PCA分析（见图8）和有监督的PLS-DA分析（见图 9）。从图中可以看出QC样本（所有组别样本的混合物）点紧密的在中心附近，说明在样品采集期间内仪器具有较高的精密度，且样品稳定。不同组别的样本之前有明显的分离，初步说明样本之间存在显著的差异。为了进一步分析组间差异，剔除QC样本后，采用有监督的PLS-DA分析多组间差异，结果显示不同品种的油菜花籽样本可以得到很好的区分，并根据VIP值>1.2筛选潜在的差异代谢物，共筛选出21个差异性成分，以饱和和不饱和脂肪酸为主（见表3），这一结果与上述代谢组学分析结果相符。据文献报道[2]，油菜籽中含有丰富脂肪酸，以饱和脂肪酸和多不饱和脂肪酸为主。其中多不

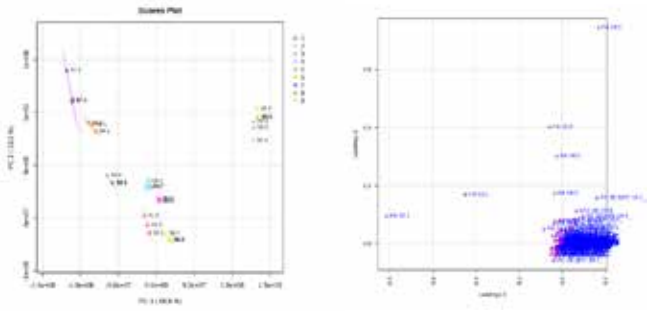

图9. PLS-DA分析结果和载荷图

RUO-MKT-02-15719-ZH-A

表3. 不同品种鉴定的差异脂质列表

Component Name	Area	RT/min	Formula	Found At Mass
FA 18:2	1.11E+08	2.33	$C_{18}H_{32}O_2$	279.2323
FA 16:0	7.89E+07	2.91	$C_{16}H_{32}O_2$	255.2325
FA 18:1	1.48E+08	3.20	$C_{18}H_{34}O_2$	281.248
FA 18:0	4.27E+07	4.37	$C_{18}H_{36}O_2$	283.2638
FA 20:1	6.77E+07	4.60	$C_{20}H_{38}O_2$	309.2799
FA 22:1	1.23E+08	6.01	$C_{22}H_{42}O_2$	337.3098
…….	…….	…….	…….	…….

进人体健康。同时脂质组学的结果显示，不同品种的油菜籽之间主要的差异化合物主要为FA 18:1、FA 18:2、FA 16:0、 FA 18:0等，该结果与代谢组学结果一致，同样证明了不同样本之间亚油酸和亚麻酸等不饱和脂肪酸含量的差异。从图（图10）中可观察到，相比于其他品种，2、7、8号油菜籽内亚油酸和亚麻酸含量偏高，初步推测2、7和8号油菜籽的营养价值相对于其他偏高。植物的生长条件会极大影响油菜籽中代谢物以及脂质代谢，所以为了防止营养成分的损失，需要对其生长环境和培育条件进行考察和优化；不仅如此，后续加工工艺的优化也是一种手段，极大地保留营养物质，发挥潜力更好的促进人体健康。

结论

本实验使用X500 QTOF高分辨质谱，采用数据依赖性采集模式和动态背景扣除，完成油菜花籽的数据采集工作。由于其具备高扫描速度，且整个组学样品采集仅需一次进样，即可获得全面高质量的一级和二级质谱图。

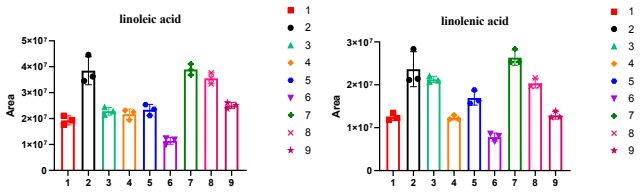

图10. 共同差异化合物的柱状图

基于X500R QTOF高分辨质谱平台对9种不同产地的油菜籽样品进行差异分析，使用SCIEX OS 软件结合天然产物、代谢物和脂质等高分辨数据库进行后续的数据处理，通过一级精确质量数、同位素分布和二级谱图匹配，快速且准确鉴定了299个代谢物和387个脂质。进一步通过统计学分析，发现硫代葡萄糖苷、黄酮、脂肪酸等多种差异代谢物，可为其营养价值的评价提供参考意义。后续可通过广泛拟靶向代谢组学对黄酮、硫代葡萄糖苷、不饱和脂肪酸等差异代谢物进行相对定量分析，深入研究不同品种油菜花组的代谢物差异。

参考文献

[1] Shen S, Zhan C, Yang C, Fernie AR, Luo J. Metabolomics-centered mining of plant metabolic diversity and function: Past decade and future perspectives. Mol Plant. 2023, 16(1): 43-63.

[2] Shen J, Liu Y, Wang X, et al. A Comprehensive Review of Health-Benefiting Components in Rapeseed Oil. Nutrients. 2023, 15(4): 999.

[3] Yang R, Deng L, Zhang L, et al. Comparative Metabolomic Analysis of Rapeseeds from Three Countries. Metabolites. 2019, 9(8): 161.

RUO-MKT-02-15719-ZH-A

Large scale targeted metabolomics assay for quantitative plasma profiling

Using the SCIEX Triple Quad™ or QTRAP® Systems

Kranthi Chebrolu, Robert Proos, Christie Hunter
SCIEX, USA

Untargeted serum metabolomics studies have detected, identified and documented over 75% of endogenous compounds.[1] However, only a handful of robust and sensitive targeted methods are in existence to quantify large panels of endogenous metabolites in a single assay. Methods for the quantification of plasma metabolites have great utility for many applications, including disease research, food omics and pharmaceutical development, among others. However, the wide structural diversity of metabolites, and hence the broad chromatographic and ionization properties of these compounds, have posed an immense challenge in developing high-throughput, large scale targeted LC-MS methods for semi-quantitative purposes.

Here, a large, high-throughput serum metabolite method consisting of 336 serum metabolites was developed and tested using SRM 1950 plasma. The chromatographic separations were performed on a Kinetex F5 (Phenomenex, CA) column using standard reversed-phase mobile phases for reliable separations of a majority of serum analytes. Development of the MRM method was done both from standards and from testing in matrix, as well as leveraging the CAS numbers, accurate mass information, compound nomenclature and groups from Human Metabolite Data Base (HMDB). Both polarity switching and the Scheduled MRM™ Algorithm were used to ensure the robust analysis of this large panel of analytes in a single injection. The assay was tested on both the SCIEX Triple Quad 7500 LC-MS/MS System – QTRAP Ready and the QTRAP 6500+ LC-MS/MS System.[3]

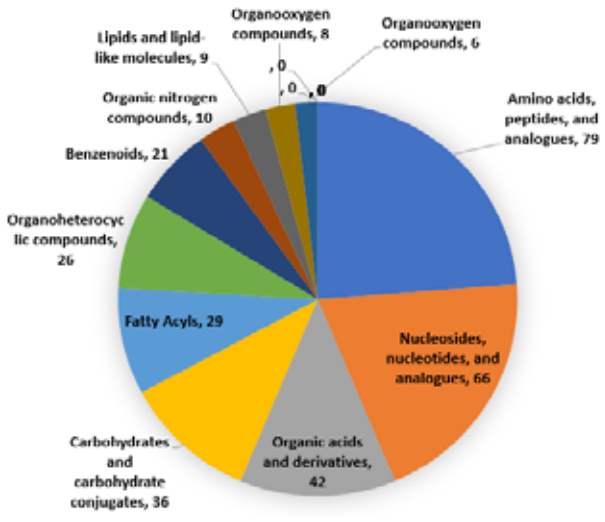

Figure 1. Broad compound class coverage. Targeted MRM assay covers a broad range of metabolites typically found in plasma/serum. The method covers 11 metabolite classes as defined in HMDB.

Key features of the targeted plasma metabolomics method

- Full solution for targeted quantitative metabolomics for easy adoption on any SCIEX Triple Quad or QTRAP System
- MRM-based assay for reproducible quantification of a broad range of metabolites in biological samples
  - ~85% of MRM transitions with <20% CV in 10 replicates for 734 MRMs in single injection
- Detailed standard operating protocol describing sample preparation through data processing
- sMRM Pro Builder tool for streamlining retention time windows, dwell time determination and assay optimization
- Targeted analysis for simplified data processing in SCIEX OS software
- High data reproducibility demonstrates robustness of the implementation on both the SCIEX 7500 System and the QTRAP 6500+ System

RUO-MKT-02-13259-A

Methods

Sample preparation: NIST SRM 1950 plasma was extracted using 8 volumes of methanol then spiked with internal standard QReSS kit (Cambridge Isotopes). After centrifugation to precipitate the proteins, the supernatant was directly analyzed. More details on the sample preparation can be found in the SCIEX How method.[4]

Chromatography: Samples were analyzed using the ExionLC™ System with a Kinetex F5 column (2.1 x 150 mm, 2.6 µm, Phenomenex). A simple linear gradient from 0 to 95% B was used with standard reversed phase mobile phases (A = 0.1% formic acid in water and B = 0.1% formic acid in acetonitrile) with a flow rate of 200 µL/min. A 1 µL injection volume was used and the column temperature was maintained at 30 ºC throughout the analysis. More details on the chromatography can be found in the SCIEX How method.[4]

Mass spectrometry: The sample extract was analyzed on both the QTRAP 6500+ System and the SCIEX 7500 System. Data were collected using methods built with the Scheduled MRM™ Algorithm as well as unscheduled methods. Finally, this high throughput method is used to analyze 336 serum metabolites (a total of 784 MRM transitions) in a 20 min run period. More details on the MS settings and the MRM transition list can be downloaded from the SCIEX How method.[4]

Data processing: All data was analyzed using the Analytics module in SCIEX OS Software 2.0.

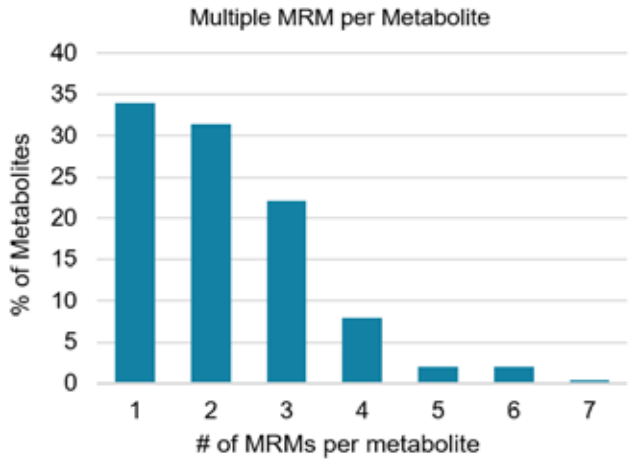

Figure 2. Robust MRM assay with multiple MRMs per metabolite. To increase assay robustness and specificity, over 65% of the 336 metabolites in the assay have more than 1 MRM transition per metabolite.

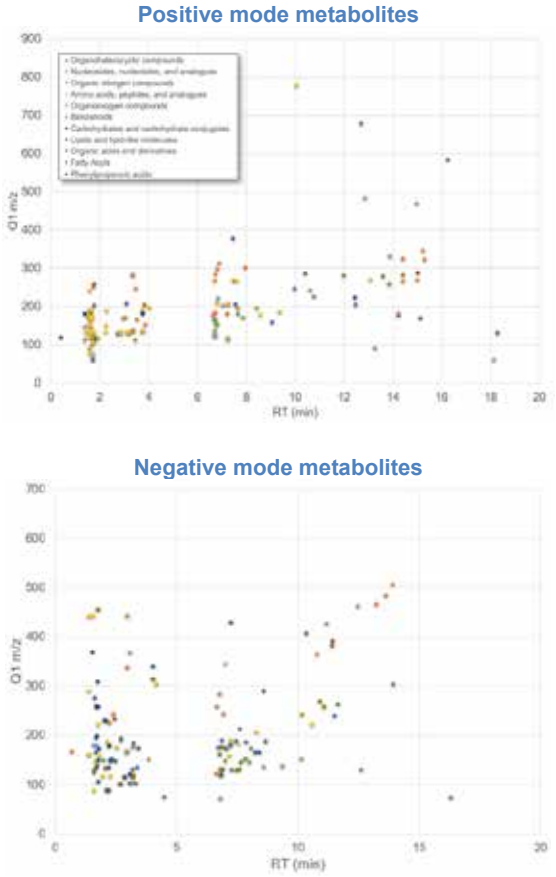

Figure 3. Reversed phase chromatography approach. The Kinetex F5 column provided good retention of the polar metabolites while also providing separation across the gradient of the many other compound classes. The top graph shows the separation of metabolites detected in positive mode and the bottom graph shows the negative mode metabolites.

Chromatography

Chromatography of metabolites can be difficult due to the broad range of properties across the compounds of interest. Balancing the retention of polar metabolites as well as separation across the gradient of many other classes of metabolites is key to the development of a generic global profiling method. A reverse-phase method with a Kinetex F5 column (Phenomenex) was used to retain both nonpolar and polar analytes in a single separation for this broad targeted metabolite assay. Figure 3 highlights the separation achieved for the metabolites detected in positive ion mode and negative ion mode, color coded by metabolite class. The retention time reproducibility was highly consistent across the 10 replicates, with an RSD of 0.38% in plasma matrix.

RUO-MKT-02-13259-A

It should be noted that the method described here is intended for use as a starter method to cover a broad range of metabolites, metabolite classes and associated pathways. Optimization of the chromatography, compounds monitored, and the specific MRM transitions and parameters could quickly be performed depending on the specific matrix, pathways, and analytes of interest.

Importance of time scheduling MRMs

Injections were performed without time scheduling in positive (blue) and negative (green) ion polarities to detect metabolites and determine retention times. Replicate injections using Scheduled MRM™ Algorithm were then performed in positive and negative ion mode to further refine retention times. The increased dwell times afforded by the use of the Scheduled MRM Algorithm provide improved peak area reproducibility across 10 replicates, as seen in Figure 4.

After removal of a small number of transitions that were poorly detected in this particular plasma sample, 264 MRM transitions were monitored in positive mode for the final dataset. A large improvement in peak area reproducibility was observed with time scheduled (blue solid) and without time scheduled (blue dotted). In the unscheduled method, a dwell time of 5 msec was set, giving a cycle time of 1.8 sec. After time-scheduling, the average dwell time was 64 msec and the target cycle time was set at 1 sec.

A more dramatic effect was observed in negative mode where a much larger number of MRM transitions (470 final MRM

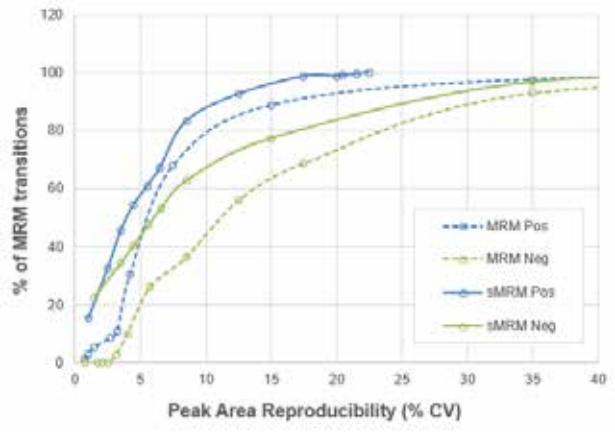

Figure 4. Improvement in data quality with time scheduling of MRM transitions. Ten replicate injections were performed without time scheduling (dotted line) to detect metabolites and to determine retention times. Then using Scheduled MRM Algorithm, 10 more replicates were injected to assess reproducibility gains due to time scheduling. In both positive ion (blue) and negative ion (green) mode, large increases in data reproducibility were observed.

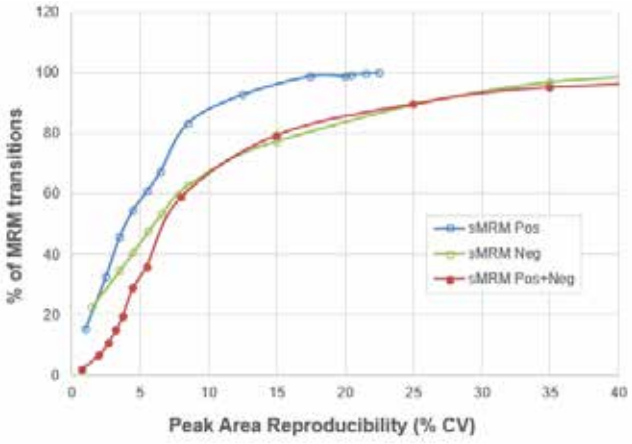

Figure 5. Fast polarity switching for broadest compound coverage in single injection assay. High data quality is maintained when both the positive and negative ion MRM transitions are combined into a single method with fast polarity switching. No decline in data quality was observed when compared to the individual single polarity methods: 80% of MRM transitions analyzed over 10 replicates has %CV < 15%, but with over 700 MRM transitions in the assay.

transitions) was monitored (Figure 4, green lines). Again, a large increase in dwell time is obtained upon using the Scheduled MRM Algorithm for scheduling such a large numbers of MRM transitions, hence the increase in data quality and reproducibility. In this case, with many more analytes, a dwell time of 5 msec was used, giving a cycle time of 3.3 sec for the unscheduled method (dotted green lines). After time-scheduling, the average dwell time was 20 msec and the target cycle time was set at 1 sec (solid green lines).

Fast polarity switching

The next step was to combine both the positive mode and negative mode analytes together into a single, final method. This was possible due to the fast polarity switching available on the SCIEX 7500 System. A total of 734 MRM transitions were combined into the final single, time-scheduled MRM assay with polarity switching, to get wide metabolite coverage in a single assay. Ten replicate injections were performed and the peak area reproducibility was compared to the previous single polarity methods (Figure 5, red line). High data quality was maintained when running the complete assay. There is no decay in the cumulative reproducibility curve from what was seen in negative mode only (470 MRMs) when compared to the full polarity switching method (734 MRMs).

In this final dataset, ~70% of analytes were reproducibly measured across 10 replicates with %CV < 10%, and ~85% were measured (or in other words, about 600 MRM transitions)

RUO-MKT-02-13259-A

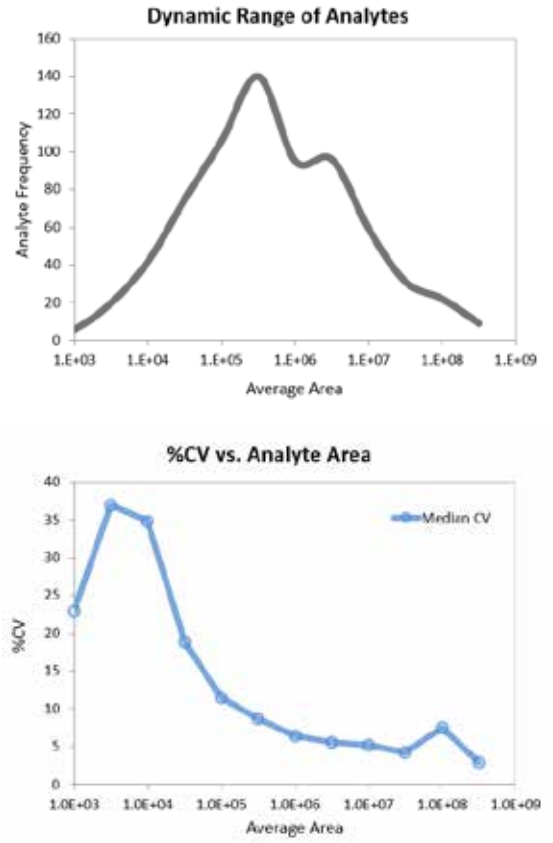

Figure 6. Reproducibility across the dynamic range. Wide dynamic range was observed in the detected metabolites using this assay, with over 4 orders of magnitude (top). As expected, the average observed peak area reproducibility across the 10 replicate injections track with peak area, with only the very lowest analytes having higher %CVs (bottom).

with %CV < 20%. The final average dwell time was 14 msec and the target cycle time was set at 1 sec.

Dynamic range and coverage

The ability to precisely quantify both the high abundant metabolites as well as the low abundant analytes in a large multiplex panel is essential for researchers. This assay covers a wide range of metabolites in plasma spread across a broad range of abundance (Figure 6, top). On both the QTRAP 6500+ System and the SCIEX 7500 System, the instrument dynamic range is very high, up to 6 orders of linear dynamic range, enabling this large assay to be performed in a single run using simple sample preparation. The reproducibility observed for the higher abundant analytes was below 5% CV in the final assay. As expected, reproducibility decreases slightly as the abundance decreases, but still remains good down to the very low abundant, difficult to detect metabolites (Figure 6, bottom).

Finally, the method encompasses compounds from 69 pathways including the TCA cycle, glycolysis, purine pyrimidine metabolism and amino acid metabolism (Figure 7).

Conclusions

The large scale polarity switching method using Scheduled MRM Algorithm has been developed to quantify ~336 serum metabolites in plasma and can be used for large scale targeted metabolomics studies.

- The sMRM Pro Builder Tool was developed to streamline optimization of the sMRM assay and provide insights on MRM assay data quality
- Time scheduling of MRMs provided significant improvements over unscheduled methods for this large of a number of MRM transitions, with 95% of positive mode data and 80% of negative mode data having peak area %CV ≤15%
- Using polarity switching to include both positive and negative ion mode metabolites in a single sMRM method also provided high quality data, with no loss in peak area reproducibility compared to individual single polarity sMRM method
- Improved sensitivity of the SCIEX 7500 System showed up to a 3-5 fold increase in signal to noise ratio over the QTRAP 6500+ System, which provides detection and quantification of ~30% more metabolites in plasma.[3]

RUO-MKT-02-13259-A

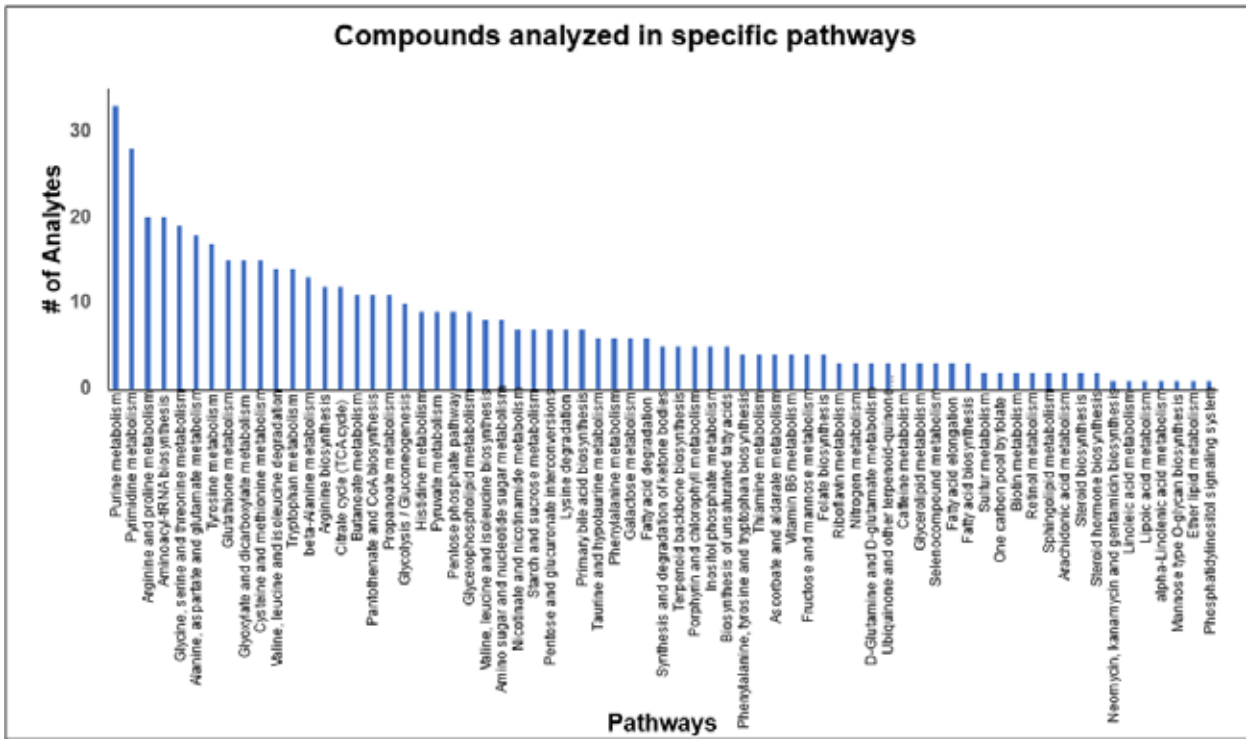

Figure 7. Targeted assay contains metabolites from 69 different metabolic pathways. The compounds present in the method were linked to the pathways they belong to using MetaboAnalyst 5.0 online tool. The compound name list was submitted in the Pathway analysis tool under Annotated features. Further, option *Homo sapiens* (SMPDB) was chosen for library search and match to run the pathway analysis tool. Later, the Patway_results.csv file was downloaded to obtain all the pathways indicated for the list of uploaded compounds.

References

1. Adam MG et al., (2021) Identification and validation of multivariable prediction model based on blood plasma and serum metabolomics for the distinction of chronic pancreatitis subjects from non-pancreas disease control subjects. *Gut 0: 1–9*.
2. Yuan M, Breitkopf SB, Yang X, Asara JM. (2012) A positive/negative ion–switching, targeted mass spectrometry–based metabolomics platform for bodily fluids, cells, and fresh and fixed tissue. *Nat Protocols.* **7(5)**, 872-81.
3. Significant sensitivity increases provides 30% more polar metabolites quantified in plasma. SCIEX technical note RUO-MKT-02-12701-A.
4. SCIEX How solution for Targeted profiling method for metabolomics. SCIEX How, RUO-MKT-02-12750-A.

RUO-MKT-02-13259-A

Significant sensitivity increases provides 30% more polar metabolites quantified in plasma

With the SCIEX Triple Quad™ 7500 LC-MS/MS System – QTRAP® Ready

Robert Proos, Darren Dumlao, Kranthi Chebrolu, Christie Hunter
SCIEX, USA

Studying the impact of biological perturbations on the metabolome requires high sensitivity and specificity, as well as the ability to multiplex large numbers of known metabolites in a single assay. The utility of LC-MS/MS analysis for the quantification of metabolites from biological samples has become widely accepted as the key analytical solution due to the aforementioned requirements.[1]

In addition to very good sensitivity and specificity, targeted analysis using multiple reaction monitoring (MRM) on triple quadrupole MS systems has the advantage of throughput and simplified data processing. By focusing on known important metabolites that are key to biology, quantitative results provide key biological insights. These platforms are capable of fast polarity switching, allowing a broad range of analytes to be interrogated in a single injection. Finally, because of broad dynamic range typically required for biological samples, high sensitivity is a critical attribute of the LC-MS system for the analytes with needing lower detection limits that were previously undetectable and for smaller sample sizes.

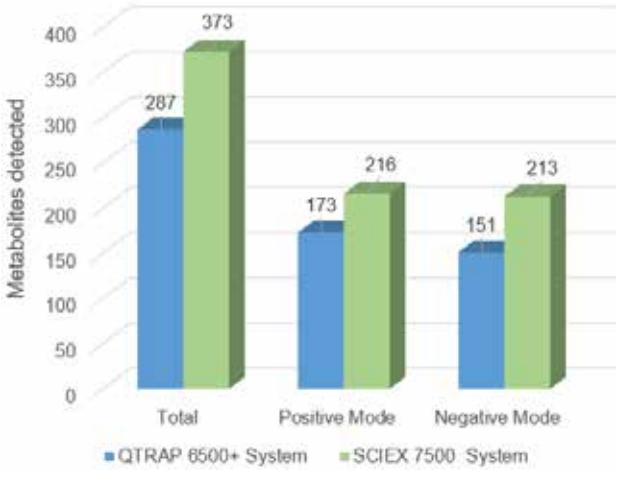

Figure 1. Increased sensitivity on the SCIEX 7500 System improved the number of metabolites detected. A similar analysis was run on both the QTRAP® 6500+ System and the SCIEX 7500 System was performed. The SCIEX 7500 System showed a 25% increase in metabolite detected was observed in positive ion mode, and a 41% increase was observed in negative mode. Note some metabolites were detected in both polarities and thus the overall gain in detected metabolites was 30%.

A targeted LC-MS/MS assay with MRM transitions for over 450 metabolites was used to assess the impact of added sensitivity on the detection and quantification of metabolites in plasma. Using a generic reversed-phase chromatography method and operating the MS systems in both positive and negative polarity modes to obtain broad coverage, a similar method was run on three separate QTRAP 6500+ systems and as well as three separate SCIEX 7500 systems under independent lab settings.

Key features of the SCIEX 7500 System for quantification of polar metabolites

- Provides significant gains in sensitivity though increased generation, capture, and transmission of ions with the:
  - OptiFlow® Pro Ion Source with E Lens™ Technology and the D Jet™ Ion Guide[2]
- NIST SRM 1950 plasma was used as reference material to compare platforms
- Higher sensitivity and S/N on the SCIEX 7500 System yielded large improvements in detected, quantifiable of metabolites- up to 30% more vs the QTRAP 6500+ System (Figure 1)
- Targeted assay is provided, complete with a standard operating protocol, an MRM list, and tools to facilitate method development (sMRM Builder template) can also integrate internal standard kits if required.[3]

RUO-MKT-02-12701-A

Methods

Sample preparation: NIST SRM 1950 plasma was extracted using 8 volumes of methanol then spiked with internal standard QReSS kit (Cambridge Isotopes). After centrifugation to precipitate the proteins, the supernatant was directly analyzed.

Chromatography: Samples were analyzed using the ExionLC™ System with a Kinetex® F5 column (2.1 x 150 mm, 2.6 µm, Phenomenex). Simple linear gradient from 0 to 95% B was used with standard reverse phase mobile phases (A = 0.1% formic acid in water and B = 0.1% formic acid in acetonitrile) with a flow rate of 200 µL/min. A 1 µL injection volume was used and the column temperature was maintained at 30 °C throughout the analysis.

Mass spectrometry: The same extracted sample was analyzed on both the QTRAP® 6500+ System and the SCIEX 7500 System. Data was collected using methods built with the Scheduled MRM™ Algorithm as well as unscheduled methods. Variations of the method were repeated on two additional instrument sets to confirm the observed sensitivity gains. Detailed method information is available in the supplementary method.[3] Finally, this high throughput method is used to analyze over 400 serum metabolites in a 20 min run period.

Data processing: All data was analyzed using the Analytics module in SCIEX OS Software.

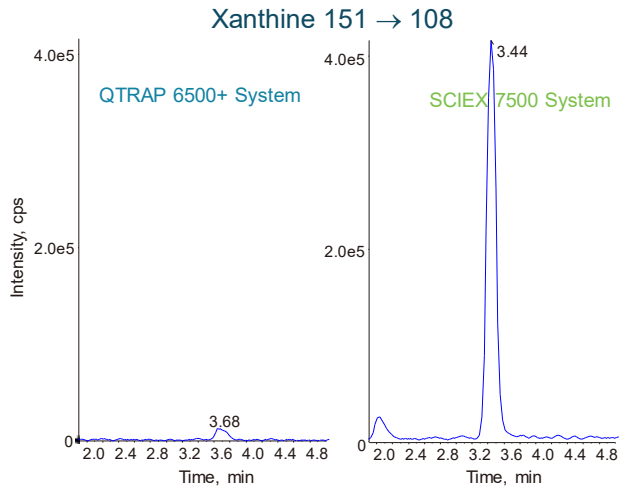

Figure 2. Signal to noise improvement for negative ion mode metabolites. Example shown here for Xanthine, created from guanine during purine degradation. Here the improved area and S/N observed when running the same assay on the SCIEX 7500 System as compared to the QTRAP 6500+ System is highlighted.

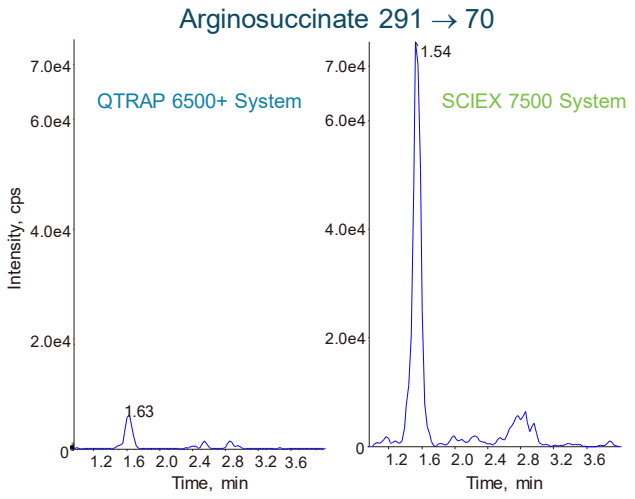

Figure 3. Signal to noise improvement for positive ion mode metabolites. Example shown here of argininosuccinate, an essential amino acid formed from citrulline in the uric acid biosynthetic pathway, highlights the improved area and S/N observed when running the same assay on the SCIEX 7500 System as compared to the QTRAP 6500+ System.

Sensitivity improvements on the SCIEX 7500 System

A number of innovations on the SCIEX 7500 System have resulted in increased sensitivity for MRM analysis. Here, the impact of these sensitivity gains on a targeted metabolomics assay was evaluated by comparing the signals observed after running a similar assay on six instruments (3 QTRAP 6500+ systems and 3 SCIEX 7500 systems). Example comparisons are shown in Figures 2 and 3 for positive and negative ion mode, highlighting the sensitivity gains on the raw signal. Xanthine analyzed in negative ion mode had a small detectable signal on the QTRAP 6500+ System but had a much improved signal on the SCIEX 7500 System (30x area and 8x S/N gains). An example for positive ion mode is argininosuccinate, showing a 13x gain in area and a 4x gain in S/N.

Perhaps more compelling was the ability to detect metabolites on the SCIEX 7500 System that were undetectable (below the noise) on the QTRAP 6500+ System. Two examples are showing in Figure 4, for both positive ion mode (retinal) and negative ion mode (pyridoxic acid). Retinal is a small molecule metabolized through oxidation of β-carotene in the human body and is essential, especially for night vision. Pyridoxic acid is a catabolic product of vitamin B6 metabolism.

RUO-MKT-02-12701-A

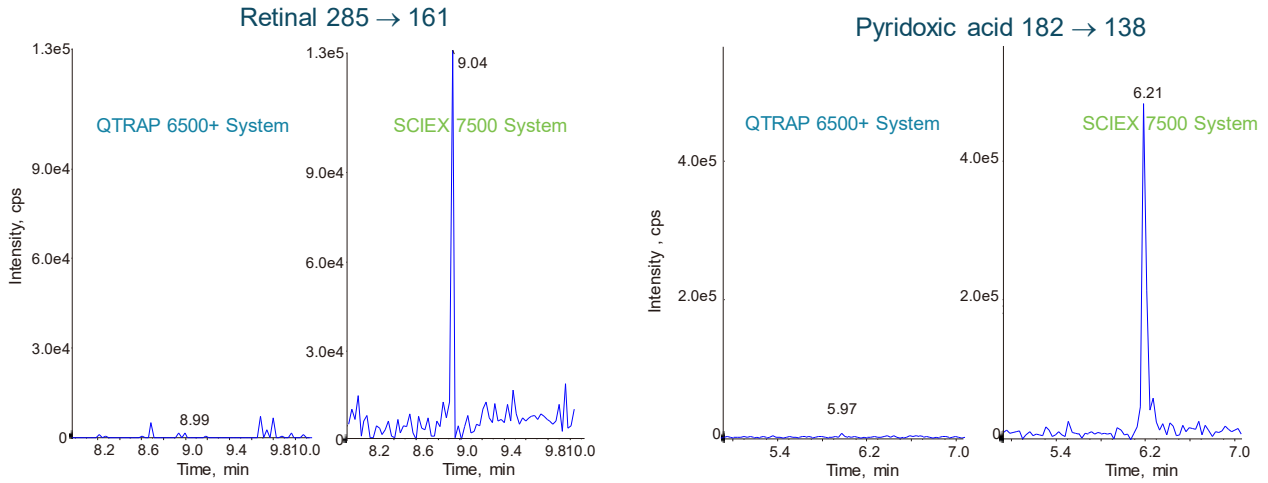

Figure 4. Improved S/N leads to quantification of additional metabolites. Compounds that were not detectable in the plasma sample on the QTRAP 6500+ System are now easily quantified on the SCIEX 7500 System. Retinal was easily quantified in positive ion mode (left) and pyridoxic acid in negative ion mode (right) also showed a large increase in signal and S/N on the SCIEX 7500 System.

Increased numbers of metabolites detected

Next, the results across the assay were compared looking at the peak areas, the peak heights and the S/N between the two instruments and by computing the fold increases for each metabolite. This allowed some general conclusions to be drawn between the two platforms (Table 1). In positive ion mode, the average peak area gain was 17x providing an overall signal / noise gain of 3x. In negative ion mode, the sensitivity increases were a bit more pronounced with a peak area gain of 40x and a S/N gain of 5x. The increased S/N and peak areas led to an increase in the number of metabolites that could be reliably detected and quantified in the assay. Peak detection used a minimum S/N value of 3.

Table 1. Average gains observed on the SCIEX 7500 System vs the QTRAP 6500+ System. The average peak area, peak height and S/N were compared between the two platforms to characterize the average observed gains.

	Average fold increase	
	Positive ion mode	Negative ion mode
Peak area	*17*	*40*
Peak height	*18*	*43*
Signal / noise	*3*	*5*

The resulting gains in metabolites detected and quantified is shown in Figure 1. In positive ion mode, 173 metabolites were detected on the QTRAP 6500+ System and 216 were detected on the SCIEX 7500 System, an increase in detected metabolites of 25%. The results were even more significant in negative mode, with 151 metabolites detected on the QTRAP 6500+ System and 213 detected on the SCIEX 7500 System - a gain of 41%. As some metabolites were measured and detected in both polarities, the overall gain in detected metabolites was 30%.

Confirmation of results on multiple instrument platforms

In order to ensure a robust conclusion, sample analysis was repeated across multiple instrument sets: a total of three QTRAP 6500+ systems and three SCIEX 7500 systems. The S/N for each metabolite detected was measured and then compared between both instruments to compute a fold increase in signal to noise. This was done across the dataset such that a normal distribution for each instrument set could be plotted (Figure 5). Due to the wide range of analytes covered in these global targeted methods, global source conditions were used on both instruments. This is likely the source of some of the larger, or smaller, than expected sensitivity differences between platforms. Nevertheless, the data demonstrated the general increase that can be expected upon translating this global metabolomics method from the QTRAP 6500+ System to the SCIEX 7500 System.

RUO-MKT-02-12701-A

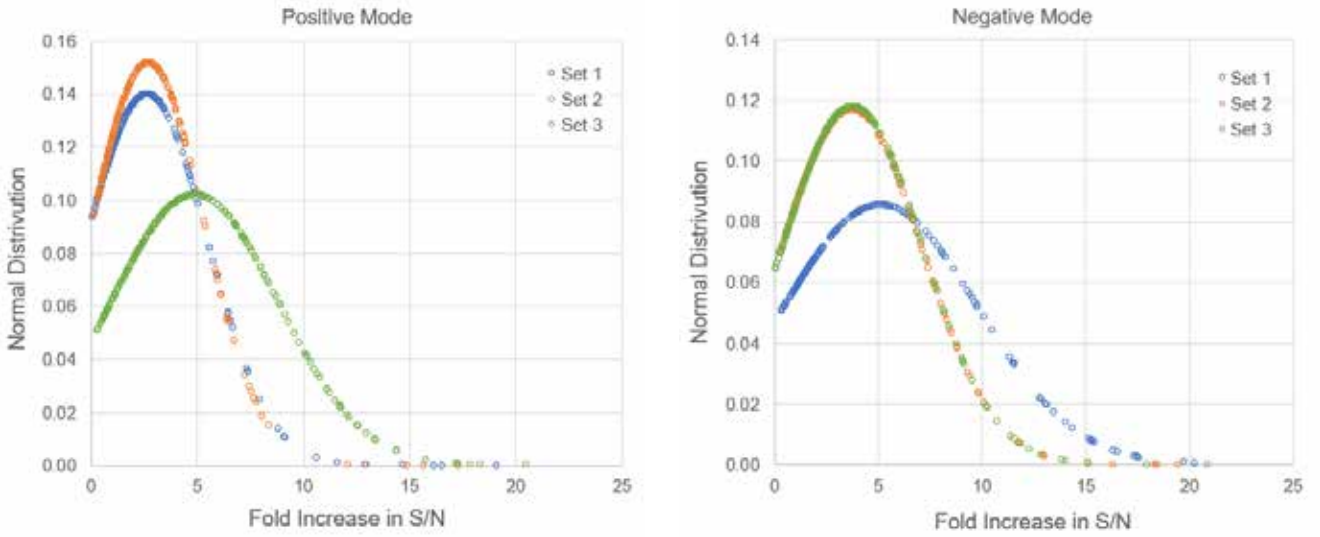

Figure 5. Repeating results on multiple instruments. To confirm the observed sensitivity gains from instrument set 1, similar methods were run on two more instrument sets. As shown in the distributions for the three instrument sets, similar sensitivity gains were observed in both polarities. On average, signal to noise gains of ~3.5 were observed for the SCIEX 7500 System for each instrument set tested. Note general source conditions must be used when monitoring such wide ranging analytes, likely resulting in the broader than expected distribution of S/N gains.

Conclusions

- A targeted MRM assay was developed and run on extracted NIST SRM 1950 plasma in order to compare the performance between the QTRAP 6500+ System and the SCIEX 7500 System
- The higher sensitivity of the SCIEX 7500 System allowed for the detection and quantification of ~30% more metabolites in plasma. Specifically, there was a 25% increase in positive mode, and a 41% increase in negative mode
- The assay was repeated on two other instrument sets to confirm the observation. Using the increase in S/N as the measure of improvement, all three instrument sets showed significant improvements in S/N for a large number of metabolites.

References

1. Yuan M, Breitkopf SB, Yang X, Asara JM. (2012) A positive/negative ion–switching, targeted mass spectrometry–based metabolomics platform for bodily fluids, cells, and fresh and fixed tissue. *Nat Protocols.* **7(5)**, 872-81.
2. Enabling new levels of quantification. SCIEX technical note RUO-MKT-02-11886-A.
3. Targeted profiling method for metabolomics.

RUO-MKT-02-12701-A

ME/TED：新一代靶向代谢组学数据分析软件及其应用

ME/TED: New Generation Software for Targeted-metabolomics Data Analysis

满卓[a]，郝亚芳[b]，司丹丹[a]，龙志敏[a]，刘冰洁[a]，陈爱明[b]
Zhuo Man[a], Yafang Hao[b], Dandan Si[a], Zhimin Long[a], Bingjie Liu[a], Aiming Chen[b]
[a] SCIEX应用支持中心，中国；[b] 大连达硕

关键词： ME/TED; Targeted Metabolomics; 重叠峰自动解析; 人工智能

前言

在生命科学、临床诊断、营养健康与植物代谢等领域，靶向代谢组学对于精准剖析生物体内特定代谢物的变化及功能至关重要。随着研究的深入，对数据分析的准确性、高效性和全面性提出了更高要求。SCIEX与大连达硕联合推出的ME/TED（MExplorer Ultimate/Targeted Engine for Data Processing）新一代靶向代谢组学数据分析软件，凭借其强大的功能为科研工作者提供了有力支持，通过以下应用案例展现其卓越性能。

基于SCIEX Triple Quad系统进行大规模靶向血浆代谢组学检测方法开发，用于定量血浆分析。通过检测336种血清代谢物，涵盖11类代谢物及69条代谢途径。样品经甲醇提取、离心后分析，采用ExionLC AE系统和Kinetex F5柱进行色谱分离，在SCIEX Triple Quad液相串联三重四极杆系统上进行质谱检测。

ME/TED软件具有以下主要特点

1. **一站式全流程分析：**ME/TED为用户提供从样本管理到数据管理、信号处理到统计分析、网络与通路分析，以及数据整合的一站式解决方案，确保研究过程连贯且高效，避免在多个软件间切换带来的麻烦与信息损失。
2. **自动化峰表提取：**运用先进算法自动进行MRM离子分析处理与多样本的峰表提取，有效减少人为误差，大幅提升数据处理的速度和准确性，确保实验结果的可靠性。
3. **重叠峰去卷积：**针对高通量样本中常见的离子对与多组分重叠问题，软件具备高效的去卷积能力，能够精准解析复杂质谱数据，使分析结果更加可靠，有效解决传统分析方法在处理复杂数据时的重复工作与困难挑战。
4. **专属数据库构建与应用：**支持用户构建专属代谢物数据库，涵盖化合物、质谱条件等关键信息，不仅提高代谢物注释准确性，还为个性化研究提供有力支撑，满足不同研究的特殊需求。
5. **不同样本类型特征性代谢物分析：**根据不同样本类型构建特征性代谢物数据库，帮助研究人员快速识别和分析样本中的特征代谢物，深入挖掘其生物学意义，为研究疾病机制和生物标志物提供便捷途径。
6. **拟靶向离子对数据库：**创新性地结合非靶向和靶向分析的优势，通过构建拟靶向离子对数据库，实现更高效的数据解析和更广泛的化合物覆盖，提升对生物样本中代谢物分析能力。

图1. ME/TED软件登录界面展示

RUO-MKT-02-34599-ZH-A

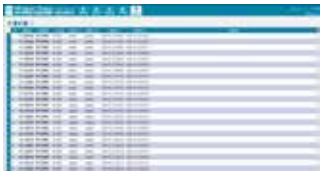

分样本类型的数据库

离子对数据库

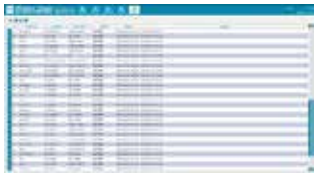

分应用场景的数据库

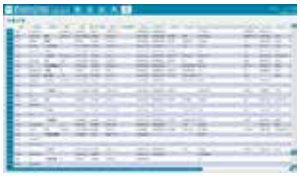

其他数据库

图2. 数据库管理界面展示

仪器设备

图3. SCIEX Triple Quad™ 三重四极杆系统

实验方法

样本制备：以NIST SRM 1950血浆为样本，加入8倍体积甲醇进行萃取，再添加内标QReSS试剂盒(Cambridge Isotopes)。经离心使蛋白质沉淀后，取上清液直接用于后续分析。

色谱分析：使用配备Kinetex F5色谱柱(2.1×150mm, 2.6 µm)的ExionLC AE系统对样品进行分析。采用从0到95%B的简单梯度，流动相为标准反相体系(A=0.1%甲酸水溶液，B=0.1%甲酸乙腈溶液)，流速为0.2 mL/min。进样量为1 µL，柱温：30℃。

质谱分析：样品提取物在SCIEX Triple Quad™ 三重四极杆系统上进行分析。数据采集采用基于动态分窗口保留时间的多反应监测(Scheduled MRM)算法构建的方法。这种高通量方法用于在20分钟运行时间内分析代谢物。

代谢组学分析流程图

图4. 靶向代谢组学分析流程图

采用上述SCIEX仪器检测获取原始数据后，ME/TED软件首先创建靶向分析项目，进入数据管理界面，导入并处理离子对和原始数据，可对数据绘图。在此基础上校正保留时间，再按参数提取色谱峰并可手动确认。定量分析时依据标准品数据构建标准曲线，将色谱峰面积转换为化合物浓度。差异物发现与通路分析通过调用One-MAP云平台服务，设定算法链与算法参数，上传数据并分析后便获得结果。

数据分析结果展示

1. 数据项目创建

运用MExplorer Ultimate软件系统分析336种血清代谢物数据。软件兼容性强，能直接导入处理SCIEX Triple Quad质谱系统采集的数据，且可实时质控，即采集时就能监控数据质量。项目创建操作简便，用户登录进入“项目管理”界面，点击“新建”按要求设定后选“靶向分析项目”类型，项目建成后自动进入“数据管理”界面，其规范的命名规则和流畅流程提升了数据管理效率，有力支持研究开展。如图5所示。

2. 数据管理与预处理

数据管理与预处理功能优势显著。在数据管理上，离子对管理可灵活导入、导出、新增、修改和删除离子对数据，契合诸如336种血清代谢物的检测需求；样本管理支持英文文件名数据导入，能精准设置实验条件、添加分类配对标签，便于样本分组对比。数据预处理方面，其数据校正基于色谱峰评分构建校准曲线校正保留时间；色谱峰提取依参数精准提取并支持人工确认调

RUO-MKT-02-34599-ZH-A

图5. 代谢组学数据分析流程图

图6. 数据管理界面

整；QC校正进一步校准峰提取结果。这些功能紧密协作，为后续定量分析和差异物发现提供高质量数据。如图6所示。

3. 色谱峰提取与校正

色谱峰提取与校正功能亮点突出。色谱峰提取能依精确参数从血清等复杂代谢物数据中智能高效提取离子对色谱峰。在重叠峰解析上，ME/TED凭借先进算法综合分析峰形、保留时间和质谱信息，精准区分重叠峰成分，减少误判。校正功能方面，数据校正通过评分选校准点构建曲线校准保留时间，QC校正进一步优化数据，二者协同降低人工定量识别峰的工作量，提升分析效率，保障研究中血清代谢物分析的准确性。如图7所示。

4. 定量分析与标准曲线构建

构建标准曲线时，简单点击按钮便能选择检测标准品的化合物，软件自动依据标准品色谱峰面积和浓度构建对应关系，确保准确性。在定量分析中，软件以标准曲线为依据，将样本色谱峰

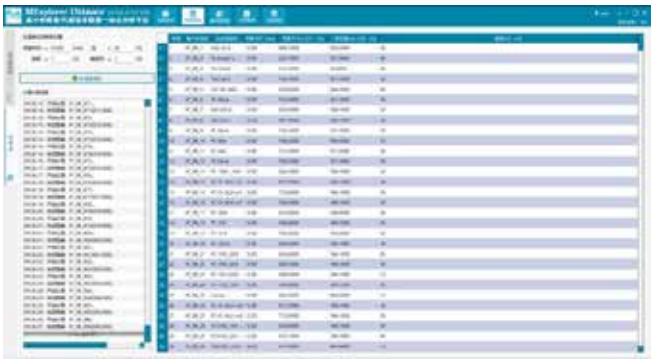

图7. 色谱峰提取界面

面积快速准确映射为化合物浓度，实现自动化批量处理，减少人工计算量和误差，为血清代谢物浓度测定提供可靠支持，助力深入研究。如图8所示。

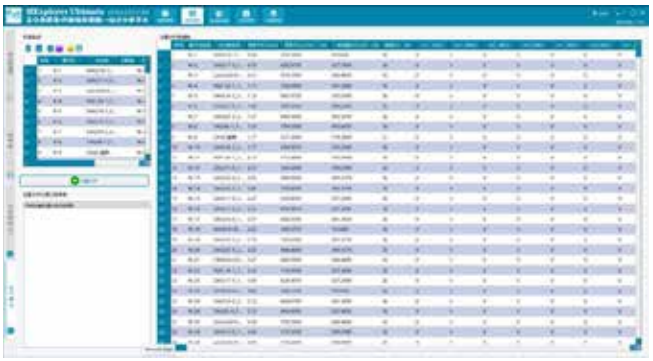

图8. 定量分析界面图

5. 整合分析(如有需要)

若研究涉及正、负离子整合分析，则可先在ME软件中创建正、负离子数据分析两个项目，进而实现高效整合分析。峰表整合时，可先从负离子项目导出峰表，再在正离子项目中设置合并名称、匹配样本后合并峰表。整合后可灵活切换原始峰表和多个整合峰表状态。整合峰表的差异物分析操作与整合前相同，能在不同峰表状态下进行，助力深入探究代谢物变化规律和代谢机制。如图9所示。

6. 差异物发现与通路分析

若研究涉及差异物发现与通路分析，ME/TED软件可调用OneOMAP云平台服务，该平台集成海量质谱库与丰富算法链，能精准分析质谱数据。用户在软件中设定对比分析项，选定或创建One-

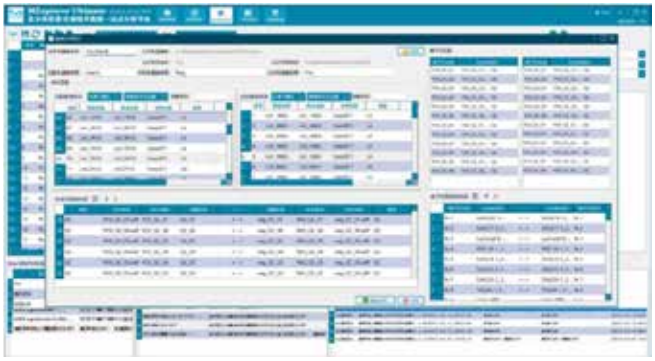

图9. 代谢组学数据分析流程图

图10. 代谢组学数据分析流程图

MAP项目及算法链后点击执行，软件自动上传峰表等信息。分析完成后，可在软件端查看差异物分析和通路分析结果。其中，差异物分析能精准找出不同样本组间的代谢物差异，通路分析则通过直观图表展示代谢物参与的生物通路，帮助研究人员深入理解血清代谢物变化在生物过程中的意义。如图10所示。

7.报告输出

最终结果以分析报表形式输出，内容全面，涵盖数据质量监控、色谱峰提取、定量分析、差异物与通路分析等多方面。ME/TED可详细记录实时质控、色谱峰参数、代谢物定性定量信息，以图表展示差异代谢物表达变化和生物通路，为研究成果呈现、论文撰写及深入研究提供有力支持，助力研究人员高效解读数据、挖掘生物学意义。如图11所示。

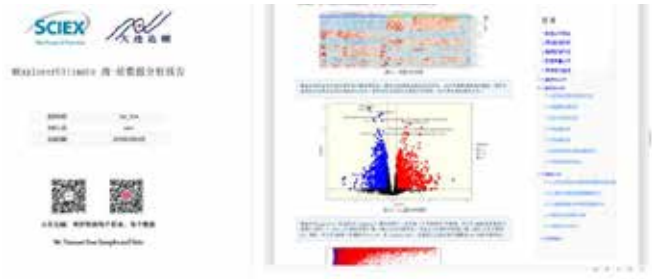

图11. ME/TED分析报告

结果与讨论

本案例成功分析336种血清代谢物，多次实验定量结果稳定，大多数离子在MRM监测下CV<20%，高丰度代谢物重现性更佳(CV<5%)。通过分析不同样本组差异代谢物，涉及69条代谢途径，为探究疾病代谢机制提供依据。ME/TED软件一站式分析、实时质控、超大规模定性及高效差异物发现功能优势明显，可极大推动代谢组学研究。

结论

靶向代谢组学分析中，ME/TED软件凭借一站式分析、重叠峰解析、精准定量以及智能化差异物发现等突出功能，可显著提升研究效率与准确性，在代谢组学研究领域展现出极大的应用价值。ME/TED软件通过精准构建标准曲线，可靠测定不同丰度代谢物浓度，重复实验数据稳定。差异物发现与通路分析功能中，软件调用One-MAP云平台，精准定位不同样本组的差异代谢物及其参与的关键代谢途径，助力深入探究生物过程的代谢变化机制。

RUO-MKT-02-34599-ZH-A

Targeted metabolomics in rat urine using Zeno MS/MS

Analysis on the SCIEX ZenoTOF 7600 system

Kranthi Chebrolu[1], Jason Causon[2], Robert Di Lorenzo[2], Christie Hunter[1]
[1]SCIEX, USA; [2]SCIEX, Canada

Often researchers in academic labs and those performing clinical trials are only given very small amounts of sample, and need to get the most information from the modest volume. This requirement drives the need for targeted assays with high sensitivity and specificity, to obtain high-quality, quantitative results in complex biological samples and to deliver biological insight. High-resolution accurate mass (HRMS) systems have excellent utility in untargeted metabolomics and compound identification in complex matrices because of their high specificity and full-scan MS/MS quality. However, HRMS instruments typically have not been the chosen instrument to perform accurate quantification of a targeted panel of analytes because of their lower sensitivity. In addition, some high resolution platforms cannot keep high resolution at the scan speeds required for fast analyses.

With the introduction of the SCIEX ZenoTOF 7600 system, scientists can now achieve quantitative results at high speeds with high mass accuracy. The core innovation on the ZenoTOF 7600 system is the Zeno trap that when activated, provides significant improvements in duty cycle due to the optimization of ion transmission from the collision cell into the accelerator.[1] This duty cycle improvement provides a substantial increase in MS/MS sensitivity and thus enables targeted high resolution workflows. Here, a small, targeted assay for metabolites in urine from a diabetic rat model was used to characterize the MRM^{HR} workflow and the impact of Zeno MS/MS on the quality of quantitative results.

Urine samples from a Zucker diabetic rat model were obtained and a targeted assay for 13 metabolites was developed. Sensitivity between the Zeno trap on and Zeno trap off methods was compared and a significant gain in MS/MS signal was observed (for example: cAMP fragment in Figure 1 shows a ~12-fold improvement). In this technical note, the complete workflow from data acquisition through to statistical analysis of results is described.

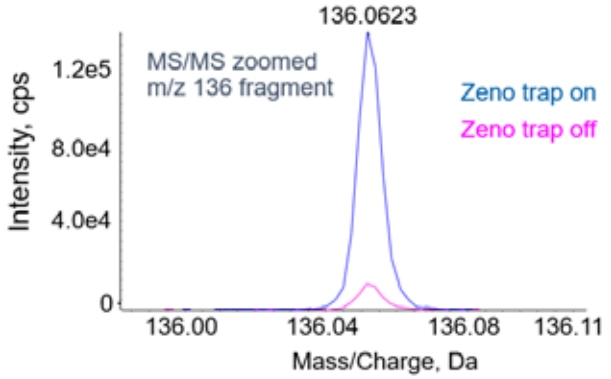

Figure 1. Significant sensitivity gains in MS/MS. Comparison of extraction ion chromatograms (XICs) for cAMP fragments obtained from MS/MS collect with Zeno trap on (blue) vs. Zeno trap off (pink). Signal/noise ratio improved ~12.5 fold when using the Zeno trap. This XIC is from a 2 µL injection of diluted urine.

Key features of the ZenoTOF 7600 system for targeted metabolomics

- Significant increases in MS/MS sensitivity due to Zeno trap, which delivers ≥90%[1] duty cycle on MS/MS fragments while still maintaining fast acquisition rates (up to 133 Hz)
- MS/MS XIC peak area gains of ~13 fold with Zeno trap activated for high-sensitivity quantification of detected metabolites
- Flexibility of a QTOF instrument for additional workflow
  - SWATH acquisition, data dependent acquisition, electron activated dissociation (EAD)
- Powerful data processing tools in SCIEX OS software for accurate quantification, followed by multivariate statistical analysis using MarkerView software

RUO-MKT-02-13297-B

Methods

Sample preparation: Urine samples were collected from four distinct rat groups: Zucker diabetic fatty (ZDF) rats, male and female; Sprague Dawley (SD) rats, male and female. Urine was collected from N=5 rats per group. 20µL of urine was aliquoted and diluted 10-fold with mobile phase A prior to LC-MS/MS analysis.

Chromatography: An ExionLC AD HPLC system (SCIEX) with a Phenomenex Luna Omega Polar C18, 3 µm 150 x 2.1 mm (00F-4760-AN) was used for sample separation. A simple linear gradient from 0 to 95% B was used with standard reverse phase mobile phases (A = 0.1% formic acid in water and B = 0.1% formic acid in acetonitrile) with a flow rate of 300 µL/min. Either a 0.2 or 2 µL injection volume was used and the column temperature was maintained at 40 °C throughout the analysis. The total run time was 13.1 min including 2 min of equilibration.

Mass spectrometry: MRM^{HR} data was acquired on the SCIEX ZenoTOF 7600 system in positive ESI mode using SCIEX OS software. The ion source conditions were as follows: CUR 35, GS1 55, GS2 55, ISVF 5500, TEM 600 °C. High resolution MS/MS was collected for each metabolite using an accumulation time of 10 msec. A collision energy (CE) of 30 was used for each MS/MS. Methods were built with the Zeno trap both activated and deactivated to enable the sensitivity comparisons. Three replicates were collected on each sample with each method.

Data processing: MS/MS interpretation, peak integration, and quantitative analysis were conducted in SCIEX OS software, then results were imported into MarkerView software for multivariate statistical analysis (Figure 2). To build a processing method for MRM^{HR} data, the MS/MS spectrum was first examined in the Explorer module to select the best fragment ion. This was also compared to the library spectrum from LibraryView software using the SCIEX Accurate Mass Metabolite Library

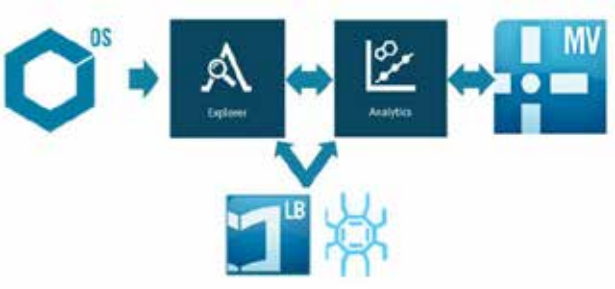

Figure 2. Workflow diagram. Data was both acquired and processed using SCIEX OS software. MS/MS was interpreted using both Explorer and Analytics, library searching was performed using the Library View and ChemSpider.

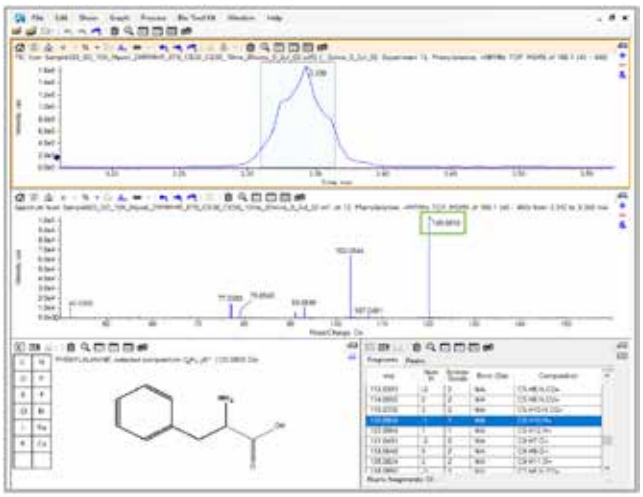

Figure 3. Explorer in SCIEX OS software for metabolite identification. The top pane shows the extracted ion chromatogram (XIC) of phenylalanine, whereas the middle pane shows the experimental accurate mass MS/MS which can be used to select the fragment mass of interest from LibraryView software. The bottom pane shows the structure obtained from ChemSpider that provided in silico (theoretical) fragmentation and accurate mass information that was later used in the calculation of mass error.

(AMMSL 2.0). Structural information from ChemSpider was also used to confirm the identity of the fragment and obtain the theoretical m/z of fragment of interest to be used. This fragment accurate mass information obtained in Explorer mode (Figure 3) was then used to build a final processing method in the Analytics module of SCIEX OS software. Peak areas of the fragment ions were then imported into MarkerView software for statistical analysis.

Zeno MRM^{HR} workflow for targeted quantification

When activated, the Zeno trap provides a significant increase in MS/MS signal on the ZenoTOF 7600 system, while maintaining very high acquisition rates, and not sacrificing mass resolution. Using a targeted MRM^{HR} assay for 13 metabolites in urine, the sensitivity gains due to the activation of the Zeno trap was explored. Extracted ion chromatograms (XICs) were compared from the data collected with the Zeno trap on and off to determine gains in sensitivity. As shown in Figure 1, cyclic AMP produces a dominant fragment ion at *m/z* 136.0618 with significant signal gains of over 10 fold observed.

To address the concerns of limited sample volume, a comparative experiment was performed using a 0.2 µL injection volume with the Zeno trap on, and a 2 µL injection volume with Zeno trap off (Figure 4). Even with ten-fold less sample injected on column, the peak area for the XIC of the *m/z* 136.0618

RUO-MKT-02-13297-B

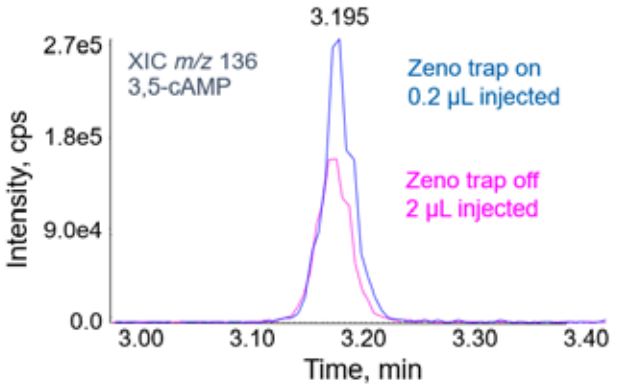

Figure 4. Better sensitivity in MS/MS with 10x less sample. Comparison of extraction ion chromatograms for cAMP fragments obtained from MS/MS collect with Zeno trap on (0.2 µL injection, blue) vs. Zeno trap off (2 µL injection, pink). Signal/noise ratio improved ~1.5 fold when using the Zeno trap. MS/MS acquisition rates are very fast (10 msec accumulation) providing 15 data points across the peak at base.

fragment mass with the Zeno trap on ~1.5 fold higher. With higher dilution factors or lower loading of complex matrices on column, matrix effects are reduced improving data quality. Also the ability to analyze much lower sample volumes can be an advantages for some researchers with very precious samples.

The comparison between Zeno trap off vs. on was done for each of the 13 metabolites analyzed and the results are summarized in Table 1. The data quality specifications such as fragment mass error, library match and area gains with the Zeno trap on are presented in Table 1. The mass error for the quantifiable fragment ions were <3ppm for 12 out of 13 compounds analyzed in this study. On average, the significant area gains obtained with the Zeno trap on for MS/MS is 14-fold higher compared to the Zeno trap off. It is important to note that the MS/MS acquisition rate was very high (10 msec accumulation time per MS/MS).

MarkerView software for statistical analysis

Here, a small sample set was explored to test the workflow from quantification to statistical analysis (Figure 5, Table 2).[3,4] Note these metabolites were selected based on previous results from a SWATH acquisition study on the same sample set.[2] Metabolites of interest were selected and included in this targeted assay study. Unsupervised principle component analysis (PCA) was used to generate the two-dimensional score plots in MarkerView software (MV). The four categories of mouse models, ZDF-male and female, SD-male and female have clustered differentially, are clearly separated, and 97% of the variance was explained by the PC1 and PC2 (Figure 5, top).

Table 1. Increased quality of MS/MS spectra due to Zeno trap. Activation of the Zeno trap provided significant MS/MS signal increase and therefore large increases in fragment ion XICs (average of 13.6 fold). High mass accuracy and very good library hits were observed for the resulting Zeno MS/MS spectra.

Metabolite	Fragment ion (m/z)	Library match	MS/MS fragment mass error (ppm)	Area gain with Zeno trap on (on/off)
Acetylglutamate	*84.0444*	√	*-0.14*	*12.51*
Arginine	*70.0651*	√	*3.73*	*13.18*
Carnitine	*103.0401*	√	*-4.52*	*11.12*
Creatine	*43.0291*	√	*3.87*	*18.11*
Cyclic AMP	*136.0618*	√	*2.56*	*10.00*
Glutamine	*84.0444*	√	*1.72*	*18.08*
Histidine	*110.0713*	√	*0.24*	*26.72**
Leucine	*69.0699*	√	*0.56*	*15.83*
Methyladenosine	*150.0778*	√	*1.28*	*10.28*
Phenylalanine	*120.0808*	√	*2.37*	*10.38*
Tryptophan	*118.0651*	√	*0.26*	*11.93*
Tyrosine	*119.0495*	√	*-3.81*	*8.89*
Uric acid	*141.0407*	√	*4.24*	*10.29*
			Average area gain:	***13.64***

**Zeno trap off peak area very low, hard to measure*

The loading plots showed four PCV groups (data not shown). Metabolites showing large changes on the loadings plot were selected and displayed as box and whisker plots across the samples (Figure 5 bottom). cAMP and methyladenosine had similar pattern of difference across the samples, while creatine showed a different pattern across the ZDF and SD urine samples.

SWATH acquisition to MRM^{HR} workflow

Here, the ability to create a SWATH acquisition to MRM^{HR} workflow for metabolomics was also demonstrated, as SWATH acquisition was performed on the same sample set on the same instrument. Metabolites that showed differences in abundance between experiment groups from the SWATH acquisition data were selected along with a few additional metabolites, and used to build a targeted MRM^{HR} method. Good correlation was observed in the fold change results between the different diabetic mice vs. the SD male sample for the eight metabolites measured in both datasets ($r^2 \geq 0.92$ for all the group comparisons, Figure 6). This highlights the feasibility of

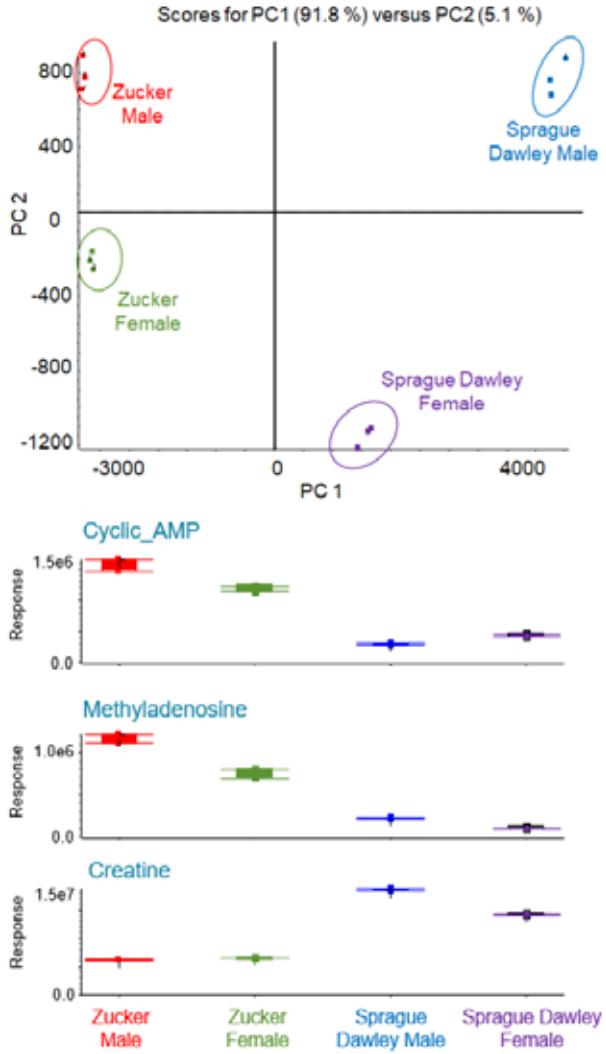

Figure 5. Principal component analysis (PCA) highlights clear differences between samples. Peak areas from MRM^{HR} data were imported into MarkerView software and PCA-PCVG was performed. (Top) Scores plot shows both good reproducibility between replicate injections and clear separation of the different rat urine samples, even with just these 13 targeted metabolites. (Bottom) Box and whisker plots for selected analytes highlights the differences seen across the samples.

performing the non-targeted screening workflow as well as a targeted quantification assay on a single HRAM system.

With the SWATH acquisition workflow, a large number of metabolites can be quantified from a single run and provide preliminary quantitative results to find differences between samples. When an MRM^{HR} assay is next developed for the same analytes, a much more narrow Q1 isolation window is used

Table 2. Differences in metabolite abundances between the rat urine samples. Using the male SD rats for comparison, the peak area fold changes (log 2 peak area ratio) were computed.

	Log2 peak area ratios		
Metabolite	**SD female / SD male**	**ZDF female / SD male**	**ZDF male / SD male**
Acetylglutamate	*-0.94*	*0.40*	*0.36*
Arginine	*-1.32*	*-4.42*	*-1.44*
Carnitine	*1.77*	*3.59*	*2.90*
Creatine	*-0.38*	*-1.53*	*-1.60*
Cyclic AMP	*0.56*	*1.97*	*2.39*
Glutamine	*3.62*	*6.34*	*4.92*
Histidine	*-0.09*	*-1.08*	*-2.33*
Leucine	*-1.35*	*-2.06*	*-2.47*
Methyladenosine	*-1.11*	*1.78*	*2.39*
Phenylalanine	*-0.76*	*-2.04*	*-3.48*
Tryptophan	*-0.51*	*-3.50*	*-3.49*
Tyrosine	*-0.83*	*-3.01*	*-3.94*
Uric acid	*0.17*	*1.71*	*0.73*

providing higher specificity of detection, and thus providing an addition confirmation of the screening results. And with the ZenoTOF 7600 system, this can be performed on the same system.

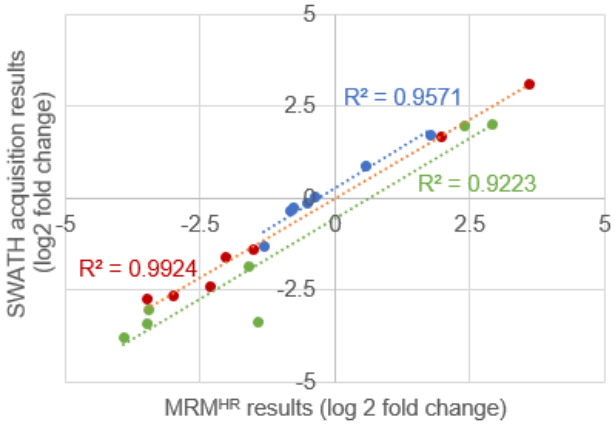

Figure 6. Correlation of quantitative results from SWATH acquisition and MRM^{HR} workflow. The log2 fold change results were computed for eight compounds across the three groups of comparisons: SD female/SD male, ZDF female/SD male and ZDF male/ SD male. Very good correlation was obtained between the two different quantitative techniques.

RUO-MKT-02-13297-B

Conclusions

Here, the targeted MRM^{HR} workflow on the ZenoTOF 7600 system has been explored for use in quantification of metabolites in biological samples.

- Zeno MS/MS provided a 13-fold average increase in MS/MS sensitivity, thus providing both high-quality, full-scan MS/MS data for each metabolite for confident compound identification as well as large increases in fragment ion XIC areas for higher sensitivity quantification
- The sensitivity improvements with the Zeno trap provides the user with more workflow options; for instance, greater sample dilution to reduce matrix effects, or to perform small injection volumes for the analysis of volume-limited samples
- Raw data processing in SCIEX OS software and multivariate statistical analysis visualization using MarkerView software delivers the complete workflow from identification to quantification
- In addition, the ability to transition from non-targeted SWATH acquisition studies to targeted MRM^{HR} workflow on a single MS instrument was demonstrated.

References

1. Qualitative flexibility combined with quantitative power - Using the SCIEX ZenoTOF 7600 LC-MS/MS system, powered by SCIEX OS software. SCIEX technical note, RUO-MKT-02-13053-A.
2. Rapid analysis and interpretation of metabolomics SWATH acquisition data using a cloud-based processing pipeline. SCIEX technical note RUO-MKT-02-13056-A.
3. What is principal component analysis and how does it work? SCIEX community post RUO-MKT-18-12137-A.
4. What is principal component variable grouping (PCVG) and how do I use it? SCIEX community post RUO-MKT-18-12137-A.

RUO-MKT-02-13297-B

液相色谱串联质谱法测定20种常见氨基酸的非衍生化方法

A Underivatized Method for the Determination of 20 Common Amino Acids by Liquid Chromatography Tandem Mass Spectrometry

陈金梅，司丹丹，龙志敏，郭立海
Chen Jinmei, Si Dandan, Long Zhimin, Guo Lihai

SCIEX应用支持中心，中国
SCIEX, China

Key words: Amino Acids, Liquid Chromatography Tandem Mass Spectrometry, Underivatized

前言

氨基酸不仅提供了合成蛋白质的重要原料，而且对于促进生长，进行正常代谢、维持生命提供了物质基础。如果人体缺乏或减少其中某一种氨基酸，人体的正常生命代谢就会受到障碍，甚至导致各种疾病的发生或生命活动终止。氨基酸检测对于研究植物在不同条件和不同生长阶段的氮代谢、氮吸收、运输、同化和营养状况的变化同样具有重要意义。因此氨基酸无论是在代谢组学研究还是临床检测都具有一定的意义，然而天然氨基酸的靶向分析存在一些挑战。因为氨基酸是分子量较小，极性较强的一类化合物。氨基酸检测已有多种检测方法，包括紫外（UV）、荧光（FL）、质谱（MS）和电化学检测等方式。通过 UV 和 FL 检测分析 AA 通常需要衍生化步骤，提高检测的分离度和灵敏度，但会导致样品制备繁琐且分析时间长。使用质谱检测方法也多使用衍生化检测方式，即使前处理变得繁琐也没有选择非衍生话的检测方式的一大原因是由于天然氨基酸在反相（RP）色谱柱上的保留较差。本文建立一种快速的氨基酸非衍生化检测方法，为代谢组学和临床检测提供方法参考。

仪器设备

液相方法

色谱柱：Luna Omega SUGAR (150 × 2.1mm, 3 µm)

流动相：A相：水 (20 mM甲酸铵+0.35%甲酸)
B相：90%乙腈 (20 mM甲酸铵+1.15%甲酸)

流速：0.30 ml/min

表1. 液相梯度

Time	Flow	B
2	0.3	95
7	0.3	80
10	0.3	10
12	0.3	10
12.1	0.3	95
15	0.3	95

RUO-MKT-02-14479-ZH-A

柱温：40 ℃

进样量：1 μL

质谱方法

离子源：ESI源，正离子模式

离子源参数：

IS电压:：3000 V　　气帘气 CUR: 20 psi

雾化气 GS1: 55 psi　　辅助加热气 GS2: 50 psi

碰撞气 CAD: Medium　　源温度 TEM: 650 ℃

表2. 化合物的质谱参数

Name	Q1	Q3	CE	DP
Alanine	90.1	44.1	16	40
L_Arginine	175.1	70.0	30	40
L_Asparagine	133.1	74.0	21	30
Aspartic Acid	134.2	88.0	14	50
L_Cystine	241.1	152.1	17	50
L_Glutamine	147.1	84.1	23	30
L_Glutamic Acid	148.1	84.0	21	40
Glycine	76.2	30.1	18	30
L_Histidine	156.1	110.0	20	40
Leucine	132.1	86.0	15	40
Isoleucine	132.1	86.0	15	40
L_Lysine	147.1	84.1	23	30
L_Methionine	150.1	104.0	14	40
L_Phenylalanine	166.2	103.0	38	40
L_Proline	116.1	70.1	21	45
L_Serine	106.0	60.1	17	25
L_Threonine	120.0	74.0	14	30
L_Tryptophan	205.1	188.0	16	30
L_Tyrosine	182.1	136.3	19	40
L_Valine	118.1	72.0	17	30

实验结果

1. 色谱图：使用上述液相色谱条件，15 min之内即可检测20种氨基酸，20种氨基酸出峰时间适中，色谱峰形较好，两对同分异构体实现分离，典型谱图如图所示。

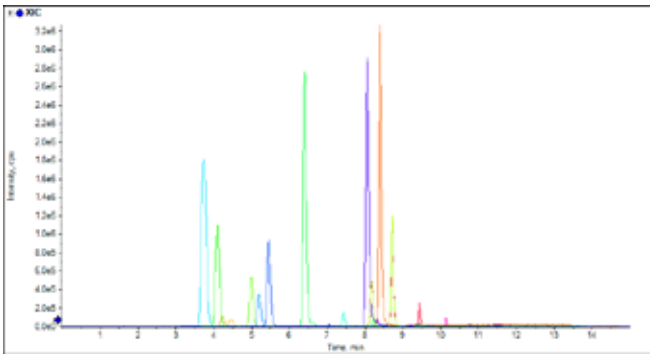

图1. 20种氨基酸的典型色谱图

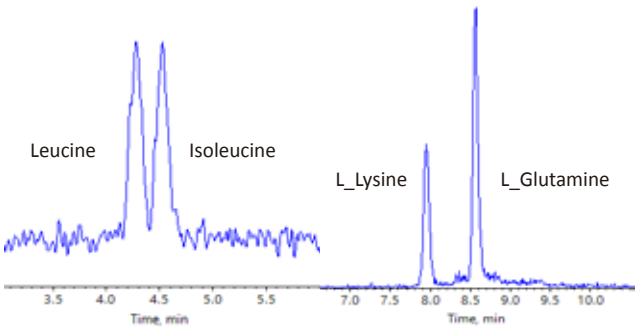

图2. 两对同分异构体的提取离子流色谱图

2. 线性范围和重现性：用水逐级稀释20个化合物的标准工作溶液至不同浓度的标准曲线，以峰面积对浓度做标准曲线。20个化合物最低定量下限样品连续进样6针，RSD在10.0%以内，结果见表3。

3.血浆中的氨基酸含量测定：使用蛋白沉淀法对血浆进行前处理后进行含量测定，大鼠血浆和人血浆样品中检测到氨基酸的含量如下表所示。

表3. 20个化合物的线性范围和相关系数和重现性结果

化合物	线性范围	相关系数	LLOQ重现性
Alanine	0.78-25nmol	0.995	8.36
L_Arginine	0.024-6.25nmol	0.991	3.77
L_Asparagine	0.024-25nmol	0.997	4.23
Aspartic Acid	0.780-25nmol	0.998	8.43
L_Cystine	0.097-12.5nmol	0.996	7.6
L_Glutamine	0.048-3.125nmol	0.996	8.45
L_Glutamic Acid	0.097-25nmol	0.998	5.57
Glycine	3.125-25nmol	0.993	8.58
L_Histidine	0.048-6.25nmol	0.991	7.60
Leucine	0.024-25nmol	0.998	4.66
Isoleucine	0.024-25nmol	0.995	7.18
L_Lysine	0.048-25nmol	0.998	7.14
L_Methionine	0.048-25nmol	0.999	4.49
L_Phenylalanine	0.024-25nmol	0.999	4.39
L_Proline	0.048-25nmol	0.999	6.12
L_Serine	0.097-25nmol	0.997	4.99
L_Threonine	0.097-25nmol	0.999	8.27
L_Tryptophan	0.048-25nmol	0.999	2.40
L_Tyrosine	0.097-25nmol	0.999	4.45
L_Valine	0.024-25nmol	0.999	6.80

表4. 氨基酸含量测定结果

Compound	Human（nmol/ml)	Mouse（nmol/ml)
Alanine	111.438	155.302
Aspartic Acid	12.144	9.986
Glycine	25.1194	42.8821
Isoleucine	24.676	23.088
Leucine	38.446	37.602
L_Arginine	43.79	46.34
L_Asparagine	3.424	7.4
L_Cystine	0.4771	0.1669
L_Glutamic Acid	93.81	30.284
L_Glutamine	95.588	157.52
L_Histidine	23.926	21.244
L_Lysine	25.43	155.368
L_Methionine	5.164	18.396
L_Phenylalanine	17.618	23.008
L_Proline	67.046	38.014
L_Serine	45.612	58.978
L_Threonine	36.418	68.266
L_Tryptophan	12.91	30.142
L_Tyrosine	24.286	26.274
L_Valine	50.248	46.626

总结

本文建立了液相色谱串联质谱法非衍生方式测定20种常见氨基酸，为组学研究和临床检测提供方法参考，可以根据需求进一步进行方法学验证。

RUO-MKT-02-14479-ZH-A

色氨酸代谢物的LC-MS/MS定量分析

Yeqing Peng[1], Huiru. Tang[1], Ting.Liu[2], Zheng.Jiang[2]

1. Human Phenome Institute, Metabonomics and Systems Biology Laboratory at Shanghai International Centre for Molecular Phenomics, Fudan University, Shanghai, China
2. SCIEX, Shanghai, China.

Keywords: Tryptophan metabolites, LC-MS/MS.

前言

色氨酸（Tryptophan, Trp）是必需氨基酸之一。色氨酸通过血清素通路（Serotonin pathway）、犬尿氨酸通路（Kynurenine pathway）和吲哚通路（Indole pathway）而产生一批具有多种生理功能的代谢物, 在生物体和植物体内发挥着重要作用（图1）。譬如，色氨酸就是按蚊的必需氨基酸，主要是由所吸的血液供应。在按蚊体内，色氨酸除了供应蛋白合成，大多数游离色氨酸通过犬尿氨酸代谢途径被氧化，从而生成犬尿酸（kynurenine, Kyn），3-羟基犬尿酸（3-hydroxykynurenine, 3-HK）和黄尿酸（xanthurenic acid, XA）。为了研究按蚊体内微生物对色氨酸和其代谢物的影响变化，本文建立了色氨酸及其15种代谢物的液相串联质谱（LC-MS/MS）定量测定方法，该方法也可应用于其他生物体或植物体的色氨酸和其代谢物的测定。

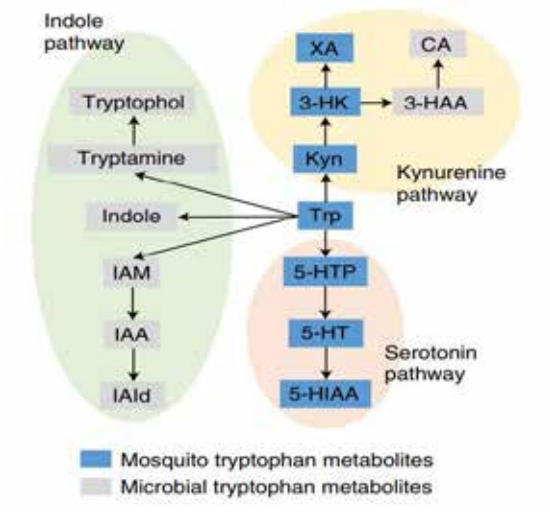

图1. 色氨酸及其主要代谢通路[1]

本文实验方法特点

1. 灵敏度高，满足多种基质的检测需求；
2. 方法覆盖率全，基本覆盖了色氨酸和其主要代谢物；
3. 方法准确性和重现性良好，符合方法学要求；

仪器设备

样品前处理

收集15只雌性按蚊（~30mg）作为1份生物样本。将样本液氮速冻，使用400 μL预冷的80%甲醇-双蒸馏水（ddH_2O）溶液(含10 μL内标，内标具体信息详见质谱方法) 匀浆样本。14000 g，4 ℃离心10 min后，保存上清，再使用400 μL预冷甲醇-双蒸馏水溶液进行2次萃取。混合所有上清液，14000g，4 ℃离心10 min。 然后，将1 mL上清液转移到新管中，冷冻干燥待用。LC-MS/MS分析前，使用200 μL 80% methanol-双蒸馏水溶液复溶样本。

液相方法

色谱柱：Agilent ZORBAX RRHD Eclipse Plus C18 (2.1mm × 50mm, 1.8 μm)；

流动相：A相：水 (0.1% 甲酸）B相：乙腈 (0.1% 甲酸)

柱温：35 ℃

自动进样器温度：4 ℃

质谱方法

质谱系统：QTRAP® 5500三重四极杆线性离子阱复合型质谱系统和QTRAP® 6500+三重四极杆线性离子阱复合型质谱系统均可进行分析；

1）QTRAP® 5500质谱系统

离子源：ESI源，正、负离子模式

RUO-MKT-02-14917-ZH-A

表1. 液相梯度

Time（min）	Flow Rate（mL/min）	A Phase（%）	B Phase（%）
0	0.3	98	2
2.95	0.3	98	2
3	0.5	98	2
6	0.5	20	80
8	0.5	20	80
8.05	0.3	98	2
10	0.3	98	2

离子源参数：

IS电压: +5500 V/ -4500 V;　　气帘气 CUR: 35 psi;

雾化气 GS1: 55 psi;　　辅助加热气 GS2: 55psi;

碰撞气源温度 TEM: 500 ℃;　　入口电压 EP: 10 V/ -10V;

碰撞池出口电压 CXP：10V/ -10V。

2）QTRAP® 6500+质谱系统

离子源：ESI源，正、负离子模式

离子源参数：

IS电压: +5500 V/ -4500 V;　　气帘气 CUR: 35 psi;

雾化气 GS1: 55 psi;　　辅助加热气 GS2: 60psi;

碰撞气源温度 TEM: 400 ℃;　　入口电压 EP: 10 V/ -10V;

碰撞池出口电压 CXP：10V/ -10V。

实验结果

化合物色谱图

色氨酸及其代谢物，色谱峰型良好。

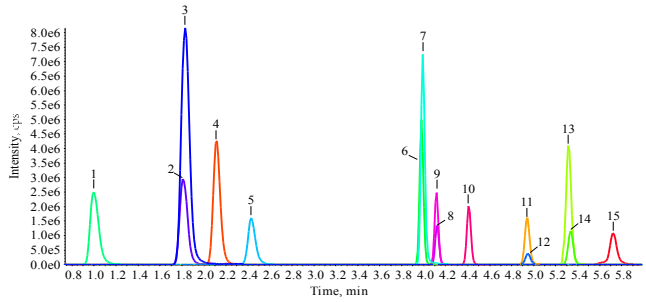

* 图中编号同表

表2. 色氨酸、15种代谢物和4种同位素内标的MRM离子对信息； 4个内标分别为：D3-羟色氨酸（5-hydroxytryptophan-4,6,7-d3），D2-5羟基吲哚乙酸（5-hydroxyindole-3-acetic-2,2-d2 acid），D2-吲哚乙酸（indole-3-acetic-2,2-d2 acid），D3-色氨酸（tryptophan-2,3,3-d3）。

Q1 (Da)	Q3 (Da)	R.T. (min)	ID	DP	CE
177.1	160.1	1.81	Serotonin	57	31
221.1	204.1	1.79	5-hydroxytryptophan	63	16
224.1	207.1	1.80	5-hydroxytryptophan-4,6,7-d3	63	16
161.1	144.1	4.12	Tryptamine	54	34
194.1	148.2	4.11	5-hydroxyindole-3-acetic-2,2-d2 acid	130	36
192.1	146.1	4.12	5-Hydroxyindole acetic acid	130	36
175.0	130.0	4.41	Indole-3-acetamide	85	27
301.1	283.1	5.71	Cinnabarinic acid	100	24
209.1	192.0	2.10	kynurenine	57	26
118.0	91.0	4.95	indole	107	30
162.2	144.1	5.31	Tryptophol	87	35
176.2	130.2	5.33	indole acetic acid	130	25
178.1	132.2	5.33	Indole-3-acetic-2,2-d2 acid	130	25
205.1	188.1	3.98	tryptophan	65	30
208.1	191.1	3.98	trytophan-2,3,3-d3	65	30
225.1	208.0	1.00	3-Hydroxy-kynurenine	65	26
206.0	160.0	3.99	xanthurenic acid	100	40
152.0	108.0	2.42	3-Hydroxyanthranilic acid	-100	-20
144.0	115.0	4.95	Indole-3-carboxaldehyde	-160	-38

灵敏度和线性范围

色氨酸及其代谢物，LOD（最低定量下线）为0.03-3.20 fmol，线性范围大于3个数量级，线性相关系数R^2均大于0.9900。

表3. 色氨酸及其代谢物LOD，线性范围和R^2。

Num.	Component Name	LOD (fmol)	Linear range (μM)	R^2
1	3-Hydroxy-L-kynurenine	0.29	0.0015 - 1.9213	0.9997
2	5-hydroxytryptophan	0.21	0.0004 - 0.4797	0.9997
3	Serotonin	0.48	0.0009 - 1.0858	0.9987
4	kynurenine	0.51	0.0032 - 4.0428	0.9998
5	3-Hydroxyanthranilic acid	3.20	0.0066 - 8.2303	0.9987
6	tryptophan	0.13	0.0025 - 3.1341	0.9993
7	xanthurenic acid	0.14	0.0002 - 0.2398	0.9993
8	Tryptamine	0.10	0.0003 - 0.4148	0.9999
9	5-Hydroxyindole acetic acid	1.50	0.0021 - 2.5735	0.9998
10	Indole-3-acetamide	0.03	0.0002 - 0.2824	0.9994
11	indole	10.64	0.0171 - 21.4189	0.9988
12	Indole-3-carboxaldehyde	0.09	0.0005 - 0.6406	0.9987
13	Tryptophol	0.70	0.0029 - 3.5893	0.9995
14	indole-3-acetic acid	2.01	0.0049 - 6.1786	0.9999
15	Cinnabarinic acid	0.37	0.0014 - 1.8027	0.9997

RUO-MKT-02-14917-ZH-A

重现性

精密度通过日内差和日间差结果来评价，采用L2，L4，L7标准溶液代表高、中、低三种浓度水平，日内差为每个浓度组分析5次的结果，日间差为连续检测三天的结果。

Analytes	Intra_day (n=5, CV%)			Inter_day (n=5, CV%)		
	C_H	C_M	C_L	C_H	C_M	C_L
3-Hydroxyanthranilic acid	1.7	0.8	4.7	1.4	1.2	2.3
3-Hydroxy-L-kynurenine	0.7	0.6	1.3	1.5	1.4	3.5
5-Hydroxyindole acetic acid	1.0	1.5	3.2	1.1	0.9	5.1
5-hydroxytryptophan	0.9	1.2	3.2	1.3	1.2	5.3
Cinnabarinic acid	0.4	0.5	9.6	0.9	1.9	9.8
indole	0.9	1.0	14.1	0.6	1.0	10.2
indole acetic acid	1.2	1.6	6.7	1.3	2.2	6.1
Indole-3-acetamide	0.9	0.4	3.6	0.8	1.2	5.3
Indole-3-carboxaldehyde	0.1	0.8	4.9	1.2	0.9	5.8
kynurenine	0.7	0.9	3.3	0.8	1.2	4.7
Serotonin	0.9	1.7	1.9	1.5	2.0	6.3
Tryptamine	0.8	0.8	8.4	1.8	1.7	5.5
tryptophan	1.0	0.7	2.8	1.8	1.7	3.3
Tryptophol	1.5	1.7	7.7	1.5	1.9	8.1
xanthurenic acid	0.9	1.3	9.5	1.1	1.6	4.2

*"C_L"表示低浓度标准品，"CM"表示中浓度标准品，"C_H"表示高浓度标准品。

总结：

本文建立了液相色谱串联质谱法测定色氨酸和其15种代谢物的方法。方法灵敏度高，色氨酸和15种化合物的LLOQ平均为：0.003 μM，线性范围跨越三个数量级，日内和日间重现性CV%<15 %, 符合方法学要求，为后期按蚊样品的测定提供了支持。

文献

1. Yuebiao Feng, Yeqing Peng, Xiumei Song, Han Wen, Yanpeng An, Huiru Tangand Jingwen Wang. Anopheline mosquitoes are protected against parasite infection by tryptophan catabolism in gut microbiota, Nature Microbiology, https://doi.org/10.1038/s41564-022-01099-8.

RUO-MKT-02-14917-ZH-A

LC-MS/MS法测定两种甲基化修饰组氨酸

Determination of two histidine methylation by LC-MS/MS

查海红，钟晨春，龙志敏，郭立海
Haihong Zha, Chenchun Zhong, Zhimin Long, Lihai Guo
SCIEX应用支持中心，中国

Keywords: histidine methylation; SCIEX Triple Quad™ System;

引言

甲基化是最丰富和最常见的翻译后修饰之一，广泛参与细胞中重要的生物学过程。组氨酸甲基化发生在咪唑环的N1或N3位置，约占蛋白质甲基化修饰的13%，这种位置特异性是由不同家族的组氨酸甲基转移酶所决定的。组氨酸甲基化在蛋白结合金属离子方面具有潜在作用，能调控细胞内金属离子浓度平衡，因此对于癌症机理的研究具有重要意义[1-2]。

本文建立了一种同时检测N1和N3位甲基化修饰组氨酸的快速检测方案，方法的定量下限可低至0.2-0.5 nM，仪器灵敏度高，重现性好，可以很好的满足蛋白质中修饰组氨酸的测定要求。

本实验方法特点：

1. 使用三重四极杆质谱（SCIEX Triple Quad™ 系统）测定2种甲基化组氨酸，具有较好的色谱保留，且两种甲基化组氨酸也能实现较好分离，见图1。
2. 本方法灵敏度低至0.2-0.5 nM，重现性好，很好的满足蛋白质中修饰组氨酸的检测需求。

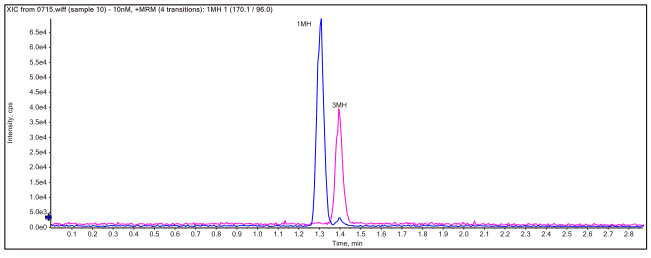

图1. 两种甲基化组氨酸的典型色谱图

仪器设备

Exion LC™ AD 系统 + SCIEX Triple Quad™ 系统

液相方法

色谱柱：Luna Omega Polar C18 150 × 2.1mm, 5 µm

流动相：A相：水（含0.001% 甲酸+ 1 mM 甲酸铵）

B相：乙腈

进样体积：1 µL

柱温：40℃；

流动相梯度：

Time (min)	Flow (ml/min)	A (%)	B (%)
0.00	0.3	99	1
2.00	0.3	99	1
3.00	0.5	10	90
4.50	0.5	10	90
5.00	0.5	99	1
6.00	0.5	99	1
6.10	0.3	99	1
7.00	0.3	99	1

RUO-MKT-02-29083-ZH-A

质谱方法

离子源：ESI源，正离子模式

离子源参数：

电喷雾电压 IS: 5500 V　　气帘气 CUR: 35 psi

雾化气 GS1: 50 psi　　辅助加热气 GS2: 50 psi

碰撞气 CAD: 8　　源温度 TEM: 500℃

表1. 两种甲基化组氨酸的质谱参数

化合物名称	Q1 Mass	Q3 Mass	DP	CE
1甲基组氨酸(1MH)	170.1	96	40	27
3甲基组氨酸(3MH)	170	124	40	19

蛋白样品前处理：

SDS-PAGE胶分离蛋白质，考马斯染色切目的条带蛋白，进行脱色胰酶消化，提取消化后的肽段；使用6M 盐酸 100℃酸解肽段成氨基酸，1.5 mL溶液氮吹干燥，150 μL水复溶，10000 rpm离心5 min，取上清进样分析

实验结果

1. 灵敏度和重复性：

两种甲基化组氨酸的最低定量下限为0.2-0.5 nM，典型色谱图见图2；两种甲基化组氨酸连续进样六针RSD小于5%。

表2. 两种甲基化组氨酸的定量下限、线性范围及重现性

	LLOQ (定量下限)	线性范围	重现性 (RSD)
1MH	0.2 nM	0.2-500 nM	4.94%
3MH	0.5 nM	0.5-500 nM	3.18%

2. 线性范围：

两种甲基化组氨酸在线性范围内线性关系良好，相关系数大于0.995（见图3），标曲各点准确度在90%-110%之间。

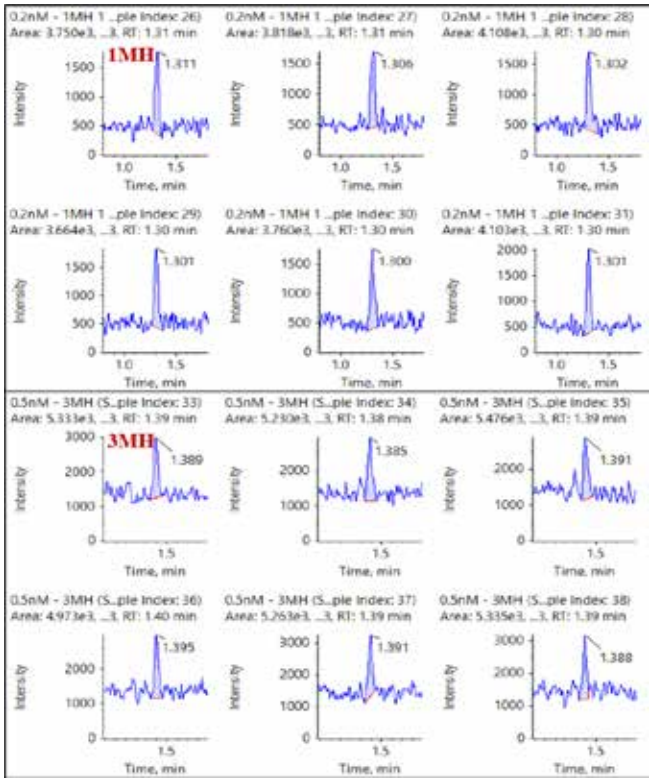

图2. 两种甲基化组氨酸最低定量限色谱图

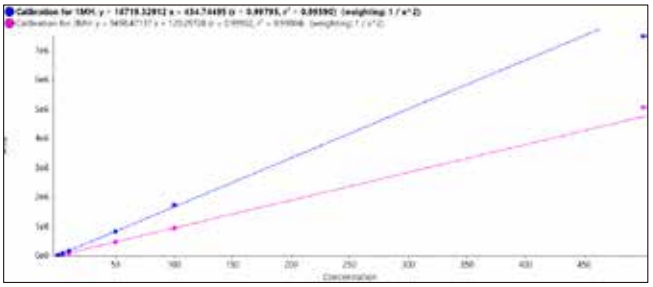

图3. 两种甲基化组氨酸的标准曲线图

3. 样品检测：

实际处理蛋白质样品中甲基化组氨酸结果见图4，可以测到蛋白质中低含量的甲基化修饰组氨酸，进而可以比较不同位点修饰的差异。

RUO-MKT-02-29083-ZH-A

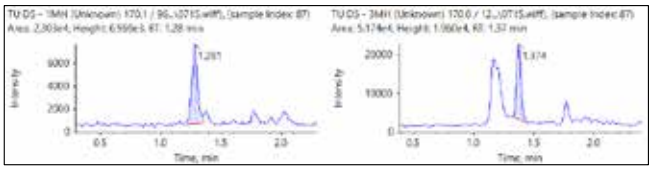

图4. 实际蛋白质样品中甲基化组氨酸检测结果图

总结

本文使用SCIEX Triple Quad™ 系统建立了蛋白质中甲基修饰组氨酸的LC-MS/MS方法。结果表明，本方法灵敏度高、重现性好，两个异构体能实现较好分离，能够满足蛋白质中甲基修饰组氨酸的检测需求。

参考文献

[1] Lv M , Cao D , Zhang L ,et al.METTL9 regulates N1-histidine methylation of zinc transporters to promote tumor growth[J].Cold Spring Harbor Laboratory, 2021.DOI:10.1101/2021.04.20.440582.

[2] Cao R , Zhang X , Liu X ,et al.Molecular basis for histidine N1 position-specific methylation by CARNMT1[J].Cell Research, 2018, 28(4).DOI:10.1038/s41422-018-0003-0.

RUO-MKT-02-29083-ZH-A

酵母细胞中乙酰辅酶A和乳酰辅酶A的定量分析检测

The Determination of Acetyl-CoA and Lactoyl-CoA in Yeast Cells Using LC-MS/MS

史晓媛，龙志敏，郭立海
Xiaoyuan Shi, Zhimin Long, Lihai Guo
SCIEX 应用支持中心，中国

Key Words： Acetyl-CoA; Lactoyl-CoA; Cells

引言

辅酶 A（Coenzyme A, 简称 CoA）是所有生物体中普遍存在且必不可少的一种辅助因子，其主要作用是在许多代谢和分解过程中作为羰基活化基团和酰基活化的载体。研究表明辅酶A的活性基团硫醇基团（-SH）能够激活含羰基的分子，在分解和合成代谢反应中，与多种羧酸结合，从而形成具有代谢活性硫酯衍生物，如乙酰辅酶 A，乳酰辅酶 A，丙二酰辅酶 A和3-羟基-3-甲基戊二酰（HMG）辅酶 A。辅酶 A 及其硫酯衍生物广泛参与中枢代谢途径，包括柠檬酸循环，脂肪酸的生物合成与氧化，氨基酸代谢，异戊二烯和肽聚糖的生物合成等。除此之外，这些衍生物还可以作为蛋白质衍生化的底物，比如赖氨酸乙酰化，琥珀酰化，丙酰化，丁酰化，这个过程已成为转录调控，细胞代谢的一种重要机制。本文建立了LC-MS/MS测定酵母细胞中乙酰辅酶A和乳酰辅酶A的方法，灵敏度高，重现性好。

图1. ExionLC™ AD系统和SCIEX Triple Quad™系统

仪器设备：

SCIEX ExionLC™ AD系统和SCIEX Triple Quad™系统

液相条件

液相系统：SCIEX ExionLC™ AD系统

色谱柱：BEH Shield RP18（100 × 2.1 mm，1.7 µm）

流动相：A: 水（含10mM甲酸铵，0.05%氨水）; B: 乙腈

流速：0.3 mL/min

柱温：40 ℃

液相梯度：

时间(min)	A(%)	B(%)
0	98	2
1.0	98	2
6.0	5	95
7.5	5	95
7.6	98	2
10.0	98	2

质谱条件

离子源：ESI，正离子模式

扫描方式：MRM多反应监测

气帘气CUR：40psi　　喷雾电压IS：5500V

RUO-MKT-02-14062-ZH-A

源温度 Tem：500℃　　雾化气Gas1：45psi

辅助气GAS2：45psi　　碰撞气 CAD：10

MRM参数：如表1

表1. 乙酰辅酶A和乳酰辅酶A的质谱参数

化合物名称（Name）	Q1	Q3	DP	CE
乙酰辅酶A 1（Acetyl-CoA 1）	810.2	303.2	85	40
乙酰辅酶A 2（Acetyl-CoA 2）	810.2	428.0	85	34
乳酰辅酶A 1（Lactoyl-CoA 1）	840.3	333.3	85	42
乳酰辅酶A 2（Lactoyl-CoA 2）	840.3	228.2	85	26

前处理方法

1. 配置甲醇：异丙醇（1:1）溶液作为提取液；
2. 加入200 µL上述提取液到样品，充分涡旋20s（在-80℃冰箱口处操作，结束后放置-80℃冰箱口）；
3. 加入二氯甲烷500 µL，充分涡旋30s，涡旋两次（在-80℃冰箱口处操作，结束后放置-80℃冰箱口）；
4. 加入200 µL H_2O，涡旋30s，将上述样品放置在4℃冰箱静置10 min，（有分层，上层为水相）；
5. 离心（4℃, 10min, 15000r/min），取上清液150 µL到进样瓶待检测。

实验结果

1. 特异性

水做为空白溶液，分别称取一定量的乙酰辅酶A和乳酰辅酶A，加入水溶解稀释，并稀释至浓度为5 ng/mL的标准工作溶液。将空白溶液和工作溶液分别进样5 µL，提取离子流图见图2。空白溶液在待测物保留时间处无干扰。2种物质峰型良好，且化合物灵敏度高。

2. 线性范围

用水逐级稀释乙酰辅酶A和乳酰辅酶A标准工作溶液至0.1 ng/mL, 0.5 ng/mL, 1 ng/mL, 5 ng/mL, 10ng/mL, 50ng/mL, 100 ng/mL以峰面积对浓度做标准曲线。图3为乙酰辅酶A和乳酰辅酶A的线性范围、线性方程和相关系数。

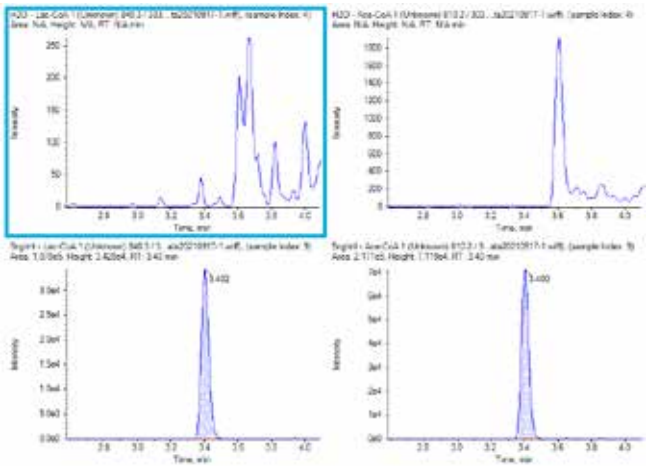

图2. 空白溶液和标准品溶液中乙酰辅酶A和乳酰辅酶A的提取离子流图

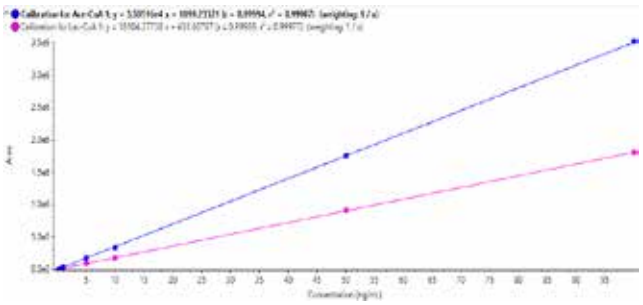

图3. 乙酰辅酶A和乳酰辅酶A标准曲线，线性回归系数r>0.999

3. LLOQ的准确度和重现性

平行制备6份0.1ng/mL浓度的标准溶液做为LLOQ溶液，进样分析。测定结果如表2。2个化合物在LLOQ浓度下的准确度在107.7-111.1%，准确度良好，RSD%在3.65-4.61%，重现性良好，色谱图见图4、图5。

RUO-MKT-02-14062-ZH-A

表2. 回收率测试结果

	最低定量限 LLOQ, ng/mL	准确度 Accuracy,%	相对标准偏差 RSD, %
乙酰辅酶A	0.1	107.7	3.65
乳酰辅酶A	0.1	111.1	4.61

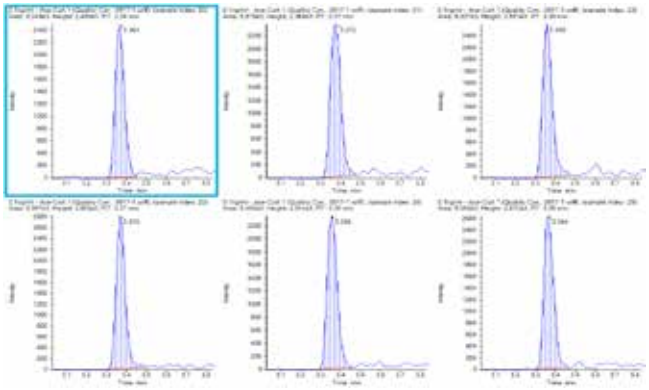

图4. 乙酰辅酶A在LLOQ浓度下重现性色谱图展示

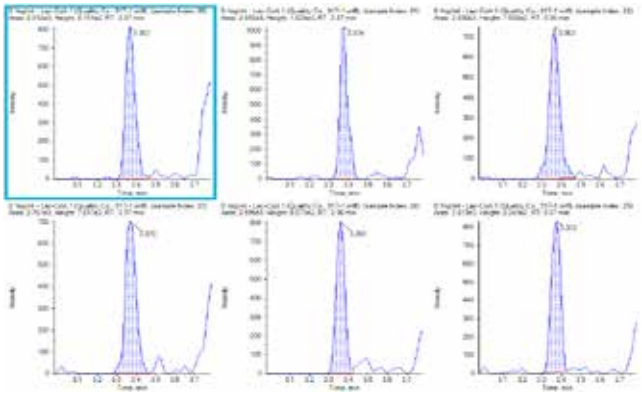

图5. 乳酰辅酶A在LLOQ浓度下重现性色谱图展示

总结

本文使用SCIEX Triple Quad™建立了LC-MS/MS 方法快速测定细胞中乙酰辅酶A和乳酰辅酶A的含量。结果表明，该方法的特异性好，无干扰；线性范围为0.1ng/mL-100 ng/mL，在线性范围内线性关系良好，相关系数大于0.999。2种物质定量下限为0.1ng/mL，在定量下限连续进样6针，RSD<5%，表明仪器灵敏度高，重现性好，该方法为辅酶A衍生物质的测定提供了参考。

RUO-MKT-02-14062-ZH-A

生物样品里中长链酰基辅酶A的方法建立

Method Establishment of Medium and Long Chain Acyl-coenzyme A in Biological Samples

查海红，龙志敏，郭立海
Zha Haihong, Long Zhimin, Guo Lihai

SCIEX China

Keywords： Medium and Long Chain Acyl-coenzyme A, Biological Samples

前言

辅酶A（coenzyme A）是一种辅酶，由泛酸、半胱氨酸和三磷酸腺苷等组成的大分子。辅酶A是体内70多种酶反应通路的辅助因子，包括糖类的分解，脂肪酸的氧化，氨基酸的分解，丙酮酸的降解，激发三羧酸循环，提供机体生命所需90%的能量，因此是调节糖、脂肪和蛋白质代谢的重要因子。同时，辅酶A还参与机体大量必需物质的合成。在脑部合成神经肌肉信使和神经递质乙酰胆碱以及促进睡眠的褪黑激素等。神经肌肉信使可在神经和肌肉之间交换资讯，神经递质可在神经与大脑之间传递情感、外界刺激、记忆、学习等方面的资讯。另外，辅酶A还是重要的乙酰基和酰基传递体。所以，通过对酰基辅酶A的检测，可以更清楚了解体内的代谢路径。

本文的目的是在没有标准品的情况下建立中长链酰基辅酶A的方法，于是先从细胞样本中提取中长链酰基辅酶A，然后采用SCIEX QTRAP®质谱特有的“线-阱”转换功能，发现并确证生物样本中的中长链酰基辅酶A，进而建立生物样本中通用的中长链酰基辅酶A的采集方法。

仪器设备

SCIEX ExionLC™系统 + QTRAP®质谱系统

液相方法

色谱柱：C18 (50 × 2.1 mm)

流动相：A相：水（10 mM 甲酸铵，0.005% 氨水）
B相：乙腈

SCIEX ExionLC™系统

流速：0.3 mL/min

柱温：30 ℃

进样量：10 µL

表1. 液相洗脱梯度

时间 (min)	A (%)	B (%)
0.0	90	10
0.3	90	10
1.0	55	45
4.5	2	98
5.0	2	98
5.1	90	10
6.0	90	10

RUO-MKT-02-12392-ZH-A

质谱方法

离子源：ESI源，正离子模式

离子源参数：

IS电压: 5500 V　　气帘气 CUR: 35 psi

雾化气 GS1: 50 psi　　雾化气 GS2: 50 psi

碰撞气 CAD: Medium　　源温度 TEM: 550 ℃

样品前处理

以细胞样品为例，配置甲醇：异丙醇:水（1:1:1）作为提取液；在冰上操作，加入200 µL提取液到样品，充分涡旋20 s，在液氮中反复冻融4次，超声（70 W, 10 s/4次，每次间隔20 s）；在冰上操作，加入二氯甲烷500 µL，充分涡旋30 s，涡旋两次；加入130 µL H_2O，涡旋30 s；将上述样品放置在4 ℃冰箱，静置10 min（有分层，上层为水相）；离心（4 ℃，10 min，15,000 g），取上清液150 µL到进样瓶待检测。

采集方法建立

本文的宗旨是在没有标准品的情况下，实现对生物样本中的中长链酰基辅酶A的检测。因此本文的思路是先从生物样本中提取出中长链酰基辅酶A，然后根据文献及化合物的裂解规律编辑MRM离子对用于发现中长链酰基辅酶A，最后利用SCIEX QTRAP®质谱独有的MRM-IDA-EPI复合扫描方式，在 MRM 出峰的同时，对色谱峰进行 MS/MS 采集，获得完整的二级质谱图帮助我们进行化合物确证。

通过文献查阅[1]以及酰基辅酶A类化合物的裂解规律，我们确定了8种酰基辅酶A的MRM离子对信息，分别为带有4碳、6碳、8碳、10碳、12碳、14碳、16碳以及18碳链长度的酰基辅酶A，即C4_COA、C6_COA、C8_COA、C10_COA、C12_COA、C14_COA、C16_COA和C18_COA，详细的质谱采集参数见表2和图1.

实验结果

我们在细胞样品中对这8种酰基辅酶A进行了检测与确证，图2展示了这8种酰基辅酶A对应的MRM离子对的色谱峰，根据酰基辅酶A出峰规律，链越长，极性越小，保留时间越靠后，初步推测了每个酰基辅酶A的出峰位置。

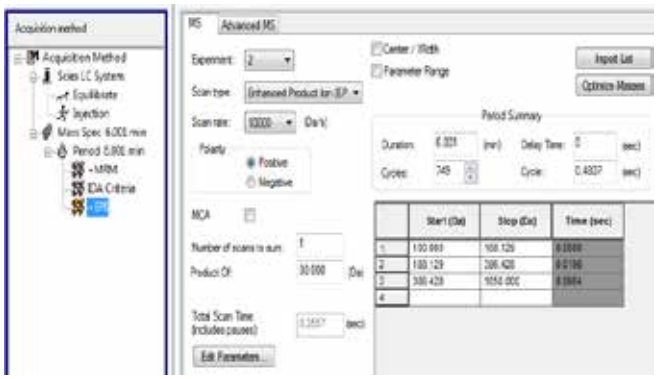

图1. MRM-IDA-EPI参数

表2. 8种酰基辅酶A的质谱参数

化合物	Q1/Q3	去簇电压（V）	碰撞能量（V）
C4_COA	838.2/331.2	130	40
C6_COA	866.2/359.2	130	40
C8_COA	894.2/387.2	130	40
C10_COA	922.2/415.2	130	44
C12_COA	950.2/443.2	130	44
C14_COA	978.2/471.2	130	44
C16_COA	1006.2/499.2	130	44
C18_COA	1034.2/527.2	130	44

接着，我们利用SCIEX QTRAP®质谱独有的MRM-IDA-EPI复合扫描方式，在 MRM 出峰的同时，可以对色谱峰进行 MS/MS 采集，从而获得完整的二级质谱图帮助我们进行化合物确证。于是，我们找到每个酰基辅酶A推测出峰位置的二级谱图进行进一步的确证，详细的二级谱图见图3。因为我们从采集的酰基辅酶A的二级质谱图中，发现明显m/z 428的特征峰和有规律的差28Da 的CH2-CH2的碎片峰， m/z 331.3(C4-CoA)\m/z 359.3(C6-CoA)\m/z 387.3(C8-CoA)\m/z 415.3(C10-CoA)\m/z 443.4(C12-CoA)\m/z 471.4(C14-CoA)\m/z 499.4(C16-CoA)\m/z 527.5(C18-CoA)，所以我们通过二级谱图对这8种酰基辅酶A得到进一步的确证。

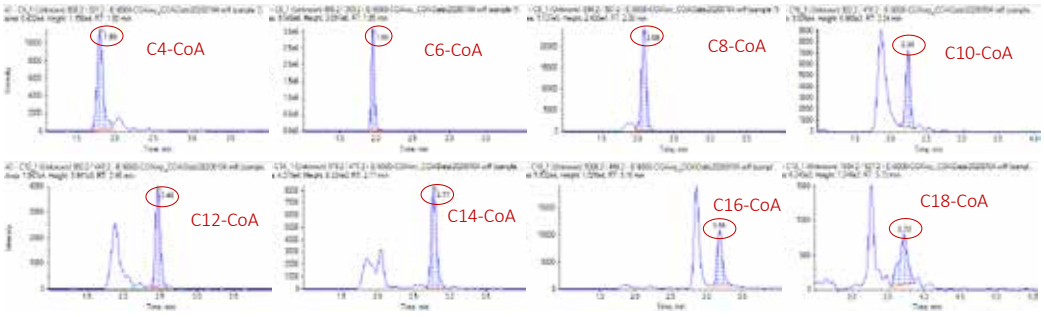

图 2. 8种酰基辅酶A在细胞中的色谱图

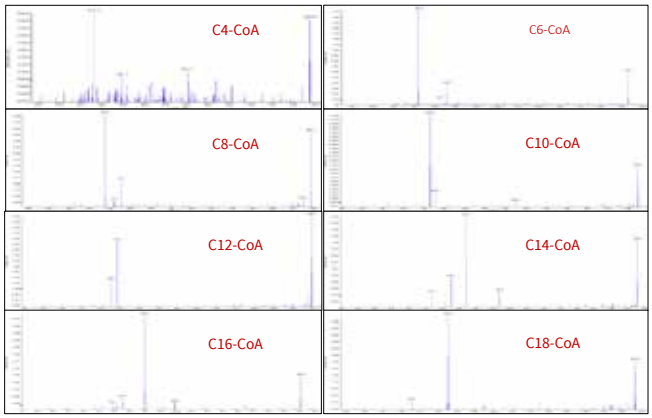

图3. 8种酰基辅酶A 的EPI二级谱图

总结

本文在没有标准品的情况下，采用SCIEX QTRAP®质谱特有的“线-阱”转换功能，在生物样品中建立中长链酰基辅酶A的方法。首先通过文献搜索及结构分析确定MRM离子对信息，进而在生物样品中通过酰基辅酶A的保留时间规律及二级谱图规律来确证酰基辅酶A，从而最终确定并建立中长链酰基辅酶A的质谱检测方法。

参考文献

[1]. Wang S , Wang Z , Zhou L , et al. Comprehensive Analysis of Short-, Medium-, and Long-Chain Acyl-Coenzyme A by Online Two-Dimensional Liquid Chromatography/Mass Spectrometry[J]. Analytical Chemistry, 2017:12902.

RUO-MKT-02-12392-ZH-A

SCIEX Triple Quad™ 系统靶向测定多巴胺合成和代谢主要通路上的8个代谢物的应用

Determination of 8 Metabolites on main Pathways of Dopamine Biosynthesis and Metabolism by SCIEX Triple Quad™ System

雷敏，龙志敏，郭立海
Lei Min, Long Zhimin, Guo Lihai
SCIEX，中国

Key Words: Dopamine Biosynthesis and Metabolism Pathway , Target Metabolomics，Dopamine and other metabolites, Biomarker

引言

多巴胺（以下简称DA）是大脑中最重要的也是最丰富的儿茶酚胺，且是其他神经递质的前体。20世纪60年代，Hornykiewicz[1,2]研究认为多巴胺的耗竭与帕金森疾病密切相关，因此通过靶向代谢组学的研究思路，探索多巴胺代谢通路上代谢物的变化与帕金森疾病之间的关系的研究者也越来越多。该技术方案旨在建立该代谢通路上主要的8个代谢物的测试方法，为研究者建立该测试方法提供参考。

涉及到多巴胺合成和代谢通路的主要步骤如下[3]。

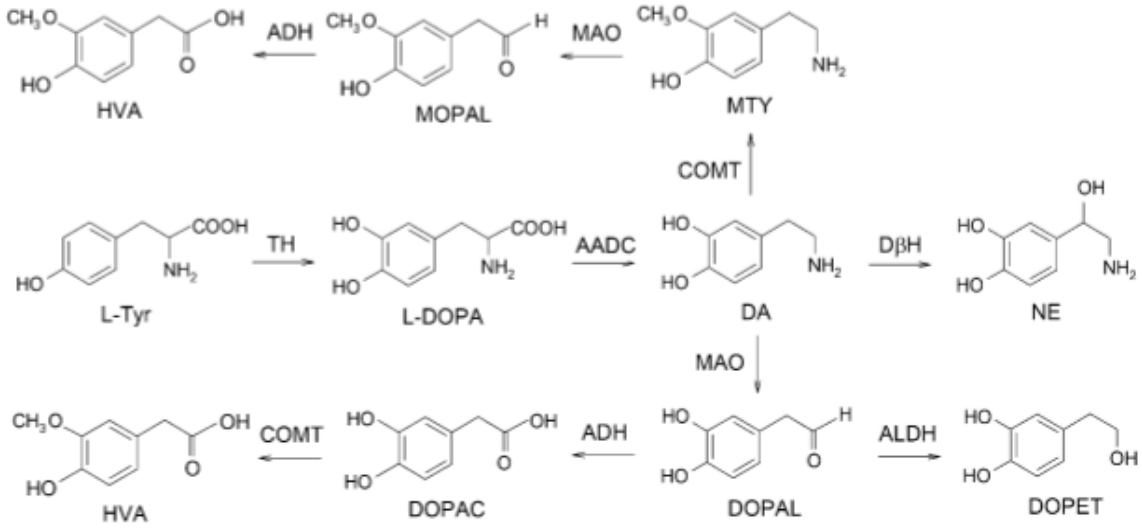

图1. 多巴胺合成和代谢的主要通路。L-Tyr 在TH和AADC作用下转变成DA；DA依次在MAO，ADH和COMT作用下，分别转变成DOPAL，DOPAC，最终到HVA。继而，DA做为NE的前体，通过DβH转变成NE。根据一个小通路上，DOPAL 通过ALDH可降解为DOPET。DA依次在COMT和ADH的作用下，途径MTY和MOPAL转变为HVA的次级代谢通路也显示在图中。

RUO-MKT-02-13256-ZH-A

本文实验方法特点

本文展示了使用SCIEX Triple Quad™ 系统对多巴胺合成和代谢通路上的多巴胺及其代谢物共8个化合物进行测定，方法具有以下特点：

1. 仪器的灵敏度高，8个化合物方法定量下限在0.2-2ng/ml之间，满足生物样本中多巴胺及其代谢物定量要求。
2. 仪器和方法的特异性好，可正负切换同时检测，仅6.5min的方法即可准确定量，检测效率高。
3. 8个化合物最低定量下限的RSD在1.97%-5.18%之间，表明仪器和方法的重现性好。
4. 该方法对多巴胺代谢通路上化合物的测试有很好的参考意义，有助于更好的研究帕金森等精神类疾病的生物标志物。

仪器设备

SCIEX Exion LC™系统 + Triple Quad™系统

液相方法

色谱柱：HSS T3 (100 × 2.1 mm, 1.8 µm)

流动相：A相：水（含0.1%甲酸）

B相：乙腈（含0.1%甲酸）

流速：0.4 ml/min

柱温：40℃；

进样量：5 µL

Time(min)	A (%)	B (%)
0.00	98	2
1.20	98	2
2.50	40	60
4.50	5	95
5.00	5	95
5.01	98	2
6.50	98	2

质谱方法

离子源：ESI源，正负离子切换同时检测-Scheduled MRM™模式

离子源参数：

IS电压: 正离子：5500V；　负离子：-4500V

气帘气 CUR: 30 psi　雾化气 GS1: 60 psi

辅助气 GS2: 60 psi　源温度 TEM: 600℃

碰撞气 CAD: Medium

表1. 质谱参数

化合物名称	极性	Q1	Q3	保留时间(min)	去簇电压（DP, eV）	碰撞能量(CE, eV)	碰撞池出口电压(CXP, eV)
HVA	负离子	180.9	122.1	3.15	-50	-19	-11
DOPAL		150.9	123	3.02	-80	-20	-11
DOPET		152.9	123	2.97	-60	-17	-8
DOPAC		123.2	93.1	2.99	-80	-18	-10
NE	正离子	152	107	0.78	50	25	7
L-DOPA		198.1	152.1	1.58	45	18	7
3-MT		168.1	119.2	2.84	45	24	7
DA		154.1	137.1	1.69	45	12	7

RUO-MKT-02-13256-ZH-A

实验结果

1. **特异性：**配制含6%高氯酸的水溶液，作为空白溶液；分别称取一定量的上述表1中8个标准品，加入一定量空白溶液溶解，并稀释至浓度为20 ng/ml的标准工作溶液。分别取上述两份溶液进样5 µl，提取离子流图如下。空白溶液中，在待测物保留时间处无干扰，见图2。20 ng/ml的标准工作溶液，见图3，8个代谢物峰形良好，且代谢物响应高，表明仪器的灵敏度高。

2. **线性范围：**用空白溶液分别逐级稀释8个代谢物至工作溶液浓度分别为0.2 ng/ml, 1 ng/ml, 2 ng/ml, 10 ng/ml, 20 ng/ml, 100 ng/ml, 200 ng/ml, 500 ng/ml，以峰面积对浓度做标准曲线。图4分别为8个代谢物的线性方程和相关系数，可见相关系数均在0.992以上，表明相关系数良好，线性良好。

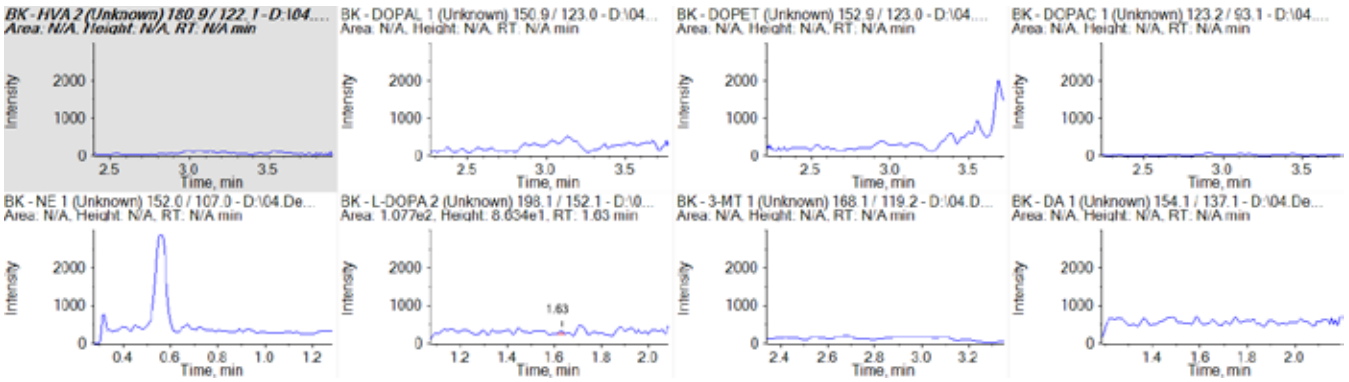

图2. 空白溶液中的提取离子流图
(从左到右，第一行分别为HVA, DOPAL, DOPET, DOPAC；第二行分别为NE, L-DOPA, 3-MT, DA)

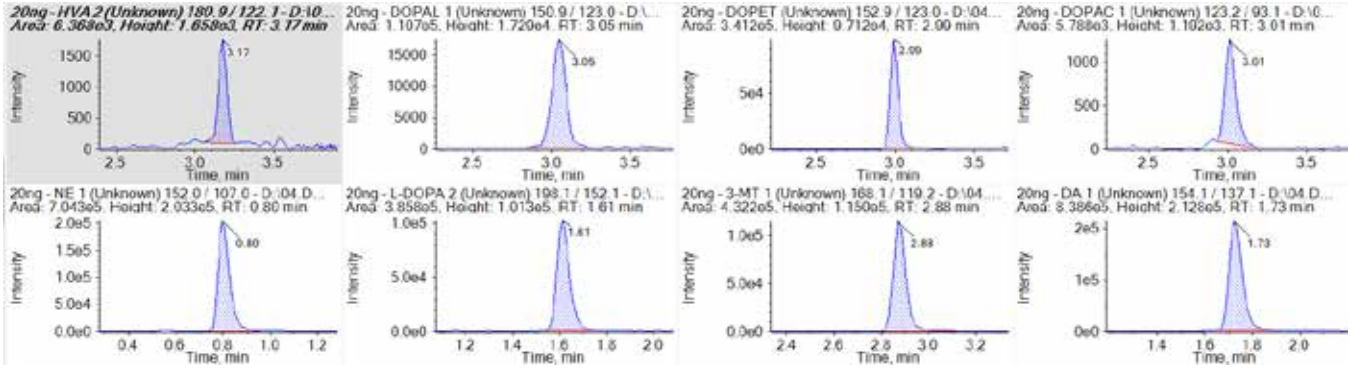

图3. 20 ng/ml溶液的提取离子流图
(从左到右，第一行分别为HVA, DOPAL, DOPET, DOPAC；第二行分别为NE, L-DOPA, 3-MT, DA)

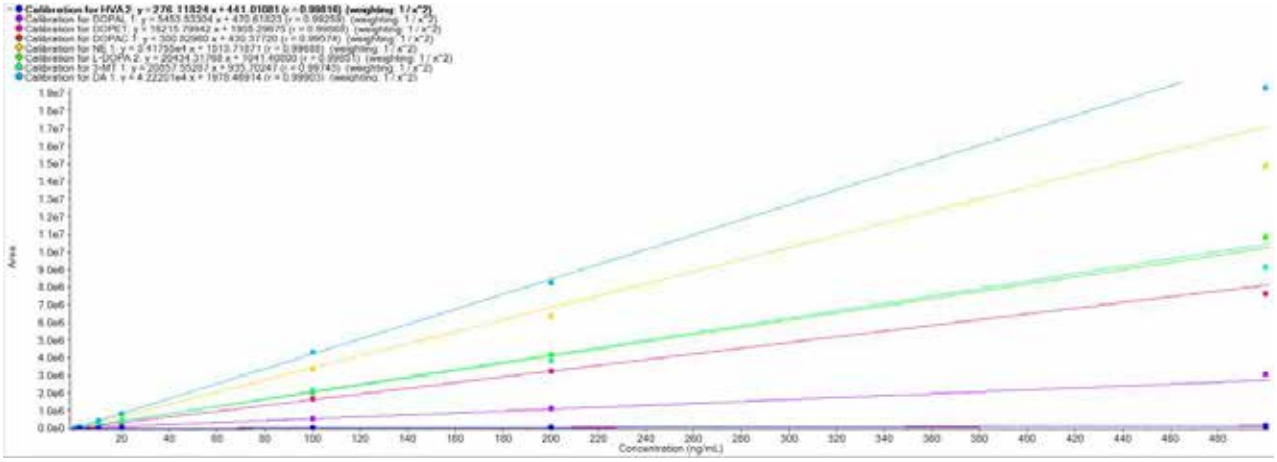

图4. 8个代谢物的标准曲线

3. **LLOQ的准确度和重现性：**平行制备3份线性最低点工作溶液作为LLOQ溶液，进样分析，测定结果如下表格2。3份平行样品中，8个化合物在不同的LLOQ浓度下的准确度在97.32%-107.26%，准确度良好；RSD%在1.97%-5.18%，RSD均满足测试要求，重现性良好。

表2. 重现性测试结果

化合物名称	最低定量限 (LLOQ, ng/ml)	准确度 (Accuracy, %)	相对标准偏差 (RSD,%)
HVA	2	98.33	4.58
DOPAL	1	107.26	3.57
DOPET	0.2	100.19	4.24
DOPAC	2	101.83	5.18
NE	0.2	99.66	2.18
L-DOPA	0.2	97.32	3.83
3-MT	0.2	98.57	4.10
DA	0.2	98.95	1.97

总结

本文使用SCIEX Triple Quad™ 建立了LC-MS/MS方法测定多巴胺通路上的多巴胺及其代谢物的含量。空白溶剂中无干扰，方法的特异性好；8个代谢物的最低定量下限在0.2-2ng/ml，表明仪器的灵敏度高。HVA和DOPAC的线性范围均为2ng/ml-500ng/ml，DOPAL的线性范围均为1ng/ml-500ng/ml, DOPET, NE, L-DOPA, 3-MT和DA的线性范围宽均为0.2ng/ml-500ng/ml，线性关系良好；8个代谢物的最低定量下限连续进样3针，RSD在1.97%-5.18%，表明仪器和方法的重现性好。该方法为开展帕金森等相关疾病上的多巴胺及其代谢物的测试工作提供了参考。

参考文献

[1] H. Ehringer,O.Hornykiewicz, Klin. Wochenschr. 1960, 38, 1236–1239.

[2] O. Hornykiewicz, Mov.Disord. 2002, 17,501–508.

[3] Angew.Chem.Int. Ed. 2019, 58,6512–6527.

RUO-MKT-02-13256-ZH-A

丹磺酰氯衍生化法检测生物样品中3种游离态多胺（腐胺，精胺和亚精胺）

Determination of Three Free Polyamines in Biological Samples by Using Dansyl Chloride Derivatization

史晓媛，龙志敏，郭立海
Shi Xiaoyuan, Long Zhimin, Guo Lihai

SCIEX应用支持中心（上海），中国
SCIEX, China

Key Words: Polyamines, Derivatization, Liquid Chromatography Tandem, Mass Spectrometry

多胺(Polyamines, PA) 是带有两个或两个以上氨基的脂肪族化合物，在生物体内广泛存在。最常见的多胺有腐胺（Putrescine）、亚精胺（Spermidine）和精胺（Spermine）等。多胺广泛存在于植物、动物、浮游植物以及海藻中，作为生物体内促进细胞生长的重要物质之一，对细胞生长、细胞增殖起着关键性的作用，能直接参与生物体内的多种生理活动，是生物体生长和细胞代谢所必需的痕量生物活性物质。

本文建立了分析生物样品中3种游离态多胺的定量方法，样品经丹磺酰氯（DNS-Cl）衍生后，多胺衍生物不需要再经过浓缩的步骤，极大地提高了分析速度。本方法具有选择性高，样品用量少，适合痕量分析等优点，能对生物样品中3种游离态多胺(腐胺、亚精胺和精胺) 进行很好的定量分析。

样品处理

1. 移取 100 µL 血浆，加入300 µL乙腈，涡旋混匀1 min，超声10 s后，离心5 min (4 ℃, 15000 r/min)。
2. 取上清液，氮气吹干。加入50 µL 丹磺酰氯溶液（5 mg/mL，乙腈溶解）及100 µL 0.1 M Na_2CO_3缓冲液（pH 11）复溶，涡旋30 s后, 避光条件下50 ℃)水浴加热 20 min。
3. 反应完成后加入3 µL甲酸，将pH值调至7左右，离心5 min(4℃, 15000 r/min)，取上清液进行LC-MS/MS测定。

液相条件

色谱柱：ACQUITY UPLC BEH C18, 1.7 µm,2.1 × 50 mm

流动相：A相:水（0.1%甲酸, 5 mM甲酸铵）
B相:乙腈：异丙醇（v:v, 2:1）

流速： 0.4 mL/min

柱温：45℃

进样量：10 µL

梯度洗脱，洗脱程序如表1：

表1. 液相梯度条件

时间（min）	A%	B%
0	50	50
0.2	50	50
2.6	20	80
3	5	95
3.5	5	95
3.6	50	50
5	50	50

RUO-MKT-02-13583-ZH-A

质谱条件

SCIEX Triple Quad™ 4500

ESI正模式检测

IS电压: 5500V　　气帘气CUR: 30 psi

雾化气GS1: 60 psi　　辅助加热气: 60 psi

碰撞气CAD: 9　　源温度TEM: 600℃

质谱参数如表2：

No.	Compound	Q1	Q3	DP	CE
1	腐胺	555.3	170.1	115	40
	Putrescine	555.3	169.2	115	39
2	亚精胺	845.3	360.3	180	51
	Spermidine	845.3	170.2	180	91
3	精胺	1135.5	360.2	220	66
	Spermine	1135.5	170.0	220	130

实验结果与讨论

1.衍生化反应原理

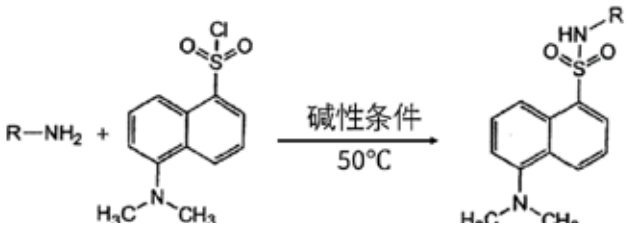

反应原理如上图，丹磺酰氯（Dansyl Chloride, DNS）在碱性条件下与酚羟基，一级胺和二级胺反应，可以提高这些分析物的反相色谱保留行为、样品稳定性以及质谱响应，从而提高检测灵敏度，得到较好的定量结果。我们发现, pH值对多胺衍生反应有很大影响，pH值在9.8附近时，衍生反应效率最高。

2. 三种多胺标准品衍生物色谱图

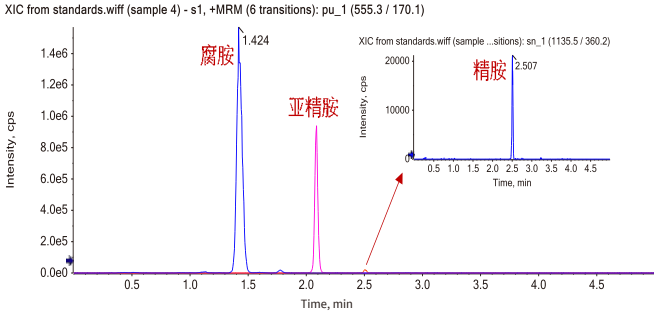

图1. 一针进样，对三种多胺进行高灵敏度分析（10 ng/mL）

3.线性结果及重复性考察

配制一系列覆盖大鼠血浆中多胺含量的标准曲线，浓度分别为1 ng/mL, 2ng/mL, 10 mg/ mL, 40 ng/mL, 50 ng/mL 3种多胺均呈良好线性关系（$R^2 > 0.99$），可满足分析大鼠血浆中多胺的需要。取上述2 ng/mL标准溶液 5 份，根据前述样品前处理方法，平行测定，峰面积的相对标准偏差小于10%。实验结果显示，衍生反应的重复性较好。

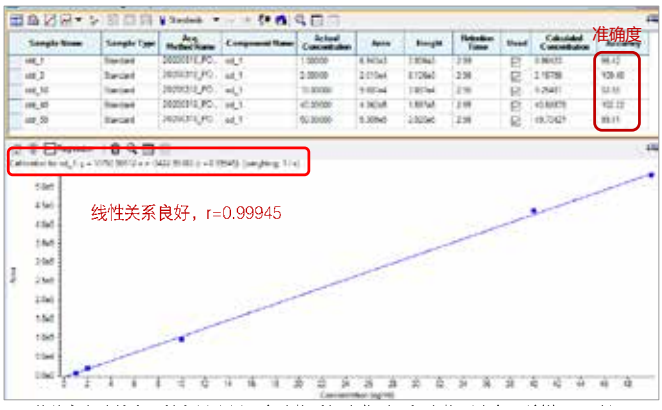

图2. 亚精胺的线性结果

RUO-MKT-02-13583-ZH-A

小结

本文针对生物样品中3种内源性游离多胺，利用丹磺酰氯衍生的方法，快速完成3种游离多胺的高灵敏定量分析。多胺物质衍生化后，衍生物更稳定，并增强了反相色谱保留行为，质谱响应提高，更容易被质谱检测到，可实现稳定可靠的定量分析。对应线性范围内，3种多胺均呈良好线性关系（$R^2 > 0.99$），5次重复样品的相对偏差均小于10%，方法具有选择性高，样品用量少，灵敏度好等特点，可为生物样品中游离态腐胺、亚精胺和精胺的痕量分析提供参考。

RUO-MKT-02-13583-ZH-A

LC-MS/MS法测定DNA中胞嘧啶及其修饰物

Determination of cytosine and its modifiers in DNA by LC-MS/MS

查海红，钟晨春，龙志敏，郭立海
Haihong Zha, Chenchun Zhong, Zhimin Long, Lihai Guo
SCIEX应用支持中心，中国

关键词： cytosine; modifiers; SCIEX Triple Quad™ System;

引言

核酸的表观遗传学修饰参与调控许多生理过程，在体内扮演着重要的角色。比如 DNA 上的 5-甲基胞嘧啶（5-methylcytosine，5-mC）与许多生理过程和疾病相关，包括衰老、癌症、X 染色体失活、分化和发育等。当基因中的5-mC 为正常水平时，抑癌基因可正常表达，而当其高度甲基化时，则会抑制抑癌基因的表达，使其沉默，从而导致癌症的发生。DNA中研究最普遍的表观遗传修饰是5-mC 及其去甲基化路径上的中间产物（图1）。哺乳细胞内，5mC/C 约3%， 5hmC/C约0.1%，5fC/C和5caC/C只有百万分之一[1-2]。

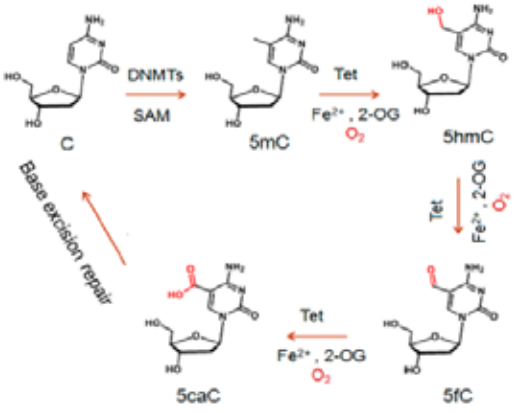

图1. 胞嘧啶 (C) 甲基化及5-mC去甲基化通路

本文建立了一种同时检测DNA中胞嘧啶及其修饰物的快速检测方案，方法的定量下限可低至 pM级别，仪器灵敏度高，可以很好的满足检测需求。

本实验方法特点：

1. 使用三重四极杆质谱（SCIEX Triple Quad™ 系统）测定DNA中胞嘧啶及其修饰物，具有较好的色谱保留，见图2。
2. 本方法灵敏度低至pM级别，灵敏度高，很好的满足检测需求。

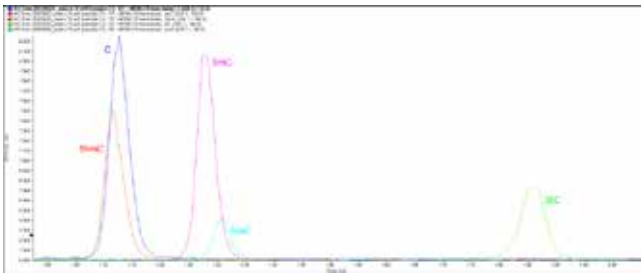

图2. 胞嘧啶及其修饰物的典型色谱图

仪器设备

Exion LC™ AD 系统 + SCIEX Triple Quad™ 系统

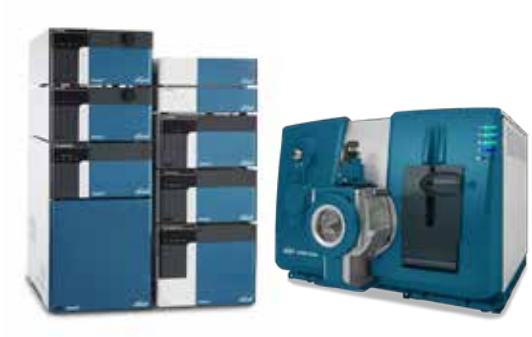

RUO-MKT-02-29097-ZH-A

液相方法

色谱柱：Kinetex Polar C18 100 × 2.1 mm, 2.6 µm

流动相：A相：水（含0.1% 甲酸）
B相：甲醇:乙腈 1:1（含0.1% 甲酸）

进样体积：10 µL

柱温：40℃；

流动相梯度：

Time (min)	Flow (ml/min)	A (%)	B (%)
0.00	0.3	95	5
1.00	0.3	95	5
3.50	0.3	5	95
4.20	0.3	5	95
4.50	0.3	95	5
6.00	0.3	95	5

质谱方法

离子源：ESI源，正离子模式

离子源参数：

电喷雾电压 IS: 5500 V　　气帘气 CUR: 40 psi

雾化气 GS1: 55 psi　　辅助加热气 GS2: 55 psi

碰撞气 CAD: 9　　源温度 TEM: 350℃

表1. 胞嘧啶及其修饰物的质谱参数

化合物名称	Q1 Mass	Q3 Mass	DP	CE
C	228.1	112	18	18
5mC	242.1	126	18	17
5hmC	258.1	142	17	14
5fC	256.1	140	17	17
5caC	272.1	156	17	17

实验结果

1. 灵敏度：

胞嘧啶及其修饰物的最低定量下限为pM级别，典型色谱图见图3。

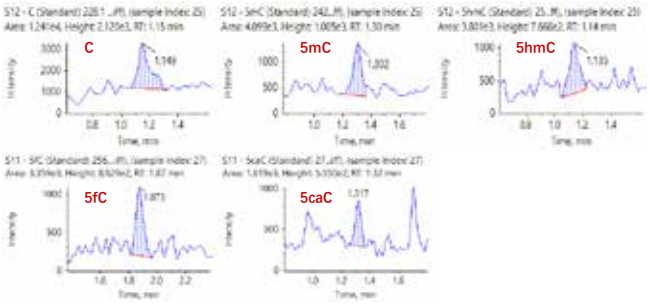

图3. 胞嘧啶及其修饰物最低定量限色谱图

表2. 胞嘧啶及其修饰物的定量下限和线性范围

	LLOQ (定量下限)	线性范围
C	11.2 pM	11.2-8200 pM
5mC	5.6 pM	5.6-12300 pM
5hmC	5.6 pM	5.6-4100 pM
5fC	16.9 pM	16.9-12300 pM
5caC	16 .9pM	16.9-111100 pM

2. 线性范围：

胞嘧啶及其修饰物在线性范围内线性关系良好，相关系数r大于0.996（见图4），标曲各点准确度在85%-115%之间。

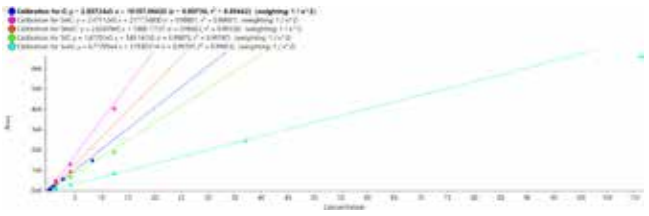

图4. 胞嘧啶及其修饰物的标准曲线图

RUO-MKT-02-29097-ZH-A

3. 样品检测：

实际DNA样品中胞嘧啶及其修饰物的检测结果见图5，所有成分都能检测到。

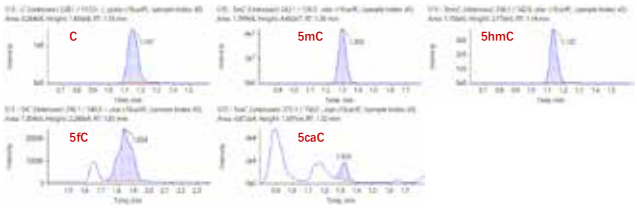

图5. 实际DNA样品中胞嘧啶及其修饰物的检测结果图

总结

本文使用SCIEX Triple Quad™ 系统建立了DNA中胞嘧啶及其修饰物的LC-MS/MS方法。结果表明，本方法灵敏度高，能够满足检测需求。

参考文献

[1] Lister, R.et al. Human DNA methylomes at base resolution show widespread epigenomic differences. Nature462, 315-322[J]. PubMed,2009.DOI:10.1038/nature08514.

[2] C.-X. Song, C. Yi, C. He, Mapping recently identified nucleotide variants in the genome and transcriptome, Nat. Biotechnol. 2012, 30, 1107-1116.

RUO-MKT-02-29097-ZH-A

利用SCIEX 液相色谱串联质谱法对细胞中的能量代谢物进行靶向分析

Targeted Analysis of Energy Metabolites in Cells by Using SCIEX Liquid Chromatography-Tandem Mass Spectrometry

史晓媛，龙志敏，郭立海
Xiaoyuan Shi, Zhimin Long, Lihai Guo
SCIEX 应用支持中心，中国

Key Words: Energy metabolites; Target Analysis; Cells

引言

细胞作为生物体结构和功能的基本单位，易获得、条件较为可控，不易受到外界因素的影响，如年龄、健康程度、外界环境改变等都会对实验结果的准确性产生影响，可以广泛运用于疾病机制研究、药理学、毒理学、细胞能量代谢研究等方面。细胞能量代谢研究可借助于各种细胞模型，鉴识细胞内源性能量代谢物, 直接反映细胞生命活动的生物标志物信息，从而揭示有关细胞的代谢途径和过程，对于体外研究药物作用下代谢物的变化及改变机制具有重要意义。能量代谢物中包含很多高能磷酸键化合物如ATP，ADP等，在进行液相质谱分析时，容易与管路中的金属离子络合导致峰型变差，灵敏度降低。本文优化了流动相条件，通过加入亚甲基二膦酸来改善峰型，建立了300多种能量代谢物的检测方法，可以进行高通量靶向分析。

仪器设备：

SCIEX ExionLC™ AD系统和SCIEX Triple Quad™ 7500系统

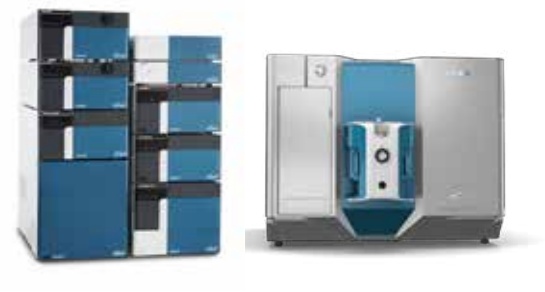

图1 . ExionLC™ AD系统和SCIEX Triple Quad™ 7500系统

液相条件

液相系统：SCIEX ExionLC™ AD系统

色谱柱：ACQUITY BEH Amide（100 × 2.1mm，1.7 μm）

流动相：A: 95%水（含20mM乙酸铵，5 μM亚甲基二膦酸）
B: 95%乙腈（含20mM乙酸铵，5 μM亚甲基二膦酸）

流速：0.3 mL/min

柱温：40 ℃

液相梯度：

时间(min)	A(%)	B(%)
0	5	95
1.0	5	95
12.0	25	75
15.0	60	40
20.0	60	40
20.1	5	95
26.0	5	95

质谱条件

离子源：ESI，正、负离子模式

扫描方式：MRM多反应监测

气帘气CUR：40psi　　喷雾电压IS：+3000V/-3000V

源温度 Tem：500℃　　雾化气Gas1：35psi

辅助气GAS2：70psi　　碰撞气 CAD：10

RUO-MKT-02-14614-ZH-A

MRM参数，如表1

表1. 部分能量代谢物的质谱参数

Component Name	Q1	Q3	Polarity
AMP	348.15	136	Positive
dAMP	332.1	136	Positive
Deoxyadenosine	252	136	Positive
Adenosine	268	136	Positive
Guanine	152.2	110	Positive
Guanosine	284.1	135	Positive
dGMP	348.1	135	Positive
GMP	364	152	Positive
Citrate	191.05	87	Negative
Isocitrate	191.02	117	Negative
Aconitate	173.05	85	Negative
Oxoglutarate	145	101	Negative
Succinate	117	73	Negative
Fumarate	115	71	Negative
Malate	133	115	Negative
Oxaloacetate	131	87	Negative

实验结果

1. 正离子模式下目标化合物的提取离子流图见图1，负离子模式各目标化合物的提取离子流图见图2。

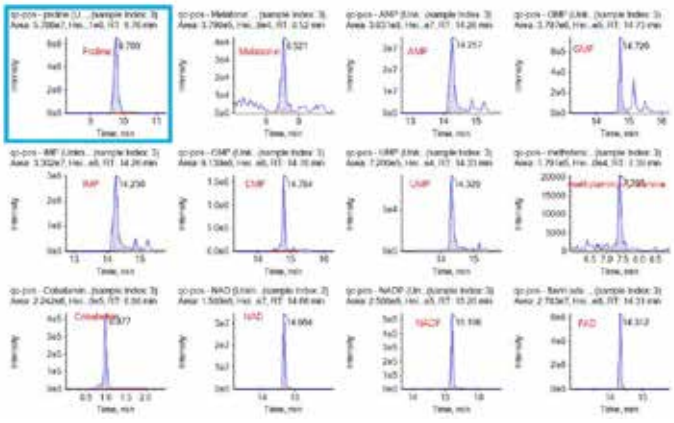

图1. 部分正模式化合物提取离子色谱图

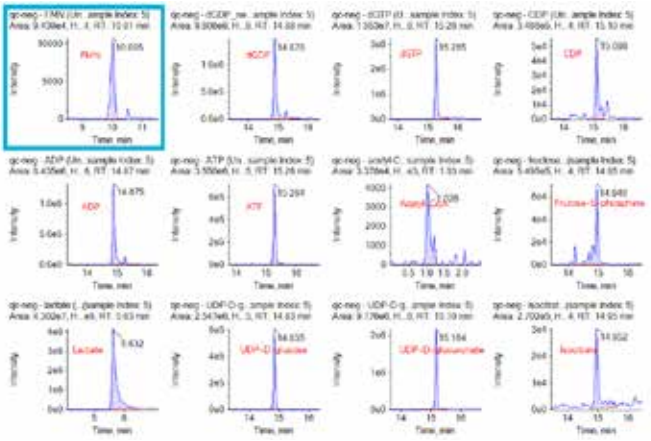

图2.部分负模式化合物提取离子色谱图

2. 数据分析

本文共检测了12个细胞样品用于差异性分析，实现该方法在靶向能量代谢组学中的应用。12个样本中6个为给药组细胞样本，另外6个为对照组样本。利用该LC-MS/MS方法对这批样本中能量代谢物进行了靶向的分析。首先，我们对这两组样品测得峰面积结果进行了PLSDA分析，从图3中可以看出这两组样品很明显的被区分开来，说明能量代谢物在给药组及对照组中有显著差异。

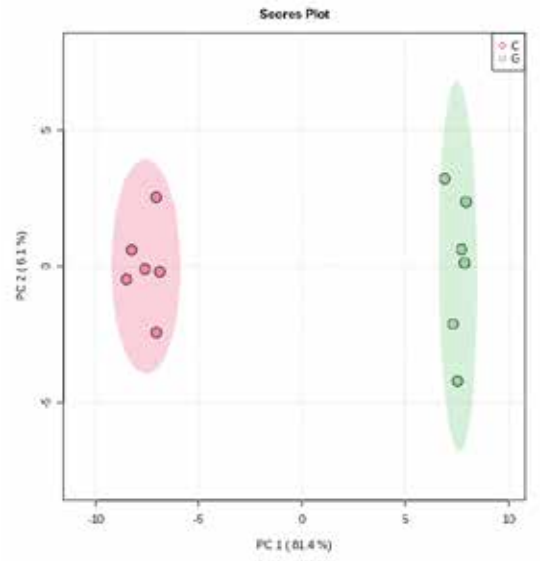

图3. 两组细胞样本的PLSDA图（G为给药组，C为对照组）

RUO-MKT-02-14614-ZH-A

为了找出变化差异明显的能量代谢物成分，我们进行了统计分析，得到每种代谢物在两组样品中的p-value和VIP值，通过p-value< 0.01和VIP>1的筛选，共有92种代谢物有显著变化（见表2）。从热图（图4）可以发现对照组与给药组有显著差异，在top25的化合物中，给药组中腺苷、鸟苷、肌苷、尿嘧啶、葡萄糖-6-磷酸等14种物质含量升高，脱氧鸟苷三磷酸、甘氨酸、肌醇、天门冬氨酸、肌氨酸等11种物质含量降低。

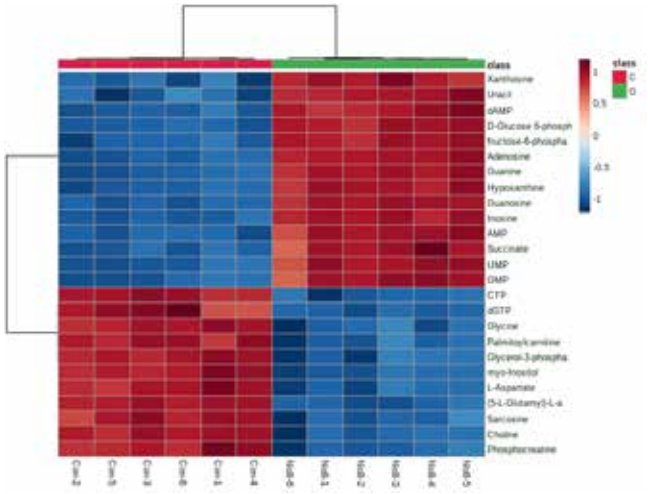

图4. 两组细胞样品的热图（top25）（G为给药组，C为对照组）

总结

本文使用SCIEX Triple Quad™ 7500系统建立了330种能量代谢物LC-MS/MS检测方法，可用于细胞中能量代谢物的靶向研究。该方法不仅能高效准确地检测出样品中的代谢物成分，而且能够提供有效地差异性分析，为高通量分析不同模型下能量代谢物的差异提供了快速可靠的方法。

表2. 部分差异化合物（top25）

No.	差异化合物名称	p.value	VIP
1	Guanosine	1.1873	1.30E-13
2	D-Glucose 6-phosphate	1.1872	1.41E-13
3	Adenosine	1.1871	2.06E-13
4	Inosine	1.187	2.23E-13
5	(5-L-Glutamyl)-L-amino acid	1.187	2.50E-13
6	Guanine	1.1864	7.75E-13
7	Hypoxanthine	1.1857	2.05E-12
8	fructose-6-phosphate	1.185	4.85E-12
9	dAMP	1.1846	8.30E-12
10	AMP	1.1841	1.35E-11
11	myo-Inositol	1.1837	1.88E-11
12	Choline	1.1833	2.57E-11
13	CTP	1.1833	2.65E-11
14	UMP	1.1825	5.01E-11
15	L-Aspartate	1.1813	1.11E-10
16	Phosphocreatine	1.1807	1.54E-10
17	Glycine	1.1806	1.64E-10
18	Xanthosine	1.1804	1.92E-10
19	Palmitoylcarnitine	1.1802	2.04E-10
20	GMP	1.1801	2.27E-10
21	Glycerol-3-phosphate	1.1795	3.02E-10
22	Uracil	1.1791	3.76E-10
23	Succinate	1.1789	4.05E-10
24	Sarcosine	1.1789	4.08E-10
25	Guanosine	1.1873	1.30E-13

RUO-MKT-02-14614-ZH-A

SCIEX三重四极杆质谱仪快速分析11种含高能磷酸键化合物

Rapid Analysis of 11 Energy Rich Phosphate Compounds by SCIEX Triple Quad Mass Spectrometer

陈俊苗，司丹丹，龙志敏
Junmiao Chen, Dandan Si, Zhimin Long
SCIEX 应用支持中心，中国

Key words: SCIEX Triple Quad 6500+, Energy Rich Phosphate Compounds, Nucleotide Compounds, dATP, dCTP, dTTP.

引言

高能磷酸化合物是指水解时可释放大量能量的一类磷酸化合物。这类化合物多含有1到3个不等的磷酸基团如三磷酸腺苷（ATP）等，它们是生物释放、储存和利用能量的媒介，是生物界直接的供能物质。该类化合物在使用液相色谱质联用仪(LC/MS)进行分析时流动相添加剂有限，色谱峰形不好导致响应较差，其他分析手段比如毛细管电泳（CE-UV）、高效液相（HPLC-UV）多采用紫外检测器导致灵敏度不够。而该类化合物在基质样品中含量较低且不够稳定更是增加了检测难度。

目前有部分文献报道采用在流动相中加入离子对试剂，虽然可提高化合物的灵敏度，但由于离子对试剂在仪器中比较容易残留很难完全清洗干净，当更换为其他非离子对试剂的项目时容易产生信号抑制等问题。而该类化合物在液相色谱中峰形不好灵敏度差的主要原因是化合物中的磷酸基团容易与系统中微量的金属尤其是铁等结合导致[1]。

本方法采用在流动相中添加亚甲基二磷酸及甲酸铵的方式改善含磷酸基团化合物的峰形，采用SCIEX Triple Quad™ 6500+系统进行高灵敏度质谱分析，定量限可达0.1ng/mL以下，部分化合物检测限可低至0.01ng/mL，完全满足该类化合物的定量分析需求。

方法优势：

1. 流动相不用离子对试剂减少仪器污染，增加方法通用性。
2. 良好的线性及灵敏度满足不同基质样品中不同浓度水平的高能磷酸化合物的准确定量。
3. 样品前处理简单，只需简单蛋白沉淀再挥干，无需固相萃取（SPE）浓缩。

仪器设备：

SCIEX ExionLC™ AD系统和SCIEX Triple Quad™ 6500系统

图1. SCIEX ExionLC™ AD系统和SCIEX Triple Quad™ 6500+系统

样品制备

商品化的标准品储备液含有氢氧化钠形成钠盐，可直接用纯水稀释标准曲线进样分析。粉末标品采用纯水溶解，若溶解不好可适量加入氨水助溶。基质样品采用甲醇：乙腈（1:1，V:V）混合溶剂提取，高速离心后取上清液挥干，再用纯水复溶，细胞样品需要先破碎细胞后再进行提取。

液相条件：

液相系统：SCIEX ExionLC™ AD系统

RUO-MKT-02-14446-ZH-A

色谱柱：Synergi 4 μm Fusion-RP, 150 × 3mm

流动相A：水（含5 mM甲酸铵，5 μM亚甲基二磷酸）

流动相B：95%乙腈水（含5 mM甲酸铵，5 μM亚甲基二磷酸）

流速：0.25 mL/min

柱温：40 ℃

进样体积：10 μL

液相梯度：

时间(min)	流速（mL/min）	A(%)	B(%)
0	0.25	99	1
2	0.25	98	2
5	0.25	90	10
8	0.25	10	90
9	0.25	10	90
9.1	0.25	99	1
13	0.25	50	1

质谱条件：

电离模式：负离子模式

扫描方式：MRM多反应监测

气帘气CUR: 25 psi　　源温度 TEM：650 ℃

雾化气Gas1：35 psi　　辅助气Gas2：60 psi

MRM参数：如表1

表1. 11种高能磷酸化合物的质谱参数

名称	Name	Q1	Q3	DP	CE
腺嘌呤核苷酸	AMP-1	346.1	134.0	-50	-40
腺嘌呤核苷酸	AMP-2	346.1	96.9	-50	-36
鸟嘌呤核苷酸	GMP-1	361.9	210.9	-50	-25
鸟嘌呤核苷酸	GMP-2	361.9	150.0	-50	-35
2'-脱氧胞苷-5'-单磷酸	dCMP-1	306.1	194.9	-50	-25
2'-脱氧胞苷-5'-单磷酸	dCMP-2	306.1	78.9	-50	-60
三磷酸胞嘧啶脱氧核苷酸	dCTP-1	466.0	159.0	-40	-35
三磷酸胞嘧啶脱氧核苷酸	dCTP-2	466.0	78.9	-40	-120
胸腺嘧啶脱氧核苷酸	dTMP-1	321.0	194.9	-50	-25
胸腺嘧啶脱氧核苷酸	dTMP-2	321.0	78.9	-50	-45
三磷酸胸腺嘧啶脱氧核苷酸	dTTP-1	481.0	159.0	-40	-45
三磷酸胸腺嘧啶脱氧核苷酸	dTTP-2	481.0	78.9	-40	-120
尿苷二磷酸	UDP-1	403.0	159.0	-50	-35
尿苷二磷酸	UDP-2	403.0	78.9	-50	-100
尿嘧啶核苷酸	UMP-1	323.1	96.9	-40	-27
尿嘧啶核苷酸	UMP-2	323.1	79.0	-40	-80
腺嘌呤核苷酸	AMP-1	346.1	134.0	-50	-40
腺嘌呤核苷酸	AMP-2	346.1	96.9	-50	-36
鸟嘌呤核苷酸	GMP-1	361.9	210.9	-50	-25
鸟嘌呤核苷酸	GMP-2	361.9	150.0	-50	-35
次黄嘌呤核苷酸	IMP-1	347.0	134.9	-40	-35
次黄嘌呤核苷酸	IMP-2	347.0	96.9	-40	-31

实验结果

灵敏度及线性：如表2所示，所有11种化合物在线性范围内线性良好，线性关系R值均可达0.999，部分化合物定量下限（LLOQ）可达0.05 ng/mL，各化合物标准曲线图如图3。图2展示了所有11种化合物在1 ng/mL浓度下的峰图，图中可看出各化合物峰形良好，且部分化合物如dTTP和UDP等响应较高，定量下限可做到更低的水平。由于本次11种化合物同时检测，根据样品中各化合物大致含量进行定量下限配制，并没有配制更低的标准品浓度进行考察。各化合物如果分开检测定量下限可比表2中所列值更低。

重现性：所有11个化合物1 ng/mL标准品溶液连续进样6针，用峰面积计算得重现性RSD均小于5%，表明该方法重现性良好。

表2. 11种化合物线性范围及灵敏度结果

名称	Name	线性范围 (ng/mL)	线性关系 (R)	定量下限 (ng/mL)
胞嘧啶苷酸	CMP-1	0.2-100	0.999	0.20
三磷酸腺嘌呤脱氧核苷酸	dATP-1	0.1-100	0.999	0.10
2'-脱氧胞苷-5'-单磷酸	dCMP-1	0.1-100	0.999	0.10
三磷酸胞嘧啶脱氧核苷酸	dCTP-1	0.1-100	0.999	0.10
胸腺嘧啶脱氧核苷酸	dTMP-1	0.1-100	0.999	0.10
三磷酸胸腺嘧啶脱氧核苷酸	dTTP-1	0.1-100	0.999	0.10
尿苷二磷酸	UDP-1	0.05-100	0.999	0.05
尿嘧啶苷酸	UMP-1	0.05-100	0.999	0.05
腺嘌呤核苷酸	AMP-1	0.2-100	0.999	0.20
鸟嘌呤核苷酸	GMP-1	0.2-100	0.999	0.20
次黄嘌呤核苷酸	IMP-1	0.2-100	0.999	0.20

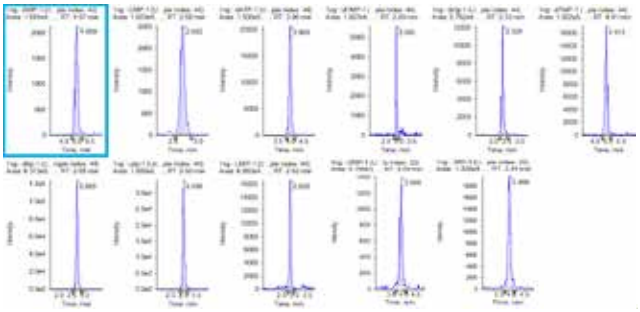

图2. 11种化合物1ng/mL峰图信息

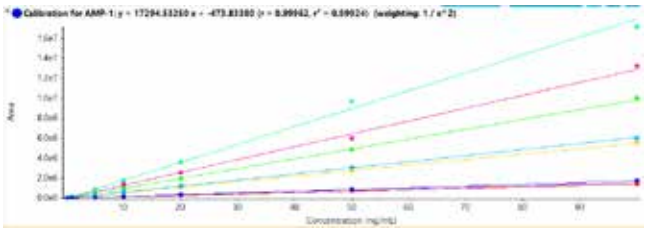

图3. 部分化合物标准曲线图

总结

本文使用SCIEX Triple Quad™ 6500+系统建立了11种含高能磷酸键化合物的定量方法，该方法流动相体系简单，无需添加离子对试剂，减少仪器污染的同时可增加方法的通用性。另外方法灵敏度及重现性好，各化合物在线性范围内线性关系良好，可以满足不同含量样品中高能磷酸化合物的定量需求。

参考文献

[1] Henryk S, Markus N, Marco H; Enhanced nucleotide analysis enables the quantification of deoxynucleotides in plants revealing connections between nucleoside and deoxynucleoside metabolism. THE PLANT CELL 2021: 33: 270–289.

RUO-MKT-02-14446-ZH-A

应用SCIEX Triple Quad™ 5500 系统检测生物样品中38种胆汁酸

Determination of 38 Bile Acids in Biological Samples on SCIEX Triple Quad™ 5500 system

查海红，陈慧敏，龙志敏，郭立海
Zha Haihong, Chen Huimin, Long Zhimin, Guo Lihai
SCIEX China

Key Words: SCIEX Triple Quad™ 5500，Bile Acids，Biological Samples

前言

胆汁酸（Bile Acids）是胆汁中存在的一类胆烷酸的总称，是一组用于胆固醇代谢、肠道营养物质吸收和胆汁脂质分泌的重要生理剂。胆汁酸按结构可分为游离型胆汁酸和结合型胆汁酸，游离型胆汁酸包括胆酸（CA）、去氧胆酸（DCA）、鹅去氧胆酸（CDCA）和少量的石胆酸（LCA）；结合型胆汁酸包括甘氨胆酸（GCA）、甘氨鹅去氧胆酸（GCDC）、牛磺胆酸（TCA）和牛黄鹅去氧胆酸（TCDCA）等。胆汁酸主要存在于肠肝循环系统并通过再循环起一定的保护作用。胆汁酸合成与代谢失调通常表明肝功能异常，因此血清中胆汁酸水平是衡量肝胆功能的重要指标。通过对生物样品中多种胆汁酸含量的检测，可以为更多的疾病找到可靠的标志物。

目前胆汁酸的分析方法主要包括气相色谱、气相色谱串联质谱、高效液相色谱、液相色谱串联质谱法（LC-MS/MS）等。其中LC-MS/MS具有方法简便、灵敏、特异性好的特点，适合大通量样本的分析，因此，本文采用SCIEX 液相色谱串联质谱系统，检测生物样品中38种胆汁酸，分别为：lithocholate (LCA), ursodeoxycholate (UDCA), hyodeoxycholate (HDCA), chenodeoxycholate (CDCA), deoxycholate (DCA), α-muricholate (αMCA), β-muricholate (βMCA), cholate (CA), glycolithocholate (GLCA), glycoursodeoxycholate (GUDCA), glycochenodeoxycholate (GCDCA), glycodeoxycholate (GDCA), glycocholate (GCA), taurolithocholate (TLCA), tauroursodeoxycholate (TUDCA), taurohyodeoxycholi acid (THDCA), taurochenodeoxycholate (TCDCA), taurodeoxycholate (TDCA), tauro-β-muricholate (TβMCA), taurocholate (TCA), murideoxycholate (MDCA), 23-nordeoxycholate (23-NDCA), hyocholate (HCA), glycohyocholate (GHCA), glycohyodeoxycholate (GHDCA), 7-ketolithocholate (7-KLCA), 12-Ketochenodeoxycholate (12-KCDCA), 7-ketodeoxycholate (7-KDCA), 3-oxocholate (3-OA), ursocholate (UCA), dioxolithocholate (DLCA), ω-muricholate (ωMCA), λ-muricholate (λMCA), allocholate (ACA), tauro-ω-muricholate (TωMCA), tauro-α-muricholate (TαMCA), tauro-λ-muricholate (TλMCA), glyco-λ-muricholate (GλMCA).

仪器设备

SCIEX ExionLC™液相系统 + Triple Quad ™ 5500质谱系统

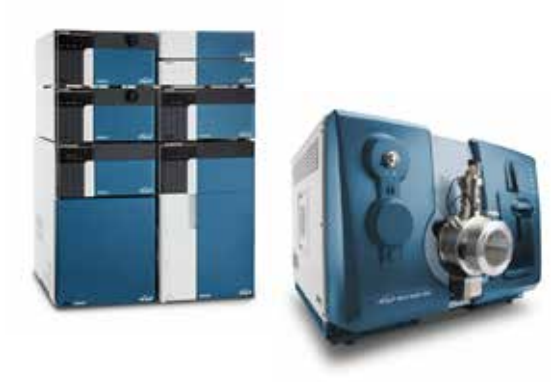

液相方法

色谱柱：Phenomenex Kinetex C18 (100 × 2.1 mm, 1.7 µm)

流动相：A相：水（0.1% 甲酸）
B相：乙腈（0.1% 甲酸）

流速：0.45 ml/min

RUO-MKT-02-10519-ZH-A

柱温：40 ℃

进样量：5 μL

表1. 液相洗脱梯度。

时间 (min)	A (%)	B (%)
0.0	90	10
1.0	90	10
2.0	75	25
12.5	60	40
14.5	2	98
16.0	2	98
16.5	90	10
18.0	90	100

质谱方法

离子源：ESI源，负离子模式

离子源参数：

IS电压: -4500 V　　气帘气 CUR: 35 psi

雾化气 GS1: 55 psi　　雾化气 GS2: 55 psi

碰撞气 CAD: Medium　　源温度 TEM: 550 ℃

实验结果

本文将该方法用于老鼠血浆样品的检测，每种胆汁酸的保留时间通过标准品以及文献[1-3]进行确定。在血浆样品中，这38种胆汁酸都能被检测到，详细的提取离子流图见图1，说明该方法能用于复杂生物样品的检测。

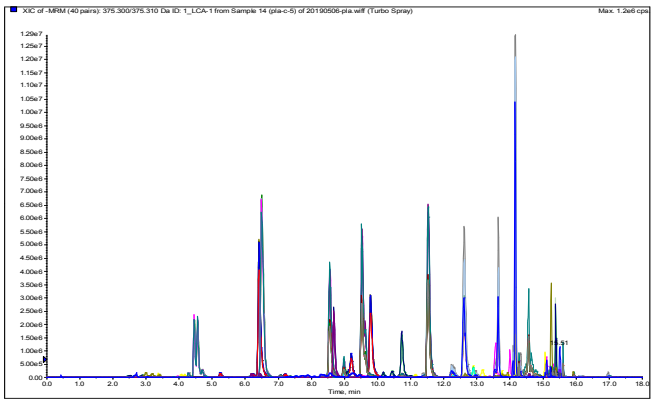

图1. 血浆样品中38种胆汁酸的提取离子流图。

表2. 38种胆汁酸的质谱参数。

Compound	Q1/Q3	DP	CE	CXP
LCA	375.3 / 375.3	-120	-23	-20
UDCA	391.4 / 391.4	-140	-30	-7
HDCA	391.3 / 391.3	-140	-30	-7
CDCA	391.3 / 391.3	-140	-27	-20
DCA	391.3 / 391.3	-140	-30	-17
α MCA	407.2 / 407.2	-150	-30	-20
β MCA	407.2 / 407.2	-150	-30	-20
CA	407.2 / 407.2	-150	-30	-20
GLCA	432.3 / 74.0	-135	-71	-19
GUDCA	448.3 / 74.1	-135	-71	-19
GCDCA	448.4 / 74.1	-140	-72	-20
GDCA	448.3 / 74.2	-140	-75	-20
GCA	464.3 / 74.1	-120	-75	-7
TLCA	482.3 / 80.0	-130	-120	-5
TUDCA	498.3 / 80.1	-120	-120	-10
THDCA	498.3 / 80.1	-120	-120	-10
TCDCA	498.3 / 80.0	-110	-120	-10
TDCA	498.2 / 80.0	-120	-120	-21
T β MCA	514.2 / 80.1	-120	-125	-20
TCA	514.2 / 80.1	-120	-125	-20
MDCA	391.3 / 391.4	-140	-30	-7
NDCA	377.3 / 377.3	-140	-20	-7
HCA	407.2 / 407.2	-150	-20	-20
GHCA	464.3 / 74.1	-120	-75	-7
GHDCA	448.3 / 74.2	-135	-71	-19
7-KLCA	389.3 / 389.3	-140	-20	-7
12-KCDCA	405.3 / 405.3	-140	-20	-7
7-KDCA	405.3 / 405.3	-140	-20	-7
3-OA	405.3 / 405.3	-140	-20	-7
UCA	407.3 / 407.3	-140	-20	-7
DLCA	403.3 / 403.3	-145	-20	-7
ω MCA	407.3 / 407.3	-140	-20	-7
λ MCA	407.3 / 407.3	-140	-20	-7
ACA	407.3 / 407.3	-140	-20	-7
T ω MCA	514.2 / 80.1	-120	-125	-20
T α MCA	514.2 / 80.1	-120	-125	-20
T λ MCA	514.2 / 80.1	-120	-125	-20
G λ MCA	464.3 / 74.1	-120	-75	-7

RUO-MKT-02-10519-ZH-A

本文共检测了24个老鼠血浆样品用于差异性分析，其中12个为正常老鼠的血浆样品，12个为患有糖尿病的老鼠的血浆样品。我们对这批老鼠血浆样品中的38种胆汁酸成分进行了定性及半定量的分析。

首先，我们对这两组样品进行了PCA分析，从图2中我们可以看出这两组样品很明显的被区分开来，说明胆汁酸在糖尿病模型中有显著变化。

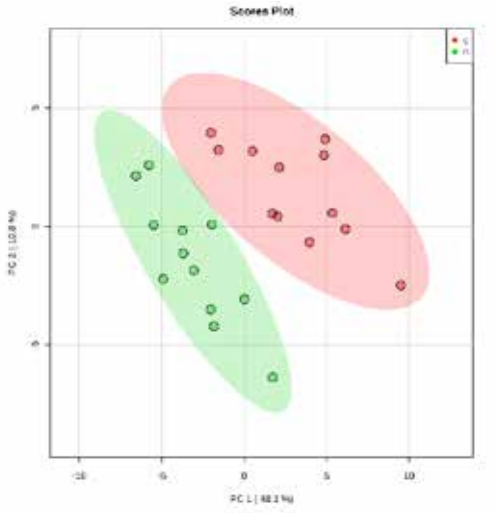

图2. 两组老鼠血浆样品的PCA图。

接着，我们将这组数据进行了热图分析，从图3中我们可以更直观地看出每种胆汁酸含量在不同组别中的变化。

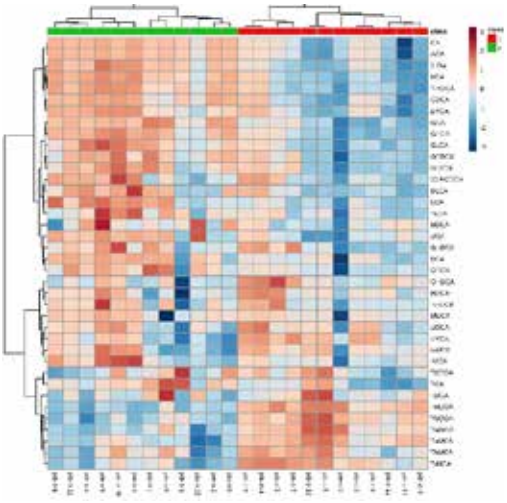

图3. 两组老鼠血浆样品的热图。

最后，为了找出变化差异明显的胆汁酸成分，我们对这38种胆汁酸进行了统计分析，得到每种胆汁酸在两组样品中的p-value和fold change（FC）值（图4），通过p-value < 0.05和FC>2的筛选，共有23种胆汁酸有显著变化，其中6种结合型胆汁酸在糖尿病模型的血浆中含量下降，17种胆汁酸的含量升高，详细见表3。说明，糖尿病对体内胆汁酸的含量有明显影响，且大部分有升高的趋势。

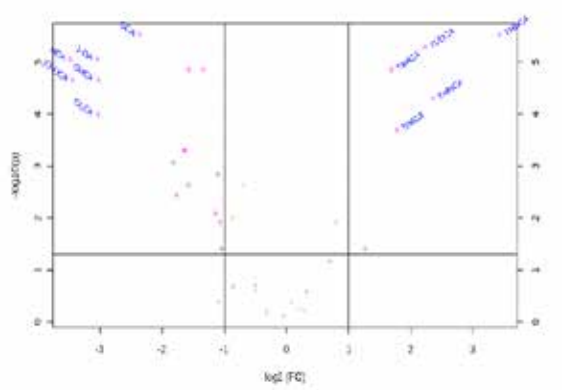

图4. 两组老鼠血浆样品中38种胆汁酸含量的火山图。

表3. 两组老鼠血浆样品中变化差异明显的23种胆汁酸。

	FC	p-value	糖尿病中的含量
THDCA	10.82	2.96E-06	down
TUDCA	4.71	5.18E-06	down
T α MCA	3.23	1.41E-05	down
T ω MCA	5.14	4.96E-05	down
T λ MCA	3.43	2.01E-04	down
GHDCA	2.40	3.87E-02	down
GCA	5.10	2.96E-06	up
HCA	11.13	8.88E-06	up
3-OA	8.21	8.88E-06	up
ACA	2.97	1.41E-05	up
CA	2.52	1.41E-05	up
7-KDCA	10.82	2.22E-05	up
GHCA	8.14	2.22E-05	up
GLCA	8.17	1.03E-04	up
GCDCA	3.12	4.96E-04	up
CDCA	3.09	4.96E-04	up
G λ MCA	3.52	8.58E-04	up
LCA	2.15	1.43E-03	up
α MCA	2.98	2.32E-03	up
GDCA	3.41	3.64E-03	up
DLCA	2.20	8.29E-03	up
TCA	2.09	1.21E-02	up
TLCA	2.06	3.87E-02	up

RUO-MKT-02-10519-ZH-A

总结

本文使用SCIEX Triple Quad™ 5500系统建立了LC-MS/MS方法测定38种胆汁酸的定性定量方法。该方法在复杂的生物样品中进行了验证，不仅能高效准确地检测出样品中的胆汁酸成分，而且能够提供有效地差异性分析，为大通量分析不同疾病中胆汁酸的差异提供了可靠的方法。

参考文献

[1] Han J , Liu Y , Wang R , et al. Metabolic Profiling of Bile Acids in Human and Mouse Blood by LC–MS/MS in Combination with Phospholipid-Depletion Solid-Phase Extraction[J]. Analytical Chemistry, 2015, 87(2):1127-1136.

[2] Wang X , Xie G , Zhao A , et al. Serum Bile Acids Are Associated with Pathological Progression of Hepatitis B-induced Cirrhosis[J]. Journal of Proteome Research, 2015:150512060716008.

[3] Xie G , Wang Y , Wang X , et al. Profiling of Serum Bile Acids in a Healthy Chinese Population Using UPLC–MS/MS[J]. Journal of Proteome Research, 2015, 14(2):850-859.

RUO-MKT-02-10519-ZH-A

应用SCIEX Triple Quad™ 4500 系统检测生物样品中90种胺类代谢物

Determination of 90 Amine- and Phenol-Containing Metabolites in Biological Samples on SCIEX Triple Quad™ 4500 system

陈慧敏，龙志敏，郭立海
Chen Huimin，Long Zhimin， Guo Lihai

SCIEX应用支持中心，中国
SCIEX, China

Keywords： SCIEX Triple Quad™ 4500 System，Amino Acids，Metabolomics，Biological Samples

引言

氨基酸及其衍生物是人类生理过程的常用生物标志物。它们在人体体液中的识别和定量提供了对人类健康的深刻见解。许多研究发现，在癌症患者和其他增生性疾病患者的生物液和受影响的组织中，多胺及其代谢物的含量明显较高。一些治疗性多胺类似物已被证明在治疗癌症和其他高增殖性疾病方面具有潜在的用途。含胺代谢物的检测可能用于癌症及其他疾病研究[1-2]。

目前利用LC-MS/MS同时检测多种含胺代谢物类的主要挑战在于生物基质中大量极性代谢物的检测。亲水性化合物在反相（RP）LC固定相上保留很差，在复杂生物基质中易发生信号抑制。在本文的研究中通过衍生化可以有效改善代谢物色谱行为和灵敏度。本文采用丹磺酰氯作为衍生化试剂对含伯胺、仲胺的代谢物进行衍生化，从而增加胺类物质在反相色谱中的保留能力，并提高在质谱检测中的离子化效率，达到提高胺类物质定量准确性和检测灵敏度的目的，并利用SCIEX Triple Quad™ 4500系统建立了15 min一针同时检测90个含胺代谢物的定量方法。该方法对胺类代谢物覆盖面广（包括氨基酸及其甲基化、乙酰化产物等），利用小鼠组织样本中检测72个胺类代谢物，提供了胺类物质代谢组的轮廓信息，并进行差异分析。另外利用该方法分别检测了小鼠血浆和尿液样本中71种和88种胺类代谢物。

仪器设备

ExionLC™ AD系统 + SCIEX Triple Quad™ 4500系统

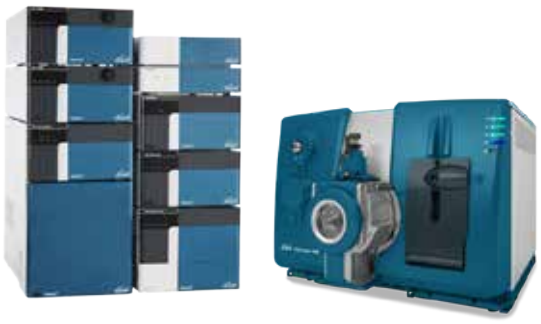

样本前处理：

血浆样本：取100 µL血浆，加入300 µL甲醇，震荡1 min，静置1 h（4 ℃），14000 rpm离心10 min，取上清冻干保存。

尿液样本：50 µL尿液用水稀释1倍，之后同血浆样本处理方法。

组织样本：样本称重20-30 mg置于EP管中，加入800 µL遇冷至-80 ℃的甲醇,匀浆破碎，4 ℃下14000 rpm离心10 min,上清转移冻干保存于-80 ℃中。

RUO-MKT-02-11082-ZH-A

衍生化反应：

复溶冻干样本，取上清液50 µL，加入30 µL丹磺酰氯乙腈溶液(10 mg/mL)和40 µL的0.5 M碳酸钠—碳酸氢钠缓冲液，封口并迅速混匀，置于60 ℃水浴反应30 min，取出加入10 µL 0.25 M NaOH，再次60 ℃水浴反应10 min。随混合物冷却至室温后加入70 µL的10%甲酸溶液，1 µL进样。整个处理过程应尽可能迅速，且避光[3]。

丹磺酰氯衍生化伯胺或仲胺的反应原理如图1a, 如果一个化合物有多个相应基团可能会和多个丹磺酰氯发生反应。经过衍生后的化合物在LC-MS/MS中的特征裂解碎片见图1b，对应质荷比分别为m/z 170和m/z 156。

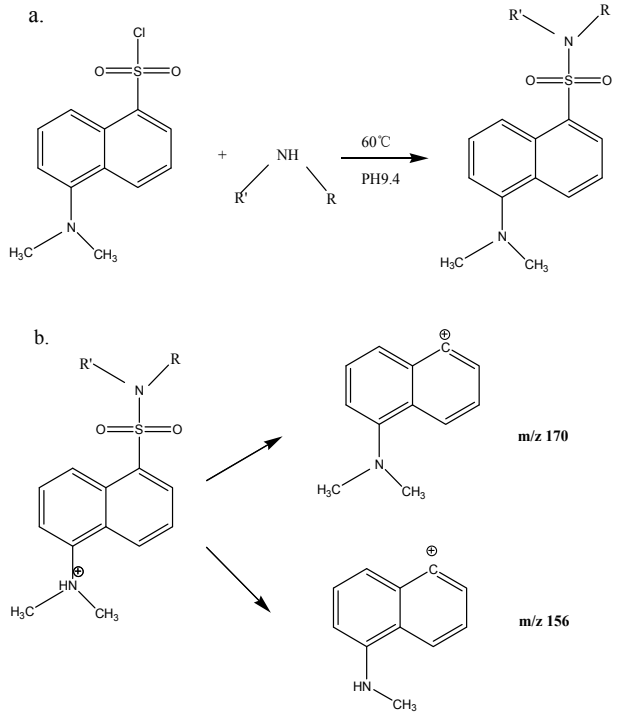

图1. a丹磺酰氯衍生化伯胺或仲胺的反应原理，b衍生后的待测物离子在LC-MSMS中易裂解产生的两个碎片。

液相条件：

色谱柱：Phenomenex Kinetex C18, 2.1 × 50 mm, 2.6 µm；

流动相：采用梯度洗脱

A为水（0.1%的甲酸）；

B为乙腈（0.1%的甲酸）；

流速：0.17 mL/min；

柱温：40 ℃；

进样量：1 µL；

表1. 液相洗脱梯度。

时间 (min)	A (%)	B (%)
2	85	15
3.5	65	35
6	60	40
8.5	58	42
10.5	40	60
11.5	5	95
12	5	95
12.5	0	100
13	0	100
13.1	85	15
15	85	15

质谱方法：

扫描方式：ESI+

ESI离子源参数：

气帘气CUR：35 psi；　　碰撞气CAD：7 psi；

IS电压：5500 V；　　源温度：550 ℃；

雾化气GAS 1：55 psi；　　辅助气GAS 2：55 psi；

实验结果：

1. 尿液，组织和血浆样本的检测结果

本文根据标准品以及相关文献[3-4] 利用SCIEX Triple Quad™ 4500系统建立了复杂生物样品中90种胺类代谢物的检测方法。图2a,b和c分别为小鼠尿液、组织和血浆中检测到的代谢物提取离子流图。其中在尿液中88种代谢物都能被检测到，而组织和血浆中分别能检测到72和71种。

RUO-MKT-02-11082-ZH-A

表2. 90种胺类代谢物的质谱参数。

Compound	Q1	Q3	Dwell Time	DP	CE
Glucosamine	413.14	170.1	8	60	35
2-Aminoadipic acid	395.13	170.1	8	60	30
4-Aminobutyric acid	337.12	170.1	8	60	30
4-Hydroxyproline	365.12	170.1	8	60	30
5-Glutamylcysteine	484.12	170.1	8	60	40
5-Oxoproline	363.10	170.1	8	60	30
Alanine	323.11	170.1	8	60	30
Alanyl-glutamine	451.16	170.1	8	60	40
Arginine	204.60	156.1	8	60	30
Asparagine	366.11	170.1	8	60	30
Aspartic acid	367.10	170.1	8	60	35
Citrulline	409.15	170.1	8	60	35
Cystathionine	345.09	170.1	8	60	35
Cysteine	355.08	170.1	8	60	35
Cystine	354.07	170.1	8	60	40
Glutamic acid	381.11	170.1	8	60	30
Glutamine	380.13	170.1	8	60	30
Glycine	309.09	170.1	8	60	30
Histidine	622.18	170.1	8	60	45
Isoleucine	365.15	170.1	8	60	30
DL-Kynurenine	442.14	170.1	8	60	30
Leucine	365.15	170.1	8	60	30
Lysine	307.10	170.1	8	60	30
Methionine	383.11	170.1	8	60	30
Methionine sulfoxide	399.10	170.1	8	60	35
N-Acetylaspartic acid	409.11	170.1	8	60	35
N-Acetylcysteine	397.09	170.1	8	60	35
Ornithine	599.20	170.1	8	60	45
Phenylalanine	399.14	170.1	8	60	35
Pipecolic acid	363.14	170.1	8	60	30
Proline	349.12	170.1	8	60	30
Serine	339.10	170.1	8	60	35
Threonine	353.12	170.1	8	60	30
Tryptophan	438.15	170.1	8	60	30
Tyrosine	208.10	156.1	8	60	35
Valine	351.14	170.1	8	60	30
4-Aminobenzoic acid	371.11	156.1	8	80	45
Guanine	385.11	170.1	8	60	30
2-Aminoethanol	295.11	170.1	8	60	30
4-Hydroxyphenyllactic acid	416.12	170.1	8	60	30
Histamine	578.19	170.1	8	60	30
O-Phosphoethanolamine	375.08	170.1	8	60	30
Boc-D-Tyr-OH	515.18	170.1	8	60	45
D-Homoserine	353.12	170.1	8	60	30
Saccharopine	510.19	170.1	8	60	45

Compound	Q1	Q3	Dwell Time	DP	CE
Argininosuccinic acid	759.25	170.1	8	60	45
β -alanine	323.11	170.1	8	60	35
L-Homoarginine	422.19	170.1	8	60	40
L-Homocitrulline	423.17	170.1	8	60	40
DL-3-Aminoisobutyric acid	337.12	170.1	8	60	30
2-Aminoisobutyric acid	337.13	170.1	8	60	25
5-Aminovaleric acid	351.13	170.1	8	60	30
L-2-Aminobutyric acid	337.13	170.1	8	60	30
DL-2,6-Diaminopimelic acid	424.15	170.1	8	60	40
6-Aminocaproic acid	365.15	170.1	8	60	30
L-Norvaline	351.14	170.1	8	60	30
D–(−)- α -Phenylglycine	385.12	170.1	8	60	35
L-Norleucine	365.15	170.1	8	60	30
Serotonin	643.20	170.1	8	80	35
Tryptamine	394.16	170.1	8	60	30
4-aminohippuric acid	428.13	170.1	8	60	40
5-Hydroxyindoleacetic acid	425.12	170.1	8	80	35
3-Aminosalicylic acid	387.11	170.1	8	60	30
Taurine	359.07	170.1	8	60	25
Hypotaurine	343.08	170.1	8	60	40
Djenkolic Acid	488.10	170.1	8	60	40
DL-Ethionine	397.13	170.1	8	60	30
DL-Homocysteine	369.09	170.1	8	60	30
DL-Lanthionine	675.16	170.1	8	60	40
L-Carnosine	460.16	170.1	8	60	30
L-Anserine	354.12	170.1	8	60	30
Ala-leu	436.19	170.1	8	60	40
Sarcosine	323.11	170.1	8	60	25
3-Methyl-L-histidine	403.14	170.1	8	60	35
N ε ,N ε ,N ε -Trimethyllysine	422.21	170.1	8	60	40
Asymmetric dimethylarginine	436.20	170.1	8	60	40
O-acetyl-L-serine	381.11	170.1	8	60	30
N α -Acetyl-L-lysine	422.17	170.1	8	60	40
DL-5-Hydroxylysine	315.11	170.1	8	60	30
5-Hydroxy-L-tryptophan	687.19	170.1	8	60	40
4-Hydroxy-L-isoleucine	381.15	170.1	8	60	30
Prolinamide	348.14	170.1	8	60	30
2-Amino-2-methyl-1-propanol	323.14	156.1	8	60	40
Methylguanidine	307.12	170.1	8	60	30
Homocarnosine	354.12	156.1	8	60	30
Aminolevulinic acid	365.12	170.1	8	60	30
Metanephrine	431.16	170.1	8	60	40
Salicyluric acid	429.11	170.1	8	60	35
3-Hydroxyanthranlic acid	387.10	170.1	8	60	30
3-Methyl-L-histidamine	359.15	170.1	8	60	35

RUO-MKT-02-11082-ZH-A

图2a

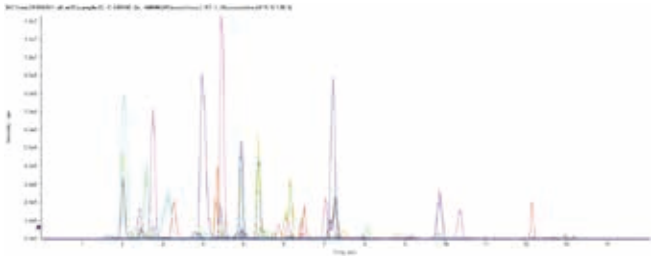

图2b

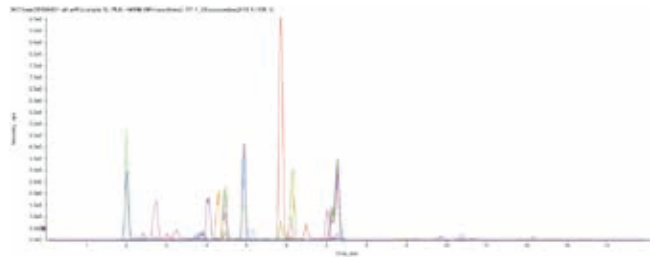

图2c

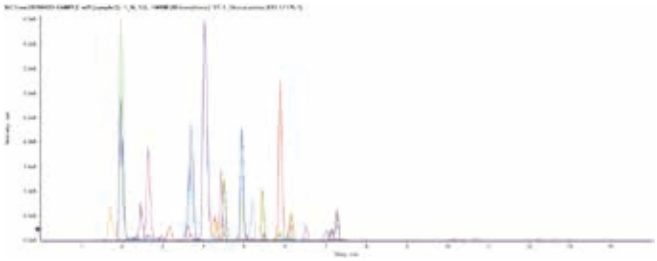

图2. a尿液、b组织和c血浆中90种胺类代谢物的提取离子流图。

另外为验证该方法在生物样品中的稳定性以及可靠性，我们利用测得的峰面积对6个批次处理组织样本（进行了批间精密度考察，另外对一个批次处理的6个平行样做了批内精密度考察。精密度考察结果中测得的所有化合物的RSD<20%。其中批内精密度考察结果内52个化合物RSD<10%，批间精密度考察结果中58个化合物RSD<10%，详细结果见表3。该结果表明该方法的稳定可靠，可用于生物样本中胺类代谢物的检测。

2. 癌组织和癌旁组织中胺类代谢物的靶向差异分析

此外，本文共检测了16个组织样品用于差异性分析，实现该方法在靶向代谢组学中的应用。16个样本中8个为癌症模型小鼠的癌组织，另外8个为对应癌旁组织。利用该LC-MS/MS方法对这批样本中胺类代谢物进行了半定量的分析。

首先，我们对这两组样品测得峰面积结果进行了PLSDA分析，从图3中可以看出这两组样品很明显的被区分开来，说明胺类代谢物在癌组织及癌旁组织中有显著差异。

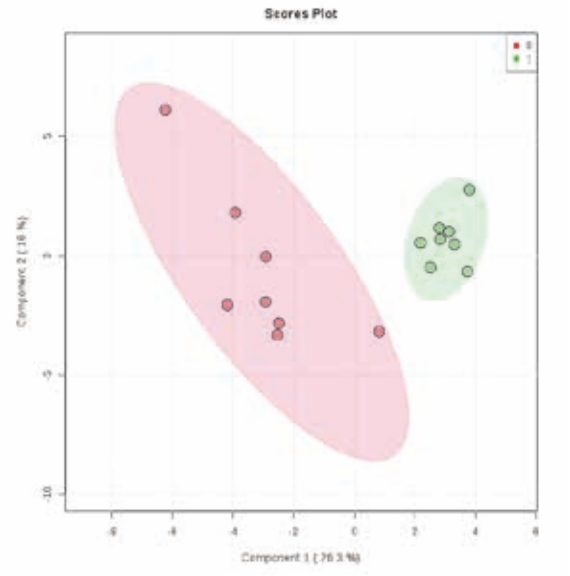

图3. 两组组织样品的PLSDA图（0对应癌组织，1对应癌旁组织）。

接着，我们对这两组数据进行了热图分析，从图4中可以更直观地看出每种代谢物含量在不同组别中的变化。

最后，为了找出变化差异明显的氨基酸成分，我们对组织中测得的胺类代谢物进行了统计分析，得到每种代谢物在两组样品中的p-value和fold change（FC）值（图5），通过p-value < 0.05和FC>2的筛选，共有7种代谢物有显著变化。癌组织中Cystathionine、Methylguanidine 、Guanine、Histamine 4种胺类代谢物含量比癌旁组织低，β -alanine、DL-Kynurenine和Aminolevulinic acid 3种胺类代谢物的含量更高，详情见表4，箱状图见图6。

RUO-MKT-02-11082-ZH-A

表3. 方法的批间和批内精密度考察。

化合物	批内精密度（n=6）		批间精密度（n=6）	
	Mean（cps）	RSD (%)	Mean（cps）	RSD (%)
D-Homoserine	2.44E+03	9.95	2.42E+03	6.97
Argininosuccinic acid	2.71E+03	16.91	5.22E+03	5.49
β -alanine	2.67E+04	7.47	6.52E+04	4.80
L-Homoarginine	6.14E+03	8.00	6.44E+03	5.83
L-Homocitrulline	4.81E+03	9.49	4.11E+03	4.36
DL-3-Aminoisobutyric acid	1.37E+04	11.57	4.00E+04	9.67
5-Aminovaleric acid	2.75E+05	6.15	3.67E+06	3.00
L-2-Aminobutyric acid	2.88E+05	8.38	2.25E+05	4.99
DL-2,6-Diaminopimelic acid	1.60E+04	9.16	1.44E+04	9.78
L-Norvaline	2.34E+06	7.17	8.47E+06	6.89
D–(−)- α -Phenylglycine	2.19E+03	13.63	1.75E+03	10.17
L-Norleucine	5.76E+04	8.35	2.87E+05	4.53
Taurine	3.04E+07	3.95	2.53E+07	7.19
Hypotaurine	2.10E+03	10.42	1.77E+03	10.42
DL-Homocysteine	8.69E+03	12.10	2.23E+04	4.83
Ala-leu	5.28E+03	6.07	5.05E+03	4.80
Sarcosine	1.05E+05	9.60	1.60E+05	1.71
3-Methyl-L-histidine	4.68E+04	7.13	5.39E+04	7.28
N ε ,N ε ,N ε -Trimethyllysine	1.22E+05	9.86	1.48E+05	2.26
Asymmetric dimethylarginine	6.93E+04	9.83	2.54E+05	6.16
N α -Acetyl-L-lysine	5.02E+04	8.46	2.02E+04	7.77
4-Hydroxy-L-isoleucine	8.63E+03	8.07	8.74E+03	13.67
Prolinamide	3.17E+04	8.44	9.31E+03	6.52
2-Amino-2-methyl-1-propanol	1.91E+03	12.93	8.76E+03	7.56
Methylguanidine	5.25E+03	9.99	1.77E+03	15.31
aminolevulinic acid	1.17E+05	6.19	3.33E+04	7.33
3-Methyl-L-histidamine	8.13E+05	3.35	1.99E+05	9.34
2-Aminoadipic acid	1.66E+04	11.35	7.50E+04	5.98
4-Aminobutyric acid	1.07E+06	6.89	6.01E+05	0.30
4-Hydroxyproline	4.26E+05	10.34	3.73E+05	3.27
5-Glutamylcysteine	2.32E+07	8.53	1.30E+07	7.79
5-Oxoproline	1.77E+04	9.64	7.11E+03	7.36

化合物	批内精密度（n=6）		批间精密度（n=6）	
	Mean（cps）	RSD(%)	Mean（cps）	RSD(%)
Alanine	9.06E+06	6.36	2.11E+07	4.55
Arginine	1.46E+05	9.26	4.82E+05	2.02
Asparagine	2.19E+05	9.53	2.53E+06	2.15
Aspartic acid	3.39E+06	2.69	6.45E+06	7.38
Citrulline	2.02E+06	6.70	4.50E+05	3.66
Cystathionine	6.01E+05	3.62	3.71E+05	7.20
Cysteine	6.20E+04	5.67	2.35E+05	5.25
Cystine	4.68E+03	9.44	1.10E+04	3.81
Glutamic acid	1.39E+07	4.18	3.66E+07	5.76
Glutamine	5.68E+06	4.88	6.47E+06	4.24
Glycine	5.89E+06	6.78	1.39E+07	1.27
Histidine	3.99E+05	7.44	6.10E+05	4.41
Isoleucine	3.59E+05	7.29	1.83E+06	4.73
DL-Kynurenine	1.45E+03	7.23	1.38E+05	11.37
Leucine	2.55E+06	7.66	8.66E+06	6.02
Lysine	1.47E+05	8.52	9.06E+05	8.30
Methionine	7.40E+05	8.45	3.84E+06	4.60
D-Methionine sulfoxide	7.32E+04	4.56	1.70E+05	8.66
N-Acetylaspartic acid	1.15E+04	13.73	6.12E+03	10.49
Ornithine	5.98E+04	12.71	4.57E+04	10.38
Phenylalanine	1.41E+06	9.05	2.27E+06	4.61
Pipecolic acid	1.02E+04	11.37	6.39E+03	5.72
Proline	4.99E+06	6.12	1.79E+07	6.09
Serine	9.34E+05	4.17	3.35E+06	4.49
Threonine	1.57E+06	7.99	5.62E+06	6.56
Tryptophan	6.50E+04	8.23	1.28E+05	12.85
Tyrosine	5.79E+04	9.20	1.02E+05	9.51
Valine	2.35E+06	8.58	8.00E+06	5.47
4-Aminobenzoic acid	1.62E+03	12.75	4.50E+03	6.90
Guanine	1.61E+04	10.38	2.20E+04	4.24
2-Aminoethanol	7.80E+05	8.17	1.57E+06	6.24
4-Hydroxyphenyllactic acid	5.93E+03	14.61	4.44E+03	8.26
Histamine	5.97E+03	6.40	2.76E+04	3.00
O-Phosphoethanolamine	6.36E+05	4.35	7.88E+06	8.91

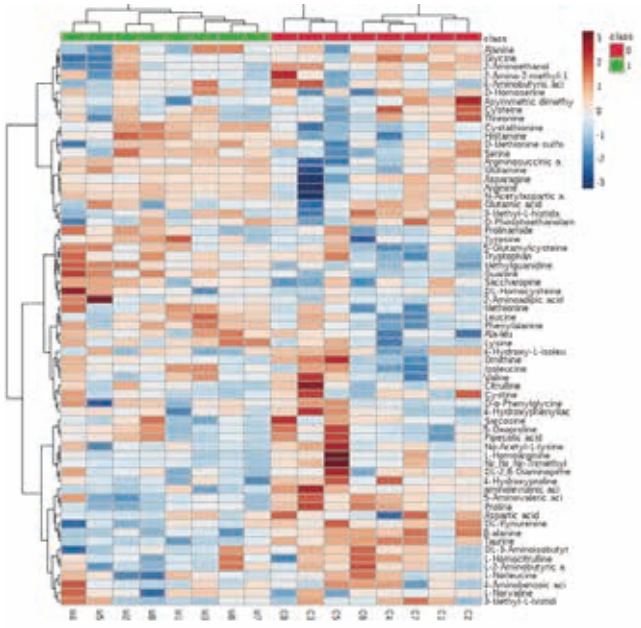

图4. 两组组织样品的热图（0对应癌组织，1对应癌旁组织）。

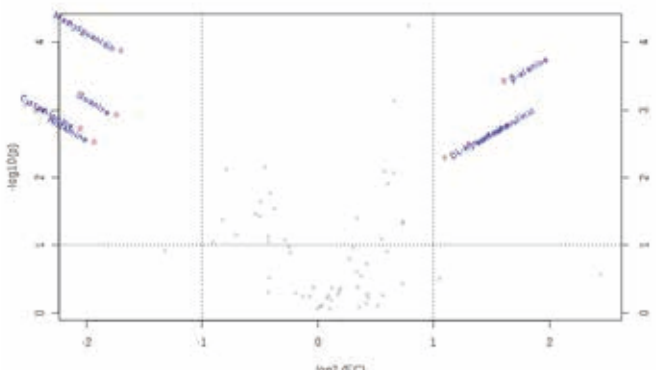

图5. 两组组织样品中胺类代谢物含量的火山图。

表4. 癌组织和癌旁组织中差异明显的化合物。

差异化合物名称	Fold Change	p.value	癌组织中含量
Cystathionine	0.24103	0.00013145	Down
Histamine	0.2617	0.00036933	Down
Guanine	0.30046	0.0011478	Down
Methylguanidine	0.30888	0.0018332	Down
β -alanine	3.0461	0.0029219	Up
Aminolevulinic acid	2.4787	0.0031365	Up
DL-Kynurenine	2.1398	0.005015	Up

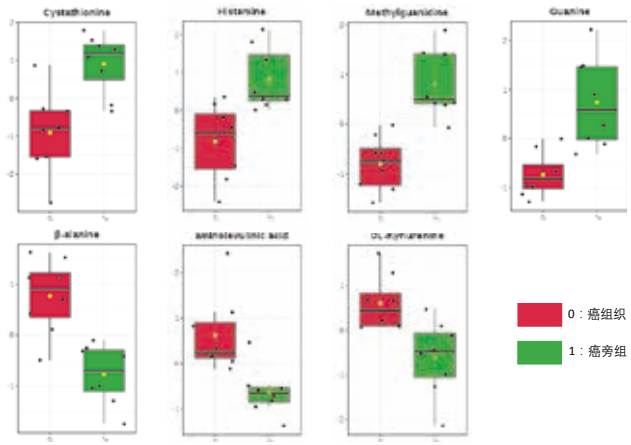

图6. 两组组织样品中7个差异化合物的箱状图。

通过该方法在靶向代谢组学中的应用，利用检测到的差异物结合体内代谢通路的分析，并结合文献分析，癌症与氨基酸代谢通路有着显著相关性，可以为癌症机制及临床治疗方案研究提供基础。

小结

本文使用SCIEX Triple Quad™ 4500系统建立了高效快速的90种胺类代谢物LC-MS/MS检测方法，可用于组织、血浆和尿液中胺类代谢物的靶向研究。该方法耗时短，所用色谱柱常规易得，并在多个复杂的生物样品中进行了验证，不仅能高效准确地检测出样品中的代谢物成分，而且能够提供有效地差异性分析，为高通量分析不同疾病模型下胺类代谢物的差异提供了快速可靠的方法。

参考文献

1. Casero, R. A., Marton, L. J. Targeting polyamine metabolism and function in cancer and other hyperproliferative diseases. Nat. Rev. Drug Discovery, 2007, 6, 373-390；
2. Khuhawar, M. Y., Qureshi, G. A. Polyamines as cancer markers : applicable separation methods. J. Chromatogr., B 2001, 764, 385-407；
3. Kevin Guo, Liang Li. Differential 12C-/13C-Isotope Dansylation Labeling and Fast Liquid Chromatography/Mass Spectrometry for Absolute and Relative Quantification of the Metabolome. Anal. Chem, 2009, 81, 3919-3932；

RUO-MKT-02-11082-ZH-A

4. Khamis M.M. et al. Comparison of accuracy and precision between multipoint calibration, single point calibration, and relative quantification for targeted metabolomic analysis. Analytical and Bioanalytical Chemistry, 2018.

RUO-MKT-02-11082-ZH-A

LC-MS/MS快速测定细胞中易挥发成分活性醛

LC-MS/MS Method for Rapid Determination of Volatile Aldehydes in Cells

汪洋

Wang Yang

SCIEX China

Key Words: API 4000™ LC-MS/MS; Tumor; Reactive aldehyde species; Derivatization

前言

氧化应激与多种病理状态相关，包括炎症、动脉粥样硬化、神经退行性疾病和癌症。细胞氧化应激通常被用于描述氧化还原状态的失衡，这种代谢紊乱不仅涉及反应性自由基，还包括过氧化氢、活性醛等非自由基。其中，脂质过氧化分解产物中的醛类，如丙二醛、乙醛和己醛等，被称为“氧化应激第二信使”，与自由基相比，活性醛半衰期较长，能够从其生成部位扩散开来，引起更广泛的影响。

目前针对醛类检测研究较多的领域，主要集中于环境食品行业。而针对肿瘤细胞中活性醛的研究一般依赖于灵敏度低的检测试剂盒，高通量检测多种醛类的方法研究却相当匮乏。虽然醛类检测使用气相质谱联用技术更具优势，但是需要固相微萃取或者顶空进样装置，对技术平台要求高。因此，我们基于LC-MS/MS技术平台，开发了适用于肿瘤细胞中十一种活性醛靶向检测方法。主要方法是采用2,4二硝基苯肼（Dinitrophenylhydrazine, DNPH）作为衍生化试剂，与活性醛生成稳定的腙类化合物进行LC-MS/MS检测，从而摆脱易挥发性物质对气相质谱联用技术检测的依赖。

试验方案：

1. 样品前处理：

处理细胞样品时，加入180 µL 50% 乙腈水溶液裂解细胞，再加入20 µL NaOH溶液，涡旋5 min后，加入20 µL $HClO_4$溶液，最后加入200 µL DNPH溶液在室温下反应4 h，离心（20000 g, 4 ℃, 15 min）后取上层清液真空挥干，200 µL ACN 复溶，离心进样检测。

2. 液相条件：

液相：Shimadzu LC 20AD^{XR}系统

色谱柱：Agilent ZORBAX SB-C18（2.1mm×50mm, 5 µm）

流速：0.3 ml/min

流动相：ESI-: A相为H_2O, 含2 mM 醋酸铵；B相为ACN, 含2 mM 醋酸铵；ESI+：A相为H_2O, 含0.1% 甲酸（Formate, FA）；B相为ACN, 含0.1% FA

柱温：40 ℃

进样量：5 µl

梯度洗脱：

Time (min)	% A（水相）	% B（有机相）
0	70	30
1	70	30
10	0	100
12	0	100
12.2	70	30
15	70	30

3. 质谱条件：

质谱扫描模式：MRM

离子源：电喷雾离子源

电离模式：负离子模式检测（ESI-) 子模式检测（ESI+)

质谱参数：

RUO-MKT-02-10543-ZH-A

质谱参数	数值
ISV	5500 / -4500 V
CUR	30 psi
TEM	450 ℃
GS1	50 psi
GS2	50 psi

表1. 活性醛衍生物MRM离子对、CE和DP参数。

Analyte	MW	Precursor ion	Product ion	CE	DP
Formaldehyde	30.0	208.9	150.9/162.8	-12	-40
Acetaldehyde	44.1	223.1	150.9/162.9	-13	-40
Pentanal	86.1	264.9	152.0/163.0	-28	-60
Hexaldehyde	100.2	279.0	151.9/162.8	-30	-50
Heptanal	114.2	293.0	162.8/177.9	-20	-90
Nonanal	142.1	321.1	151.9/162.9	-30	-90
Glyoxal	58.0	417.1	181.8/233.9	-28	-75
4-HNE	156.2	335.1	166.9/181.7	-28	-70
Retinal	284.4	465.3	268.2/373.2	34	55
Methylglyoxal	72.1	433.1	250.3	20	60
Malondialdehyde	72.1	235.0	259.0/189.0	29	50

4. 活性醛的DNPH衍生化

活性醛化学性质活泼，稳定性差，物理性质易挥发，因此在样品处理过程中易出现损失，造成结果偏差。我们采用衍生化的方法，将活性醛与DNPH反应生成稳定的腙类化合物进行LC-MS/MS检测。衍生化反应如下：

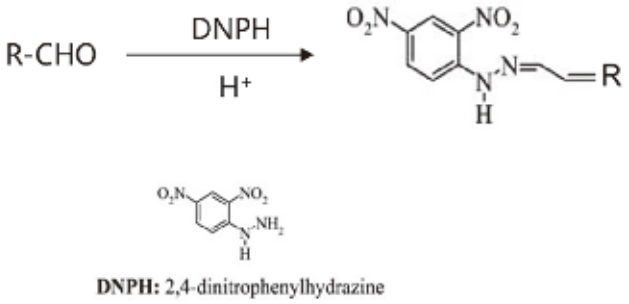

DNPH: 2,4-dinitrophenylhydrazine

实验结果：

1. C18色谱柱分离获得的典型色谱图

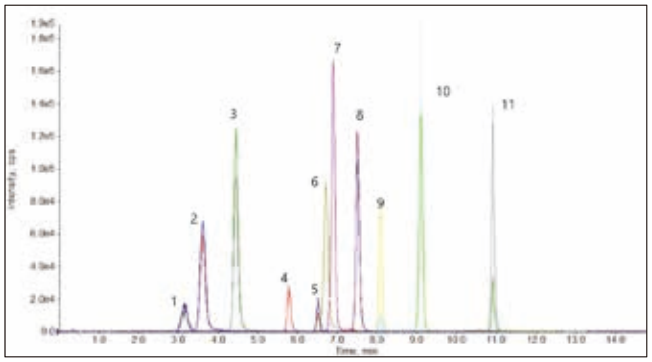

图1. 11种醛类衍生物的色谱峰。

以上色谱峰为各个醛类物质的衍生物色谱峰，对应的醛类物质如下：

1. Malondialdehyde; 2. Formaldehyde; 3. Acetaldehyde; 4. Methylglyoxal; 5. 4-HNE; 6. Glyoxal; 7. Pentanal; 8. Hexaldehyde; 9. Heptanal; 10. Nonanal; 11. Retinal

2. 线性范围：

11种活性醛在各自线性范围内线性良好（r > 0.99），线性范围宽，保证不同浓度水平样品的准确定量（如表2）。

表2. 测定11种活性醛的标准曲线。

Number	Analyte	Calibration range (ng/ml)	Regression equation	Linearity (r)
1	Malondialdehyde	50-1000	y=0.00195x-0.0109	0.9978
2	Formaldehyde	10-500	y=0.00308x+0.265	0.9953
3	Acetaldehyde	10-500	y=0.00754x+0.113	0.999
4	Methylglyoxal	10-500	y=0.000519x-0.00196	0.9975
5	4-HNE	5-100	y=0.000908x+0.0133	0.998
6	Glyoxal	10-500	y=0.00716x+0.104	0.9946
7	Pentanal	1-50	y=0.0089x+0.0284	0.9981
8	Hexaldehyde	1-50	y=0.00611X+0.0292	0.9988
9	Heptanal	2-100	y=0.000524x+0.00158	0.9985
10	Nonanal	5-100	y=0.00662x+0.274	0.9904
11	Retinal	20-500	y=0.00644x-0.0318	0.9934

RUO-MKT-02-10543-ZH-A

3. 回收率

制备得到低/高浓度的质控样品，经过与样品相同的前处理过程后，经LC-MS/MS检测，回收率为70.26-90.34 %（见图2），重现性（n=3）RSD为1.30-7.37%（见图3）。

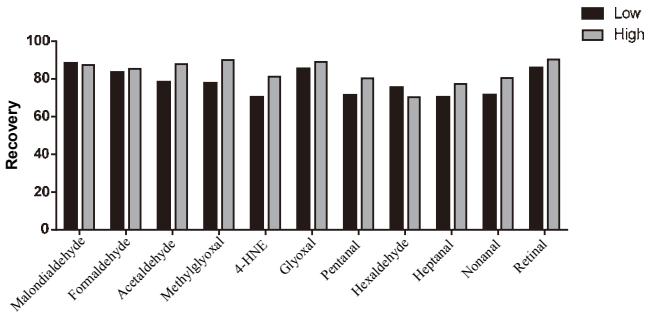

图2. 11种活性醛质控样品的回收率。

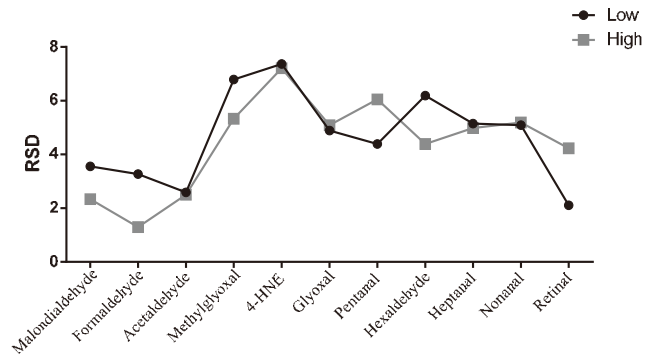

图3. 11种活性醛质控样品的分析重现性。

总结

本文在SCIEX API 4000™ LC-MS/MS 系统平台上，通过衍生化法前处理获得活性醛稳定腙类衍生物，建立了一套测定肿瘤细胞中11种活性醛的LC-MS/MS检测方法。该方法虽然经过衍生化处理，但是整个处理过程较为简单方便，拓宽了LC-MS/MS检测的化合物种类，展示了LC-MS/MS对挥发性物质检测的新方向。该方法灵敏度高，细胞中的定量限可达ng级，样品回收率高，重现性RSD < 8%，可对生物细胞中微量活性醛进行快速处理分析。

RUO-MKT-02-10543-ZH-A

液质联用结合化学衍生技术测定生物体内短链脂肪酸(SCFA)

Analysis of short-chain fatty acids (SCFAs) by LC-MS/MS coupled with chemical derivatization

江汉鹏，龙志敏，郭立海
Hanpeng Jiang, Zhimin Long, Lihai Guo
SCIEX应用支持中心，中国

Keywords: Short-chain fatty acids (SCFAs), LC/MS，化学衍生

前言

短链脂肪酸（SCFA，乙酸，丙酸，丁酸等）是生物体内很常见的物质，由于其分子结构小且稳定，其在CID下产生的碎片离子少且强度低，所以在液质联用MRM检测下往往基线较高，限制其灵敏度，碎片离子少导致MRM离子对少，通常使用MIM的模式检测，既Q1和Q3均扫描母离子，在基质干扰下无法区分干扰峰和目标峰，也限制了其检测准确度。所以在使用液质联用技术检测短链脂肪酸仍然有一定的难度。

因此，本文使用液质联用结合化学衍生技术测定生物体内SCFAs。使用化学衍生技术，将叔胺基团衍生至脂肪酸结构上，既可以将负离子模式下检测的脂肪酸转变为正离子模式检测，其衍生化后的产物，又可产生强度高并且稳定的碎片离子，提高了其检测灵敏度和准确度。

方法特点

1. 通过稳定的化学衍生技术，可在正离子模式下检测脂肪酸，衍生后产物可产生稳定高强度的碎片离子，即每种脂肪酸至少有二对以上MRM离子对对其检测，不仅提高了检测灵敏度也提高的准确度。仅需不到1 µL即可检测到SCFAs。
2. 该衍生化试剂可产生稳定的中性丢失离子，可对样品中羧酸类化合物靶向刷查。

样品及试剂

用于化学衍生的试剂为N,N-二甲基1,4-丁二胺（DMBA），反应所需催化剂为2-氯-1-甲基吡啶碘化物（CMPI）和三乙胺（TEA）。

样品前处理

血浆样本前处理流程如下。对于提取SCFAs，10µL血浆加入40 µL乙腈沉淀蛋白，蛋白充分沉淀后，放置低温（4℃）离心机，高速（12000 rpm）离心10 min，取上清，N^2吹干后备用。

化学衍生流程参考以下文献[1]，反应流程如下（图1），过前处理吹干生物样品用100 µL的ACN进行复溶。加入10 µL CMPI (20 µmol/mL) 和20 µL TEA (20 µmol/mL)混匀，随后加入20 µL DMBA (20 µmol/mL) 进行化学衍生。将反应液置于40 ℃下以1400 rpm的速度震荡1 h。待反应完成后，氮气吹干，除去溶剂和过量的衍生化试剂。用1mL纯水复溶后纯水稀释500倍后进样。

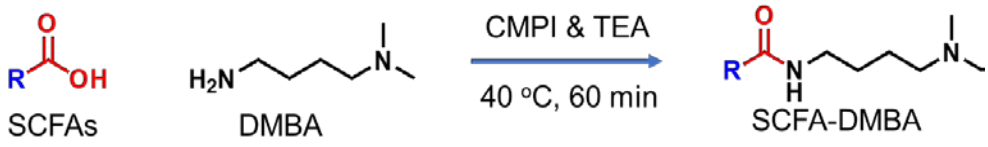

图1. SCFAs化学衍生反应

RUO-MKT-02-15699-ZH-A

仪器设备

ExionLC™ AD系统+ SCIEX Triple Quad™ LC-MS/MS系统

液相条件：

色谱柱：Phenomenex Kinetex C18 (100mm × 2.1 mm, 2.6μm)

柱温：40 ℃

进样体积：1 μL

流动相：A为水（含0.1%甲酸，v/v），B为乙腈

流速：0.4 mL/min

梯度如下：见表1

表1. SCFA色谱分离梯度

Time [min]	A.Conc [%]	B.Conc [%]
0.00	95.0	5.0
0.50	90.0	10.0
3.00	5.0	95.0
4.00	5.0	95.0
4.10	95.0	5.0
6.00	95.0	5.0

质谱条件

离子源：ESI源；POS模式；

扫描方式：MRM

离子源参数：

IS电压: 5500 V；　　气帘气CUR：35 psi；

雾化气GS1：60 psi；　　辅助气GS2：65 psi；

离子源温度为550 ℃；　　碰撞气：Medium

MRM参数如表2所示（SCFA*：定量离子对）

表2. SCFA的MRM参数

ID	Q1	Q3	DP	CE
AA-DMBA-1	159.1	114	10	17
AA-DMBA-2*	159.1	100.1	10	19
AA-DMBA-3	159.1	72.1	10	21
BA-DMBA-1	187.1	142.1	15	19
BA-DMBA-2*	187.1	100	15	23
BA-DMBA-3	187.1	72.1	10	24
PA-DMBA-1*	215.1	170.2	20	21
PA-DMBA-2	215.1	100.1	20	25
PA-DMBA-3	215.1	72.1	15	26

数据处理及数据分析

使用Analyst软件采集数据，SCIEX OS软件对采集的数据进行分析。

实验结果与讨论

1. 化学衍生后质谱碎裂规律

脂肪酸通常在负离子模式下进行检测，由于短链脂肪酸分子的结构特征，其无法产生强度高并且典型的碎片离子，往往采用SIM模式或者MIM模式对其检测，既仪器扫描时只选择母子，这往往导致了基线过高，并且色谱流动的弱酸性会抑制其在ESI 源内的电离，进一步的影响了检测灵敏度。另一方面，检测时，没有至少两对离子对来辅助定性，在复杂的生物基质下，杂峰也会干扰定性，造成假阳性结果。为了解决以上问题，本文采用化学衍生的方法，方法如图2，将含有叔胺和四个碳链的基团标记在脂肪酸上，标记后化合物可以在正离子模式下检测，解决了负离子离子化抑制的问题；其次，衍生产物由于碳数的增加，使得使用反相色谱时，其衍生产物的保留增强，解决了短链脂肪酸在反

RUO-MKT-02-15699-ZH-A

相色谱上保留差的问题，避免了共流出产生的相互干扰和信号抑制；最后衍生产物可以产生稳定且强的碎片离子（图2），比如稳定的45Da的中性丢失，以及质荷比100和72俩个碎片离子，所以，对于SCFAs的检测，每种SCFAs的检测MRM离子对，增加至3对，由于不是SIM和MIM方式，其大大的降低了基线，提升了检测灵敏度，并且有多个离子对辅助定性，在复杂的生物基质下，造成假阳性概率大大降低。

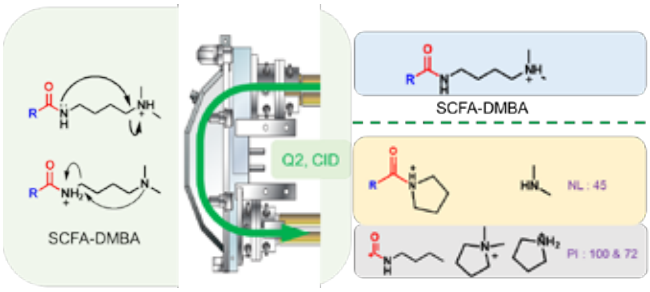

图2. 衍生化产物在质谱碰撞池中碎裂模式

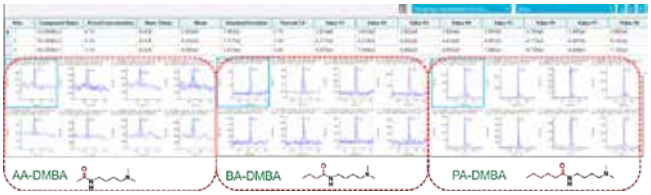

图4. 0.1 ng/mL浓度下连续进样8针色谱图及稳定性

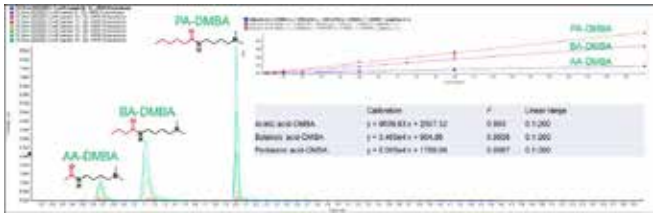

图3. 乙酸，丁酸，戊酸的色谱图，标准曲线及线性范围

2. 血浆中SCFAs检测

以乙酸（AA），丁酸(BA)和戊酸（PA）为例，对人和小鼠的血浆建立分析方法。色谱图，标曲和线性范围如图3所示。三种SCFAs线性良好，r^2>0.99。0.1ng/mL浓度下重复8次RSD均小于5%（3.6%）,提取离子色谱图如图4所示，三种浓度（0.1, 10和200 ng/mL）下准确度在85.0%至111.5%之间，重复性和准确度良好，如表3所示。方法对于乙酸，丁酸和戊酸的定量下限分别为0.01, 0.05和0.1ng/mL。

建立分析方法后，对人及小鼠血浆内三种SCFA进行了定量检测。色谱图如图5所示。血浆稀释50000倍后，仍然可检测到，仅需不到1 μL即可检测到血浆中的SCFAs，可用于痕量血浆中中SCFAs的检测。最后定量小鼠和人血浆中三种SCFA，浓度在120.5至490.2 mg/L范围内，如表4所示。

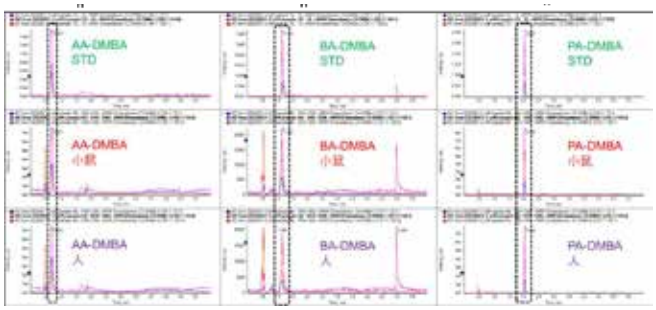

图5. 标准品，小鼠和人血浆中乙酸，丁酸，戊酸衍生产物色谱图

表3. 乙酸，丁酸，戊酸的LOQ，准确度和重复性

	Linear range ng/ml	LOQ ng/ml	Accuracy (ng/mL, %)			Repeatability (RSD%, n=8)
			0.1	10	200	0.1 ng/mL
Acetic acid-DMBA	0.1-200	0.01	111.5	97.4	100.7	2.7
Butanoic acid-DMBA	0.1-200	0.05	85.0	113.4	99.1	3.6
Pentanoic acid-DMBA	0.1-200	0.1	107.7	99.4	97.2	3.6

RUO-MKT-02-15699-ZH-A

表4. 小鼠和人血浆中乙酸，丁酸，戊酸浓度

	人血浆 (mg/L)	小鼠血浆(mg/L)
Acetic acid	484.8	490.2
Butanoic acid	104.5	120.5
Pentanoic acid	158.3	173.4

结论

本文运用前处理结合化学衍生的方法，检测到了生物体系中的SCFAs，该方法衍生简单，灵敏度高，稳定，重现好。对于检测SCFAs，仅用不到1微升血浆即可检测出其中的SCFAs，后期可运用于痕量生物样本——比如干血斑——中SCFAs的检测。

参考文献

1. Huang Y.Q., Wang Q.Y., Liu J.Q., Hao Y.H., Yuan B.F., Feng Y.Q., Isotope labelling – paired homologous double neutral loss scan-mass spectrometry for profiling of metabolites with a carboxyl group, Analyst, 2014, 139, 3446

RUO-MKT-02-15699-ZH-A

液相色谱串联质谱法测定植物中的激素成分

Determination of Plant Hormones in Plants by Liquid Chromatography Tandem Mass Spectrometry

陈金梅，司丹丹，龙志敏，郭立海
Chen Jinmei, Si Dandan, Long Zhimin, Guo Lihai

SCIEX应用支持中心，中国
SCIEX, China

Key Words: Plant Hormones, Liquid Chromatography Tandem Mass Spectrometry, ABA, SA, IAA, JA

前言

植物激素（Phytohormone）亦称植物天然激素或植物内源激素，是一组天然存在的激素，在低浓度下会影响生理过程的有机物质。它们虽然都是些简单的小分子有机化合物，但它们的生理效应却非常复杂、多样。从影响细胞的分裂、伸长、分化到影响植物发芽、生根、开花、结实、休眠和脱落等。所以植物激素对植物的生长发育有重要的调控作用。目前用于植物激素检测的方式有放射免疫分析法、酶联免疫吸附分析法，方法灵敏度高但特异性和准确度低；火焰离子化法、紫外分光光度法、荧光或电化学检测灵敏度和特异性低，无法满足植物体内植物激素水平检测需求；气相色谱串联质谱法需要衍生化操作，液相色谱串联质谱法具有高的灵敏度、特异性、准确性和重复性，更适合植物体内植物激素的检测。

本文实验方法特点

本文使用液相色谱串联质谱法对脱落酸（ABA），水杨酸（SA），吲哚乙酸（IAA）和茉莉酸（JA）进行检测，方法具有以下特点：

1. 仪器的灵敏度高，满足植物提取液中植物激素的检测需求。
2. 仪器和方法的特异性好，9 min的方法即可准确定量，检测效率高。
3. 使用各个化合物同位素标准品作为内标，内标法定量分析，使用溶剂标准曲线可以对样品进行准确的含量测定。

仪器设备

液相方法

色谱柱：BEH C18 100A (100 × 3.0mm, 1.8 µm)

流动相：A相：水 (0.001mMol乙酸铵)
B相：乙腈

流速：0.3 ml/min

柱温：40 ℃

进样量：2 µL

RUO-MKT-02-13364-ZH-A

表1. 液相梯度

Time	Flow	B
0.3	0.3	5
3.5	0.3	65
4.5	0.3	65
5	0.3	95
7	0.3	95
7.1	0.3	5
9	0.3	5

质谱方法

离子源：ESI源，负离子模式

离子源参数：

IS电压:- 4500 V　　气帘气 CUR: 35 psi

雾化气 GS1: 50 psi　　辅助加热气 GS2: 50 psi

碰撞气 CAD: Medium　　源温度 TEM: 500 ℃

表2. 化合物的质谱参数

	Q1 Mass (Da)	Q3 Mass (Da)	Dwell Time (msec)	ID	DP (volts)	CE (volts)
1	263.200	153.200	50.0	ABA	-40.000	-14.000
2	269.200	156.100	50.0	ABA_D6	-40.000	-14.000
3	137.200	93.000	50.0	SA	-40.000	-23.000
4	141.100	97.000	50.0	SA_D4	-40.000	-23.000
5	174.000	130.100	50.0	IAA	-30.000	-13.000
6	176.000	132.100	50.0	IAA_D2	-30.000	-13.000
7	209.100	59.200	50.0	JA	-35.000	-15.000
0	214.100	61.000	50.0	JA_D5	-35.000	-15.000

实验结果

1. **线性范围**：用50 %甲醇逐级稀释ABA、D6-ABA、SA、D4-SA、IAA、D2-IAA、JA、D5-JA的标准工作溶液至1-200 ng/ml，以峰面积比值对浓度做标准曲线。图2为四个化合物的线性范围、线性方程和相关系数。

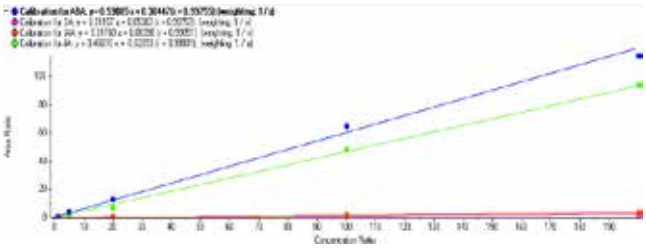

图1. 四个化合物的标准曲线

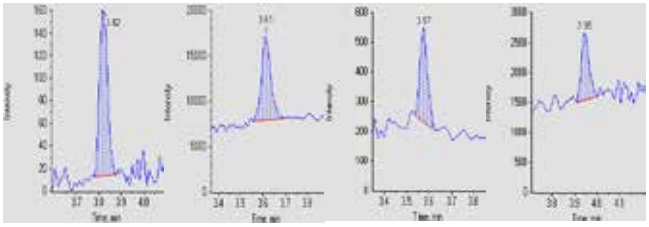

图2. LLOQ浓度下色谱图展示

2. **LLOQ的重现性**：平行制备六份LLOQ溶液，进样分析，测定结果如下所示。ABA、SA、IAA、JA四个化合物LLOQ分别为0.01 ng/ml、0.1 ng/ml、0.2 ng/ml、0.1 ng/ml，峰面积的重现性RSD%分别为7.88%、 2.98%、4.94%、4.82%，重现性好。

3. **植物提取液中植物激素的含量测定**：使用液液萃取法对植物进行提取后上样分析，使用内标法计算样品中含量，结果如表3所示。

表3. 植物提取液中植物激素的含量测定结果

Sample Name	Component Name	Area	IS Area	Calculated Concentration
8	ABA	475001.6	65282.0	10.947
8	SA	626808.2	2867168.1	13.917
8	IAA	7752.5	382831.9	0.968
8	JA	54483.2	54200.9	2.121
18	ABA	697685.1	63755.8	16.518
18	SA	2402753.7	3199760.5	58.470
18	IAA	109267.5	370171.3	16.391
18	JA	132849.8	49523.3	5.883
COL_3	ABA	211546.3	54443.3	5.797
COL_3	SA	4052759.0	3658578.8	88.336
COL_3	IAA	340410.3	310947.5	61.243
COL_3	JA	569798.9	37077.2	34.335

RUO-MKT-02-13364-ZH-A

总结

本文建立了液相色谱串联质谱法测定植物中的植物激素。方法灵敏度高，脱落酸（ABA），水杨酸（SA），吲哚乙酸（IAA）和茉莉酸（JA）四个化合物LLOQ分别为0.01 ng/ml、0.1 ng/ml、0.2 ng/ml、0.1 ng/ml，可满足植物中植物激素的检测需求。

RUO-MKT-02-13364-ZH-A

液相色谱串联质谱法测定15种植物内源激素成分

Fifteen Plant Endogenous Hormone Components Were Determined Using Liquid Chromatography Tandem Mass Spectrometry

陈金梅，司丹丹，龙志敏，郭立海
Chen Jinmei, Si Dandan, Long Zhimin, Guo Lihai

SCIEX应用支持中心，中国
SCIEX, China

Key Words: Plant Endogenous Hormone, Liquid Chromatography Tandem Mass Spectrometry, Auxins, Gibberenllins, Cytokinins, Abscisic acid

前言

植物激素（Phytohormone）亦称植物天然激素或植物内源激素，是一组天然存在的激素，在低浓度下会影响生理过程的有机物质。目前被科学界公认的六大类内源激素有植物生长素类（auxins）、赤霉素类（gibberenllins）、细胞分裂素类（cytokinins）、乙烯（ethylene）、脱落酸（abscisic acid）、油菜素甾醇类（brassinosteroids）。其中生长素、赤霉素、细胞分裂素、油菜素甾醇属于生长促进剂，脱落酸和乙烯属于生长抑制剂。除六大类激素之外，近年来科学家陆续发现了其他多种对植物生长发育有调控作用的物质，如多胺、茉莉酸、水杨酸类等。目前用于植物激素检测的方式有放射免疫分析法、酶联免疫吸附分析法，方法灵敏度高但特异性和准确度低；火焰离子化法、紫外分光光度法、荧光或电化学检测灵敏度和特异性低，无法满足植物体内植物激素水平检测需求；气相色谱串联质谱法需要衍生化操作，液相色谱串联质谱法具有高的灵敏度、特异性、准确性和重复性，更适合植物体内植物激素的检测。

仪器设备

SCIEX ExionLC™系统+ SCIEX Triple Quad™ 7500系统

液相方法

色谱柱：Phenomenex Kinetex F5 (100 × 2.1mm, 2.6 µm)

流动相：A相：水 (0.01%乙酸）B相：乙腈

流速：0.35 ml/min

柱温：40 ℃

进样量：2 µL

表1. 液相梯度

Time	Flow	B
1	0.3	5
8	0.3	95
9	0.3	95
9.1	0.3	5
11	0.3	5

RUO-MKT-02-14422-ZH-A

质谱方法

离子源：ESI源

一针正负离子切换模式

离子源参数：

IS电压:：2500 V (POS)/1750 V(NEG)　　气帘气 CUR: 40 psi

雾化气 GS1: 25 psi　　辅助加热气 GS2: 60 psi

碰撞气 CAD: Medium　　源温度 TEM: 500 ℃

表2. 化合物的质谱参数

Compound	Q1	Q3	CE
IAA_1	176.1	130.1	21
IAA_2	176.1	103.0	40
MeJA_1	225.2	151.1	19
MeJA_2	225.2	133.1	21
TZR_1	352.2	136.1	43
TZR_2	352.2	148.0	32
2-IP_1	204.0	136.0	22
2-IP_2	204.0	119.0	46
IBA_1	204.0	158.0	28
IBA_2	204.0	144.2	31
ABA_1	263.1	153.2	-18
ABA_2	263.1	204.1	-26
SA_1	137.0	93.0	-21
SA_2	137.0	65.0	-37
GA3_1	345.1	239.2	-20
GA3_2	345.1	143.1	-35
JA_1	209.0	59.2	-16
JA_3	209.0	41.0	-50
GA7_1	329.2	223.2	-25
GA7_2	329.0	211.2	-35
GA4-1	331.1	243.2	-26
GA4-2	331.1	213.1	-38
MT_1	231.0	216.1	-20
MT_2	231.0	144.0	-36
CK_1	224.0	133.0	-28
CK_2	224.0	106.1	-45
TZ_1	218.0	188.0	-21
TZ_2	218.0	134.0	-24
ICA_1	144.0	115.0	-37
ICA_2	144.0	126.0	-31

实验结果

1. **线性范围**：用80 %甲醇逐级稀释15个化合物的标准工作溶液至不同浓度的标准曲线，以峰面积对浓度做标准曲线。表3为15个化合物的线性范围，图1 为线性方程和相关系数。

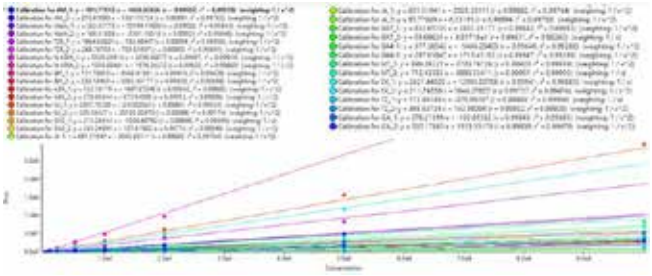

图1. 15个化合物的标准曲线

2. **灵敏度和重现性**：平行制备六份LLOQ溶液，进样分析， 15个化合物LLOQ浓度和峰面积的重现性如下表所示，重现性好。

表3. LLOQ浓度下重现性展示

Compound	线性范围	LLOQ 6针RSD	Compound	线性范围	LLOQ 6针RSD
IAA	10pg-10ng	6.88	JA	50pg-10ng	4.58
MeJA	100pg-10ng	5.89	GA7	50pg-10ng	8.13
TZR	10pg-10ng	4.18	GA4	50pg-10ng	7.02
2-IP	10pg-10ng	4.07	MT	10pg-10ng	4.8
IBA	50pg-10ng	8.43	CK	10pg-10ng	4.46
ABA	10pg-10ng	6.47	TZ	10pg-10ng	3.38
SA	100pg-10ng	6.09	ICA	10pg-10ng	6.69
GA3	10pg-10ng	6.82			

3. **植物提取液中植物激素的含量测定**：取出冷冻的植物样品，研磨至粉末，称取50 mg粉末，加入1 ml甲醇-水-甲酸提取液提取，涡旋混匀，超声10 min，至4度离心机12000 r/min离心10 min，取上清液至真空冷冻干燥机冻干，使用100 µl的80%甲醇溶液复溶，过0.22 µm滤膜过滤于自动进样小瓶中，样品中检测到10种植物内源植物激素。

RUO-MKT-02-14422-ZH-A

表4. 植物提取液中植物激素的含量测定结果

化合物	含量
IAA	150pg/ml
MeJA	4ng/ml
TZR	150pg/ml
N-6DIA	25pg/ml
ABA	5.5ng/ml
SA	206pg/ml
GA3	5.1ng/ml
JA	30ng/ml
MT	3ng/ml
ICA	950pg/ml

总结

本文建立了液相色谱串联质谱法测定植物中的15种植物内源激素成分。方法灵敏度高，可满足植物中植物激素的检测需求，为植物激素检测提供方法参考。

RUO-MKT-02-14422-ZH-A

SCIEX 液相色谱串联质谱法对小麦苗中183种代谢物进行靶标代谢组学分析

Targeted-metabonomics analysis of 183 metabolites in wheat seedling by SCIEX Liquid Chromatography-Tandem Mass Spectrometry

侯朋艺，肖梦晴，龙志敏
Pengyi Hou, Mengqing Xiao, Zhimin Long
SCIEX应用支持中心，中国

Keywords : SCIEX LC-MS/MS, Targeted-metabonomics, Wheat seedling

引言

代谢组学（Metabonomics）旨在研究生物体或组织甚至单个细胞中的糖类、脂类、氨基酸、核苷酸等全部小分子代谢物成分及其动态变化[1]。植物内源性代谢物对植物的生长发育有重要作用。植物中代谢物超过20万种，有维持植物生命活动和生长发育所必须的初生代谢物，还有利用初生代谢物生成的与植物抗病和抗逆关系密切的次生代谢物，所以对植物代谢物进行分析是十分必要的。

靶向代谢组学 (Targeted Metabonomics) 是代谢组学研究的重要组成部分，也是全代谢组研究的延伸与拓展。相对于全代谢组分析而言，靶向代谢组分析具有特异性强，检测灵敏度高和定量准确等几个特点。靶向代谢组学可以用于：验证有非靶向代谢组学实验提出的假说；进行基于假说的探索性实验，针对特定代谢物，研究代谢模型。 靶向代谢组学分析成功的关键因素是准确度、高通量和可靠性。靶向代谢组学一般采用三重四极杆 LC-MS/MS 系统上用多反应监测 (MRM) 进行靶向 MS/MS。MRM 是进行质谱定量的选择方法，具有高灵敏度、特异性好的特点，可以产生独特的碎片离子，可对非常复杂基质中的目标化合物进行监测和定量。

本文在前期利用高分辨质谱TripleTOF™ 6600+系统将小麦苗中成分进行表征的基础上，开发并验证了一种LC-MS/MS方法，即在一针进样、正负离子同时监测模式下，对小麦苗中183种代谢物的靶标定量分析。结果表明，该方法专属性好，灵敏度高、稳定性好。

供试品溶液制备

在前期提取好的小麦苗样品中，加入乙腈:水 (1:1) 混合溶液1 ml，涡旋5 min，15000 rpm离心5 min后，取上清液，直接进样分析。

液相条件

色谱柱：Waters ACQUITY UPLC HSS T3 (100 × 2.1 mm, 1.8 µm)

流动相：A: 水（含有0.01%甲酸）B: 乙腈

流速：0.3 ml/min

柱温：50 ℃

进样体积：2 µl

梯度条件：

RUO-MKT-02-13585

Time (min)	A (%)	B (%)
0	100	0
0.5	100	0
10	60	40
18	5	95
27	5	95
27.1	100	0
30	100	0

质谱条件

离子源：电喷雾电离 (ESI)，正负离子切换模式

扫描方式：sMRM多反应监测

MRM检测窗口 (MRM detection window): 100 sec

气帘气 (CUR)：40 psi　　离子喷雾电压(IS)：5500V(+)/-4500V(-)

加热温度 (TEM)：500℃　　雾化气 (GS 1)：50 psi

辅助气 (GS2)：50 psi　　碰撞气 (CAD)：9

去簇电压 (DP): 80 V　　入口电压 (EP): 10 V

碰撞池出口电压 (CXP): 10 V　　碰撞能 (CE): 35 V

sMRM参数：如表1

实验结果

正离子模式下各目标化合物的提取离子流图见图1，负离子模式下各目标化合物的提取离子流图见图2。

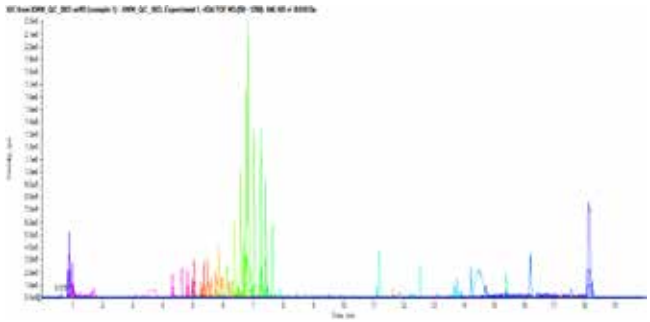

图1. 小麦苗正离子模式下各目标化合物的提取离子流图

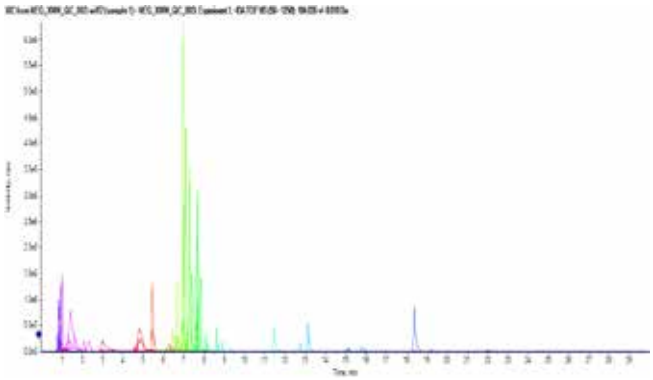

图2. 小麦苗负离子模式下各目标化合物的提取离子流图

表1. 小麦苗部分成分的质谱参数

Component Name	Q1	Q3	Polarity	Component Name	Q1	Q3	Polarity
Spermidine	146.17	72.08	POS	(S)-ibuprofen	207.14	91.05	POS
Arg	175.12	70.07	POS	3,4-dimethoxy-benzaldehyde	167.07	95.06	POS
GLUTAMINE	147.08	84.04	POS	Dihydrocapsiate	309.21	109.10	POS
L-alanin	90.06	44.05	POS	benzene-1,2-diol	111.04	57.93	POS
DL-threonine	120.07	74.06	POS	Olivetol	181.12	105.07	POS
Pyroglutamic acid	130.05	84.04	POS	Saccharopine	277.14	93.07	POS
Glutamic acid	148.06	84.04	POS	(+)-(S)-dehydrovomifoliol	223.13	191.00	POS

RUO-MKT-02-13585

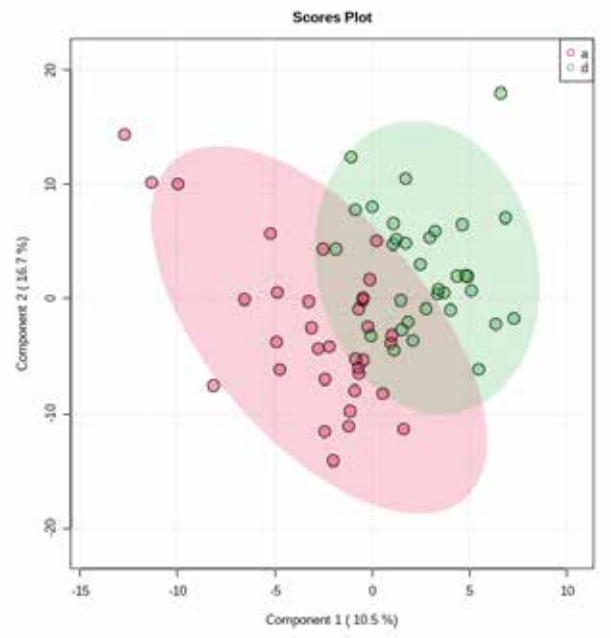

图3. 不同组小麦苗样品间主成分分析 (PCA) 图

总结

本文使用SCIEX LC-MS/MS系统建立了小麦苗中183种成分同时检测的靶标代谢组学方法，同时该方法对前期建立的基于SCIEX TripleTOF™ 6600+系统进行非靶向代谢组学的试验结果进行了验证，证明了非靶向代谢组学结果标记物查找的可靠性。本文所建立的靶向代谢组学方法的特点是采用一针进样、正负离子同时监测模式进行样品采集，专属性好，灵敏度高，满足小麦苗大队列样本的检测需求。

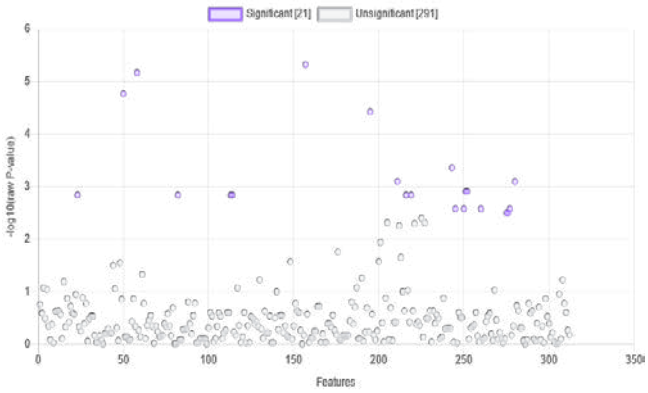

图4. 不同组小麦苗样品间含量具有显著性差异的离子

参考文献

[1] Oliver F, Joachim K, Peter D, et al. Metabolite profiling for plant functional genomics [J]. Nature Biotechnology, 2000, 18 (11): 1157-1161.

RUO-MKT-02-13585

High sensitivity quantification of acylcarnitines using the SCIEX 7500 system

Mackenzie Pearson
SCIEX, USA

Carnitine and acylcarnitines play an important role in the trafficking of fatty acids from the cytosol to the mitochondrial matrix with the additional responsibility of keeping the balance of CoA and acyl-CoA levels within the cell. Acylcarnitines are acetylated forms of L-carnitine produced from carnitine acyltranferases. These acyltransferases cover the entire range of fatty acid lengths, and depending on their chain length specificities, can be found in different tissue types.[1]

In many laboratories across the world, acylcarnitines and related molecules from a variety of sample types are quantified to investigate metabolic conditions, such as organic acidemias and fatty acid oxidation defects.[2] They have also been investigated as potential biomarkers for Type 2 Diabetes and other related conditions.[3] Whole blood from dried blood spots (DBS) is most commonly analyzed during screening, however, plasma, serum and urine are other common matrices used for analysis.

Carnitines and acylcarnitines vary in their hydrophobicity, ranging from small, polar carnitine to acylcarnitines with very long acyl chain lengths. This variability poses a unique challenge for chromatographic method development. To overcome this, chemical derivatization techniques are often needed to aid in the retention of these compounds on a reverse phase column.

The detection and quantification of acylcarnitine compounds can be challenging since many species occur as isomers and are found at very low concentrations in biological samples. Here, several acylcarnitine compounds were quantified in matrix, using diluted standards and the SCIEX 7500 system. Linearity, lower limits of quantification (LLOQ) and dynamic range were characterized and the sensitivity and reproducibility of the SCIEX 7500 system were evaluated. These experiments were performed without derivatization and with minimal sample preparation to quantify these low-level analytes in a biological matrix.

Key features of the SCIEX 7500 system for the quantification of acylcarnitines

- A high-throughput LC-MS method able to quantify acylcarnitine species
- A highly sensitive method that does not require derivatization of samples before analysis
- A robust method with high sensitivity and reproducibility and broad dynamic range (LDR)

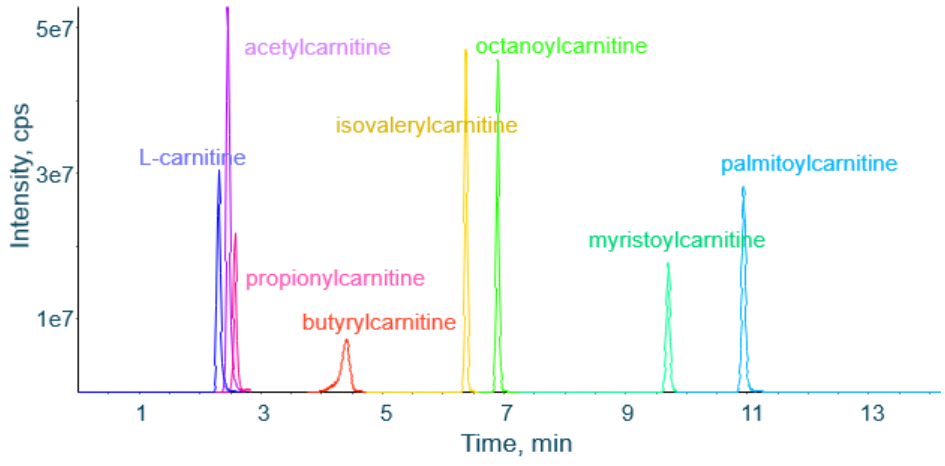

Figure 1. Extracted ion chromatogram (XIC) for 8 unlabeled acylcarnitine compounds.

RUO-MKT-02-13839-A

Methods

Sample preparation: Labeled and unlabeled standards were purchased from Cambridge Isotopes (p/n: NSK-B-1, NSK-B-US-1). The unlabeled standards were serially diluted from stock solutions to concentrations ranging from 1:50 to 1:1,000,000. Labeled standards were spiked in at a 1:100 dilution across all samples.

Ten µL of Wistar rat plasma was extracted using 490 µL of 80:20 methanol:water and then vortexed. The samples were spun for 10 minutes at 15000 rpm. An insert vial was loaded with 150 µL of supernatant and 1 µL was injected. Triplicate injections were analyzed.

Chromatography: An ExionLC system with a Phenomenex Kinetex column (C18, 2.6 µm, 150x4.6 mm; p/n 00F-4462-E0) was used to perform the separation. The total run time was 15.5 min. A 1.0 µL injection was used. Table 1 shows the chromatographic gradient used.

Table 1. Chromatographic gradient.

Time (min)	Flow (µL/min)	B Conc (%)	B Curve
3.0	*600*	*15.0*	*0*
3.5	*600*	*75.0*	*0*
11.0	600	*99.0*	*0*
12.5	*600*	*99.0*	*0*
13.50	*600*	*15.0*	*0*

Mobile phase A: 99:1 water:methanol with 0.1% Formic Acid
Mobile phase B: 1:99 water:methanol with 0.1% Formic Acid

Mass spectrometry: Samples were analyzed on the triple quadrupole version of the SCIEX 7500 system using the Scheduled MRM algorithm in the positive ion mode. Table 2 lists the source conditions for analysis.

Table 2. Source conditions for the SCIEX 7500 system.

Parameter	Value
CUR	*45*
CAD	*10 (medium)*
Temp	*475*
IS	*1400*
GS1	*45*
GS2	*70*

Data processing: All data were acquired and processed using SCIEX OS software 2.1.0.

Quantification results

Figure 1 shows extracted ion chromatograms for 8 unlabeled acylcarnitine compounds in diluted 1:50 neat solution. Compounds ranging in size from L-carnitine toand short-chain acetylcarnitine, to medium-chain octanoylcarnitine, to long-chain palmitoylcarnitine in neat solution at the 1:50 dilution, to highlight the optimized separation.

Next, the standards were diluted into extracted rat plasma across a broad concentration range to determine the sensitivity of the method. Lower limits of quantification (LLOQs) were calculated for all 8 analytes. Table 3 lists all LLOQs for each standard in the assay. The MRM signals observed at the lowest concentration analyzed for 4 of the analytes are shown in Figure 2. These are integrated peaks for the 1:1,000,000 dilution of the unlabeled L-carnitine, acetylcarnitine (short-chain), octanoylcarnitine (medium-chain) and myristoylcarnitine (long-chain) compounds. While the 1:1,000,000 dilution was the final point in the calibration curve, the response from some analytes in the assay suggest that quantification at even lower concentrations might be possible.

In Figure 3, 5 analytes that exhibited 4.5 orders of linear dynamic range (LDR) are shown. The LDR value for each analyte is shown in Table 3. These values were calculated for each analyte based on 3 replicates at each dilution, ranging from 1:50 to 1:1,000,000, of the stock solutions of the commercially available standards.

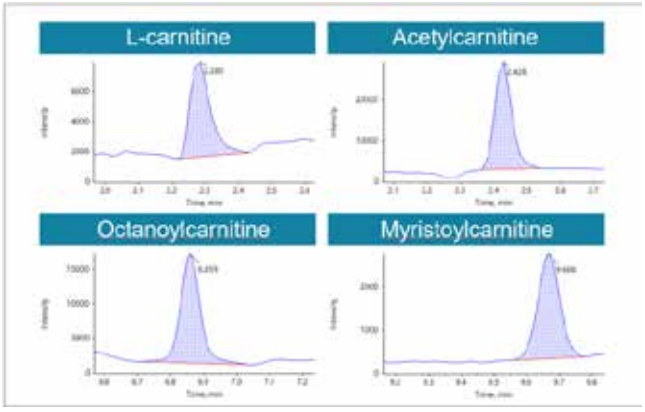

Figure 2. MRM chromatograms for the 1:1,000,000 dilution point in the concentration curve. Examples of the signals obtained at the lowest concentration measured. Signal was generated at the following concentrations: 152 pM L-carnitine, 38 pM acetylcarnitine, 7.6 pM octanoylcarnitine and 7.6 pM myristoylcarnitine.

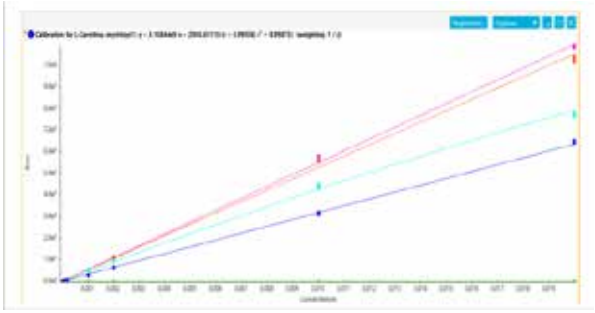

Figure 3. Linear dynamic range for several acylcarnitine compounds. Selected compounds exhibited 4.5 orders of linear dynamic range. Note that wider LDR might be possible for some compounds, as detection at lower concentrations is possible based on observed signals.

To assess reproducibility and robustness, 3 replicates of carnitine and acylcarnitines at their respective LLOQ concentrations in matrix were analyzed. A summary of the accuracy and %CV results is shown in Table 3. The reproducibility observed at the LLOQ was <6% across all the analytes, indicating strong reproducibility. The LDR observed for some analytes was 4.5 orders.

Table 3. Calibration curve statistics. The observed LLOQ, accuracy and %CV at the LLOQ and LDR of the calibration for acylcarnitine compounds in matrix is reported.

Name	LLOQ* (pM)	Accuracy	%CV	LDR
L-carnitine	*152*	*106.51*	*5.88*	*4.5*
acetylcarnitine	*38*	*107.13*	*5.67*	*4.5*
propionylcarnitine	*15.2*	*113.43*	*3.81*	*4*
butyrylcarnitine	*76*	*119.45*	*0.94*	*3.5*
isovalerylcarnitine	*15.2*	*92.98*	*0.44*	*4*
octanoylcarnitine	*7.6*	*119.31*	*2.2*	*4.5*
myristoylcarnitine	*14.13*	*91.46*	*3.87*	*4.5*
palmitoylcarnitine	*15.2*	*99.8*	*4.45*	*4.5*

**calculated concentration from calibration curve*

Next, the endogenous levels of carnitine and acylcarnitines in 10 µL of extracted Wistar rat plasma were assessed. In brief, this plasma was diluted 1:20 utilizing a simple sample preparation, without derivatization or SPE extraction was employed, and 1 µL of plasma was injected on the column. Table 4 illustrates the sensitivity of the SCIEX 7500 system using this minimal extraction protocol. The concentrations of each acylcarnitine compound range from low µM to high nM and provide excellent reproducibility in a biological matrix.

Table 4. Concentration and %CV for endogenous acylcarnitine compounds in extracted Wistar rat plasma.

Name	Concentration (µM)	%CV
L-carnitine	*0.8085*	*2.11*
acetylcarnitine	*0.7183*	*4.61*
propionylcarnitine	*0.0956*	*5.91*
butyrylcarnitine	*0.0879*	*8.89*
isovalerylcarnitine	*0.0067*	*1.52*
octanoylcarnitine	*0.0007*	*2.12*
myristoylcarnitine	*0.0033*	*2.44*
palmitoylcarnitine	*0.0131*	*6.32*

Conclusions

- The SCIEX 7500 system can quantify acylcarnitine species using LC-separation, yielding a high-throughput, robust and reproducible method that does not require derivatization of samples before analysis
- The SCIEX 7500 system provides unparalleled sensitivity and could be utilized to quantify other low-level acylcarnitines that are present in biological matrices without the need for extensive sample preparation or derivatization
- Since the SCIEX 7500 provides greater depths of sensitivity using plasma, researchers could further dilute the sample or require less sample for extraction, allowing consideration of alternative sample types for analysis.

RUO-MKT-02-13839-A

References

1. Meierhofer D. (2019) Acylcarnitine profiling by low-resolution LC-MS. *PLoS ONE*, **14(8)**, 1-11.

2. Han J, Higgins R, Lim MD, *et al.* (2018) Isotope-labeling derivatization with 3-nitrophenylhydrazine for LC/multiple-reaction monitoring-mass-spectrometry-based quantitation of carnitines in dried blood spots. *Analytica Chimica Acta. 1037: 177-187*.

3. Shuo Z, Xiao-Fei, F, Ting H, *et al*. (2020) The Association Between Acylcarnitine Metabolites and Cardiovascular Disease in Chinese Patients With Type 2 Diabetes Mellitus. *Frontiers in Endocrinology*, **11**, 212.

RUO-MKT-02-13839-A

Separation of hexose phosphate isomers using differential mobility spectrometry (DMS)

Separation of five hexose phosphate isomers using the SelexION device on the QTRAP 6500+ system

Catherine S. Lane[1], Denise Mehl[2], Arno van Rooij[3], Alain J. van Gool[3], Richard J.T. Rodenburg[3], Dirk J. Lefeber[3], Marek J. Noga[3]

[1]SCIEX, United Kingdom; [2]SCIEX, Germany; [3]Translational Metabolic Laboratory, Radboud Consortium for Glycoscience, Radboudumc, Nijmegen, The Netherlands

Sugar phosphates are important metabolites in many biosynthesis pathways including glycolysis, glycogenolysis and biosynthesis of nucleotide sugar building blocks for glycosylation. As such, the determination of their abundances is of key importance for quantitative metabolic profiling experiments and investigation of some metabolic disorders such as congenital disorders of glycosylation (CDG) and defects in glycolysis and gluconeogenesis.[1,2] However, analytical measurement of these compounds is far from trivial due in part to the presence of structural isomers with similar MS/MS fragmentation patterns. In addition, their highly hydrophilic nature makes their separation by conventional reversed-phase HPLC highly problematic.[3] Here, differential mobility spectrometry (DMS) was employed for the separation of five isomeric hexose phosphate isomers glucose 1-phosphate (Glc1P), mannose 1-phosphate (Man1P), fructose 6-phosphate (Fru6P), glucose 6-phosphate (Glc6P) and galactose 6-phosphate (Gal6P).

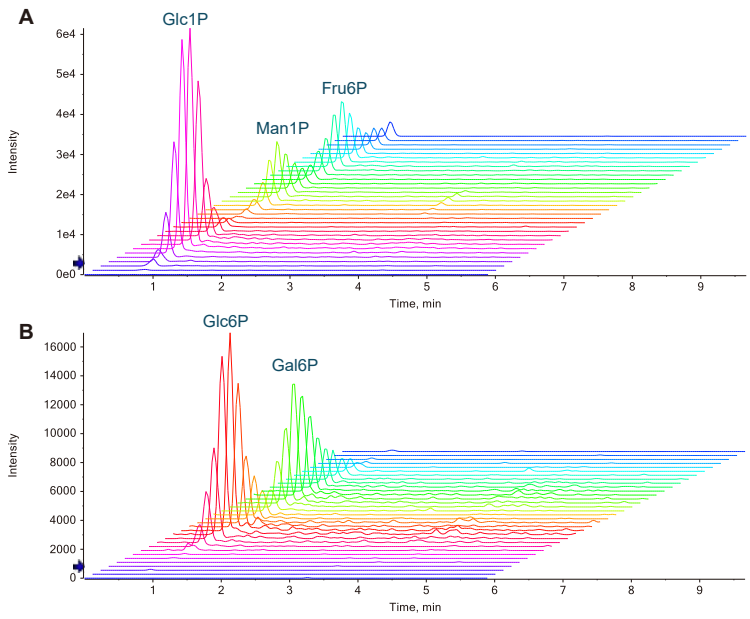

Figure 1. LC-DMS-MS/MS analysis of mixtures of hexose phosphate isomers (200 µg/mL) in the absence of chemical modifier, using the generic MRM 259->79 with 33 settings of CoV spanning the range 6.2 to 12.6 V. SV = 4100 V, resolution gas = Medium. Each colored trace shows the MRM 259->79 extracted ion chromatogram at a different value of CoV. **(A)** Glc1P, Man1P, Fru6P; **(B)** Glc6P, Gal6P.

Key features of DMS for distinguishing hexose phosphate isomers

- The analysis of hexose phosphates is challenging due to their isomeric and highly hydrophilic nature
- Differential mobility spectrometry using the SelexION device allows near-baseline separation of Glc1P, Man1P and Fru6P; and Glc6P and Gal6P without the use of chemical modifier
- When all 5 isomers are analysed together separation into three groups is observed: Glc1P/Glc6P, Man1P/Gal6P, Fru6P
- The introduction of chemical modifiers into the DMS cell maximizes the possibilities for isomer separation
- 1-Propanol chemical modifier enhances separation of Man1P from other isomers at the expense of reduced resolution for Glc1P and Gal6P

RUO-MKT-02-14374-A

Methods

***Sample preparation*:** Isomeric hexose phosphates were purchased from Sigma-Aldrich as disodium salts. They were diluted in 10 mM ammonium bicarbonate, 20% acetonitrile in water or 10 nM ammonium bicarbonate in water to concentrations of between 2 and 200 µg/mL for infusion or LC-DMS-MS/MS analysis. Compounds were analyzed both individually and as mixtures.

SelexION device conditions: Experiments were performed using a QTRAP 6500+ system equipped with a SelexION device (Figure 2), the fundamental properties of which have been described elsewhere.[4-6] The DMS cell was mounted between the sampling orifice of the mass spectrometer and the ion source. The temperature of the DMS cell was maintained at 150ºC, with nitrogen curtain gas operated at 30 psi. Resolving gas (nitrogen) was employed to enhance the separation of the isomers. The DMS cell was used both with and without chemical modifier (1-propanol) added into the curtain gas flow at 1.5% (mole ratio). For DMS infusion experiments, samples were infused at 7 µL/min in 10 mM ammonium bicarbonate, 20% acetonitrile in water. Separation Voltage (SV) was stepped between values of 0 and up to 4200 V. At each value of SV, compensation voltage (CoV) was scanned over values in the range -80 V to +20 V. At each value of CoV, full scan linear ion trap CID MS/MS data were acquired for the sugar isomers. The resulting plots reveal the optimal CoV at which a particular ion is transmitted through the DMS cell at a fixed value of SV. After determination of optimal CoV values for DMS-separated isomers, CoV values can be fixed to allow the selective transmission of individual isomers in a mixture.

***LC conditions*:** Multiple reaction monitoring (MRM) transitions were optimized targeting fragment ions either common to all 5 hexose phosphate isomers, or unique to/predominantly found in one or a subset of the isomers. These MRMs were used to explore DMS separation on an LC timescale. A SCIEX ExionLC AD system with a Phenomenex Kinetex F5 column (2.6 µm, 100 x 2.1 mm) at 30 ºC with a gradient of 2% to 20% mobile phase B in 1.8 min (total analysis time 6 min) was used at a flow rate of 300 µL/min. Mobile phase A was 10 mM ammonium bicarbonate in water and mobile phase B was 10 mM ammonium bicarbonate in 80% acetonitrile, 20% water. The injection volume was set to 10 µL.

Figure 2. Configuration of the SelexION device. The DMS cell is mounted in the atmospheric region between the ion source and sampling orifice of the mass spectrometer, allowing the user to easily install the DMS device in minutes.

DMS separation of hexose phosphate isomers by infusion

DMS-MS was employed for the analysis of deprotonated molecules of Glc1P, Man1P, Fru6P, Glc6P and Gal6P, with and without the presence of 1-propanol chemical modifier. The controlled addition of 1-propanol vapor in the DMS cell induces different shifts in optimal CoV for individual isomers, resulting in separation in CoV space that can be orthogonal to the separation obtained when no chemical modifier is employed. Isomers were analysed both individually and as mixtures.

Without modifier, baseline separation of Glc1P/Glc6P, Man1P/Gal6P and Fru6P was observed. Only partial separation of Glc1P from Glc6P was observed, and Gal6P behaved similarly to Man1P (Figure 2). With 1-propanol modifier, separation of Glc1P/Gal6P, Man1P, Glc6P and Fru6P was observed, but Gal6P behaved similarly to Glc1P (Figure 3).

RUO-MKT-02-14374-A

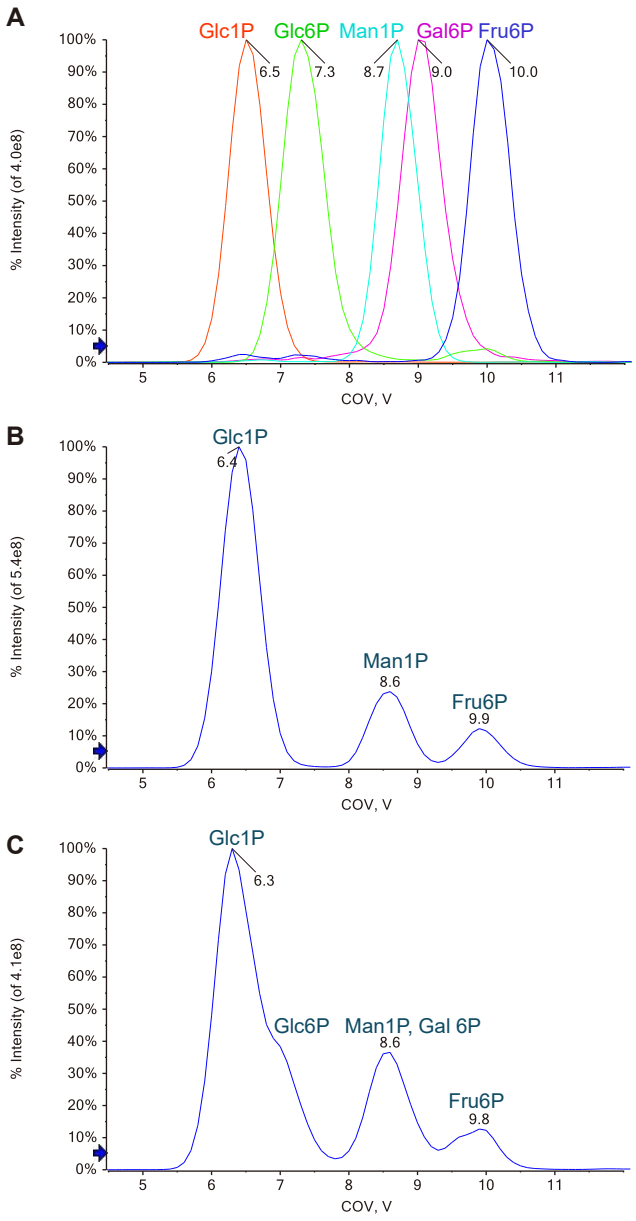

Figure 3 Separation of hexose phosphate isomers in the absence of chemical modifier. Isomers were infused individually at 2 µg/mL (A) or as mixtures at 5 µg/mL (B & C) using SV = 4100 V; resolving gas set to High.

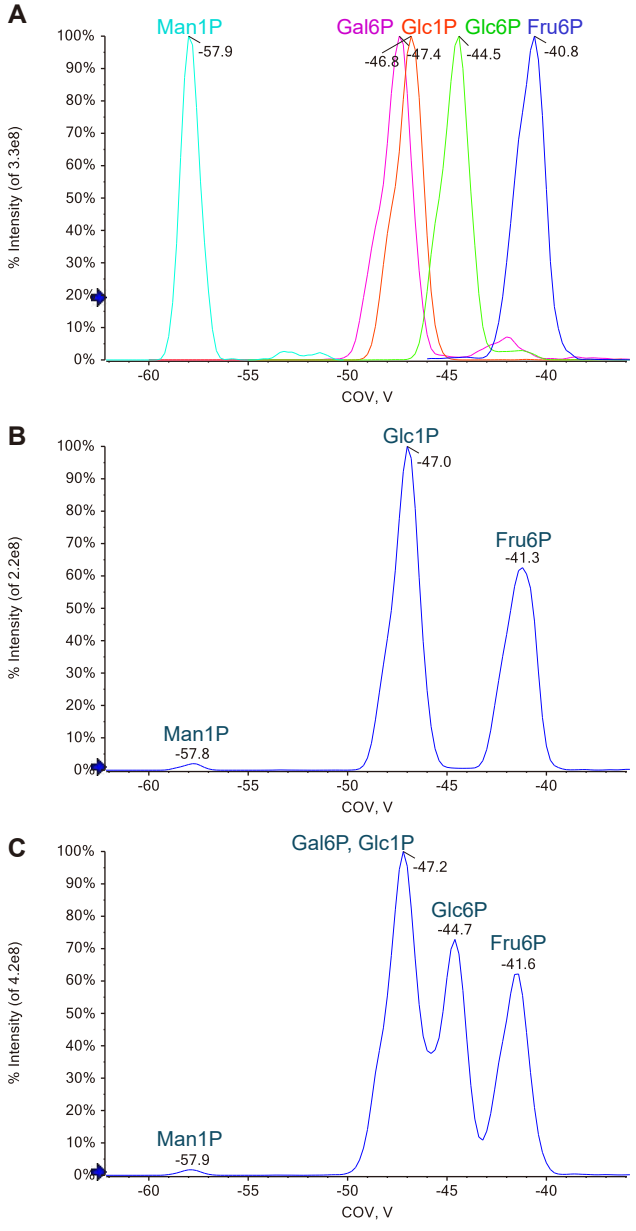

Figure 4 Separation of hexose phosphate isomers in the presence of 1-propanol chemical modifier. Isomers were infused individually at 5 µg/mL (A) or as mixtures (B & C) at 5 µg/mL using SV = 3750 V; resolving gas set to Medium.

RUO-MKT-02-14374-A

LC-DMS-MS/MS analysis of hexose phosphate isomers

LC-DMS-MS/MS was used for the analysis of hexose phosphate isomers individually and as mixtures. Experiments were performed in the absence of chemical modifier; SV was set to 4100 V; resolving gas was set to Medium. For initial experiments, the MRM transition 259->79 (common to all isomers and corresponding to the parent ion to PO3- fragment ion transition) was monitored using 33 different values of CoV spanning the range 6.2 V to 12.6 V with a step size of 0.2 V. The hexose phosphate isomers, chromatographically indistinguishable under these conditions, could be separated in CoV space (Figures 1 and 5).

The specificity of the LC-DMS-MS/MS separation for Glc1P, Man1P and Fru6P was calculated by observing the amount of non-specific, or breakthrough, signal for the generic 259->79 MRM transition at optimal CoV values for each of the three isomers during single-isomer analysis. Non-specific signal is reported as the area of any breakthrough peak as a percentage of the MRM peak area at the isomer's optimal CoV (Table 1).

Table 1. The specificity of the LC-DMS-MS/MS separation of Glc1P, Man1P and Fru6P. Non-specific signal observed for the MRM 259->79 as peak area percentage of signal observed at optimized CoV for LC-DMS-MS/MS analysis of individual isomers. SV = 4100 V, resolution gas = Medium.

	Glc1P CoV 7 V	Man1P CoV 9.2 V	Fru6P CoV 11 V
Glc1P 200 µg/mL	-	*0.11%*	*0.07%*
Man1P 200 µg/mL	*0.29%*	-	*0.02%*
Fru6P 200 µg/mL	*0.08%*	*0.16%*	-

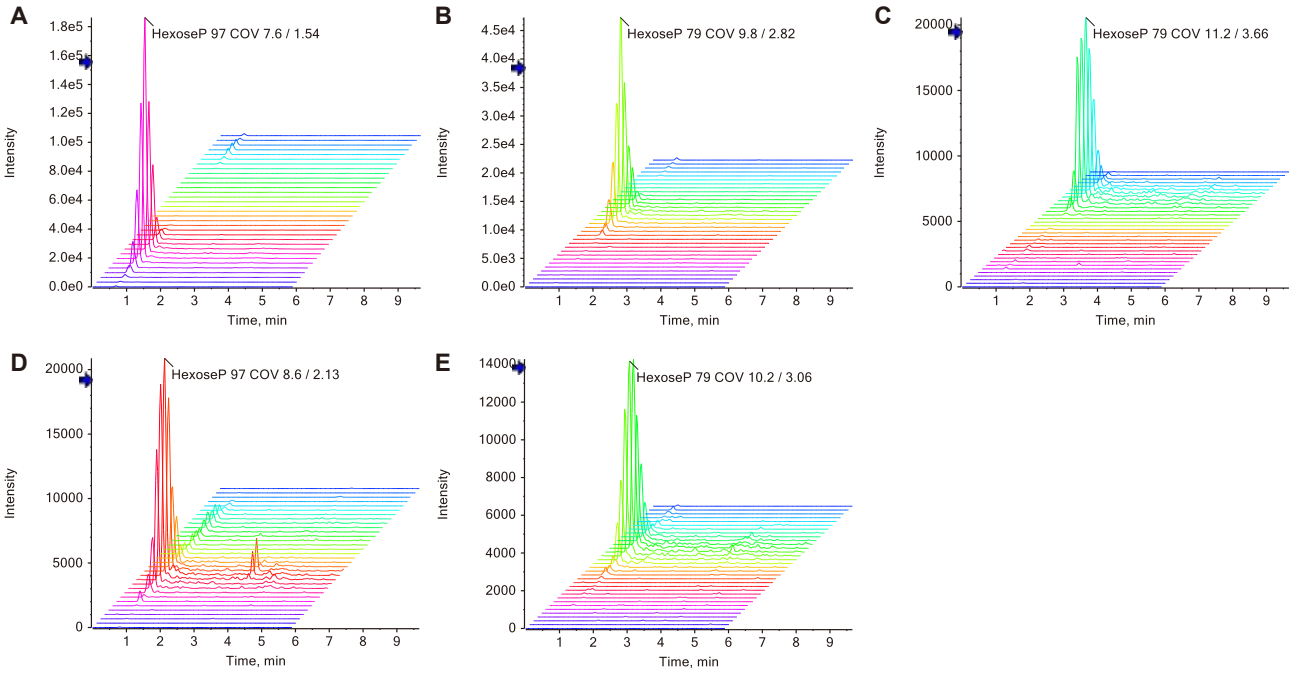

Figure 5. Determination of optimal CoV values for LC-DMS-MS/MS analysis. LC-DMS-MS/MS analysis of individual hexose phosphate isomers (200 µg/mL) in the absence of chemical modifier, using the generic MRM 259->79 with 33 settings of CoV spanning the range 6.2 to 12.6 V. SV = 4100 V, resolution gas = Medium. Results for the individual experiments are shown as follows: (A) Glc1P, (B) Man1P, (C) Fru6P, (D) Glc6P, (E) Gal6P.

RUO-MKT-02-14374-A

Conclusions

Here, differential mobility spectrometry (DMS) has been used for the analysis of five hexose phosphate isomers. Baseline separation of a mixture of three isomers, Glc1P, Man1P and Fru6P, was observed both in the absence and presence of 1-propanol chemical modifier. Likewise, when Glc6P and Gal6P were analysed together, they could be separated under both sets of conditions. The DMS separations were demonstrated both by infusion and by LC-DMS-MS/MS analysis.

When all five isomers were analysed as a mixture in the absence of chemical modifier, baseline separation of Glc1P/Glc6P, Man1P/Gal6P and Fru6P was observed. With 1-propanol modifier, separation of Glc1P/Gal6P, Man1P, Glc6P and Fru6P was observed. Future work will focus on the evaluation of a wider range of chemical modifiers to establish whether a set of conditions can be found under which Glc1P and Gal6P can be separated from the other isomeric forms.

References

1. Orvisky E *et al.* (2003) Phosphomannomutase activity in congenital disorders of glycosylation type Ia determined by direct analysis of the interconversion of mannose-1-phosphate to mannose-6-phosphate by high-pH anion-exchange chromatography with pulsed amperometric detection. *Anal. Biochem.* **317(1),** 12-18.
2. Tegtmeyer LC *et al.* (2014) Multiple Phenotypes in Phosphoglucomutase 1 Deficiency. *N. Engl. J. Med.* **370(6),** 533-542.
3. Hinterwirth H *et al.* (2010) Selectivity issues in targeted metabolomics: Separation of phosphorylated carbohydrate isomers by mixed-mode hydrophilic interaction/weak anion exchange chromatography. *J. Sep. Sci.* **33**, 3273-3282.
4. Shvartsburg AA, (2008) Differential Ion Mobility Spectrometry. CRC Press, Boca Raton *https://doi.org/10.1201/9781420051070*.
5. Krylov EV, Nazarov EG, Miller RA. (2007) Differential mobility spectrometer: Model of operation. *Int. J. Mass Spectrom.* **226,** 76-85.
6. Schneider BB, *et al*. (2017) Maximizing Ion Transmission in Differential Mobility Spectrometry. *J. Am. Soc. Mass Spectrom*. **28**, 2151-2159.RUO-MKT-02-3251-C.

RUO-MKT-02-14374-A

Simultaneous quantification of trimethylamine oxide and its precursors from gut microbial metabolic pathway

Using the QTRAP 4500MD system

Cui Jingwen[1], Zhang Yuanyuan[1] and Li Guoqing[1]
[1]SCIEX, China

Trimethylamine N-oxide (TMAO), a gut microbiota-derived metabolite, is found in higher concentrations in plasma after ingestion of L-carnitine and phosphatidylcholine. Ingestion of choline, L-carnitine, betaine and foods such as red meat cause significant increase in trimethyl amine (TMA) due to the enzymatic activity of gut microbiota. TMA is absorbed into the bloodstream and metabolized by flavin-containing mono oxygenase (FMO) enzymes to trimethylamine oxide (TMAO) in the liver. TMAO has been implicated in the pathology of multiple diseases, including heart failure.[1]

Therefore, establishing a rapid and accurate quantitative method for routine monitoring of metabolites involved in TMAO production is needed to support gut microbiome research and screening of hundreds samples from a large research cohorts.

Here, an LC-MS/MS method for the simultaneous quantification of acetyl-carnitine, carnitine, choline, TMAO and betaine in plasma has been developed. All target compounds were extracted using a simple sample extraction procedure then diluted before analysis using LC-MS/MS.[2]

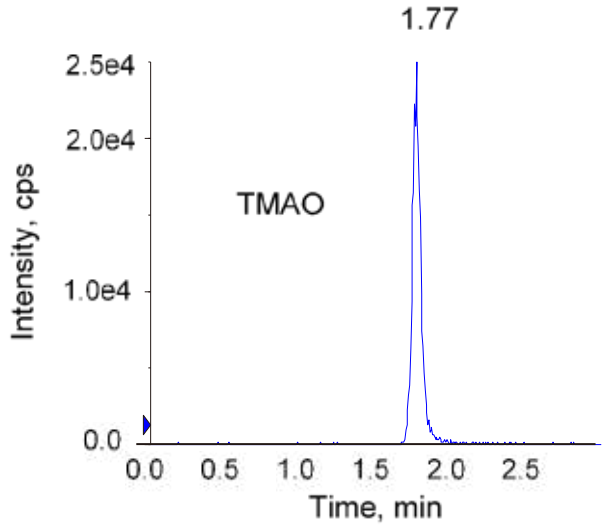

Figure 1. Fast chromatography. A chromatographic peak of trimethylamine N-oxide Q1/Q3 76.1/58.1 using a rapid 5.5 min method for quantification.

Key features of QTRAP 4500MD system for gut microbiome studies

- Robust LC-MS/MS system for routine quantification studies with the Turbo V ion source and Curtain Gas interface
- Simplified plasma sample preparation, using a one-step extraction and dilution
- Fast, reversed-phase chromatography provides good separation of the target analytes
- High accuracy and precision values for all analytes monitored, meeting bioanalytical requirements.

RUO-MKT-02-13913-A

Methods

Sample preparation: A 20 µL plasma sample was extracted with 100 µL of acetonitrile and further spiked with 100 µL of a 5 ng/mL deuterated internal standard mixture. The sample mixture was centrifuged at 14000 rpm for 5 min, then 5 µL of the supernatant was injected on the column for analysis. The intra-day and inter-day variability over 5 days of the assay was evaluated.

Chromatography: A Jasper HPLC system (SCIEX) with a Phenomenex Kinetex C18, 2.6 µm, 2.1x100 mm column (00D-4462-AN) was used for sample separation using gradient conditions (Table 1) and a flow rate of 0.6 mL/min. A 5 µL injection volume was used and the column temperature was maintained at 40°C throughout the analysis. The total run time was 5.5 min.

Mass spectrometry: A QTRAP 4500MD system with a Turbo V ion source was used in positive ionization mode. All source and compound parameters were optimized and are outlined in the SCIEX How method.[3] The MS method included optimized MRM transitions for multiple analytes.

Data processing: The method development and data acquisition was carried out using Analyst MD software. Data processing was performed using MultiQuant MD software.

Table 1. Fast gradient conditions.

Time	Mobile phase A	Mobile phase B
0	*10*	*90*
3.5	*50*	*50*
3.6	*10*	*90*
5.5	*10*	*90*

Mobile phase A – water with 0.1% formic acid in 10 mM ammonium formate.
Mobile phase B - 90% acetonitrile with 0.1% formic acid in 10 mM ammonium formate

Rapid analysis of TMAO and related species

First, phosphate buffered saline (PBS) was used to dilute the standards to make a standard calibration curve and obtain a first rough assessment of sensitivity. The concentration range evaluated and the linearity of the calibration curves is outlined in Table 2 along with the observed LLOQ concentrations for TMAO, betaine, L-carnitine, acetyl-carnitine, and choline. All analytes showed good gaussian peak shape (Figure 2).

Triplicate injections of TMAO, betaine, L-carnitine, acetyl-carnitine and choline were each analyzed at different concentrations and across 5 days, as outlined in Table 3. The intra-day reproducibility was analyzed across triplicate injections from a single day. The accuracy for each metabolite ranged from 89.87% to 112.03% and the %RSD ranged from 1.81% to

Table 2. Concentration curves. Compounds were diluted with phosphate buffered saline (PBS) to create standard concentration (ng/mL) curves for each analyte. Good linearity was achieved for each of the standards. Observed lower limits of quantification in buffer are highlighted in bold, using standard bioanalytical requirements of <20% CV and ±20% accuracy.

Series	Acetyl-carnitine	Carnitine	Betaine	Choline	TMAO
STD1	***0.03***	***0.05***	***0.05***	***0.05***	***0.13***
STD2	*0.05*	*0.1*	*0.1*	*0.1*	*0.25*
STD3	*0.1*	*0.2*	*0.2*	*0.2*	*0.5*
STD4	*0.25*	*0.5*	*0.5*	*0.5*	*1.25*
STD5	*1.25*	*2.5*	*2.5*	*2.5*	*6.25*
STD6	*2.5*	*5*	*5*	*5*	*12.5*
STD7	*5*	*10*	*10*	*10*	*25*
STD8	*10*	*20*	*20*	*20*	*20*
Linear equation	*Y=1.54803x-0.009*	*Y=1.43472x+0.04162*	*Y=0.63080X+0.00622*	*Y=0.93725X-0.00116*	*Y=9.55724x-0.54357*
Correlation coefficient	*0.9999*	*0.99118*	*0.99713*	*0.99987*	*0.99792*

RUO-MKT-02-13913-A

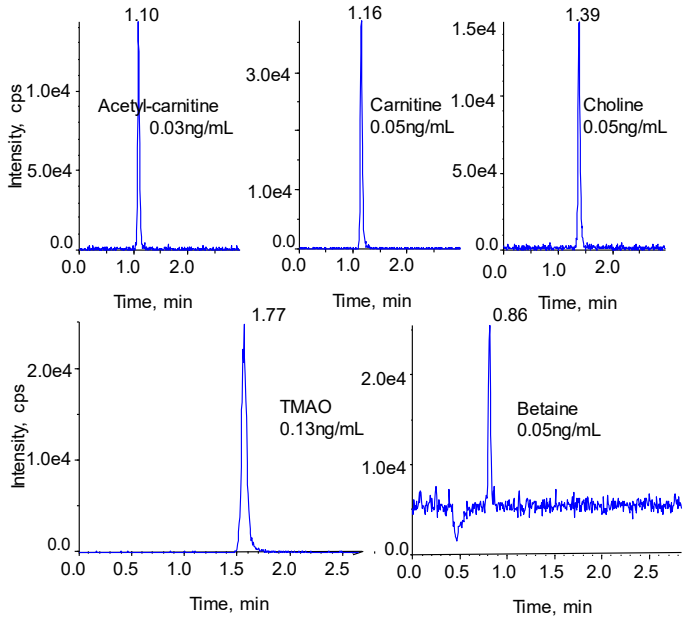

Figure 2. Lower limits of quantification (LLOQ) for acetyl-carnitine, L-carnitine, choline, TMAO and betaine. Good peak shape and signal/noise were observed at the LLOQ for each analyte in PBS matrix.

8.87%. The inter-day reproducibility was measured by comparing results from triplicate injections across days. The inter-day accuracy ranged from 92.93% to 107.15% and the %RSD ranged from 1.77% to 8.01%. The LLOQs observed for each analyte are marked in bold in Table 2. Standard bioanalytical requirements were followed.

Next, this rapid LC-MS method was tested in plasma. A simple extraction protocol was used, which provided good detection and good signal/noise of TMAO and its precursors analytes in plasma (Figure 3).

Table 3. Quantification results. Inter-day and intra-day results for the analysis of acetyl-carnitine, carnitine, choline, TMAO and betaine in PBS. Precision and accuracy results for a few of the low concentrations points are shown.

Compound Name	Theoretical concentration	Inter-day			Intra-day		
	ng/mL	Mean (ng/mL)	RSD%	Accuracy%	Mean (ng/mL)	RSD%	Accuracy%
Acetyl-carnitine	*0.08*	*0.08*	*4.88%*	*95.97%*	*0.078*	*4.29*	*97.32*
	0.15	*0.15*	*6.44%*	*96.96%*	*0.141*	*4.91*	*94.33*
	7.5	*7.36*	*7.01%*	*98.14%*	*6.74*	*3.16*	*89.87*
Carnitine	*0.15*	*0.16*	*8.01%*	*103.33%*	*0.143*	*7.89*	*95.57*
	0.3	*0.31*	*6.78%*	*103.22%*	*0.291*	*8.28*	*97.03*
	15	*13.94*	*1.77%*	*92.93%*	*13.971*	*1.97*	*93.14*
Choline	*0.15*	*0.16*	*4.53%*	*107.15%*	*0.166*	*3.45*	*110.55*
	0.3	*0.32*	*5.07%*	*105.63%*	*0.336*	*2.04*	*112.03*
	15	*14.91*	*2.88%*	*99.40%*	*14.509*	*2.3*	*96.73*
TMAO	*0.38*	*0.38*	*5.18%*	*100.35%*	*0.402*	*2.93*	*105.9*
	0.75	*0.71*	*3.53%*	*94.71%*	*0.716*	*3.75*	*95.52*
	37.5	*37.06*	*6.91%*	*98.83%*	*35.023*	*1.81*	*93.4*
Betaine	*0.15*	*0.15*	*7.89%*	*101.26%*	*0.15*	*8.87*	*100.04*
	0.3	*0.32*	*5.45%*	*106.87%*	*0.327*	*2.27*	*108.99*
	15	*14.14*	*3.95%*	*94.26%*	*13.788*	*4.11*	*91.92*

Conclusions

Here, a method for the rapid quantification of TMAO, betaine, L-carnitine, acetyl-carnitine and choline in plasma has been developed on the QTRAP 4500MD system. This method has the advantages of high specificity, linearity and high accuracy. As shown, this method is suitable to support rapid monitoring of TMAO metabolites:

- Rapid 5.5-minute run time provided good peak separation for detection in a shorter run time than several recently published methods for faster screening.[4]
- Consistent quantification results were obtained for all standards tested, with correlation coefficients ranging from 0.991 to 0.999
- Inter- and intra-day reproducibility and accuracy meet standard bioanalytical requirements of %CV less than ≤ 15% in for all analytes analyzed in plasma
- Method was evaluated in plasma matrix using a simple extraction protocol and good signal/noise was observed.

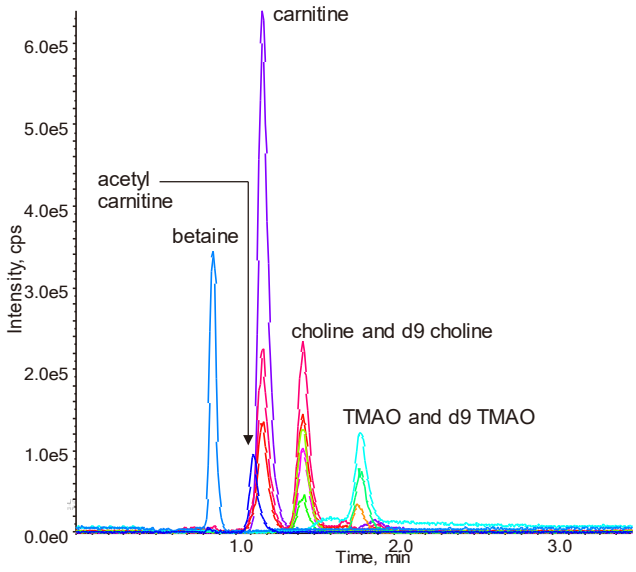

Figure 3. Detection in plasma. The extracted ion chromatograms (XIC) show the separation of TMAO and its precursors in 3.5 min run time from extracted from a plasma sample.

References

1. The gut, the heart, and TMAO. Cleveland clinic website.
2. Velasquez MT, et al. (2016) Trimethylamine N-oxide: The good, the bad and the unknown. *Toxins* **8**, 326.
3. SCIEX How link
4. *Katrina et al.,* (2021) A simplified LC-MS/MS method for the quantification of the cardiovascular disease biomarker trimethylamine-N-oxide and its precursors. *J. Pharma. Anal.* **11,** 523-528.

RUO-MKT-02-13913-A

SWATHtoMRM: 高覆盖靶向代谢组学方法

SWATHtoMRM: Development of High-Coverage Targeted Metabolomics Method Using SWATH® Technology for Biomarker Discovery

查海红[1]，蔡玉萍[2,3]，尹岩东[2,3]，王卓众[2,4]，李康[4]，朱正江[2,3]，郭立海[1]

[1] SCIEX，亚太应用支持中心，中国；[2]中科院上海有机化学研究所生物与化学交叉研究中心，中国
[3] 中国科学院大学，中国；[4] 哈尔滨医科大学，中国

Haihong Zha[1], Yuping Cai[2,3], Yandong Yin[2,3], Zhuozhong Wang[2,4], Kang Li[4], Zheng-Jiang Zhu[2,3], Lihai Guo[1]

[1]SCIEX, China; [2]Interdisciplinary Research Center on Biology and Chemistry, Shanghai Institute of Organic Chemistry, Chinese Academy of Sciences, China
[3]University of Chinese Academy of Sciences, China; [4]Harbin Medical University, China

Key Words: Targeted metabolomics; multiple-reaction monitoring (MRM); high coverage; SWATH-MS; biomarker discovery; colorectal cancer (CRC)

前言

代谢组学的目标是系统性定量检测所有代谢物的动态变化。由于生物样品中的代谢物结构多样，且浓度跨度范围广，对大规模定量研究这些代谢物带来极大的挑战。基于MRM技术的靶向代谢组学具有最佳的定量能力，但是其覆盖度极为有限。为此，本文开发了一个新的方法 —— SWATHtoMRM，利用SWATH®技术的高覆盖特点来建立高覆盖的靶向代谢组学方法。

首先，运用SWATH技术对一个混合的生物样本进行非靶向的检测来获得样品中所有代谢物的二级谱图信息；然后，利用SWATHtoMRM软件从SWATH®数据中提取高质量的1000-2000个代谢物的离子对用于靶向分析检测；接着，本文从覆盖率，重现性，灵敏度以及线性范围几个方面阐述了SWATHtoMRM方法在定量分析中的优势；最后，本文将该方法运用于寻找结直肠癌疾病的潜在生物标志物的研究中。利用一针进样，同时靶向分析1303个代谢物的方法来检测结直肠癌病人的癌旁和癌组织样本，在组织样本中，发现并验证了20个潜在的结直肠癌的生物标志物。其中，17种潜在的代谢标志物在结直肠癌病人的血浆样本中进一步被验证与肿瘤切除相关，对于评估结直肠癌病人术后的预后效果有着极大的潜力。

SWATHtoMRM技术是一种新的高覆盖的靶向代谢组学方法，将促进靶向代谢组学在疾病生物标志物研究中的应用。

RUO-MKT-02-8700-ZH-A

仪器设备

SCIEX TripleTOF® 6600+ 三重四极杆质谱系统

液相方法

色谱柱：Waters BEH Amide, 1.7 µm, 100 mm × 2.1 mm

流动相：A相：水（25 mM 醋酸铵 + 25 mM 氨水）
B相：乙腈

流速：0.3 mL/min

柱温：40℃；

流动相梯度：

Time(min)	A (%)	B (%)
0.00	5	95
1.00	5	95
14.00	35	65
16.00	60	40
18.00	60	40
18.10	5	95
23.00	5	95

质谱方法

SWATH

离子源参数：

离子源：ESI正离子模式　　GS1: 60 psi

GS2: 60 psi　　气帘气 CUR: 30 psi

源温度 TEM: 550℃　　喷雾电压 ISVF: 5000 V

去簇电压 DP: 60 V　　碰撞能量 CE: 30 V

质谱采集参数：

一级质量范围: 100-700 Da　　一级扫描时间: 100 ms

二级窗口数: 24　　二级扫描时间: 35 ms

二级质量范围: 25-700 Da

DDA

离子源参数：

离子源：ESI正离子模式　　GS1: 60 psi

GS2: 60 psi　　气帘气 CUR: 30 psi

源温度 TEM: 550℃　　喷雾电压 ISVF: 5000 V

去簇电压 DP: 60 V　　碰撞能量 CE: 30 V

质谱采集参数：

一级质量范围: 100-700 Da　　一级扫描时间: 100 ms

二级采集数: 24　　二级扫描时间: 35 ms

二级质量范围: 25-700 Da

Scheduled MRM

采集窗口: 60 s　　循环时间: 990 ms

RUO-MKT-02-8700-ZH-A

数据处理

SWATHtoMRM流程

SWATHtoMRM的数据处理流程已整理成R包，主要用于从SWATH®数据中大规模提取MRM离子对信息（图 1a），该R包目前可以免费使用，下载地址为： http://www.zhulab.cn/software.php。整个数据处理流程分为两步：SWATH®数据的分析以及MRM离子对的生成。

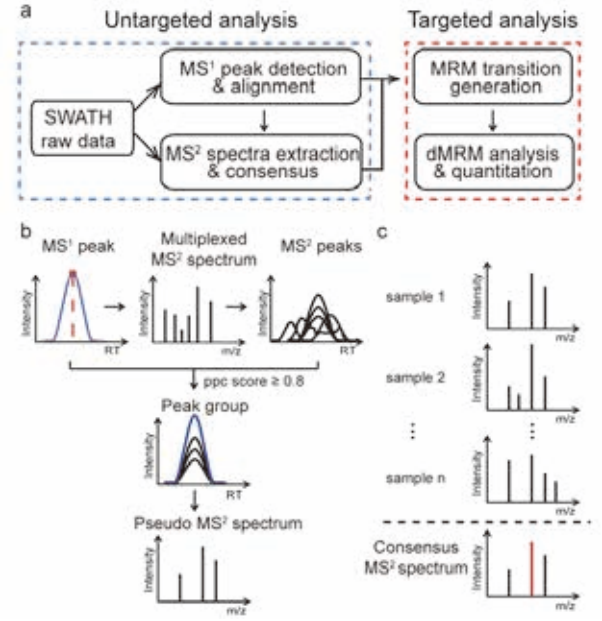

图1. (a) SWATHtoMRM流程概览。(b) 从SWATH®数据中提取伪MS²图谱。(c) 将来自多个样品的MS²谱图合并为consensus 谱图，保留出现频率超过50%的碎片离子，并用于生成MRM离子对。

1. SWATH数据处理

首先，将原始数据（.wiff文件）通过“msconvert”转化成mzXML格式的文件，然后将多个数据文件放至一个文件夹内通过SWATHtoMRM处理。对于SWATH®数据的处理主要分为以下四步：

首先是MS¹色谱峰的提取与筛选。MS¹的峰检测是通过XCMS的CentWave算法完成的，R包中的CAMERA被用来对峰进行注释。然后对于每个检测到的MS¹色谱峰进行筛选，去除同位素峰和响应低于1,000 counts的峰。对于多个数据文件，用XCMS中的OBI-Warp算法进行对齐。

然后是MS²的质谱峰与色谱峰的提取。对于每一个MS¹色谱峰，在峰的顶点提取对应SWATH®窗口下的复合MS²质谱图（图1b），然后对该谱图做去噪处理，去除响应低于200 counts的峰、质荷比大于母离子的峰以及同位素峰，再对剩下的碎片离子

提取色谱峰；

接着是MS^1与MS^2的峰匹配。通过计算每一个碎片离子色谱峰与母离子色谱峰之间的相关性得分（PPC score），将得分大于0.8的碎片离子归属为对应母离子产生的子离子，然后生成一张该母离子的伪二级谱图（图 1b）。

最后是生成一个consensus的二级谱图。将来自多个样品中的同一个母离子的二级谱图进行consensus，只保留在所有样品中出现频率超过50%的碎片离子（图 1c）。接着将最终生成的consensus谱图导出用于后续的MRM离子对的生成。

2. MRM离子对生成

对于每个代谢物的consensus谱图中的子离子还将进一步评估后再生成MRM离子对。选取的3个原则为：（1）母离子与子离子的差值要大于14 Da，即至少相差一个“CH_2”基团；（2）去除脱水、脱羧和脱氨的子离子；（3）在剩下的子离子中挑选响应最高的组成MRM离子对。每个代谢物只选取了一个MRM离子对用于靶向检测。

实验结果

1. SWATHtoMRM 工作流程

首先，本文在多种生物样本中（人类尿液，结直肠癌组织以及Jurket细胞）测试了SWATHtoMRM的可行性与实用性。

下面，以人类尿液样本为例，从SWATH数据中检测到3554个MS^1峰，其中有950个峰因为是同位素峰或响应低而被过滤。在剩下的2604个代谢特征峰中，2091（80.3%）个代谢物有合适的MRM离子对生成。靶向检测这2091个代谢物离子对后，通过手动分析，确证有1614（77.2%）个代谢物能在尿液样本中检测到（图 2a）。

图 2b是以代谢物牛磺酸为例，详细展示了通过SWATHtoMRM构建MRM离子对的过程。首先，包含多个代谢物子离子的复合二级谱图被提取出来。然后，提取每个子离子的色谱峰，计算与母离子色谱峰之间的相关性PPC，保留得分大于0.8 的子离子离子。随后，将6个样本的牛磺酸的二级谱图合并，得到一张包含13个碎片离子的consensus二级谱图。最后，挑选响应最高的子离子（m/z = 44.0496 Da）构建MRM离子对（Q1/Q3， 126.0/44.0）。

同时，本文还将SWATHtoMRM方法应用于其他种类的生物样本，在靶向检测中成功检测到的比例都在75%以上（图 2c）。因此，该方法能从不同的生物样本中提取大规模可靠的离子对信息。此外，本文只展示了正离子模式的数据，该方法同样适用于负离子模式。

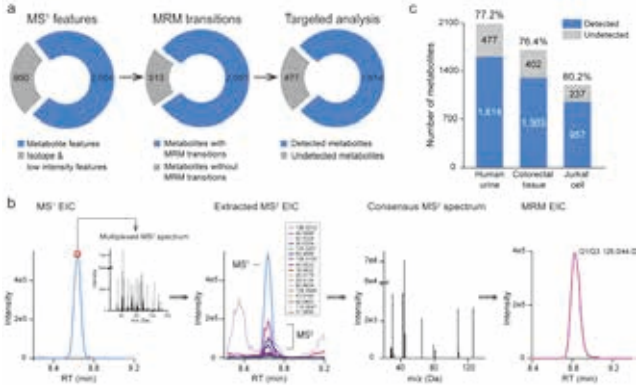

图2. (a) 人尿液样本中大规模MRM离子对的生成。(b) 代谢物牛磺酸的离子对生成过程。(c) 从不同类型生物样本（尿液，组织和细胞）中检测到的MRM离子对个数。

2. SWATHtoMRM 覆盖度

为了展示SWATHtoMRM方法的宽广的覆盖范围，本文将该方法与从DDA数据中提取MRM离子对的方法进行了比较（图 3）。为了保证比较的公平性，选用了相同的尿液样本进行采集，质谱采集参数以及后续的数据分析参数也都保持一致。

从相同的尿液样本中，SWATH 和DDA分别检测出2604和2149个峰（图 3a, 3b）。比较两者的二级覆盖度，SWATH（2105, 80.8%）显著高于DDA（1174, 54.6%）（图 3b）。对于两者共有的1539个峰的二级覆盖度，SWATH（84.9%）也显著高于DDA（61.1%）（图 3a）。

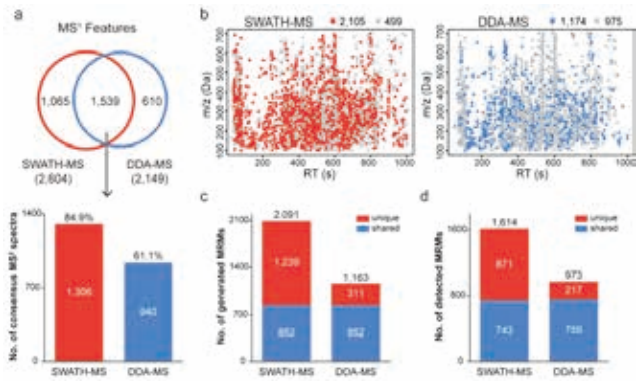

图3. 从SWATH数据中生成的MRM离子对具有很广的覆盖度。(a) 韦恩图展示了SWATH与DDA技术检测到的共有和特有的峰。(b) SWATH与DDA数据中MS^1和MS^2的分布图。红/蓝=有MS^2，灰色=无MS^2。(c) 两种方法构建的MRM离子对数目比较。(d) 两种方法检测到的代谢物数目比较。

RUO-MKT-02-8700-ZH-A

SWATH与DDA分别有2091和1163个代谢物生成MRM离子对，其中有852个代谢物是在两者都有生成离子对（图 3c）。对于这852个代谢物，分别有87.2%（SWATH）和88.7%（DDA）的检出率，两种方法具有相近的检出率，进一步说明通过SWATHtoMRM生成的离子对是可靠的（图 3d）。另外，从总检出数上来看，SWATH比DDA多检测到66%的代谢物。因此，通过SWATHtoMRM生成的MRM离子对比从DDA数据生成的离子对有更广的覆盖度。

3. SWATHtoMRM 定量效果

为了评估SWATHtoMRM的定量效果，本文对比了SWATHtoMRM，SWATH-MS¹以及SWATH-MS² 3种技术间的灵敏度、动态范围和重现性。首先，将尿液样本梯度稀释至1024倍，并对这些稀释的样本分别进行SWATHtoMRM和SWATH采集，然后随机选择629个检测到的代谢物进行比较。

灵敏度：通过比较不同稀释浓度的样本中检测到的代谢物个数来评估。结果显示，SWATHtoMRM的灵敏度明显好于SWATH-MS¹和 SWATH-MS²（图4a），因为QQQ的灵敏度好于TOF。通过进一步比较不同丰度的代谢物在稀释样本中的检测情况， 发现SWATHtoMRM在所有浓度点都表现出最好的灵敏度，尤其在低丰度代谢物中（图 4b）。

动态范围：通过比较629个代谢物在整个稀释范围内的R^2来评估。结果显示，SWATHtoMRM 的线性范围比 SWATH-MS¹和SWATH-MS²都要更广，且SWATHtoMRM中R^2> 0.8的代谢物超过了80%，而SWATH-MS¹和SWATH-MS²则不到60%（图 4c）。图4d展示了代谢物2-氨基己二酸和酪氨酸在3个模式下的线性范围比较。

重现性：通过比较相邻稀释倍数的代谢物检出强度的比值分布来评估。统计629个代谢物在两组相邻稀释浓度间的检出强度比值（4× ：16×、16× ：64×），图 4e展示的强度比值分布图中，SWATHtoMRM的离散程度比 SWATH-MS¹和SWATH-MS²小，说明SWATHtoMRM的定量重现性更好，尤其是在低浓度时。

综上，SWATHtoMRM方法具有高的灵敏度，宽的动态范围以及好的重现性，适合于定量分析代谢物。

4. SWATHtoMRM 的应用

为了进一步展示SWATHtoMRM方法的实用性，本文将该技术运用于结直肠癌（CRC）诊断的潜在生物标志物的研究中。研究对象为CRC病人的癌旁和癌组织（18对样本作为训练集，42对样本用作验证集）。

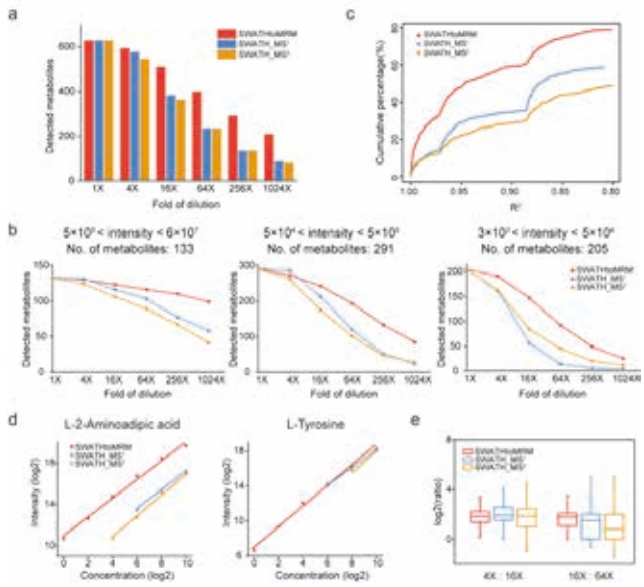

图4. SWATHtoMRM定量效果。(a) 3个模式在不同稀释浓度中的检测到的代谢物个数比较。 (b) 3个模式在不同丰度范围内检测到的代谢物个数比较。(c) 3个模式的R^2累积分布比较图。(d) 两种代谢物的线性范围比较。(e) 相邻两个稀释梯度间的比值分布图。

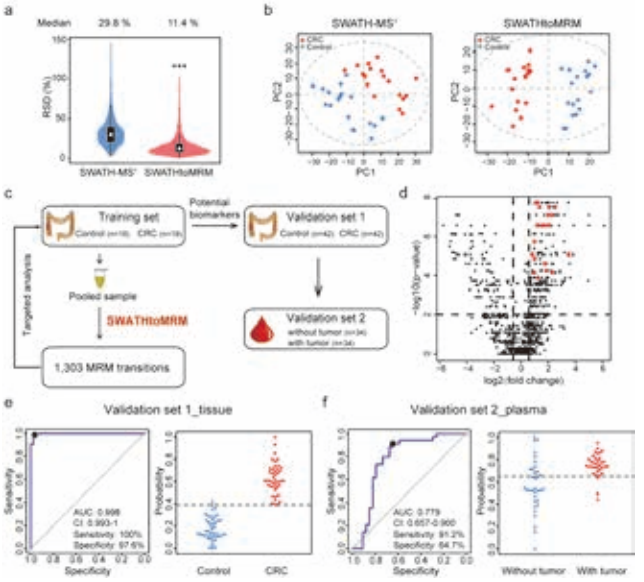

图5. (a) QC样品中检测到的1213个代谢物RSD分布图。(b) SWATH-MS¹和SWATHtoMRM检测得到的癌旁和癌组织中代谢物的PCA图。(c) 基于SWATHtoMRM的CRC潜在生物标志物研究的实验流程。(d) 检测到的1213个代谢物的火山图，红点表示20个潜在的生物标志物。(e) 组织样本验证集中，基于20个潜在标志物构建的PLS预测模型的ROC曲线（左）和概率分布图（右）。(f) 血浆样本验证集中，基于17个潜在标志物构建的PLS预测模型的ROC曲线（左）和概率分布图（右）。

RUO-MKT-02-8700-ZH-A

首先，利用训练集的QC样本采集了SWATH数据，并构建了1705个MRM离子对，其中1303（76.4%）个代谢物被成功检测到。通过对训练集样本的采集和分析，共有1213（93.1%）个代谢物至少在4个实际组织样品中被检测到，这些代谢物被用于后续统计分析。为了在实际样本中进一步比较，针对训练集样本也采集了SWATH数据。

从QC样本的RSD分布以及训练集样本的PCA分析结果来看，SWATHtoMRM在重现性和灵敏度方面显著优于SWATH-MS[1]，主要表现在更小的RSD值和较窄的RSD分布（图 5a），以及PCA图中更小的组内离散度和更大的组间区分度（图 5b）。

图 5c展示了基于SWATHtoMRM的CRC潜在生物标志物研究的实验流程。在寻找潜在生物标志物阶段，训练集检测到的1303个代谢物中，有358个代谢物具有统计学差异（fold-change ≥ 1.5，p-value < 0.01，图 5d），其中67个被成功鉴定。随后，使用PLS-DA模型分析了CRC癌旁和癌组织的代谢物差异，VIP值排名最高的20个代谢物被定义为潜在的生物标志物，并且在训练集中具有极好的辨别能力（AUC = 1）。接下来，本文在验证集样本中检测了这20个代谢物，并评估了其预测精度，结果发现这些代谢物在验证集样本中同样具有极好的辨别能力（AUC = 0.998，sensitivity = 100%，specificity = 97.6%， 图 5e）。

因为在临床应用中，血浆样本更易获得，因此，本文最后通过CRC病人手术切除前后的血浆样本来评估这些代谢物作为评价预后效果的标志物的潜力。在血浆样本中，17个代谢物能检测到。这17个代谢物同样表现出可靠的预测能力（AUC = 0.779，sensitivity = 91.2%，specificity = 64.7%，图5f）。

综上，SWATHtoMRM方法能在未来应用于临床样本的检测，以及疾病的生物标志物的研究中。

总结

本文基于SCIEX TripleTOF® 6600建立了一种新的靶向代谢组学方法—SWATHtoMRM，可同时检测高达1000-2000个代谢物。与DDA相比，SWATHtoMRM方法能够在保障提取的离子对质量的同时，构建更多的MRM离子对。而与SWATH-MS技术相比，SWATHtoMRM具有更好的重现性、更高的灵敏度和更广的线性范围。并且通过实际案例的应用，说明该方法在疾病的代谢物生物标志物的研究中具有巨大的潜力。

RUO-MKT-02-8700-ZH-A

从IDA到MRM: 高覆盖结合高准确代谢组学方法

IDA to MRM: High Coverage Combined with High Accuracy Metabolomics

陈金梅，司丹丹，龙志敏，郭立海
Chen Jinmei, Si Dandan, Long Zhimin, Guo Lihai

SCIEX应用支持中心，中国
SCIEX, China

Key Words: TripleTOF® 5600+ LC-MS/MS System, QTRAP® 6500+ LC-MS/MS System, Information Dependent Acquisition (IDA) Scanning, MRM, Metabolomics

前言

代谢组学是继基因组学和蛋白质组学之后新近发展起来的一门学科，是系统生物学的重要组成部分。之后得到迅速发展并渗透到多项领域，比如疾病诊断、医药研制开发、营养食品科学、毒理学、环境学，植物学等与人类健康护理密切相关的领域。非靶向代谢组学和靶向代谢组学是代谢组学两种主要应用形式，各具优劣势。现如今比较前沿的研究是高覆盖结合高准确代谢组学方法。运用TripleTOF® 5600+ LC-MS/MS 系统的非靶向方法发现样品中存在的代谢物，并锁定其保留时间和检测的离子对，将其转化为QTRAP® 6500+ LC-MS/MS系统的多反应离子监测（MRM）模式对样品采集，这种将非靶向代谢组学和靶向代谢组学结合起来的研究方式，利用各自的优势，既保证了覆盖全面性同时解决了结果准确性问题，使得该方法具有独特的亮点。

本实验采用数据依赖采集+动态背景扣除（IDA+DBS）和MRM数据采集模式结合的方式，对疾病组和正常组的尿液样品完成采集和数据分析工作。准确鉴定并筛选出数百种差异代谢物，获得覆盖度很高的显著的差异代谢通路，为组学研究提供新思路。

技术特点

1. TripleTOF® 5600+ 系统，配备 Turbo V™ 离子源获得稳定喷雾，提高离子化效率，同时减少污染，更大程度提高稳定性、可靠性和维持正常运行时间，非常适合大样本组学研究
2. TripleTOF® 5600+ 系统是集扫描速度，分辨率和灵敏度于一体的高分辨质谱仪，超快的扫描速度保证获取全面的质谱信息和稳定的信号DBS功能保证采集到有效的二级图谱，全轴的高分辨率一级和二级数据，为鉴定可靠的生物标志物提供保障
3. QTRAP® 6500+系统在具有高灵敏度同时保证数据稳定性的体系。可以提供理想的定量限（LOQ），具有更宽的线性范围，能对复杂基质中浓度差异较大的化合物进行检测和定量分析。只需一次进样，正负模式切换检测所有差异代谢物，提高通量

仪器设备

SCIEX ExionLC™系统+QTRAP® 6500+系统+TripleTOF® 5600+系统

液相方法

色谱柱：ACQUITY UPLC® HSS T3(100 × 2.1 mm, 1.8 µm)

流动相：A相：水（0.03%甲酸）
B相：甲醇：乙腈（1:1, 0.03%甲酸）

流速：0.3 mL/min

柱温：40℃

进样量：5 µL

RUO-MKT-02-11799-ZH-A

表1. 液相梯度。

Time(min)	A (%)	B (%)
0.00	95	5
17.00	5	95
21.00	5	95
21.10	95	5
25.00	95	5

TripleTOF® 5600+ 系统质谱方法

离子源：DuoSprayTM离子源（ESI+/-）

扫描模式：TOF MS-IDA-TOF MS/MS

扫描范围：m/z 100-1200

CDS自动校正

动态背景扣除（DBS）开启

离子源参数：

ISVF电压: 5500 V/-4500 V　　气帘气 CUR: 35 psi

雾化气 GS1: 50 psi　　雾化气 GS2: 55 psi

源温度：550℃　　DP电压：±80 V

碰撞能量：35 ± 15 V

QTRAP® 6500+系统质谱方法

离子源：IonDrive Turbo V 离子源（ESI+/-）

扫描模式：MRM

离子源参数：同上

实验结果

1.主成分（PCA）分析

基于非靶向高分辨率数据（正负离子模式）进行PCA分析，探索正常组和疾病组之间的潜在生物标志物，PCA结果表明，QC聚类离散度小，说明仪器稳定性良好，正常组和疾病组区分明显，组内差异较大，说明个体差异较大。

2.潜在差异代谢物

对XCMS plus软件提取得到的feature进行统计学分析，筛选出adjusted p-valve<0.05,VIP>1的feature，检索标准品建立的内源性代谢物二级数据库鉴定，正负离子模式共鉴定出300个差异代谢物。

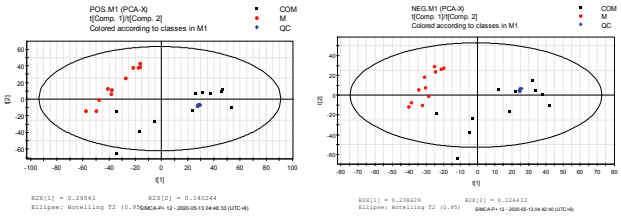

POS　　NEG

图1. PCA得分图 图注：红色为正常组 黑色为疾病组 蓝色为QC组。

3.差异代谢物确认

利用QTRAP® 6500+系统的高灵敏度和高通量的优势，将鉴定出的差异代谢物和初步得到的差异代谢通路上的化合物均转化成MRM方法，使用QTRAP® 6500+系统检测，一针进样正负切换模式检测潜在差异代谢物，进行统计学分析，筛选出adjusted p-valve<0.05,VIP>1的代谢物，做为差异代谢物。

4.差异代谢通路寻找

对差异代谢物分析，得到差异代谢通路，具有显著差异，覆盖率较高的通路为图中绿色标注的2条代谢通路。

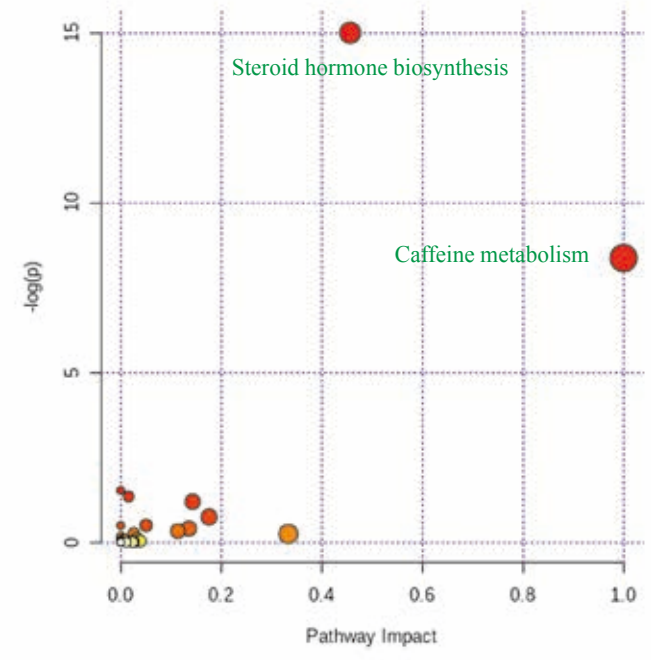

图2. 差异代谢通路。

RUO-MKT-02-11799-ZH-A

5.差异代谢通路中化合物上下调情况

以咖啡酸代谢通路为例分析疾病组相比于正常组化合物的上下调情况，该通路上疾病组相比于正常组所有化合物均呈下调趋势，为后续研究提供方向。

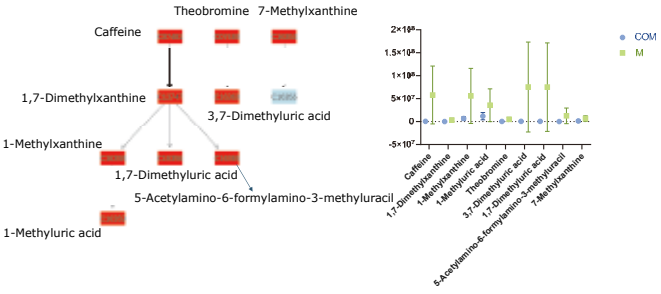

图3. Caffeine metabolism代谢通路及通路中化合物上下调情况。
图注：绿色为正常组，蓝色为疾病组

总结

本实验展示了TripleTOF® 5600+系统结合QTRAP® 6500+系统方案在代谢组学领域的优势。TripleTOF® 5600+系统数据采集模式（IDA+DBS扫描模式），只需一针进样，可获得高分辨的一级和有效的二级质谱数据，减少分析人员手动扣除基质背景和多次采集数据的烦恼，大大缩短了数据采集的时间，提高效率。QTRAP® 6500+系统在复杂基质中代谢物定量方面表现出高灵敏度、高通量、线性范围宽的优势，二者互为验证和补充，结合标准品建立的内源性代谢物数据库，可以鉴定出几百种差异代谢物，大大提高组学研究结果的覆盖度和准确度，是组学研究的发展趋势。

RUO-MKT-02-11799-ZH-A

基于ZenoTOF™ 7600系统的高质量二级质谱数据建立拟南芥广靶代谢组学检测方法

Establishment of Wide Target Metabolomics Detection Method for Arabidopsis Thaliana Based on High-quality secondary mass spectrometry data of Zeno TOF™ 7600 System

陈金梅，司丹丹，龙志敏，郭立海
Chen Jinmei, Si Dandan, Long Zhimin, Guo Lihai

SCIEX应用支持中心，中国
SCIEX, China

Key Words： ZenoTOF™ 7600 System, QTRAP® 6500+ System, Information Dependent Acquisition (IDA) Scanning, Zeno™ Trap, Scheduled MRM, Metabolomics, Arabidopsis thaliana

前言

代谢组学是继基因组学和蛋白质组学之后新近发展起来的一门学科，是系统生物学的重要组成部分。近年来在植物研究领域受到广泛关注。植物中代谢物超过20万种，有维持植物生命活动和生长发育所必需的初生代谢物及利用初生代谢物生成的与植物抗病和抗逆关系密切的次生代谢物，所以对植物代谢物进行分析是十分必要的。非靶向代谢组学和靶向代谢组学是代谢组学两种主要应用形式，各具优劣势。现如今将二者优势结合起来的是高覆盖结合高准确代谢组学方法，也就是广泛靶向/拟靶向/类靶向代谢组学较为流行。

本实验采用ZenoTOF™ 7600系统的非靶向方法，数据依赖采集+动态背景扣除+ Zeno™ 阱开启（IDA+DBS+Zeno™ Trap on）数据采集模式，使用SCIEX OS软件对拟南芥完成数据采集和数据分析工作，鉴定出拟南芥中代谢物成分。运用发现样品中存在的代谢物，并锁定其保留时间和检测的离子对，将其转化为QTRAP® 6500+系统的分窗口多反应监测（Scheduled MRM™）模式对样品采集，既保证了覆盖全面性同时解决了结果准确性问题，使得该方法具有独特的亮点。

技术特点

1. ZenoTOF™ 7600系统，配备Zeno™ Trap，提高离子占空比，富集MS/MS碎片离子，提高MS/MS灵敏度，特别是对低含量化合物，也能获得优异的数据库匹配，提升代谢物覆盖度；
2. ZenoTOF™ 7600系统是集扫描速度，分辨率和灵敏度于一体的高分辨质谱仪，配合133 Hz快速扫描速度，保证化合物的覆盖率和MS/MS谱图质量的前提下，可以缩短样品运行时间；
3. QTRAP® 6500+系统是具有高灵敏度同时保证数据稳定性的体系。可以提供理想的定量限，具有更宽的线性范围，能对复杂基质中浓度差异较大的化合物进行检测和定量分析。5毫秒极性切换能力可以在保证点数的前提下实现一针正负切换，样品只需进样一针，实现高通量检测。

仪器设备

SCIEX ExionLC™系统+QTRAP® 6500+系统+ ZenoTOF™ 7600系统

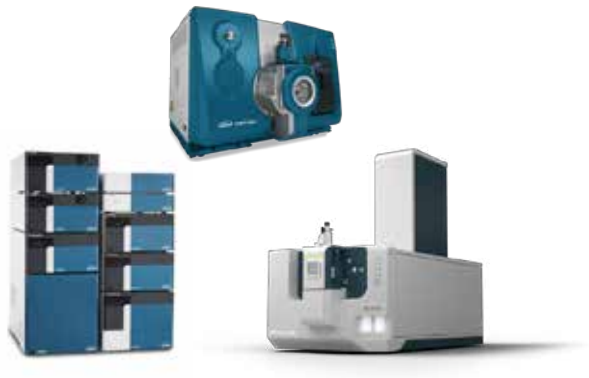

RUO-MKT-02-14255-ZH-A

液相方法

色谱柱：Luna Omega Polar C18 (100 × 3.0mm, 3 µm)

流动相：A相：水（0.03%甲酸）
B相：甲醇：乙腈（1:1，0.03%甲酸）

流速：0.3 mL/min

柱温：40 ℃

进样量：2 µL

表1. 液相梯度

Time(min)	A (%)	B (%)
1.00	95	5
7.00	50	50
22.00	2	98
27.00	2	98
27.10	95	5
30.00	95	5

ZenoTOF™ 7600系统质谱方法

扫描模式：ESI+/- TOF MS-IDA-20TOF MS/MS

扫描范围：一级m/z 50-1500 二级m/z 30-1500

CDS自动校正

动态背景扣除（DBS）开启

Zeno on

离子源参数：

喷雾电压: 5500V/-4500 V　　气帘气 CUR: 35 psi

雾化气 GS1: 50 psi　　雾化气 GS2: 55 psi

源温度：550 ℃　　DP电压：± 60 V

碰撞能量：± 35 ± 15 V

QTRAP® 6500+ 系统质谱方法

扫描模式：一针正负切换的Scheduled MRM

离子源参数：

喷雾电压: 5500V/-4500 V　　气帘气 CUR: 35 psi

雾化气 GS1: 50 psi　　雾化气 GS2: 55 psi

源温度：550 ℃　　DP电压：± 60 V

碰撞能量：三个能量中的最优值

实验流程

ZenoTOF™ 7600 系统的IDA+DBS+Zeno on数据采集模式得到高分辨数据后，使用SCIEX OS软件结合二级数据库（SCIEX）结合已报到的文献，使用非靶向，半靶向和靶向流程对样品完成快速、准确、全面的鉴定，建立数据库，并将其转化成离子对，使用QTRAP® 6500+系统的 Scheduled MRM一针正负切换数据采集模式采集批量样品数据。

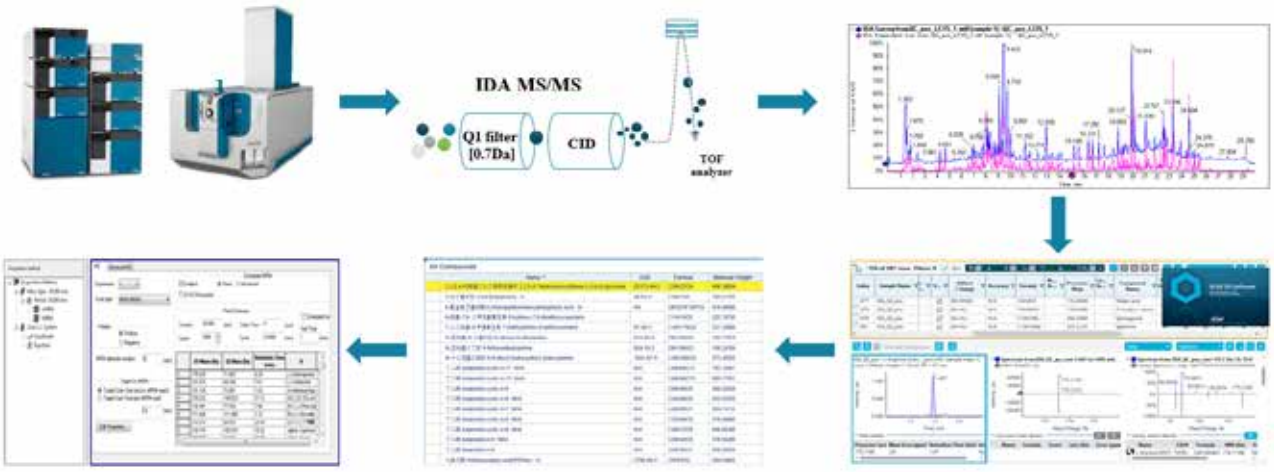

图1. 实验流程

RUO-MKT-02-14255-ZH-A

实验结果

1. 采用非靶向，半靶向和靶向流程正负离子共鉴定到538个化合物，并建立本地数据库，代谢物主要包括酚类，氨基酸及其衍生物，有机酸，糖及糖苷等类别。

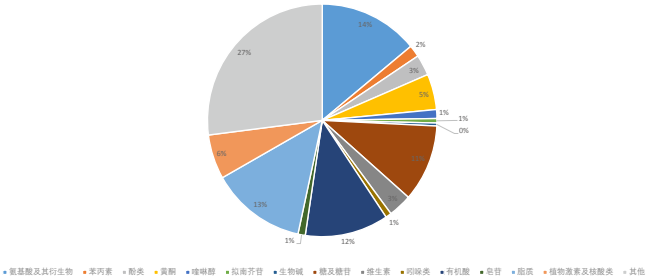

图2. 代谢物类别

2. 采用建立好的一针正负切换的Scheduled MRM方法采集数据，每10针穿插一针QC，37针的TIC图重现性良好，QC样品中加入的内标化合物，时间偏移在0.05 min之内，峰面积的RSD为5.70%。

总结

本实验展示了ZenoTOF™ 7600系统结合QTRAP® 6500+系统方案在植物代谢组学领域的优势。ZenoTOF™ 7600系统数据采集模式（IDA+DBS+Zeno on扫描模式），只需一针进样，可获得高分辨的一级和高质量有效的二级质谱数据，减少分析人员手动扣除基质背景和多次采集数据的烦恼，大大缩短了数据采集的时间，提高效率，Zeno on的功能使低含量化合物依旧可以得到高质量的二级，用于鉴定分析。QTRAP® 6500+系统在复杂基质中代谢物定量方面表现出高灵敏度、高通量、线性范围宽的优势，二者互为验证和补充，大大提高组学研究结果的覆盖度和准确度，是组学研究的发展趋势。

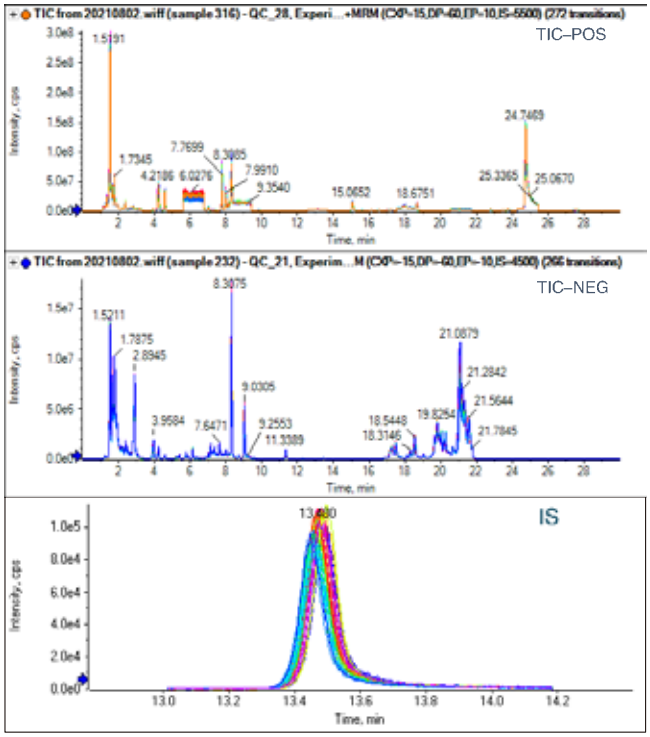

图3. QC样品和内标化合物重现性谱图

RUO-MKT-02-14255-ZH-A

基于高分辨质谱X500R QTOF系统番茄广靶代谢组学分析

Metabolic Profiling of Solanum lycopersicum by X500R QTOF High Resolution Mass Spectrometry

江汉鹏，龙志敏
Han-Peng Jiang, Zhimin Long
SCIEX应用支持中心，中国

Keywords: X500R QTOF, LC/MS, Metabolomics, Solanum lycopersicum

前言

代谢组学是一门新兴的学科，作为系统生物学的一个分支，在1999年才被首次提出[1]，主要研究生物体内受到内外环境扰动后产生的小分子代谢物的变化。代谢组处于基因调控和蛋白质执行这一网络的下游，往往提供了生物学的终端信息[2, 3]，所以，代谢组学研究为探索其上游的机理和相应调控方式提供着重要的线索。目前已被广泛应用于基础医学，药理学、植物学、微生物学和食品安全等研究领域。

植物生理过程相比与动物的，亦尤为复杂，植物及其相关的微生物群落可以产生数以百万计的代谢物，其中据推测它们可能具有新的生物活性的物质大部分尚未被鉴定[4]。过去的几十年研究中，代谢分析与其他组学工具的整合已经被证明是非常有效的鉴定功能基因和阐明生理途径的手段[5]，所以对植物的代谢物进行分析十分重要。

番茄是世界上价值较高的水果和蔬菜作物，对人类饮食有很大的营养贡献。收获期的番茄果实是多种代谢产物的综合体现，所以通过分析和鉴定番茄果实中的代谢产物为番茄果实品质改良提供了知识基础，也为植物代谢生物学研究提供了丰富的资源。

本实验采用高分辨质谱X500R QTOF系统的非靶向分析方法，结合数据依赖采集和动态背景扣除采集方法。使用SCIEX OS软件对番茄完成数据采集和数据分析工作，通过一级质谱及同位素分布信息鉴定到可能代谢物3944种，其中有二级图谱确认代谢物330种。最后将所鉴定的成分信息及二级质谱图谱转化为数据库及MRM离子对列表，为之后的研究提供了数据基础。

方法特点

1. X500R QTOF系统继承了SCIEX仪器经典工业化的、抗污染的离子源设计，具有高分辨率，高质量准确度，高灵敏度，高采集速度和高定量线性动态范围，可同时采集高质量的MS和MS/MS图谱，满足定性和定量需要。本文提供完整前处理方法，结合X500R QTOF系统的数据依赖采集和动态背景扣除采集方法，无需重复进样即可得到番茄非靶向代谢组学信息。
2. 定性结果生成数据库文件及MRM离子对列表，为之后鉴定及靶向分析提供数据支持。

样品及试剂

实验用番茄样品如下：普通番茄（大），普通番茄（小），有机番茄（大），粉番茄（大），草莓番茄（小），糖心番茄（小），绿番茄（小），黄番茄（小）。

样品前处理

约20g鲜重番茄样本置于冻干仪中冻干。取冻干样品，使用研磨机研磨，研磨10秒，停10秒，重复4次至冻干番茄变成粉末。取1g冻干粉末，加入10毫升甲醇和水混合溶液（50/50，v/v），放置于-20度过夜提取。提取完后，取上清，4度，12000rpm离心后，取上清即可进样。

仪器设备

ExionLC™ 系统 + SCIEX高分辨质谱X500R QTOF系统

RUO-MKT-02-15354-ZH-A

液相条件

色谱柱：Waters HSS T3 (100mm × 2.1 mm, 1.8μm)

柱温：40 ℃

进样体积：2 μL

流动相：A为水（含0.025%甲酸，v/v），

B为甲醇和乙腈（1:1，含0.025%甲酸，v/v）

流速：0.3 mL/min

梯度：见下表

Time [min]	A.Conc [%]	B.Conc [%]
0.00	98.0	2.0
2.00	98.0	2.0
20.00	2.0	98.0
25.00	2.0	98.0
25.10	98.0	2.0
28.00	98.0	2.0

质谱条件

SCIEX高分辨质谱X500R QTOF系统

离子源：ESI源；

扫描模式：ESI +/- TOF MS – IDA 15 TOF MS/MS；

扫描范围：MS1, m/z, 40-1500; MS2, m/z, 40-1500

CDS自动校正

动态背景扣除（DBS）开启

离子源参数：

IS电压: 5500 V / -4500 V；　　气帘气CUR：35 psi；

雾化气GS1：55 psi；　　辅助气：55 pis；

离子源温度为550 ℃；　　碰撞气：7 psi

DP电压：±60；　　碰撞能量：±40 ± 20

数据处理及数据分析

使用SCIEX OS软件对番茄完成数据采集，代谢物定性和相对定量。使用Library View™软件建立代谢物数据库。

实验结果与讨论

1. 番茄代谢物定性分析

实验采用数据依赖采集（IDA）和动态背景扣除采集方法，使用SCIEX OS软件采集，无需重复进样即可获得样本中一级和二级图谱信息，二级图谱可直接导入Library View™ 软件生成本地数据库，分析流程见图1。

数据处理和采集使用为同一软件，数据处理采用非靶向，半靶向和靶向流程正负离子共鉴定到可能代谢物3944个。其中330个代谢物获得了高质量二级图谱，被准确定性，定性示例见图2，并利用这些二级图谱建立本地数据库。对于数据库中没有的代谢物，对其MS/MS图谱进行了解析，图3列举了部分茄类代谢物MS/MS图谱解析。

番茄的代谢物主要包括茄类典型代谢物（番茄碱、番茄红素、番茄皂苷等）（见表1），酚酸类，氨基酸及其衍生物，有机酸，核苷（酸）类，糖及糖苷等。通过这些二级图片，即可将数据转化为MRM离子对信息，为之后靶向筛查提供基础。

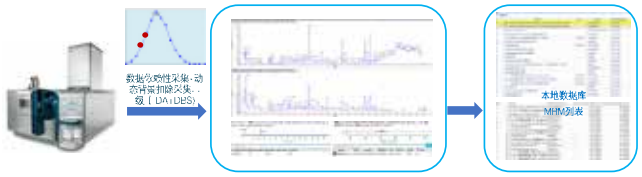

图1.分析流程

RUO-MKT-02-15354-ZH-A

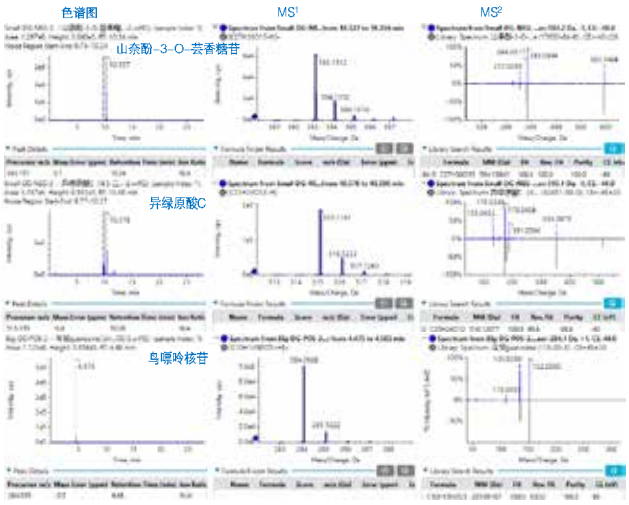

图2.数据库定性分析示例

2. 代谢产物的统计分析

用所鉴定到的化合物将所测试的8种番茄作组成份分析（图3）。QC很好的聚类，说明该方法可信度高。8种番茄初步可以分为四类。第一类为大番茄，包含普通大番茄和有机大番茄；第二类为普通小番茄，通常也称为千禧果，水果番茄；第三类为粉番茄（大）；第四类为市场上特殊品种，都是小番茄，包括草莓番茄、黄番茄、绿番茄和糖心番茄。这些分类也符合从品种上对番茄的分类，说明该方法具有科学性。但是目前使用的番茄样本数量较少，后续需要扩大样本量以更好的验证，并且找出具有生理学意义的差异代谢物。

表1.定性到的茄类特有代谢物

No.	代谢物	化学式	ESI模式	保留时间	理论 m/z	检测 m/z	质量偏差（ppm）	MS/MS碎片离子信息
1	Dehydrofilotomatine	$C_{50}H_{81}NO_{21}$	+	10.35	1032.5370	1032.5401	2.7	414.3370; 145.0502
2	Dehydrolycoperoside A	$C_{58}H_{93}NO_{29}$	+	9.4	1268.5910	1268.5936	2.4	1208.5735
3	Dehydrolycoperoside F	$C_{58}H_{93}NO_{29}$	+	9.94	1268.5910	1268.5942	2.8	1208.5735; 1106.5413; 1088.4976; 1046.5421
4	Dehydrolycoperoside G	$C_{58}H_{93}NO_{29}$	+	10.34	1268.5910	1268.5948	3	1208.5735
5	Dehydrotomatine isomer (25R)	$C_{50}H_{81}NO_{21}$	+	11.73	1032.5370	1032.5402	2.8	414.3418
6	Hydroxytomatidenol	$C_{27}H_{43}NO_3$	+	10.12	430.3320	430.3325	2.3	412.3226; 162.1290
7	Hydroxytomatidine	$C_{27}H_{45}NO_3$	+	10.34	432.3470	432.3482	2.2	414.3373; 273.2223; 161.1335
8	Lycoperodine	$C_{12}H_{12}N_2O_2$	+	7.27	217.0970	217.0975	1.5	200.1323; 144.0810; 84.0455
9	Lycoperoside F	$C_{58}H_{95}NO_{29}$	+	10.11	1270.6060	1270.6060	-0.2	1210.5857; 1090.5473; 1030.5273
10	Tomatidine	$C_{27}H_{45}NO_2$	+	12.01	416.3523	416.3530	1.6	398.3431; 273.2230; 255.2108; 161.1333
11	Tomatine	$C_{50}H_{83}NO_{21}$	+	12.01	1034.5530	1034.5555	2.4	578.4010; 416.3650; 298.3321
12	Solasodine	$C_{27}H_{43}NO_2$	+	10.03	414.3370	414.3378	2.8	255.2188; 161.1331; 112.0753
13	(Hydroxy- α -Tomatine) FA I	$C_{50}H_{83}NO_{22}HCOOH$	-	13.45	1096.5530	1096.5600	-6	577.3912; 61.9886
14	(Hydroxy- α -Tomatine) FA II	$C_{50}H_{83}NO_{22}HCOOH$	-	14.93	1096.5530	1096.5600	-6	934.507
15	Esculeoside A	$C_{58}H_{95}NO_{29}$	+	10.11	1270.6060	1270.6060	-0.2	1210.5857; 1090.5473
16	Esculeoside B	$C_{56}H_{93}NO_{28}$	+	8.65	1228.5960	1228.5981	1.9	1210.5896; 610.3971; 430.3397
17	α -tomatine	$C_{50}H_{83}NO_{21}$	+	12.01	1034.5530	1034.5555	2.4	578.4010; 398.3321; 416.3650
18	γ -tomatine	$C_{39}H_{65}NO_{12}$	+	12.01	740.4580	740.4599	2.6	578.4111; 175.1494
19	δ -tomatine	$C_{34}H_{51}N_5O_3$	+	12.01	578.4060	578.4058	-1.1	560.3961; 435.2771; 255.2111; 161.1331
20	Dehydrolycoperoside A/F/G	$C_{58}H_{93}NO_{29}$	+	9.95	1268.5910	1268.5942	2.8	1208.5735; 572.3516; 470.3320
21	Dehydrotomatine	$C_{50}H_{81}NO_{21}$	+	11.73	1032.5370	1032.5402	2.8	414.3418; 145.0502
22	Tomatidine-O-rhamnoside	$C_{41}H_{38}O_2$	+	10.76	563.2940	563.2948	0.6	490.3541; 430.3228; 325.1113; 295.1064; 163.0599
23	Acetyl hydroxy tomatidine-di-O-hexoside	$C_{41}H_{67}NO_{15}$	+	10.11	814.4580	814.4579	-0.5	754.4367; 634.3967; 574.3745; 435.2760; 255.2115

RUO-MKT-02-15354-ZH-A

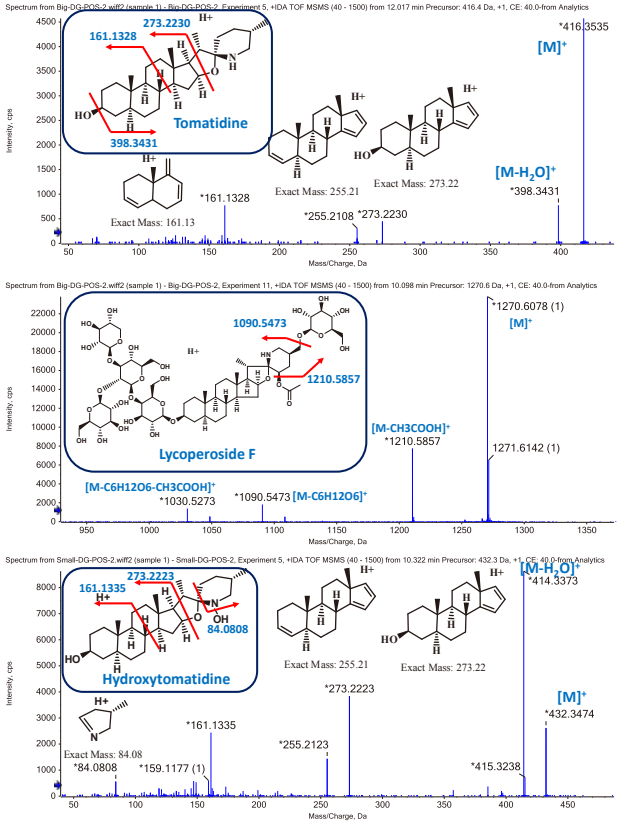

图3.部分茄类代谢物MS/MS图谱解析

结论

本实验采用数据依赖采集和动态背景扣除采集方法。使用高分辨质谱X500R QTOF系统和SCIEX OS软件对番茄完成数据采集和数据分析工作，通过一级质谱及同位素分布信息鉴定到可能代谢物3944种，其中有二级图谱确认代谢物330种。最后将所鉴定的成分信息及二级质谱图谱转化为数据库及MRM离子对列表，并且做了初步的主成分分析。后续需要扩大样本量以更好的验证，找出具有生理学意义的差异代谢物。

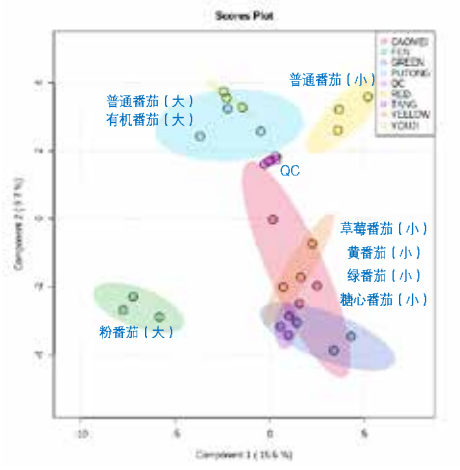

图4. 8种番茄组成份分析

参考文献

[1] Nicholson JK, Lindon JC, Holmes E., "'Metabonomics': understanding the metabolic responses of living systems to pathophysiological stimuli via multivariate statistical analysis of biological NMR spectroscopic data," Xenobiotica, 1999, 29, 1181-9

[2] Rinschen MM, Ivanisevic J, Giera M, Siuzdak G., "Identification of bioactive metabolites using activity metabolomics," Nat Rev Mol Cell Biol., 2019, 20, 353-367

[3] Wishart DS, Tzur D, Knox C, Eisner R, Guo AC, et al, "HMDB: the Human Metabolome Database," Nucleic Acids Res, 2007, 35, D521-6

[4] Tsugawa H, Rai A, Saito K, Nakabayashi R., "Metabolomics and complementary techniques to investigate the plant phytochemical cosmos," Nat Prod Rep, 2021, 38, 1729-1759

[5] Kusano M, Tabuchi M, Fukushima A, Funayama K, Diaz C, Kobayashi M, Hayashi N, Tsuchiya YN, Takahashi H, Kamata A, et al, "Metabolomics data reveal a crucial role of cytosolic glutamine synthetase 1;1 in coordinating metabolic balance in rice," Plant J., 2011, 66, 456-66

RUO-MKT-02-15354-ZH-A

SCIEX QTRAP®系统在紫薯高覆盖靶向代谢组学中的应用

Development of a High Coverage metabolomics method of Ipomoea batatas (L.) Lam by SCIEX QTRAP® System

雷敏，龙志敏，郭立海
Lei Min, Long Zhimin, Guo Lihai
SCIEX，中国

Key word: Ipomoea batatas (L.) Lam，High coverage metabolomics method, Plant metabolomics, Biomarker

引言

高覆盖靶向代谢组学[1, 2]研究思路，目前是很多代谢组学实验室开展的一种新的代谢组学研究思路。该研究方法的特点是，既结合了SCIEX TripleTOF™系统的高覆盖度，同时也结合了SCIEX QTRAP®(或SCIEX Triple Quad ™) 系统高通量，高稳定性和宽线性范围的特点，为代谢组学研究提供了一种高覆盖度及高效的研究方法。

本文中，紫薯中的代谢物MRM方法建立的流程如下，先在SCIEX TripleTOF ™系统上建立IDA方法对紫薯提取物进行高覆盖度的测定，然后将鉴定到的化合物建立MRM离子对，在SCIEX QTRAP®(或SCIEX Triple Quad ™) 系统进行靶向代谢组学的测定。

本文使用高覆盖靶向代谢组学的思路测定2个不同生长阶段的紫薯中的代谢物，然后再进行统计分析，筛选其中的差异代谢物，以挖掘紫薯生长阶段的代谢物差异或生长信息 。

本文实验方法特点

本文展示了使用SCIEX QTRAP® (或SCIEX Triple Quad ™) 系统建立了紫薯的高覆盖靶向代谢组学方法，方法具有以下特点：

1. 仪器的灵敏度高，检测速度快，同时检测紫薯中的203个代谢物，包括氨基酸，核苷，糖类，脂质，黄酮及黄酮苷类，花青素类，酚酸类等成分。其中，正离子检测93个化合物，负离子检测110个化合物，化合物覆盖度高。
2. 仪器和方法的特异性好，可正负切换同时检测，结合Scheduled MRM™功能，仅35min的方法即可完成一针样品中的203个化合物的检测，检测效率高。
3. QC样本203个化合物中的RSD结果，91%化合物的RSD在15%%之内，满足代谢组学QC样本重复性要求，表明仪器和方法的重现性好。
4. 该方法为SCIEX QTRAP®系统或SCIEX Triple Quad ™系统的用户开展高覆盖靶向代谢组学提供思路，以及为开展紫薯高覆盖靶向代谢组学研究的用户提供方法，便于快速筛选差异物。

仪器设备

SCIEX Exion LC™系统 + QTRAP®系统 (或SCIEX Triple Quad™系统)

液相方法

色谱柱：HSS T3 (100 × 2.1 mm, 1.8 µm)

RUO-MKT-02-13860-ZH-A

流动相：A相：水（含0.05%甲酸和5 mmol/L 醋酸铵）
B相：乙腈

流速：0.3 ml/min

柱温：40℃；

进样量：2 μL

Time(min)	A (%)	B (%)
0.00	100	0
0.50	100	0
10.0	70	30
20.0	5	95
30.0	5	95
30.1	100	0
35.0	100	0

质谱方法

离子源：ESI源，正负离子切换同时检测-Scheduled MRM™模式

离子源参数：

IS电压: 正离子：5500V；　　负离子：-4500V

气帘气 CUR: 35 psi　　雾化气 GS1: 50 psi

辅助气 GS2: 50 psi　　源温度 TEM: 500℃

碰撞气 CAD: Medium

循环时间（正离子/负离子）：0.4 s / 0.4 s

表1. 部分MRM离子对列表展示
表1.1. 部分正离子列表

No.	Q1	Q3	Compound name	DP	EP	CE	CXP
1	317.07	153.02	异鼠李素 Isorhamnetin	80	10	35	7
2	403.14	373.09	川陈皮素Nobiletin	80	10	35	7
3	463.11	301.07	芍药花青素+Glc 1	80	10	35	7
4	463.12	301.07	芍药花青素+Glc 2	80	10	35	7
5	465.1	303.05	金丝桃苷 Hyperin	80	10	35	7
6	627.16	303.05	槲皮素+2Glc	80	10	35	7
7	641.14	317.07	Methylquercetin+2Glu 1	80	10	35	7
8	641.17	317.07	Methylquercetin+2Glu 2	80	10	35	7
9	769.22	287.06	矢车菊素+乙酰基+Glc+Rha+xyl	80	10	35	7
10	773.2	287.06	矢车菊素+3Glc	80	10	35	7
11	787.2	301.07	芍药花青素+2Glc+Caffeoyl 1	80	10	35	7
12	787.21	301.07	芍药花青素+2Glc+Caffeoyl 2	80	10	35	7
13	787.22	301.07	芍药花青素+2Glc+Caffeoyl 3	80	10	35	7
14	787.23	301.07	芍药花青素+3Glc	80	10	35	7
15	789.21	303.05	槲皮素+3Glc 1	80	10	35	7
16	789.22	163.04	槲皮素+3Glc 2	80	10	35	7
17	789.23	163.04	槲皮素+3Glc 3	80	10	35	7
18	791.2	305.06	二氢槲皮素+ 3Glc	80	10	35	7
19	801.21	301.07	芍药花青素+2Glc+Feruoyl 1	80	10	35	7
20	801.22	301.07	芍药花青素+2Glc+Feruoyl 2	80	10	35	7
21	805.22	319.08	羟基槲皮素+3 Glc	80	10	35	7
22	893.23	287.06	矢车菊素+3Glc+salicylacyl	80	10	35	7
23	907.25	301.07	芍药花青素+3Glc+salicylacyl	80	10	35	7
24	909.28	303.09	槲皮素+3Glc++salicylacyl	80	10	35	7

表1.2. 部分负离子列表

No.	Q1	Q3	Compound name	DP	EP	CE	CXP
1	465.11	303.04	二氢槲皮素+ Glc 1	-80	-10	-35	-11
2	465.12	303.04	二氢槲皮素+ Glc 2	-80	-10	-35	-11
3	465.13	303.04	二氢槲皮素+ Glc 3	-80	-10	-35	-11
4	465.14	303.04	二氢槲皮素+ Glc 4	-80	-10	-35	-11
5	465.15	303.04	二氢槲皮素+ Glc 5	-80	-10	-35	-11
6	337.05	191.06	1-pCoQA	-80	-10	-35	-11
7	337.06	119.05	5-pCoQA	-80	-10	-35	-11
8	353.07	191.06	1-CQA 1	-80	-10	-35	-11
9	353.08	191.06	1-CQA 2	-80	-10	-35	-11
10	353.09	191.06	5-CQA	-80	-10	-35	-11
11	353.04	191.06	1-CQA 3	-80	-10	-35	-11
12	353.03	191.06	1-CQA 4	-80	-10	-35	-11
13	353.02	191.06	1-CQA 5	-80	-10	-35	-11
14	355.1	175.04	1-O-feruloyl-β-D-glucose	-80	-10	-35	-11
15	367.1	173.05	5-FQA	-80	-10	-35	-11
16	367.11	173.05	4-FQA	-80	-10	-35	-11
17	457.11	137.02	水杨酸酰基奎宁酸+ Coumaroyl 1	-80	-10	-35	-11
18	457.12	137.02	水杨酸酰基奎宁酸+ Coumaroyl 2	-80	-10	-35	-11
19	473.1	173.04	水杨酸酰基奎宁酸+ cafferoyl 3	-80	-10	-35	-11
20	473.11	173.04	水杨酸酰基奎宁酸+ cafferoyl 4	-80	-10	-35	-11
21	487.11	173.05	5-FQA+salicylacyl 3	-80	-10	-35	-11
22	473.13	173.04	水杨酸酰基奎宁酸+ cafferoyl 1	-80	-10	-35	-11
23	487.12	137.03	5-FQA+salicylacyl 1	-80	-10	-35	-11
24	487.13	137.02	5-FQA+salicylacyl 2	-80	-10	-35	-11

实验结果

1. **空白溶液和QC样品溶液**：配制含50%乙腈溶液，作为空白溶液，考察专属性，提取离子流图如图1；分别从所有样品中取30 µl溶液混合，作为QC样本，考察仪器的稳定性。提取离子流图如图2。A样本的提取离子流图见图3。

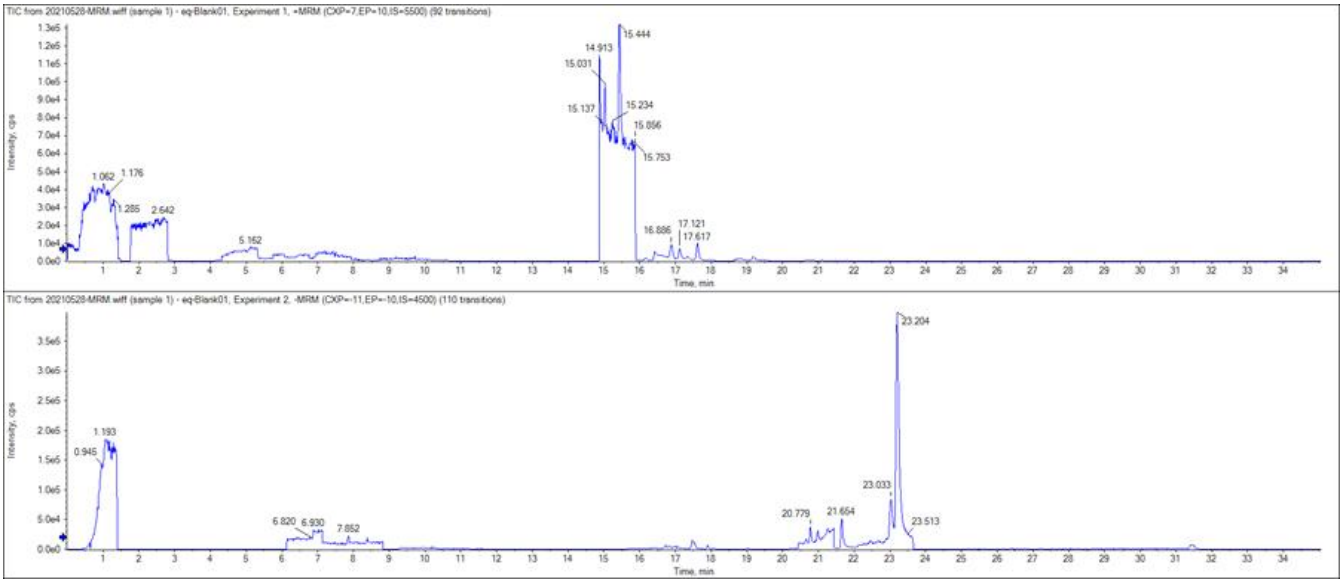

图1. 空白溶液中的总离子流图
(从上到下，上图为正离子的总离子流图，下图为负离子的总离子流图)

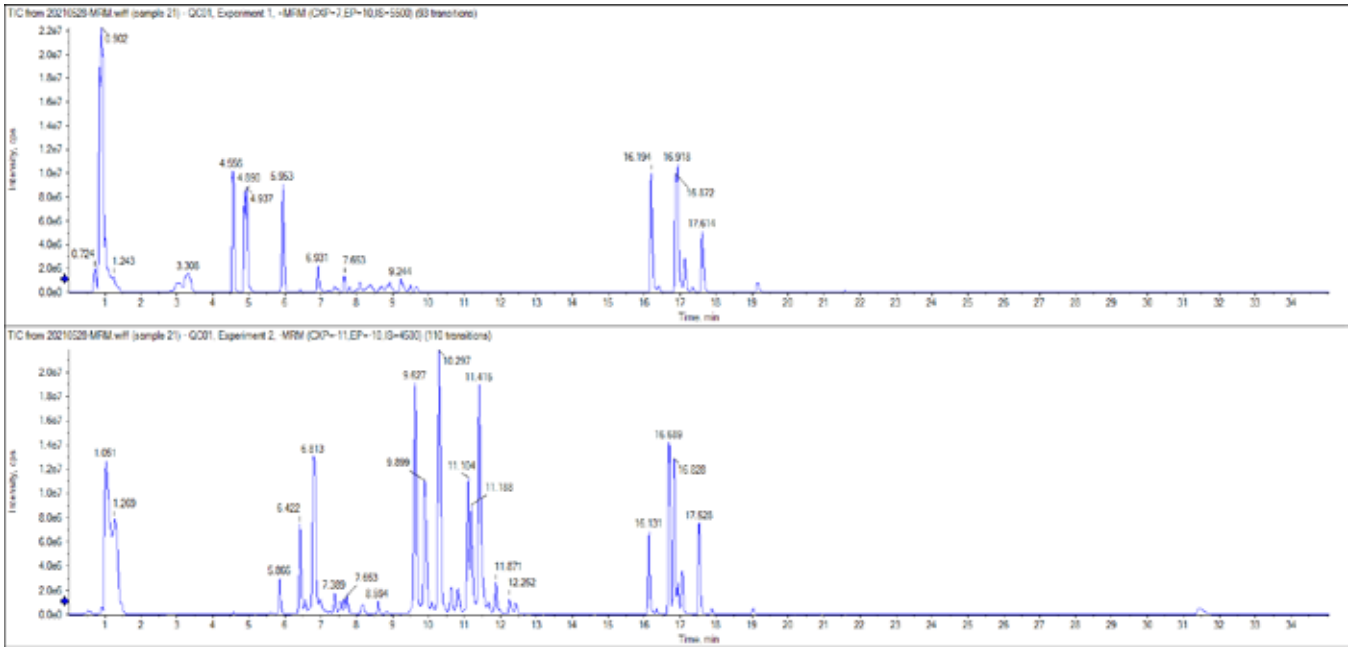

图2. QC样品总离子流图
(从上到下，上图为正离子的总离子流图，下图为负离子的总离子流图)

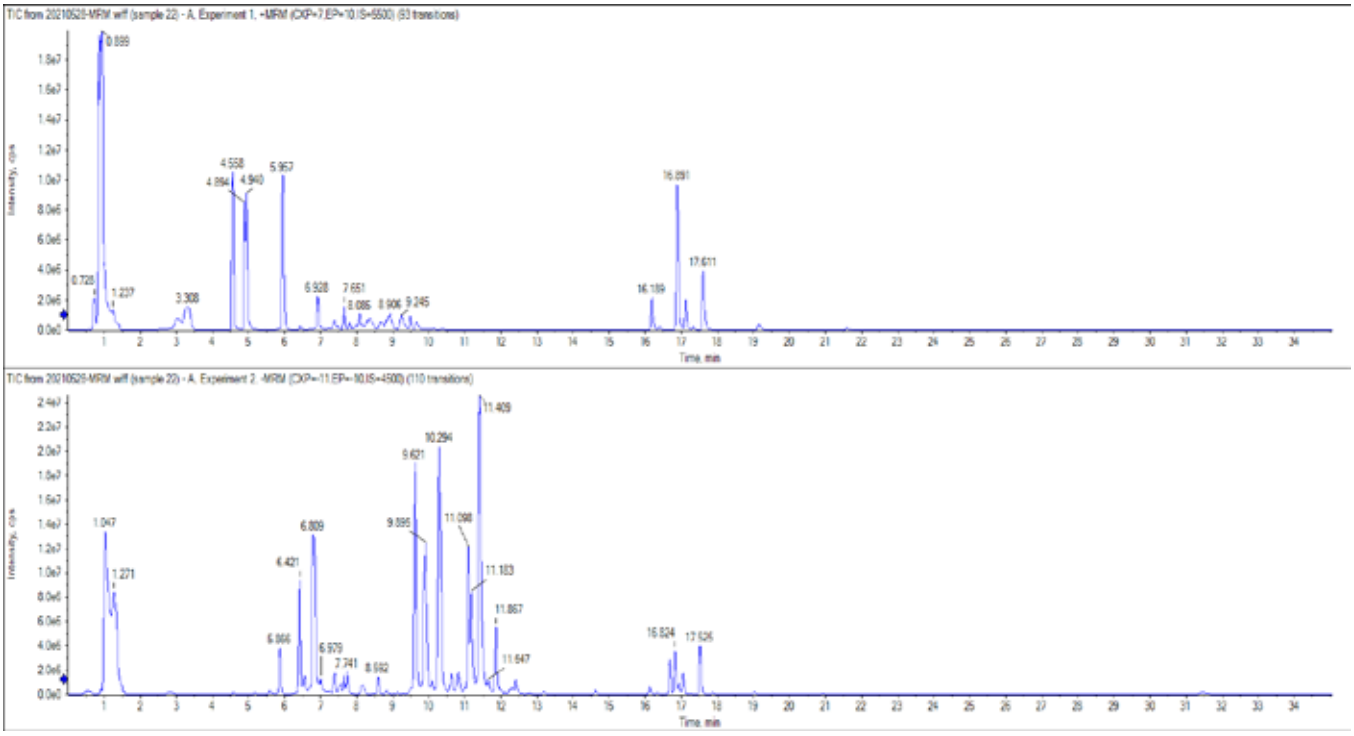

图3. A样品总离子流图
(从上到下，上图为正离子的总离子流图，下图为负离子的总离子流图)

2. QC样本重现性评估：

QC样本穿插在进样序列中，每三针样品中穿插一针QC样品，最后使用QC样品来评估序列进样中仪器的稳定性和重复性。

首先，3针QC样品的重叠图，见图4。从重叠图中可以看出，化合物保留时间和响应强度的总离子流图重叠好。

其次，对3针QC样品中203个化合物RSD%进行计算，来评估重现性。91%的化合物在15%%之内，满足代谢组学QC样本重复性要求，且表明仪器的重现性良好。

从以上两方面考察结果来看，仪器在序列运行过程中，状态稳定，样品结果可用于代谢组学分析。

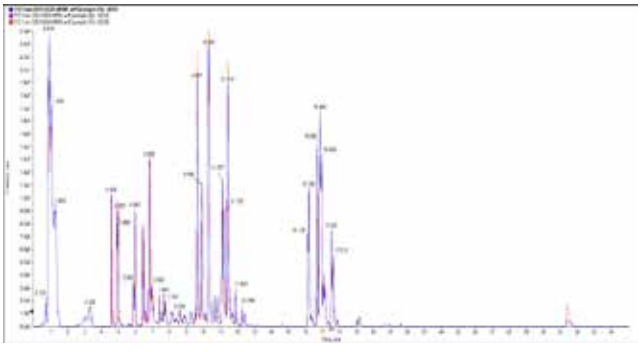

图4. 3针QC样品总离子流重叠图

RUO-MKT-02-13860-ZH-A

3. 统计结果：

2个不同阶段的紫薯样本，每组3个样本，每个样本进样1针，最后寻找两个阶段的差异代谢物。本文中的数据使用Markerview (版本号1.3, SCIEX)和MetaboAnalyst (版本号5.0，https://www.metaboanalyst.ca) 对203个代谢物进行统计，筛选差异物。

使用MetaboAnalyst软件对2组样本进行PLS-DA统计，PLS-DA得分图见图5。从PLS-DA得分图可以看出2组样本有明显的区分，表明样本之间有明显的差异。使用Markerview软件对2组样本分别进行t-检验， t-检验结果及其中一个化合物的箱体图展示见图6。使用MetaboAnalyst进行t-test，Fold Change及PLS-DA分析，以p值<0.01，Fold change>2或<0.5，及VIP>1筛选两组间的差异物。Fold Change图见图7。两组间的差异物总共是135个，列表见表3，包括14个氨基酸及其他类小分子，20个脂质化合物，50个酚酸类化合物，51个黄酮苷和花青素苷类化合物。

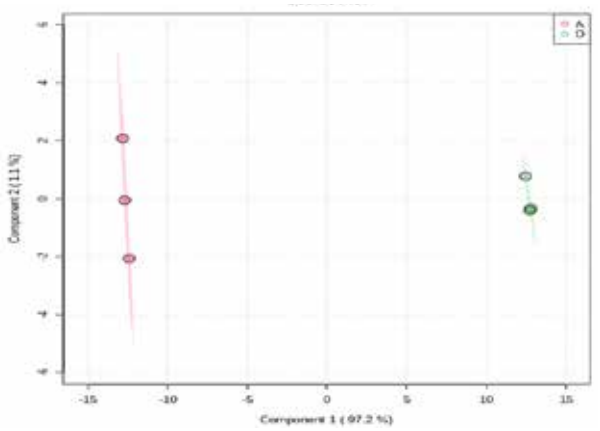

图5. PCA-DA得分图

Row	Index	Peak Name	m/z	Ret. Time	Group	Use	t-value	p-value	Mean 1	Mean 2	Median 1	Median 2	Sigma 1	Sigma 2	Delta	Fold Change	Log (Fold Change)
1	128	128	N/A	N/A		☑	211.18	5.3642e-9	2.280e7	8.662e6	2.281e7	8.643e6	7.393e4	8.929e4	1.413e7	2.632e0	4.202e-1
2	85	85	N/A	N/A		☑	-327.92	5.8782e-9	7.669e6	6.004e7	7.638e6	6.001e7	1.537e5	2.300e5	-5.237e7	1.277e-1	-8.937e-1
3	170	170	N/A	N/A		☑	461.98	1.7535e-8	7.709e5	1.729e5	7.700e5	1.734e5	1.980e3	1.052e3	5.980e5	4.460e0	6.493e-1
4	121	121	N/A	N/A		☑	189.59	3.8553e-8	3.917e7	7.674e6	3.904e7	7.630e6	2.390e5	1.603e5	3.150e7	5.104e0	7.079e-1
5	82	82	N/A	N/A		☑	-153.50	4.3836e-8	1.776e7	4.129e7	1.786e7	4.127e7	2.150e5	1.559e5	-2.353e7	4.301e-1	-3.664e-1
6	104	104	N/A	N/A		☑	221.14	5.0269e-8	5.910e5	9.144e3	5.902e5	1.039e4	3.887e3	2.379e3	5.818e5	6.463e1	1.810e0
7	75	75	N/A	N/A		☑	91.68	9.6716e-8	8.925e5	3.870e5	8.923e5	3.873e5	6.415e3	7.077e3	5.055e5	2.306e0	3.629e-1
8	95	95	N/A	N/A		☑	317.77	1.0999e-7	8.184e7	9.901e6	8.170e7	9.985e6	3.523e5	1.721e5	7.194e7	8.266e0	9.173e-1
9	15	15	N/A	N/A		☑	75.62	2.1599e-7	7.024e5	1.161e5	6.973e5	1.210e5	8.942e3	1.002e4	5.863e5	6.051e0	7.818e-1
10	18	18	N/A	N/A		☑	126.83	5.6200e-7	8.211e5	7.461e4	8.214e5	7.615e4	8.866e3	5.031e3	7.465e5	1.100e1	1.042e0
11	100	100	N/A	N/A		☑	55.19	1.6639e-6	4.606e5	1.282e5	4.621e5	1.312e5	6.193e3	8.396e3	3.324e5	3.593e0	5.555e-1
12	157	157	N/A	N/A		☑	-427.79	1.8754e-6	1.558e7	5.060e7	1.563e7	5.060e7	1.384e5	3.090e4	-3.501e7	3.080e-1	-5.115e-1
13	57	57	N/A	N/A		☑	137.75	2.2163e-6	9.651e5	3.249e4	9.709e5	3.413e4	1.071e4	4.764e3	9.326e5	2.970e1	1.473e0
14	123	123	N/A	N/A		☑	160.19	2.7593e-6	1.949e7	1.542e6	1.953e7	1.522e6	1.805e5	7.139e4	1.795e7	1.264e1	1.102e0

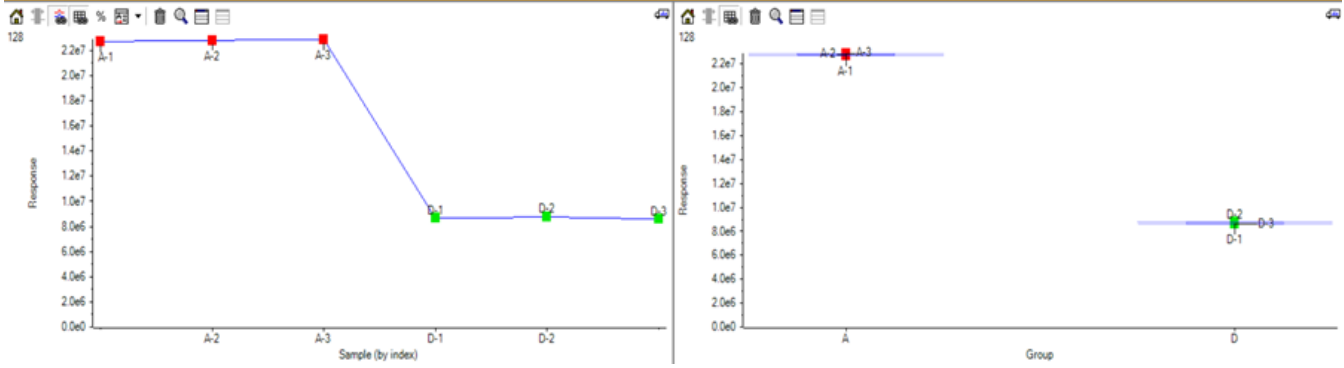

图6. t-检验结果及箱体图

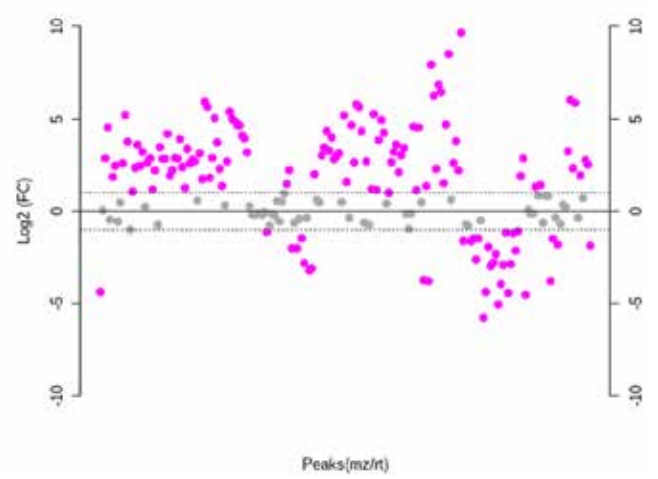

图7. Fold Change图

总结

本文展示了使用SCIEX QTRAP® 系统建立了紫薯的高覆盖靶向代谢组学方法。该方法可同时检测紫薯中的203个代谢物，包括氨基酸，核苷，糖类，脂质，黄酮及黄酮苷类，花青素类，绿原酸等成分。其中，正离子检测93个化合物，负离子检测110个化合物，化合物覆盖度高。仪器和方法的特异性好，可正负切换同时检测，结合Scheduled MRM™功能，仅35min的方法即可完成一针样品中的203个化合物的检测，检测效率高。QC样本中203个化合物的RSD，91%的化合物在15%之内，表明仪器和方法的重现性好。该方法为SCIEX QTRAP®系统或SCIEX Triple Quad ™的用户开展高覆盖靶向代谢组学提供思路，以及为开展紫薯代谢组学研究的用户提供方法，便于快速筛选差异物。

参考文献

[1] F Zheng, X Zhao, Z Zeng, L Wang, G Xu, Development of a plasma pseudotargeted metabolomics method based on ultra-high-performance liquid chromatography-massspectrometry. Nature Protocols. 2020.

[2] Zhou S, Kremling KA,et al.Metabolome-Scale Genome-Wide Association Studies Reveal Chemical Diversity and Genetic Control of Maize Specialized Metabolites. Plant Cell. 2019,31(5):937-955.

RUO-MKT-02-13860-ZH-A

表3. A组和D组之间的差异物列表

化合物名称	化合物名称	化合物名称
新蛇床内酯	1-pCoQA	木犀草素+3Glc+Feruoyl
JA	Sucrose+Caffeoyl 1	羟基槲皮素+4 Glc +GlcUA
JA-Lle	4C,5FCQA	异鼠李素 Isorhamnetin
姜糖脂B Gingerglycolipid B +HCOOH 1	1-CQA 3	矢车菊素+3Glc+salicylacyl
12-OPDA	Sucrose+Caffeoyl 2	二氢槲皮素+ Glc 4
异东莨菪内酯	3,4-diCQA+Glc	芍药花青素+2Glc+Feruoyl 1
SA	3,4-diCQA	山奈素+3Glc+Rha+salicylacyl
鸟苷guanosine	Sucrose+Caffeoyl 3	羟基槲皮素+4 Glc 1
姜糖脂B Gingerglycolipid B +HCOOH 2	3C,5FCQA	木犀草素+3Glc+Caffeoyl 3
ABA	1-O-feruloyl-β-D-glucose-O-glucose +s	羟基槲皮素+4 Glc 2
麦芽五糖Maltopentaose	Sucrose+2Caffeoyl 3	木犀草素+3Glc+ 2Caffeoyl
CA	水杨酸酰基奎宁酸+ cafferoyl 3	木犀草素+3Glc+Caffeoyl 1
烟酸nicotinic（Nicotinic acid）	水杨酸酰基奎宁酸+ cafferoyl 4	山奈素+3Glc+Caffeoyl+Feruoyl
阿魏酸 Ferulic Acid	1-pCoQA+Feryoyl 4	芍药花青素+2Glc+Caffeoyl 3
FFA 18:2-2O	3,4-diCQA+Rha	山奈素+3Glc+Cafferoyl 1
LPC 18:0	3F,5CQA	Methylquercetin+2Glu 1
LPE 16:0	Ferulic acid O-hexoside	木犀草素+4Glc+GlcUA
LPE 18:3 1	Sucrose+Caffeoyl 4	木犀草素+ 4 Glc + salicylacyl
LPE 20:3 1	水杨酸酰基奎宁酸+ Coumaroyl 1	槲皮素+3Glc 3
LPC 18:3	1-pCoQA+Feryoyl 5	芹菜素+ 4 Glc + salicylacyl
LPE 20:2 1	3C,4FQA+Glc	槲皮素+3Glc++salicylacyl
LPE 18:2 1	水杨酸酰基奎宁酸+ cafferoyl 2	芍药花青素+Glc 2
LPE 18:0	Sucrose+2Caffeoyl 1	槲皮素+3Glc 2
FFA 18:1-2O	1-pCoQA+Feryoyl 3	槲皮素+2Glc
LPE 20:0	1-pCoQA+Feryoyl 2	芍药花青素+3Glc+salicylacyl
LPC 16:0	5-pCoQA	二氢槲皮素+ 3Glc + Feruoyl
FFA 18:3	3,4-diCQA+Caffeoyl 1	槲皮素+3Glc 1
LPE 20:3 2	Sucrose+2Caffeoyl 4	羟基槲皮素+3 Glc
LPE 18:2 2	1-CQA+Coumaroyl 4	山奈素+3Glc+Feruoyl 1
FFA 16:0	1-CQA+Coumaroyl 2	芍药花青素+3Glc+Rha+GlcUA
FFA 18:2	3,4-diCQA+Caffeoyl 2	矢车菊素+2Glc+Xyl+2Caffeoyl 1
FFA 18:1	3,4-diCQA+Glc+Feruoyl	芍药花青素+2Glc+Caffeoyl 1
LPE 18:3 2	1-CQA+Coumaroyl 1	山萘素+3Glc+Cafferoyl 2
FFA 18:3-O	5-FQA+Feruoyl 3	二氢槲皮素+ Glc 5
1-CQA 1	1-O-feruloyl-β-D-glucose	芍药花青素+Glc 1
5-FQA+salicylacyl 2	水杨酸酰基奎宁酸+ cafferoyl 1	木犀草素+2Glc+Rha+2Caffeoyl 1
5-FQA+Feruoyl 2	水杨酸酰基奎宁酸+ Coumaroyl 2	芍药花青素+3Caffeoyl +Rha+Feruo
1-CQA 2	1-CQA 5	山奈素+3Glc+Feruoyl 2
5-CQA	3C,4FQA+Caffeoyl 1	芍药花青素+2Glc+Rha+Caffeoyl
3,4-diCQA-去乙酰基+3,4-diCQA	槲皮素+4Glc	羟基槲皮素+3 Glc+GlcUA 2
5-FQA+Feruoyl 1	羟基槲皮素+5 Glc	矢车菊素+2Glc+Xyl+2Caffeoyl 2
4,5-diCQA	山奈素+4Glc+salicylacyl 1	二氢槲皮素+ 3Glc
4-FQA	山萘素+3Glc+2Caffeoyl	山萘素+3Glc+Cafferoyl 4
3,5-diCQA	矢车菊素+3Glc+Caffeoyl 2	山奈素+4Glc+salicylacylc2
4-FQA+Glc+Caffeoyl	山奈素+3Glc+Cafferoyl 3	芍药花青素+2Glc+Caffeoyl 2

备注：JA为茉莉酸，JA-Lie为茉莉酸异亮氨酸，12-OPDA为12-Oxo phytodienoic acid，SA为水杨酸，ABA为脱落酸，CA为肉桂酸，CQA为咖啡酰奎宁酸，FQA为魏酰奎宁酸，Salicylacyl为水杨酸酰基，pCoQA ，pCo或Coumaroyl为香豆酰奎宁酸，DiCQA 双咖啡酰奎宁酸，Feruoyl 或F为阿魏酰基，Caffeoyl 或C为咖啡酰基，Sucrose为蔗糖，Rha为鼠李糖，Ferulic acid 阿魏酸，Glc 为葡萄糖，GlcUA为葡萄糖醛酸。

SCIEX ZenoTOF™ 7600系统中两种裂解技术产生碎片的互补性研究

Two different activated dissociation techniques provide complementary and information rich for structure elucidation based on SCIEX ZenoTOF™ 7600 system

刘婷[1]；郭立海[1]

[1] *Sciex 中国应用部*

CAD (Collision-activated dissociation, 碰撞活化解离)技术 是LC-MS/MS（液质联用质谱）常用的碎片裂解模式；这种传统的裂解技术是一种接近热力学平衡条件下的解离技术，断裂位点主要是对化合物的弱键进行断裂；其局限性表现在无法获得更多的结构诊断离子。EAD（Electron activated dissociation， 电子活化解离）技术通常能提供与CAD互补的碎片信息，该技术远离热力学平衡，是一种电子自由基的解离技术，可以对化合物进行选键裂解。

SCIEX ZenoTOF 7600 系统（简称7600系统）标配CAD和EAD两种裂解技术； 不同于其他商用的、具有EAD碎裂功能的质谱，7600系统的EAD碎裂，因为其电子能量可调，其碎裂模式随着电子能量的不同，可分为ECD（Electron Capture Dissociation,电子捕获解离）碎裂（0-5 eV）、Hot ECD（Hot Electron Capture Dissociation, 活跃电子捕获解离）(5-10 eV) 碎裂和EIEIO（Electron impact excitation of ions from organics，电子碰撞的激发离子）(>10eV) 三种碎裂方式，分别应用于肽段和蛋白解析，蛋白翻译后修饰和二硫键解析，单电荷小分子结构解析。正因如此，7600系统的EAD碎裂覆盖了大分子到小分子的全方位解决方案（图1）。

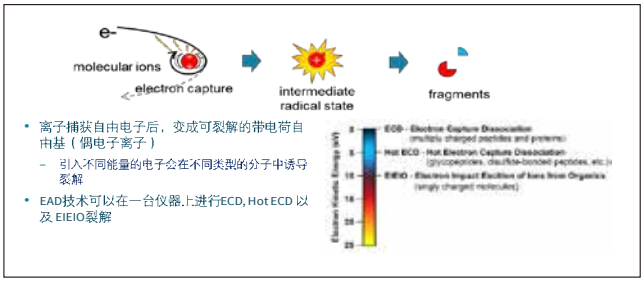

图1. EAD碰撞原理和EAD在不同电子能量下的应用范围

7600系统的EAD碎裂原理和应用研究，已有材料报道[1-5]。本文将就EAD与CAD碎裂的互补性， EAD和EI（Electron ionization, 电子电离）碎裂的相似性等方面进行阐述，以便更加了解EAD的碎裂方式，更好地应用该技术。

Zeno TOF 7600系统 EAD技术特点

- 电子能量可调，可覆盖大分子到小分子应用；
- 与CAD碎裂技术有良好互补性，加强化合物结构解析；
- 结合7600系统的Zeno™ Trap（Zeno 阱）的富集功能， 提供高质量的EAD MS/MS谱图；
- 使用方便，不需要任何额外试剂；

液相和质谱条件

柱上上样量0.1 ng 利血平；液相条件和质谱源参数见表1；分别采集CAD MS/MS谱图和EAD MS/MS 谱图；CAD模式下，CE (Collision energy，轰击能量) 为45 eV；EAD 模式下Current beam（电流束）设定为3500 V；KE（Kinetic energy，电子能量）为14 eV;

EAD 碎片 与CAD碎片的互补性

对比EAD MS/MS和CAD MS/MS谱图，碎片离子存在差异，且有明显互补性。从图2中可以看出，EAD模式下，可获得了很多CAD无法获得的碎片信息，如：m/z 251.1176， m/z 381.1814, m/z 414.2135, m/z550.2637, m/z594.2564。其中碎片m/z 414.2135是母离子断裂m/z 195.0682后产生的另一个碎片，在CAD碎裂模式中，这个碎片无法发现，但在EAD模式下，却很明显。

RUO-MKT-02-14197-ZH-A

表1. 液相条件和质谱源参数

液相条件		质谱参数	
流动相A相：	水	气体1（Gas1）, 气体2（Gas2）	55 psi, 55 psi
流动相B 相:	异丙醇	离子源温度(Tem)	600 ℃
色谱柱：	Phenomen Kenetic C18 30×2.1, 2.6 µm	喷雾电压（SV）	5500 V
柱温：	40 ℃	去簇电压（DP）	50 V

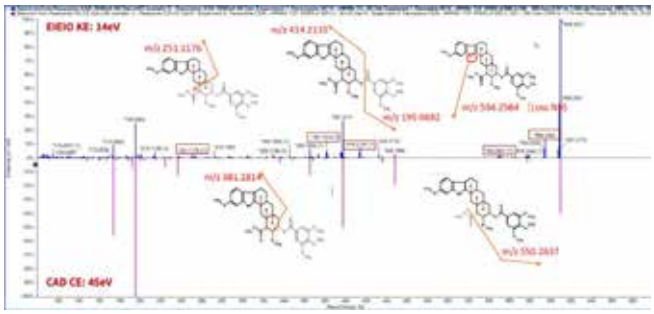

图2. EAD (KE 14eV）MS/MS谱图（上图）和CAD（CE 45eV）MS/MS谱图（下图），差异碎片使用红框表示，使用SCIEX OS软件解析EAD断裂位点

EAD碎片和EI碎片的相似性

EI碎裂是GC-MS（气相质谱）中常见的碎裂模式。在实验中，我们发现利血平的EAD碎片和EI碎片有一定的相似性，这可能与他们在原理上，都是使用电子和小分子作用有关系。

查询HMDB（human metabolome database，人类代谢组学数据库），获得利血平EI 图谱（https://hmdb.ca/spectra/c_ms/100080），导出该谱图为text文本，获得碎片m/z和intensity%（百分比强度）表格。再分别导出EAD和CAD的主要碎片m/z和intensity%表格。将EI谱图中强度<1%的碎片离子过滤掉，再观察其他EI碎片是否分别在EAD和CAD谱图中存在，获得表2。从表2中，可以发现：在EAD 模式下，可获得区别于CAD的特有碎片，和EI碎裂模式下获得的碎片很相似（图3）。 这可以从一个侧面说明EAD碎裂原理和EI碎裂可能有某种相似性，因为EI碎裂原理较为成熟，也许为我们解析EAD碎裂方式提供了一种有效途径。

表2. GC-MS-EI模式下获得的主要碎片，在LC-MS/MS-EAD碎裂模式下，大概率也被发现；

m/z	GC-MS-EI Intensity%	LC-MS/MS-EAD Intensity%	LC-MS/MS-CAD Intensity%
195	100.0	25.0	100.0
251	38.0	1.7	NF
265	15.0	NF	NF
381	25.0	3.0	NF
397	25.0	10.5	53.0
414	20.0	2.7	NF
593	10.0	3.8	NF

结论

- EAD碎裂和CAD碎裂具有互补性；在应用中，多种碎裂模式对结构的解析更具有优势；
- 该实验提示：EAD碎裂和EI碎裂获得的碎片，具有一定的相似性；

RUO-MKT-02-14197-ZH-A

参考文献

1. 贾伟，应万涛，钱小红. (2007) 另辟蹊径 —— 串联质谱肽段断裂的新军“电子捕获解离”. 质谱学报，2007. Vol 18. No. 1 : 55-64.
2. 石磊，刘淑莹. (2011) 电子捕获解离技术在生物质谱中的作用. 化学进展，2011. Vol 28. No. 8: 1710-1718
3. Complete structural elucidation of lipids in a single experiment using electron activated dissociation (EAD). SCIEX technical note, RUO-MKT-02-13050-ZH-B.
4. Tunable electron activated dissociation (EAD) MS/MS to preserve particularly labile post-translational modifications. SCIEX technical note, RUO-MKT-02-13006-ZH-B.
5. Comprehensive peptide mapping of biopharmaceuticals utilizing electron activated dissociation (EAD). SCIEX technical note, RUO-MKT-02-12639-ZH-B.

RUO-MKT-02-14197-ZH-A

Quantitative analysis and structural characterization of bile acids using the ZenoTOF 7600 system

Paul RS Baker[1], Robert Proos[1], Maxim D Seferovic[2] and Thomas D. Horvath[3,4]

[1]SCIEX, USA; [2] Dept of Obstetrics and Gynecology, Baylor College of Medicine, Houston, TX; [3]Dept of Pathology, Texas Children's Hospital, Houston, TX; [4]Dept of Pathology & Immunology, Baylor College of Medicine, Houston, TX

This technical note demonstrates the power and capability of the ZenoTOF 7600 hybrid time-of-flight mass spectrometry (TOFMS) system to sensitively detect, quantify, and structurally characterize the bile acid content of biological specimens. Analysis of bile acids by nominal mass instruments, such as triple-quadrupole MS (TQMS) systems, is challenging because of the high chemical background found in several precursor ions to precursor ion-based multiple-reaction monitoring (MRM) transitions used in current state-of-the-art assays (1-4). High-resolution mass spectrometry (HRMS) generates a full product ion spectrum for each targeted bile acid, and extracting fragment ions with a narrow mass-to-charge (*m/z*) window can reduce background chemical interferences and improve the signal-to-noise (S/N) of the assay. The detection of individual bile acid isomers currently depends on chromatographic resolution; collision-induced dissociation (CID)-based fragmentation cannot distinguish these isomeric metabolites. Electron-activated dissociation (EAD; 5-7) is a complementary fragmentation mode to CID that can provide structurally diagnostic fragment ions to differentiate bile acid isomers (**Figure 1)**.

Herein, the ZenoTOF 7600 system was used to quantify the bile acid content of human plasma sample extracts with a sensitivity comparable to that of high-end TQMS systems. Furthermore, the EAD-based fragmentation generated several structurally diagnostic fragment ions that are capable of distinguishing between the bile acid isomers. These data demonstrate the capability of the ZenoTOF 7600 system to perform highly sensitive and selective analysis of endogenous bile acid content in human plasma.

Key features of bile acid analysis on the ZenoTOF 7600 system

- The ZenoTOF 7600 system can detect and quantify bile acids with a sensitivity comparable to that of high-end TQMS instruments
- The narrow fragment ion extraction window possible with HRMS improves assay sensitivity by reducing background chemical interferences and, consequently, increases the S/N of the assay
- EAD can generate diagnostic fragment ions to enable the distinction between bile acid isomers, which improves the overall specificity of the analysis

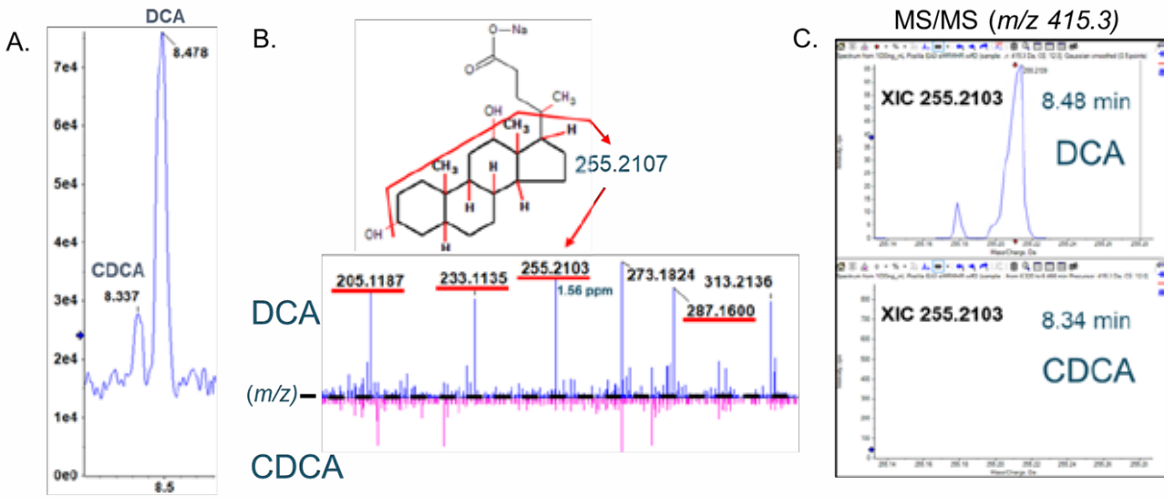

Figure 1. Bile acid isomer structural characterization by electron-activated dissociation (EAD). Bile acids have multiple structural isomers per each subclass. Deoxycholic acid (DCA), chenodeoxycholic acid (CDCA), and ursodeoxycholic acid (UDCA) have the same empirical formula and exact mass, but they differ structurally with the position and/or stereochemistry of their hydroxyl functional groups. **(A)** The TOFMS total ion chromatogram (TIC) for *m/z* 415.3 (DCA sodium adduct) shows the importance of chromatography to resolve bile acid isomers. **(B)** The EAD MS/MS spectra for DCA+Na and CDCA+Na are presented in an inverted overlay. Underlined in red are EAD-based fragments unique to DCA+Na; the proposed fragmentation of the DCA+Na fragment with m/z 255.2107 is shown on the DCA+Na structure. **(C)** The DCA+Na-specific fragment at *m/z* 255.2107 shows no interference in the XIC for chromatographically resolved CDCA+Na. These data suggest EAD fragmentation may be used instead of chromatographic systems with long gradients to distinguish bile acid isomers.

MKT-30747-B

Introduction

Primary bile acids are cholesterol-derived molecules that are synthesized in the liver and are collected and pre-concentrated in the bile contained in the gall bladder (8). During gastric emptying, bile is secreted into the duodenum via the common bile duct, where bile acids play a crucial role in emulsifying and absorbing dietary fats (8,9). The two primary bile acids, cholic acid (CA) and chenodeoxycholic acid (CDCA) are bioconverted into chemically distinct, bacterially produced secondary bile acids and an expanding list of microbially-conjugated bile acids (MCBAs) by host microbiota (10-16). Of considerable recent interest is the potential role of these bacterial-derived secondary bile acids in human physiology and their contributions to pathologies such as inflammatory bowel disease and cancer. Consequently, there is great interest in identifying and quantifying these compounds in diverse samples.

Multiple methods for bile acid analysis have been reported in the literature (1-4). These methods are typically TQMS-based, and their effectiveness highly depends on sample prep, instrument sensitivity, and chromatography to deliver high-quality bioanalytical results. One common drawback of these published methods is that they often use the negative ion mode. At the mass range of interest (~400-500 Da), there is considerable isobaric chemical interference from the matrix and the mobile phase solvents, depending on their source. This is especially problematic for low-resolution TQMS instruments (Rs ~100-150 equating to ±0.1 Da mass error). HRMS offers a potential solution to this problem due to its high mass accuracy and high resolution. Fragment ions can be extracted from a high-resolution MS/MS spectrum using a narrow *m/z* tolerance window (~ 20 mDa), which may exclude many isobaric interferences that cause the high background in TQMS instruments. The ZenoTOF 7600 system can acquire data in this mass range with a mass accuracy of ± 2ppm and a resolution of >35K.

Bile acids are cholesterol-derived amphipathic molecules of saturated hydroxylated C-24 sterols. As shown in **Figure 2**, the location and stereochemistry of the hydroxyl functional groups define the different isomers within each sub-class. CID-based fragmentation of bile acids primarily yields product ions related to the bile acid head group, and relatively few fragments are generated from the ring structure; hence, CID alone does not generate diagnostically useful fragment ions for identification or quantification purposes. Using chromatography to resolve bile acid isomers requires relatively long chromatographic gradients, which are not conducive to high-throughput analysis. An alternative to lengthy chromatographic gradients and CID-based fragmentation is EAD. EAD-based fragmentation provides ample fragments derived from the sterol ring structure (**Figure 1A & 1B)**, and it can distinguish the isomers of each bile acid subclass without extensive chromatographic method development.

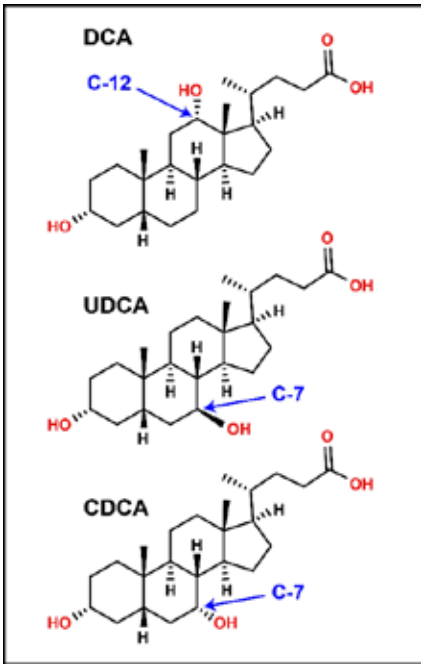

Figure 2. The deoxycholic acid sub-class of bile acids. Bile acids are cholesterol-derived amphipathic molecules of saturated hydroxylated C-24 sterols. DCA has a hydroxyl moiety at carbon 12 (C-12) whereas UDCA and CDCA are hydroxylated at carbon-7 (C-7). The latter two isomers are characterized by a different stereochemistry at the number 7 carbon.

The ZenoTOF 7600 system has an EAD cell that provides complimentary fragmentation that can be activated and scheduled within a typical quantitative bioanalytical method to provide structural characterization of bile acids. In this technical note, the speed and sensitivity of the ZenoTOF 7600 system were leveraged to quantify bile acids in prepared plasma samples. These results were compared to those acquired on the QTRAP 7500 instrument. To demonstrate the power of EAD for structural characterization, the DCA sub-class was structurally characterized to identify EAD-specific fragments for each isomer.

Methods

Materials: Bile acid standard mixtures were purchased from Cambridge Isotopes Laboratories. The stable isotope-labeled bile acid mixes (unconjugated, cat# MSK-BA1; conjugated, MSK-BA2) were used as internal standards, and unlabeled bile acid mixes (unconjugated, cat# MSK-BA1-US; conjugated, MSK-BA2-US) were used as primary reference standards. All solvents were LCMS grade and obtained from Burdick and Jackson and Fisher Scientific.

Sample preparation: Human blood (research use only) was collected into tubes containing potassium ethylenediamine tetraacetic acid (K_2EDTA) anti-coagulant following the procedure outlined in the institutional review board (IRB) protocol #_____. The

Table 1: Chromatographic gradient (flow rate = 0.30 mL/min)

Time (min)	Mobile phase A (%)	Mobile Phase B (%)
0.0	75	25
1.5	75	25
13	20	80
14.5	20	80
14.6	75	25
17	75	25

plasma was isolated from the red blood cell fraction by centrifugation. A 50 µL volume of each plasma sample was pipetted into individual 0.6 mL Eppendorf tubes, and a 200 µL volume of methanol was added to precipitate plasma proteins (primary DF=5-fold). All samples were vortex-mixed for 30 seconds and centrifuged at 17,000*g* for 5 minutes, and the supernatant for each clarified plasma extract sample was transferred into fresh vials.

A 50 µL volume of each clarified plasma extract sample was transferred into fresh glass vials. A 450 µL volume of an internal standard solution (10 nM deuterated BAs) was added to each sample vial (DF=50-fold overall), and the vials were capped and vortex-mixed for 30 seconds. The final volume of each sample was split into two identically labeled glass autosampler vials (w/ inserts), with each set being injected on the QTRAP 7500 and the ZenoTOF 7600, respectively.

Chromatography: Extracted metabolites were resolved using two different HPLC systems. For the ZenoTOF 7600-based system, an Exion UHPLC instrument equipped with a Phenomenex Kinetex XB-C18 column (100 x 2.1 mm; 2.6 µm particle size) was used. For the QTRAP 7500 TQMS-based system, a Nexera 40 Series UHPLC system equipped with a Restek Raptor C18 column (100 x 2.1 mm; 5.0 µm particle size) and an Ultra C18 guard column (10 x 2.1 mm i.d., 5 µm; Restek) was used. The two different columns produced similar but not identical chromatographic elution profiles. Notably, both columns entirely resolved the multiple bile acid isomers. The autosampler sample bay was maintained at 10 °C for both systems, and a 15 µL sample volume was injected on column. The column oven temperature was kept at 50°C with a constant mobile phase flow rate of 0.3 mL/min for a total run time of 17 min. The mobile phase compositions were (A) 10 mM ammonium formate in water and (B) pure acetonitrile. Gradient details are shown in **Table 1**

Mass spectrometry: Extracted sample extracts were analyzed using the ZenoTOF 7600 system with an OptiFlow Turbo V ion source and a QTrap 7500 system with an OptiFlow Pro Turbo V ion source using

Table 2: ZenoTOF 7600 and QTRAP 7500 systems source and method parameter settings

Parameter	ZenoTOF 7600 system	QTRAP 7500 instrument
Curtain gas (CUR)	35	40
Ion source gas 1 (GS1)	60	35
Ion source gas 2 (GS2)	80	70
CAD Gas (CAD)	7	9
Source temperature (TEM)	250 °C	500 °C
Ion spray voltage (IS)	-4500 V/+5000V (CID/ EAD)	-2000 V
Declustering Potential (DP)	-80 V/+80V (CID/EAD)	N/A
CID Accumulation/dwell time	Variable ($sMRM^{HR}$)	Variable (sMRM)
CID Collision energy (CE)	Molecule-dependent	Molecule-dependent
Q1/Q3 Mass Resolution	N/A	Unit/Unit
EAD Accumulation/dwell time	40 ms	N/A
CE for TOF MS	-10 V/+10V (CID/EAD)	N/A
TOF MS mass range	70-1000 Da	N/A
TOF MS/MS mass range	40-400 Da	N/A
Time bins to sum	6	N/A
EAD Collision energy (CE)	12 V	N/A
Electron kinetic energy (KE)	13 eV	N/A
Zeno pulsing for MS/MS	Yes	N/A
Zeno threshold	20000	N/A

Table 3: ZenoTOF 7600 and QTRAP 7500 systems compound parameter settings

	ZenoTOF 7600 System			QTRAP 7500 System	
Bile acid	RT (min)	DP	CE	RT (min)	CE
LCA	11.9	-80	-5	10.7	-23
UDCA	7.4	-80	-5	6.2	-23
CDCA	9.0	-50	-5	7.9	-24
DCA	9.3	-40	-49	8.1	-47
CA	7.1	-40	-49	5.9	-47
GLCA	9.6	-80	-48	6.7	-46
GUDCA	5.6	-80	-82	3.6	-76
GCDCA	7.15	-80	-82	5.1	-80
GDCA	7.4	-80	-82	5.4	-80
GCA	5.7	-150	-48	3.9	-46
TLCA	7.4	-80	-137	6.6	-135
TUDCA	4.5	-80	-142	3.8	-145
TCDCA	5.8	-80	-142	5.2	-145
TDCA	6	-80	-142	5.4	-136
TCA	4.7	-190	-66	4.1	-64

Table 4. Bile acid standards. Mixtures of labeled and unlabelled bile acids were obtained from Cambridge Isotopes Laboratories. Bile acids were analyzed in the negative ion mode, targeting the [M – H]- ions for quantitation. For qualitative analysis of bile acids using EAD, the $[M+Na]^+$ ion was used. In cases where the precursor and the product ion were the same in the $sMRM^{HR}$ transition, the TOFMS spectrum was used for quantitation.

Bile Acid	Molecular formula	Abbreviation	[M - H]-	$[M - H]^-$ Product ion	$[M + Na]^+$
Lithocholic Acid	C24H40O3	**LCA**	375.290	375.290	399.288
D4-Lithocholic Acid	C24H36[2H]4O3	**D4-LCA**	379.316	379.316	403.313
Ursodeoxycholic Acid	C24H40O4	**UDCA**	391.285	391.285	415.283
D4-Ursodeoxycholic Acid	C24H36[2H]4O4	**D4-UDCA**	395.310	395.310	419.308
Chenodeoxycholic Acid	C24H40O4	**CDCA**	391.285	391.285	415.283
D4-Chenodeoxycholic Acid	C24H36[2H]4O4	**D4-CDCA**	395.310	395.310	419.308
Deoxycholic Acid	C24H40O4	**DCA**	391.285	391.285	415.283
D4-Deoxycholic Acid	C24H36[2H]4O4	**D4-DCA**	395.310	395.310	419.308
Cholic Acid	C24H40O5	**CA**	407.280	343.266	431.278
D4-Cholic Acid	C24H36[2H]4O5	**D4-CA**	411.305	411.305	435.303
Glycolithocholic Acid	C26H43NO4	**GLCA**	432.312	388.324	456.309
D4-Glycolithocholic Acid	C26H39[2H]4NO4	**D4-GLCA**	436.337	392.349	460.335
Glycoursodeoxycholic Acid	C26H43NO5	**GUDCA**	448.307	74.025	472.304
D4-Glycoursodeoxycholic Acid	C26H39[2H]4NO5	**D4-GUDCA**	452.332	74.025	476.329
Glycochenodeoxycholic Acid	C26H43NO5	**GCDCA**	448.307	74.025	472.304
D4-Glycochenodeoxycholic Acid	C26H39[2H]4NO5	**D4-GCDCA**	452.332	74.025	476.329
Glycodeoxycholic Acid	C26H43NO5	**GDCA**	448.307	74.025	472.304
D4-Glycodeoxycholic Acid	C26H39[2H]4NO5	**D4-GDCA**	452.332	74.025	476.329
Glycocholic Acid	C26H43NO6	**GCA**	464.302	402.302	488.299
D4-Glycocholic Acid	C26H39[2H]4NO6	**D4-GCA**	468.327	406.331	492.324
Taurolithocholic Acid	C26H45NO5S	**TLCA**	482.295	79.958	506.292
D4-Taurolithocholic Acid	C26H41[2H]4NO5S	**D4-TLCA**	486.320	79.958	510.317
Tauroursodeoxycholic Acid	C26H45NO6S	**TUDCA**	498.289	79.958	522.287
D4-Tauroursodeoxycholic Acid	C26H41[2H]4NO6S	**D4-TUDCA**	502.315	79.958	526.312
Taurochenodeoxycholic Acid	C26H45NO6S	**TCDCA**	498.289	79.958	522.287
D4-Taurochenodeoxycholic Acid	C26H41[2H]4NO6S	**D4-TCDCA**	502.315	79.958	526.312
Taurodeoxycholic Acid	C26H45NO6S	**TDCA**	498.289	79.958	522.287
D4-Taurodeoxycholic Acid	C26H41[2H]4NO6S	**D4-TDCA**	502.315	79.958	526.312
Taurocholic Acid	C26H45NO7S	**TCA**	514.284	124.008	538.282
D4-Taurocholic Acid	C26H41[2H]4NO7S	**D4-TCA**	518.310	124.007	542.307

A scheduled, high-resolution multiple reaction monitoring ($sMRM^{HR}$) or a scheduled multiple reaction monitoring (sMRM) scan mode, respectively. In some cases, a pseudo-MRM transition was used (i.e., precursor ion to precursor ion). On the QTRAP 7500 system, these molecules were quantitated at the MS/MS level with low CE. However, for the data acquired for these bile acids on the ZenoTOF 7600 system, the TOFMS data were used.

To structurally characterize bile acids, an MRM-triggered data-dependent acquisition (DDA) scan mode was used to acquire EAD-based product ion spectra in the positive ion mode (standards only). Although EAD-based fragmentation is possible in the negative ion mode, it is relatively inefficient compared to the positive ion mode; consequently, the EAD-based analysis was performed in the positive ion mode. Because bile acids are anionic, the sodium adduct for each

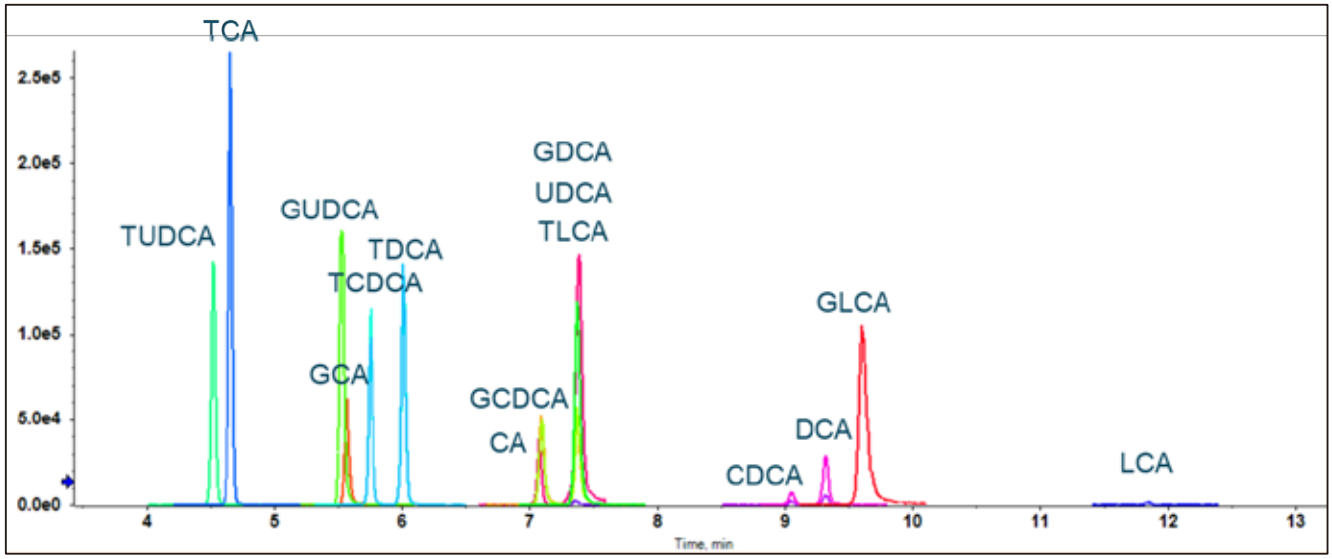

Figure 3. Chromatographic resolution of bile acids. Bile acid standards were analyzed using the ZenoTOF 7600 instrument. Chromatography was designed to separate bile acid isomers (e.g., DCA, UDCA, and CDCA) with baseline resolution.

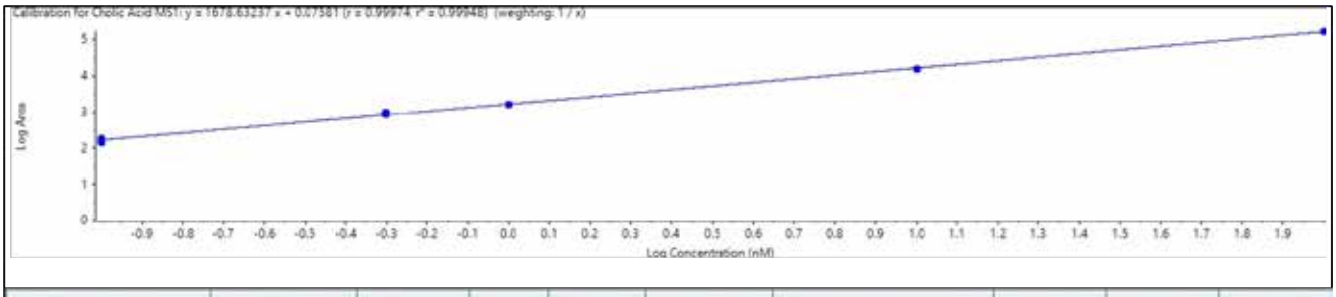

Component Name	Actual Concentration	Num. Values	Mean	Standard De...	Percent CV	Average Accuracy across Replicates	Value #1	Value #2	Value #3
Cholic Acid MS1	0.10	3 of 3	9.752e-2	1.297e-2	13.30	97.52	1.101e-1	8.423e-2	9.818e-2
Cholic Acid MS1	0.50	3 of 3	5.494e-1	3.442e-2	6.26	109.89	5.442e-1	5.862e-1	5.180e-1
Cholic Acid MS1	1.00	3 of 3	9.848e-1	1.668e-2	1.69	98.48	9.689e-1	9.834e-1	1.002e0
Cholic Acid MS1	10.00	3 of 3	9.350e0	1.985e-1	2.12	93.50	9.184e0	9.295e0	9.570e0
Cholic Acid MS1	100.00	3 of 3	1.006e2	3.304e-1	0.33	100.62	1.003e2	1.005e2	1.010e2

Figure 4. Standard curve for cholic acid (CA). The detection of CA was linear over a 4 orders of magnitude concentration range, with a LOQ calculated to be 0.613 nM in a neat internal standard curve preparation.

was monitored and isolated for fragmentation. A summary of the MS instrument parameters is presented in **Tables 2 and 3**, and a comprehensive list of the compounds studied is shown in **Table 4**.

Data processing: All data were processed using SCIEX OS software. The Analytics module was used for quantitation, and the Explore module was used to structurally characterize bile acids from EAD-based MS/MS spectra. Limits of detection (LOD) and of quantitation (LOQ) estimates were calculated using the standard deviation of the y-intercepts and the mean slope of the 3 (ZenoTOF 7600 system) or 4 (QTRAP 7500 instrument) calibration curves calculated for each analyte as the previously described in the ICH harmonized tripartite guideline (17). The internal standard concentration (9 nM) was included in the linear regression calculations performed using SCIEX OS; consequently, the LOQ and LOD equations were modified to the following formats:

$$LOD = [BA](nM_{BA}) = [D_x - BA]\left(nM_{D_x-BA}\right)\frac{3.3 * \sigma_{y-intercept}}{\bar{m}}$$

$$LOQ = [BA](nM_{BA}) = [D_x - BA]\left(nM_{D_x-BA}\right)\frac{10 * \sigma_{y-intercept}}{\bar{m}}$$

Where [BA]=the bile acid concentration with units of nM_{BA}; [D_x-BA]= IS concentration with units of $nM_{Dx\text{-}BA}$. This correction is necessary to offset the LOQ and LOD when the [IS] is used, which otherwise would generate artifactual values when [IS] ≠ 1.

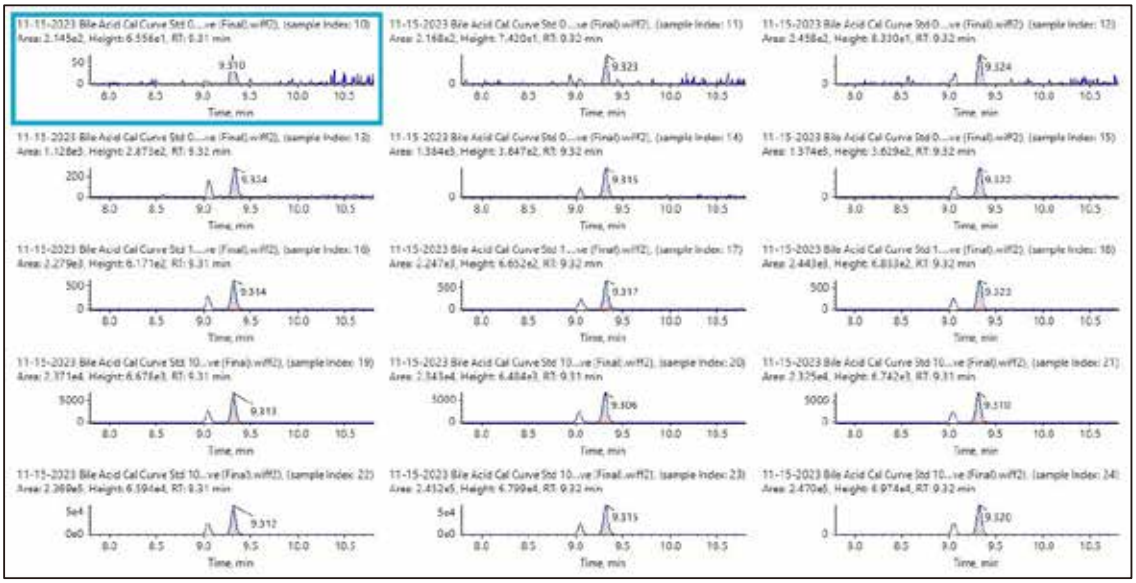

Figure 5. Standard curve chromatograms for DCA. On the ZenoTOF 7600-based LC/HRMS system, DCA eluted at 9.3 min; its isobar, CDCA, eluted at 9.1 min. Presented here are the individual runs for each standard (in triplicate, from left to right) at each concentration of the standard curve. Data were smoothed once for both presentation and integration purposes. Data for 0.01 and 0.05 nM are not shown for DCA and were not included in the standard curve calculations.

Results and Discussion

A bile acid standard curve was generated neat in solvent and analyzed on the QTRAP 7500 and the ZenoTOF 7600 systems. The parameter settings were optimized for each instrument, as detailed in Tables 2 and 3, and the chromatographic gradient conditions resulted in the separation of each isomeric bile acid with baseline resolution **(Figure 3)**. The concentrations within the internal standard curve ranged from 0.01 to 1000 nM, covering a dynamic range > 5 orders of magnitude. Due to the sensitivity of the QTRAP 7500 instrument, the 1000 nM concentration standards caused detector saturation; this was not an issue on the ZenoTOF 7600 system. Consequently, to better match the conditions on each instrument, the final standard curve calculations and subsequent *in vivo* measurements were truncated to a linear dynamic range of 0.1 to 100 nM. Due to this consideration, it is important to note that the results presented here do not necessarily reflect the maximum extent of the dynamic range capability of the instrument for the measurement of bile acids. The range tested, however, was sufficient to measure bile acids in rat plasma. An example curve acquired for cholic acid on the ZenoTOF 7600 system and its associated ion statistics are presented in **Figure 4**.

The individual chromatograms for each injection of the standard curve from 0.1 to 100 nM DCA are presented in **Figure 5.** Its isomer, CDCA, appears in the chromatogram at ~9.1 min, but the chromatographic resolution is sufficient so that there is no interference in the measurement of these two analytes. The measurement of DCA was performed at the TOFMS level rather than

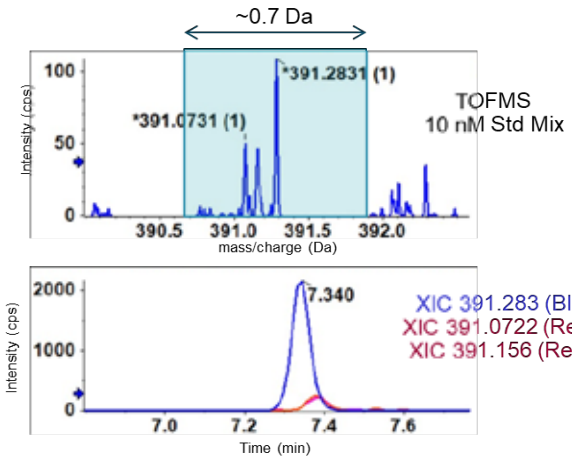

Figure 6 Benefits of a narrow XIC window with HRMS. (Top) The TOFMS mass spectrum of DCA is zoomed around its mass of 391.2854. the blue box overlaid on the spectrum represents the resolution window of a typical QTMS system. The three peaks in the spectrum would all contribute to the overall calculated concentration if analyzed at the MS1 level on the QTMS. (Bottom) Using HRMS, only the peak associated with DCA (Blue)is considered, which reduces interference and chemical background noise (Red 1 and 2). For presentation purposes, the spectral and chromatographic peaks have been smoothed.

the sMRM^{HR} level because even at very low CE values (-5 V), the precursor ion peak intensity was significantly reduced. Some collision energy is required, even in precursor ion to precursor ion transitions, because this voltage helps push ions through Q2 to the Zeno trap and the pulser (for a better understanding of the ZenoTOF 7600 system ion path, see reference 18). The power of HRMS at the MS1 level of analysis is shown in **Figure 6**. In the top spectrum, the

DCA peak is 391.2831 Da. Two potentially interfering peaks are very close to DCA, located at 391.0722 Da and 391.1560 Da, respectively. These two contaminating peaks would be included in any MS1 level analysis on a TQMS system because the isolation width of a nominal mass instrument is ~ 0.7Da, as indicated by the transparent blue box overlaid on the spectrum. These additions to DCA's total peak area calculation would affect its measurement accuracy. However, because it is possible with HRMS to extract a narrow window around the ion of interest (XIC width of 0.020 Da), these contaminants, as shown in red in the bottom chromatogram, can be excluded, and the correct peak area for DCA can be determined, which increases the overall accuracy of the assay. TQMS systems rely on analysis at the MS2 level to reduce this type of interference.

A standard curve for each analyte for each injection (triplicate injections) was generated, and the data were used to calculate the LOD and LOQ of each bile acid measured with the ZenoTOF 7600 system or the QTRAP 7500 instrument (**Table 5**). These values were computed using the standard deviation of the y-intercepts and the mean slope for each calibration curve (17) to estimate best the instruments' relative sensitivity for bile acid analysis. With the exceptions of CA, GLCA and GUDCA, the sensitivity of the ZenoTOF 7600 system is comparable to that of the QTRAP 7500 instrument. The QTRAP 7500 had an approximately 10-fold better sensitivity for the three noted exceptions. Still, the LOQs for all compounds on both systems indicate that either instrument can measure bile acids in rat

Table 5. LOD and LOQ calculations for bile acids measured on the ZenoTOF 7600 system and the QTRAP 7500 instrument

	ZenoTOF 7600 system		*QTRAP 7500 instrument*	
Bile acid	***LOD (nM)***	***LOQ (nM)***	***LOD (nM)***	***LOQ (nM)***
LCA	*0.134*	*0.405*	*0.0552*	*0.167*
UDCA	*0.047*	*0.144*	*0.0263*	*0.080*
CDCA	*0.098*	*0.297*	*0.0941*	*0.285*
DCA	*0.041*	*0.125*	*0.0184*	*0.056*
CA	*0.202*	*0.613*	*0.0279*	*0.085*
GLCA	*0.221*	*0.669*	*0.0145*	*0.044*
GUDCA	*0.044*	*0.135*	*0.0035*	*0.010*
GCDCA	*0.028*	*0.0851*	*0.0144*	*0.044*
GDCA	*0.017*	*0.0518*	*0.0182*	*0.055*
GCA	*0.069*	*0.210*	*0.0536*	*0.162*
TLCA	*0.070*	*0.211*	*0.0264*	*0.080*
TUDCA	*0.025*	*0.0743*	*0.0256*	*0.078*
TCDCA	*0.102*	*0.309*	*0.0252*	*0.076*
TDCA	*0.033*	*0.101*	*0.0107*	*0.032*
TCA	*0.084*	*0.254*	*0.0460*	*0.139*

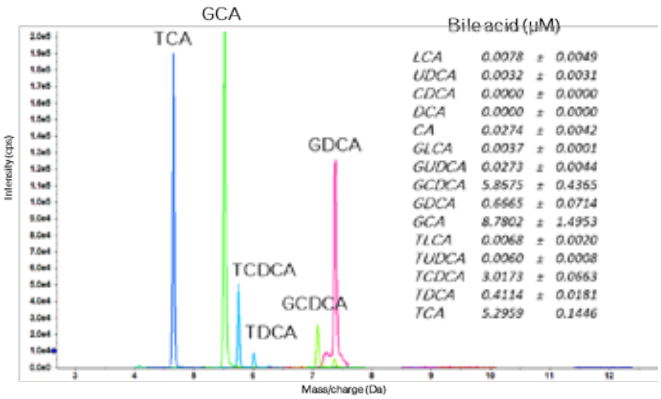

Figure 7. XIC chromatogram of bile acids in human plasma. Eleven of 15 targeted bile acids were detected in a single rat plasma sample. In the figure, the major peaks are labeled, and the concentrations (μM) of each bile acid ± the standard deviation are shown in the inset table.

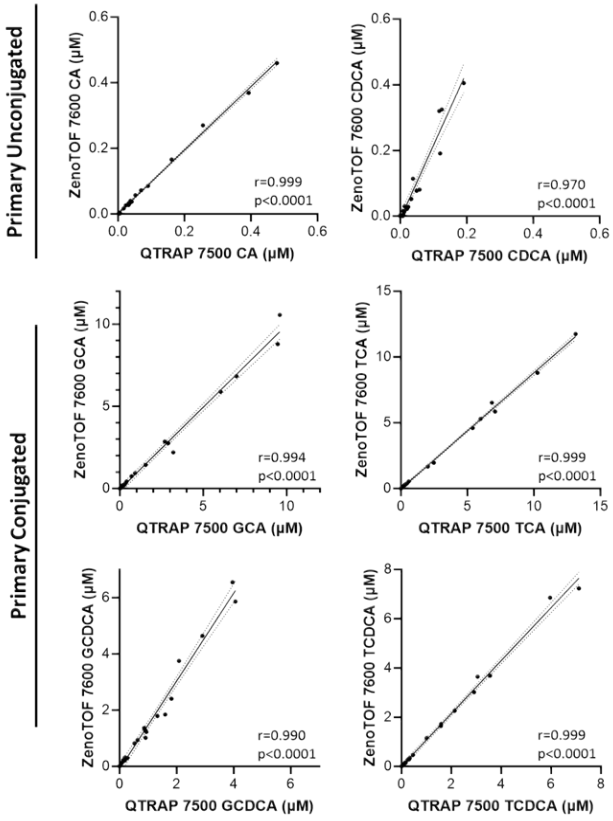

Figure 8. Pearson correlation plot. A Pearson correlation calculation was performed on the quantitative plasma data acquired using the ZenoTOF 7600 system and the QTRAP 7500 instrument. Show here are plots, for multiple primary conjugated and unconjugated bile acids. All plots show a strong linear correlation between the two differently acquired data sets indicating that these two instruments are equally capable of measuring endogenous bile acids in plasma.

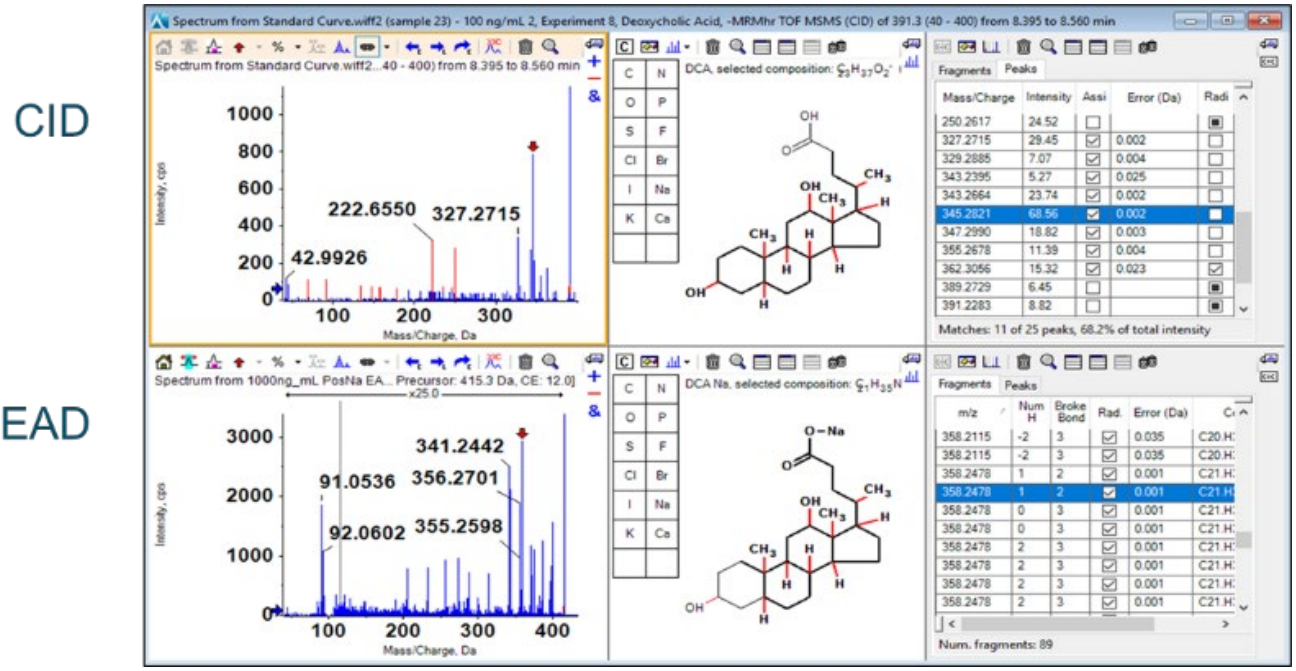

Figure 9. Product ion analysis of deoxycholic acid (DCA). A DCA standard (100 nM) was analyzed using the ZenoTOF 7600 system by CID- and EAD-based fragmentation (left panels). The middle panels show the .mol file for DCA, and the panels on the right show the theoretical fragments for CID (i.e., heterolytic fragmentation) and EAD (radical-based fragmentation). The highlighted fragment in blue corresponds to structure highlighted in bold on the middle figures and is indicated by a red arrow in the MS/MS spectra on the left.

plasma. **Figure 7** shows the XIC chromatogram for a single rat plasma extract. The concentrations of each targeted bile acid are displayed to the right of the peaks. Only the major peaks are labeled, but 11 of the 15 bile acids were detected *in vivo* using the ZenoTOF 7600 system. Similar data were obtained using the QTRAP 7500 instrument. **Figure 8** shows a Pearson correlation plot of the bile acid concentration data acquired from the plasma samples using the two different instrument types. The plots show a linear correlation between the two data sets for multiple primary conjugated and unconjugated bile acids in plasma. The r values of >0.99 and the p values <0.0001 indicate the data sets are equivalent and that both instruments are equally capable of measuring bile acids in plasma.

The EAD-based fragmentation functionality of the ZenoTOF 7600 system can provide significantly more structural details than that generated by CID-based fragmentation. **Figure 9** shows the product ion spectrum for DCA. This experiment analyzed a DCA standard (100 nM) using the ZenoTOF 7600 system by CID- and EAD-based fragmentation. The CID spectrum in the top left panel has relatively few fragments compared to the EAD-based spectrum in the bottom left panel. The middle panels show the .mol files for DCA and indicate the highlighted fragment in the right panels in bold. This feature of SCIEX OS, called fragment pane, enables the structural characterization of compounds by matching the actual MS/MS data to *in silico*-generated fragments based on the .mol file. The predicted CID fragments are shown in red in the top left panel. Note that most of these fragments are not present in the spectrum. However, all the predicted fragments appear for DCA fragmented via EAD. This ability to generate fine structural detail was extended to determine whether EAD-based fragmentation could distinguish bile acid isomers.

Figure 2 shows that DCA, CDCA, and UDCA have the same empirical formula and exact mass but differ structurally in the position and stereochemistry of their hydroxyl functional groups. **Figure 1A** shows the TOFMS total ion chromatogram (TIC) for *m/z* 415.3 (DCA sodium adduct) and the importance of chromatography in resolving bile acid isomers. Using EAD-based fragmentation, unique fragment ions were identified for DCA and CDCA, the two isomers that elute closely (**Figure 1B**). These fragments are underlined in red on the spectra. Notably, the DCA-specific fragment at *m/z* 255.2107 shows no interference in the XIC for chromatographically resolved CDCA. Thus, the *m/z* fragment at 255.2017 Da can be used as a DCA-specific fragment for sMRM^{HR} analysis and may enable a shorter gradient for higher throughput. EAD-based fragmentation may enable the complete structural characterization of these molecules without requiring purification or other structural diagnostic tools. More importantly, this type of fragmentation may help identify novel conjugated bile acids (10-15). For example, Quinn et al. recently reported the discovery of several new MCBAs (specifically phenylalanocholic acid (Phe-CA), tyrosocholic acid (Tyr-CA), and leucocholic acid (Leu-CA)) that were discovered in the intestinal contents collected from mice (11). Another study found evidence of

MKT-30747-B

the amino acids glutamate, glutamine, aspartate, asparagine, methionine, histidine, lysine, serine, tryptophan, valine, alanine, and arginine forming conjugates with CDCA, DCA, or CA (12). Considering the emerging importance of MCBAs in human disease (19-20) and the critical role of mass spectrometry in their characterization (21), the quantitative sensitivity and qualitative capabilities of the ZenoTOF 7600 may prove invaluable to the growth of bile acid metabolism research.

Conclusions

- **The specific method details are provided for the analysis of endogenous bile acids using the ZenoTOF 7600 system and the QTRAP 7500 instrument**
- **The ZenoTOF 7600 system is capable of measuring endogenous bile acids with comparable sensitivity to the QTRAP 7500 system**
- **The narrow XIC window possible on HRMS systems enables the MS1-based collection of data without the inclusion of chemical background interferences**
- **EAD-based fragmentation provides structural characterization of molecules and may abrogate the need for extensive chromatographic separation of isomers to ensure specificity**

References

1. Liu D, Li G, Liu D, Shi W, Wang H, Zhang Q, Shen M, Huang X, Lin H. *Quantitative Detection of 15 Serum Bile Acid Metabolic Products by LC/MS/MS in the Diagnosis of Primary Biliary Cholangitis.* Chem Biodivers. 2023; Mar;20(3):e202200720. doi: 10.1002/cbdv.202200720
2. Gao T, Hu S, Xu W, Wang Z, Guo T, Chen F, Ma Y, Zhu L, Chen F, Wang X, Zhou J, Lv Z, Lu L. *Targeted LC-MS/MS profiling of bile acids reveals primary/secondary bile acid ratio as a novel biomarker for necrotizing enterocolitis.* Anal Bioanal Chem. 2024; Jan;416(1):287-297. doi: 10.1007/s00216-023-05017-7
3. Yang J, Lin J, Wang A, Yang X, Wang Y, Zhang Y, Dong H, Tian Y, Zhang Z, Wang M, Song R. *Study on the effect of calibration standards prepared with different matrices on the accuracy of bile acid quantification using LC-MS/MS.* J Pharm Biomed Anal. 2024; 237:115785. doi: 10.1016/j.jpba.2023.115785.
4. Engevik MA, Thapa S, Lillie IM, Yacyshyn MB, Yacyshyn B, Percy AJ, Chace D, Horvath TD. *Repurposing dried blood spot device technology to examine bile acid profiles in human dried fecal spot samples.* Am J Physiol Gastrointest Liver Physiol. 2024; 326:G95–G106. Doi: 10.1152/ajpgi.00188.2023
5. Baba T, Campbell JL, Le Blanc JCY, Baker PRS, Hager JW, Thomson BA. *Development of a Branched Radio-Frequency Ion Trap for Electron Based Dissociation and Related Applications.* Mass Spectrom (Tokyo). 2017;6(1):A0058. doi: 10.5702/massspectrometry.A0058.
6. Che P, Davidson JT, Kool J, Kohler I. *Electron activated dissociation - a complementary fragmentation technique to collision-induced dissociation for metabolite identification of synthetic cathinone positional isomers*. Anal Chim Acta. 2023; 1283:341962. doi: 10.1016/j.aca.2023.341962
7. Baba T, Campbell JL, Le Blanc JCY, Baker PRS. *Distinguishing Cis and Trans Isomers in Intact Complex Lipids Using Electron Impact Excitation of Ions from Organics Mass Spectrometry.* Anal Chem. 2017 Jul 18;89(14):7307-7315. doi: 10.1021/acs.analchem.6b04734. Epub 2017 Jun 28. PMID: 28613874.
8. Russell DW. *The enzymes, regulation, and genetics of bile acid synthesis.* Annu Rev Biochem. 2003; 72:137-74. doi: 10.1146/annurev.biochem.72.121801.161712
9. Ridlon JM, Kang DJ, Hylemon PB. *Bile salt biotransformations by human intestinal bacteria.* J Lipid Res. 2006 ;47(2):241-59. doi: 10.1194/jlr.R500013-JLR200
10. Guzior DV, Quinn RA. *Review: microbial transformations of human bile acids.* Microbiome. 2021; 9(1):140. doi: 10.1186/s40168-021-01101-1
11. Quinn RA, Melnik AV, Vrbanac A, Fu T, Patras KA, Christy MP, Bodai Z, Belda-Ferre P, Tripathi A, Chung LK, Downes M, Welch RD, Quinn M, Humphrey G, Panitchpakdi M, Weldon KC, Aksenov A, da Silva R, Avila-Pacheco J, Clish C, Bae S, Mallick H, Franzosa EA, Lloyd-Price J, Bussell R, Thron T, Nelson AT, Wang M, Leszczynski E, Vargas F, Gauglitz JM, Meehan MJ, Gentry E, Arthur TD, Komor AC, Poulsen O, Boland BS, Chang JT, Sandborn WJ, Lim M, Garg N, Lumeng JC, Xavier RJ, Kazmierczak BI, Jain R, Egan M, Rhee KE, Ferguson D, Raffatellu M, Vlamakis H, Haddad GG, Siegel D, Huttenhower C, Mazmanian SK, Evans RM, Nizet V, Knight R, Dorrestein PC. *Global chemical effects of*

MKT-30747-B

the microbiome include new bile-acid conjugations. Nature. 2020; 579(7797):123-129. doi: 10.1038/s41586-020-2047-9

12. Lucas LN, Barrett K, Kerby RL, Zhang Q, Cattaneo LE, Stevenson D, Rey FE, Amador-Noguez D. *Dominant Bacterial Phyla from the Human Gut Show Widespread Ability To Transform and Conjugate Bile Acids*. mSystems. 2021; e0080521. doi: 10.1128/mSystems.00805-21

13. Foley MH, Walker ME, Stewart AK, O'Flaherty S, Gentry EC, Patel S, Beaty VV, Allen G, Pan M, Simpson JB, Perkins C, Vanhoy ME, Dougherty MK, McGill SK, Gulati AS, Dorrestein PC, Baker ES, Redinbo MR, Barrangou R, Theriot CM. *Bile salt hydrolases shape the bile acid landscape and restrict Clostridioides difficile growth in the murine gut.* Nat Microbiol. 2023; 8(4):611-628. doi: 10.1038/s41564-023-01337-7

14. Gentry EC, Collins SL, Panitchpakdi M, Belda-Ferre P, Stewart AK, Carrillo Terrazas M, Lu HH, Zuffa S, Yan T, Avila-Pacheco J, Plichta DR, Aron AT, Wang M, Jarmusch AK, Hao F, Syrkin-Nikolau M, Vlamakis H, Ananthakrishnan AN, Boland BS, Hemperly A, Vande Casteele N, Gonzalez FJ, Clish CB, Xavier RJ, Chu H, Baker ES, Patterson AD, Knight R, Siegel D, Dorrestein PC. Reverse metabolomics for the discovery of chemical structures from humans. Nature. 2024; 626(7998):419-426. doi: 10.1038/s41586-023-06906-8

15. Guzior DV, Okros M, Shivel M, Armwald B, Bridges C, Fu Y, Martin C, Schilmiller AL, Miller WM, Ziegler KM, Sims MD, Maddens ME, Graham SF, Hausinger RP, Quinn RA. *Bile salt hydrolase acyltransferase activity expands bile acid diversity.* Nature. 2024; Online Ahead of Print. doi: 10.1038/s41586-024-07017-8.

16. Horvath TD, Haidacher SJ, Hoch KM, Auchtung JM, Haag AM. *A high-throughput LC-MS/MS method for the measurement of the bile acid/salt content in microbiome-derived sample sets.* MethodsX. 2020; 7:100951. doi: 10.1016/j.mex.2020.100951

17. *ICH harmonized tripartite guideline: validation of analytical procedures: text and methodology Q2(R1)*, International Conference of harmonization of technical requirements for registration of pharmaceuticals for human use, 2005

18. Baker, PRS and Proos R. Untargeted data-dependent acquisition (DDA) metabolomics analysis using the ZenoTOF 7600 system. SCIEX technical note, RUO MKT-02-15367-A

19. 19McDonald D, Hyde E, Debelius JW, Morton JT, Gonzalez A, Ackermann G, Aksenov AA, Behsaz B, Brennan C, Chen Y, DeRight Goldasich L, Dorrestein PC, Dunn RR, Fahimipour AK, Gaffney J, Gilbert JA, Gogul G, Green JL, Hugenholtz P, Humphrey G, Huttenhower C, Jackson MA, Janssen S, Jeste DV, Jiang L, Kelley ST, Knights D, Kosciolek T, Ladau J, Leach J, Marotz C, Meleshko D, Melnik AV, Metcalf JL, Mohimani H, Montassier E, Navas-Molina J, Nguyen TT, Peddada S, Pevzner P, Pollard KS, Rahnavard G, Robbins-Pianka A, Sangwan N, Shorenstein J, Smarr L, Song SJ, Spector T, Swafford AD, Thackray VG, Thompson LR, Tripathi A, Vázquez-Baeza Y, Vrbanac A, Wischmeyer P, Wolfe E, Zhu Q; *The American Gut Consortium; Knight R. American Gut: an Open Platform for Citizen Science Microbiome Research*. mSystems. 2018; 3(3):e00031-18. doi: 10.1128/mSystems.00031-18

20. Lloyd-Price J, Arze C, Ananthakrishnan AN, Schirmer M, Avila-Pacheco J, Poon TW, Andrews E, Ajami NJ, Bonham KS, Brislawn CJ, Casero D, Courtney H, Gonzalez A, Graeber TG, Hall AB, Lake K, Landers CJ, Mallick H, Plichta DR, Prasad M, Rahnavard G, Sauk J, Shungin D, Vázquez-Baeza Y, White RA 3rd; IBDMDB Investigators; Braun J, Denson LA, Jansson JK, Knight R, Kugathasan S, McGovern DPB, Petrosino JF, Stappenbeck TS, Winter HS, Clish CB, Franzosa EA, Vlamakis H, Xavier RJ, Huttenhower C. *Multi-omics of the gut microbial ecosystem in inflammatory bowel diseases*. Nature. 2019; 569(7758):655-662. doi: 10.1038/s41586-019-1237-9

21. Wang M, Jarmusch AK, Vargas F, Aksenov AA, Gauglitz JM, Weldon K, Petras D, da Silva R, Quinn R, Melnik AV, van der Hooft JJJ, Caraballo-Rodríguez AM, Nothias LF, Aceves CM, Panitchpakdi M, Brown E, Di Ottavio F, Sikora N, Elijah EO, Labarta-Bajo L, Gentry EC, Shalapour S, Kyle KE, Puckett SP, Watrous JD, Carpenter CS, Bouslimani A, Ernst M, Swafford AD, Zúñiga EI, Balunas MJ, Klassen JL, Loomba R, Knight R, Bandeira N, Dorrestein PC. *Mass spectrometry searches using MASST*. Nat Biotechnol. 2020; 38(1):23-26. doi: 10.1038/s41587-019-0375-9

MKT-30747-B

Quantitative and qualitative bile acid analysis on the ZenoTOF 8600 system using EAD

Paul RS Baker[1], Remco van Soest[1], Santosh Kapil[1], Robert Proos[1], Maxim D Seferovic[2] and Thomas D. Horvath[3,4]

[1]SCIEX, USA; [2] Dept of Obstetrics and Gynecology, Baylor College of Medicine, Houston, TX; [3]Dept of Pathology, Texas Children's Hospital, Houston, TX; [4]Dept of Pathology & Immunology, Baylor College of Medicine, Houston, TX

This technical note demonstrates the power and capability of the ZenoTOF 8600 system to sensitively detect, quantify, and structurally characterize the bile acid content in human plasma.

The analysis of bile acids in human samples has become increasingly important as insights into the prominent biological role of this class of molecules are discovered [1,2]. Analysis of bile acids by triple-quadrupole MS (TQMS) systems is challenging because of the high chemical background found in several precursor ions to precursor ion-based multiple-reaction monitoring (MRM) transitions used in current state-of-the-art assays (1-4). High-resolution mass spectrometry
(HRMS) enables the extraction of fragment ions with a narrow mass-to-charge (*m/z*) window, which can reduce background chemical interferences and improve the signal-to-noise (S/N) of the assay as previously demonstrated [3].

The detection of individual bile acid isomers currently depends on chromatographic resolution because collision-induced dissociation (CID)-based fragmentation cannot distinguish these isomeric metabolites. However, a novel fragmentation method, electron-activated dissociation (EAD) can generate unique fragments, even among isomers that may help reduce the time required for analysis.

Here, the ZenoTOF 8600 system was used to quantify the bile acid content of human plasma sample extracts using both CID- and EAD-based fragmentation methods. EAD-based fragmentation was strategically used when isomeric pairs overlapped to provide specificity and enable faster analysis times.

Key features of bile acid analysis on the ZenoTOF 8600 system

- The ZenoTOF 8600 system can detect and quantify bile acids with an approximately 12-fold better sensitivity than the ZenoTOF 7600 system
- The narrow fragment ion extraction window possible with HRMS improves assay sensitivity by reducing background chemical interferences and, consequently, increases the S/N of the assay
- EAD can generate diagnostic fragment ions to enable the distinction between bile acid isomers, which improves the overall specificity and speed of the analysis

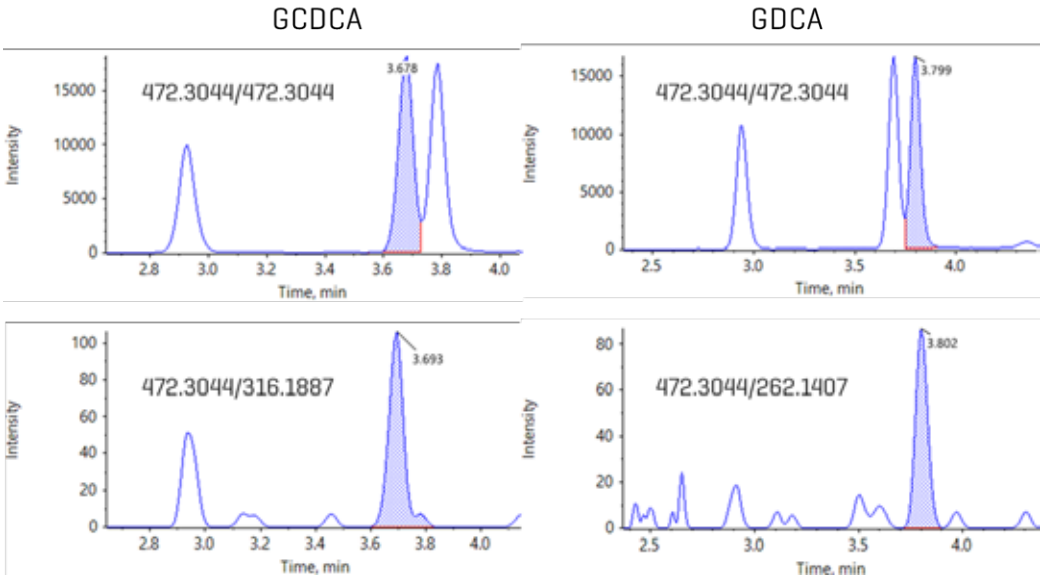

Figure 1. Detection and quantitation of bile acid isomers in human plasma using EAD. Using a fast, 10-minute gradient, bile acids were analyzed on the ZenoTOF 8600 system, Isomers such as GCDCA and GDCA are indistinguishable using CID-based fragmentation. Using EAD, unique, diagnostic fragments were enabled their accurate quantitation despite the chromatographic overlap. The upper panels show the two isomers overlapping when using a ; the lower panels show the ability to isolate each isomer separately when a unique, EAD-based fragment is used.

RUO-MKT-35189-A

Introduction

Bile acids are amphipathic steroidal molecules synthesized in the liver from cholesterol and play a crucial role in the digestion and absorption of dietary lipids [1]. Primary bile acids, such as cholic acid and chenodeoxycholic acid, are conjugated with glycine or taurine before being secreted into bile. Once released into the intestinal lumen, these acids undergo microbial transformation to form secondary bile acids like deoxycholic acid and lithocholic acid that are collectively termed microbially conjugated bile acids (MCBAs). Enterohepatic circulation maintains a dynamic balance of bile acid synthesis, secretion, reabsorption, and excretion. Beyond their digestive functions, bile acids are now recognized as signaling molecules involved in metabolic regulation and immune responses, acting through nuclear receptors such as FXR and membrane-bound G-protein coupled receptors [2].

Mass spectrometry (MS) has become the analytical method of choice for the quantitation and profiling of bile acids due to its sensitivity, specificity, and ability to differentiate structurally similar compounds. [3-5] The use of HPLC ESI-MS/MS allows for the simultaneous detection of multiple bile acid species, including conjugated and unconjugated forms, in biological matrices such as plasma, bile, and feces. Targeted MS approaches using multiple reaction monitoring (MRM) provide high-throughput and quantitative data essential for clinical and research applications in liver disease, metabolic disorders, and gut microbiome studies.

Recently, we reported the analysis of bile acids using the ZenoTOF 7600 system, which is a hybrid quadrupole time of flight instrument (QTOF) that measures compounds with high resolution (~35K) and mass accuracy (<2 ppm) [TN ref]. In the negative ion mode, bile acid analysis by nominal mass instruments is challenging due to solvent-based high chemical background noise. With accurate mass systems, this issue can be mitigated using narrow product ion extraction windows (XIC), which minimize noise and enable a similar calculated LOQ for the ZenoTOF 7600 system as with the highly sensitive triple quadrupole SCIEX 7500 system. Using the ZenoTOF 8600 system, these studies were extended to capitalize on the instrument's improved sensitivity.

The ZenoTOF 8600 system has unique design features that make it particularly suited for targeted bile acid analysis. First, the instrument has a complementary fragmentation mode, EAD, that provides unparalleled structural characterization of small molecules [6-10]. Second, improved hardware, such as the front end with the Optiflow Pro source, a larger instrument orifice, and an advanced optical detector, enables higher sensitivity compared to the ZenoTOF 7600 system. Third, the instrument's front end is equipped with a DJET+ with Mass Guard, which has been shown to reduce instrument contamination on the SCIX 7500+ system [11], an important consideration for lipid and metabolite analysis, especially in the

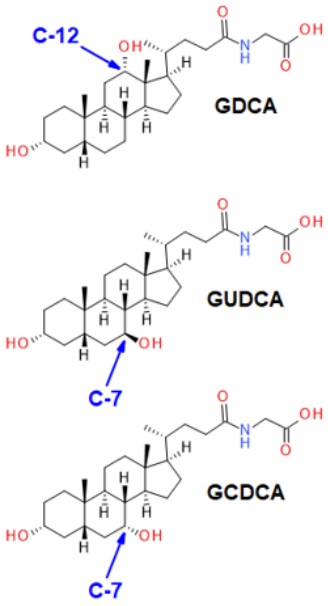

Figure 2. The glucodeoxycholic acid subclass of bile acids. Bile acids are cholesterol-derived amphipathic molecules of saturated hydroxylated C-24 sterols. GDCA has a hydroxyl moiety at carbon 12 (C-12), whereas GUDCA and GCDCA are hydroxylated at carbon 7 (C-7). The latter two isomers are characterized by a different stereochemistry at the number 7 carbon. Quantitative specificity for this class of molecules is highly dependent on chromatographic resolution when analyzed using CID-based fragmentation.

complex matrices common to bile acid analysis, including plasma, feces, and bile.

Bile acids are cholesterol-derived amphipathic molecules of saturated hydroxylated C-24 sterols. As shown in **Figure 2**, the location and stereochemistry of the hydroxyl functional groups define the different isomers within each sub-class. CID-based fragmentation of bile acids primarily yields product ions related to the bile acid head group, and relatively few fragments are generated from the ring structure; hence, CID alone does not generate diagnostically useful fragment ions for identification or quantitation purposes. Using chromatography to resolve bile acid isomers requires relatively long chromatographic gradients, which are not conducive to high-throughput analysis. An alternative to lengthy chromatographic gradients and CID-based fragmentation is EAD. EAD-based fragmentation provides ample fragments derived from the sterol ring structure, and it can distinguish the isomers of each bile acid subclass without extensive chromatographic method development.

In this technical note, the speed and sensitivity of the ZenoTOF 8600 system were leveraged to quantify bile acids in prepared plasma samples. To demonstrate the power of EAD to improve structural specificity during quantitative analysis, unique EAD-based fragments were identified for potentially co-eluting isomer pairs and used strategically in conjunction with CID-based fragmentation to enable a

RUO-MKT-35189-A

faster assay while maintaining quantitative specificity, accuracy, and precision.

Methods

Materials: Bile acid standard mixtures were purchased from Cambridge Isotopes Laboratories. The stable isotope-labeled bile acid mixes (unconjugated, cat# MSK-BA1; conjugated, MSK-BA2) were used as internal standards, and unlabeled bile acid mixes (unconjugated, cat# MSK-BA1-US; conjugated, MSK-BA2-US) were used as primary reference standards. All solvents were of LC-MS grade and obtained from Burdick and Jackson and Fisher Scientific.

Sample preparation: Human blood (research use only) was collected into tubes containing potassium ethylenediamine tetraacetic acid (K_2EDTA) anti-coagulant following the procedure approved by the institutional review board (IRB) of BCM. The plasma was isolated from the red blood cell fraction by centrifugation. A 50 µL volume of each plasma sample was pipetted into individual 0.6 mL Eppendorf tubes, and a 200 µL volume of methanol was added to precipitate plasma proteins (primary DF=5-fold). All samples were vortex-mixed for 30 seconds and centrifuged at 17,000*g* for 5 minutes, and the supernatant for each clarified plasma extract sample was transferred into fresh vials. A 50 µL volume of each clarified plasma extract sample was transferred into fresh glass vials. A 450 µL volume of an internal standard solution (10 nM deuterated BAs) was added to each sample vial (DF=50-fold overall), and the vials were capped and vortex-mixed for 30 seconds. And prepared for analysis by HPLC ESI-MS/MS.

Chromatography: Extracted metabolites were resolved using a Nexera 40 Series UHPLC system equipped with a Restek Raptor C18 column (100 x 2.1 mm; 5.0 µm particle size). The autosampler sample bay was maintained at 10 °C , and a 5 µL sample volume was injected on column. The column oven temperature was kept at 50°C with a constant mobile phase flow rate of 0.3 mL/min for a total run time of 17 min. The mobile phase compositions were (A) 10 mM ammonium formate in water and (B) pure acetonitrile. Gradient details are shown in **Table 1.** Alternatively, the gradient was altered to enable a 10 min total run time (**Table 2**) in which EAD-based fragmentation was selectively employed to maintain compound specificity for co-eluting isomers that are not distinguishable using CID-based fragmentation, an example of which is shown in **Figure 1**.

Table 1. Chromatographic gradient conditions

Time (min)	Mobile phase A (%)	Mobile Phase B (%)
0	75	25
1.5	75	25
13	20	80
14.5	20	80
14.6	75	25
17	75	25

Table 2. 10-minute chromatographic gradient conditions

Time (min)	Mobile phase A (%)	Mobile Phase B (%)
0	75	25
1.5	75	25
6	20	80
7.5	20	80
7.6	75	25
10	75	25

Mass spectrometry: Sample extracts were analyzed using the ZenoTOF 8600 system with an OptiFlow ProTurbo V ion source and a scheduled, high-resolution multiple reaction monitoring (sMRMHR) scan mode. CID-based fragmentation was used for the initial assessment of the system's performance using the 17-minute gradient. This experiment was repeated using EAD-based fragmentation. To speed up the experiment and reduce the total time to 10 min, an sMRMHr experiment was performed using mixed-mode fragmentation. For isomers that overlapped when the gradient was shortened, an EAD-based fragment that is diagnostic for the overlapping isomers was used. Otherwise, CID was used for analysis due to its greater sensitivity and shorter accumulation times. MS instrument parameters are presented in **Table 3**, and a comprehensive list of the compounds studied is shown in **Table 4**.

Table 3. Instrument parameter settings

Parameter	ZenoTOF 8600 system
Curtain gas (CUR)	35
Ion source gas 1 (GS1)	60
Ion source gas 2 (GS2)	80
CAD Gas (CAD)	7
Source temperature (TEM)	250 °C
Ion spray voltage (IS)	-4500 V/+5000V (CID/ EAD)
Declustering Potential (DP)	-80 V/+80V (CID/EAD)
CID Accumulation/dwell time	Variable (sMRM^{HR})
CID Collision energy (CE)	Molecule- dependent
Q1/Q3 Mass Resolution	N/A
EAD Accumulation/dwell time	40 ms
CE for TOF MS	-10 V/+10V (CID/EAD)
TOF MS mass range	70-1000 Da
TOF MS/MS mass range	40-400 Da
Time bins to sum	6
EAD Collision energy (CE)	12 V
Electron kinetic energy (KE)	13 eV
Zeno pulsing for MS/MS	Yes
Zeno threshold	20000

Table 4. Bile acid compound parameters

Bile Acid	Abbreviation	[M - H]-	[M - H]⁻ Product ion	[M + Na]⁺	Collision energy (V)
Lithocholic Acid	LCA	375.29	375.29	399.288	-5
D4-Lithocholic Acid	D4-LCA	379.316	379.316	403.313	-5
Ursodeoxycholic Acid	UDCA	391.285	391.285	415.283	-5
D4-Ursodeoxycholic Acid	D4-UDCA	395.31	395.31	419.308	-5
Chenodeoxycholic Acid	CDCA	391.285	391.285	415.283	-5
D4-Chenodeoxycholic Acid	D4-CDCA	395.31	395.31	419.308	-5
Deoxycholic Acid	DCA	391.285	391.285	415.283	-49
D4-Deoxycholic Acid	D4-DCA	395.31	395.31	419.308	-49
Cholic Acid	CA	407.28	343.266	431.278	-49
D4-Cholic Acid	D4-CA	411.305	411.305	435.303	-49
Glycolithocholic Acid	GLCA	432.312	388.324	456.309	-48
D4-Glycolithocholic Acid	D4-GLCA	436.337	392.349	460.335	-48
Glycoursodeoxycholic Acid	GUDCA	448.307	74.025	472.304	-82
D4-Glycoursodeoxycholic Acid	D4-GUDCA	452.332	74.025	476.329	-82
Glycochenodeoxycholic Acid	GCDCA	448.307	74.025	472.304	-82
D4-Glycochenodeoxycholic Acid	D4-GCDCA	452.332	74.025	476.329	-82
Glycodeoxycholic Acid	GDCA	448.307	74.025	472.304	-82
D4-Glycodeoxycholic Acid	D4-GDCA	452.332	74.025	476.329	-82
Glycocholic Acid	GCA	464.302	402.302	488.299	-48
D4-Glycocholic Acid	D4-GCA	468.327	406.331	492.324	-48
Taurolithocholic Acid	TLCA	482.295	79.958	506.292	-137
D4-Taurolithocholic Acid	D4-TLCA	486.32	79.958	510.317	-137
Tauroursodeoxycholic Acid	TUDCA	498.289	79.958	522.287	-142
D4-Tauroursodeoxycholic Acid	D4-TUDCA	502.315	79.958	526.312	-142
Taurochenodeoxycholic Acid	TCDCA	498.289	79.958	522.287	-142
D4-Taurochenodeoxycholic Acid	D4-TCDCA	502.315	79.958	526.312	-142
Taurodeoxycholic Acid	TDCA	498.289	79.958	522.287	-142
D4-Taurodeoxycholic Acid	D4-TDCA	502.315	79.958	526.312	-142
Taurocholic Acid	TCA	514.284	124.008	538.282	-66
D4-Taurocholic Acid	D4-TCA	518.31	124.007	542.307	-66

During sMRMHr analysis, a full product ion spectrum is acquired. To identify diagnostic, EAD-based fragments for co-eluting bile acid isomers such as GCDCA and GDCA,

The Analytics module within SCIEX OS software was used for quantitation, and the Explore module was used to structurally characterize bile acids from EAD-based MS/MS spectra. The limit of quantitation (LOQ) was determined from the lowest standard injected with the %CV value < 15 and an accuracy within 85% and 115% of the expected values for the internal standard curve.

Results and Discussion

A bile acid standard curve was generated neat in solvent and analyzed on the ZenoTOF 8600 system. The parameter settings were optimized, as detailed in **Tables 3 and 4**, and the chromatographic gradient conditions resulted in the separation of each isomeric bile acid with baseline resolution **(Figure 3)**. The concentrations within the internal standard curve ranged from 0.011 to 100 nM, covering a dynamic range of > 4 orders of magnitude. An example curve acquired for gylcoursodeoxycholic acid (GUDCA) is presented in **Figure 4 (panel A)**, and the individual chromatograms for each injection of the standard curve from 0.011 to 50 nM GUDCA are shown (**panel B**). The associated quantitative statistics for GUDCA quantitation are shown in **Table 5.** The data derived from the internal standard curves were used to calculate the LOQ of each bile acid measured with the ZenoTOF 8600 system (**Table 6**). These values were determined as the lowest concentration standard injected that gave a %CV value <15% and an accuracy within the range of 85% to 115% of the expected value.

The LOQ values for the ZenoTOF 7600 system were calculated in a different way [BA TN] than they were in this report [see above]. Additionally, on the ZenoTOF 7600 system, a 15 µL sample was injected, whereas only 5 µL was injected onto the ZenoTOF 8600

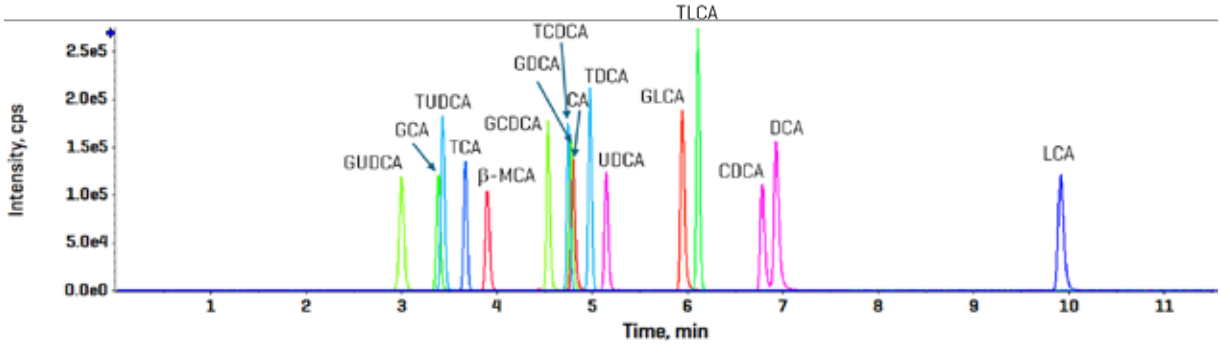

Figure 3. Elution profile of targeted bile acids using CID-based fragmentation in the negative ion mode. The 50 nM standard was injecte3d and analyzed using the sMRMHr scan mode. Total run time was 17 min.

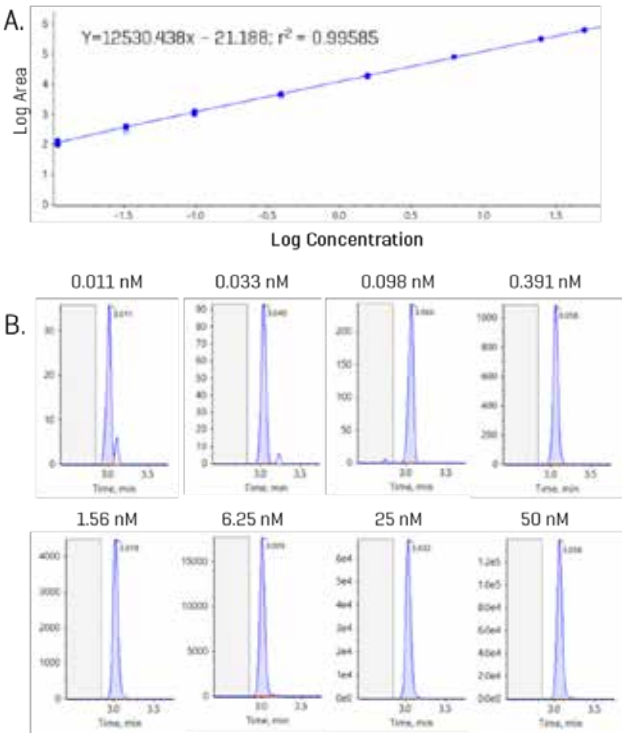

Figure 4. Example internal standard curve with representative peaks for GUDCA. **(A)** Internal standard curve for GUDCA from 0.011 to 50 nM. **(B)** Example chromatograms at each concentration level of the curve; blank region highlighted in grey.

system. To compare the relative sensitivity of the two different systems, the on-column injection amount at the LOQ was used as a reference (**Table 7**). The data show that the ZenoTOF 8600 system is an average of ~20-fold more sensitive than the ZenoTOF 7600 system (range = 1.1 to 61-fold improvement). The wide range may be, in part, due to the difference in the sources used with the two instruments. The ZenoTOF 7600 system is equipped with the Turbo V twin spray source, which optimizes differently and may have a different ionization capacity, or a differential ionization efficiency compared to the Optiflow Pro Turbo V ion source on the ZenoTOF 8600 system. The ion path of the ZenoTOF 8600 system is also different from the previous version, which may also slightly affect transmission in a compound-dependent manner.

The assay developed using neat standards was used to measure endogenous bile acids in human plasma. **Figure 5** shows the combined XIC data for all targeted bile acids measured with the sMRMHr workflow in human plasma extract. Except for lithocholic acid (LCA), all bile acids were detected and quantified using the ZenoTOF 8600 system. The data shown here were collected using the CID-based fragmentation mode, and the LC gradient extended over 17 minutes. The concentrations of bile acids detected in two representative plasma samples are shown in **Table 8**. The same experiment was performed using EAD-based fragmentation for all compounds (not shown), and those data were used to identify diagnostic fragment ions for bile acid isomers that co-elute using the faster, 10 min gradient.

Table 5. Quantitative statistics for GUDCA

Standard	*Standard concentration (nM)*	*Calculated concentration (nM)*	*Std dev*	*%CV*	*Average accuracy (n = 5)*
GUDCA	*0.011*	*0.011*	*0.0014*	***12.9***	***100.4***
GUDCA	*0.033*	*0.033*	*0.0017*	***5.13***	***101.0***
GUDCA	*0.098*	*0.093*	*0.0074*	***7.90***	***95.0***
GUDCA	*0.391*	*0.385*	*0.0087*	***2.27***	***98.5***
GUDCA	*1.56*	*1.57*	*0.0873*	***5.58***	***100.3***
GUDCA	*6.25*	*6.39*	*0.1008*	***1.58***	***102.3***
GUDCA	*25*	*26*	*0.6598*	***2.59***	***102.0***
GUDCA	*50*	*50*	*1.3860*	***2.76***	***100.5***

Table 6. LOQ values for bile acids on the ZenoTOF 8600 system

Bile acid	*LOQ (nM)*
LCA	0.098
UDCA	0.098
CDCA	0.033
DCA	0.033
CA	0.033
GLCA	0.033
GUDCA	0.011
GCDCA	0.011
GDCA	0.011
GCA	0.098
TLCA	0.033
TUDCA	0.011
TCDCA	0.033
TDCA	0.033
TCA	0.033

Table 7. Comparison of on-column injection load at LOD between the ZenoTOF 7600 and 8600 systems

Bile Acid	fmol on-column injection at LOQ		Fold-increase in sensitivity
	ZenoTOF 7600 system	ZenoTOF 8600 system	
LCA	6.075	0.490	12.4
UDCA	2.160	0.490	4.4
CDCA	0.446	0.165	2.7
DCA	0.188	0.165	1.1
CA	9.195	0.165	55.7
GLCA	10.035	0.165	60.8
GUDCA	2.025	0.055	36.8
GCDCA	1.277	0.055	23.2
GDCA	0.777	0.055	14.1
GCA	3.150	0.490	6.4
TLCA	3.165	0.165	19.2
TUDCA	1.115	0.055	20.3
TCDCA	4.635	0.165	28.1
TDCA	1.515	0.165	9.2
TCA	3.810	0.165	23.1

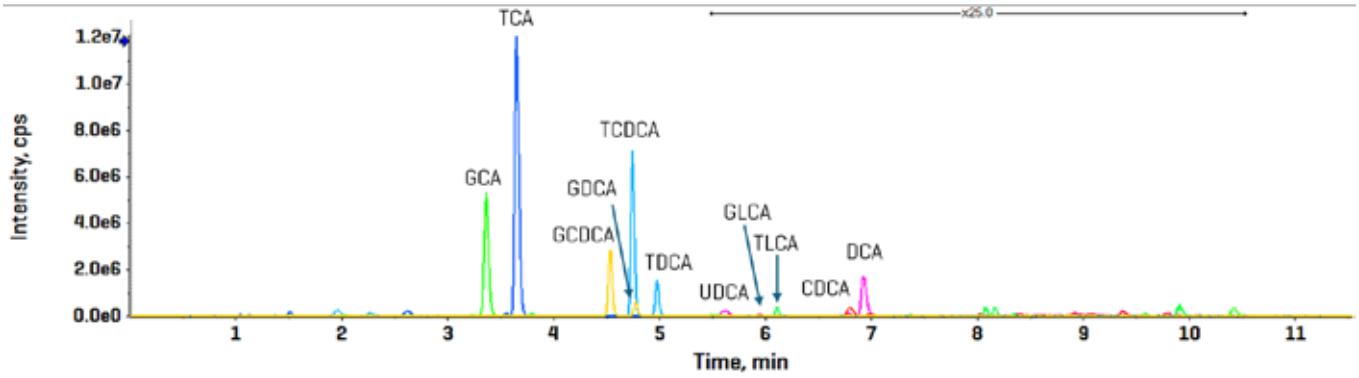

Figure 5. Bile acid detection and quantitation in human plasma using sMRMHr analysis on the ZenoTOF 8600 system

Table 8. Example quantitative results from 2 different human plasma samples

Bile Acid	Abbreviation	Sample 1		Sample 2	
		Concentration (nM)	%CV (n=3)	Concentration (nM)	%CV (n=3)
Lithocholic Acid	LCA	ND	N/A	ND	N/A
Ursodeoxycholic Acid	UDCA	0.714	4.9	0.490	4.3
Chenodeoxycholic Acid	CDCA	12.4	1.7	0.612	1.1
Deoxycholic Acid	DCA	12.3	2.4	0.708	6.0
Cholic Acid	CA	6.03	2.4	5.32	7.2
Glycolithocholic Acid	GLCA	0.395	6.0	0.041	14
Glycoursodeoxycholic Acid	GUDCA	0.181	1.0	2.48	1.0
Glycochenodeoxycholic Acid	GCDCA	797	1.4	112	3.7
Glycodeoxycholic Acid	GDCA	146	3.8	0.863	6.1
Glycocholic Acid	GA	1570	2.7	206	0.9
Taurolithocholic Acid	TLCA	1.13	0.89	0.093	3.7
Tauroursodeoxycholic Acid	TUDCA	2.41	4.3	1.53	4.1
Taurochenodeoxycholic Acid	TCDCA	1510	0.37	344	6.0
Taurodeoxycholic Acid	TDCA	246	2.5	254	0.30
Taurocholic Acid	TCA	3780	1.2	313	3.7

The EAD-based fragmentation functionality of the ZenoTOF 7600 system can provide significantly more structural details than that generated by CID-based fragmentation. Previously, we reported the identification of unique fragments for the bile acid isomers CDCA and

RUO-MKT-35189-A

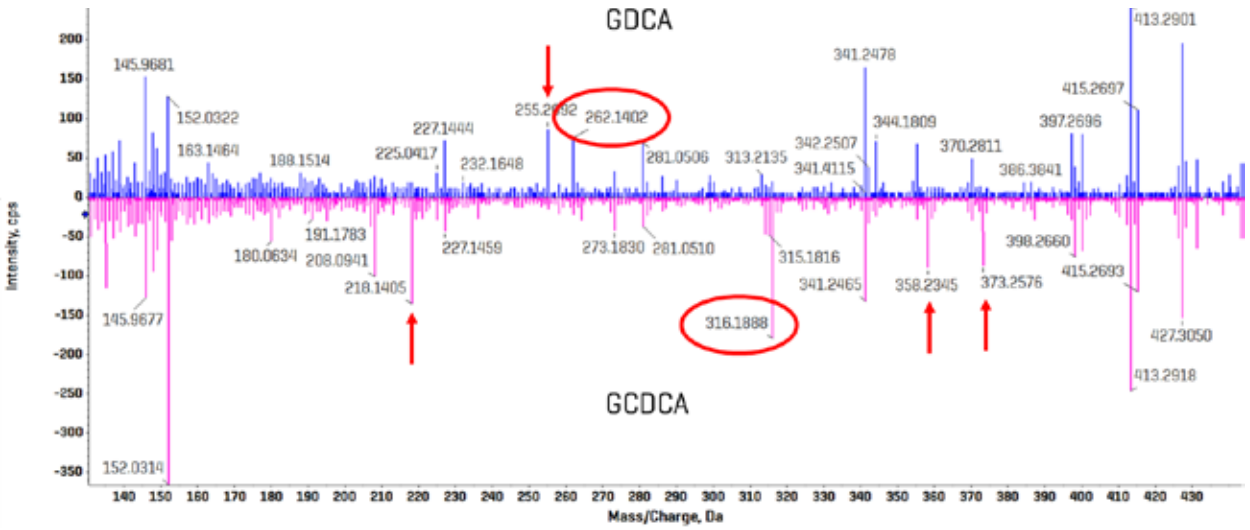

Figure 6. Comparison of EAD-based fragmentation of GDCA and GCDCA. A portion of the product ion spectra for GCDCA and GDCA is highlighted, with the spectrum for GDCA overlaid and inverted. Multiple fragments were identified for each bile acid isomer that appear to be unique and could serve as a selective fragment ion during analysis (red arrows). The fragment ions with *m/z* 262.1403 and 316.1888 were chosen for GDCA and GCDCA, respectively, due to their relatively high abundances.

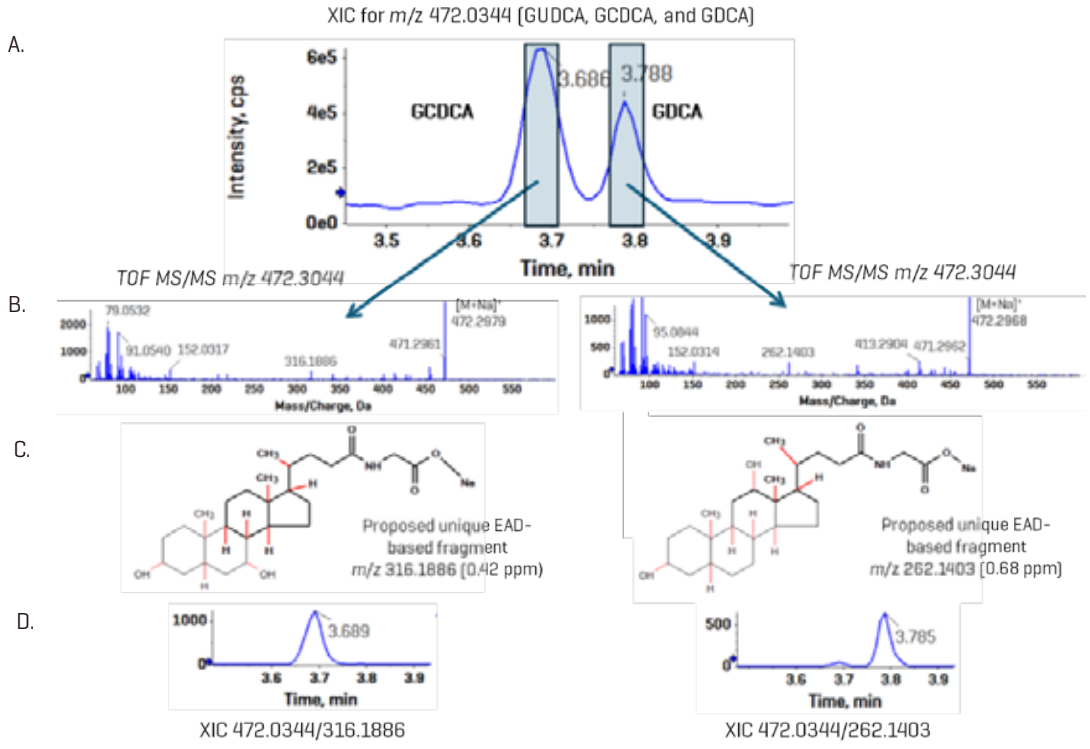

Figure 7. Resolution of bile acid isomers using EAD-based fragmentation. GCDCA and GDCA are bile acid isomers that have identical CID-based MS/MS spectra. Using EAD, unique, diagnostic fragments were observed for each isomer (A and B) in a standard mixture (6.56 nM). Using the fragments pane in SCIEX OS, structures for each fragment, *m/z* 316.1886 and 262.1403, were proposed for GUDCA and GDCA, respectively (C). Using a 10 mDa XIC window, panel D shows the improved specificity of the analysis for the two standards.

DCA [TN BA]. These isomers elute very closely and are responsible, in part, for the relatively long analysis time so that they remain chromatographically resolved. It was hypothesized that using EAD-based fragmentation for these isomer pairs would allow for a truncated chromatographic gradient and enable faster sample analysis. Here, we extended these findings using the ZenoTOF 8600

system and leveraged the ~10-fold increase in sensitivity to strategically use EAD-based fragmentation for specific bile acids during sMRMHr analysis. **Figure 6** shows a region of the EAD-derived product ion spectrum for GCDCA and GDCA acquired as neat standards; the spectrum for GCDCA is inverted so the differences in the spectra are more apparent. Fragment ions at *m/z* 262.1403 and 316.1888 were identified as unique, diagnostic ions for GDCA and GCDCA, respectively. Other apparently unique fragment ions for each bile acid isomer are indicated with red arrows. Having multiple unique fragment ions may help with quantitation, as fragment intensities can be added during quantitative processing in the Analytics module of SCIEX OS software.

Using the faster, 10-min gradient, the bile acid standards were analyzed using EAD-based fragmentation. **Figure 7, panel A,** shows the elution profile of GCDCA and GDCA using neat standards, with the peak-to-peak retention time difference of ~12 s. The product ion spectra are shown in **panel B**, with the diagnostic ion for each apparent in its respective spectrum. The fragment panel app within the SCIEX OS Explore module proposed 2 possible structures of the fragments, as shown in **Panel C**. In **Panel D**, the XICs for GCDCA and GDCA show minimal to no interference when the EAD-specific fragments are used.

To test whether this technique can be used to measure bile acids in plasma, the same 10-minute, EAD-based method used for **Figure 7** was applied to the analysis of human plasma extracts (**Figure 1).** In contrast to the results with neat standards, in the plasma matrix, the isomers GCDCA and GDCA are not baseline resolved when using a common fragment—in this case, the precursor-to-precursor MRMHr transition. However, when the data were processed using the unique EAD-based fragments, the individual bile acids were completely resolved, allowing for accurate quantitation.

In the data reported here, the ZenoTOF 8600 system was able to measure bile acids in human plasma with ~10-fold greater sensitivity than the ZenoTOF 7600 system using CID-based fragmentation. Of note, for this particular assay, a choice has to be made whether to maximize sensitivity and run the samples using the longer gradient in the negative ion mode with CID-based fragmentation, or to maximize speed and specificity by running the assay with the fast gradient using EAD-based fragmentation and sacrifice ~ 100-fold sensitivity compared to the longer assay. For the isomers in question here, GDCA, GCDCA, and GUDCA, the EAD-based method was appropriate for biological analysis. Currently, a study is underway to measure amino acid conjugates of bile acids. These molecules are measured in the positive ion mode and are amenable to a combined analysis of CID- and EAD-based analysis, using EAD only when needed to improve specificity.

Conclusions

- **The ZenoTOF 8600 system is ~ 20-fold more sensitive for the analysis of bile acids compared to the ZenoTOF 7600 system narrow XIC window possible on HRMS systems enables the MS1-based collection of data without the inclusion of chemical background interferences**
- **EAD-based fragmentation provides structural characterization of molecules and may abrogate the need for extensive chromatographic separation of isomers to ensure specificity**

References

1. Collins, S. L., Stine, J. G., Bisanz, J. E., Okafor, C. D., & Patterson, A. D. (2023). Bile acids and the gut microbiota: metabolic interactions and impacts on disease. *Nature reviews. Microbiology*, *21*(4), 236–247. https://doi.org/10.1038/s41579-022-00805-x
2. Lin, S., Wang, S., Wang, P., Tang, C., Wang, Z., Chen, L., Luo, G., Chen, H., Liu, Y., Feng, B., Wu, D., Burrin, D. G., & Fang, Z. (2023). Bile acids and their receptors in regulation of gut health and diseases. *Progress in lipid research*, *89*, 101210. https://doi.org/10.1016/j.plipres.2022.101210
3. Baker, PRS., Proos, R., Sefevoric, MD., and Horvath, TD. Quantitative analysis and structural characterization of bile acids using the ZenoTOF 7600 system. SCIEX technical note MKT-30747-B. https://sciex.com/tech-notes/life-science-research/metabolomics/quantitative-analysis-and-structural-characterization-of-bile-ac
4. Liu, D., Li, G., Liu, D., Shi, W., Wang, H., Zhang, Q., Shen, M., Huang, X., & Lin, H. (2023). Quantitative Detection of 15 Serum Bile Acid Metabolic Products by LC/MS/MS in the Diagnosis of Primary Biliary Cholangitis. *Chemistry & biodiversity*, *20*(3), e202200720. https://doi.org/10.1002/cbdv.202200720
5. Gao, T., Hu, S., Xu, W., Wang, Z., Guo, T., Chen, F., Ma, Y., Zhu, L., Chen, F., Wang, X., Zhou, J., Lv, Z., & Lu, L. (2024). Targeted LC-MS/MS profiling of bile acids reveals primary/secondary bile acid ratio as a novel biomarker for necrotizing enterocolitis. *Analytical and bioanalytical chemistry*, *416*(1), 287–297. https://doi.org/10.1007/s00216-023-05017-7
6. Yang, J., Lin, J., Wang, A., Yang, X., Wang, Y., Zhang, Y., Dong, H., Tian, Y., Zhang, Z., Wang, M., & Song, R. (2024). Study on the effect of calibration standards prepared with different matrix on the accuracy of bile acid quantification using LC-MS/MS. *Journal of*

RUO-MKT-35189-A

pharmaceutical and biomedical analysis, 237, 115785. https://doi.org/10.1016/j.jpba.2023.115785

7. Baba T, Campbell JL, Le Blanc JCY, Baker PRS, Hager JW, Thomson BA. *Development of a Branched Radio-Frequency Ion Trap for Electron Based Dissociation and Related Applications.* Mass Spectrom (Tokyo). 2017;6(1):A0058. doi: 10.5702/massspectrometry.A0058

8. Baba, T., Campbell, J. L., Le Blanc, J. C., & Baker, P. R. (2016). In-depth sphingomyelin characterization using electron impact excitation of ions from organics and mass spectrometry. *Journal of lipid research*, *57*(5), 858–867. https://doi.org/10.1194/jlr.M067199

9. Baba, T., Campbell, J. L., Le Blanc, J. C., & Baker, P. R. (2016). Structural identification of triacylglycerol isomers using electron impact excitation of ions from organics (EIEIO). *Journal of lipid research*, *57*(11), 2015–2027. https://doi.org/10.1194/jlr.M070177

10. Baba, T., Campbell, J. L., Le Blanc, J. C. Y., Baker, P. R. S., & Ikeda, K. (2018). Quantitative structural multiclass lipidomics using differential mobility: electron impact excitation of ions from organics (EIEIO) mass spectrometry. *Journal of lipid research*, *59*(5), 910–919. https://doi.org/10.1194/jlr.D083261

11. Baba T, Campbell JL, Le Blanc JCY, Baker PRS. Distinguishing Cis and Trans Isomers in Intact Complex Lipids Using Electron Impact Excitation of Ions from Organics Mass Spectrometry. Anal Chem. 2017 Jul 18;89(14):7307-7315. https://doi: 10.1021/acs.analchem.6b04734

12. Selen, E., Baghla, R., Moore, I., Galermo, E., Zhang, Z., and Jones, E. Redefine bioanalysis with enhanced robustness on the SCIEX 7500+ system. SCIEX technical note MKT-31350-A. https://sciex.com/tech-notes/pharma/bioanalysis-pk/redefine-bioanalysis-with-enhanced-robustness-on-the-sciex-7500-plus-system

基于激光显微切割-液质联用技术的微量细胞广靶脂质组学分析

High-coverage Targeted Lipidomics Analysis of Trace Cells based on Laser Microdissection-LC-MS/MS Method

钟晨春[1]，龙志敏[1]，高天龙[2]，郭立海[1]

[1] *SCIEX中国 应用支持中心；* [2] *徕卡生命科学*

Key words: lipidomics; single cell; laser microdissection; Triple Quad 7500; MRM

活细胞无时不在与外界进行着物质和能量的交换，其代谢水平应是其生命体征的主要表现。在健康和疾病中，代谢程序和它们所支持的特定生理功能之间有着密切的联系。这些核心代谢功能的失调与许多现代疾病有关，包括癌症和慢性炎症性代谢疾病，如糖尿病、肥胖、动脉粥样硬化和类风湿关节炎。然而，由于疾病的复杂性和所涉及的细胞表型甚多，对于发生在致病环境中的代谢重塑的详细了解还很缺乏。营养水平的改变、供能系统的变化以及信号因子的存在以及与邻近细胞的相互干扰，都会诱导代谢变化，使细胞在其特定的组织微环境中发挥作用。由于每个细胞都生活在一个独特的环境中，我们体内没有一个细胞在新陈代谢、表型和功能上完全相同。在单细胞分辨率下，解决代谢的时空异质性和阐明这一复杂性将推动代谢领域向前发展，允许转换到临床应用和理解体内系统代谢组学变化的基础。

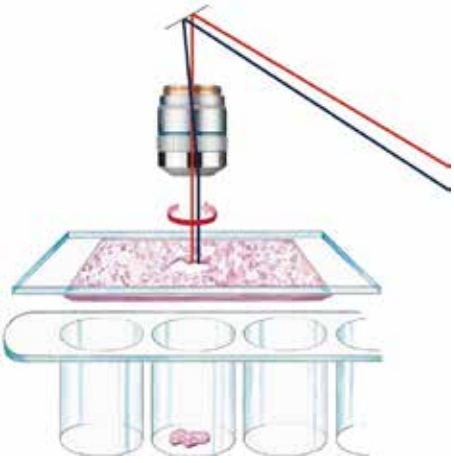

图1. 徕卡激光捕获显微切割采用移动激光的显微切割技术。徕卡显微系统采用高精确度的光学部件并借助棱镜沿着组织上所需的切割线对激光束进行操纵，可垂直于组织实施切割，从而获得切割精确、无污染的分离体。

对于单细胞代谢组学来说，单细胞样品制备、鉴定细胞内代谢产物和数据分析都需要复杂的技术和模型来进行。由于细胞代谢会对环境变化产生响应，因此在单细胞样品制备过程中面临的一个主要问题就是如何在样品制备过程中尽量避免或减少对细胞代谢的影响，其中一种方法就是在制备过程中将细胞尽可能地维持在天然环境中。组织切片伴随着显微镜技术等的发展而得到广泛的应用，而激光显微切割 (LMD, Laser Microdissection)技术可以方便地对其进行特定的单个细胞或整个组织区域的分离（图1）。

相比DNA和RNA，细胞内的代谢物无法扩增，单个细胞能够提供的用于分析的代谢物浓度低体积小，一些极为稀少的代谢物需要更加灵敏的检测方法。SCIEX 7500 系统是SCIEX的新一代高端定量工作平台。在继承以往产品耐用性的同时，SCIEX 7500系统灵敏度的提高可以应对诸如单细胞代谢组学这些极具挑战性的分析工作。

实验方法

样品制备：由制备好的脑组织切片样本置于激光显微切割载物台；接收端放置PCR管，其管盖用于分离体的接收。从5倍显微镜物镜开始，寻找到合适的视野并调节焦距，直至切换至40倍放大视野。在确定好焦距平面后，将视野移动到空白区域，进行激光切割位置校准，再将视野移动到待切割的细胞区域；选择合适的细胞数目或切割面积 (如 ~2000 μm^2)，在调节好相关参数（Power 49、Aperture 5、Speed 13、Bridge size 4）后开始进行切割（图2）。切割完成后，小心将PCR管取出，由管底倒扣至管盖盖紧，防止管盖中收集的样品遗落。

样品提取：装有样品的PCR管在vortex中振荡5s，由点甩小型离心机将微量样品离心至管底，小心打开管盖，加入30 µL提取溶

RUO-MKT-02-14573-ZH-A

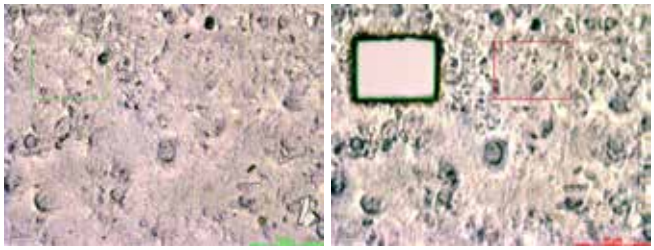

图2. 脑组织切片样本用于激光显微切割分离体制备。鉴于脑组织细胞排列致密，在显微镜观察中对于细胞数目较难计算，故而在40倍放大视野中选取合适的面积，约2000 μm^2（左）进行切割分离并用于后续分析；一份样品切割分离完成后（右），可继续选择其他区域进行操作。

液（异丙醇:乙腈:水 30:65:5 v/v/v），振荡混匀，超声15 min，离心后将全部溶液转移至进样小瓶中待LC-MS/MS分析。

LC-MS条件：样品通过ExionLC™系统串联SCIEX 7500系统，进行分析。详尽分析条件列于表1、2和3。详细的质谱分析方法及脂质化合物列表见 广泛靶向的全面脂质组学分析方法（Comprehensive Targeted Method for Global Lipidomics Screening）[1]

数据处理：数据通过SCIEX OS 软件2.1中的定量功能（点击“Analytics”）进行处理。

表1. 色谱条件

参数	数值
色谱柱	Phenomenex Kinetex C18, 100 × 2.1 mm, 2.6 μm
流动相A	含2 mM乙酸铵的甲醇
流动相B	含2 mM乙酸铵的甲醇:二氯甲烷 (2:1, v/v)
流速	300 μL/min
柱温	45 ℃
进样体积	10 μL

表2. 梯度条件

时间（min）	流动相A（%）	流动相B（%）
0	95	5
1	95	5
13	2	98
14	2	98
14.1	95	5
17	95	5

表3. SCIEX 7500系统的质谱参数

参数	数值	参数	数值
气帘气	40 psi	源温度	350 ℃
雾化气	85 psi	辅助气	70 psi
碰撞诱导解离气	9	离子喷雾电压	2400 V

高覆盖靶向脂质组学分析

该方法提供了众多的多反应监测(Multiple reactions monitoring, MRM)离子对用于多种脂类物质的靶向检测。化合物列表中可以检测约1900种脂质分子，包括磷脂酰胆碱（phosphatidylcholine, PC）/溶血磷脂酰胆碱（lyso-phosphatidylcholine, LPC），磷脂酰乙醇胺（Phosphatidyl ethanolamine, PE）/ 溶血磷脂酰乙醇胺（lyso-phosphatidylethanolamine, LPE），磷脂酰丝氨酸（phosphatidylserine, PS）/溶血磷脂酰丝氨酸（lyso-phosphatidylserine, LPS），磷脂酰肌醇（phosphatidylinositol, PI）/溶血磷脂酰肌醇（lyso-phosphatidylinositol, LPI），磷脂酰甘油（phosphatidylglycerol, PG）/溶血磷脂酰甘油（lyso-phosphatidylglycerol, LPG），甘油单酯（monoacylglycerol, MAG），甘油二酯（diacylglycerol，DAG），甘油三酯（triglyceride, TAG），胆固醇酯（cholesterol ester, CE），神经酰胺（ceramide, CER），二氢神经酰胺（dihydroceramide, DCER），葡萄糖酰神经酰胺（glucosylceramide, HCER），乳酰神经酰胺（lactosylceramide, LCER），鞘脂（sphingolipids, SM）。当前的脂质质谱库可以充分覆盖哺乳动物的血浆、组织和细胞中的常见脂质。另外，针对特定的待测物质，也可直接在MRM列表中添加其它想要检测分析的脂质化合物离子对。

靶向分析结果

在分离的微量细胞中(组织切片约2000 μm^2)，共检测到285个脂质化合物，包括鞘脂SM、胆固醇酯CE、甘油三酯TAG、甘油二酯DAG、磷脂酰乙醇胺PE、磷脂酰胆碱PC、神经酰胺Cer7类（图3）。

对于微量细胞中检测到的脂质化合物的判定，主要基于与空白提取溶剂（阴性对照）和血浆脂质提取样本（阳性对照）共同比较，并且结合各类脂质标准品出峰位置情况、同类脂质化合物有较为接近的出峰位置，而同类脂质化合物连接脂肪酸链越长保留时间越靠后、连接相同碳数的脂肪酸链上不饱和键数越多保留时间越靠前的规律，对微量样本中检出的脂质化合物做定性判断（图4）。

RUO-MKT-02-14573-ZH-A

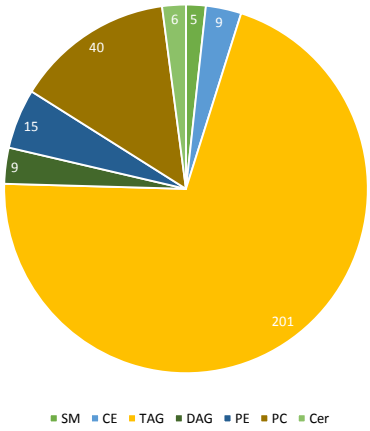

图3. 微量脑组织切片中测得的不同种类脂质化合物的数量。基于LC-MS/MS的靶向脂质组学方法快速分析基质中的多种脂类物质。

小结

- 通过徕卡激光切割显微镜LMD7获取微量样本技术与SCIEX 7500系统高灵敏度检测相结合，实现微量细胞高覆盖靶向脂质组学分析检测。在约2000 μm^2 组织切片样品中检测到脂质化合物数目285个，符合组学分析对化合物覆盖度的需求。
- 徕卡LMD7系统使用“光束移动切割”技术，进行高精度的直接、实时地切割，可以理想地切割任何类型、大小或形状的组织，保证了微量样本的精确获取。
- SCIEX 7500系统优异的灵敏度保证痕量化合物的良好检出，同时高扫描速度使得一针分析能覆盖尽量多的检测通道，保证珍贵的微量样品靶向组学分析成为可能。
- 可将此方案应用于其他细胞切片样本，助力精准代谢组学研究的开展。

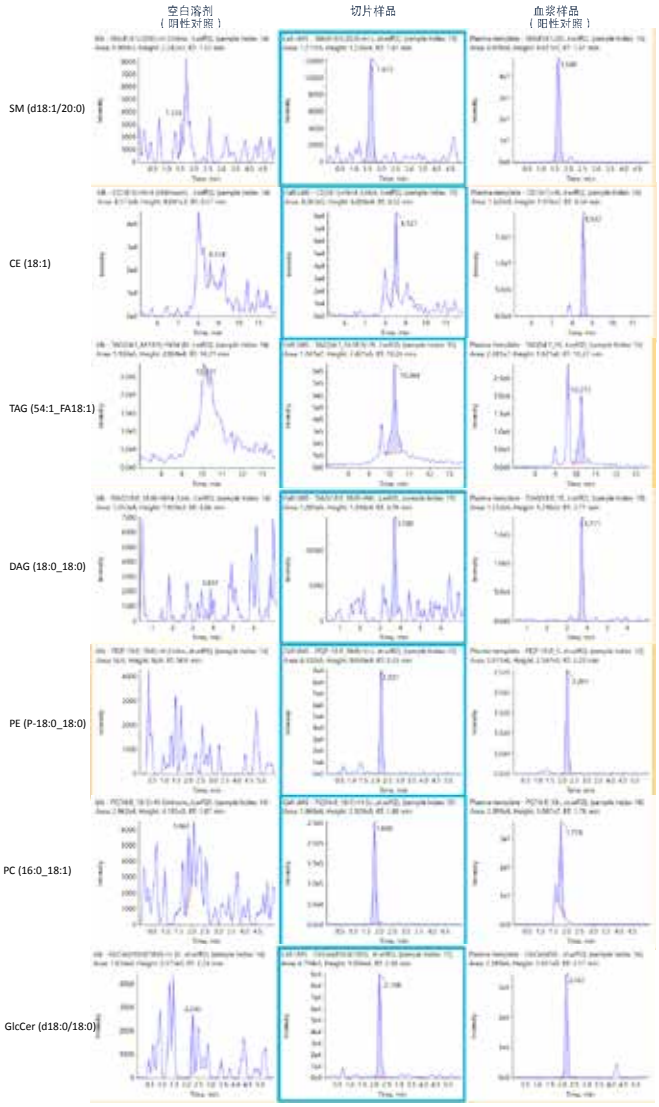

图4. 微量脑组织切片中测得的脂质化合物示例图。通过LC-MS/MS测得的7类脂质化合物在空白提取溶剂中（左）均不存在，而与阳性对照血浆样本（右）中出峰行为一致。

参考文献：

1. Download method information.

RUO-MKT-02-14573-ZH-A

基于激光显微切割-液质联用技术的空间代谢组学分析完整流程

Comprehensive Workflow for Spatial Metabolomics based on Laser Microdissection-LC-MS/MS Method

查海红[1]，钟晨春[1]，龙志敏[1]，高天龙[2]，郭立海[1]

[1] SCIEX中国 应用支持中心；[2] 徕卡生命科学

关键词： comprehensive workflow; spatial metabolomics; laser microdissection; ZenoTOF® 7600

引言

代谢组学作为系统生物学的分支，主要定性定量分析生物体内所有代谢物的含量变化。代谢组学的研究更直观反映生物体的表型，更有利于发现并解释疾病发生的机理。随着代谢组学研究技术的不断更新，空间代谢组学应运而生，满足大家探究更小单元的代谢物差异的需求，比如单个细胞甚至细胞器的差异，以及同一组织不同空间位置的差异。肿瘤是临床研究中最为关注的一个方向，肿瘤器官中不同空间位置的肿瘤微环境是有差异的，这些空间变异也会对临床预后和治疗产生深远影响。通过空间代谢组学能够解决代谢的时空异质性，推动代谢领域向前发展，并能应用到临床，从而阐述体内系统代谢组学变化的机理。

传统代谢组学分析技术受样品空间分辨率以及分析灵敏度的限制，无法精准获取靶向部位，而对其中特异代谢物的差异表征就更加困难。近来，激光显微切割技术（Laser Microdissection, LMD）作为组织微区组学分析前的原位采样技术，受到了广泛认可，利用这项技术可以将样品组织或细胞样品进行精确切割，从而获得特定位点的多细胞或单细胞水平均一的样品（图1）。后续结合高覆盖度和高灵敏度的液质联用检测技术， 将空间定位准确的微区样品进行全面准确的代谢组学分析。相比DNA和RNA，细胞内的蛋白质和代谢物无法扩增，组织微区内提供的用于分析的代谢物浓度低、 体积小，一些极为稀少的代谢物需要更加灵敏的检测方法。高分辨质谱ZenoTOF® 7600系统的Zeno™ trap技术可提供超过90%的占空比循环，显著提升二级质谱灵敏度，提供更加丰富的MS/MS数据，进而提升信息覆盖度。

本文应用徕卡激光显微切割系统结合SCIEX的ZenoTOF® 7600质谱进行空间代谢组学分析，对猪肺组织中感兴趣的区域进行了显微切割，经常规代谢组学前处理后，使用高分辨质谱获得了超过390个代谢物定性信息，作为一套完整的工作流程，可为空间代谢组学相关研究方法提供理论依据，为了解肿瘤发生发展机制，以及为癌症的防御与治疗提供新的视角。

图1. 徕卡激光捕获显微切割采用移动激光的显微切割技术。徕卡显微系统采用高精确度的光学部件并借助棱镜沿着组织上所需的切割线对激光束进行操纵，可垂直于组织实施切割，从而获得切割精确、无污染的分离体。

实验方法

RUO-MKT-02-33006-ZH-A

激光显微切割样品包埋与制备：本次实验选取猪肺组织进行方法开发，切割的面积为40w平方微米，厚度为10微米厚，并在同一张切片选取三个重复区域以进行生物学重复采集与分析。包埋与切割流程如下：

取新鲜的猪肺组织，切成0.5cm左右的方块，放入低温冰箱速冻。1小时后取出，修剪成规则形状，用4度预冷的OCT包裹组织块，粘在冷冻切片机的样品托上，一起放入冷冻切片机冷冻。

切片时，低于室内温度-15℃ ~ -20℃。切片过程中注意保持刀片和样品台干净，及时清理OCT和组织碎屑，减少OCT对组织的粘连。切下的组织用PET frameSlide膜片粘附，放在室温静置10分钟左右。放入LMD进行精确取样。

将制备好的肺组织切片样本置于激光显微切割载物台，接收端放置PCR管，其管盖用于分离体的接收。选择合适的切割面积，调节好相关参数后开始进行切割（图2）。切割完成后，小心将PCR管取出，由管底倒扣至管盖盖紧，防止管盖中收集的样品遗落。

因为粘附在膜片上的标本带有少量OCT，在取样时，分布收集了PBS清洗和未清洗的两组样品，每组3个重复，放入-80℃冰箱保存。

样品提取：装有样品的PCR管在vortex中振荡5s，由点用小型离心机将微量样品离心至管底，小心打开管盖，加入50 µL提取溶液（甲醇:乙腈:水 2:2:1 v/v/v），振荡混匀，低温反复冻融三次，离心后将全部溶液转移至进样小瓶中待LC-MS/MS分析。

LC-MS条件：样品通过ExionLC™系统串联ZenoTOF® 7600系统进行代谢物鉴定分析。详尽分析条件列于表1、2和3。

数据处理：数据通过SCIEX OS 软件3.3中的定性、定量功能（点击“Analytics”）进行处理。

代谢物鉴定

组织中代谢物成分复杂多样，且有较多同分异构体，因此，仅有准确的高分辨一级无法对化合物进行确证。针对大量样本，SCIEX OS软件可自动进行峰提取和搜库，通过一级质量数、同位素丰度和二级碎片的匹配对样本中的代谢物进行鉴别（图3），使筛查流程快速准确。

实验结果

两组样本经过SCIEX OS处理后，在PBS未清洗的样本中共鉴定到400个化合物，在PBS清洗的样本中共鉴定到396个化合物，包括氨基酸类、核苷类、吲哚类、脂肪酸类等。从鉴定个数上，两种收样方式差别不大。于是，进一步比较了两种处理方式采集到的信号响应强弱，以及三个重复间的CV值（图4）。通过比较，PBS未清洗的样本检测的信号响应更高一些，且三个重复间的CV值<30%的代谢物个数更多一些。总体比较下来，建议后续开展相关实验不需要用PBS清洗。

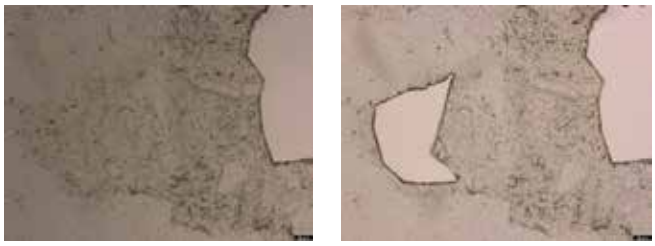

图2. 肺组织切片样本用于激光显微切割分离体制备。未进行切割分离的样品（左）；按需切割任意形状面积的样品（右）。

表1. 色谱条件

参数	数值
色谱柱	HSS T3, 100 × 2.1 mm, 1.8 µm
流动相A	含0.1% FA的水
流动相B	含0.1% FA的乙腈
流速	300 µL/min
柱温	40 ℃
进样体积	10 µL

表2. 梯度条件

时间（min）	流动相A（%）	流动相B（%）
0	99	1
1.5	99	1
13	1	99
16.5	1	99
16.6	99	1
20	99	1

表3. SCIEX 7500系统的质谱参数

参数	数值	参数	数值
气帘气	40 psi	源温度	550 ° C
雾化气	55 psi	辅助气	55 psi
碰撞诱导解离气	7	离子喷雾电压	5500 V/-4500 V
去簇电压	60 V	碰撞能量	30 V

RUO-MKT-02-33006-ZH-A

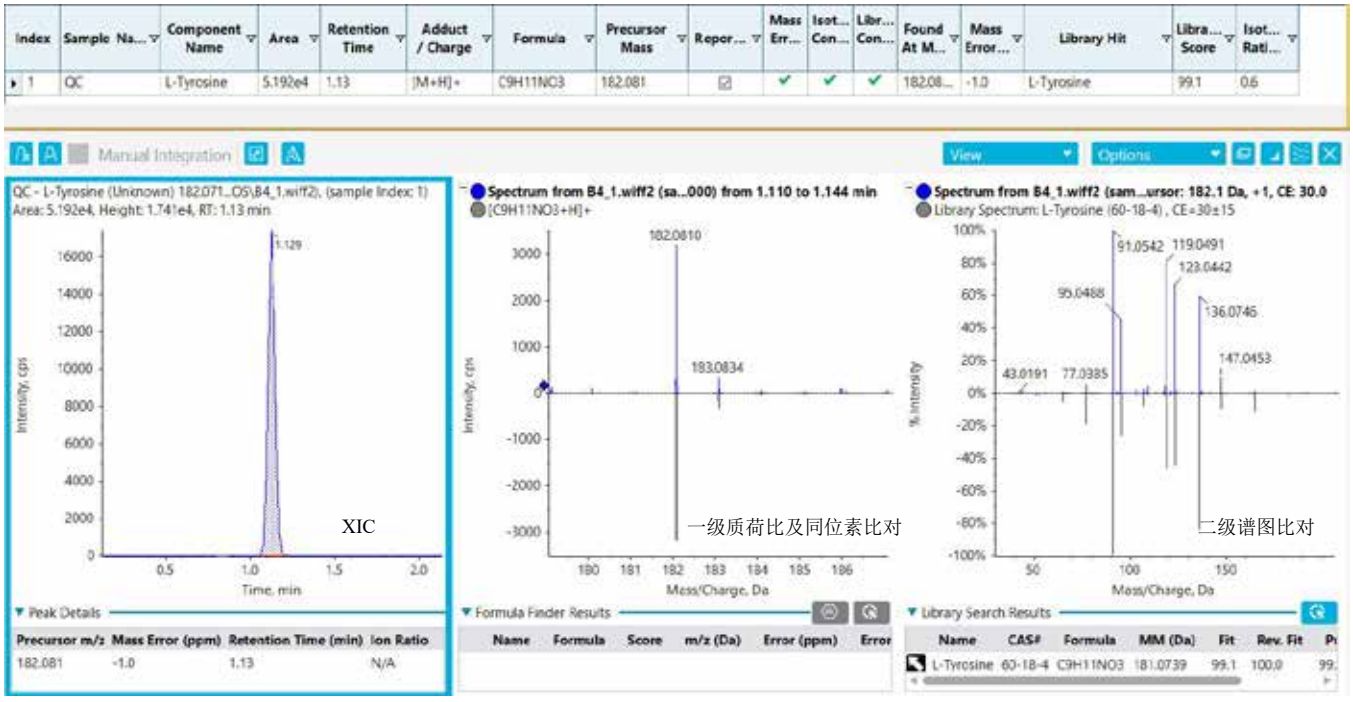

图3. 代谢物鉴定界面示例。以样本中鉴定到的酪氨酸（Tyrosine）为例，酪氨酸分子式为$C_9H_{11}NO_3$，检测到的MS信号与理论质荷比相比，质量数偏差为-1.0 ppm，同位素丰度比与理论值偏差为0.6%，MSMS与代谢物库中酪氨酸的标准谱图匹配度为99.1，以此可判定鉴定到的信号为酪氨酸。

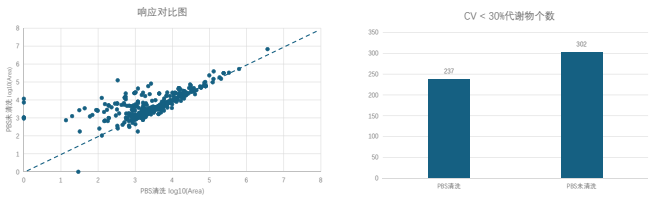

图4. PBS清洗与未清洗样品比较。左图为两种处理方式鉴定到的所有代谢物响应比较图，虚线上方表示未清洗样品含量更高，下方表示清洗样品含量更高；右图为两种处理方式的CV<30%的代谢物个数。

小结

通过对组织切片进行激光显微切割获取空间定位准确的微量样本，并与SCIEX ZenoTOF® 7600系统相结合，实现微量组织样品的全面表征以及高灵敏度组学分析。

- 徕卡激光显微切割系统使用“光束移动切割”技术，进行高精度的直接、实时地切割，可以理想地切割任何类型、大小或形状的组织，保证了微量样本的高通量精确获取。
- 通过不同前处理方式的比较，建议在样品收集过程中不用PBS清洗，保障更多的样品信息获取。
- 可将此套完整方案流程应用于其他组织切片样本，助力空间代谢组学研究的开展。

RUO-MKT-02-33006-ZH-A

基于激光显微切割-液质联用技术的微量样本的高通量分析方法

High Throughput Analysis for Trace samples based on Laser Microdissection-LC-MS/MS Method

查海红[1]，钟晨春[1]，龙志敏[1]，高天龙[1]，郭立海[1]

[1] SCIEX中国 应用支持中心；[2] 徕卡生命科学

关键词： high throughput; trace samples; laser microdissection; ZenoTOF® 7600

引言

代谢组学作为系统生物学的分支，主要定性定量分析生物体内所有代谢物的含量变化。代谢组学的研究更直观反映生物体的表型，更有利于发现并解释疾病发生的机理。肿瘤是临床研究中最为关注的一个方向，肿瘤器官中不同空间位置的肿瘤微环境是有差异的。肿瘤微环境的变化，可能导致不同细胞区室的基因、蛋白表达及信号通路的改变，进而能够影响抗肿瘤免疫和癌症上皮细胞的迁移。针对肿瘤微环境的检测和表征研究也可为癌症治疗提供新的思路。其中代谢谱是免疫微环境的重要调节因子，可能通过影响癌细胞的增殖潜能和适应环境而发挥作用。代谢特征的异质性有助于了解肿瘤免疫微环境的异质性。

传统代谢组学分析技术受样品空间分辨率以及分析灵敏度的限制，无法精准获取靶向部位，而对其中特异代谢物的差异表征就更加困难。近来，激光显微切割技术（Laser Microdissection, LMD）作为组织微区组学分析前的原位采样技术，受到了广泛认可，利用这项技术可以将样品组织或细胞样品进行精确切割，从而获得特定位点的多细胞或单细胞水平均一的样品（图1）。

由于组织微区样本量少，且珍贵，本文提供了一种可以同时收集代谢组和脂质组成分的前处理方式，后续结合高覆盖度和高灵敏度的SCIEX ZenoTOF® 7600质谱系统进行代谢组和脂质组的分析， 将空间定位准确的微区样品进行全面准确的代谢组学分析。本文选用微量猪肺组织实施整套流程，可以检测到395个代谢物和349个脂质，展示了整套流程的可行性，可以实现微量样本的一次取样，一种前处理，同时获得代谢和脂质的全面信息，提升了微量样本检测的覆盖度和通量，为后续微量样本的前处理方法提供参考。

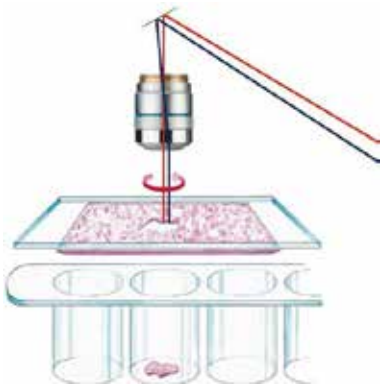

图1. 徕卡激光捕获显微切割采用移动激光的显微切割技术。徕卡显微系统采用高精确度的光学部件并借助棱镜沿着组织上所需的切割线对激光束进行操纵，可垂直于组织实施切割，从而获得切割精确、无污染的分离体。

实验方法

激光显微切割样品制备： 本次实验选取猪肺组织进行方法验证，切割的面积为40w平方微米，厚度为10微米厚，并在同一张切

RUO-MKT-02-33007-ZH-A

片选取三个重复区域以进行生物学重复采集与分析。将制备好的肺组织切片样本置于激光显微切割载物台，接收端放置PCR管，其管盖用于分离体的接收。选择合适的切割面积，调节好相关参数后开始进行切割。切割完成后，小心将PCR管取出，由管底倒扣至管盖盖紧，防止管盖中收集的样品遗落。

样品提取：装有样品的PCR管在vortex中振荡5s，由点甩小型离心机将微量样品离心至管底，小心打开管盖后加提取溶剂。先加入25 µL水，低温反复冻融3次；再加30 µL甲醇和100 µL 甲基叔丁基醚（MTBE）；涡旋，14,000 rpm离心10 min；上层MTBE层取100 µL，吹干，50 µL 甲醇:二氯甲烷 1:1复溶后转移至进样小瓶中待LC-MS/MS分析脂质成分；下层水层取40 µL至进样小瓶中待LC-MS/MS分析代谢成分。

LC-MS条件：样品通过ExionLC™系统串联ZenoTOF® 7600系统进行代谢和脂质成分鉴定分析。详尽分析条件列于表1-6。

数据处理：代谢数据通过SCIEX OS 软件3.3中的定性、定量功能（点击“Analytics”）进行处理，脂质数据结合MSDIAL和SCIEX OS软件鉴定确证。

表1. 代谢组学-色谱条件

参数	数值
色谱柱	HSS T3, 100 × 2.1 mm, 1.8 µm
流动相A	含0.1% FA的水
流动相B	含0.1% FA的乙腈
流速	300 µL/min
柱温	40 ℃
进样体积	10 µL

表2. 代谢组学-梯度条件

时间（min）	流动相A（%）	流动相B（%）
0	99	1
1.5	99	1
13	1	99
16.5	1	99
16.6	99	1
20	99	1

表3. 代谢组学-SCIEX 7600系统的质谱参数

参数	数值	参数	数值
气帘气	40 psi	源温度	550 ℃
雾化气	55 psi	辅助气	55 psi
碰撞诱导解离气	7	离子喷雾电压	5500 V/-4500 V
去簇电压	60 V	碰撞能量	30 V

表4. 脂质组学-色谱条件

参数	数值
色谱柱	Phenomenex Kinetex C18, 100 × 2.1 mm, 2.6 µm
流动相A	含5 mM醋酸铵的甲醇:乙腈:水 (1:1:1 v/v/v)
流动相B	含5 mM醋酸铵的异丙醇
流速	300 µL/min
柱温	45 ℃
进样体积	10 µL

表5. 脂质组学-梯度条件

时间（min）	流动相A（%）	流动相B（%）
0	80	20
0.5	80	20
1.5	60	40
3	40	60
13	2	98
14.5	2	98
14.6	80	20
17	80	20

表6. 脂质组学-SCIEX 7600系统的质谱参数

参数	数值	参数	数值
气帘气	40 psi	源温度	550 ℃
雾化气	55 psi	辅助气	55 psi
碰撞诱导解离气	7	离子喷雾电压	5500 V/-4500 V
去簇电压	80 V	碰撞能量	45 ± 20 V

RUO-MKT-02-33007-ZH-A

实验结果

代谢物鉴定：组织中代谢物成分复杂多样，且有较多同分异构体，因此，仅有准确的高分辨一级无法对化合物进行确证。针对大量样本，SCIEX OS软件可自动进行峰提取和搜库，通过一级质量数、同位素丰度和二级碎片的匹配对样本中的代谢物进行鉴别（图2），使筛查流程快速准确。在代谢组学的样本中共鉴定到395个代谢物，包括氨基酸类、核苷类、吲哚类、脂肪酸类等。

脂质鉴定：脂质数据通过MSDIAL软件鉴定后，在SCIEX OS上进一步确证，共鉴定到349个脂质成分，包括脂肪酸、神经酰胺、甘油磷脂、甘油酯等（图3）。

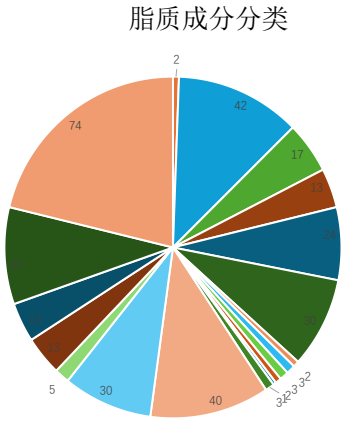

图3. 微量肺组织切片中测得的不同种类脂质化合物的数量。

图2. 代谢物鉴定界面示例。以样本中鉴定到的牛磺酸（Taurine）为例，牛磺酸分子式为$C_2H_7NO_3S$，检测到的MS信号与理论质荷比相比，质量数偏差为-2.0 ppm，同位素丰度比与理论值偏差为1.2%，MSMS与代谢物库中牛磺酸的标准谱图匹配度为100，以此可判定鉴定到的信号为牛磺酸。

RUO-MKT-02-33007-ZH-A

小结

- 本文采用MTBE:CH_3OH:H_2O (10:3:2.5 v/v/v)的提取溶剂，同时获得微量样本的代谢成分与脂质成分用于后续分析，提高了微量样本的检测通量和覆盖度。
- 本文通过对组织切片进行激光显微切割获取空间定位准确的微量样本，并与SCIEX ZenoTOF® 7600系统相结合，实现微量组织样品的全面表征以及高灵敏度组学分析。
- 对于同一微量样本提取的代谢和脂质组分，经过质谱检测和分析，分别能鉴定到超过300个的代谢物和脂质成分，证明了该方法运用到组学研究的可靠性。
- 可将此套完整提取分析方案应用于其他微量组织切片样本，助力空间代谢组学研究的发展。

RUO-MKT-02-33007-ZH-A

空间代谢组学方法表征肿瘤微环境异质性

Spatial metabolomics method to characterize heterogeneity in tumor micro-environment

钟晨春，龙志敏，郭立海

SCIEX中国，应用支持中心

Keywords: spatial omics; metabolomics; lipidomics; heterogeneity; tumor micro-environment; laser microdissection; ZenoTOF™ 7600

肿瘤的发展除了与癌细胞自身基因突变导致的恶性增殖有关以外，还与肿瘤微环境息息相关。在癌症中，正常组织中和谐的细胞相互作用关系被破坏，原本保护正常细胞生存的微环境在肿瘤细胞的影响下，逐渐演变成适应肿瘤生长的条件。肿瘤微环境的变化，可能导致不同细胞区室的基因、蛋白表达及信号通路的改变，进而能够影响抗肿瘤免疫和癌症上皮细胞的迁移。针对肿瘤微环境的检测和表征研究也可为癌症治疗提供新的思路。

肿瘤微环境的特征主要由肿瘤和非肿瘤成分决定。它们的定位或丰度/活性在空间上是不同的，包括抑制性免疫检查点的表面表达、免疫抑制或促炎细胞因子的分泌、免疫抑制或效应细胞的浸润、血管系统的状态、边缘区域的空间距离，以及代谢营养素的分布。这些空间变异也会对临床预后和治疗反应产生深远影响。代谢谱是免疫微环境的重要调节因子，可能通过影响癌细胞的增殖潜能和适应环境而发挥作用。代谢特征的异质性似乎有助于肿瘤免疫微环境的异质性。

传统分析技术受样品空间分辨率以及分析灵敏度的限制，无法精准获取靶向部位，而对其中特异代谢物的差异表征就更加困难。组织切片伴随着显微镜技术等的发展而得到广泛的应用，而激光显微切割（LMD, laser microdissection）技术可以方便地对特定的组织区域的精确分离。结合高灵敏度的液质联用检测技术，从而将空间定位准确的微区细胞代谢谱进行全面准确的表征。

实验方法

样品制备：由制备好的肿瘤组织切片样本置于徕卡LMD7激光显微切割载物台；接收端放置PCR管，其管盖用于分离体的接收。在确定好焦距平面后，将视野移动到空白区域，进行激光切割位置校准，再将视野移动到待切割的细胞区域；选择合适切割面积（~20,000 μm^2）开始进行切割（图1）。切割完成后，小心将PCR管取出，由管底倒扣至管盖盖紧，防止管盖中收集的样品遗落。共收集到来自10个病人的原位癌（25份）、浸润癌（18份）、癌旁组织（13份）样本共46份，每一份在平行的两张张切片上同样位置分别收集作为代谢组学和脂质组学分析。

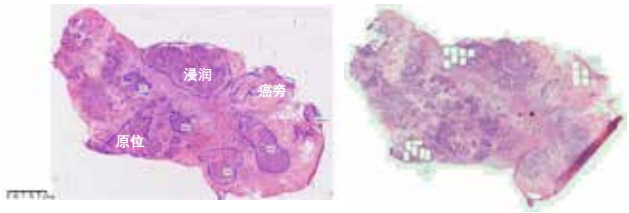

图1. 组织切片样本用于激光显微切割分离体制备。经过苏木精-伊红（HE）染色确定组织切片中不同类型的细胞区域（左）包括原位癌、浸润癌和癌旁细胞，在平行的未染色组织切片中的相应位置进行激光显微切割获得分离体（右）。

样品提取：装有样品的PCR管在vortex中振荡5s，由小型离心机将微量样品离心至管底，小心打开管盖，加入50 μL提取溶液（代谢组学样本:甲醇:乙腈:水 2:2:1, v/v；脂质组学样本:二氯甲烷:甲醇 1:1, v/v），振荡混匀，超声15 min，离心后将全部溶液转移至进样小瓶中待LC-MS/MS分析。

LC-MS条件：样品通过ExionLC™系统串联SCIEX ZenoTOF™ 7600系统进行代谢物鉴定和差异代谢物分析。

数据处理：数据通过SCIEX OS 软件3.1中的定性、定量功能（点击“Analytics”）进行处理。

RUO-MKT-02-15648-ZH-A

表1. 代谢组学-色谱条件

参数	数值
色谱柱	Phenomenex Kinetex F5, 150 × 2.1 mm, 2.6 µm
流动相A	含0.1%甲酸的水
流动相B	含0.1%甲酸的乙腈
流速	200 µL/min
柱温	40 ℃
进样体积	10 µL

表2. 代谢组学-梯度条件

时间（min）	流动相A（%）	流动相B（%）
0	100	0
1	100	0
13	2	98
14	2	98
14.1	100	0
18	100	0

表3. 脂质组学-色谱条件

参数	数值
色谱柱	Phenomenex Kinetex C18, 100 × 2.1 mm, 2.6 µm
流动相A	含2 mM乙酸铵的甲醇
流动相B	含2 mM乙酸铵的甲醇:二氯甲烷 (2:1, v/v)
流速	300 µL/min
柱温	45 ℃
进样体积	10 µL

表4. 脂质组学-梯度条件

时间（min）	流动相A（%）	流动相B（%）
0	95	5
1	95	5
13	2	98
14	2	98
14.1	95	5
17	95	5

表5. SCIEX ZenoTOF™ 7600系统的质谱参数

参数	数值	参数	数值
气帘气	35 psi	源温度	350 ℃
雾化气	55 psi	辅助气	55 psi
碰撞诱导解离气	9	离子喷雾电压	5500 V/-4500V
去簇电压	60 V	碰撞能量	35 ± 15 V

代谢物鉴定

组织细胞中代谢物成分复杂多样，且有较多同分异构体，因此，仅有准确的高分辨一级无法对化合物进行确证。针对大量样本，SCIEX OS软件可自动进行峰提取和搜库，通过一级质量数、同位素丰度和二级碎片的匹配对样本中的代谢物进行鉴别（图2），使筛查流程快速准确。在代谢组学的样本中共鉴定173个化合物，包括氨基酸类、核苷类、吲哚类、脂肪酸类等。

图2. 代谢物鉴定界面示例。以样本中鉴定到的脯氨酸（Proline）为例，Proline分子式为$C_5H_9NO_2$，检测到的MS信号与理论质荷比相比，质量数偏差为-0.3ppm，同位素丰度比与理论值偏差为1.3%，MSMS与代谢物库中Proline的标准谱图匹配度为100，以此可判定鉴定到的信号为Proline。

在脂质组学分析样本中共鉴定到550个脂质化合物，基于ZenoTOF™ 7600系统特有的电子活化解离（EAD）碎裂模式，可以鉴定出其中一些脂质化合物的精细结构，如脂肪酸链连接的具体位置（sn1或sn2）以及连接的不饱和脂肪酸双键的具体位置（图3）；对于样本中检测到的脂质化合物包括固醇酯类、神经酰胺类、溶血磷脂胆碱类、磷脂胆碱类、溶血磷脂乙醇胺类、磷脂乙醇胺类、磷脂肌醇类、磷脂丝氨酸类、鞘酯类、甘油二酯类、甘油三酯类。

RUO-MKT-02-15648-ZH-A

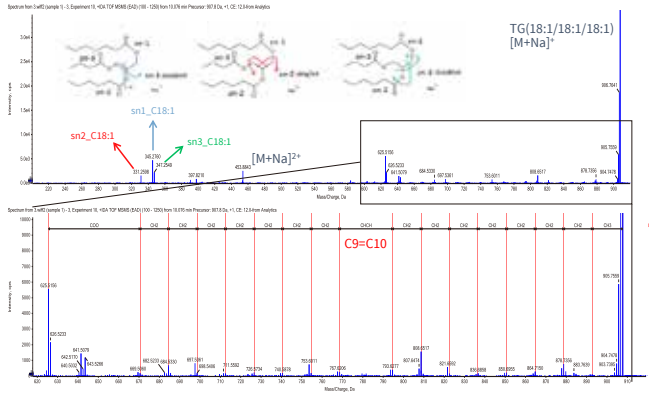

图3. 脂质化合物精细结构鉴定示例。以甘油三酯TG (18:1/18:1/18:1)为例，在EAD碎裂模式下，化合物[M+Na]+峰可以产生特征的碎片离子，帮助解析甘油三个羟基各自所连接的脂肪酸组成，以及在高质荷比区域产生的连续CH2断裂碎片确定不饱和键的位置（C9和C10间为双键）。

差异代谢物分析

在质控样本（quality control, QC, 所有样本等体积混合，整个分析批次中每6个样本穿插一针QC样本进样）中化合物峰面积RSD%不超过30%（n=8），在代谢组学样本中共检出100个代谢物，脂质组学样本中共检出502个代谢物，并将这些化合物在所有的样本包括原位癌组织、浸润癌组织、癌旁组织进行峰面积提取。

将获得的各种组织中化合物含量信息进行生物统计学分析，以浸润癌组织v.s.癌旁组织为例，寻找表征区分这两种组织的差异代谢物。以t-检验p-value值小于0.05以及PLSDA分析VIP值不小于1作为筛选条件，对这两种组织的区分，共找到84个差异代谢物（图4）。经过后续进一步生物学验证，确定的差异代谢物可以帮助开展癌细胞在空间定位及异质性的精准区分工作，更好的理解例如肿瘤转移的起源和发展、侵袭能力、对药物的敏感性等方面的特点，从而制定个体化的精准治疗方案。

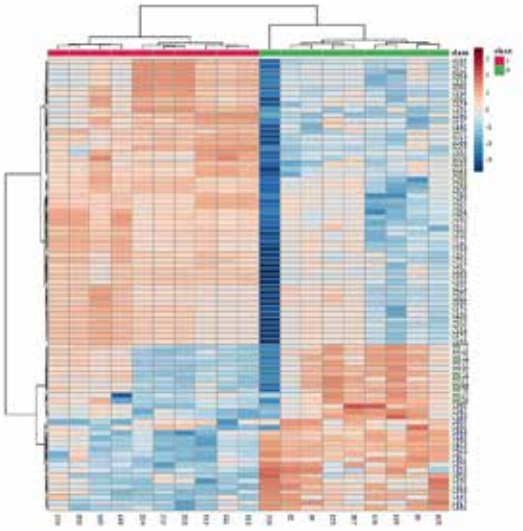

图4. 浸润癌组织v.s.癌旁组织中的差异代谢物热图。通过统计学分析，包括t-test的p值小于0.05以及PLSDA计算的VIP值不小于1作为筛选条件，获得了84个差异代谢物。

小结

- 通过对组织切片进行激光显微切割获取空间定位准确的微量样本，并与SCIEX ZenoTOF™ 7600系统相结合，实现微量细胞水溶性和脂溶性代谢物的全面表征以及高灵敏度组学分析。
- 徕卡LMD7系统使用“光束移动切割”技术，进行高精度的直接、实时地切割，可以理想地切割任何类型、大小或形状的组织，保证了微量样本的高通量精确获取。
- SCIEX ZenoTOF™ 7600系统对代谢物可以进行精准全面的鉴定，尤其是特有的EAD碎裂技术，可以对例如脂质化合物的精细结构进行解析，获取更精准的定性信息。
- 可将此方案应用于其他组织切片样本，助力空间组学研究的开展。

RUO-MKT-02-15648-ZH-A

MEMI原位同步离子化成像系统结合SCIEX高分辨质谱应用于植物组织切片的空间代谢组学

Application of MEMI Desorption Electrospray Ionization System and SCIEX High Resolution Mass Spectrometry in Imaging Metabolomics of Plant section

肖梦晴； 钟晨春；龙志敏；刘冰洁
Xiao Mengqing; Zhong Chenchun; Long Zhimin; Liu Bingjie

SCIEX应用支持中心（上海）
SCIEX Application and Support Center (Shanghai)

Key words: imaging mass spectrometry, plant section, MEMI, spatial metabolomics

引言

MEMI原位同步离子化成像系统是基于电喷雾电离原理的常压离子化技术，可以通过对原位固相样品的分析，检测样本中代谢物的相对含量，并进行分子成像。MEMI的原理是通过直流高压电使溶剂带上过量电荷，雾化气一边干燥溶剂，使带电液滴表面电荷密度增加，发生库伦爆炸，一边将带电液滴喷射至样品表面，并与表面分析物产生质子转移反应，从而产生分子离子，进入质谱产生电喷雾信号（图1）。

质谱成像技术在揭示天然产物的时空分布和代谢物-基因关系方面均可发挥重要作用，也就是说，质谱成像技术能够对复杂植物组织进行高分辨率的空间化学分析，进而将植物组织中的代谢物在空间层面的分布可视化，有助于揭示植物代谢产物的形成机制和生物合成机制等。

本文通过MEMI原位同步离子化成像系统与SCIEX ZenoTOF® 7600高分辨质谱系统联合，对组织切片样本进行原位质谱成像检测，以检测到的化合物的峰面积的强弱进行可视化图像分析，实现对复杂植物组织进行高分辨率的空间化学分析，有助于研究天然产物生物合成及代谢变化等。

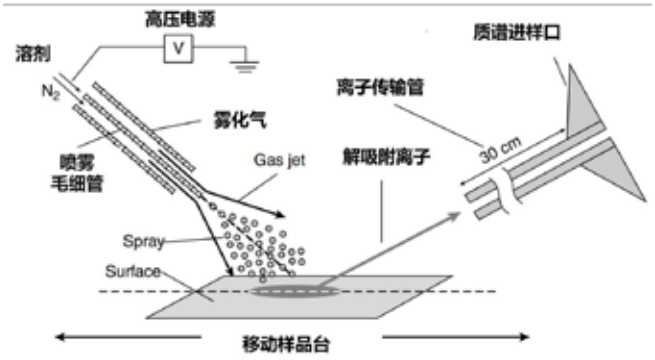

图1. MEMI工作原理示意图

方法特点

本方法在成像过程中无需使用基质，也不需要复杂的样品制备过程，可保持样品形态无损。使用时，仅需移除质谱的电喷雾离子源，无需卸真空或重启质谱，即可方便快速的换上MEMI成像源，进行成像分析。实验完成后，仅需几分钟即可还原为液相色谱 - 质谱仪。可灵活搭配高分辨质谱和三重四极杆质谱，完成定性或定量工作。

MKT-34548-A

仪器设备

MEMI原位同步离子化成像系统 + ZenoTOF® 7600高分辨质谱系统

方法条件

1. 质谱检测一级质量范围TOF MS, m/z 100-1000, accumulation time, 0.25 s
2. 质谱源气参数：IS电压，3000 V（-3000 V）；碰撞气，7
3. MEMI气流：1 mPa 高纯氮气
4. MEMI溶剂：含0.1% 三氟乙酸的甲醇溶液，流速10 µL/min
5. 空间分辨率：100 µm

实验结果

1.MEMI成像操作流程

MEMI设备与ZenoTOF® 7600连接完成后，需要通过对喷针位置的调整，使信号响应达到最佳。调试时，首先打载液泵开关，确保喷针中喷雾正常，然后使用具有稳定分子量化学成分的载玻片，打开质谱方法，通过调整垂直、水平、高度、倾角旋钮调整喷针位置，使TOF MS中信号达到相对稳定且较高的响应。调试完成后，待测切片置于样品台，对载玻片上的样本切片进行定位，设置起始和终止位点，保证样本切片完全置于定位区域中。定位完成后，需要设置扫描参数，样品台位移速度及行距，位移速度决定了X轴方向的成像分辨率，行距决定了Y轴方向的成像分辨率。设置完成后进行复位-定位操作，使喷针重新位于扫描起始点，即可开始质谱数据采集。

2.植物组织切片成像分析

在进行成像分析之前，先对该部位组织进行常规的代谢组学前处理，通过液相质谱联用系统进行定性分析，所得鉴定结果作为基础代谢物数据库，成像所得信息通过数据库进行质荷比匹配定性，本实验中成像的样本为银杏根茎切片，成像检测中，化合物的金属加合物响应更高，在银杏根茎中存在的白果内酯、银杏内酯等天然成分均可检出（图2）。

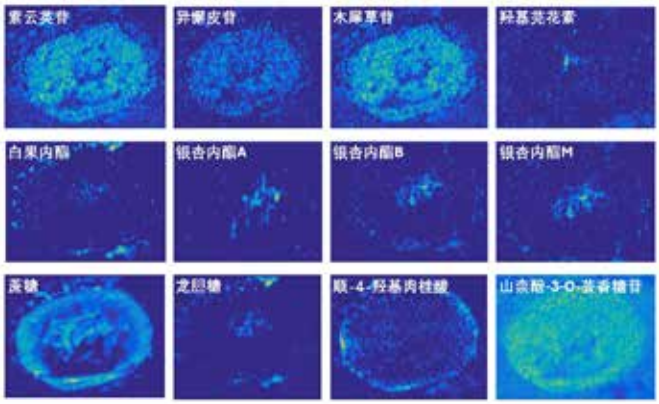

图2. 部分代谢物在银杏叶根茎组织切片中的成像图

小结

本文采用MEMI原位同步离子化成像系统和ZenoTOF® 7600高分辨质谱系统对植物组织切片中多种代谢物进行快速原位分析，为银杏根茎中的天然产物提供了空间分布信息，实现了对植物组织进行高分辨率的空间化学分析，为植物组织中代谢物合成途径的调控机制提供了一个更加直观的解决思路，该应用可扩展至植物的生长发育、抗逆机制、病虫害防治以及植物与环境的相互作用等研究。

MKT-34548-A

MEMI原位同步离子化成像系统结合SCIEX高分辨质谱应用于小鼠组织切片的空间代谢组学

Application of MEMI Desorption Electrospray Ionization System and SCIEX High Resolution Mass Spectrometry in Imaging Metabolomics of Mouse tissue section

肖梦晴； 钟晨春；龙志敏；郭立海
Xiao Mengqing; Zhong Chenchun; Long Zhimin; Guo Lihai

SCIEX应用支持中心（上海）
SCIEX Application and Support Center (Shanghai)

Key word: Phospholipid, Phosphatidic Acid, Phosphatidylserine, imaging mass spectrometry

引言

质谱成像技术是一种结合了质谱分析和影像分析的分子成像技术，待测样本制备成切片进行数据采集，在获取样本中不同化合物丰度信息的同时，还可以直接的获得其空间分布信息。质谱成像技术按照技术分类主要分为三种：基质辅助激光解析电离质谱成像（MALDI）、二次离子质谱成像（SIMS）和解析电喷雾电离质谱成像（DESI）。

MEMI原位同步离子化成像系统是基于电喷雾电离原理的常压离子化技术，可以通过对原位固相样品的分析，检测样本中代谢物的相对含量，并进行分子成像，在动植物组织的内源性代谢物、药物及其代谢物、多肽、脂质等分布分析（如区分癌组织和癌旁组织），或材料表面残留物或污染物分析（如潜指纹成像）方面具有优良的表现。MEMI的原理是通过直流高压电使溶剂带上过量电荷，雾化气一边干燥溶剂，使带电液滴表面电荷密度增加，发生库伦爆炸，一边将带电液滴喷射至样品表面，并与表面分析物产生质子转移反应，从而产生分子离子，进入质谱产生电喷雾信号（图1）。

本文通过MEMI原位同步离子化成像系统与SCIEX ZenoTOF® 7600高分辨质谱系统联合，对组织切片样本进行原位质谱成像检测，以检测到的化合物的峰面积的强弱进行可视化图像分析，通过对不同化合物的图像比对，发现原位差异代谢物，为传统代谢组学分析提供一个全新的可视化视角，有助于获得更精确的代谢信息，发现更深层的潜在生物标志物。

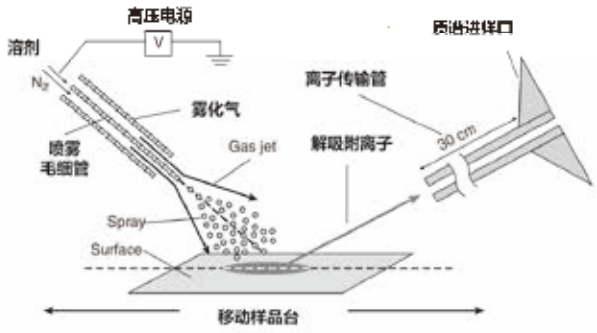

图1. MEMI工作原理示意图

方法特点

1. 本方法在成像过程中无需使用基质，也不需要复杂的样品制备，可保持样品形态无损。使用时，仅需移除质谱的电喷雾离子源，无需卸真空或重启质谱，即可方便快速的换上MEMI成像源，进行成像分析。实验完成后，仅需几分钟即可还原为液相色谱-质谱仪。可灵活搭配高分辨质谱和三重四极杆质谱，完成定性或定量工作。

MKT-33672-A

2. MEMI通过样品台的移动，使样品的不同位置被电离进入质谱系统，形成质谱图，获得样品的成像信息。相比传统的解吸附电喷雾离子源，MEMI通过精确同步电喷雾的启动和暂停，有效地使分析物离子产生与质谱的离子注射时间同步，最大化离子利用率，从而提高灵敏度，扩展可覆盖的分析物数量。

仪器设备

MEMI原位同步离子化成像系统 + ZenoTOF® 7600高分辨质谱系统

方法条件

1. 质谱检测一级质量范围TOF MS, m/z 100-1000, accumulation time, 0.25 s
2. 质谱源气参数：IS电压，3000 V（-3000 V）；气帘气CUR，35 psi；雾化气GS1，20 psi；辅助气GS2，0；离子源温度为0；碰撞气，7
3. MEMI气流：1 mPa 高纯氮气
4. MEMI溶剂：含0.1% 甲酸的甲醇溶液，流速10 µL/min
5. 空间分辨率：100 µm

实验结果

1. 小鼠组织脂质成像

脂质在能量存储、细胞膜形成和细胞信号通路方面发挥着重要作用，并且在癌症、神经系统疾病和免疫疾病均涉及大量脂质的异常代谢。因此，研究生物组织中脂质的相对含量和空间分布，将有助于发现人类疾病的生物标志物。有些脂质在组织中丰度较低或电喷雾过程中离子化效率低，难以检测，或者产生大量钠、钾加合离子，造成质谱峰分裂，不利于谱图解析和后续定量分析，因此需要进一步提高检测灵敏度、简化谱图。本实验中使用0.1%甲酸添加到甲醇喷雾溶剂中，使提高了脂质在MEMI中的离子化效率，图2为使用该方法检测磷脂酰丝氨酸的部分结果，本次实验共检测到89种PS。

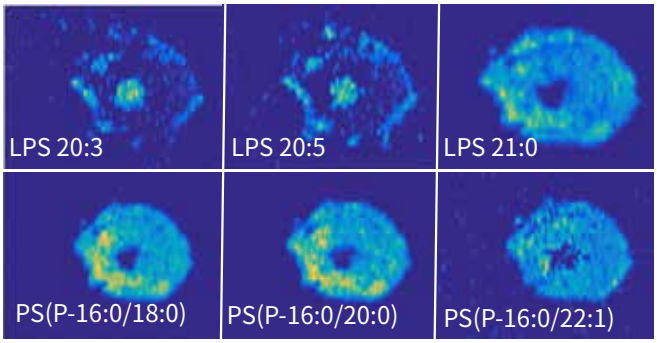

图2. 部分磷脂酰丝氨酸PS在小鼠组织切片中的成像图

2. 野生型（WT）和基因敲除型（KO）小鼠脑组织切片差异代谢物分析

上文中通过对溶剂的优化明显提高代谢物的灵敏度，扩展可覆盖的分析物数量，有了这一基础，接下来我们进一步在野生型和基因敲除型小鼠的脑组织切片中进行质谱成像分析，旨在通过质谱成像技术快速发现在不同基因型小鼠样本中，是否存在差异代谢物。WT样本中共检测到164种物质，KO样本中共检测到178种物质，其中大部分脂质的检出和分布在两者中一致性较高，部分物质存在差异性。图3可以直观的看到差异化合物在WT和KO组中的分布情况，以及在脑组织切片中不同区域的分布情况。

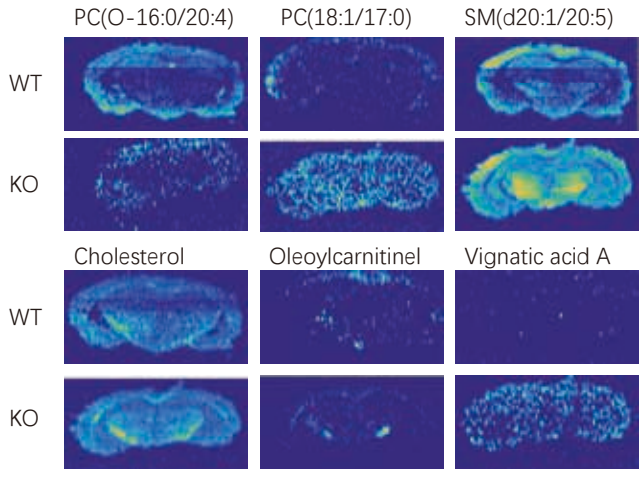

图3. WT和KO组小鼠脑组织切片差异化合物分布情况对比

MKT-33672-A

小结

本文采用MEMI原位同步离子化成像系统和ZenoTOF® 7600高分辨质谱系统对动物组织切片进行快速原位定性分析，通过酸增强模式提升信号，进而提升了代谢物的成像效果，并通过对野生型和基因敲除型小鼠脑组织切片的分析，发现了在两个样本之间存在明显空间分布差异的代谢物，验证了MEMI可以作为可靠的非靶向分析差异化合物的方法，为代谢组学分析提供一个更加直观的解决思路。

MKT-33672-A

基于SinCell-100 —— Zeno TOF® 7600平台的单细胞代谢组学分析完整流程

Complete process of single cell metabolomics analysis based on SinCell-100 and Zeno TOF® 7600 platform

陈俊苗[1]，娄港归[2]，陈安琪[2]，司丹丹[1]，龙志敏[1]，刘冰洁[1]
Junmiao Chen[1], Ganggui Lou[2], Anqi Chen[2], Dandan Si[1], Zhimin Long[1], Bingjie Liu[1]

[1] *Sciex 应用技术中心，中国*
[2] *宁波华仪宁创智能科技有限公司，中国*

Key word: Single cell; metabolomics; Zeno TOF® 7600; Sincell-100;

引言

代谢组学作为系统生物学的分支，旨在定性定量分析生物体内所有代谢物的含量变化。传统的代谢组学技术以群体细胞作为研究对象，但细胞之间存在显著的异质性。在群体细胞分析的策略框架下，任一独立细胞的特征属性可能被群体细胞的平均属性掩盖，难以满足全面而精准的评价需求。

单细胞代谢组学是代谢组学发展的前沿。单细胞代谢组学以细胞中代谢物信息为切入点，在单个细胞精度实现了细胞亚群的精准分析，能够揭示过去由于群体细胞采样而被掩盖和遗漏掉的重要信息，使研究者对生物体模型的探索更准确和全面。然而，由于代谢物无法扩增，且单个细胞能够提供的用于分析的代谢物浓度极低，使得单细胞中代谢物的准确分析难度极大。另外，单细胞分析方法学的复杂性也为单细胞代谢组学的分析研究带来诸多困难。

本文建立了基于SCIEX Zeno TOF® 7600 和华仪宁创SinCell-100的单细胞质谱检测平台，实现了高灵敏、高通量的单细胞代谢分析。华仪宁创SinCell-100采用萃取式技术路线，可全自动地完成亚微米级单细胞定位、皮升级萃取、皮升电喷雾离子化等环节。SCIEX Zeno TOF® 7600系统的Zeno™ trap技术可提供超过90%的占空比循环，显著提升二级质谱灵敏度，提供更加丰富的MS/MS数据，进而提升单细胞代谢组学覆盖度。另外，基于该单细胞平台对膀胱癌耐药性进行了研究，建立了一套完整的单细胞代谢组学分析流程，为探索膀胱癌发生发展机制、药物的干预与治疗提供全新的视角。

单细胞检测平台特点：

- SinCell-100全自动单细胞前处理系统具有单细胞定位、皮升级萃取、皮升级电喷雾功能，提升了单细胞代谢分析前处理环节的效率和稳定性。
- Zeno TOF® 7600拥有高分辨多重反应检测（MRM^{HR}）扫描技术、Zeno™ trap技术，显著提升了二级质谱灵敏度，提供更加丰富的MS/MS谱图信息。
- 基于SinCell-100 —— Zeno TOF® 7600单细胞质谱检测平台，在膀胱癌单细胞中检出260余种代谢物，为膀胱癌耐药细胞的表征与鉴别提供了数据支撑。
- 此套应用方案具备较强的普适性，可迁移应用于其他对于单细胞代谢组学有需求的生命科学和临床医学场景，助力研究者开展高水平研究工作。

图1. 单细胞质谱仪器平台架构 SinCell全自动单细胞前处理系统负责单细胞定位、代谢物萃取、皮升电喷雾；SCIEX Zeno TOF® 7600系统负责高分辨质谱谱图采集。

MKT-33682-A

实验方法

总体实验流程

膀胱癌单细胞的代谢分析流程如图2所示。总体流程包括细胞样本的采集和制备、单细胞代谢检测、数据分析等环节。具体包括：

取对数生长期的单细胞，加入适量胰酶消化1 min，加入3 ml培养基吹打细胞，使贴壁细胞脱落；以2000 rpm转速4℃离心5 分钟；弃掉上清；加入5 mL专用缓冲液溶液，轻缓吹打并洗涤细胞；重复上述离心、洗涤步骤2次，重悬并制备1 mL细胞悬浮液；显微计数，将细胞悬浮液浓度稀释至10^4cells/mL，吸取上述细胞悬浮液，采用甩片法或沉降法制备细胞涂片；使用10倍显微镜检查细胞涂片，确认已获得清晰可见的单细胞形态且干扰杂质较少。完成制片后，将样品上机检测。（注：其他类型的样本，例如组织解离细胞、流式分选细胞等，均可按各自处理流程先制备成细胞悬浮液，再参照上述流程制备细胞涂片并样品上机检测。）

图2. 膀胱癌单细胞代谢分析流程 通过细胞培养制备、单细胞代谢物提取、单细胞代谢物检测及数据分析等流程，实现单细胞代谢物的全流程分析。

SinCell-100单细胞前处理条件

采用华仪宁创SinCell-100全自动单细胞前处理系统进行采样，参数如下：萃取液加载时间：2s；萃取液调控压力：200mbar；萃取时间：2s；电喷雾模式：正离子模式；电喷雾电压：+2.5kV；电喷雾时长：40s。

Zeno TOF® 7600质谱条件

采用MRM^{HR}模式，靶向正离子采集，累积时间Accumulation time：100ms；TOF MS扫描范围Scan range：100-1000m/z；雾化气GAS1：0 psi；辅助气GAS2：0 psi；气帘气Curtain GAS：0 psi；源温度Ion Source Temperature：0 ℃。Zeno Trap开启，部分MRM^{HR}参数见表1。

表1. 部分靶向代谢物检测参数

Name	TOF MS	TOF MSMS	DP	CE
Choline	104.1	60.0809	50	21
Creatinine	114.1	44.0494	50	14
Proline	116.1	70.0656	50	13
L-Valine	118.1	72.0807	40	15
Cysteine	122	58.995	50	29
Creatine	132.1	90.0552	50	14
L-Isoleucine	132.1	69.0697	30	30
Leucine	132.1	86.0965	50	13
Dl-Asparagine	133.1	87.0995	40	13
Glycerophosphocholine	258.1	104.1073	50	16
Glutathione	308.1	162.0218	50	21
AMP	348.1	136.0621	50	21
NAD	664.1	428.0369	50	32
NADP	744.1	136.0611	50	50
Pyruvate	87	43.0207	-50	-20
Lactate	89	43.0212	-50	-16
Fumaric Acid	115	45.0005	-50	-13
Succinate	117	72.9723	-50	-12
Taurine	124	79.9598	-50	-18
Oxaloacetate	131	86.9965	-50	-14
Malate	133	115.0063	-50	-14
Isocitrate	191	117.0213	-50	-19
Citrate	191.1	87.0114	-50	-22
D-Gluconate	195	129.0221	-50	-17
Uridine	243	111.0069	-50	-21
D-Glucose 6-Phosphate	259	138.9447	-50	-40
Glutathione	306	143.0477	-50	-19

实验结果

本次实验分别构建并培养了两组膀胱癌细胞系，分别为TCCSUP (人膀胱癌细胞) 和TCCSUP-CDDP（顺铂耐药的人膀胱癌细胞）。待细胞生长稳定后，制备单细胞涂片进行单细胞质谱检测。

采用高分辨多重反应检测（MRM^{HR}）扫描方法对膀胱癌细胞进行单细胞靶向代谢检测，基于质谱峰精确离子质量的母子离子对匹配（图3），同时与空白对照比较，共检测出260余种明确细胞来源的靶向代谢物质，详细代谢物参数设置如表1所示。

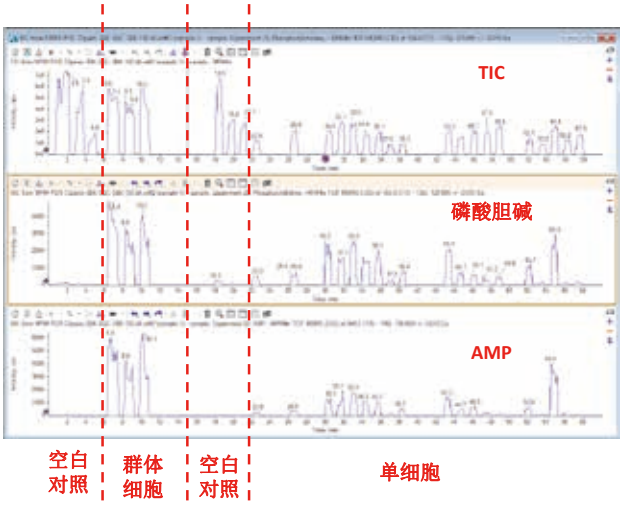

图3. 单细胞代谢物检出 与空白对照相比，群体细胞和单细胞中均可以显著检出细胞来源的代谢物，如磷酸胆碱、AMP、肌酸、腺苷、谷胱甘肽等。

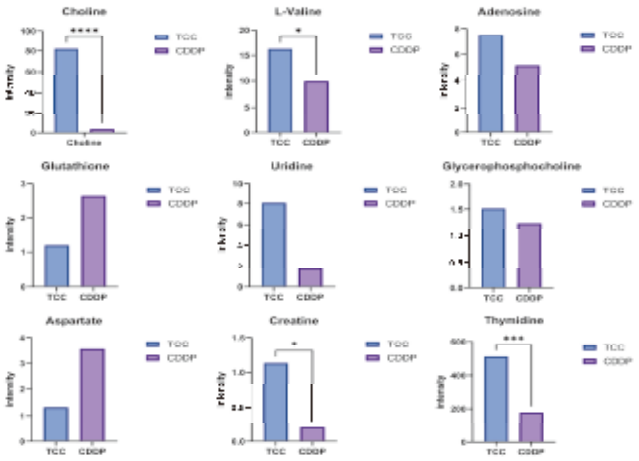

图4. 单细胞代谢物的分布特征 部分代谢物在TCCSUP 和 TCCSUP-CDDP两类细胞中相对含量的分布特征。

基于扫描模式，可通过单个细胞水平对不同亚型的膀胱癌细胞进行代谢分析，提取每个单细胞的代谢特征离子进行OPLS-DA聚类分析。结果显示，TCCSUP 和 TCCSUP-CDDP的两类细胞亚型之间存在着显著的代谢差异（图5），基于数据降维和火山图分析，分别从两组数据中筛选到了多种差异代谢物，可以实现TCCSUP 和TCCSUP-CDDP两组细胞的准确分型。

通过SCIEX OS软件提取每个单细胞中目标代谢物离子的平均强度，该强度可用于代谢物的相对定量。如图4所示，提取并计算相关代谢物的含量及分布特征。靶向检测的代谢物中Choline、L-Valine、Adenosine、Uridine、Creatine、Glycerophosphocholine和Thymidine在TCCSUP组中的含量高于TCCSUP-CDDP组，Glutathione和Aspartate在TCCSUP组中的含量低于TCCSUP-CDDP组。其中Choline、L-Valine、Creatine和Thymidine存在显著的统计学差异（$p<0.05$）。

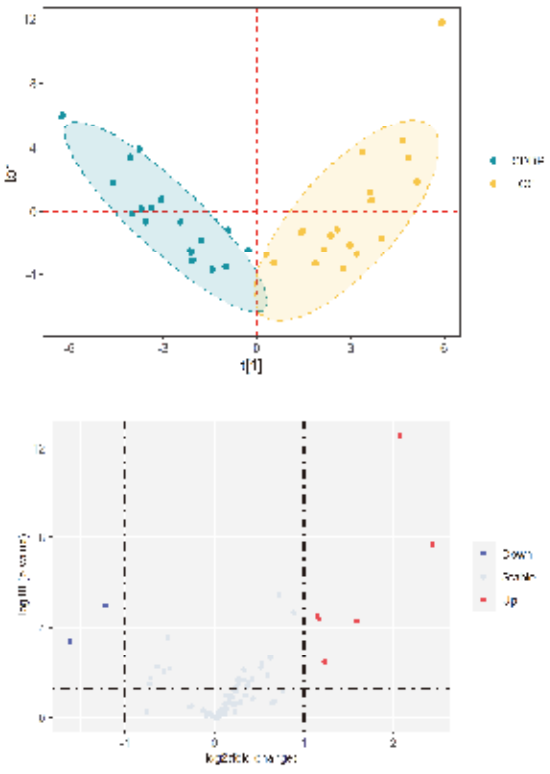

图5. TCCSUP 和 TCCSUP-CDDP的单细胞代谢差异分析 通过OPLS-DA的聚类结果（左图）可以有效区分两组细胞，基于火山图（右图）可筛选到存在显著差异的差异代谢物。

MKT-33682-A

总结

本研究建立了SinCell-100和Zeno TOF® 7600联用的单细胞质谱检测平台，实现了单细胞中代谢物的高效分析，基于该平台对TCCSUP 和 TCCSUP-CDDP的两类细胞亚型进行了单细胞水平的靶向分析，筛选到多种差异代谢物。该项工作为膀胱癌耐药性研究提供了数据支撑，也为生命科学及临床医学领域的其他单细胞代谢分析应用提供参考。

MKT-33682-A

基于流式细胞分选结合高灵敏度液质联用分析的肿瘤微环境代谢表征

Metabolic characterization of the tumor microenvironment based on flow cell sorting combined with high-sensitive LC-MS analysis

钟晨春[1]，龙志敏[1]，张毅[2]，郭立海[1]

[1] *SCIEX中国，应用支持中心*
[2] *贝克曼库尔特生命科学*

Key word: metabolomics; flow cell sorting; MRM; LC-MS; tumor microenvironment;

肿瘤微环境中免疫细胞复杂的合成和分解代谢对于免疫细胞产生免疫应答能力是至关重要的。为了维持巨大的合成代谢需求，肿瘤细胞采用一种特殊的代谢方式使得肿瘤微环境通常是酸性、缺氧、缺乏营养物质、积累免疫抑制性代谢物。这种微环境利于肿瘤细胞的生存和增殖，但不利于免疫细胞的生存和抗肿瘤效应。如何控制肿瘤和免疫细胞的代谢，如糖类、脂肪酸、氨基酸等代谢途径的变化，对于提高免疫细胞的抗肿瘤效应具有重要的意义。

每种免疫细胞都具有特定的功能，以识别和清除肿瘤细胞。在实验室中鉴定及分离不同免疫细胞亚群通常需要进行复杂的多色免疫表型分析实验，以区分细胞表面标志物的细微差异，然后进行不同亚群的分选。该操作流程在一定程度上会影响分选所得细胞活性，进而对后续实验带来一定影响。Beckman CytoFLEX SRT流式细胞分选仪是一种基于低压力系统设计的仪器，在确保高活性分选的前提下，能够高速、高纯度的分选实体瘤组织及血液肿瘤样品。由于技术上的限制，流式分选的单功能细胞检测通常严重依赖于较大的细胞量，并且需要在体外孵育激活。而随着高灵敏度液质联用技术应用的出现，研究人员现在可以方便、准确的对于代谢临床样本中单功能免疫细胞状态进行评估。基于SCIEX Triple Quad 7500系统，我们将流式分选出的单功能细胞进行代谢组学分析，建立了对肿瘤感染条件下不同免疫细胞精准表征的工作流程，以推动治疗靶点发现、精准诊断等领域向前发展。

样品制备：

流式分选白血病人和正常人的相关细胞由江苏省人民医院提供。

样品提取：向装有样品的EP管中加入50 µL提取溶液（甲醇:乙腈:水 2:2:1, v/v/v），振荡混匀，超声15 min，离心后将全部溶液转移至进样小瓶中待LC-MS/MS分析。

LC-MS条件：样品通过ExionLC™系统串联SCIEX 7500 系统，进行分析。详尽分析条件列于表1、2和3。

数据处理：数据通过SCIEX OS 软件2.1中的定量功能（点击“Analytics”）进行处理。

表1. 色谱条件

参数	数值
色谱柱	Acquity BEH Amide, 100 × 2.1 mm, 1.8 µm
流动相A	含10 mM乙酸铵的水
流动相B	含10 mM乙酸铵的乙腈:水 (9:1, v/v)
流速	300 µL/min
柱温	40 ℃
进样体积	10 µL

表2. 梯度条件

时间（min）	流动相A（%）	流动相B（%）
0	5	95
1	5	95
13	2	98
14	2	98
14.1	95	5
17	95	5

MKT-32209-A

表3. SCIEX 7500系统的质谱参数

参数	数值	参数	数值
气帘气	40 psi	源温度	350° C
雾化气	85 psi	辅助气	70 psi
碰撞诱导解离气	9	离子喷雾电压	± 3000 V

高灵敏度的靶向代谢组学分析方法建立

该方法提供了众多的多反应监测(Multiple reactions monitoring, MRM)离子对用于多种代谢物的靶向检测。对于肿瘤微环境研究来说，感兴趣的化合物包括能量代谢相关途径的中间体，如糖酵解、磷酸戊糖途径、三羧酸循环、氨基酸代谢，以及能量和氧化还原辅助因子，如ATP和NADH。另外，针对特定关注的待测物质，如某个代谢通路上的化合物，也可直接在MRM列表中添加该化合物的MRM离子对。

同时，该方法灵活性强，基于不同的分析对象或者分析化合物的积累，可以对其中具体的MRM通道进行拓展和优化。

表4. 靶向代谢物MRM离子对检测列表

序号	代谢物	母离子	子离子	碰撞能量(V)
1	Glycine	76.1	30.5	18
2	Isobutyrylglycine	146.0	72.0	22
3	Serine	106.0	60.0	15
4	Homoserine	120.2	44.2	32
5	3-Phospho-Serine	186.0	88.0	12
6	Phosphoserine	186.0	88.0	10
7	O-Acetyl-L-Serine	148.0	106.0	14
8	Betaine	118.0	58.0	36
9	Betaine Aldehyde	102.0	58.0	21
10	Dimethylglycine	104.0	58.0	21
11	Threonine	120.0	74.0	13
12	Lysine	147.0	67.0	32
13	Pipecolic Acid	130.0	84.0	18
14	Cadaverine	190.0	69.0	10
15	Carnitine	162.1	103.0	20
16	Acetylcarnitine	204.0	85.0	19
17	L-Alpha-Aminoadipate	163.0	73.0	37
18	Acetyllysine	189.0	84.0	23
19	Alanine	90.1	44.2	13
20	Asparagine	133.1	74.0	19
21	Aspartate	134.0	74.0	17
22	Phenylalanine	166.1	103.0	30
23	Tyrosine	182.1	77.0	39
24	Dopamine	154.0	137.0	16
25	Normetanephrine	184.0	166.0	13
26	Diiodothyronine	525.5	352.8	31
27	Valine	118.1	55.2	13
28	2-Oxo-3-Methyl-Butyrate	117.0	85.0	25
29	Methylhydroxyisobutyrate	119.0	87.0	12
30	Leucine	132.1	86.0	13
31	Lipoamide	206.0	189.0	15
32	Methyl Oxo Pentanoate	131.0	99.0	10
33	Methylsuccinic Acid	131.9	86.9	25
34	Methionine	150.1	133.0	12
35	Methionine Sulfoxide	166.0	74.0	14
36	Phosphorylcholine	184.0	125.0	23
37	Choline	104.0	60.0	21
38	Glycerophosphocholine	258.1	104.0	16
39	Dimethyl-L-Arginine	203.0	70.0	24
40	Taurine	296.1	172.1	15
41	Cystine	241.0	74.0	32
42	Cysteine	122.1	59.1	29
43	Homocysteine	136.1	90.1	17
44	L-Cystathyonine	223.0	149.0	29
45	Cystathionine	223.0	134.0	11
46	Cysteamine	78.0	61.0	16
47	Methylcysteine	136.0	119.0	12
48	S-Adenosyl-L-Homocysteine	385.1	136.0	21
49	S-Adenosyl-L-Methionine	399.1	250.0	15
50	S-Adenosyl-L-Methioninamine	355.0	250.0	20
51	Glutathione	308.1	162.0	21
52	Glutathione Disulfide	613.0	231.0	35
53	S-Ribosyl-L-Homocysteine	268.0	88.0	31

MKT-32209-A

表4. 靶向代谢物MRM离子对检测列表（续）

序号	代谢物	母离子	子离子	碰撞能量 (V)
54	Creatine	132.0	90.0	14
55	Creatinine	114.0	44.2	14
56	Arginine	175.0	60.0	16
57	1,4-Diaminobutane	87.0	45.0	21
58	Ornithine	133.0	70.0	14
59	Citrulline	176.0	159.0	14
60	Allaontoin	159.0	99.0	11
61	Putrescine	89.0	72.0	12
62	Urea	61.1	44.2	12
63	Spermine	202.1	129.1	19
64	Spermidine	146.0	112.0	13
65	Sarcosine	90.0	44.1	20
66	L-Arginino-Succinate	291.0	70.0	37
67	N-Acetylputrescine	131.0	114.0	12
68	Carnosine	397.2	171.0	21
69	N-Acetyl-L-Ornithine	175.0	115.1	16
70	N-Carbamoyl-L-Aspartate	177.1	74.0	19
71	Histidine	156.1	110.1	14
72	Histidinol	142.1	95.0	20
73	3 Methyl Histidine	340.2	171.0	21
74	1-Methylhistamine	126.0	109.0	20
75	Imidazoleacetic Acid	127.0	81.0	15
76	1-Methyl-Histidine	170.1	124.0	20
77	N-Glycyl-L-Proline	216.1	70.0	21
78	Proline	116.1	70.1	13
79	Hydroxyproline	132.0	68.2	19
80	Glutamine	147.1	84.1	17
81	Glutamate	148.1	84.1	17
82	N-Acetyl-Glutamine	189.1	130.0	17
83	N-Acetyl-Glutamate	190.1	84.1	24
84	Phenylacetylglutamine	265.0	129.0	22
85	Tryptophan	205.0	146.0	18
86	Kynurenine	209.0	146.0	25
87	4-Aminobutyrate	104.0	69.0	22
88	5-Methoxytryptophan	235.0	176.0	22
89	Indole	118.0	91.0	26
90	GABA	274.1	171.0	21
91	Beta Amino Butyric Acid	274.1	172.0	21
92	Anthranilate	181.0	90.0	20
93	Melatonin	233.0	174.0	18
94	Metanephrine	198.0	181.0	13
95	Gamma-Aminoisobutyrate	104.1	86.0	16
96	Tryptophanol	162.0	144.0	19
97	3-OH-Anthranilate	154.0	136.0	18
98	Hydroxy-Tryptophan	221.0	204.0	18
99	Glucosamine	180.0	162.0	18
100	N-Acetyl-Glucosamine	222.0	138.0	16
101	D-Glucosamine-6-Phosphate	260.0	126.0	17
102	D-Glucosamine-1-Phosphate	260.1	162.1	17
103	Acadesine	259.0	110.0	24
104	Aminoimidazole Carboxamide Ribonucleotide	339.0	110.0	32
105	Adenosine	268.2	136.1	29
106	1-Methyladenosine	281.8	150.0	27
107	S-Methyl-5-Thioadenosine	298.0	136.0	29
108	Adenine	136.0	119.0	27
109	AMP	348.2	136.0	21
110	dAMP	332.1	136.0	23
111	Deoxyadenosine	252.0	136.0	22
112	ATP	506.0	408.0	47
113	Guanine	152.2	110.0	20
114	Guanosine	284.1	135.0	33
115	dGMP	348.1	135.0	38
116	GMP	364.0	152.0	19
117	Deoxyguanosine	268.1	152.0	17
118	7-Methylguanosine	298.0	166.0	24
119	Xanthosine	285.0	153.0	20
120	Xanthosine-5-Phosphate	365.0	97.0	13
121	Hypoxanthine	137.0	110.0	10
122	Purine	121.0	94.0	19

MKT-32209-A

表4. 靶向代谢物MRM离子对检测列表（续）

序号	代谢物	母离子	子离子	碰撞能量(V)
123	Inosine	269.0	137.0	14
124	IMP	349.0	137.0	21
125	Inosione	269.0	137.0	14
126	Deoxyinosine	253.0	137.0	12
127	Thymine	127.1	110.0	19
128	DMP	323.0	81.0	19
129	Thymidine	243.0	127.0	35
130	Cytidine	244.1	112.0	14
131	Cytosine	112.1	95.0	19
132	CMP	324.0	112.0	18
133	dCMP	308.0	112.0	18
134	Uracil	113.0	70.0	23
135	UMP	325.0	97.0	14
136	Deoxyuridine	229.0	113.0	11
137	N-Carbamoyl-Beta-Alanine	133.0	115.0	12
138	XMP	365.0	153.0	23
139	3-Amino Isobutanoate	104.0	86.0	25
140	Amino Adipic Acid	332.3	171.1	21
141	Beta Hydroxybutyrate	105.0	87.0	15
142	Mesaconic Acid	128.9	84.9	10
143	Mevalonic Acid	148.0	107.0	10
144	Mevalonolactone	131.0	69.0	19
145	2-Aminooctanoic Acid	160.0	55.3	21
146	Ethanolamine	62.1	44.2	18
147	Imidazole	69.0	42.2	23
148	Methylamino-L-Alanine	258.0	116.0	21
149	L-Alpha-Aminobutyrate	104.0	58.0	17
150	Cobalamin	678.0	147.0	52
151	Pyridoxine	170.0	134.0	22
152	Pyridoxamine	169.0	134.0	25
153	Flavone	223.0	121.0	29
154	Biotin	245.1	227.0	20
155	Thiamine Phosphate	345.0	122.0	18
156	Thiamine	265.0	122.0	13
157	Riboflavin	377.0	243.0	26
158	Folate	442.0	295.1	16
159	7,8 Dihydrofolate	444.0	178.1	30
160	5 Methyl THF	460.0	313.0	19
161	Nicotinamide	123.1	80.0	22
162	Niacinamide	123.0	80.0	30
163	NAD	664.1	428.0	32
164	NADH	666.1	514.0	28
165	NADP	744.2	136.0	50
166	NADPH	746.2	729.0	18
167	Nicotinamide Ribotide	335.0	123.0	30
168	Methylnicotinamide	137.0	94.0	20
169	Dephospho-CoA	688.0	348.0	27
170	Coenzyme A	768.0	261.0	39
171	Flavin Adenine Dinucelotide	786.0	348.0	26
172	Acetyl-CoA	810.0	303.0	30
173	Propionyl-CoA	824.1	317.1	35
174	Acetoacetyl-CoA	852.0	345.0	36
175	Malonyl-CoA	854.0	347.0	28
176	Succinyl-CoA	868.1	361.1	40
177	FMN	455.0	213.0	19
178	Penicillin	335.0	160.0	20
179	6-Phospho-gluconate	275.0	97.0	11
180	Glyoxylate	73.0	45.0	-22
181	Glycolate	75.0	45.2	-13
182	Acetoacetate	101.1	57.2	-14
183	Cholesteryl Sulfate	465.2	97.0	-39
184	Glycerate	105.0	75.0	-15
185	Sn-Glycerol-3-Phosphate	171.0	79.0	-15
186	Geranyl Pp	313.0	79.0	-18
187	Farensyl Diphosphate	381.0	79.2	-21
188	Homocysteic Acid	182.0	80.0	-23
189	Uric Acid	167.0	124.0	-17
190	GSH	308.1	162.0	-19
191	Glutathione	306.0	143.0	-19
192	Carbamoyl Phosphate	140.0	79.0	-24

MKT-32209-A

表4. 靶向代谢物MRM离子对检测列表（续）

序号	代谢物	母离子	子离子	碰撞能量 (V)
193	Carbamaoyl Asparatate	175.0	132.0	-12
194	Maleic Acid	115.0	71.0	-13
195	Parahydroxybenzoate	137.0	93.0	-21
196	Acetylphospahte	139.0	79.0	-22
197	2-Keto-Isovalerate	115.1	71.1	-13
198	Methylmalonic Acid	117.0	73.1	-13
199	Pyroglutamic Acid	128.0	82.1	-19
200	Citraconic Acid	129.0	85.1	-13
201	2-Ketohaxanoic Acid	129.0	101.3	-13
202	N-Acetyl-L-Alanine	130.0	88.0	-14
203	Hydroxyisocaproic Acid	131.0	85.1	-16
204	p-Aminobenzoate	136.1	92.0	-18
205	p-Hydroxybenzoate	137.0	93.0	-23
206	Acetylphosphate	139.0	79.0	-24
207	Phenylpropiolic Acid	145.0	101.0	-18
208	2-Hydroxy-2-Methylbutanedioic Acid	147.0	85.1	-17
209	3-Methylphenylacetic Acid	149.0	105.0	-12
210	Hydroxyphenylacetic Acid	151.0	107.0	-18
211	2,3-Dihydroxybenzoic Acid	153.0	109.0	-19
212	Allantoin	157.1	114.0	-17
213	Indole-3-Carboxylic Acid	160.0	116.0	-20
214	Phenylpyruvate	163.0	91.0	-13
215	Atrolactic Acid	165.0	119.0	-21
216	Phenyllactic Acid	165.0	103.1	-21
217	Allantoate	175.0	132.0	-14
218	2-Isopropylmalic Acid	175.0	115.0	-19
219	Pyrophosphate	176.8	158.6	-16
220	Hydroxyphenylpyruvate	179.1	107.0	-13
221	4-Pyridoxic Acid	182.0	138.0	-18
222	Indoleacrylic Acid	186.0	142.0	-20
223	Xanthurenic Acid	204.0	160.0	-19
224	Lipoate	205.0	171.0	-13
225	Orotate	155.0	111.0	-15
226	Orotidine-5-Phosphate	367.0	323.0	-18
227	Dihydroorotate	157.0	113.0	-14
228	Deoxyribose-Phosphate	213.0	79.0	-35
229	UDP	403.0	305.0	-15
230	Uridine	243.0	200.0	-21
231	dTDP	411.0	159.0	-29
232	GDP	442.0	159.0	-19
233	GTP	522.0	424.0	-23
234	dGTP	506.1	159.0	-30
235	CDP	402.0	159.0	-29
236	CDP-Choline	487.0	428.0	-21
237	Adenosine 5-Phosphosulfate	426.0	346.0	-22
238	ADP	426.0	134.1	-24
239	X5P	365.0	97.0	-11
240	Cyclic-AMP	328.0	134.1	-33
241	3-Hydroxybutyryl-Coa	852.2	408.0	-43
242	D-Glucose	179.1	89.1	-12
243	Hexose Phosphate	259.0	79.0	-40
244	Glucose-6-Phosphate	259.0	97.1	-15
245	F6P	259.0	97.1	-17
246	Fructose-6-Phosphate	259.0	169.0	-16
247	Fructose-1,6-Bisphosphate	339.0	97.0	-30
248	D-Glyceraldehdye-3-Phosphate	169.1	97.0	-10
249	Dihydroxy-Acetone-Phosphate	169.0	79.0	-40
250	1,3-Bisphopshoglycerate	265.0	79.1	-20
251	1,3-Diphopshateglycerate	265.0	79.0	-37
252	3-Phosphoglycerate	185.0	97.5	-35
253	PGA	184.9	97.1	-20
254	2-Phosphoglycerate	185.5	97.1	-35
255	Phosphoenolpyruvate	167.0	79.0	-41
256	Pyruvate	87.0	43.0	-20
257	Lactate	89.0	43.2	-16
258	Gluco-D-Lactone	177.0	129.0	-13
259	6-Phospho-D-Gluco-1,5-Lactone	257.0	97.0	-22
260	6-Phospho-D-Gluconate	275.0	97.0	-13
261	Ribulose-5-Phosphate	229.0	79.4	-26
262	Ribose-Phosphate	229.0	79.0	-42

MKT-32209-A

表4. 靶向代谢物MRM离子对检测列表（续）

序号	代谢物	母离子	子离子	碰撞能量 (V)
263	5-Phosphoribosyl-1-Pyrophosphate	389.0	291.0	-18
264	Phosphoribosyl Pyrophosphate	389.0	291.1	-18
265	D-Erythrose-4-Phosphate	199.0	97.0	-19
266	S7P	289.0	97.0	-12
267	G3P	169.0	89.0	-15
268	D-Sedoheptulose-1-7-Phosphate	289.0	97.0	-27
269	Sedoheptulose 1,7-Bisphosphate	369.0	97.0	-25
270	Gluconate	201.0	134.0	-17
271	D-Gluconate	195.0	129.0	-17
272	2-Deoxyglucose-6-Phosphate	243.2	97.1	-18
273	Glucose-1-Phosphate	259.0	241.0	-16
274	N-Acetyl-Glucosamine-1-Phosphate	300.0	79.0	-34
275	UDp-D-Glucose	565.0	323.0	-25
276	UDp-D-Glucuronate	579.0	403.0	-26
277	ADp-D-Glucose	588.0	346.0	-24
278	UDp-N-Acetyl-Glucosamine	606.0	385.0	-28
279	Citrate	191.1	87.0	-22
280	Isocitrate	191.0	117.0	-19
281	Aconitate	173.1	85.0	-17
282	Oxoglutarate	145.0	101.0	-13
283	Succinate	117.0	73.0	-12
284	Fumarate	115.0	71.0	-13
285	Malate	133.0	115.0	-14
286	Oxaloacetate	131.0	87.0	-14
287	2-Hydroxygluterate	147.1	128.7	-17
288	Ascorbic Acid	175.0	87.0	-19
289	Myo-Inositol	179.0	161.0	-17
290	Pantothenate	218.0	146.0	-21
291	Thiamine Pyrophosphate	423.1	302.0	-21

代谢组学分析结果

通过对流式细胞分选仪挑选出的肿瘤细胞和正常细胞开展代谢组学分析，对其中包含的代谢物含量进行测定，经过统计学分析（t-test、fold change、PLSDA），筛选出差异代谢物。

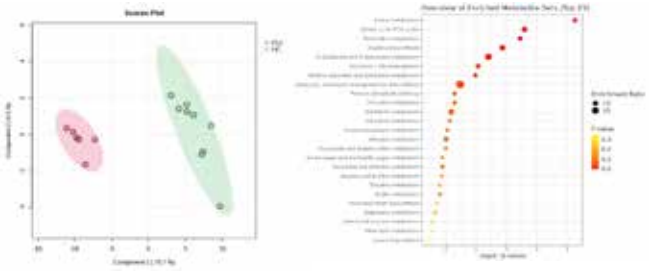

图1. 基于代谢组学分析的差异代谢表征。左，主成分分析图，CLL为癌细胞组，HC为正常细胞组。从主成分分析图可以看出，在差异代谢物表征的情况下，两组细胞样本可以显著的区分；右，代谢通路富集，差异的代谢物集中于相关的代谢通路，如三羧酸循环、糖酵解通路等。

基于测定的代谢物在肿瘤细胞和正常细胞中各自的差异，从主成分分析图（PCA）可以看出（见图1左），正常细胞和肿瘤细胞的代谢物有显著差异；根据这些差异代谢物通过通路富集分析发现（见图1右）。

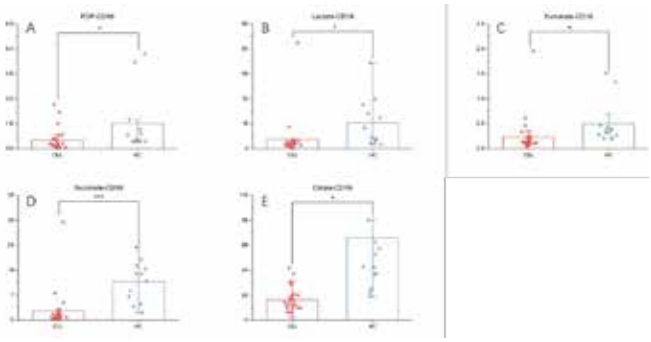

图2. 部分差异代谢物含量对比。CLL为癌细胞组，HC为正常细胞组；两组细胞之间与能量代谢相关的部分化合物有显著差异，如富马酸、柠檬酸等（*, p<0.05, ***, p<0.0001）。

MKT-32209-A

这两组细胞之间能量代谢相关通路有显著差异，而通路上的相关具体代谢物含量也有显著差异（见图2）

小结

- 通过Beckman CytoFLEX SRT流式分选系统与SCIEX 7500系统高灵敏度检测相结合，实现微量单功能细胞高覆盖靶向代谢组学分析检测。
- Beckman CytoFLEX SRT流式分选系统基于创新的光路及流路设计，在智能化操作的前提下，可实现多色、高灵敏度、高纯度、高活性的细胞及外泌体样本分析/分选，全面支持各种类型生物样本的流式分析/分选实验的开展。
- SCIEX 7500系统优异的灵敏度保证痕量化合物的良好检出，同时高扫描速度使得一针正负切换进样分析模式能覆盖尽量多的检测通道，保证珍贵的微量活细胞样品靶向组学分析成为可能。
- 可将此方案应用于其他细胞或生物基质样本，助力精准代谢组学研究和临床医学转化的开展。

MKT-32209-A

应用SCIEX Echo® MS+系统对生物样本中的脂质化合物进行快速分析

Rapid Analysis of Lipids Components in Biological Sample by SCIEX Echo® MS+ System

肖梦晴； 钟晨春；龙志敏；刘冰洁
Xiao Mengqing; Zhong Chenchun; Long Zhimin; Liu Bingjie

SCIEX应用支持中心（上海）
SCIEX Application and Support Center (Shanghai)

Key words: Lipids, SCIEX Echo® MS+

引言

脂质化合物具有重要的生物学功能，因此越来越被关注，在大量的样本中快速获取结果，进一步通过统计分析发现具有显著组间差异的化合物的手段也是脂质组学研究中最基础，也是最重要的研究手段之一。通过对大量样本的调查，所获取的结果往往可以更好的揭示脂质代谢与细胞、组织和器官的生理病理关系。

传统的液相色谱质谱联用技术进行脂质组学分析时，每个样本分析需要约17分钟。对于大型样本集，这种方法的操作成本高，同时也会降低研究效率。SCIEX Echo® MS+系统采用声波激发技术实现高通量的样品采集和数据获取，可兼容ZenoTOF® 7600系统，实现非靶向脂质组学定性和定量分析，并且在不同的进样模式下均可实现几秒钟内快速进样，检测时间上大大提升样本分析速度，使高通量脂质分析更加快速便捷。

SCIEX Echo® MS+ 系统的主要特点

1. 1~10秒快速进样，实现高通量节约时间成本。
2. 声波激发无接触式进样，在快速分析样品的同时确保无残留影响，测定结果更加准确。
3. 纳升级进样，降低基质影响，前处理简单化。

仪器设备

SCIEX Echo® MS+系统+ ZenoTOF® 7600高分辨质谱系统

声波激发条件

声波激发样品液滴需要一种合适的载体溶剂（Carrier Solvent），将样品板中被激发出来的小液滴样品带入至开放端口接口（Open Port Interface, OPI），然后通过电极（Electrode）将带有样品的载体溶剂引入到电喷雾离子源中。本实验选取的乙腈:水（1:4, 含0.1%甲酸）溶液作为载体溶剂；载体流速：350 µl/min。

质谱条件

1. 一级质量范围TOF MS, m/z 300-1100, accumulation time, 0.2 s

MKT-35277-A

2. TOF MS was followed by 100 product ion scan, with accumulation time of 15 ms
3. 二级质量范围MS/MS (CID); m/z 100 – 1100
4. 源气参数：IS电压，5000 V；气帘气CUR，35 psi；雾化气GS1，90 psi；辅助气GS2，45 psi；离子源温度为350 ℃；碰撞气，8

实验结果

1. 脂质成分鉴定

通过Echo®MS+系统进行脂质定性分析，在质谱方法中，candidates ion参数设置为100，即一个循环包含1次一级扫描和100次二级扫描，为了保证数据质量，在声波激发时采用infusion的方式，将注射时间设置为15秒，延长样本进样的时间，这种模式可以保证采集更多的二级数据信息用来进行化合物鉴定分析，以增强对低丰度化合物的检测，同时还可以保证脂质化合物的采集点数足够（大于10个），确保数据质量（图1）。 由于进样方式的不同，观察到色谱峰峰型和传统的色谱峰存在差异，尽管如此，所有的鉴定都通过MS/MS验证（图2）。

最终，通过相同分子式的脂质异构体去重复，鉴定出302种脂质化合物。主要包括甘油三酯（TG）、甘油二酯（DG）、鞘磷脂（SM）、磷脂酰胆碱（PC）、溶血磷脂酰胆碱（LPC）、磷脂酰乙醇胺（PE）、溶血磷脂酰乙醇胺（LPE）、磷脂酸（PA）、神经酰胺（Cer）、糖脂（HexCer）。

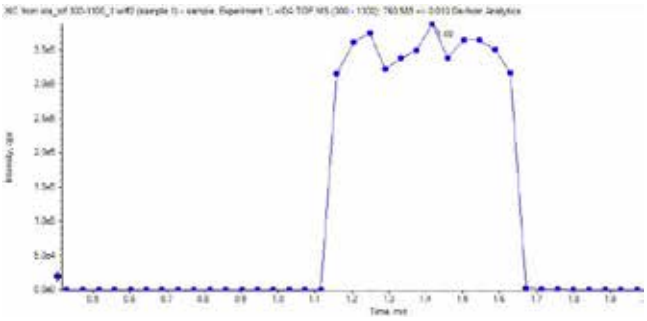

图1. 化合物一级谱图点数示意图

2. 样本中脂质化合物相对定量分析

QC样品和化合物表得到定性结果后，所有样品依次进样，进行TOFMS数据采集。对目标化合物对应的前体色谱进行提取和积分，并利用峰面积作为相对定量的结果。我们使用Echo® MS+系统和三重四极杆平台对相同的样品进行平行分析，以验证Echo®MS+系统是否能够得出与已建立的三重四极杆系统一致的结论。

鉴于脂质组学分析主要采用相对定量方法进行组间比较，我们选择了野生型小鼠和HCC肝细胞癌（HCC）模型小鼠作为样本，以验证Echo®MS+系统和已建立的三重四极杆系统的组间差异分析的一致性。图3显示了所有样品的TIC，其中QC样品5个，对照样品10个，HCC样品10个，用于数据分析。

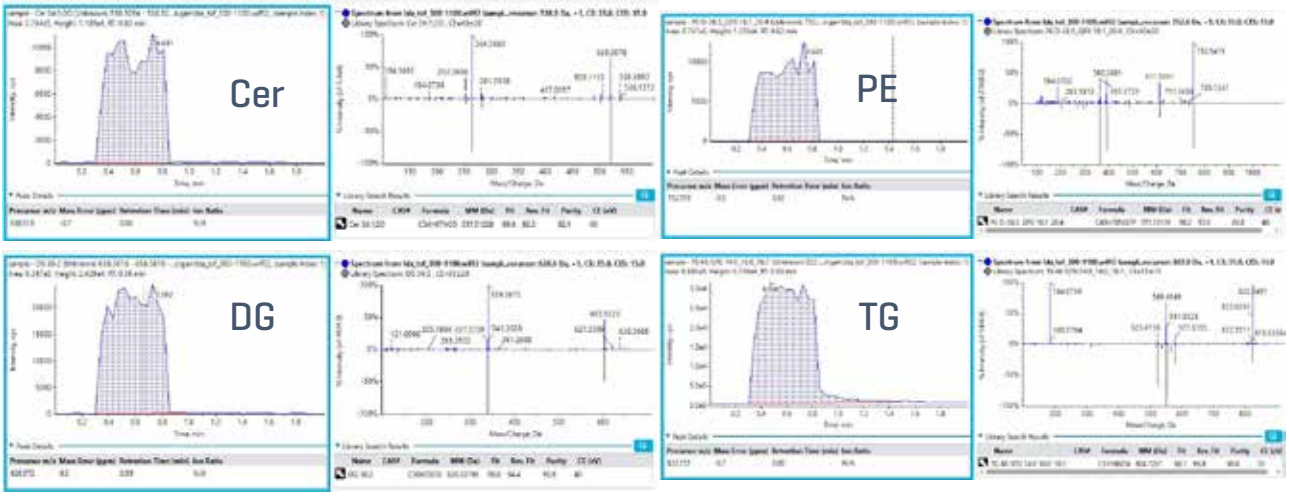

图2. 各脂质组分的一级和二级谱图。Cer、神经酰胺；PE、磷脂酰乙醇胺；DG、二酰甘油；TG、三酰甘油。TOF MS的XIC以蓝框显示，而提取的TOF MSMS则以无蓝框显示。在MS/MS数据显示中，上方的蓝色谱为实验获得的碎片化图谱，下方的灰色谱为数据库中对应化合物的参考MS/MS谱。

MKT-35277-A

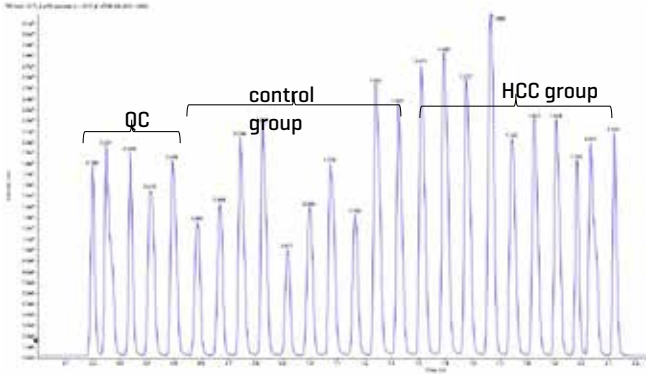

图3. 25个样本的TIC图

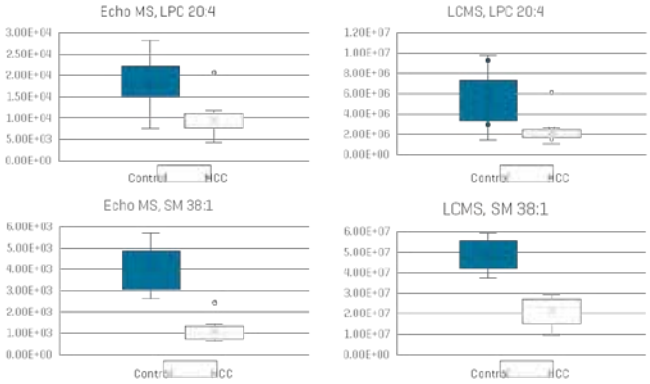

图4. LPC 20:4和SM 38:1的箱型图，在Echo TOFMS系统和三重四极杆系统中均表现出一致的趋势

图3显示了25个样本在Echo® MS+系统下采集到的原始数据的总离子流图。SCIEX OS可以对该谱图进行拆分，便于后续的定量分析。拆分后，一个数据文件下有26个样本数据信息（一张所有样本的一级谱图和25张单个样本的一级谱图），这样就可以对每一个样本通过其一级数据信息进行峰面积定量，再通过组间差异分析找到差异化合物，与常规的脂质组学分析流程一致。

同时，我们还通过液相色谱质谱联用系统进行靶向脂质组学方法对以上结果进行验证，通过MRM方法对相同样品进行分析。两个数据集的比较分析显示，HCC组溶血磷脂酰胆碱（LPC）和鞘磷脂（SM）水平有显著下降趋势。值得注意的是，LPC 16:0、LPC 18:2、LPC 20:4、SM 32:1、SM 34:1、SM 38:1、SM 41:2和SM 42:1在Echo TOFMS系统和三重四极杆系统中表现出一致的趋势（图4）。

Echo® MS+系统采用50 nL的进样量，而LCMS系统采用1 µL的进样量，后者的响应信号明显更高。这种反应差异被他们不同的定量方法进一步放大：Echo® MS+系统采用一级定量，而LCMS系统是基于MRM的定量。尽管平台之间的反应存在显著差异，但我们观察到一致的化合物特异性变化，证明了基于Echo® MS+系统的脂质组学分析的可靠性。此外，QC样本具有良好的重现性，超过90%的化合物的相对标准偏差小于0.3。

小结

本文采用SCIEX Echo® MS+系统联合ZenoTOF® 7600高分辨质谱系统建立了组织样本快速高通量的脂质组学检测方法，共鉴定到脂质12类302种，一级定量分析结果显示，对照组和HCC组在某些甘油三酯和磷脂方面存在显著差异，这与在三重四极杆上使用MRM方法获得的结果一致。

该方法为脂质组学提供了一种新的方法，即对大样本队列进行快速脂质分。一次进样仅需纳升级样本量，且单个样本检测时间仅需10s左右，样本经过一次IDA采集后可进行脂质化合物鉴定，得到的鉴定结果可用于相同批次样本的定性分析，在超大样本量检测时，可仅采集一级数据进行样本的定量分析，进一步缩短检测时间至每个样本1s左右，满足高通量脂质样本分析的需求。

MKT-35277-A

SCIEX Echo® MS+ 结合ZenoTOF® 7600系统快速分析20种氨基酸

Rapid and High-throughput Analysis of 20 Amino Acids by SCIEX Echo® MS+ System with ZenoTOF® 7600 system

冷向阳，钟晨春，龙志敏，郭立海
Xiangyang Leng, Chenchun Zhong, Zhimin Long, Lihai Guo
SCIEX 应用支持中心，中国

Key Words: SCIEX Echo® MS+ System, ZenoTOF® 7600 system, High-throughput, Amino Acids

引言

氨基酸作为生命体的基本组成单位，是机体不可或缺的重要物质。氨基酸不仅是蛋白质合成的基石，也是正常细胞生长、分化和功能所必需的结构元素和能量来源。如果机体内的氨基酸代谢异常，可能会导致生理功能紊乱，影响机体正常代谢，导致各种疾病的发生。氨基酸除了在生物体的功能外，在各个领域都扮演着重要角色。如在医药领域，氨基酸被用作药物的原料或辅料；在食品领域，氨基酸被添加到食品中以增强营养价值等。因此氨基酸的检测无论是在研究方向还是临床检测等，都具有非常重要的意义。

SCIEX Echo® MS+系统采用声波液滴激发技术实现快速、高通量的样品采集和数据获取。本方法中采用SCIEX Echo® MS+系统结合ZenoTOF 7600系统对20种氨基酸进行快速分析，采用TOFMS的采集方式，实现1.1秒1个样品的快速分析，且保证信号峰的点数在12个以上，确保数据重复性良好。此方法可以满足血浆等复杂生物基质中氨基酸检测需求，方法简单高效、样品用量小，适用于大队列样本中氨基酸化合物的快速分析。

SCIEX EchoMS系统优势：

1. 1.1秒1个样品快速分析，实现高通量节约时间成本。
2. nL级进样，降低基质影响，前处理简单化。
3. 声波激发无接触式进样，在快速分析样品的确保无残留影响。

仪器设备

SCIEX Echo® MS+ 系统结合ZenoTOF® 7600系统

图1. SCIEX Echo® MS+ 7600系统

样品制备

氨基酸的标准品采用纯水稀释配置系列浓度；血浆样本使用蛋白沉淀法处理，离心，取上清液采用纯水稀释5倍后，取50 µL置于384孔板中进样分析。

声波激发条件

载液：甲醇（含0.01%甲酸）

流速： 400 µL/min

进样模式： AQ模式

质谱条件

离子源：ESI源，正离子模式

扫描方式：TOFMS；扫描范围（m/z）：75-210

RUO-MKT-02-33693-ZH-A

累计时间：0.08s；去簇电压（DP）：40 V

离子源参数：

电喷雾电压IS: 5000 V　　气帘气 CUR: 25 psi

雾化气 GS1: 90 psi　　辅助加热气GS2: 45 psi

碰撞气 CAD: 7　　源温度 TEM: 350℃

化合物信息见表1

表1. 20种氨基酸分子式信息及线性范围、重复性

化合物名称	分子式	LLOQ (μM)	线性范围	相关系数 (R)	LLQO重复性(n=6, RSD%)
甘氨酸	$C_9H_{11}NO_2$	1	1-100	0.996	8.45
丙氨酸	$C_{11}H_{12}N_2O_2$	0.5	0.5-50	0.994	7.6
丝氨酸	$C_6H_{13}NO_2$	0.2	0.2-20	0.996	8.82
脯氨酸	$C_6H_{13}NO_2$	0.5	0.5-100	0.995	4.5
缬氨酸	$C_5H_{11}NO_2S$	0.5	0.5-100	0.993	5.05
苏氨酸	$C_5H_9NO_2$	0.5	0.5-20	0.996	6.14
半胱氨酸	$C_9H_{11}NO_3$	1	1-100	0.997	6.97
亮氨酸	$C_5H_{11}NO_2$	0.2	0.2-100	0.996	6.47
异亮氨酸	$C_3H_7NO_2S$	0.2	0.2-100	0.996	6.47
天冬酰胺	$C_3H_7NO_2$	0.2	0.2-20	0.996	5.28
天冬氨酸	$C_4H_9NO_3$	0.5	0.5-20	0.995	6.48
谷氨酰胺	$C_5H_9NO_4$	0.2	0.2-100	0.997	6.97
赖氨酸	$C_4H_7NO_4$	0.2	0.2-20	0.996	5.73
谷氨酸	$C_2H_5NO_2$	0.2	0.2-20	0.995	4.63
甲硫氨酸	$C_5H_10N_2O_3$	0.2	0.2-20	0.997	8.3
组氨酸	$C_3H_7NO_3$	0.2	0.2-50	0.997	4.58
苯丙氨酸	$C_4H_8N_2O_3$	0.2	0.2-100	0.994	4.02
精氨酸	$C_6H_9N_3O_2$	0.2	0.2-20	0.994	4.18
酪氨酸	$C_6H_{14}N_2O_2$	0.2	0.2-20	0.995	4.34
色氨酸	$C_6H_{14}N_4O_2$	0.5	0.5-50	0.992	4.52

实验结果

20种氨基酸在线性范围内，线性关系良好，相关系数R均大于0.99，定量下限 (LLOQ) 连续6次进样的 %RSD 小于8.8%，重复性良好。线性范围和重复性详细结果见表1。采用TOFMS的采集方式，实现1.1秒内对20种氨基酸进行快速分析且保证信号峰的点数在12个以上，结果见图1。典型化合物标准曲线图见图2。同时并采用此方法对大鼠血浆的氨基酸进行检测，该方法可以很好的满足实际血浆中的氨基酸检测需求，结果图见3。

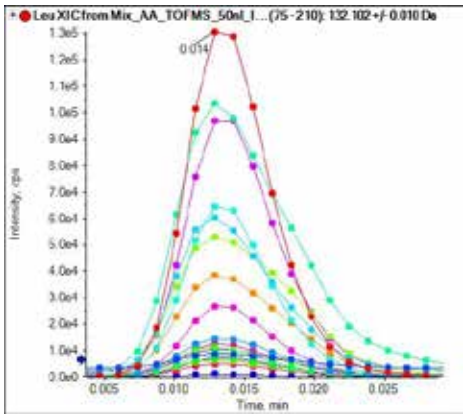

图1. 同时检测20种氨基酸

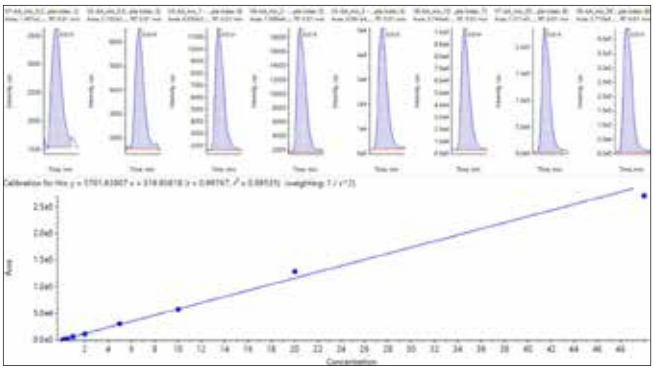

图2. 典型氨基酸标准曲线图

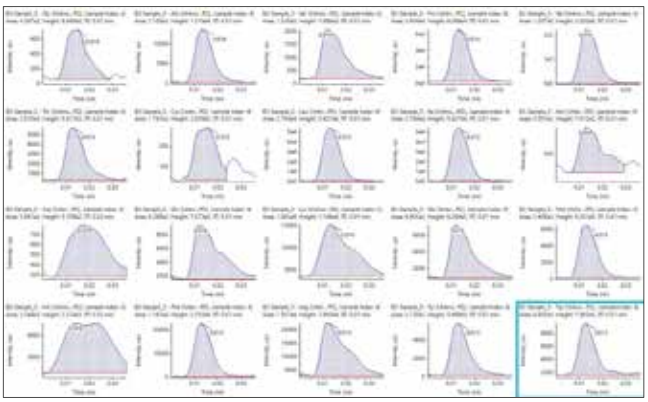

图3. 大鼠血浆中20种氨基酸检测结果

RUO-MKT-02-33693-ZH-A

总结

本文使用 SCIEX Echo® MS+ 系统结合ZenoTOF® 7600系统建立了20种氨基酸的快速高通量检测分析方法。结果表明，各化合物在线性范围内性关系良好，定量下限重现性高，可以用于实际血浆样本的快速高通量检测。SCIEX Echo® MS +系统在实现高通量样品采集同时，保证数据的高质量，实现简单的样品前处理即可满足目标物快速准确定量需求。

RUO-MKT-02-33693-ZH-A

ZenoTOF® 7600系统一次进样同时进行非靶向代谢组和靶向暴露组分析

Simultaneously Untargeted Metabolome and Targeted Exposome Analysis in One Injection by ZenoTOF® 7600 system

陈俊苗[1*]，管朋维[2*]，王宇婷[2]，许国旺[2]，刘心昱[2]，司丹丹[1]
Junmiao Chen[1*], Pengwei Guan[2*], Yuting Wang[2], Guowang Xu[2], Xinyu Liu[2], Dandan Si[1]

[1] *SCIEX中国应用支持中心；[2] 中国科学院大连化学物理研究所*
[*] *共同第一作者，本文章摘译自参考文献[1]*

Key words: Untargeted metabolome; Targeted exposome analysis; ZenoTOF® 7600

引言

遗传和环境因素在人类疾病的发生发展过程中共同发挥作用。世界卫生组织数据显示，高达 70% 的疾病以及 40% 的死亡都和环境因素紧密相关。血清中的外源性化合物与多种疾病存在密切关联，比如多氟烷基物（PFAS）会诱发慢性炎症等疾病，内分泌干扰物（EDCs）会影响生殖健康等。糖尿病作为全球性健康难题，环境因素在其发病过程中往往起着更为关键的作用。

代谢组 - 暴露组关联研究（mEWAS）聚焦于探索体内暴露、代谢表型变化和疾病风险之间的联系，为揭示环境暴露对健康的影响提供了有效途径。然而，人体内源性代谢物和外源性化学残留物不仅数量庞大、理化性质差异大，而且浓度范围跨度广泛。目前，mEWAS研究中，为平衡质谱检测的覆盖度和灵敏度，代谢组学常用高分辨率质谱（HRMS）分析，暴露组学则多采用针对特定暴露类别的靶向方法分析，这限制了研究的通用性和覆盖范围，在实际应用中存在分析通量低、耗时耗样的问题，对于体积有限/珍贵难获得的生物样品来说问题更为严重。

SCIEX ZenoTOF® 7600高分辨系统搭载Zeno trap离子阱技术，可使TOF的占空比高达 90%，显著提升了灵敏度，还能在单次分析中同时采集 HRMS 和 MRM 数据。基于此，研究团队提出了一种基于 LC-HRMS-MRM MS 模式的新方法，可在一次进样中同时进行非靶向代谢组和靶向暴露组分析。这种方法极大地简化了 mEWAS 流程，有望突破现有研究困境，推动 mEWAS 方法学取得新进展。

血清样本采集及处理

以 2 型糖尿病（T2DM）为示范研究，收集了 226 份空腹血清样本，其中包括 72 例 T2DM 患者、41 例糖尿病前期受试者和 113 例健康对照者，这些样本在性别、年龄和 BMI 方面进行了匹配。样本分类基于空腹血糖（FPG）和糖化血红蛋白水平。

取 100 µL 血清样品，加入含内标的甲醇 / 乙腈（1:1，v/v）进行蛋白质沉淀。涡旋振荡 60 s 后，在 14000 g、4 ℃ 条件下离心 15 min。收集两份 200 µL 上清液用于后续分析。通过混合实际血清样品制备实际样品来源的 QC（RSQC），同时纳入实验室血清 QC（Lab QC）用来优化条件。每 15 个样品间隔加入一个 RSQC，以确保分析系统的稳健性。

LC-HRMS-MRM MS 分析

采用 Zeno SWATH 技术收集 RSQC 和 Lab QC 样品的TOF MS和TOF MSMS信息，以最大化 MS2 信息的丰富度，并注释血清中的内源性代谢物和外源性化合物。使用 MS-DIAL 进行解卷积，然后通过数据库搜索，对代谢物和外源性化合物进行注释。内部数据库 OSI - SMMS 和暴露组数据库也分别用于内源性代谢物和外源性化合物的精确注释。

为了实现代谢物和外源性化合物的全面分离，首先使用添加了外源性标准品的 Lab QC 样品优化液相色谱洗脱梯度。优化后，在 ACQUITY UPLC BEH C18 柱（柱温50 ℃；正离子模式）和 ACQUITY UPLC HSS T3 柱（柱温55 ℃；负离子模式）上的分析时间分别为 32 min 和 26 min。

MKT-34449-A

基于已识别的外源性化合物，并结合文献调研确定靶向的外源性化合物，优化碰撞能量和去簇电压，生成 MRM 列表。最终的 LC-HRMS-MRM 方法将 HRMS 用于非靶向代谢组学分析，将 MRM MS 用于靶向暴露组学分析。详细的 LC-HRMS-MRM MS 参数见文献[1]。

统计分析

基于HRMS-MRM MS的非靶向代谢组学分析，使用 SCIEX 公司的MarkerView 软件从原始数据中获取对齐的峰表，并将所有峰的相对响应归一化到合适的内标。使用 Multi Experiment Viewer进行非参数检验，使用 SIMCA - P 14.1 软件进行正交偏最小二乘法判别分析（ OPLS - DA ）。基于 R 包进行中介效应分析和混合暴露模型分析。

对于基于HRMS-MRM MS的靶向暴露组学分析，根据 QC 样品中每个离子特征的最小相对标准偏差（ RSD ）原则，使SCIEX OS 软件获取的外源性化合物峰面积归一化到合适的内标。对于定量方法学表征，在低、中、高浓度下评估回收率，标准为在 100 ± 20% 范围内。浓度低于 LLOQ 的值赋值为 LLOQ/2。符合方法学验证标准的外源性化合物纳入后续的Spearman 相关性分析和二元逻辑回归分析。

全景代谢组和暴露组的采集与鉴定

为扩大代谢组和外源性化合物的覆盖范围，使用 ZenoTOF® 7600结合超高效液相色谱，以 Zeno SWATH 和数据依赖型采集（ DDA ）模式分析实际样品来源的质量控制（ RSQC ）和 Lab QC 样品，生成全面的原始数据（ 图 1B ）。对于代谢物和外源性化合物的注释，收集并检索在线数据库，包括 MoNA 数据库、NIST 标准参考数据库和 MS DIAL数据库。此外，还使用内部 OSI-SMMS 数据库和暴露组数据库，以尽可能多地发现代谢物和潜在的外源性化合物。在 MS DIAL 和 OSI-SMMS 软件中，通过将实际的 MS1、MS2 数据和保留时间与数据库中的数据进行比对，来进行注释（ 图 1C ）。为确保注释的准确性，所有注释的代谢物和外源性化合物都基于结构 - 保留关系和特征碎片进行人工核对。

在 Zeno SWATH 模式下，共成功鉴定出 1190 种代谢物（ 正离子模式 892 种，负离子模式 298 种 ），超过了 DDA 模式下鉴定出的 668 种代谢物（ 正离子模式 482 种，负离子模式 186 种 ）。这意味着代谢组覆盖范围显著提升，在正离子模式下代谢组分析的覆盖范围提高了 1.85 倍，在负离子模式下提高了 1.60 倍，其中有 463 种代谢物重叠（ 图 1D ）。此外，利用 Zeno SWATH 成功鉴定出 43 种血清外源性化合物，而 DDA 模式仅鉴定出 20 种（ 图 1E ），这证明了 Zeno SWATH 的高效性。它显著增强了 MS2 强度和碎片丰度，从而提升了代谢物和外源性化合物的定性和定量能力。然而，低丰度化合物的 MS2 覆盖范围有限，阻碍了更多外源性化合物的鉴定，这凸显了在暴露组研究中基于 MRM 的高灵敏度分析的必要性。随后，将从 RSQC 和 Lab QC 中确定的 43 种外源性化合物，以及从文献检索中获得的 205 种在人体中报道浓度较高或检测频率较高的农药、兽药和化学污染物，整合到MRM 列表中，并准备了全面的代谢组列表，用于后续实际样品的分析。

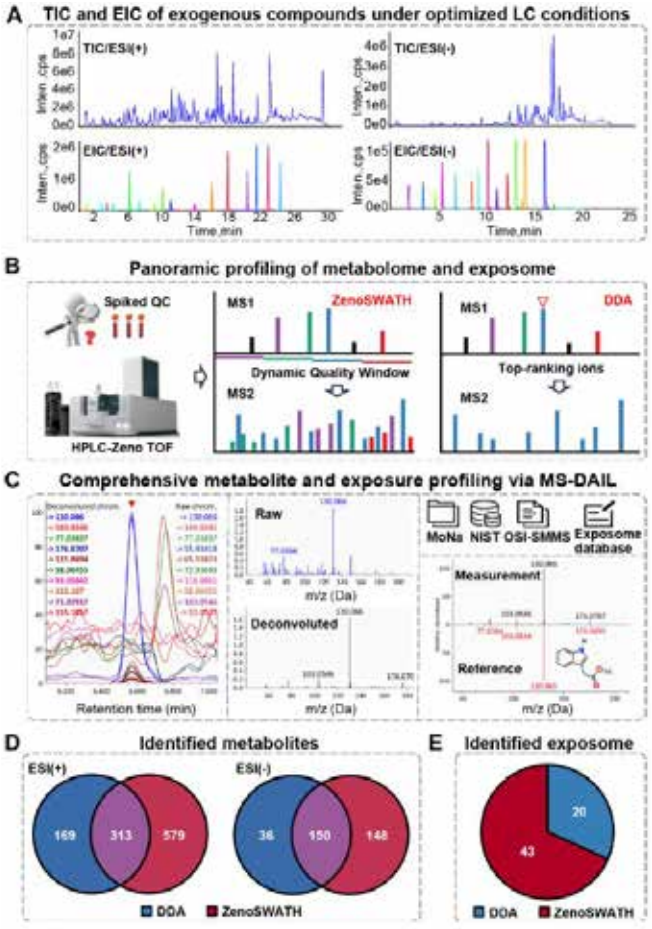

图1. HRMS-MRM MS方法构建工作流程

用于非靶向 / 靶向整合分析的 LC-HRMS-MRM MS 方法构建

为拓宽小分子的覆盖范围，采用飞行时间质谱扫描范围为 100-1000Da 的 HRMS 方法进行非靶向代谢组学分析。由于 MRM 方

MKT-34449-A

法具有高灵敏度和高选择性，适合低浓度的血清外源性化合物绝对定量。基于前期鉴定及文献报道确定了所有外源性化合物的离子对，并在SCIEX Triple Quad 6500 仪器上进行了CE和DP电压优化，以建立暴露组 MRM 方法。结果显示，与 HRMS 相比，MRM 模式显著提高了外源性化合物的检测灵敏度。在低浓度 10ng/mL（添加到胎牛血清中）时，有 15 种外源性化合物在 HRMS 中无法检测到，但在 MRM 模式下可以检测到；与 HR 模式相比，有 54 种和 79 种外源性化合物的灵敏度分别提高了 10 倍以上和 3-10 倍（图 2A-D）。尽管血清中外源性化合物的浓度通常比代谢组低 2-3 个数量级，但它们在 MRM 中的信号响应与代谢物在 HRMS 中的信号响应达到相当的水平（图 2C-F），这突出了 HRMS-MRM MS 模式有效检测低浓度外源性化合物和内源性代谢物的能力。图 2G 展示了本研究中高频检测到的暴露物在 MRM 模式下响应强度的显著提升，强调了其在综合暴露组分析中的有效性。

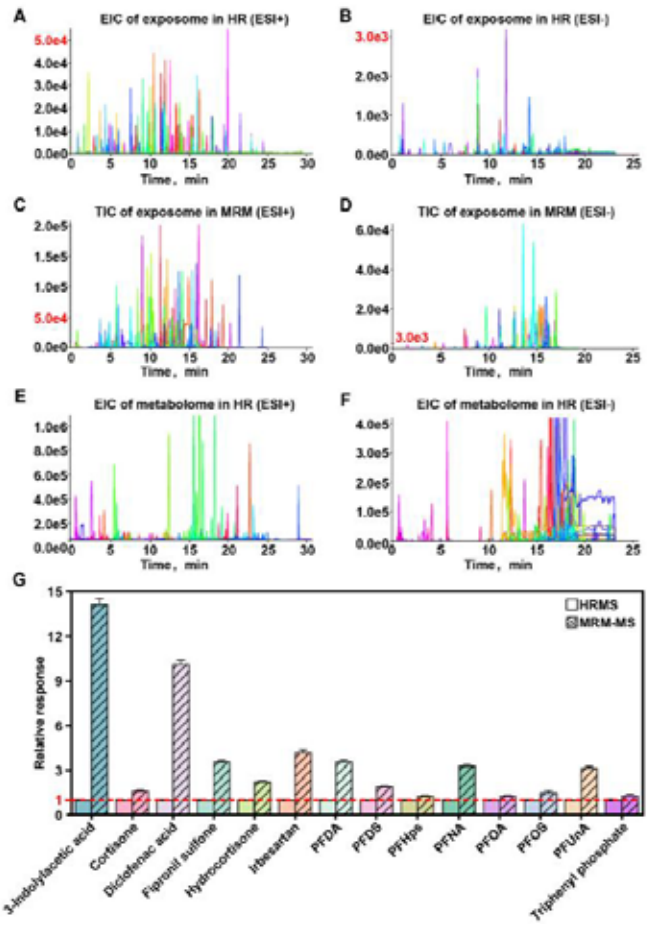

图2. HRMS模式及MRM模式的灵敏度对比

LC-HRMS-MRM MS 方法的表征

根据上述三部分研究内容，基于 ZenoTOF® 7600平台上的 Zeno SWATH 技术，建立了使用 HRMS-MRM MS 模式的非靶向 / 靶向整合方法，该方法可用于基于 HRMS 的非靶向代谢组学分析和基于 MRM 的靶向暴露组学分析。结果显示，超过 90% 的代谢特征的日内重复性相对标准偏差（RSD）小于 20%，约 89% 的代谢特征的日间 RSD 小于 20%，这证实了本研究中基于 HRMS 的代谢组学具有强大的重复性和稳定性。

对于靶向暴露组学，进行了系统深入的方法学分析，以确保定量准确。共使用 248 种外源性标准品和 21 种内标进行方法验证。结果显示，210 种外源性标准品回收率良好，RSD 小于 30%，且大多数回收率在 80%-120% 之间。此外，靶向模式下所有外源性化合物的定量范围较宽，定量下限（LLOQ）为 0.1-25ng/mL，定量上限（HLOQ）为 2.5-1000ng/mL，证实了该方法强大的定量能力。此外，使用外源性标准品对基于 MRM-MS 的暴露组学分析进行表征，超过 99% 的外源性标准品日内 RSD 小于 15%，超过 95% 的外源性标准品日间和重复性 RSD 小于 20%，这表明 MRM-MS 方法具有出色的重复性和稳定性。随后，从 10 个化学类别中选择符合既定标准的 210 种外源性标准品，用于实际样品中血清暴露组的定量分析。

外源性化合物与内源性代谢物之间的关联：

为探究外源性化合物与内源性代谢物之间的相互作用，进行相关性分析，以探究 T2DM 中外源性化合物风险背后的代谢机制。结果显示，环拉酸、氢化可的松、PFOA 和 PFOS 与脂质之间存在强正相关，脂质包括大多数长链脂肪酸（FAs）、酰基肉碱、LPC，以及一些鞘磷脂（SMs）、神经酰胺（Cers）和甘油二酯（DGs）。有证据表明，血清中 PFOA 和 PFOS 的积累与脂质升高呈正相关。本研究结果表明，PFOA 和 PFOS 通过干扰 LPC、SMs、Cers、DGs 和 CARs 等脂质代谢物，可能是 T2DM 的潜在风险因素。此外，作为一种人工甜味剂，环拉酸也被发现对脂质代谢有正向影响，这为研究环拉酸与 T2DM 之间潜在的致病机制提供了思路。

结论

血清中同时存在的内源性代谢物和环境来源的小分子与人类健康密切相关。由于这些小分子数量众多、理化性质差异大且浓度范围广，全面分析和定量这些小分子是一项巨大的挑战。在本研究中，基于SCIEX ZenoTOF® 7600系统建立了一种 HRMS-MRM MS 模式的非靶向 / 靶向整合方法。结果表明，该方法能够同时实现广

MKT-34449-A

泛覆盖的代谢组分析和精确的暴露组定量，大多数外源性化合物的检测灵敏度高于 HR 模式，特别适用于分析体积有限或珍贵难获取的生物样品。随后，该方法应用于 T2DM 的暴露组全关联研究，以识别风险因素、代谢重编程特征及其关联。本研究首次实现了一种统一的方法，可同时对内源性代谢物进行非靶向分析，并对 210 种外源性化合物进行靶向分析，为代谢组 - 暴露组全关联研究（mEWAS）提供了一种新方法，显著提高了研究效率。

参考文献

[1]. Pengwei Guan, Yuting Wang, Tiantian Chen, Jun Yang, Xiaolin Wang, Guowang Xu, Xinyu Liu; Novel Method for Simultaneously Untargeted Metabolome and Targeted Exposome Analysis in One Injection. Analytical Chemistry. 2025, 97(7): 3996-4004. https://doi.org/10.1021/acs.analchem.4c05565

MKT-34449-A

Targeted flux analysis through the Mass Isotopomer Multi-Ordinate Spectral Analysis (MIMOSA) Workflow

Using the QTRAP 6500+ LC-MS/MS System with SelexION® Technology and Elucidata Software

Darren Dumlao[1], Tiago Alves[2] and Richard Kibbey[2]
[1]SCIEX, USA, [2]Yale University, New Haven, USA

Fluxomics is a relatively recent application of mass spectrometry-based techniques that employs the use of stable labeled isotopes to trace how specific metabolites and molecules are metabolized through biological pathways. Commonly, ^{13}C or ^{15}N labeled precursor molecules are fed into a biological system and allowed to be metabolized for a given amount before the experiment is quenched. The experimental design can include a single time point once the system reaches a steady-state or a series of time points for a kinetic understanding of how the metabolites are changing over time. Unlike isotope labeling experiments, which mainly focus on the incorporation of labeled atoms into certain metabolites, the output of a flux experiment is a rate. A flux rate reveals details about how a biological system changes between 2 or more cohorts. For a metabolite with an increased enrichment of label, a flux rate can distinguish if this is due to the pathway speeding up and forming more product, or accumulation due to subsequent steps in the pathway slowing down. While fluxomics is a powerful technique in understanding the dynamic changes in metabolism, these experiments require

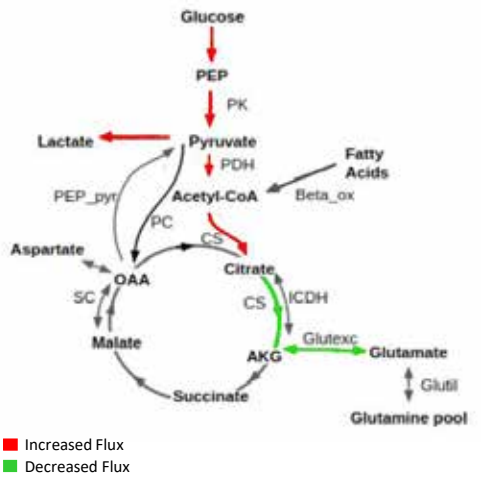

Figure 1. Fluxes were mapped to central carbon pathways to summarize the metabolic changes that occur in response to T-cell activation. The pathway map was generated in the Polly LC-MS/MS labeled workflow (Elucidata). Red indicates increases in flux and green indicates decreases in activated T-cells.

an expert level of understanding of the pathways and are mathematically rigorous.

The Kibbey lab has developed a targeted fluxomics technique, designated M.I.M.O.S.A. (Mass Isotopomer Multi-Ordinate Spectral Analysis), which is focused on energy metabolism.[1] The MIMOSA technique utilizes a targeted MRM-based method to understand each isotopologue as well as the position of the labeled carbon atoms. For separation of the glycolytic and TCA cycle intermediates, the method employs two 5-min LC gradients in conjunction with differential mobility separation. MIMOSA has been fully incorporated into the Polly software (Elucidata) with their LC-MS/MS labeled workflow. This automated workflow has removed the barriers and improved the rigor for fluxomics research.

Key features of MIMOSA fluxomics

- Uses the QTRAP® 6500+ System with SelexION® Technology for high sensitivity and specificity
- Describes fluxes for glycolytic and TCA cycle intermediates for energy metabolism studies
- Deconvolves the labeling patterns at the MS/MS level to measure positional enrichment
- Experimental output calculates normalized rates, pathway directionality, and dynamic metabolic changes between cohorts
- Polly software fully automates the data processing (natural abundance correction, absolute % enrichment, background correction, flux calculations) and data visualization which dramatically reduces the sample-to-graph time

RUO-MKT-02-12698-A

- Polly is flexible and customizable and is capable of handling other stable labeled isotopes

Methods

Sample preparation: A protocol detailing the isolation, culture, and activation of primary human CD4+ T-cells is described in Hiemer *et al*.[4] Briefly, cells were unstimulated or stimulated with ImmunoCult. Cells were harvested and incubated with fresh cold media without glucose or glutamine (MP Biomedicals) that had been supplemented with sodium bicarbonate (3.7 g/L), 10 mM HEPES, 0.2% essentially FFA free BSA (Sigma), 0.05 mM sodium pyruvate, 4 mM glutamine, and 0.45 mM L-lactate for 1 h. Cells were washed with PBS and resuspended in ^{13}C-glucose labeled media that consisted of 5.5 mM [U-$^{13}C_6$]-D-glucose (CLM-2001; Cambridge Isotopes). Cells were incubated in glucose labeling media for 4 h. Cells were subsequently washed with ice-cold PBS, and cellular metabolism was quenched with ice-cold 20% methanol in 0.1% formic acid supplemented with 10 µM d_4-taurine (Cambridge Isotopes), 3 mM sodium fluoride (Sigma), 1 mM phenylalanine (Sigma), and 100 µ M EDTA. Cells were frozen in V-bottom plates (Bioexpress, Cat #T-3025-8B) and lyophilized overnight to dryness. Samples were resuspended in water and 2 µL were injected on column.

Chromatography: The M.I.M.O.S.A chromatography has been described in Alves *et al*.[1] In short, glycolytic intermediates were analyzed using an Amino Acid 50 x 2.1 mm, 3 µm column (Imtakt) . The TCA cycle intermediates were analyzed using a Hypercarb 100 x 2.1 mm column (Thermofisher). The gradient conditions for both are described in Table 1.

Mass spectrometry: MS analysis was performed on the QTRAP 6500+ System equipped with SelexION Technology and an IonDrive™ Turbo V Ion Source. The details of the MS experiments have been described in Alves *et al*.[1] Briefly, the instrument parameters for the glycolytic intermediates experiment were the following: CAD 9, Curtain gas 30, IonSpray Voltage -3000, Temp 450, GS1 60, GS2 60, DMS modifier flow 250 µL/min, DMS temp low, SV 2200, DR off, DMS Modifier 2-propanol, DMS Modifier Composition low, Dwell 10 msec, Pause 3 msec. The instrument parameters used for the TCA cycle intermediates were: CAD 9, Curtain gas 30, IonSpray Voltage -3000, Temp 450, GS1 55, GS2 55, DMS modifier flow 325 µ L/min, DMS temp medium, SV 2600, DR open, DMS Modifier 2-propanol, DMS Modifier Composition low, Dwell 10 msec, Pause 3 msec.

Table 1. Chromatography gradients used.

Glycolytic intermediates		TCA cycle intermediates	
Time (mins)	%B	Time (mins)	%B
Flow rate = 600 µL/min		*Flow rate = 400 µL/min*	
0	*90*	*0*	*0*
0.75	*90*	*1*	*0*
2	*70*	*1.5*	*20*
3.6	*70*	*3.2*	*20*
4	*90*	*3.3*	*0*
5	*90*	*4*	*0*
Mobile phase A – 100 mM ammonium acetate, pH 6.9 Mobile phase B – acetonitrile		*Mobile phase A – 15 mM ammonium formate, 20 µL of 0.5 mM EDTA pH 6.9 Mobile phase B – acetonitrile*	

Data processing: The output .wiff data files were converted to mzML using MSConvert (version 3.0.19172, Proteowizard). Peak alignment and integration were performed using El-Maven v0.12.0. Natural abundance correction, fractional enrichment, background correction, flux calculations, and graphical data visualization were calculated using Polly LC-MS/MS labeled workflow (Elucidata).

Flux analysis on T-cells

T-cells are known to employ a different metabolic program depending upon their activation state.[2] While in their resting state, T-cells utilize B-oxidation of fatty acids as a major energy source. Once stimulated, T-cells exhibit the Warburg effect and switch to aerobic glycolysis producing increased amounts of lactate. The uptake of glucose, glutamine, and fatty acids from the exogenous environment is required for T-cells to rapidly divide and mount an immune response.[3] Here, the steady state metabolic changes that occur in human T-cells 24 hours after activation was studied using a targeted MIMOSA fluxomic approach with SCIEX QTRAP 6500+ System equipped with SelexION Technology and the Polly platform for data processing and visualization.

Data processing using El-Maven

Flux data acquired on QTRAP 6500+ System with SelexION Technology were converted to mzML to process in EL-Maven for peak alignment and peak integration. Alternatively, MultiQuant™ Software (SCIEX) could have been used for peak integration, then uploaded into Polly as a .csv file with the proper format. In Figure 2 (topl), M+2 glutamate (148/43) is used to showcase how the data are visually represented in a single plot with multiple overlaid traces. The bar graph on the right side denotes the peak area for each sample allowing for collective assessment of the data. Viewing the data in this manner allows for fast peak review, instead of the hundreds or thousands of mouse clicks performed when reviewing each scan independently. Importantly, manual integrations of the data can

RUO-MKT-02-12698-A

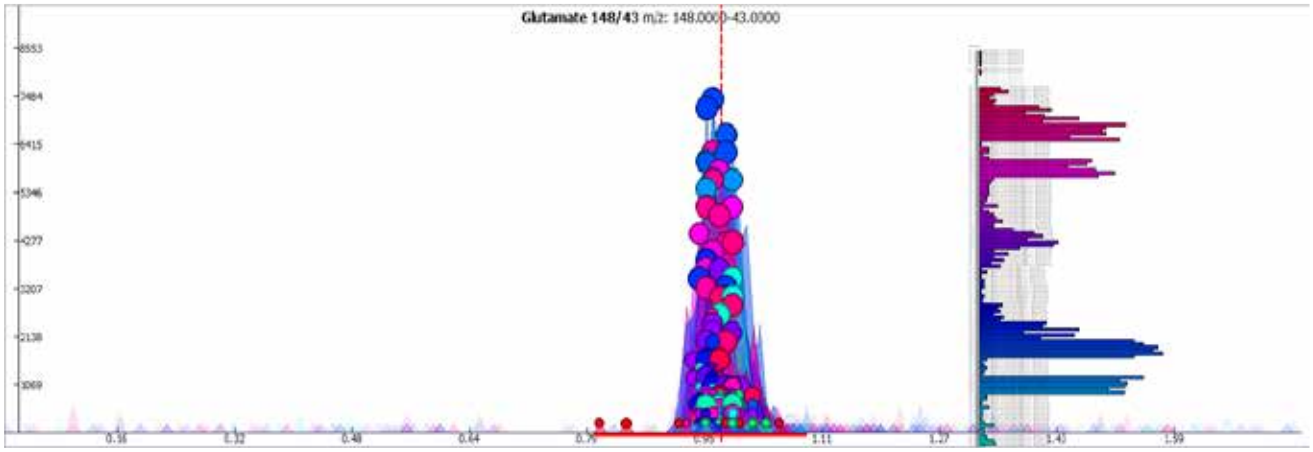

B

#	ID	Observed m/z	Expected m/z	rt	rt delta	#peaks	#good	Max Width	Max AreaTop	Max S/N	Max Quality	MS2 Score	#MS2 Events	Rank
12	Glutamate 146/41	41.0000	41.0000	0.97	0.00	156	153	24	5.14e+04	905	0.85	0.00	0	2.324764e-02
28	Glutamate 146/128	128.0000	128.0000	1.00	0.03	156	153	28	3.11e+06	259	0.84	0.00	0	1.737465e-02
13	Glutamate 147/41	41.0000	41.0000	0.97	0.00	155	134	14	3.07e+03	440	0.85	0.00	0	3.169159e-02
10	Glutamate 147/42	42.0000	42.0000	0.97	0.00	153	104	13	1.87e+03	260	0.85	0.00	0	3.381147e-02
27	Glutamate 147/129	129.0000	129.0000	1.00	0.03	156	148	28	2.27e+06	1380	0.85	0.00	0	1.739360e-02
9	Glutamate 148/41	41.0000	41.0000	0.97	0.00	149	68	14	3.45e+04	800	0.84	0.00	0	2.449962e-02
8	Glutamate 148/42	42.0000	42.0000	0.96	0.01	142	8	11	1.6e+03	320	0.84	0.00	0	3.553732e-02
7	Glutamate 148/43	43.0000	43.0000	0.97	0.00	149	72	13	5.73e+03	740	0.85	0.00	0	2.912987e-02
26	Glutamate 148/130	130.0000	130.0000	0.98	0.01	155	134	24	1.65e+06	2381	0.85	0.00	0	1.761282e-02
6	Glutamate 149/41	41.0000	41.0000	0.96	0.01	117	9	9	733	140	0.84	0.00	0	4.008596e-02
5	Glutamate 149/42	42.0000	42.0000	0.98	0.01	81	6	12	867	160	0.79	0.00	0	4.619921e-02
4	Glutamate 149/43	43.0000	43.0000	0.98	0.01	147	18	11	1.07e+03	160	0.83	0.00	0	3.836824e-02
25	Glutamate 149/131	131.0000	131.0000	1.26	0.29	150	40	19	2.27e+03	320	0.83	0.00	0	3.480655e-02
24	Glutamate 149/131	131.0000	131.0000	0.97	0.00	153	126	25	7.26e+04	3983	0.85	0.00	0	2.233860e-02
29	Glutamate 150/43	43.0000	43.0000	0.97	0.00	90	19	10	933	160	0.83	0.00	0	3.994110e-02
23	Glutamate 150/132	132.0000	132.0000	0.98	0.01	137	71	21	4.2e+04	2161	0.85	0.00	0	2.351062e-02
22	Glutamate 151/133	133.0000	133.0000	0.98	0.01	132	49	16	1.35e+04	800	0.85	0.00	0	2.672518e-02
57	Glutamine 145/127	127.0000	127.0000	1.04	0.00	156	156	32	1.71e+06	57	0.84	0.00	0	1.804220e-02
63	Glutamine 146/128	128.0000	128.0000	1.00	0.04	156	153	28	3.11e+06	259	0.84	0.00	0	1.737465e-02
18	Glutamine 147/129	129.0000	129.0000	1.00	0.04	156	148	28	2.27e+06	1380	0.85	0.00	0	1.739360e-02

Figure 2. The output from Polly LC-MS/MS labeled workflow after natural abundance correction. Additional tabs include fractional enrichment data, background correction, and a merged table. All data can be easily exported as a .csv file.

be performed as needed. El-Maven outputs processed data as a table that contains detailed information about MRM transitions, peak area, retention time, S/N, and number of peaks detected as how many are considered good peaks (Figure 2, bottom). This table is used to QC the data where the user can denote a detected metabolite as either good or bad with a checkmark or an X, respectively. The data can be automatically transferred to Polly using El-Maven's upload to the cloud function which requires an active Polly account.

Polly LC-MS/MS labeled workflow

The required files for workflow include a peak areas file (El-Maven output), a metadata file detailing the metabolites detected (molecular formula, fragment, isotope label), and a sample metadata file that denotes which cohort each sample belongs to for comparison. After the files are uploaded, the user can access the NA correction tool to perform the natural abundance correction. Natural abundance correction involves numerous calculations that considers the natural occurrence of the isotope (^{13}C = 1.1%), the number of carbons in the parent molecular and resultant fragment with all the possible labeling combinations. Setting up these calculations is laborious, time consuming, and the introduction of user error at this step is quite common. In contrast, with this automated workflow, natural abundance is calculated with a single mouse click (Figure 3).

RUO-MKT-02-12698-A

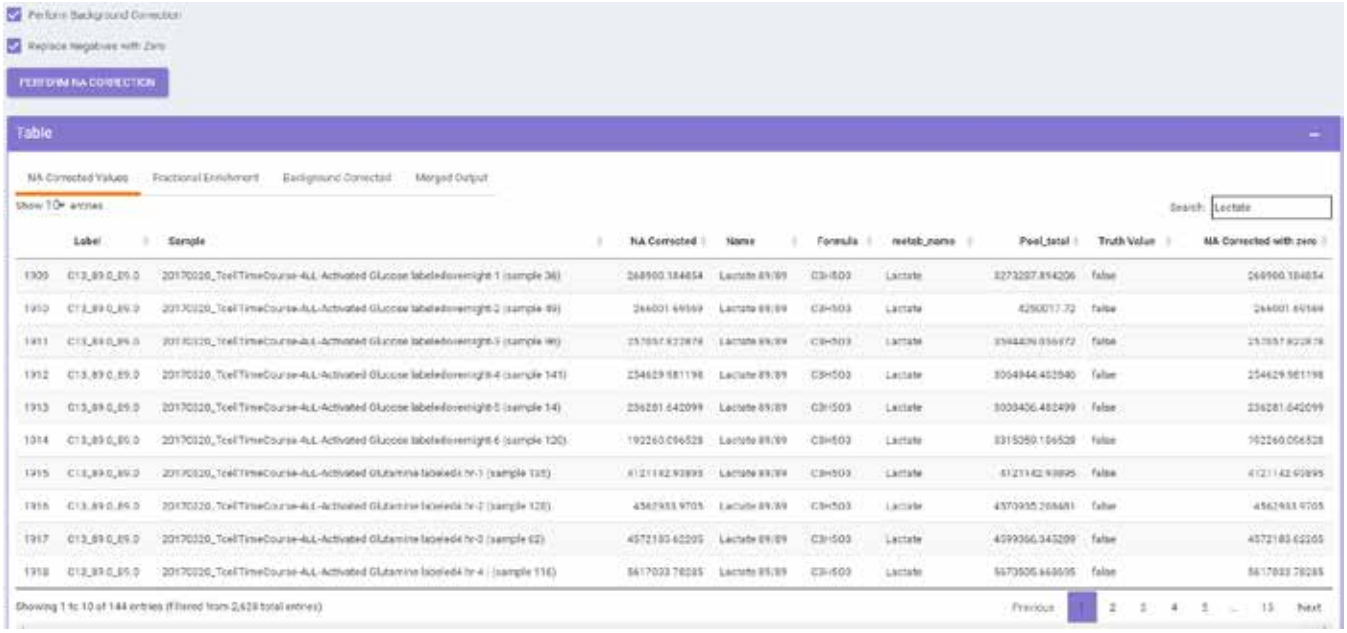

Figure 3. The output of stable isotope enrichment results calculated using Polly LC-MS/MS labeled workflow Phi (Beta).

In addition, the workflow also calculates the fractional enrichment of metabolite species and performs a background correction. The embedded search function allows the table to be filtered to only display the desired metabolite. The data can be represented graphically using the built-in visualization tools, Figure 4 shows the natural abundance corrected data for lactate. The natural abundance corrected data (represented as peak area, Figure 4A) for lactate and its isotopologues show that all isotopologue species have increased in activated T-cells (blue) compared to rested T-cells (orange). The fractional enrichment data (represented as the percentage of total lactate pool) show similar amounts of M+3 species between activated and resting T-cells (Figure 4B). An increased relative flux from glucose through lactate is suggested in activated T-cells by the lower dilutions from other non-labeled pathways. Further examination of the fractional enrichment profile of TCA intermediates show complex labeling patterns (Figure 4C and D). Citrate has an increased amount of ^{13}C incorporated into the M+2 species in general but there is more dilution between citrate and malate in activated T-cells indicating. While these data are suggestive of different utilization patterns of citrate, a more definitive interpretation requires the interpretation of positional enrichment differences between precursor and product metabolites (see below). All the data (tables and graphs) can be easily exported in a .csv or .png picture file, respectively. This fully automated workflow removes the time consuming rigorous manual labor involved in processing these types of experiments.

Phi – Flux calculations

Once the data is corrected for naturally occurring isotopes, the individual flux rates (Phi or ϕ) can be calculated. This is accomplished in the Polly Phi (Beta) tab that contains three subtabs: Calculate Phi, Results: Glucose Labeled, and Results: Generic Labeled. The Calculate Phi tab is used to define the labeled isotopes used and to display the different cohorts. Also, Polly offers customizable options for metabolites with different labeling schemes and fragmentation patterns. The two results tabs display the phi values in table and graph form for glucose and generic (used for other labeled precursors like glutamine), respectively.

In this fluxomics experiment, only uniformly ^{13}C labeled glucose ([U-$^{13}C_6$]-D-glucose) was used. Figure 5 depicts the results for the glucose labeled output with the different phi values (rows) for each sample (columns) listed. Here 45 individual phi values and positional isotopomers were calculated when using [U-$^{13}C_6$]-D-glucose as the tracer and these can be expanded to include others by user. Polly has built-in visualization tools to graphically display the flux data. Representative graphs with the expression formulas are shown to highlight the changes in metabolic flux between activated and rested cells (Figure 6). Activated T-cells

RUO-MKT-02-12698-A

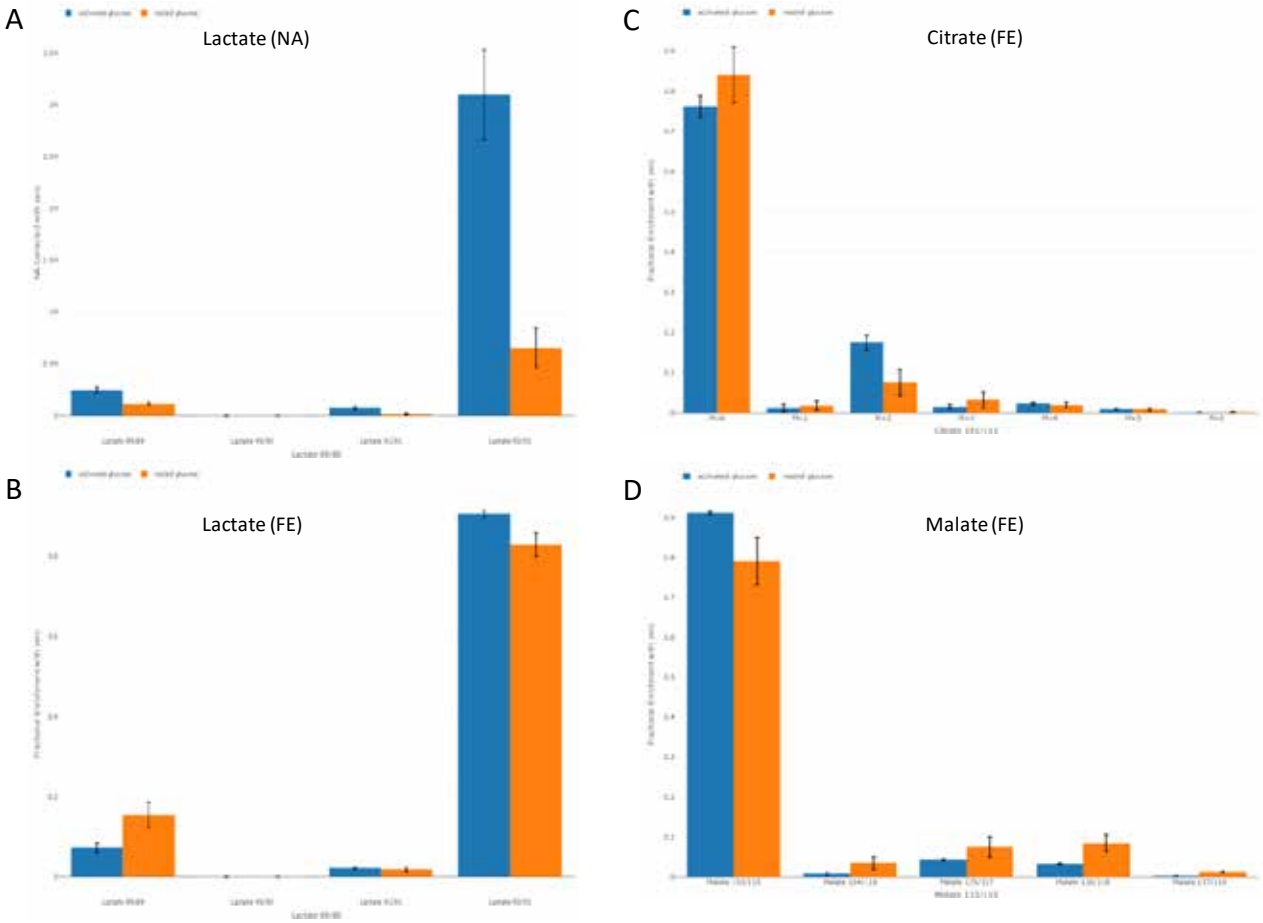

Figure 4. Visualization of natural abundance correction (NA) and fractional enrichment (FE). Representative graphs using Polly's built-in visualization tools for natural abundance correction (NA) and fractional enrichment (FE) in activated (blue bars) and rested (orange bars) T-cells. (A) depicts the natural abundance corrected isotope profile for lactate. The data is reported as average peak area. (B, C, and D) are the fractional enrichment plots for the isotope profiles of lactate, citrate, and malate, respectively. The data is reported as % of total metabolite pool. Each cohort had an n value = 6.

were observed to have a 2.5-fold increased enrichment in the pyruvate dehydrogenase (PDH) derived carbons of citrate (Figure 6A) despite only a slightly greater enrichment in lactate (Figure 4B). This identifies a greater contribution of carbohydrate oxidation to overall TCA flux in the activated cells. In contrast, there is a 70% greater loss of ^{13}C enrichment between Acetyl CoA (carbons C1,2) and those same carbons in glutamate (C4,5, Figure 6C). The same observations made by an independent calculation quantitatively validated this dramatic finding (Figure 6B). To represent the data in a biological context, metabolic flux changes that occurred in response to T-cell activation were mapped to central carbon pathways (Figure 1). Representing the data in this fashion can be useful for understanding metabolic changes, nutrient utilization, and pathway directionality.

Discussion

T-cells undergo a metabolic reprogramming when activated by a stimulus event. Using [U-$^{13}C_6$]-D-glucose, these metabolic changes were assessed after 24 hours of activation. An elevated flux of glucose through glycolysis (compared to other pyruvate generating fluxes) was observed in activated T-cells with the accumulation of ^{13}C-carbon in lactate. The dependence on glycolysis, which can rapidly generate energy, is thought to be in response to the cell's accelerated growth in mounting an immune response. Glucose was also utilized to generating citrate via PDH by a greater extent, but reduced label incorporations were seen in other TCA cycle intermediates and metabolites (malate and glutamate). One explanation of this observation is that a dilution of ^{13}C-carbon is occurring after citrate. Consistent with this, it has been reported that activated T-cells exhibit increased uptake of exogenous glutamine. Unlabeled glutamine could be

responsible for the observed dilution entering the TCA via glutamate to α-ketoglutarate exchange. A flux experiment using labeled glutamine (for instance, [1,2-^{13}C]-L-glutamine) would be needed to provide an orthogonal confirmation.

This experiment was used to showcase the utility of a targeted fluxomics approach to better understand the dynamic metabolic changes that occur during T-cell activation. The sensitivity and speed of the QTRAP 6500+ System enabled the highest quality data to be collected for the 100+ MRMs within the method. The orthogonal separation of the SelexION Technology was instrumental in separating many of the isobaric compounds in glycolysis and the TCA cycle.

The Polly LC-MS/MS labeled workflow removed many of the barriers and bottlenecks associated with processing fluxomic data. This was accomplished by streamlining the processing from peak integration to natural abundance correction. In addition to reducing data processing time, the automated workflow eliminated user derived errors commonly associated with multi-tab spreadsheets. Another positive feature of Polly is the visualization tools. Comparisons between different cohorts can quickly be selected and graphed. The data and graphs are easily exported for use in manuscripts, posters, or presentations. The reducing the time from sample to graph allows the user to spend more time in understanding the biological impact of their experiment.

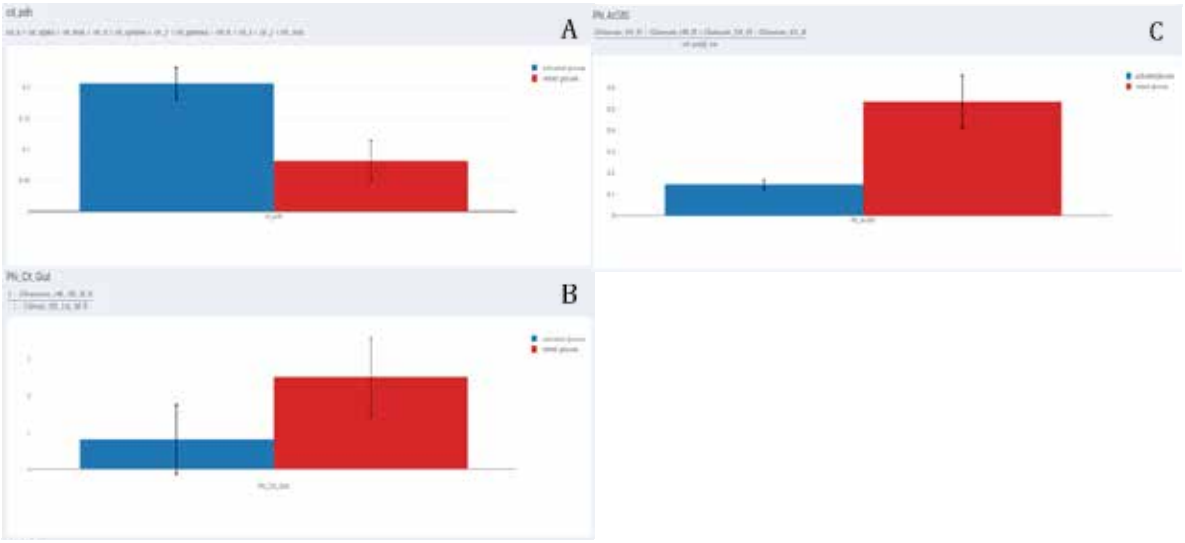

Figure 6. Representative graphs using Polly's built-in visualization tools for calculated fluxes (Phi values) for activated (blue) and rested (red) T-cells. (**A**) A greater enrichment in the pyruvate dehydrogenase (PDH) derived carbons of citrate was observed in activated T-cells. The next segment of the TCA cycle showed the opposite, namely there was a greater entry of glutamate carbon (via GDH or transamination pathways) in activated T-Cells as demonstrated by two independent calculations from citrate to glutamate (**B**) Phi_Cit_Glut and from Acetyl-CoA to citrate to glutamate (**C**) Phi_AcCitG, respectively. Each cohort had an n = 6.

RUO-MKT-02-12698-A

Figure 5. Phi results for TCA cycle calculated from MIMOSA deconvolved isotopomers from [U $^{13}C_6$]-D-glucose tracer labeling of T-Cells in Polly Phi (beta). Shown are 10 of the 45 Phi calculations (identifier column) for the different T-Cell samples. Individual mathematical descriptions of the different Phis shown in a different tab (see Figure 6). Data from individual samples (identifier descriptions provided) are shown as fractional values (multiply x 100 for percent).

References

1. Alves, TC *et al.* (2015) Integrated, Step-Wise, Mass-Isotopomeric Flux Analysis of the TCA Cycle. *Cell Metab.* **22**, 936-947.
2. Geltink, RIK, Kyle, RL, & Pearce. (2018) Unraveling the Complex Interplay Between T Cell Metabolism and Function. *Annu. Rev. Immunol.* **36**, 461-488.
3. van der Windt, GJW & Pearce, EL (2012) Metabolic switching and fuel choice during T-cell differentiation and memory development. *Immunol. Rev.* **249**, 27-42.
4. Heimer S *et al.* (2019) Integrated Metabololmic and Transcriptomic Profiling Reveals Novel Activation-Induced Metabolic Network in Human T cells, Pre-publication.

SCIEX Echo™ MS系统快速分析11种高能磷酸化合物

Rapid analysis of 11 energy-rich phosphate compounds by SCIEX Echo™ MS System

陈俊苗，司丹丹，龙志敏
Junmiao Chen, Dandan Si, Zhimin Long
SCIEX 应用支持中心，中国

Keywords: SCIEX Echo™ MS System, Energy Rich Phosphate Compounds, Nucleotide Compounds, dATP, dCTP, dTTP.

引言

高能磷酸化合物是指水解时可释放大量能量的一类磷酸化合物。这类化合物多含有1到3个不等的磷酸基团如三磷酸腺苷（ATP）等，它们是生物释放、储存和利用能量的媒介，是生物界直接的供能物质。该类化合物在使用液相色谱质联用仪（LC/MS）进行分析时流动相添加剂有限，色谱峰形不好导致响应较差，目前有部分文献报道采用在流动相中加入离子对试剂，虽然可提高化合物的灵敏度，但由于离子对试剂在仪器中比较容易残留很难完全清洗干净，当更换为其他非离子对试剂的项目时容易产生信号抑制等问题。而该类化合物在液相色谱中峰形不好灵敏度差的主要原因是化合物中的磷酸基团容易与系统中微量的金属尤其是铁等结合导致[1]。而在常规液质联用分析中需要考虑在色谱柱上的保留和分离通常需要加入特殊的添加剂，比如离子对试剂或者亚甲基二磷酸[2]等来减小其在色谱系统中的吸附从而改善峰型。

SCIEX Echo™ MS系统采用声波激发耦合质谱系统（Acoustic Ejection Mass Spectrometry，AEMS）进行样品采集，是一个高通量、基于电喷雾电离质谱的系统。SCIEX Echo™ MS系统使用声波激发进样技术（ADE）来精准控制从样品板转移样品到开放式探针接口（OPI），该开放式探针接口直接连接到SCIEX Triple Quad™ 6500+系统。这种非接触式进样方式确保进样过程无残留的同时可做到每秒分析1个样品，在多个离子通道同时检测时甚至可达到每秒3个样品的超快采集速度。同时Echo MS特殊的进样设计使得样本进样过程无需接触金属管路进而减少磷酸基团和金属的吸附作用，也因此无需在流动相系统中添加特殊添加剂就可以得到很好的峰型进行定量分析。

本方法采用SCIEX Echo™ MS系统建立了一套含高能磷酸键化合物的定量方案，其中包括三磷酸腺嘌呤脱氧核苷酸（dATP）等11种化合物。本方法流动相简单、样品用量小、分析时间短且通量高，适合含高能磷酸键化合物的快速高通量分析。

SCIEX Echo MS系统检测含高能磷酸化合物的优势：

1. 以1秒每个样品的速度分析样品，真正实现高通量分析大量样本。
2. 良好的线性及灵敏度满足不同浓度水平化合物的准确定量（表1）。
3. 样品流动相简单，不需要特殊的流动相添加剂。
4. 非接触式进样方式在快速分析样品的同时确保无残留影响（图2）。

仪器设备：

SCIEX Echo™ MS系统

图1. SCIEX Echo™ MS系统

RUO-MKT-02-15681-ZH-A

样品制备

所有化合物的标准品采用纯水稀释配置不同的浓度，取50 µl加入384孔样品板中，进样体积 25 nL。

ADE方法：声波激发进样方法需要一种合适的载体溶剂把样品液滴带入到OPI开放探针端口然后进入离子源，类似于高效液相方法中的流动相。本实验选择含2 mM氟化铵的70%乙腈作为载体溶剂，最佳流速为450 µL/min。

质谱条件：

电离模式：负离子模式

扫描方式：MRM多反应监测

气帘气CUR: 25psi

源温度 Tem：350℃

雾化气Gas1：90psi

辅助气Gas2: 70psi

MRM参数：如表1

实验结果

线性及重复性：11种化合物的质谱方法及重复性结果见表1，所有化合物在线性范围内线性良好，线性关系R值均大于0.995，线性范围可达1000倍。 所有化合物均进行了重现性考察及残留考察，结果显示0.05 µg/mL浓度下连续进样6次所有化合物的RSD均小于10%，在5 µg/mL高浓度连续进样6次后再进空白溶液，11个化合物均没有残留。图2举例展示了CMP的原始峰图，其中包含各标准曲线浓度点、空白溶剂连续6次进样的谱图，从图中可以看出各浓度点响应成比例变化，且在高浓度5 µg/mL样品连续进样6次后直接进样空白溶剂没有发现样品残留。图3中举例列举其中4个化合物的标曲图，可看出化合物的线性范围较宽，线性关系良好。

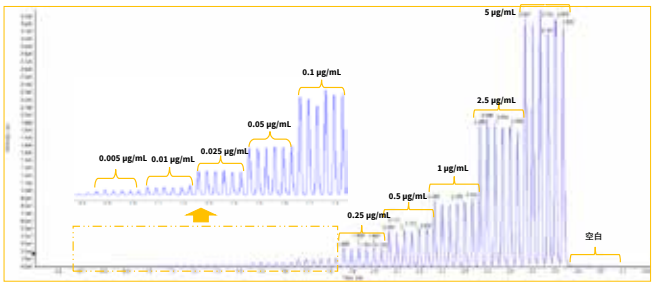

图2. CMP标准品原始峰图信息

表1. 11种高能磷酸化合物的线性范围及重复性

名称	Name	Q1	Q3	DP	CE	线性范围（µg/mL）	线性关系（R）	重复性（RSD,N=6）
胞嘧啶苷酸	CMP	322.0	96.9/78.9	-40/-90	-25/-80	0.0025-2.5	0.996	4.7%
三磷酸腺嘌呤脱氧核苷酸	dATP	490.0	159.0/78.9	-40/-40	-30/-120	0.01-5	0.995	9.2%
2'-脱氧胞苷-5'-单磷酸	dCMP	306.1	194.9/78.9	-50/-50	-25/-60	0.0025-2.5	0.996	6.4%
三磷酸胞嘧啶脱氧核苷酸	dCTP	466.0	159.0/78.9	-40/-40	-35-120	0.01-5	0.996	9.8%
胸腺嘧啶脱氧核苷酸	dTMP	321.0	194.9/78.9	-50/-50	-25/-45	0.005-2.5	0.998	3.8%
三磷酸胸腺嘧啶脱氧核苷酸	dTTP	481.0	159.0/78.9	-40/-40	-45/-120	0.01-5	0.997	9.7%
尿苷二磷酸	UDP	403.0	159.0/78.9	-50/-50	-35/-100	0.0025-1	0.995	5.8%
尿嘧啶苷酸	UMP	323.1	96.9/78.9	-40/-40	-27/-80	0.005-2.5	0.995	3.2%
腺嘌呤核苷酸	AMP	346.1	134.0/96.9	-50/-50	-40/-36	0.005-5	0.998	6.8%
鸟嘌呤核苷酸	GMP	361.9	210.9/150	-50/-50	-25/-35	0.005-2.5	0.995	4.6%
次黄嘌呤核苷酸	IMP	347.0	134.9/96.9	-40/-40	-35/-31	0.0025-1	0.998	5.7%

RUO-MKT-02-15681-ZH-A

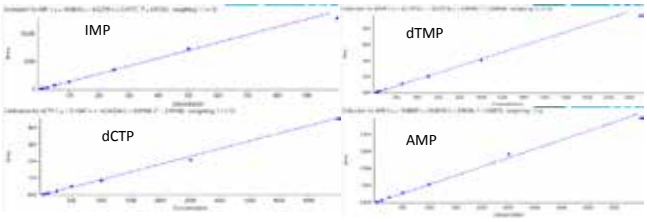

图3. 部分化合物标准曲线

总结

本文使用SCIEX Echo™ MS系统建立了11种含高能磷酸键化合物的快速高通量定量方法。各化合物线性范围宽，线性关系良好，无任何残留问题。结果表明Echo™ MS系统能够快速产生高质量的数据结果，确保只在简单的流动相条件下对含高能磷酸键的化合物进行快速准确定量。该方法线性范围宽、重现性好、定量准确、通量高，流动相简单。整个实验只需要1小时就可以完成整个384孔板上所有化合物的数据采集，而此类化合物用普通LC-MS方法需要至少5 min的液相梯度走一个样本，384个样本需要超过32小时才能完成。Echo MS系统可用于该类化合物的快速高通量分析。

参考文献

[1]. Henryk S, Markus N, Marco H; Enhanced nucleotide analysis enables the quantification of deoxynucleotides in plants revealing connections between nucleoside and deoxynucleoside metabolism. THE PLANT CELL 2021: 33: 270–289.

[2]. Rapid Analysis of 11 Energy Rich Phosphate Compounds by SCIEX Triple Quad Mass Spectrometer. SCIEX technical note RUO-MKT-02-14446-ZH-A.

RUO-MKT-02-15681-ZH-A

SCIEX Now™支持网络

一站式满足您各种支持需求

产品和数据安全

合规性服务提升您的信心，帮助您保护数据安全，确保数据完整性，以及数据管理系统的溯源性。

新手上路

我们将帮助您在SCIEX Now 学习中心在线注册，邀请您在SCIEX Now 学习中心注册学习，并向您发送欢迎电子邮件。

实验室增强服务

SCIEX实验室增强服务计划，为您的实验室提供整体服务解决方案，以提高工作效率并减少系统停机时间。

SCIEX Now 学习中心

优质的内容，个性化的学习方式 - 使用全新的科学记忆方式设计的课程。

自我学习资源

我们的知识库和社区，将帮助您提升科学知识水平，并从SCIEX专家或者同行那里找到您所需要的答案。

全工作流程技术支持

只要您在实验过程中，遇到困难挑战，SCIEX 支持团队都会帮助您高效地解决问题，实现科学目标。

立即开始成功之路：sciex.com.cn/support

SCIEX
The power of precision

SCIEX 中国

北京分公司
北京市昌平区生命科学园科学园路18号院
A座一层
电话：010-5808-1388
传真：010-5808-1390
全国咨询电话：800-820-3488，400-821-3897

上海公司及中国区应用支持中心
上海市长宁区福泉北路518号
1座502层
电话：021-2419-7201
传真：021-2419-7333
官网：sciex.com.cn

广州办公室
广州国际生物岛星岛环北路1号
B2栋501、502单元
电话：020-8842-4017

官方微信：SCIEX-China

danaher